AD 611259

WT-1453

AEC Category: HEALTH AND SAFETY
Military Category 30

OPERATION PLUMBBOB

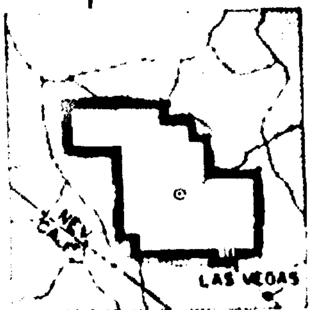

NEVADA TEST SITE
MAY-OCTOBER 1957

Project 30.6

TEST OF FRENCH UNDERGROUND PERSONNEL SHELTERS

Issuance Date: June 10, 1962

CIVIL EFFECTS TEST GROUP

NOTICE

This report is published in the interest of providing information which may prove of value to the reader in his study of effects data derived principally from nuclear weapons tests.

This document is based on information available at the time of preparation which may have subsequently been expanded and re-evaluated. Also, in preparing this report for publication, some classified material may have been removed. Users are cautioned to avoid interpretations and conclusions based on unknown or incomplete data.

PRINTED IN USA
[redacted] Available from the Office of
Technical Services, Department of Commerce,
Washington 25, D. C.

USAEC Division of Technical Information Extension, Oak Ridge, Tennessee

Report to the Test Director

TEST OF FRENCH UNDERGROUND PERSONNEL SHELTERS

By

Edward Cohen

and

Norval Dobbs

Approved by: H. J. JENNINGS
Director
Program 30

Approved by: R. L. CORSBIE
Director
Civil Effects Test Group

Ammann & Whitney
New York, New York
June 1960

ABSTRACT

The objective of this project was to investigate the predicted behavior of French underground personnel shelters, equipment, and instrumentation. Data obtained will be used for the evaluation and improvement of present designs and for the establishment of design criteria.

Five reinforced-concrete underground structures designed by French engineers were tested: one cast-in-place rectangular structure, one precast circular shelter, two entranceways at approximately the 116-psi peak overpressure range, and one entranceway at approximately the 105-psi range.

Reinforcing steel, doors, ventilation equipment, precast rings for the circular structure, and instrumentation were shipped from France and incorporated in the shelters.

Preshot and postshot precise-location surveys were made to determine the total lateral and vertical motions of the structures as a result of the blast.

Blast instrumentation consisting of Ballistic Research Laboratories (BRL) self-recording pressure gauges, French self-recording peak dynamometers, glass disk diaphragms, low-pressure manometers, recording barometers, and electronic-tube manometers and pressure gauges were used in the shelters and entranceways. Free-field measurements were recorded along the blast line. Structural response was recorded by French self-recording deformeters; recording pendulum and table; choc marts (shock impulse); electronic deflection, acceleration, and strain gauges; and seismograph.

A recording hygrometer to measure the humidity, a dust collector, self-recording fluxmeters, and peak thermometers and electronic temperature gauges to record thermal variations were also furnished from France and used in the test.

Radiation measurements were obtained by U. S. gamma-radiation film dosimeters, gamma-radiation chemical dosimeters, neutron detectors, and telemetering gamma dosimeters. Additional gamma measurements were made along the blast line and with French film badges and dosimeter recorders.

Mice were used for biological tests in all five shelters to determine the environmental aspects of the structures when subjected to nuclear blast.

PREFACE

The policy of the U. S. Government in furnishing the governments of friendly nations with unclassified information on nuclear effects led to the participation of the Service National de la Protection Civile (SNPC) of France in Operation Plumbbob. The invitation to participate in the test was extended by the Federal Civil Defense Administration (FCDA), now the Office of Civil and Defense Mobilization, in response to a request from the French Government. French participation was correlated by, and was under the sponsorship of, the FCDA

From their own resources and the unclassified information made available through NATO and elsewhere, the SNPC developed shelter designs for the protection of personnel from the effects of atomic explosions and proposed an extensive test program for inclusion in Operation Plumbbob, the 1957 test series at the Nevada Test Site. The program was planned to obtain information and data of a highly varied nature which would be of value to the FCDA as well as the SNPC.

The SNPC engaged the firm of Ammann & Whitney, Consulting Engineers, as their agent to pursue the outlined program to its completion here in the United States. The services of Ammann & Whitney included establishing and maintaining liaison with FCDA, making payments, translating and developing the contract drawings, receiving the equipment from France and arranging shipment to the site, providing field supervision during construction, and inspecting and reporting the results in accordance with AEC and FCDA requirements in a form that could be made available to the SNPC.

French participation in the test was accepted with the understanding that only such information would be made available to the SNPC as would be consistent with the national security requirements of the U. S. Government.

Edward Cohen was in charge of the work for Ammann & Whitney and served as Project Officer. Norval Dobbs served as Assistant Project Officer.

The SNPC structures were tested in the Smoky shot of Operation Plumbbob at 5:30 a.m., Aug. 31, 1957. The test was a 43-kt nuclear device mounted on a 700-ft steel tower.

In December 1957 Ammann & Whitney prepared and distributed a limited number of copies of an interim summary of test results to AEC, FCDA, and SNPC. In September 1958 a comprehensive preliminary report containing results of all data available to that date was prepared and distributed to these agencies. A supplement to this report was distributed in August 1959.

ACKNOWLEDGMENTS

The authors wish to express sincere appreciation to the following individuals for their cooperation in behalf of this project:

Civil Effects Test Group

R. L. Corsbie, U. S. Atomic Energy Commission, Director, Civil Effects Test Group

Federal Civil Defense Administration

E. R. Saunders, Director, Civil Defense Test Operation
H. J. Jennings, Director, Program 30
L. N. FitzSimons, Engineering Representative

Service National de la Protection Civile (France)

A. Martin, Conseiller Technique, Ingeniéur en Chef des Ponts et Chausséis
Capt. M. Saunois, SNPC, Armee de l'Air (France)

Ballistic Research Laboratories

J. J. Meszaros, Project Officer, Project 30.5
J. G. Schmidt, Assistant Project Officer, Project 30.5b

Lovelace Foundation of Medical Education and Research

C. S. White, Director, Program 33
D. R. Richmond, T. L. Chiffelle, R. T. Sanches, and J. D. Ward, Assistant Project Officers, Project 33.6

Ammann & Whitney, Consulting Engineers

E. Laing, A. Anderson, A. Bottenhofer, G. Pecone, and J. Fernandez, Structural Engineers
F. Wendling, J. Shirvell

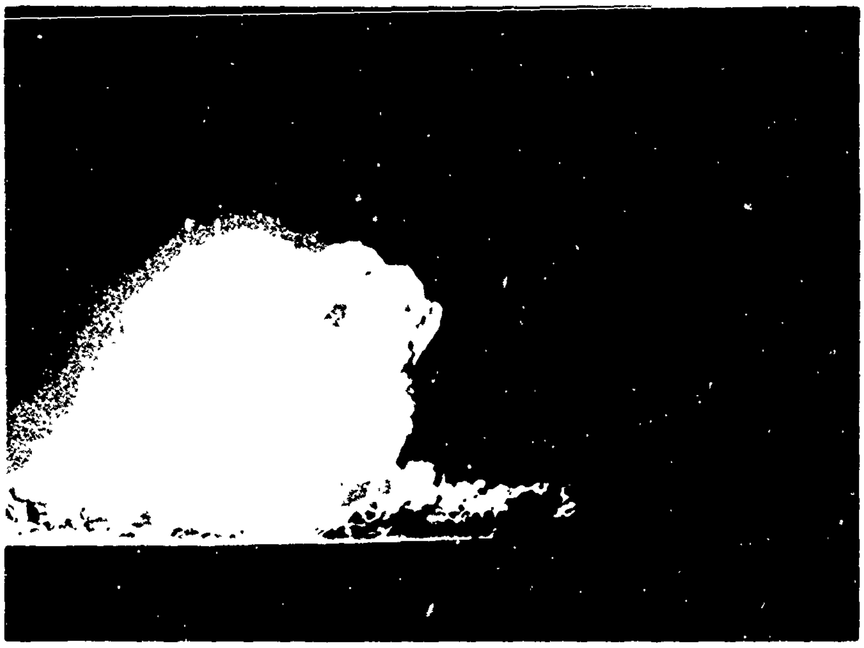

Smoky shot fireball.

Preshot photograph of tower T-2c.

CONTENTS

ABSTRACT 5

PREFACE 6

ACKNOWLEDGMENTS 7

CHAPTER 1 INTRODUCTION 19

1.1 Objectives 19
1.2 Background 19
1.2.1 Scope 19
1.2.2 Location 20
1.2.3 Orientation 20
1.3 Description of Structures 20
1.3.1 Rectangular Concrete Shelter, Type 60, Structure II-1 20
1.3.2 Cylindrical Shelter, Type 50, Structure II-2 22
1.3.3 Entrances and Entrance Chambers, Type 65, Structures II-3, II-4, and II-5 23
1.3.4 Comparative Tests 23
1.4 Design Considerations 24
1.4.1 Structural 24
1.4.2 Radiation 24

CHAPTER 2 PROCEDURE 42

2.1 Surveys 42
2.2 Instrumentation 42
2.2.1 General 42
2.2.2 French Instrumentation 42
2.2.3 U. S. Pressure Instrumentation 43
2.2.4 U. S. Radiation Instrumentation 43
2.3 Ground-shock Spectra 43
2.3.1 General 43
2.3.2 Theory 44
2.3.3 Instrumentation 44
2.4 Biological Test 45
2.4.1 General 45
2.4.2 Animals 45
2.4.3 Location 45
2.4.4 Time of Placement 45

CHAPTER 3 BLAST RESULTS 61

3.1 Structural Blast Damage 61
3.1.1 Rectangular Concrete Shelter, Type 60, Structure II-1 61

CONTENTS (Continued)

3.1.2 Cylindrical Shelter, Type 50, Structure II-2 . . . 63
3.1.3 Entrance and Entrance Chamber, Type 65, Structure II-3 . . . 65
3.1.4 Entrance and Entrance Chamber, Type 65, Structure II-4 . . . 66
3.1.5 Entrance and Entrance Chamber, Type 65, Structure II-5 . . . 67
3.2 Instrumentation . . . 68
3.2.1 French Instrumentation . . . 68
3.2.2 U. S. Pressure Instrumentation . . . 69
3.2.3 U. S. and French Radiation Instrumentation . . . 69
3.3 Ground-shock Spectra . . . 71
3.4 Biological Test Results . . . 71
3.4.1 General . . . 71
3.4.2 Mortality . . . 71

CHAPTER 4 SUMMARY . . . 142

4.1 Ground and Structure Displacements . . . 142
4.2 External Pressure . . . 142
4.3 Internal Pressure . . . 142
4.4 Structural Damage . . . 142
4.5 Radiation . . . 143
4.6 Thermal Effects . . . 143
4.7 Debris and Dust . . . 143
4.8 Limitations in Application of Test Results . . . 144

APPENDIX A CONSTRUCTION . . . 145

A.1 General . . . 145
A.2 Materials . . . 145
A.2.1 Concrete . . . 145
A.2.2 Concrete Components . . . 146
A.2.3 Concrete Forms . . . 146
A.2.4 Reinforcing Steel . . . 146
A.2.5 Structural Steel and Steel Wire . . . 146
A.3 Soil Tests and Description . . . 147
A.4 The Construction of the Structures Through Their Component Items . . . 147
A.4.1 General . . . 147
A.4.2 Excavation . . . 147
A.4.3 Floor Slabs . . . 147
A 4.4 Walls and Roof Slabs . . . 148
A.4.5 Post-Tensioning of Structure II-2 . . . 148
A.4.6 Patching . . . 149
A.4.7 Doors . . . 149
A.4.8 Ventilation Equipment . . . 149

APPENDIX B SNPC DESIGN CALCULATION FOR RECTANGULAR CONCRETE SHELTER, TYPE 60 . . . 168

B.1 General . . . 168
B.2 Main Body of the Shelter . . . 169
B.2.1 Applied Forces . . . 169
B.2.2 Roof of the Shelter . . . 169
B.2.3 Floor of the Shelter . . . 172
B.2.4 Walls of the Shelter . . . 172
B.2.5 Partition Walls . . . 174
B.2.6 Lintel Beams . . . 175

CONTENTS (Continued)

B.3 Emergency Exit Tunnel and Shaft 182
B.3.1 General 182
B.3.2 Emergency Exit Tunnel 183
B.3.3 Emergency Exit Shaft 186

APPENDIX C AS-BUILT DRAWINGS 187

APPENDIX D ANALYSIS OF RECTANGULAR CONCRETE SHELTER, TYPE 60, STRUCTURE II-1 276

D.1 General 276
D.2 Blast Loading 276
D.3 Strength Criteria 276
D.4 Analysis 277
D.5 Design and Structure 277

APPENDIX E TECHNIQUES FOR FILM-BADGE MEASUREMENT 289

E.1 General 289
E.2 Calibration 289
E.3 Handling of Film Badge 290
E.4 Film Processing 290
E.4.1 Problems of Processing Control 291
E.4.2 Controlled Processing of Radiation Film Badges 291
E.4.3 Processing Procedure 292
E.5 Analysis 292

ILLUSTRATIONS

CHAPTER 1 INTRODUCTION

1.1 Rectangular Shelter, Type 60, Structure II-1, Architectural Layout 25
1.2 Circular Shelter, Type 50, Structure II-2, Architectural Layout 26
1.3 Entrance and Entrance Chamber, Structure II-3, Architectural Layout . . 27
1.4 Entrance and Entrance Chamber, Structure II-4, Architectural Layout . . 28
1.5 Entrance and Entrance Chamber, Structure II-5, Architectural Layout . . 29
1.6 Location and Orientation of Structures, Project 30.6 30
1.7 Above-ground View of Sand Filter After Backfilling 31
1.8 Above-ground View of Intake and Exhaust Stacks 31
1.9 Nessi Ventilation System, Structure II-1 32
1.10 Dumoulin Type Blast Door 32
1.11 Forward Room of Main Chamber, Structure II-1 33
1.12 Rear Room of Main Chamber, Structure II-1 33
1.13 Ventilation Room, Structure II-1 34
1.14 Exterior View of Structure II-2 Before Backfilling 34
1.15 Above-ground View of Structure II-2 After Backfilling 35
1.16 Main Entrance, Vertical Shaft, Structure II-2 35
1.17 Nessi Ventilation System, Structure II-2 36
1.18 Interior View of Main Chamber, Structure II-2 36
1.19 Exterior View of Structure II-3 37
1.20 Exterior View of Structure II-4 37
1.21 Exterior View of Structure II-5 38
1.22 Interior View of Structure II-3 38
1.23 Interior View of Structure II-4 39

ILLUSTRATIONS (Continued)

1.24 Interior View of Structure II-5 39
1.25 Typical Entrance Structures II-3, II-4, and II-5 40
1.26 Interior View of Society Cheops Doors, Structure II-4 40
1.27 Bauche Doors, Structure II-3 41
1.28 Interior End of Ventilation System, Structure II-5 41

CHAPTER 2 PROCEDURE

2.1 Rectangular Shelter, Type 60, Structure II-1, Survey Points 47
2.2 Circular Shelter, Type 50, Structure II-2, Survey Points 48
2.3 Entrance and Entrance Chamber, Structure II-3, Survey Points 49
2.4 Entrance and Entrance Chamber, Structure II-4, Survey Points 50
2.5 Entrance and Entrance Chamber, Structure II-5, Survey Points 51
2.6 Rectangular Shelter, Type 60, Structure II-1, Instrumentation Layout . . 52
2.7 Circular Shelter, Type 50, Structure II-2, Instrumentation Layout . . . 53
2.8 Entrance and Entrance Chamber, Structure II-3, Instrumentation Layout . . 54
2.9 Entrance and Entrance Chamber, Structure II-4, Instrumentation Layout . . 55
2.10 Entrance and Entrance Chamber, Structure II-5, Instrumentation Layout . . 56
2.11 Location of Radiation-detection Equipment 57
2.12 Single-Degree-of-Freedom Spring-Mass System 58
2.13 Shock Gauge 59
2.14 Mouse Cage 59
2.15 Location of Biological Specimens 60

CHAPTER 3 BLAST RESULTS

3.1 Roof-slab Crack Pattern, Structure II-1 85
3.2 Floor-slab Crack Pattern, Structure II-1 86
3.3 Entrance Crack Pattern, Structure II-1 87
3.4 Blast Damage of Forward Room Floor Slab 88
3.5 Blast Damage of Lintel Beam at Main Partition Opening 88
3.6 Blast Damage of Rear Room Floor Slab 89
3.7 Roof-slab Cracks of the Rear Section of the Main Chamber 89
3.8 Roof-slab Cracks of the Rear Section of the Main Chamber 90
3.9 Blast Results of Interior End of Intake Ventilation Pipe 90
3.10 Over-all View of Blast Results of Interior End of Exhaust Pipe . . . 91
3.11 Internal Blast Results of Interior End of Exhaust Pipe 91
3.12 Blast Damage to Ventilation Duct Connections 92
3.13 Roof-slab Cracks of Forward Section of Main Chamber 92
3.14 Blast Damage of Main Entrance 93
3.15 Blast Damage of Main Entrance 93
3.16 Debris Resulting from Blast at the Main Entrance 94
3.17 Blast Debris and Damage of the Entrance Facing Away from GZ . . . 94
3.18 Cracks Formed in Roof Slab of Landing 95
3.19 Blast Results of Exit Tunnel 95
3.20 Debris and Damage Produced by the Blast Wave in the Entrance Facing Away from GZ 96
3.21 Detail View of Chipped-out Section at Top of Entrance Facing Away from GZ 96
3.22 Postshot View of Sand Pit and Main Entrance 97
3.23 Postshot View of Sand Pit 97
3.24 Postshot View of the Corner of the Sand-pit Facing GZ 98
3.25 Developed Vertical Elevation Facing GZ, Structure II-2 99
3.26 Developed Vertical Elevation Facing Away from GZ, Structure II-2 . . . 99

ILLUSTRATIONS (Continued)

3.27 Spalling and Cracking on GZ Side of Ring 10 100
3.28 Cracking of Ring 10 on Side Facing Away from GZ 100
3.29 Vertical Movement of Ring 10 in Relation to Ring 11 at Their Crowns . . 101
3.30 Cracking and Spalling of Joint 8-9 and Ring 8 at Crown 101
3.31 Spalling and Cracking of Rings 2 and 3 at Their Crowns 102
3.32 Spalling and Cracking on the Side of Rings 2 and 3 Facing GZ 102
3.33 Separation of Joint Between Rings 2 and 3, Side Facing GZ 103
3.34 Separation of Concrete Seats Between Rings 3 and 4, Side Facing GZ . . 103
3.35 Interior End of Exhaust Pipe After Detonation 104
3.36 Detail View of Intake-pipe Flap Plate After Detonation 104
3.37 General View of Interior End of Intake Pipe After Detonation 105
3.38 Postshot View of the Above-ground Portion of the Exhaust Stack and Exit Shaft 105
3.39 Sand Blasting of Exhaust Stack, Facing GZ 106
3.40 Blast Damage to the Exhaust Stack, Side Parallel to Blast Line . . . 106
3.41 Blast Damage to Exposed Surface of Front Reflection Shield of Sand-pit 107
3.42 Blast Damage to Unexposed Surface of Front Reflection Shield of Sand-pit 107
3.43 Blast Damage to Above-ground Portion of Structure Facing GZ . . . 108
3.44 Detail View of Blast Damage to Main Entrance and Sand-pit 108
3.45 General View of Above-ground Portion of the Structure, Facing Away from GZ 109
3.46 Entrance Crack Pattern, Structure II-3 110
3.47 Entrance Crack Pattern, Structure II-3 110
3.48 Interior End of Exhaust Valve After Detonation 111
3.49 Postshot View of Interior End of Intake Pipe 111
3.50 Blast Damage to Roof Slab of Entrance Landing 112
3.51 Blast Damage to Walls of Entrance Facing GZ 112
3.52 Detail View of End of Roof Slab of Entrance Facing GZ 113
3.53 Blast Damage of Entrance Facing GZ 113
3.54 Blast Debris Deposited on Stairs of Entrance Facing GZ 114
3.55 Blast Damage to Surface Section of Entrance Facing Away from GZ . . . 114
3.56 Blast Debris Deposited on Stairs of Entrance Facing Away from GZ . . . 115
3.57 Entrance Crack Pattern, Structure II-4 116
3.58 Entrance Crack Pattern, Structure II-4 116
3.59 Blast Debris and Damage of Entrance Facing Away from GZ 117
3.60 Blast Results of Ball Type Antiblast Valve 117
3.61 Entrance Crack Pattern, Structure II-5 118
3.62 Entrance Crack Pattern, Structure II-5 118
3.63 Postshot View of Interior Surface of Main Blast Door 119
3.64 Blast Damage to Upper Portion of Entrance Facing Structures II-3 and II-4 119
3.65 Blast Debris and Damage to Lower Portion of Entrance Facing Structures II-3 and II-4 120
3.66 Blast Damage to Upper Portion of Entrance Facing Blast Line 120
3.67 Record, Recording Pendulum, Structure II-1 121
3.68 Record, Recording Pendulum, Structure II-2 121
3.69 Record, Recording Pendulum, Structure II-3 121
3.70 Record, Recording Pendulum, Structure II-5 121
3.71 Pressure Vs. Time; Self-recording Pressures Gauge Records 122
3.72 Blast-line Pressure Vs. Distance Curve 130

3.73 Blast-line Pressure, Mach Number Vs. Time; Self-recording Dynamic Pressure Gauge Records . . . 131
3.74 Blast-line Pressure vs. Time; Electronic and Self-recording Pressure Gauge Records . . . 135
3.75 Blast-line Pressure Vs. Time; Self-recording Pressure Gauge Records . . . 136
3.76 Approximate Total Gamma Dosages During First 52 Hr After Detonation . . . 138
3.77 Blast-line Total Gamma Dose Vs. Distance Curve . . . 139
3.78 Displacement Shock Spectrum, Vertical Direction . . . 140
3.79 Displacement Shock Spectrum, Horizontal Direction . . . 141

APPENDIX A CONSTRUCTION

A.1 Structure II-1, Partially Erected Base Slab Formwork . . . 157
A.2 Structure II-1, Partially Placed Base Slab Reinforcement . . . 157
A.3 Structure II-1, Base Slab Poured; Interior Formwork Partially Erected . . . 158
A.4 Structure II-1, Roof Slab and Wall Reinforcement Placed . . . 158
A.5 Structure II-1, Concrete Placement for Structure Above Base Slab . . . 159
A.6 Structure II-2, Precast Circular Segments Placed . . . 159
A.7 Structure II-2, Reinforcement of Upper Section of Shaft T-1 . . . 160
A.8 Structure II-2, Erecting Exterior Formwork for Shaft T-2 . . . 160
A.9 Structure II-2, During Backfilling . . . 161
A.10 Structure II-2, Typical Backfill Saturation Procedure . . . 161
A.11 Structure II-2, Standard Compaction Procedure Near Structure . . . 162
A.12 Structure II-3, Erecting Base Slab Formwork . . . 162
A.13 Structure II-3, Stripping Base Slab Formwork . . . 163
A.14 Structure II-3, Concrete Placement in Walls and Roof Slab . . . 163
A.15 Structure II-3, Before Backfilling . . . 164
A.16 Structure II-4, Base Slab Formwork with Ventilation Pipe in Place . . . 164
A.17 Structure II-4, Stripping Exterior Formwork . . . 165
A.18 Structure II-5, Concrete Placement in Base Slab . . . 165
A.19 Structure II-5, Before Concrete Placement . . . 166
A.20 Typical Excavation Equipment . . . 166
A.21 Structures II-1, II-2, II-3, II-4, and II-5, Excavation . . . 167

APPENDIX C AS-BUILT DRAWINGS

C.1 Rectangular Shelter, Type 60, Title Sheet . . . 189
C.1.1 Rectangular Shelter, Type 60, Dimensional Plan and Section . . . 190
C.1.2 Rectangular Shelter, Type 60 Partial Dimensional Plan and Door Locations . . . 191
C.1.3 Rectangular Shelter, Type 60, Main Reinforcement Roof and Floor Slabs . . . 192
C.1.4 Rectangular Shelter, Type 60, Sections and Reinforcing Details . . . 193
C.1.5 Rectangular Shelter, Type 60, Roof and Floor Slab Stirrup Details, Main Wall Reinforcement . . . 194
C.1.6 Rectangular Shelter, Type 60, Reinforcement for Air Intake and Exhaust Structures . . . 195
C.1.7 Rectangular Shelter, Type 60, Reinforcement for Emergency Exit Tunnel and Shaft . . . 196
C.1.8 Rectangular Shelter, Type 60, Reinforcing Details at Door Locations S1 and S2 . . . 197
C.1.9 Rectangular Shelter, Type 60, Reinforcement at Door Locations F1 and F2 . . . 198

C.1.10 Rectangular Shelter, Type 60, Entrance Stairs, Sections and Details 199
C.1.11 Rectangular Shelter, Type 60, Bar List 200
C.1.12 Rectangular Shelter, Type 60, Spiral Reinforcement for Ventilation Ducts and Door Anchorages 201
C.1.13 Rectangular Shelter, Type 60, Mounting Details for Concrete Deformeter and Pendulum 202
C.1.14 Rectangular Shelter, Type 60, Inserts and Anchor Bolts for Instrumentation 203
C.1.15 Rectangular Shelter, Type 60, Instrumentation Layout 204
C.1.16 Rectangular Shelter, Type 60, Cable Layout for Recorder 3.5.4 . . . 205
C.1.17 Rectangular Shelter, Type 60, Scheme of Installation of Mechanical Equipment 206
C.1.18 Rectangular Shelter, Type 60, Scheme of Installation and Bill of Materials 207
C.1.19 Rectangular Shelter, Type 60, Details of Equipment 208
C.1.20 Rectangular Shelter, Type 60, Details of Equipment 209
C.1.21 Rectangular Shelter, Type 60, Blast-resistant Door FIBY, Structure II-1, at Location F1 210
C.1.22 Rectangular Shelter Type 60, Blast-resistant Door FIBX, Structure I-1, at Location F1 211
C.1.23 Rectangular Shelter, Type 60, Gastight Door at Location F1 . . . 212
C.1.24 Rectangular Shelter, Type 60, Fire Door at Location F1 213
C.1.25 Rectangular Shelter, Type 60, Anchorages for Doors at Location F1 214
C.1.26 Rectangular Shelter, Type 60, Blast-resistant Door at Location F2 215
C.1.27 Rectangular Shelter, Type 60, Gastight Door at Location F2 . . . 216
C.1.28 Rectangular Shelter, Type 60, Anchorage for Blast-resistant and Gastight Doors at Location F2 217
C.1.29 Rectangular Shelter, Type 60, Blast-resistant Emergency Exit Door at Location S2 218
C.1.30 Rectangular Shelter, Type 60, Gastight Emergency Exit Door at Location S2 219
C.1.31 Rectangular Shelter, Type 60, Anchorage for Blast-resistant and Gastight Doors at Location S2 220
C.1.32 Rectangular Shelter, Type 60, Blast-resistant Door and Anchorage at Location S1 221
C.1.33 Rectangular Shelter, Type 60, Door Operating Mechanism for Doors S1TX and S1TY 222
C.2 Circular Concrete Shelter, Type 50, Title Sheet 223
C.2.1 Circular Concrete Shelter, Type 50, Structures I-2 and II-2, Dimensional Plan and Sections 224
C.2.2 Circular Shelter, Type 50, Structures I-2 and II-2, Layout of Entrance Shaft T2 225
C.2.3 Circular Concrete Shelter, Type 50, Structures I-2 and II-2, Layout of Emergency Exit Shaft T1 226
C.2.4 Circular Concrete Shelter, Type 50, Structures I-2 and II-2, Details of Precast Units 227
C.2.5 Circular Shelter, Type 50, Structures I-2 and II-2, Emergency Exit Shaft (T1) Reinforcing Details 228
C.2.6 Circular Shelter, Type 50, Structures I-2 and II-2, Emergency Exit Shaft (T1) Reinforcing Details 229

ILLUSTRATIONS (Continued)

C.2.7 Circular Shelter, Type 50, Structures I-2 and II-2, Emergency Exit Shaft (T1) Reinforcing Details 230
C.2.8 Circular Shelter, Type 50, Structures I-2 and II-2, Main Entrance Shaft (T2) Reinforcing Details 231
C.2.9 Circular Shelter, Type 50, Structures I-2 and II-2, Main Entrance Shaft (T2) Reinforcing Details 232
C.2.10 Circular Shelter, Type 50, Structures I-2 and II-2, Main Entrance Shaft (T2) Reinforcing Details 233
C.2.11 Circular Shelter, Type 50, Structures I-2 and II-2, Main Entrance Shaft (T2) Reinforcing Details 234
C.2.12 Circular Shelter, Type 50, Structures I-2 and II-2, Main Entrance Shaft (T2) Reinforcing Details 235
C.2.13 Circular Shelter, Type 50, Structures I-2 and II-2, Main Entrance Shaft (T2) Reinforcing Details 236
C.2.14 Circular Shelter, Type 50, Structures I-2 and II-2, Main Entrance Stair Details 237
C.2.15 Circular Shelter, Type 50, Structures I-2 and II-2, Inserts and Anchor Bolts for Instrumentation 238
C.2.16 Circular Concrete Shelter, Type 50, Structure II-2, Equipment, Benches, and Inserts for Instruments 3.1.1.3 and 3.4.1.1 239
C.2.17 Circular Shelter, Type 50, Structure II-2, Instrumentation Layout 240
C.2.18 Circular Shelter, Type 50, Structures I-2 and II-2, Layout of Ventilation Equipment and Bill of Materials 241
C.2.19 Circular Shelter, Type 50, Structures I-2 and II-2, Ventilation Equipment 242
C.2.20 Circular Shelter, Type 50, Structures I-2 and II-2, Installation and Details of Ventilation Equipment 243
C.2.21 Circular Shelter, Type 50, Structures I-2 and II-2, Frame for Door S3BZ 244
C.2.22 Circular Shelter, Type 50, Structures I-2 and II-2, Frame for Door S3BU 245
C.2.23 Circular Shelter, Type 50, Structures I-2 and II-2, Door Operating Mechanism for Doors S3BZ and S3BU 246
C.2.24 Circular Shelter, Type 50, Structures I-2 and II-2, Door Operating Mechanism for Doors S1DZ and S1TU 247
C.2.25 Circular Shelter, Type 50, Structures I-2 and II-2, Doors F1BZ and F1BU Air Filter Covers S4Z and S4U 248

C.3 Entrance and Entrance Chamber, Type 65, Structures 3, 4, and 5, Title Sheet . 249
C.3.1 Entrance and Entrance Chamber, Type 65, Structure 3, Dimensional Plan and Sections 250
C.3.2 Entrance and Entrance Chamber, Type 65, Structure 3, Main Reinforcement Roof and Floor Slabs 251
C.3.3 Entrance and Entrance Chamber, Type 65, Structure 3, Main Wall Reinforcement 252
C.3.4 Entrance and Entrance Chamber, Type 65, Structure 3, Entrance Wall and Slab Reinforcement 253
C.3.5 Entrance and Entrance Chamber, Type 65, Structure 3, Reinforcement for Air Intake and Exhaust Structures 254
C.3.6 Entrance and Entrance Chamber, Type 65, Structure 3, Door Anchorage, Frame Installation, and Reinforcement at Door Location 255

ILLUSTRATIONS (Continued)

C.3.7 Entrance and Entrance Chamber, Type 65, Structure II-3, Instrument Layout, Location of Anchor Bolts, and Inserts 256
C.4.1 Entrance and Entrance Chamber, Type 65, Structure II-4, Dimensional Plan and Sections 257
C.4.2 Entrance and Entrance Chamber, Type 65, Structure II-4, Main Reinforcement Roof and Floor Slabs 258
C.4.3 Entrance and Entrance Chamber, Type 65, Structure II-4, Main Wall Reinforcement 259
C.4.4 Entrance and Entrance Chamber, Type 65, Structure II-4, Entrance Wall and Slab Reinforcement 260
C.4.5 Entrance and Entrance Chamber, Type 65, Structure II-4, Reinforcement for Ventilation Stack 261
C.4.6 Entrance and Entrance Chamber, Type 65, Structure II-4, Door Frame Installation and Reinforcement at Door Location 262
C.4.7 Entrance and Entrance Chamber, Type 65, Structure II-4, Instrument Layout, Location of Anchor Bolts, and Inserts 263
C.5.1 Entrance and Entrance Chamber, Type 65, Structure 5, Dimensional Plan and Sections 264
C.5.2 Entrance and Entrance Chamber, Type 65, Structure 5, Main Reinforcement Roof and Floor Slabs 265
C.5.3 Entrance and Entrance Chamber, Type 65, Structure 5, Main Wall Reinforcement 266
C.5.4 Entrance and Entrance Chamber, Type 65, Structure 5, Entrance Wall and Slab Reinforcement 267
C.5.5 Entrance and Entrance Chamber, Type 65, Structure 5, Reinforcement for Air Intake and Exhaust Structures 268
C.5.6 Entrance and Entrance Chamber, Type 65, Structure 5, Spiral Reinforcement for Ventilation Ducts and Door Anchorages 269
C.5.7 Entrance and Entrance Chamber, Type 65, Structure 5, Reinforcement at Door Location Fl 270
C.5.8 Entrance and Entrance Chamber, Type 65, Structure II-5, Instrument Layout, Location of Anchor Bolts, and Inserts 271
C.6.1 Power Cable Layout, Structures I-4, II-1, II-2, II-3, II-4, and II-5 272
C.6.2 Measuring Instruments 3.1.1.1, 3.1.1.4, and 3.1.1.5 273
C.6.3 Measuring Instruments 3.1.1.2, 3.2.1.1, and 3.3.1.1 274
C.6.4 Measuring Instrument 3.1.1.3 275

APPENDIX D ANALYSIS OF RECTANGULAR CONCRETE SHELTER-STRUCTURE II-1 .

D.1 Resistance Vs. Deflection Curve 288
D.2 Free-Field Pressure Vs. Time Curve 288

APPENDIX E FILM BADGE MEASUREMENT TECHNIQUES

E.1 Cobalt-60 Gamma Calibration System 293
E.2 Du Pont Film Packet and EG&G Film Badge 293
E.3 EG&G Taping Machine 294
E.4 Densitometer 294

ILLUSTRATIONS (Continued)

E.5 Effect of Development Time on the Shape of the Characteristic Curve of a Typical Medium-speed Film 295
E.6 Comparison of White Light and Gamma Radiation Exposure Densities . . 295

TABLES

CHAPTER 2 PROCEDURE

2.1 Summary of French Instrumentation 46

CHAPTER 3 BLAST RESULTS

3.1 Diametrical Postshot Measurement of Precast Rings and Joints . . . 72
3.2 Results of French Instrumentation 73
3.3 Data from Maximum Dynamometer (3.2.1.1) 74
3.4 Results of Glass-disk Pressure Indicator (3.2.1.5) 75
3.5 Results Obtained by Caisson Manometer (3.2.2.2) 75
3.6 Results of Recording Barometer (3.2.2.3) 75
3.7 Data from Lateral Gauges (3.1.1.1) 76
3.8 Data from Door Deformeter (3.1.1.2) 77
3.9 Data from Concrete Deformeter (3.1.1.3) 78
3.10 Temperature Measurements Using Maximum Thermometer (3.3.1.2) . . 78
3.11 Results Obtained by Recording Thermometer (3.3.2.1) 78
3.12 Summary of Performance of Electronic Recorder 79
3.13 Results of BRL Self-recording Pressure Vs. Time Gauges 80
3.14 Blast-line Measurements of Peak Dynamic Pressure 81
3.15 Blast-line Measurement of Peak Overpressure 81
3.16 Comparison of French and EG&G Dosimetry 82
3.17 Blast-line Goal-Post Data 82
3.18 Displacement Shock Spectrum 83
3.19 Mortality Results of Biological Test 84

APPENDIX A CONSTRUCTION

A.1 Schedule of Construction (1957) 151
A.2 Laboratory Test Results (Cylinders) 151
A.3 Laboratory Test Results (Cubes) 152
A.4 Laboratory Test Results (Beams) 152
A.5 Average Values of Concrete Test Data 153
A.6 Concrete Hammer Tests (Equivalent Cylinder Strength, psi) 153
A.7 Typical Concrete-Mix Design 154
A.8 Laboratory Test Results of Reinforcement and Post-Tensioning Wires 154
A.9 In-Place Density Test Results 155
A.10 Over-all Length of Precast Cylinders During Post-Tensioning Operation 155
A.11 Gauge Length During Post-Tensioning Operation 156
A.12 Relative and Absolute Elongation, and Stresses of Post-Tension Cables . . 156

APPENDIX D ANALYSIS OF RECTANGULAR CONCRETE SHELTER, STRUCTURE II-1

D.1 Dynamic Analysis No. 2 287

APPENDIX E TECHNIQUES FOR FILM-BADGE MEASUREMENT

E.1 Film-badge Calibration 292

Chapter 1

INTRODUCTION

1.1 OBJECTIVES

The main objectives of the program, as presented by the Service National de la Protection Civile (SNPC), were to verify the predicted effects of a nuclear explosion on civilian construction and to obtain as much basic data as possible to assist in future planning of protective construction. By subjecting structures and experiment, designed in accordance with French codes and practices and constructed by methods and with materials used in France, to an actual blast, it was hoped to substantiate the interpretations, hypotheses, and conclusions made from unclassified information and data previously made available and used for the test designs.*

It was planned that data would be obtained concerning the characteristics of the blast wave; structural strains; deflections and deformations; soil displacements; and interior and exterior pressures, temperatures, heat, and radioactivity. These were to be obtained within the limits of the extensive instrumentation provided by SNPC and supplemented by U. S. agencies. Gross physical characteristics and structural behavior were to be determined by visual observation and inspection.

1.2 BACKGROUND

1.2.1 Scope

The SNCP outlined an extensive program that would provide highly detailed data on all the phenomena produced by the test. However, the extent of this program was so great that the construction could not be completed within the test schedule, and the program had to be greatly reduced.

Although the reduced program sacrificed some of the completeness of the original program, it was expected that careful planning, systemized observation, and extensive instrumentation would still provide the basic data and information desired.

The final program consisted in the exposure of the following five structures:

Structure II-1, rectangular concrete shelter, type 60
Structure II-2, circular shelter, type 50, with precast units
Structure II-3 }
Structure II-4 } entrances and entrance chambers, type 65
Structure II-5 }

Architectural drawings showing the general features of these structures are shown in Figs. 1.1 to 1.5.

* *The Effects of Atomic Weapons*, U. S. Government Printing Office, Washington, D. C.

1.2.2 Location

The structures were placed at two locations with respect to Ground Zero (GZ). Structures II-1, II-2, II-3, and II-4 were placed at location II, with a predicted overpressure of 132 psi; and structure II-5 was placed at location III, with a predicted overpressure of 118 psi.

Approximately 50-ft clearance was provided in a lateral direction between the structures, except II-1 and II-2 which had a 100-ft separation.

Figure 1.6 shows the site layout of the structures and the blast-line instrumentation of the French program.

1.2.3 Orientation

All structures except II-5 were oriented similarly with the longitudinal axis of the chamber perpendicular to the blast line (Fig. 1.6); thus the entranceways were in line with the direction of the blast. This orientation minimized the reflected pressure that would occur on the main blast door. Structure II-5 at location III was oriented at 90° to the structures at location II; so its longitudinal axis was parallel to the blast line.

1.3 DESCRIPTION OF STRUCTURES

1.3.1 Rectangular Concrete Shelter, Type 60, Structure II-1

Structure II-1 is a complete protective shelter (Figs. 1.7 and 1.8) designed for a capacity of 50 persons with 60 cu ft of space provided for each person sheltered. It consists of the entrance stairs, an antechamber, the main body of the shelter, an emergency exit tunnel, and an emergency exit shaft. The ventilation system is a Nessi type, and the doors are made by Dumoulin (Figs. 1.9 and 1.10).

The shelter, in general, is 46 ft 7 in. by 13 ft 9 in. by 11 ft $5\frac{1}{2}$ in. high and is constructed of poured-in-place reinforced concrete. It was designed for an overpressure of 147 psi, with 1 ft $11\frac{1}{2}$-in.-thick main walls and slabs and approximately 0.3 per cent reinforcement.

The entrance is a through type with two stairways, 3 ft $3\frac{1}{2}$ in. wide, meeting at the bottom in a common entry landing. The roof slab over the stairs and the stairway walls and slabs are $11\frac{3}{4}$ in. thick; the roof slab over the landing, as well as the landing, is 1 ft $3\frac{3}{4}$ in. thick; and the exterior wall of the landing is 1 ft $11\frac{1}{2}$ in. thick.

The main entrance from the landing into the antechamber consists of an opening 2 ft $3\frac{1}{2}$ in. wide by 4 ft $10\frac{7}{8}$ in. high which is closed by three doors. On the exterior face of the wall opening is a $1\frac{9}{16}$-in. structural-steel flat-plate blast door, hung on a steel frame which is set before pouring. This door was designed for 147-psi overpressure. On the inside face of the wall opening, a $8\frac{11}{16}$-in. concrete fire-resistant door and a $\frac{3}{16}$-in. structural-steel gastight door are provided on a single frame. Recesses in the concrete are provided to receive the anchorage lugs of this common frame, which is set and grounted in after pouring.

Radiation attenuation is provided by a 3-ft 11-in. earth cover over the main body of the structure.

Two reinforced-concrete air-exhaust stacks extend 9 ft $3\frac{1}{2}$ in. above grade, and two air-intake stacks extend only 2 ft $8\frac{1}{2}$ in. above ground level. These intake and exhaust stacks are used in the natural-ventilation system only and are expendable.

The pipes for these ventilation systems are fitted with an automatic ball type dual-action antiblast valve, a protective grill against small animals at their outer opening, and a gastight stop flap at the opening inside the shelter.

Normal ventilation is provided by air drawn in from the outside, either directly by gravity through the intake vents or, when the system is operated electrically, through one of the exhaust stacks, through a simple dust filter, and into an intake fan that propels the air into the chamber. Three quick-acting shut-off valves located between the exhaust stacks and the intake fan control the electrically operated system. The output is 15,891.5 cu ft/hr, providing a complete air change every 30 min.

The superstructure of the shelter, which rises to grade near the entrance, accommodates two pits filled with sand for the filtered-air system. Each filter contains about 35.3 cu ft of clean graded sand in a 2-ft layer over the air-intake apparatus. The system, which has an output of 3178.3 cu ft/hr, draws air in through the two sand filters in parallel; the air is then passed through an activated-carbon filter and aerosol paper into the shelter.

An air-exhaust system is provided to prevent build-up of pressure within the main chamber due to the mechanical ventilation. The exhaust system consists of a series of pipe sleeves embedded in the walls of the antechamber. A pipe between the main chamber and antechamber expels the excess pressure from the main room to the antechamber. The build-up in pressure in the antechamber is relieved by means of a vent pipe leading from the antechamber to a point located between the blast and fire doors. A third pipe then runs from the space between the doors to the entranceway. The second pipe has a valve at the antechamber end of the sleeve; the pipe leading to the exterior has a ball type antiblast valve at its midpoint.

The ventilators can be controlled either electrically, from the power for lighting, or manually.

Because the ventilation system may place the shelter under overpressure, provision was made for conduits to evacuate the build-up of the ventilation pressure, with an internal safety valve operating under 6 mm of water, an overpressure gauge, and an antiblast double-action ball type valve protecting the safety valve.

The condensation water in the filter sand gathers at a low point and is accumulated at the bottom of the filters. It is then brought into the shelter by a pipe fitted with a siphon. This siphon, which is filled with water, prevents the ventilator from drawing air from the shelter interior through the siphon pipe rather than outside air through the sand filter.

Excess water from the siphon drains into the shelter drain pit. The air-distribution system inside the shelter is fitted with blow-offs for the disposal of condensation water.

Neither the natural nor the emergency ventilation system of this shelter was in operation during the test since this shelter was highly instrumented. Individual components of the Nessi type ventilation were tested in the less extensively instrumented structures II-2, II-4, and II-5.

For the test, the shelter was equipped with an electrical system; the power was supplied by one of two generators located in shelter II-2. The system comprised the electrical power supply for the ventilation and lighting arrangement. The lighting equipment consisted of six 150-watt incandescent bulbs mounted on a cable and strung from the ceiling of the main chamber. An additional 150-watt bulb was connected to an extension cable and hung on the wall of the main chamber facing GZ.

The antechamber, which is 8 ft $6^1/_4$ in. by 2 ft $3^1/_2$ in. by 7 ft $6^1/_2$ in. high, has an opening 5 ft $10^7/_8$ in. by 2 ft $3^1/_2$ in. leading to the main chamber of the structure. This opening is equipped with a $1^1/_4$-in. blast door and a $^3/_{16}$-in. gastight structural-steel door. The blast door has a steel frame that was placed before the pouring of the concrete walls; grout pockets were provided for the frame of the gastight door.

The main chamber, which has an over-all floor area of approximately 266.4 sq ft, is divided into two major sections by a 1-ft $3^3/_4$-in. by 6-ft 6-in. partition. The forward and rear sections of the main chamber are shown in Figs. 1.11 and 1.12, respectively, and the ventilation room is shown in Fig. 1.13.

At the opposite end of the shelter from the main entrance, access to the emergency exit tunnel is provided by means of an opening 1 ft $11^5/_8$ in. wide and 2 ft $7^1/_2$ in. high. This opening is closed by a $1^3/_{16}$-in. steel blast door and a $^3/_{16}$-in. steel gastight door, one on either side of the opening. Heat protection is obtained by filling the space between the doors with sandbags.

The emergency exit tunnel has an interior cross section 2 ft $7^1/_2$ in. wide by 3 ft $3^1/_2$ in. high; for this test the tunnel was 13 ft $3^1/_2$ in. long. It terminates at a 2-ft $7^1/_2$-in.-square vertical shaft that provides the means of exit to the ground level above. The opening at the top of the shaft is covered by a horizontal $^3/_8$-in. checkered-plate blast door, also designed for an overpressure of 147 psi. The door is so arranged that it can be opened from either the inside or the outside of the shaft.

1.3.2 Cylindrical Shelter, Type 50, Structure II-2

The cylindrical shelter, structure II-2 (Figs. 1.14 and 1.15), is designed to accommodate a maximum of 32 persons. It consists of a main entrance shaft, an entrance antechamber, a main precast body, an exit chamber, and an emergency exit shaft.

The shelter is entered by means of a spiral steel stair (Fig. 1.16) in a vertical shaft 5 ft $10^3/_4$ in. by 3 ft $11^1/_4$ in., with walls 1 ft $3^3/_4$ in. thick. The shaft is closed at the top (at grade level) by a horizontally sliding steel-plate blast door $1^9/_{16}$ in. thick. At the bottom of the shaft another blast door $1^1/_4$ in. thick and a gastight door permit access through a 2-ft $3^1/_2$-in.-wide by 5-ft 11-in.-high opening into a 5-ft 11-in. by 3-ft $11^1/_4$-in. by 7-ft $2^3/_4$-in.-high antechamber.

Natural ventilation is provided by a Nessi system, which is similar in type and design to that used in structure II-1 (Fig. 1.17). The intake air is drawn down a pipe that is located in the exterior wall of the antechamber. The pipe is equipped with a ball type dual-action anti-blast valve to protect the safety valve and the intake fan against blast. The air is forced, either by gravity or by an electrical intake fan, into the main chamber of the structure. A quick-acting shut-off valve governs the method of intake. Air exhaust is accomplished by means of an exhaust stack. The interior end of the stack is fitted with overpressure and anti-blast valves. The air-change capacity of the system is 1.5 times per hour. The natural ventilation system was not in operation during the test.

A sand-filter pit containing a filtered-air system, which is normally in operation during blast conditions, is located above the antechamber. The air is drawn through 34.5 cu ft of sand, consisting of a 2-ft-thick layer over the air-intake apparatus, by means of the intake fan. The air is passed through an activated-carbon filter and aerosol paper before it is passed to the main chamber. The condensation formed in the sand filter, as in structure II-1, is accumulated at the bottom of the pit and is removed from the pit by a drain with a siphon connected at its end. The water in the siphon prevents the air from being drawn out of the shelter. The siphon also acts as an overflow to deliver the condensation water to the drain of the structure.

The forced-ventilation system, which can be either electrically or manually controlled, was in operation during the test. Electrical power during the test was supplied by one of two gasoline-engine-driven generators located in the main chamber. The generator also operated a lighting system, which consisted of one 150-watt bulb mounted on an extension cable and hung on the main chamber wall facing away from GZ. The exhaust system of the generator set was connected to an exhaust pipe placed at the position usually occupied by the overpressure valve at the interior end of the exhaust stack. The overpressure valve was removed to minimize the chance that the exhaust gases might back up in the chamber and stall the generator engine.

The main body, 19 ft $6^3/_8$ in. long, is composed of 12 circular precast reinforced-concrete elements 8 ft $10^1/_4$ in. in OD, 10 in. thick and 1 ft $6^1/_2$ in. long (Fig. 1.18). These elements are aligned concentrically during construction on a concrete-setting bed and are post-tensioned together with 8 cables by the Freyssinet method.* The $1^1/_2$-in. joints between precast elements are filled with slow-setting concrete mortar. A bearing stress of 122 psi is obtained on the faces of each element by the tensioning of the cables.

After the post-tensioning operation, the entrance and exit shafts are poured in place.

The earth cover above the main structure was 4 ft 9 in. for this test.

At the exit end of the shelter, there is an exit chamber 4 ft $7^1/_4$ in. by 3 ft $3^1/_4$ in. by 6 ft $9^1/_2$ in. high, above which is the air exhaust stack. This stack, projecting 7 ft $8^1/_2$ in. above ground level, is of reinforced concrete.

Access from the exit chamber to the vertical exit shaft is by a 1-ft $11^3/_4$-in. by 2-ft $7^1/_2$-in. opening, which is closed with a $^{13}/_{16}$-in. steel blast door on one side and a $^3/_{16}$-in. steel gastight door on the other. The frame of the blast door is placed before pouring, and the frame for the gastight door is set after the concrete is poured by grouting the anchorages into the recesses that are provided.

---

* *Freyssinet Prestressing Units*, Intercontinental Equipment Co., Inc., 120 Broadway, New York 5, N. Y.

The vertical exit shaft, 2 ft 9½ in. by 3 ft 3½ in. with 1-ft 3¾-in.-thick walls, provides an exit to the ground above. The top of the shaft is closed with a ⅜-in.-thick door designed for an overpressure of 147 psi. This door, like that of structure II-1, can be opened either from the inside or the outside. This structure and the blast doors are designed for an overpressure of 147 psi.

1.3.3 Entrances and Entrance Chambers, Type 65, Structures II-3, II-4, and II-5

The entrances and entrance chambers for all three structures are of poured-in-place reinforced concrete and are similar in design and size to the entrance and entrance chamber used for structure II-1 (Figs. 1.19 to 1.21). These structures represent entrances for typical shelters; they consist only of the stairs and one antechamber. Ventilation systems, which normally would not be placed in the antechamber of a typical structure, were added to these structures for this test. These structures were included in the test for comparative evaluation of the adequacy and effectiveness of three different types of doors, as well as the added ventilation equipment, which is also different in each entrance chamber. The reinforcement pattern for the entrances of the three structures differs only in the detailing.

Interior views of the antechambers are shown in Figs. 1.22 to 1.24, and a general view of an entrance is given in Fig. 1.25.

(a) *Doors.* The doors for structure II-5 are the same as two of the Dumoulin doors (blast and gastight) used at the entrance of structure II-1 (Fig. 1.10). Structure II-4 has entrance doors made by Society Cheops; these include a blast door and a combination fire-resistant gastight door at the opening to the chamber. The blast door on the exterior side of the opening and the combination fire-resistant gastight door on the interior side of the opening are bolted tight to the concrete by bolts passing through sleeves provided in the concrete around the perimeter of the opening (Fig. 1.26).

Bauche doors are used for structure II-3. These consist of blast, fire-resistant, and gastight doors, each on a separate frame (Fig. 1.27). Frames for the doors are installed after the main structural concrete pours are made.

(b) *Ventilation.* The ventilation systems provided in the entrance chambers were included in this test for comparison of the different types and of the efficiency of operation at the different locations.

The ventilation of structure II-3, made by Aeric, consisted of two pipes (intake and exhaust) protected by reinforced-concrete stacks. The stacks extended 3 ft above the ground surface. Each pipe contained a back-pressure flap valve that was closed by the blast pressure and remained closed until the external pressure approached the natural atmospheric condition.

The Nessi ventilation system of structure II-5 was similar to the ventilation in structures II-1 and II-2. It consisted of one air intake and one exhaust pipe, both protected by reinforced concrete. The intake and exhaust stacks extended 2 ft 7 in. above the ground surface. The pipes of the ventilation system were fitted with ball type automatic antiblast valves.

Structure II-4 was provided with a second Nessi type ventilation system, similar to the ventilation system located in structures II-1, II-2, and II-5, consisting of a single reinforced-concrete stack containing one 2-ft 7½-in.-diameter pipe with a ball type antiblast valve.

The interior end of the vent stacks in structure II-5 is shown in Fig. 1.28. The interior ends of the ventilation systems for structures II-3 and II-4 were similar.

1.3.4 Comparative Tests

Structures II-1 and II-2 at location II provided primarily a comparison of effects on shape of structure (rectangular vs. cylindrical) and method of construction (poured-in-place vs. precast elements).

Because the orientation and location of structures II-1, II-3, and II-4 were the same with respect to GZ, direct comparison of the adequacy of the different door types could be made. Also, the effectiveness of the horizontal door of structure II-2 could be compared with that of the vertical door of structure II-1.

The different orientation of similar doors in structures II-1 and II-5 allowed a comparison to be made of pressures resulting in each case.

Structures II-1 and II-5 were positioned at different locations; this provided data for different pressure levels and indicated the effectiveness of the ventilation systems and doors at these different pressures.

Structures II-1, II-3, and II-4 gave comparisons of different types of ventilation systems, as described previously, and the effectiveness of each.

1.4 DESIGN CONSIDERATIONS

1.4.1 Structural

The designs of all structures were made by French engineers in accordance with French design and construction practices to provide protection against the effects of atomic and thermonuclear detonations. The criteria used were those of a static loading condition, and the required thickness of concrete and quantity of reinforcement was obtained by an ultimate-strength method of design. The dynamic effects upon the stresses of the members, the additional strain energy available in the elasto-plastic and plastic ranges, and the pressure-time variation were not considered in the actual design. The structures were designed to withstand a uniform static overpressure of 147 psi at ultimate stress. The roofs, floors, and walls of the structures were designed for the same overpressure. A uniform negative pressure of 10 psi was also considered in the design for reversal.

The following stresses were used for design:

Concrete	
Compression (cylinder strength)	3,560 psi (ultimate)
Shear (diagonal tension)	140 psi
Reinforcing steel	
Tor (tension)	57,000 psi (yield)
(compression)	57,000 psi (yield)
(tension)	71,200 psi (ultimate)
(compression)	85,400 psi (ultimate)
AD_x	41,000 psi (yield)
Bond (Tor steel)	470 psi

Actual conditions that would exist in France were simulated by utilizing procedures of construction similar to those used in France and by using reinforcing and structural steel, doors, and ventilation equipment shipped from France.

A postshot dynamic analysis of the roof slab of the rectangular type 60 shelter is included as Appendix D of this report.

1.4.2 Radiation

Initial radiation doses of 2 to 7×10^4 r on the ground surface were assumed to be consistent with design overpressure. It was hoped that an attenuation factor of 1000 would be obtained by using earth covers of 3 ft 11 in. and 4 ft 9 in. above the roofs of the structures. The allowable radiation within the structures was taken as 20 to 70 r. It was assumed that 12 cm of concrete or 20 cm of earth would reduce the initial radiation 50 per cent.

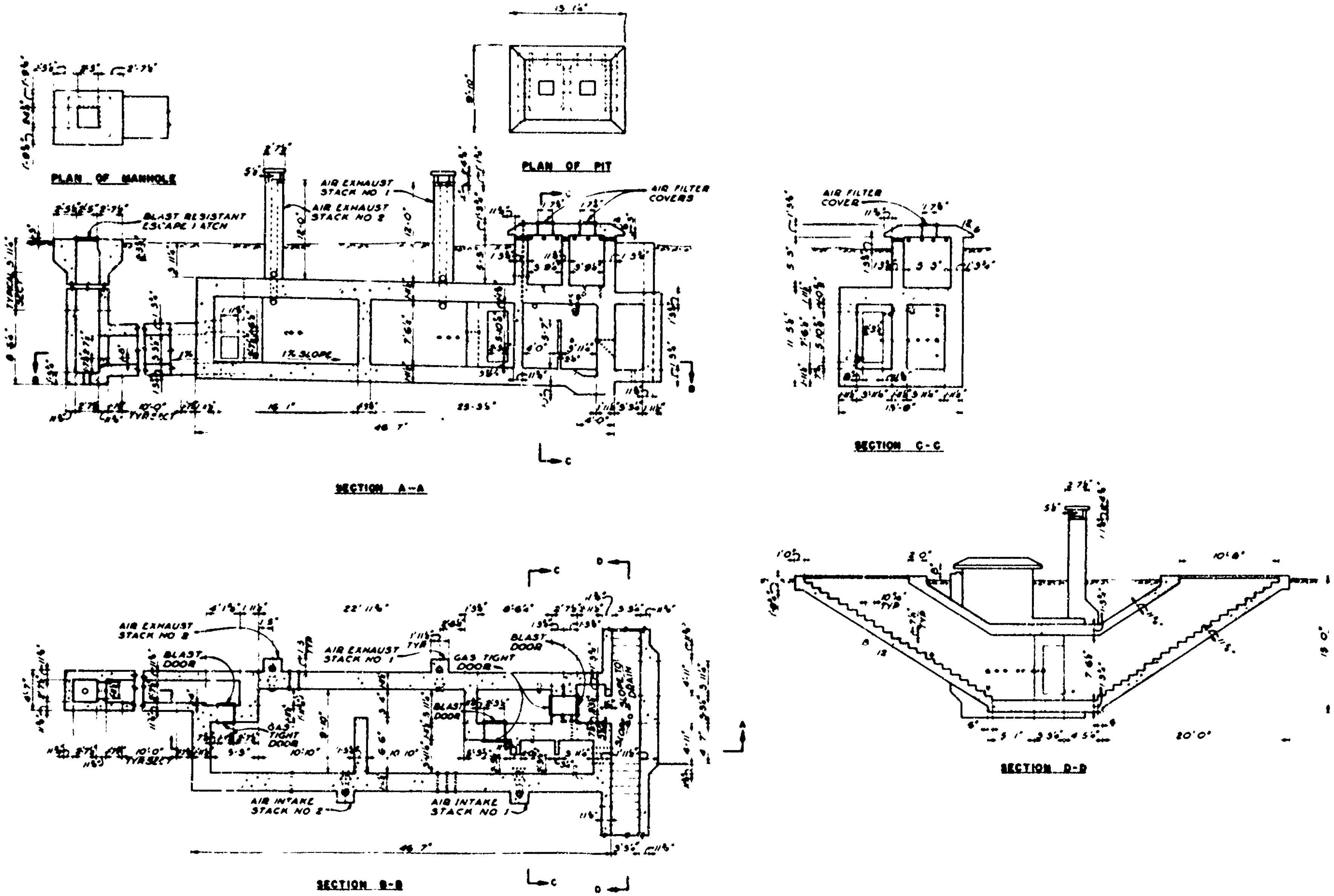

Fig. 1.1 —Rectangular shelter, type 60, structure II-1, architectural layout.

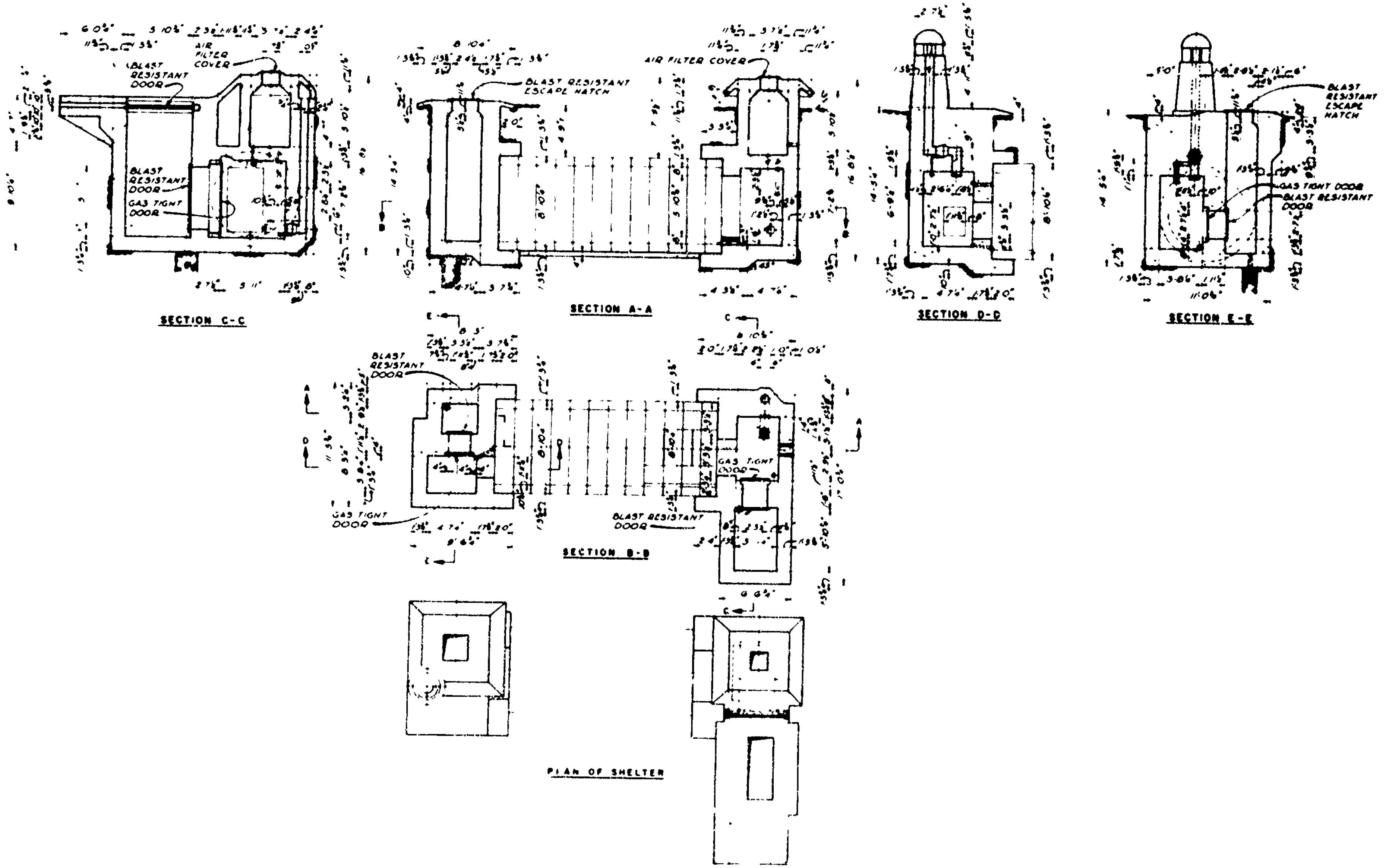

Fig. 1.2—Circular shelter, type 50, structure II-2, architectural layout.

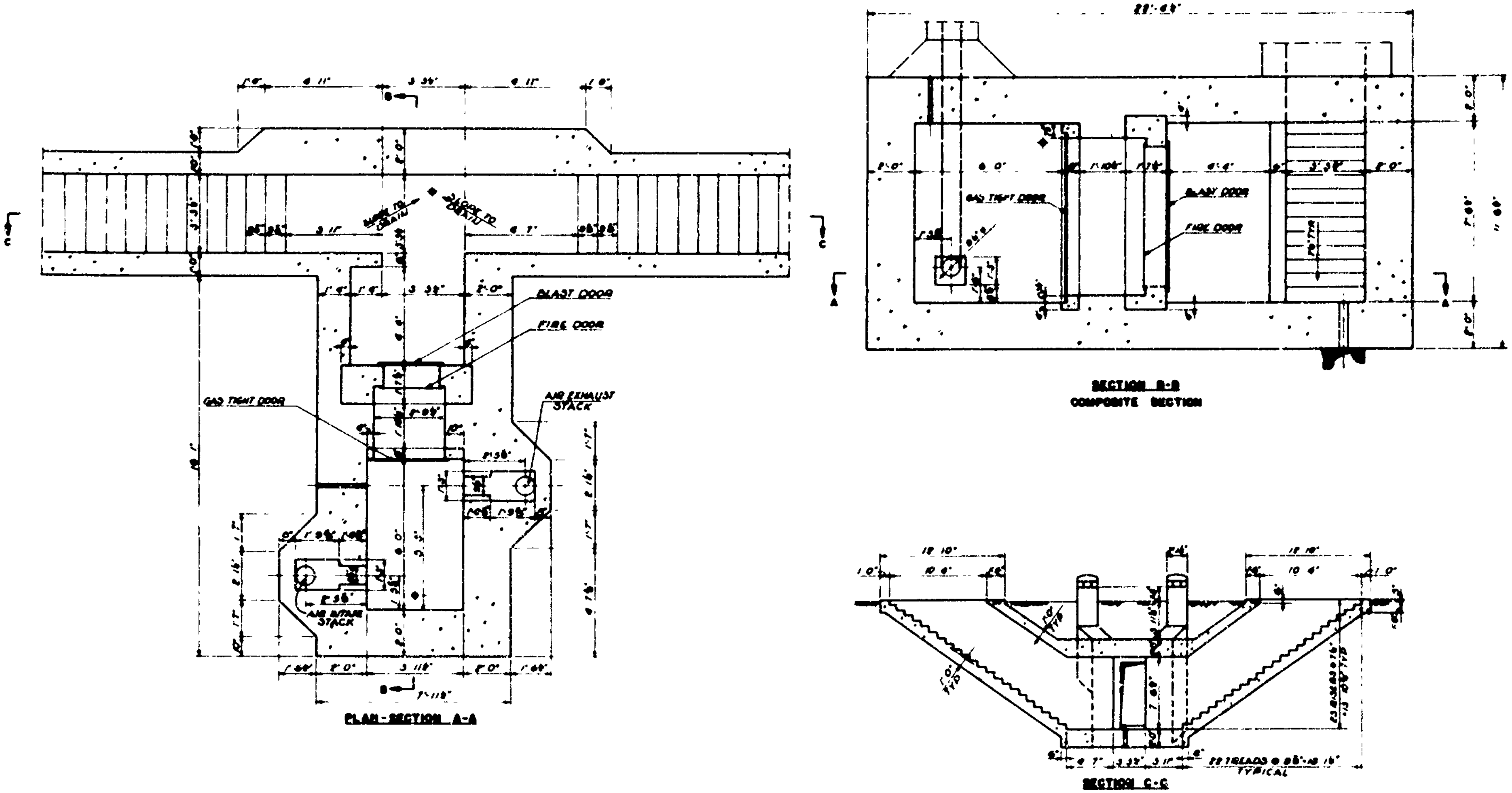

Fig. 1.3—Entrance and entrance chamber, structure II-3, architectural layout.

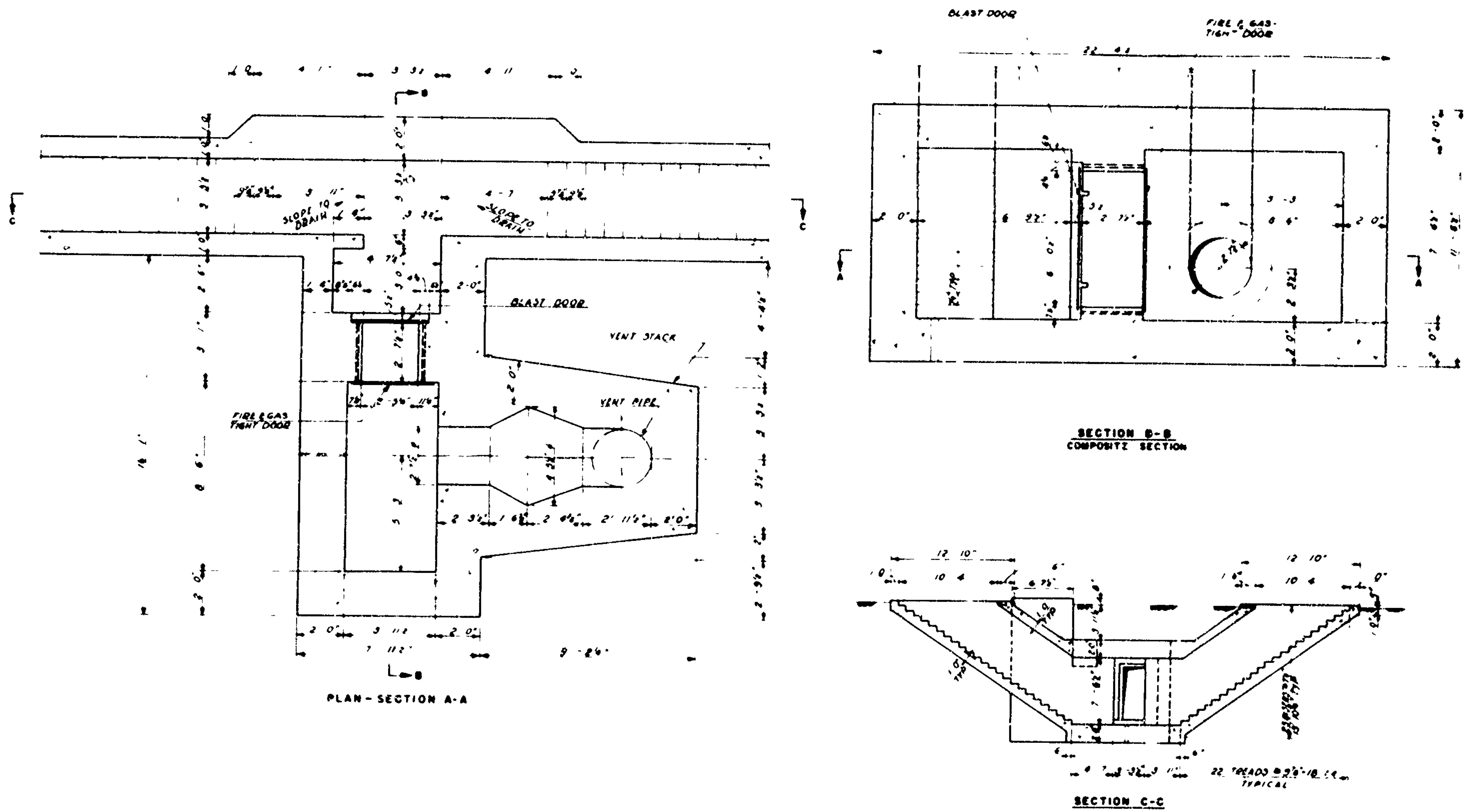

Fig. 1.4—Entrance and entrance chamber, structure II-4, architectural layout.

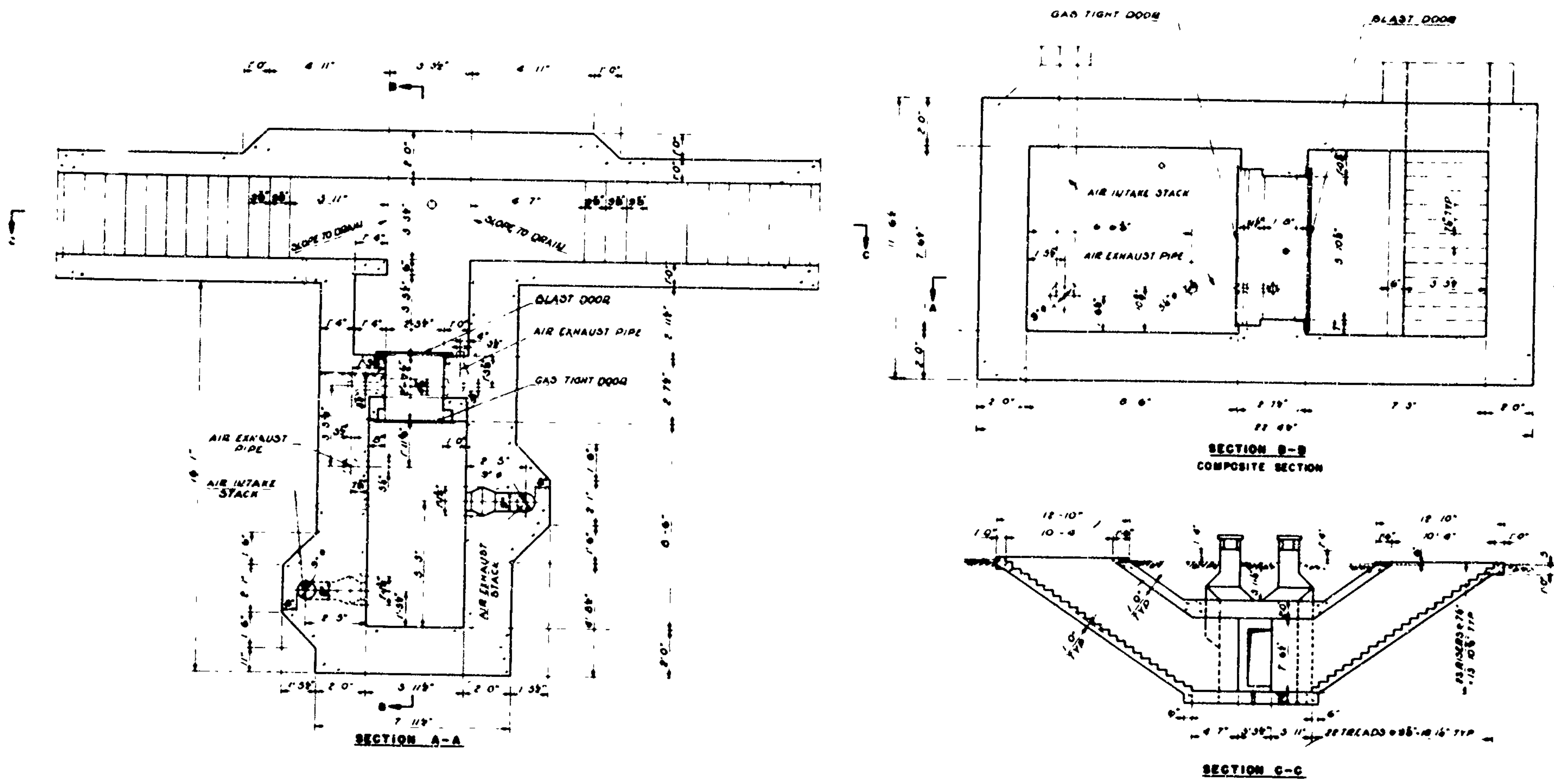

Fig. 1.5—Entrance and entrance chamber, structure II-5, architectural layout.

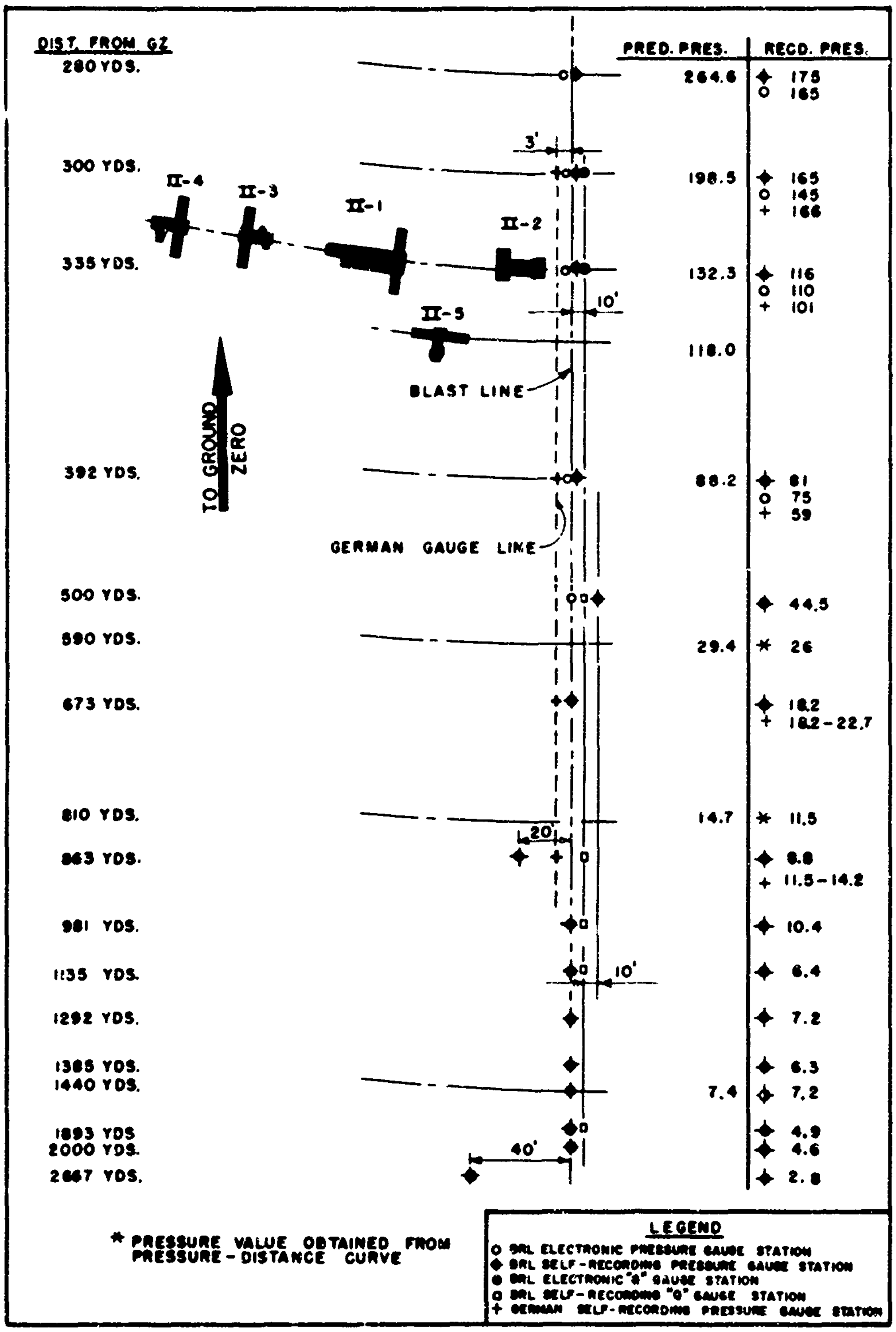

Fig. 1.6—Location and orientation of structures, Project 30.6.

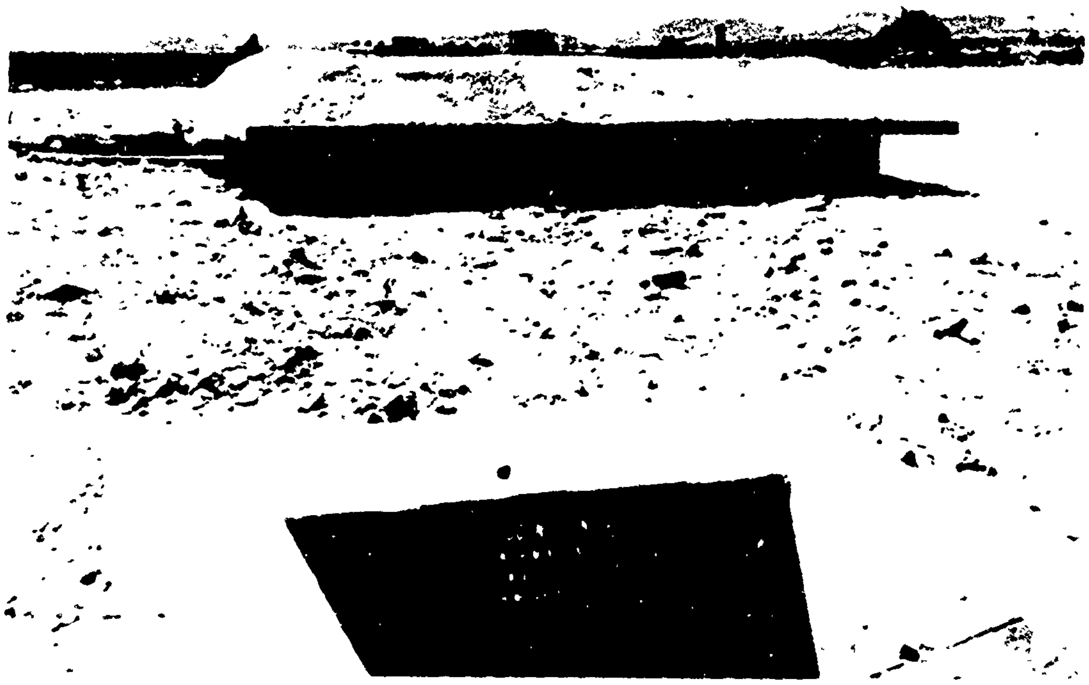

Fig. 1.7—Above-ground view of sand filter after backfilling.

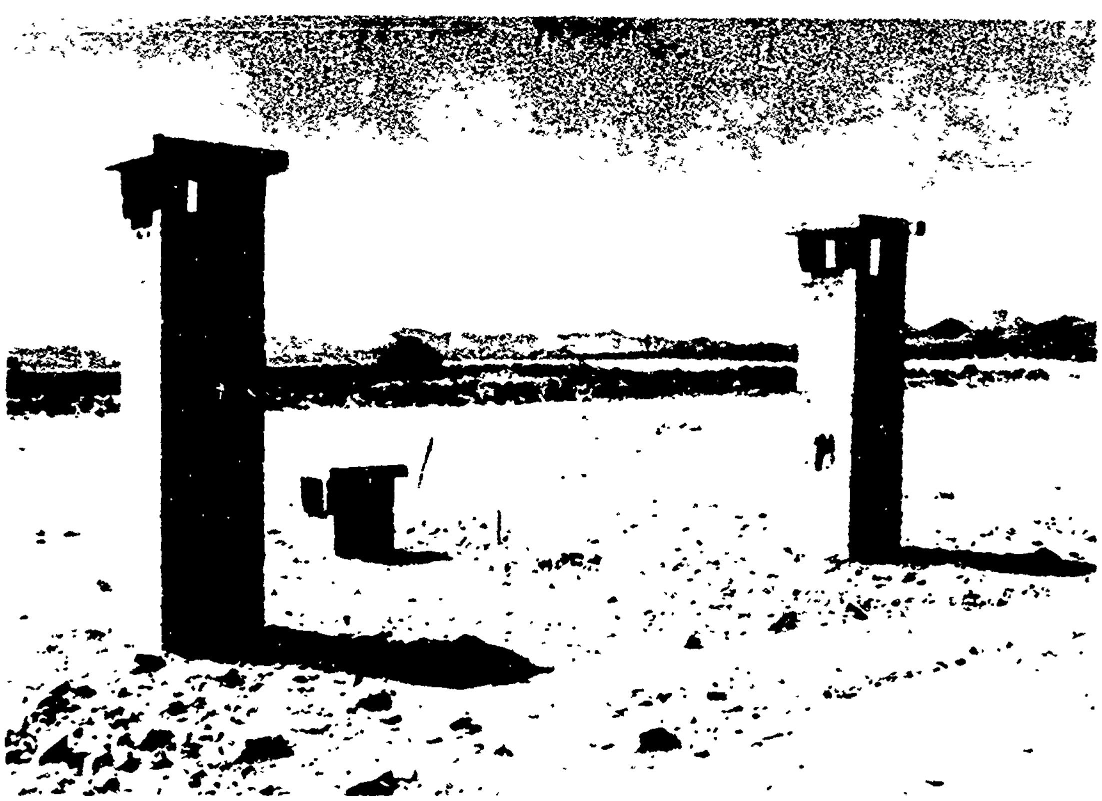

Fig. 1.8—Above-ground view of intake and exhaust stacks.

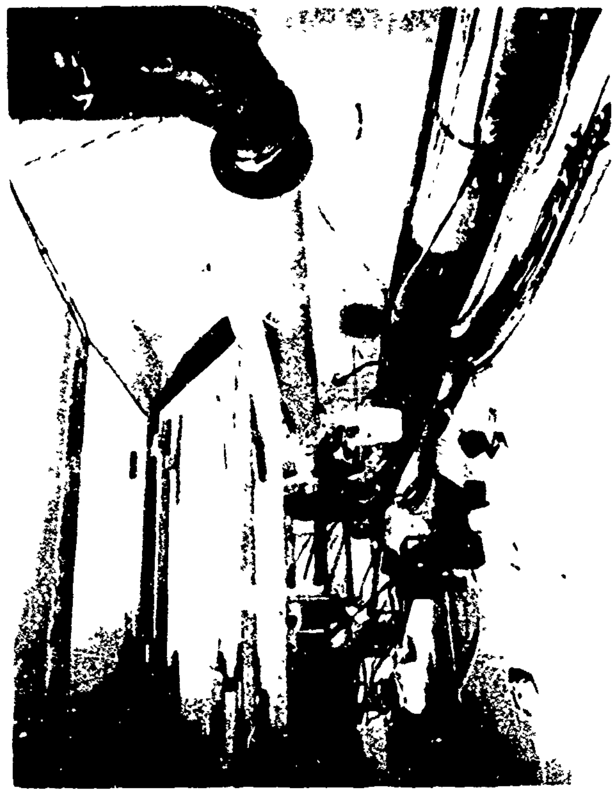

Fig. 1.9—Nessi ventilation system, structure II-1.

Fig. 1.10—Dumoulin type blast door.

Fig. 1.11—Forward room of main chamber, structure II-1.

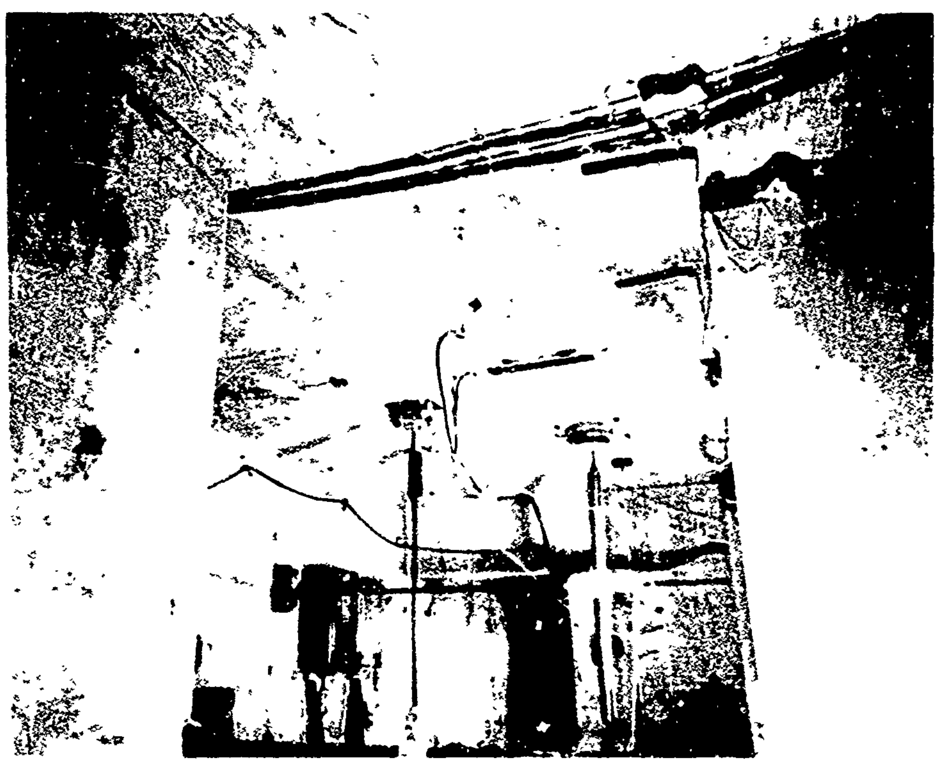

Fig. 1.12—Rear room of main chamber, structure II-1.

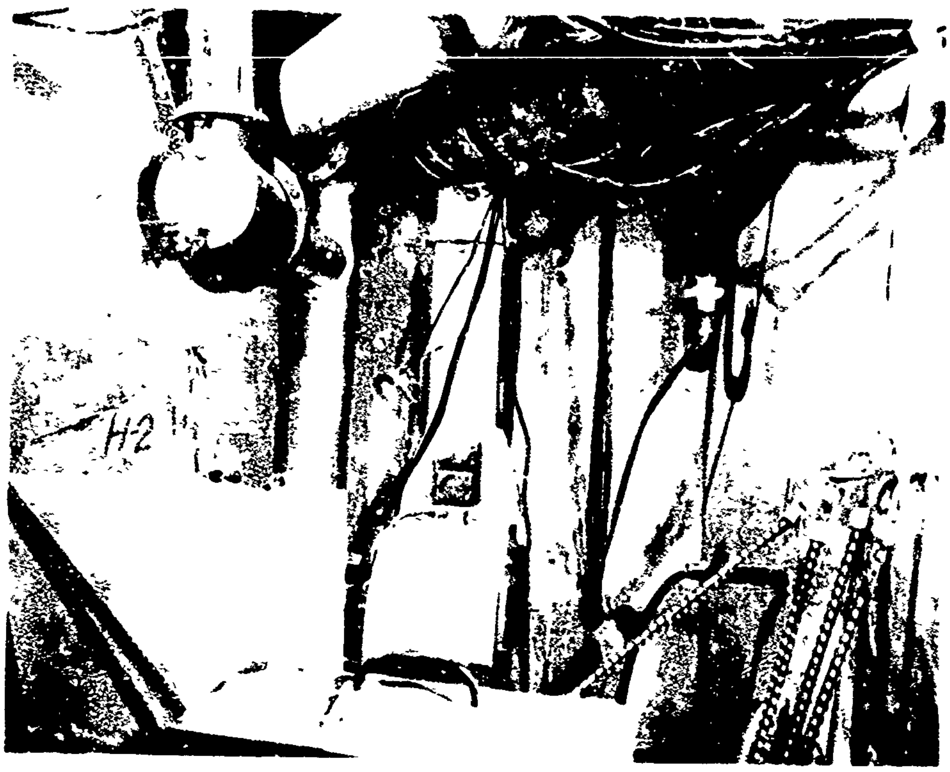

Fig. 1.13 — Ventilation room, structure II-1.

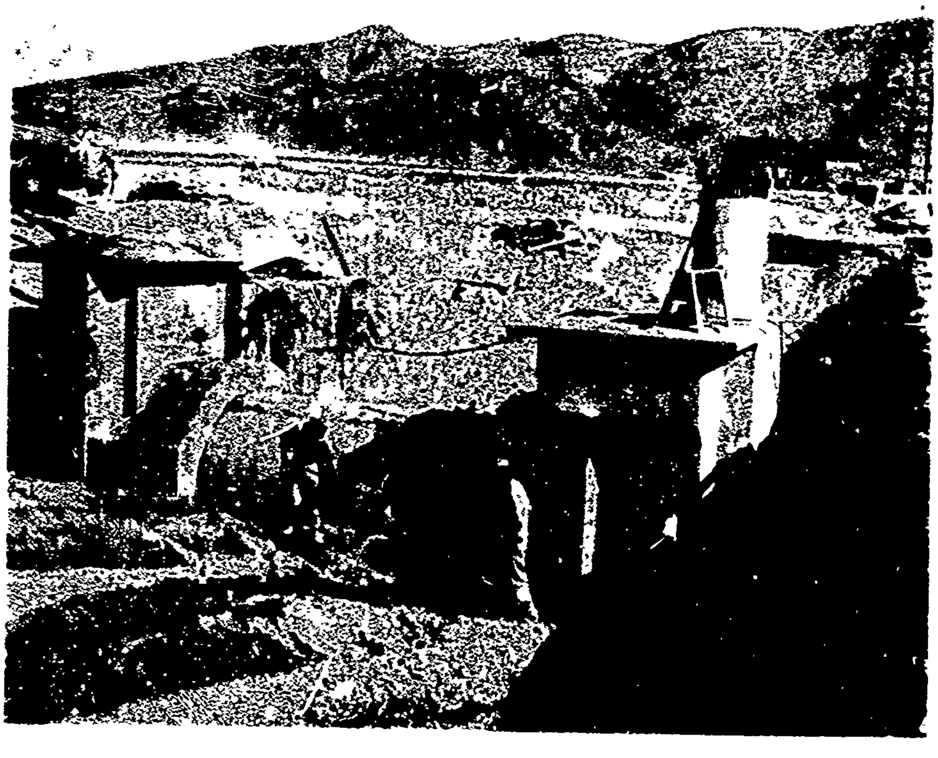

Fig. 1.14 — Exterior view of structure II-2 before backfilling.

Fig. 1.15—Above-ground view of structure II-2 after backfilling.

Fig. 1.16—Main entrance, vertical shaft, structure II-2.

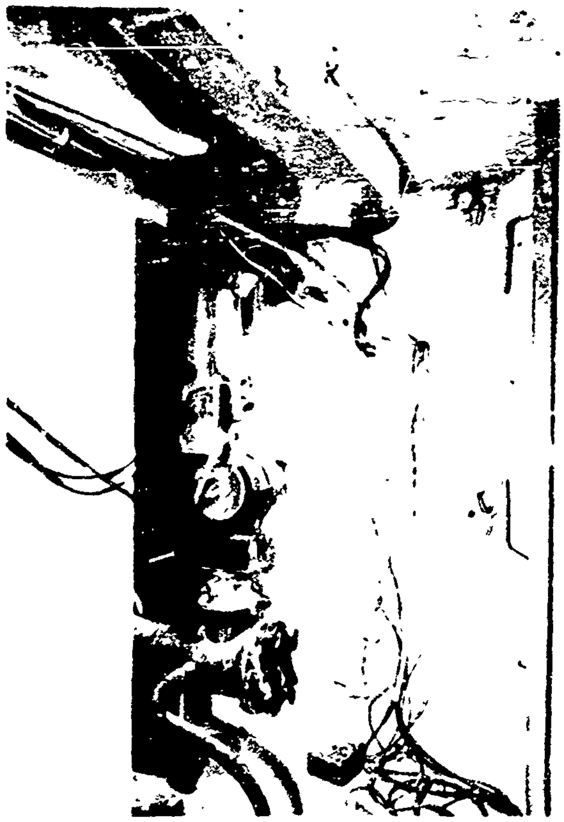

Fig. 1.17 — Nessi ventilation system, structure II-2.

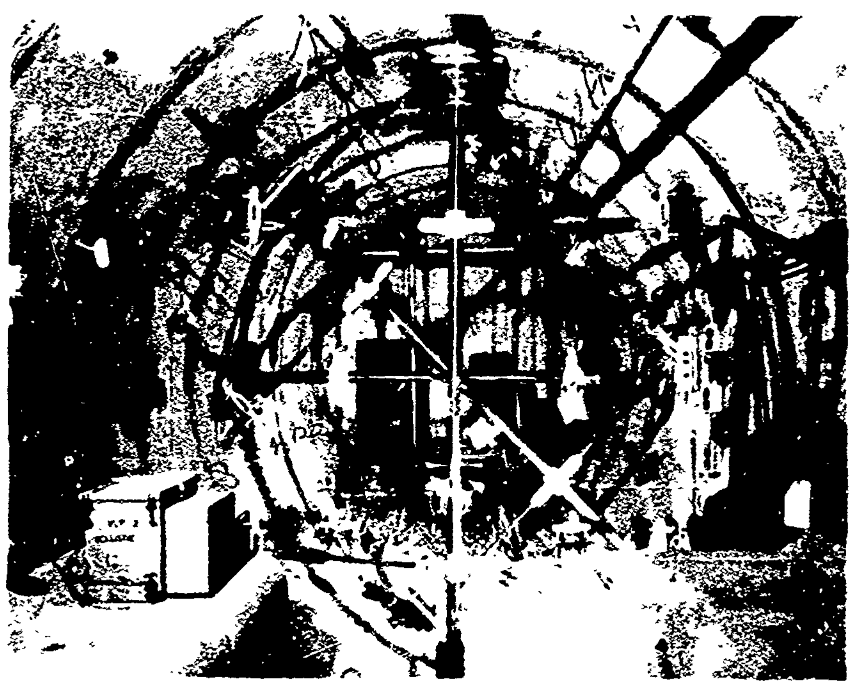

Fig. 1.18 — Interior view of main chamber, structure II-2.

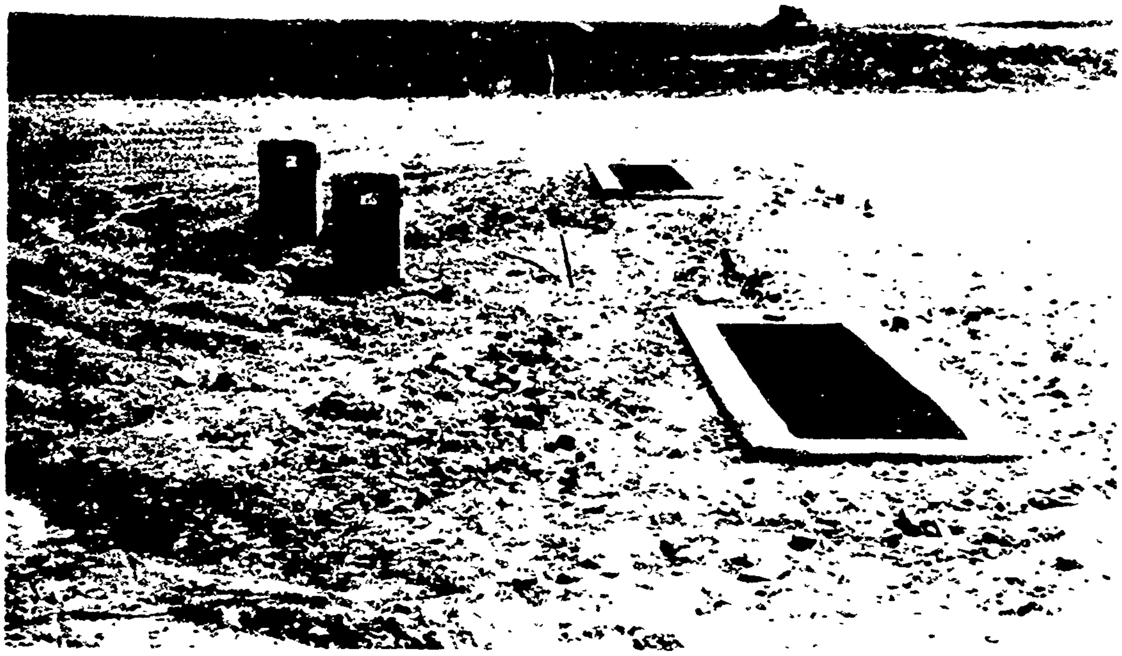

F g. 1.19 — Exterior view of structure II-3.

Fig. 1.20 — Exterior view of structure II-4.

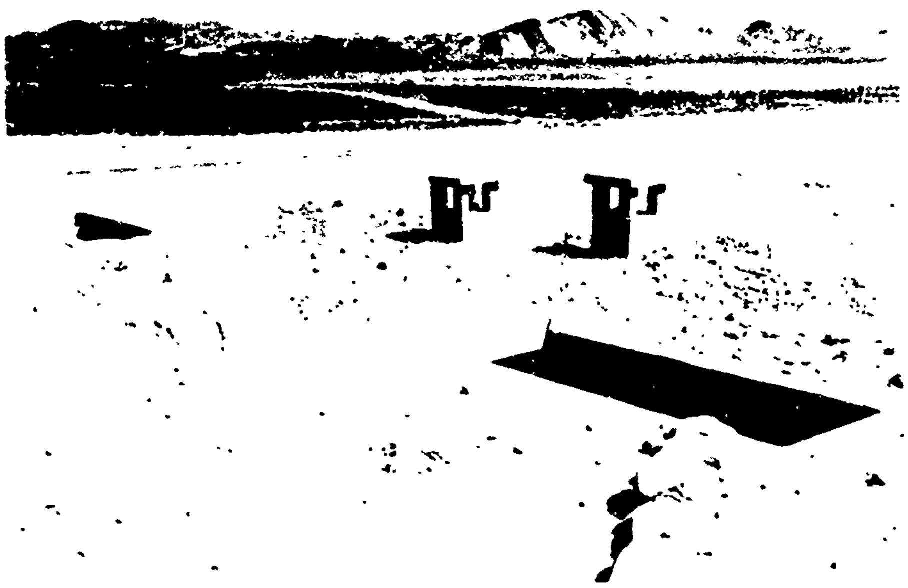

Fig. 1.21—Exterior view of structure II-5.

Fig. 1.22—Interior view of structure II-3.

Fig. 1.23—Interior view of structure II-4.

Fig. 1.24—Interior view of structure II-5. Note door deformeter gauge in place.

Fig. 1.25—Typical entrance, structures II-3, II-4, and II-5.

Fig. 1.26—Interior view of Society Cheops doors, structure II-4.

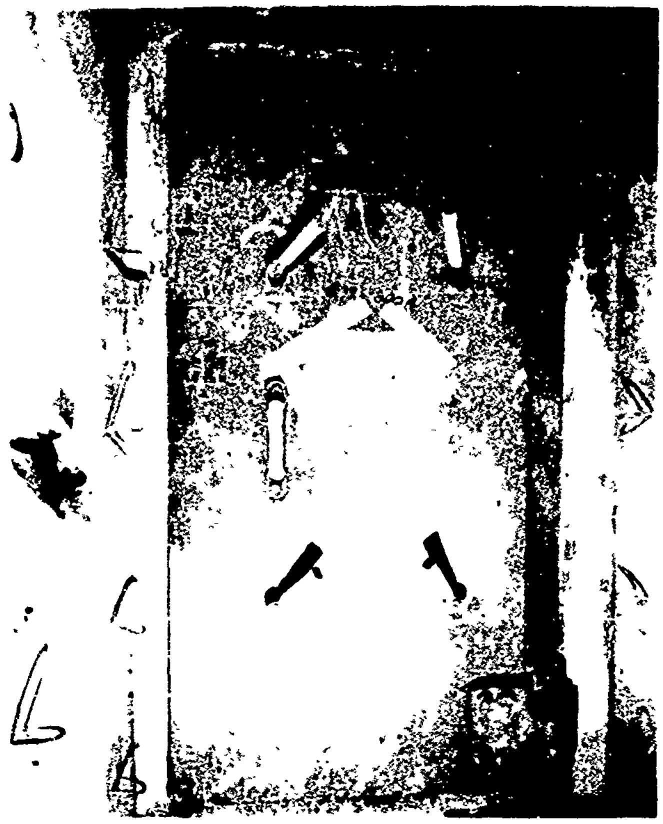

Fig. 1.27—Bauche doors, structure II-3.

Fig. 1.28—Interior end of ventilation system, structure II-5.

Chapter 2

PROCEDURE

2.1 SURVEYS

Preshot and postshot field surveys of the horizontal and vertical coordinates of the survey points, designated Y_1, Y_2, etc., were required to allow a determination of the absolute and relative lateral and vertical movements of the structures during the blast.

A second set of survey points, X_1, X_2, etc., was located in the structures to allow a determination of the relative movements of component parts of the structures.

The survey points are shown in Figs. 2.1 to 2.5.

2.2 INSTRUMENTATION

2.2.1 General

An extensive instrumentation program was developed and provided by SNPC. In addition to the equipment furnished from France, U. S. instrumentation was included for comparison purposes.

2.2.2 French Instrumentation

Instruments were provided from France to take the following measurements:

1. Pressure.
2. Deformations and vibrations.
3. Stresses and strains.
4. Heat (cal/cm^2) and temperature (°F or °C).
5. Nuclear radiation and contamination.
6. Miscellaneous (communications, lighting, etc.).

The designation, description, type, reading, and instrument number for the French instrumentation included in each structure are given in Table 2.1. In addition to the instruments indicated in the table, there was also an electronic multiple recorder placed in structure II-1 to record the signals from pressure, heat, deflection, and vibrations received from registering heads in the various other structures.

Power requirements for the operation of the equipment and instruments were of two types. A 2-kw a-c power system for the lighting system, operation of the dust collectors, and operation of the ventilation system of structure II-2 was provided by a 3-hp generator.

Direct-current power for the electronic instruments and recorder was obtained from batteries provided with the recorder (3.5.4, Table 2.1) in structure II-1.

French instrumentation was installed in the shelters by members of Project 30.5b. The equipment was assembled and placed in the structures as outlined by French instrumentation specifications and at meetings between SNPC representatives and members of Project 30.5b.

Instrument descriptions and installation procedures are more fully covered in reports WT-1535, WT-1466, and ITR-1509. The locations of all French equipment are shown in Figs. 2.6 to 2.10. The WT-1535 designation for some of the gauges listed in Table 2.1 differs from the original designation indicated on Figs. 2.6 to 2.10. The designations from report WT-1535 are listed in Table 2.1 in order to simplify any correlation of reports.

2.2.3 U. S. Pressure Instrumentation

As stated in Sec. 2.2.1, U. S. instrumentation was placed in the five shelters to obtain results with which to compare the measurements obtained from the French equipment. The U. S. instruments were provided by the FCDA and were installed by members of Project 30.5b.

The equipment consisted of 33 BRL self-recording pressure-time (SRPT) gauges and 2 self-recording very low pressure-time (VLP) gauges. The gauges, which were placed both inside and outside the shelters and in the entranceways, were distributed among the structures in the following manner: structure II-1, 9 SRPT gauges and 1 VLP gauge; structure II-2, 4 SRPT gauges and 1 VLP gauge; structure II-3, 2 SRPT gauges; structure II-4, 11 SRPT gauges; and structure II-5, 7 SRPT gauges.

The locations of the self-recording gauges, described in report WT-1535, are shown in Fig. 2.6 to 2.10.

In addition to the instrumentation in the structures, U. S. blast-line pressure data are available for determining both the free-field surface overpressures and the dynamic pressures to which the structures were subjected.

The maximum values and the location of the blast-line instrumentation are shown in Fig. 1.6. A more complete description and evaluation of the blast-line instrumentation is given by Project 30.5b in report WT-1535.

2.2.4 U. S. Radiation Instrumentation

Additional radiation-detection equipment, other than that supplied by the French, was incorporated into the test. The radiation measurements were made with U. S. gamma radiation film dosimeters, gamma-radiation differential chemical dosimeters, and neutron detectors. Two telemetering dual-unit gamma dosimeters were located in structure II-1 and on the blast line at a predicted pressure level of 88 psi. The telemetering equipment acted as a remote radiation detector transmitting gamma-time records to a central receiving station.

Five gamma-radiation differential chemical dosimeters were placed with the German (Project 30.7) pressure gauges along the blast line, Fig. 1.6, as a part of the radiation program for Project 30.7.

The installation of all radiation-recording instruments, including the French equipment, was performed by Projects 30.5b, 39.9, and 39.1a.

A more complete description of the U. S. and French radiation instrumentation is given in reports WT-1466 and ITR-1509. The layout and locations of the radiation detection equipment are shown in Fig. 2.11.

2.3 GROUND-SHOCK SPECTRA

2.3.1 General

Displacement spectra of ground shocks produced by nuclear devices, from which the velocity and acceleration spectra can be derived, were obtained by Project 1.9, which participated in shots Smoky, Whitney, Galileo, Charleston, and Stokes. A ground-shock response spectrum is a convenient method for interpreting free-field earth motions with regard to the relative effects in a structure or the effects on equipment within a structure placed in the soil. A response spectrum can be used to describe the behavior of a simple dynamic system as a function of its frequency.

2.3.2 Theory

A ground-shock spectrum is a plot of the maximum responses of single-degree-of-freedom systems (reed gauges) vs. the natural frequencies of the systems. The response is due to ground-induced motion of the reed-gauge base and is measured in the tests as peak instantaneous displacement. Acceleration and velocity spectra are derived from the measured displacement spectra. The following mathematical relations are the bases for the response spectra.

Figure 2.12 illustrates a single-degree-of-freedom spring-mass system (neglecting damping); (a) shows the system at rest, and (b) shows the system in motion in the x direction as a result of an acceleration of the base.

$\mu = x - y$ = the displacement of the mass relative to the base

x = displacement of the base

y = displacement of the mass

ω_n = undamped natural circular frequency for *nth* single-degree-of-freedom system (or *nth* mode of a multi-degree-of-freedom system)

The general differential equation of motion for a system having an acceleration input is

$$\ddot{\mu} + \omega_n^2 \cdot \ddot{\mu} = \ddot{x}$$

where superscript dots denote differentiation with respect to time.

The system responses have the following relations:[1]

μ_{max} = D, the displacement (response) spectrum

$\omega_n^2 \cdot \mu_{max}$ = V, the velocity (response) spectrum

$\omega_n^2 \cdot \mu_{max}$ = A, the acceleration (response) spectrum

The displacement-response spectrum corresponds to the values recorded in the test for the various frequencies and is the maximum displacement of the n masses relative to the base. The acceleration-response spectrum is the maximum absolute accelerations of the n masses. The velocity spectrum is composed not of the actual peak velocity of the *nth* mass relative to the base but is a pseudo relative velocity that is nearly the same as the peak relative velocity. The velocity spectrum is useful, however, in the determination of an upper bound of the strain energy in structures.

2.3.3 Instrumentation

Twelve shock gauges and protecting canisters were used on the tests. The shock gauge is a completely self-contained mechanical unit requiring no electronic or communication channels. Essentially, it consists of 10 masses attached to cantilever springs mounted on two sides of a vertical plate (Fig. 2.13). The natural frequencies of the spring-mass system are approximately 3, 10, 20, 40, 80, 120, 160, 200, 250, and 300 cps.

Peak responses to the shock input for each spring-mass system are obtained on polished, smoked record plates, which are marked by the movement of a stylus attached to each mass.

The gauge is protected by a cylindrical canister 2 ft in diameter and approximately 2 ft deep. Transmission of shock input to the gauge (either in the vertical or horizontal direction) is secured by bolting the gauge in the desired position to the 1-in. base plate of the canister.

Vertical and radial gauges to record free-field effects were placed approximately 1 ft below the ground surface at various distances from GZ during shots Smoky, Whitney, Galileo, Charleston, and Stokes. During shot Smoky one radial and one vertical gauge were placed in the underground rectangular structure of Project 30.7 at the 1005-ft range. The canisters were bolted to the floor slab of the structure. One radial and two vertical gauges were placed adjacent to the structure; a distance of 5 ft was used between gauges.

2.4 BIOLOGICAL TEST

2.4.1 General

After extensive consultation it was agreed that Project 33.6 would make a biological asessment of the internal environment of the structures of Project 30.6 when subjected to nuclear blast. The objectives of the test were twofold: (1) to place biological specimens in the structures and to follow their mortality rate over a 60-day period postshot and (2) if possible, to relate the cause of death, if any, to a specific environmental factor.

The test consisted in placing five samples of 20 mice each; one sample was placed in each of the five structures.

The biological data presented here have been abstracted from the Project 33.6 report, WT-1507.

2.4.2 Animals

The animals used in the study were mice of the RAP strain whose body weights were between 20 and 25 g and whose ages were approximately six weeks. In addition to the samples used in the structures, two samples were kept as controls. Each sample of 20 mice was placed in a wire-mesh cage (approximately 9 by 15 by 9 in.) (see Fig. 2.14). The cages contained copious amounts of food (Purina Laboratory Chow) and two water bottles. In the event the blast should jar the water bottles from the cage, each cage had sliced raw potatoes to act as a source of moisture. Control tests had shown that animals under these circumstances could survive for four days unattended.

2.4.3 Location

The cage in structure II-1 was located on the floor of the main chamber. The cage in structure II-2 was placed on the top landing of the main entrance (Fig. 1.16) to protect the specimens from the effects of the exhaust fumes of the gasoline generators located in the shelter. The cages in structures II-3 through II-5 were located on spring-suspended plates in the antechamber sections of these structures. The suspended plate was approximately 3 ft above the floor surface.

The locations of the test samples for the five shelters are shown in Fig. 2.15.

2.4.4 Time of Placement

The animals were placed in the structure three and four days before the shot. Each day thereafter the food and water supply was replenished up to, and including, the day before the shot.

REFERENCE

1. Y. C. Fung and M. V. Barton, Some Characteristics and Uses of Shock Spectra, Report AM No. 6-14, The Ramo-Wooldridge Corporation, California, Oct. 15, 1956.

Table 2.1 — SUMMARY OF FRENCH INSTRUMENTATION

Designation	Description	Type*	Reading†	Instrument No ‡ II-1	II-2	II-3	II-4	Ii	Remarks
3 2 1 1	Max dynamometer (piston, spring, and segment)	NE	P	1-8	1-5 (9-13)	1-6 (14-19)	1-6 (20-25)	1-6 (26-31)	
3 2 1 5	Glass disk diaphragms (glass disk mounted on circular plate)	NE	P	6	10	9	11	12	
3 2 2 1	Low-pressure manometer (recording cylinder and pen)	NE	T	2					
3 2.2 2	Caisson manometer (Bourdon tube and recording pen)	NE	T			4	5	6	
3 2 2 3	Recording barometer (classic barometer with thermometer and hygrometer)	NE	P	6	4	8	9	10	
3 2 3 1	Tube manometer (Bourdon tube and recording pen)	NE	T	2					
3 5 4	Pressure gauge (3 5 4 recorder)	E	T	50 to 56 48 57,59 (43 49 50 52-56,59)				67,33 (67)	
3 1 1 1	Door lateral gauge (steel punch and lead plate)	NE	P	1 to 10	1 to 8 (11 to 18)	41 and 42 (19 and 20)	45 and 46 (21 and 22)	49 and 50 (23 and 26)	
3 1 1 2	Door deformeter (group of 5 lateral gauges)	NE	P	3 and 4 (B3 and B4)	5 (B5)	8 (B8)		10 (B10)	5 lead plates on each
3 1 1 3	Cone deformeter (punch and lead disk)	NE	P	1 and 2	1 to 3 (3,4,5)	1 (6)	1 (7)	1 (8)	
3 1 1 4	Recording pendulum (pencil fixed on mass, marks swing on table)	NE	P	1	1	1	1	1	
3 1 1 5	Choc mart (steel balls and layer of bituminous material)	NE	P	1 to 3		1	1	1	5 tubes in each
3 5 4	Seismograph (3 pendulums oscillating around spring)	E	T	4					
3 5 4	Acceleration gauge (3 5 4 recorder)	E	T	37,60 and 38,62					
3 5 4	Deflection gauge (3 5 4 recorder)	E	T	42 to 44				47	
3 5 4	Strain gauge (3 5 4 recorder)	E	T	8 to 11					
3 3 1 1	1-Unit fluxmeter (metallic plates varying in thickness)	NE	P	1 to 5	1 to 3	1 and 2	1 and 2	1 and 2	[illegible] flux-meters in each unit
3 3 1 2	Peak thermometer (medical thermometer)	NE	P	3 and 4	6			8	
3 3 1 4	12-Unit fluxmeter (heat-sensitive paint)	NE	P	8 and 10		11		12	
3 3 1 4	9-Unit fluxmeter (heat-sensitive paint)	NE	P	17 and 22	14, 15, and 24		13		
3 . . 7	Recording thermometer (meteorological type)	NE	T	6 and 12	7 and 14	8	4	10	
3 3 2 2	Recording hygrometer (meteorological type)	NE	T	2					
3 5 4	Temperature gauge (3 5 4 recorder)	E	T	15 and 27 22 to 25	20 and 21			35 (35)	
3 4 1 1	Film badges (polyethylene bags)	NE	P	47 and 48 51 to 57	58 to 64	45 and 46 49 and 50	67 to 70	37 and 43 71 to 74	§
3 4 1.3	Dosimeter recorder (plastic bags)	NE	P	2	4	2	1	6	
2.1 2.1.4	Antenna and cable (plastic-coated cable)			H1, H2, H3	H1, H2, H3				
2 1 5 2	Radio sets (fixed transmitter receiver, portable transmitter-receiver)			1 and 2	1				
3 4 3 1	Dust collectors (vacuum tube)			1	1 and 2	1	1	1	
3 4 3 1	Lighting equipment (light bulbs)			6	1	1	1	1	
3 5 4	Temperature and pressure (3 5 4 recorder)	E	T	16,30 74 26,73 31,72	19,77				
3 5 4	Temperature, pressure, and accelerator (3 5 4 recorder)	E	T	14,40 61,75					

* NE, nonelectronic, E electronic
† P, peak value, T, time record
‡ Instrument numbers in parentheses are designations used in Report WT-1535
§ For actual locations of instrument No 3 4 1 1 see "as-built drawings" in Appendix C

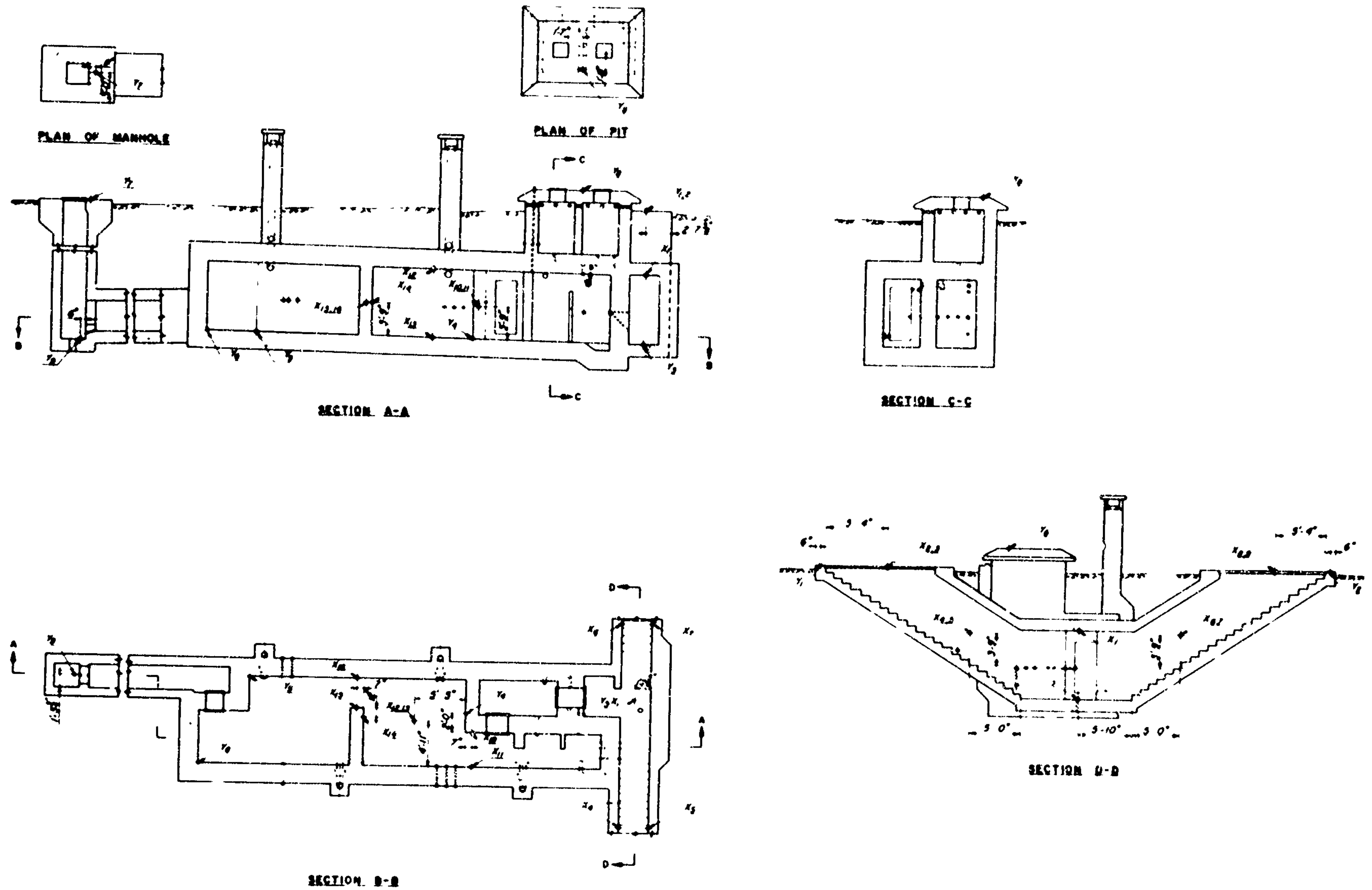

Fig. 2.1—Rectangular shelter, type 60, structure II-1, survey points.

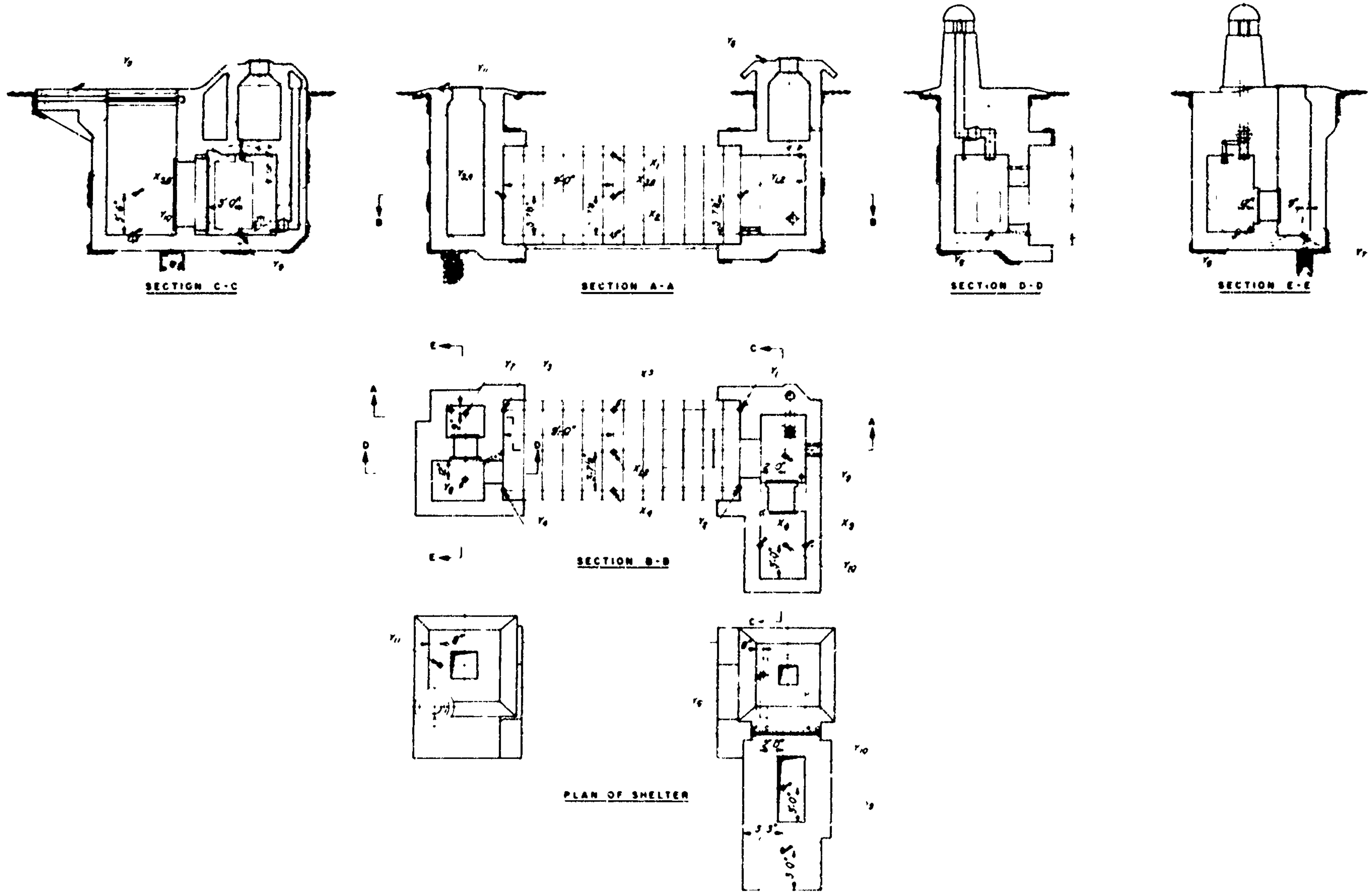

Fig. 2.2—Circular shelter, type 50, structure II-2, survey points.

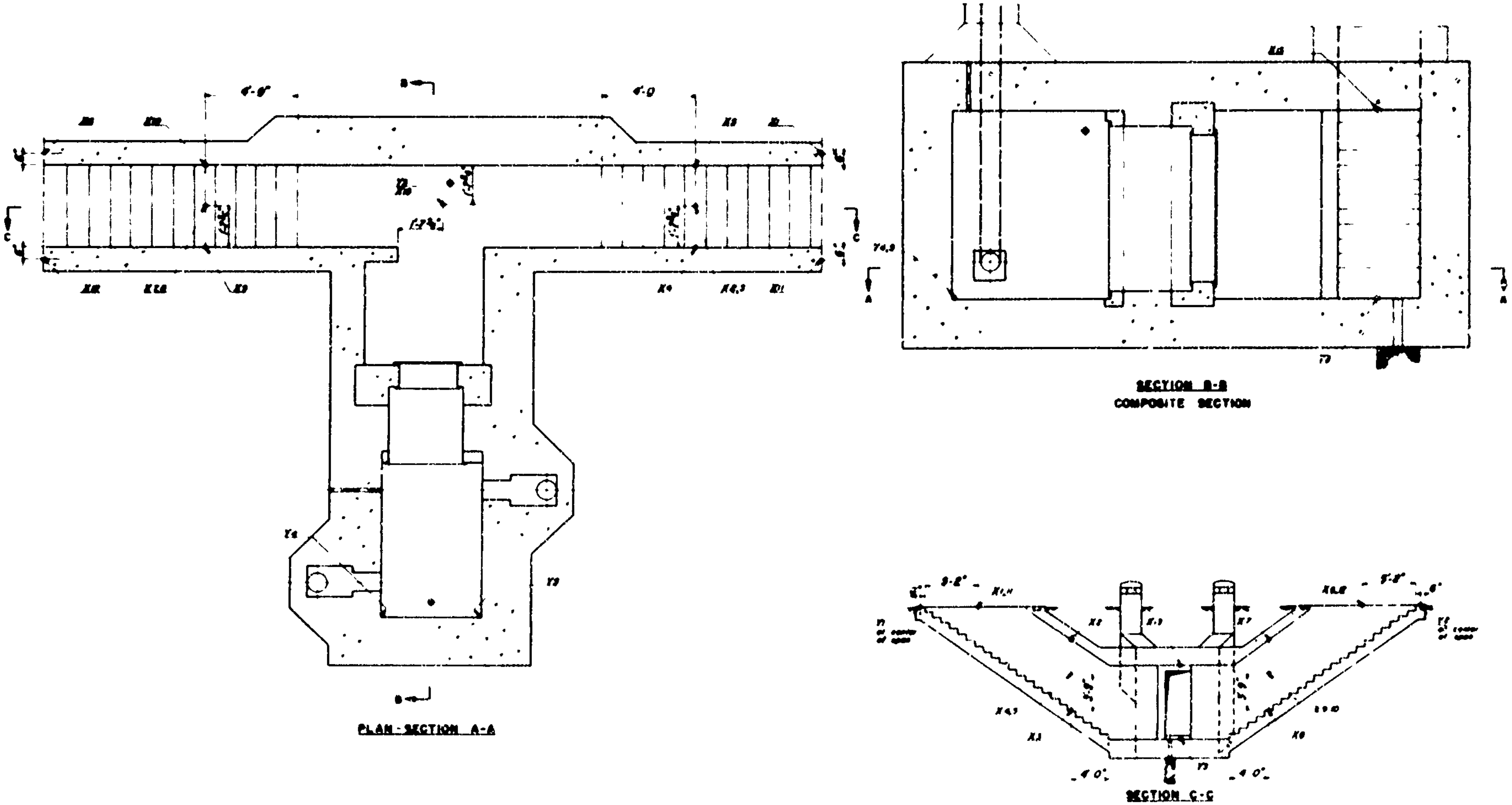

Fig. 2.3—Entrance and entrance chamber, structure II-3, survey points.

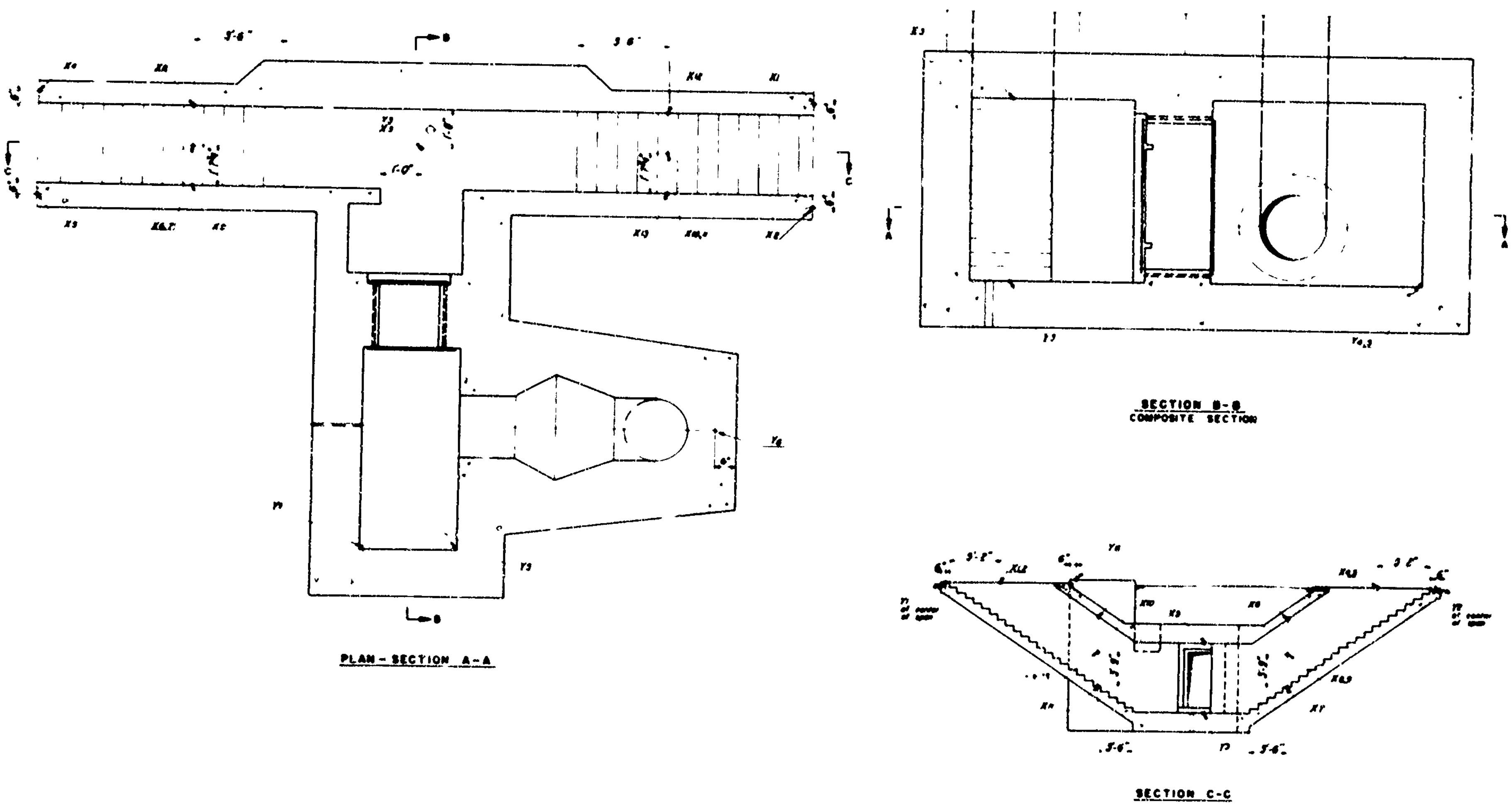

Fig. 2.4—Entrance and entrance chamber, structure II-4, survey points.

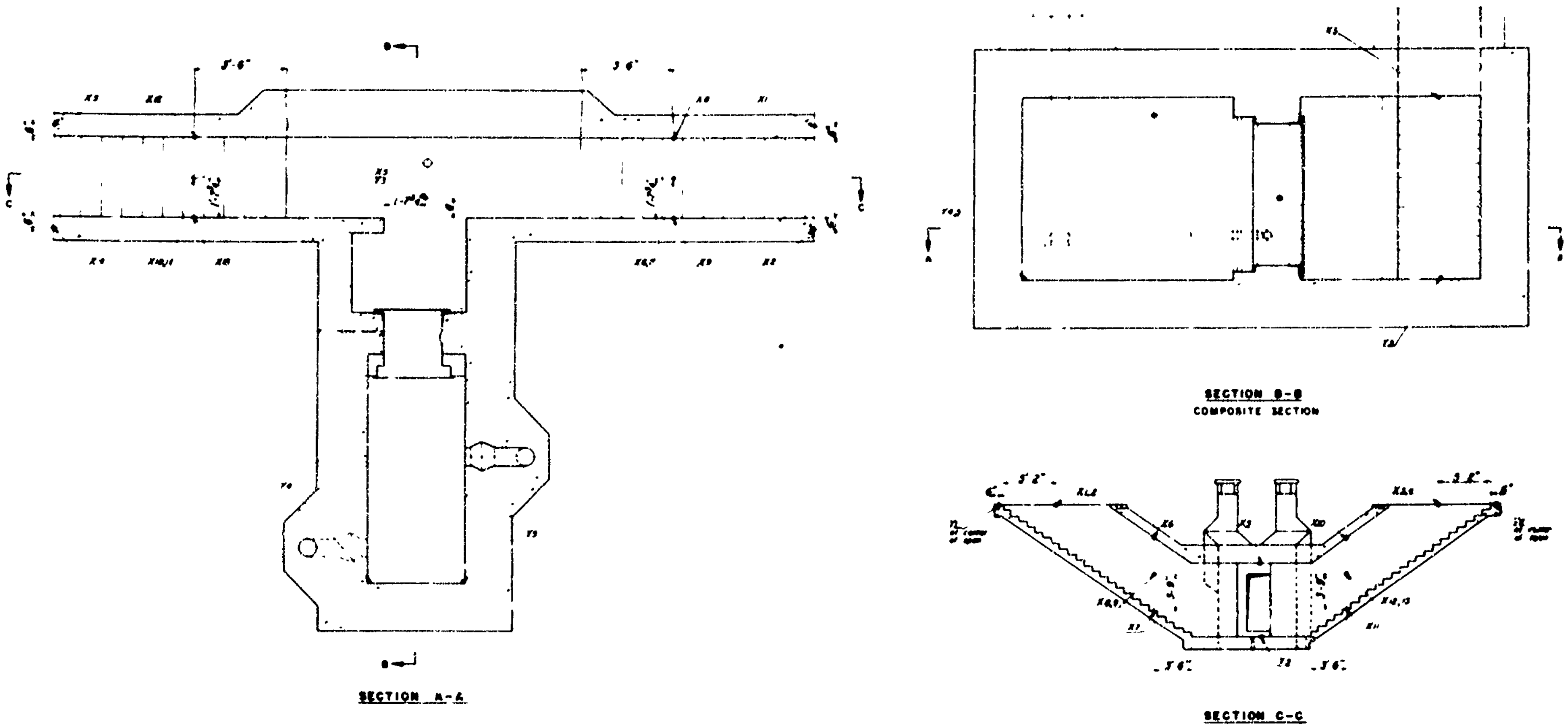

Fig. 2.5—Entrance and entrance chamber, structure II-5, survey points.

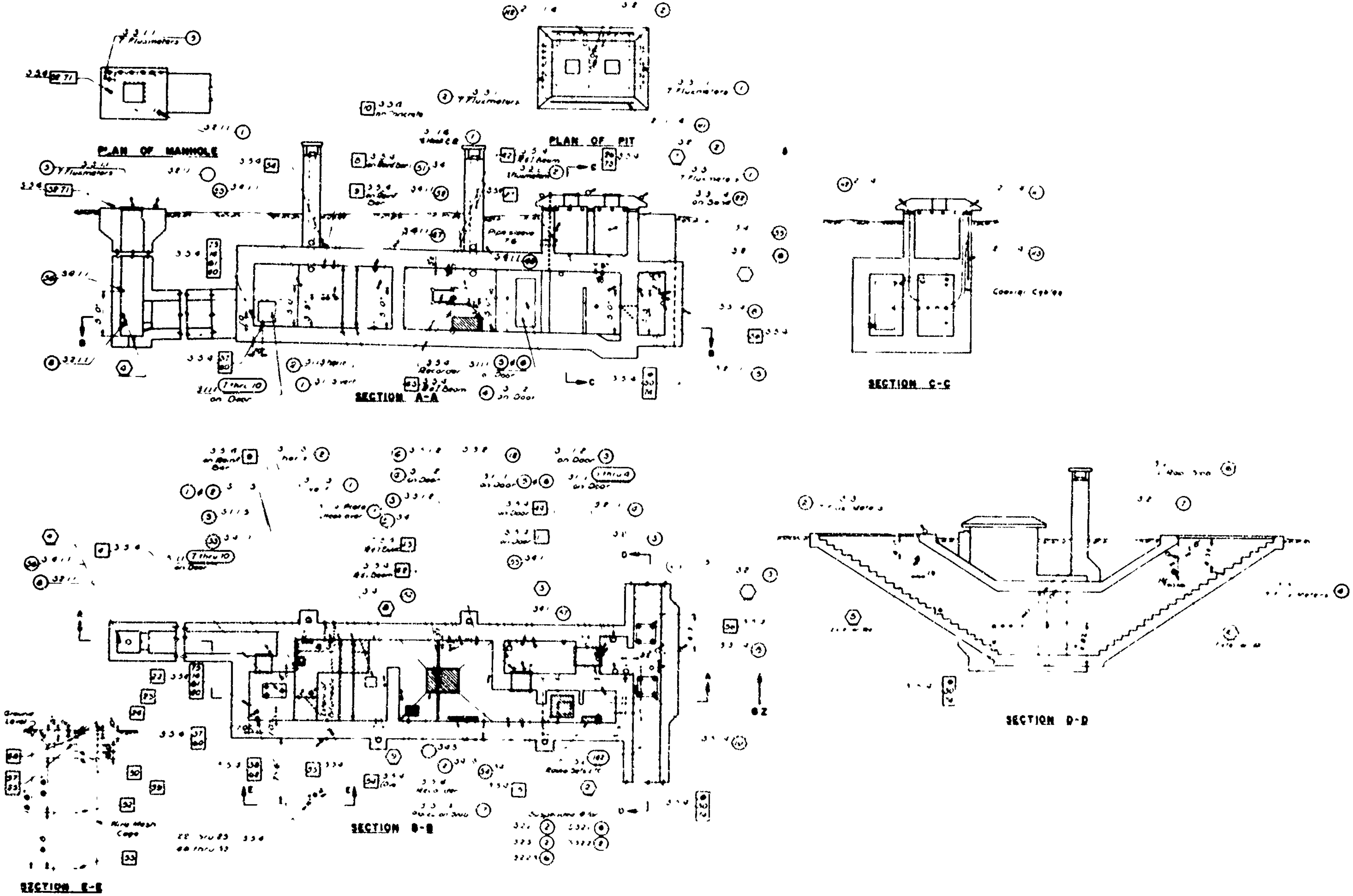

Fig. 2.6—Rectangular shelter, type 60, structure II-1, instrumentation layout.

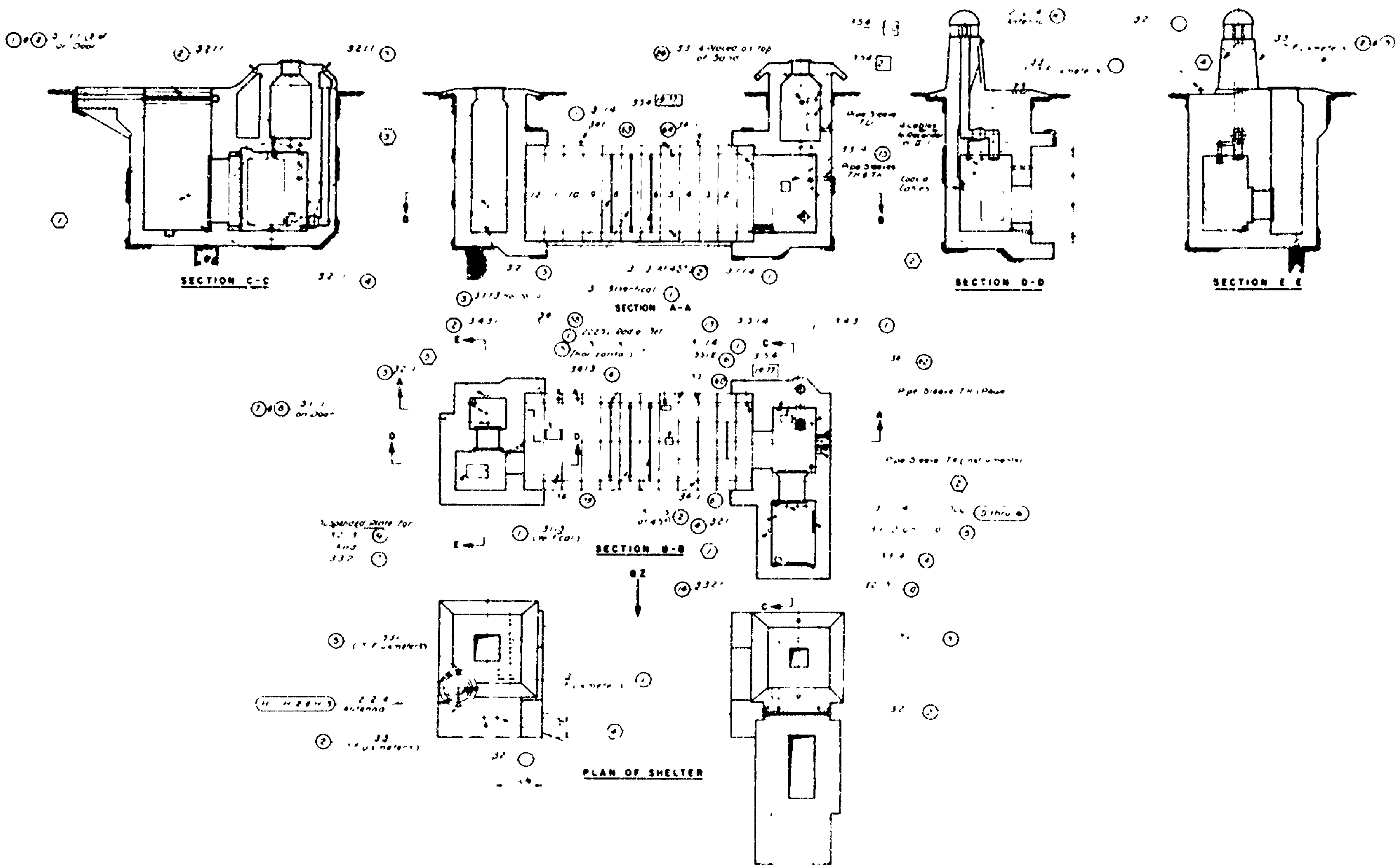

Fig. 2.7—Circular shelter, type 50, structure II -2, instrumentation layout.

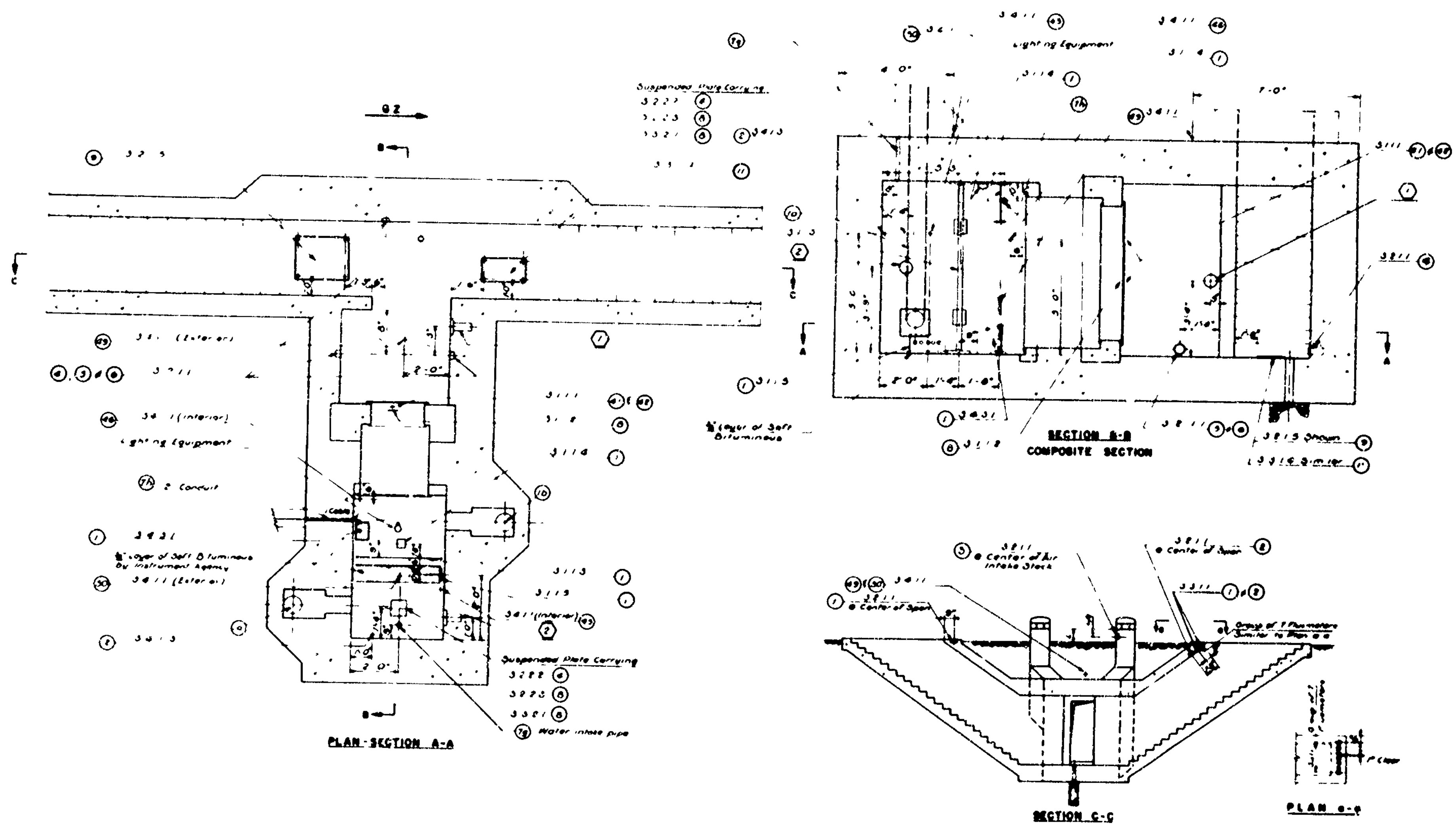

Fig. 2.8—Entrance and entrance chamber, structure II-3, instrumentation layout.

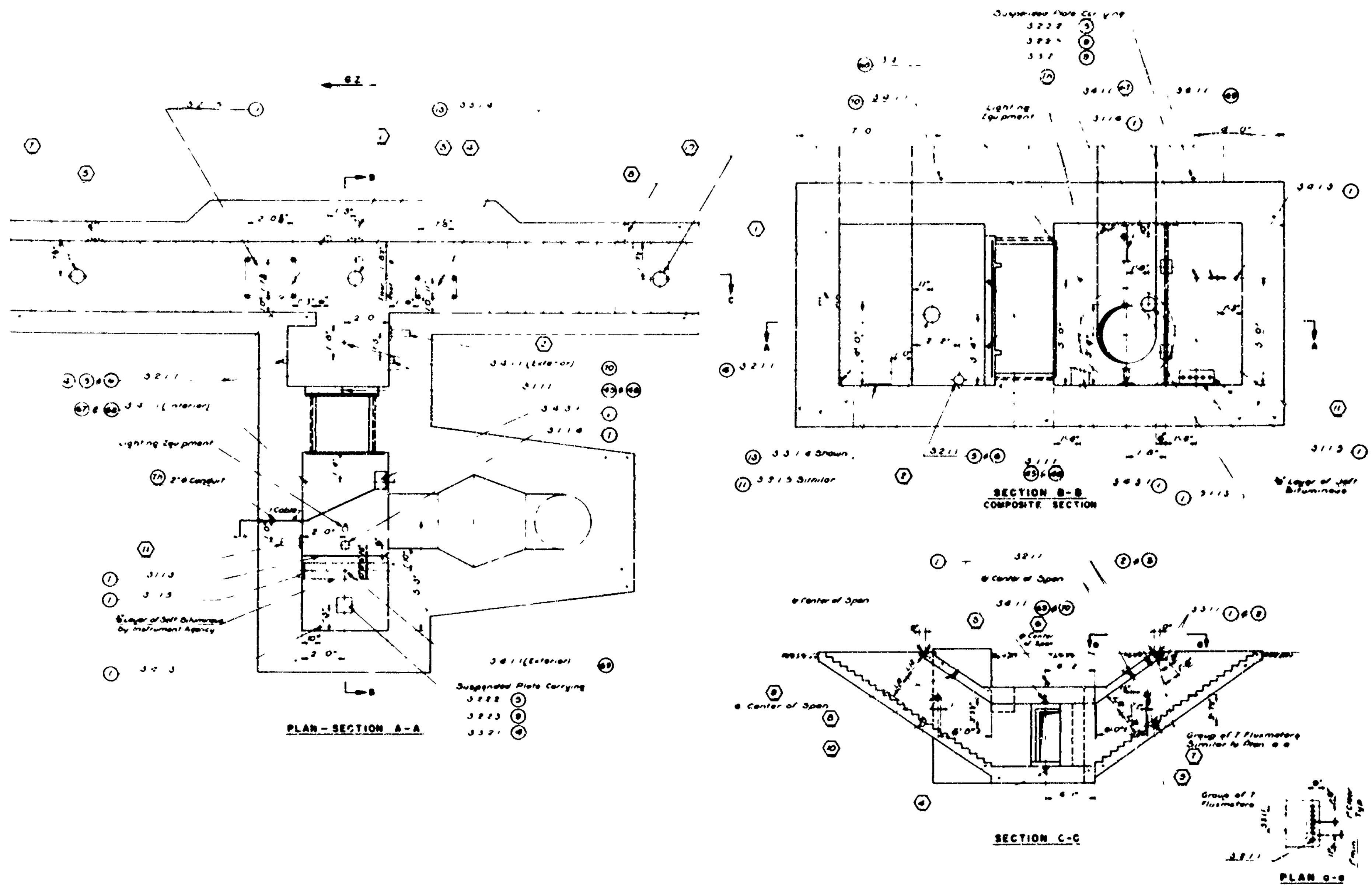

Fig. 2.9—Entrance and entrance chamber, structure II-4, instrumentation layout.

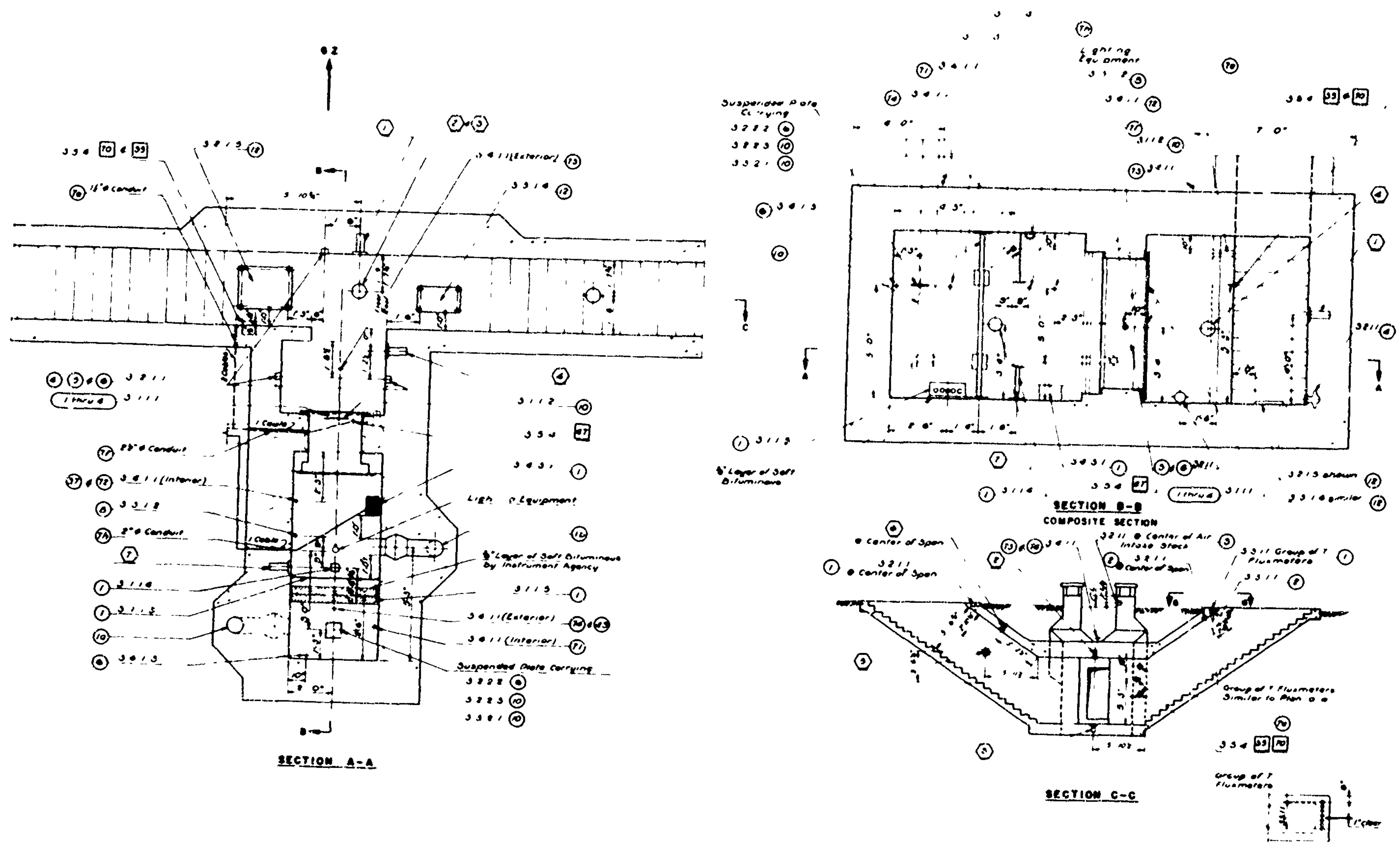

Fig. 2.10—Entrance and entrance chamber, structure II-5, instrumentation layout.

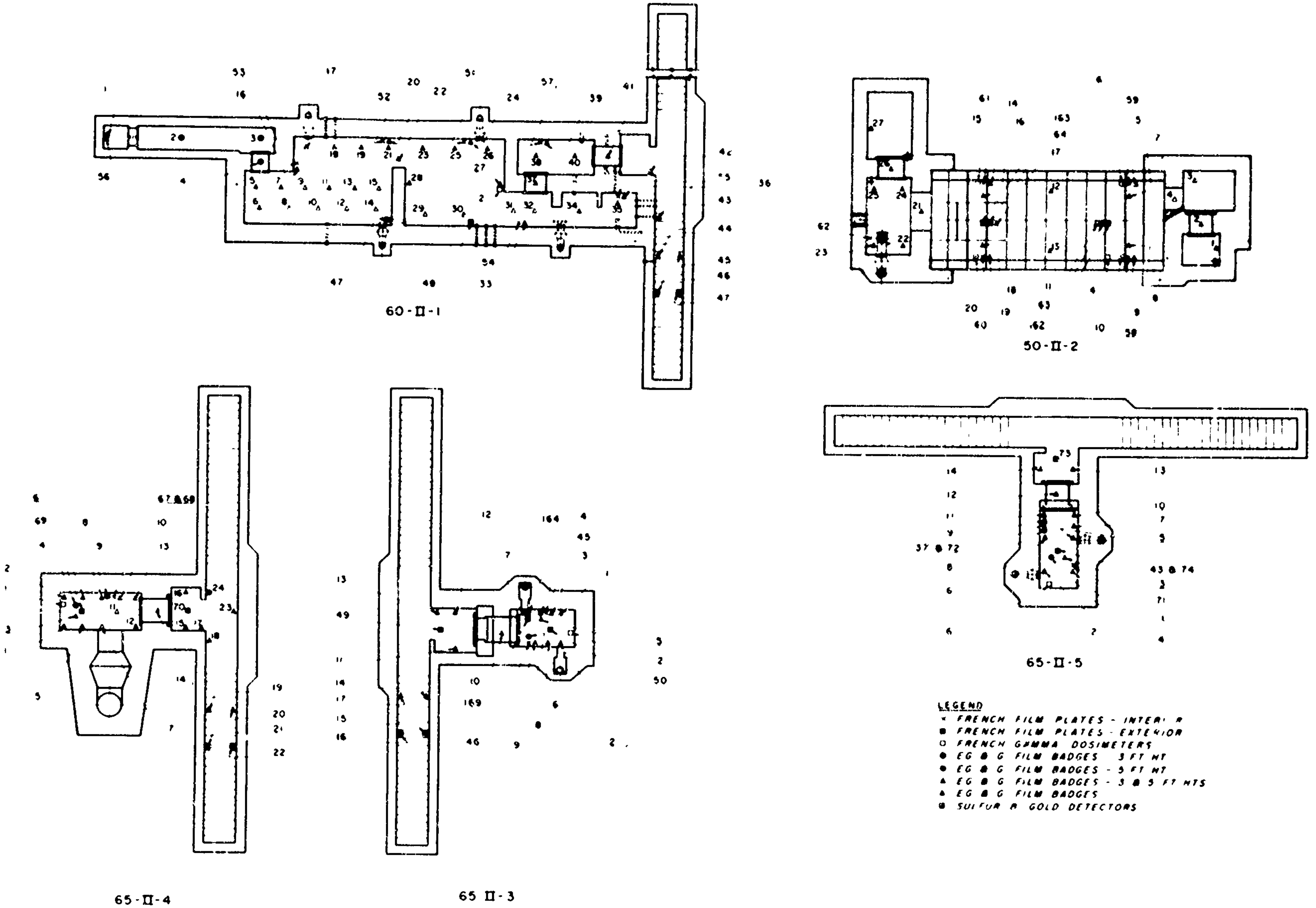

Fig. 2.11—Location of radiation-detection equipment.

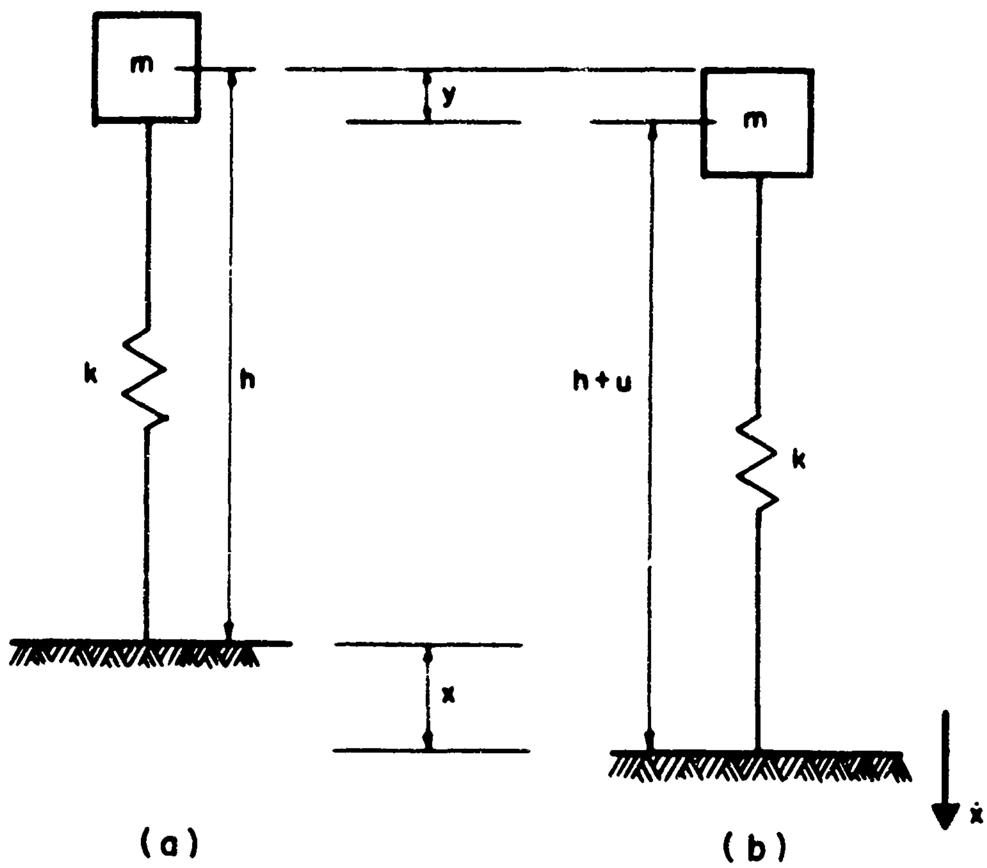

Fig. 2.12—Single-degree-of-freedom spring-mass system.

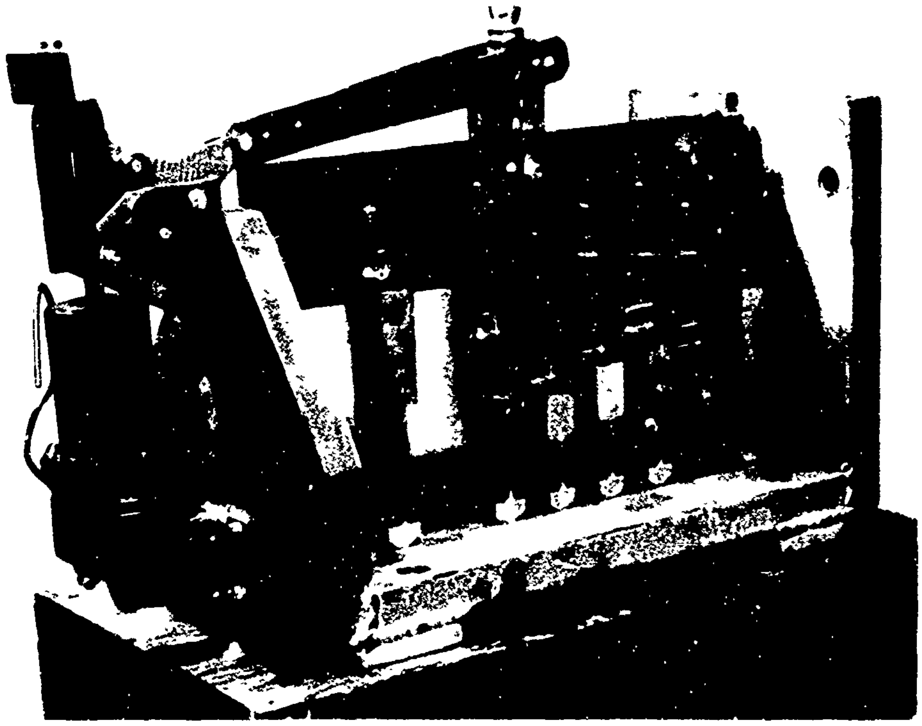

Fig. 2.13—Shock gauge.

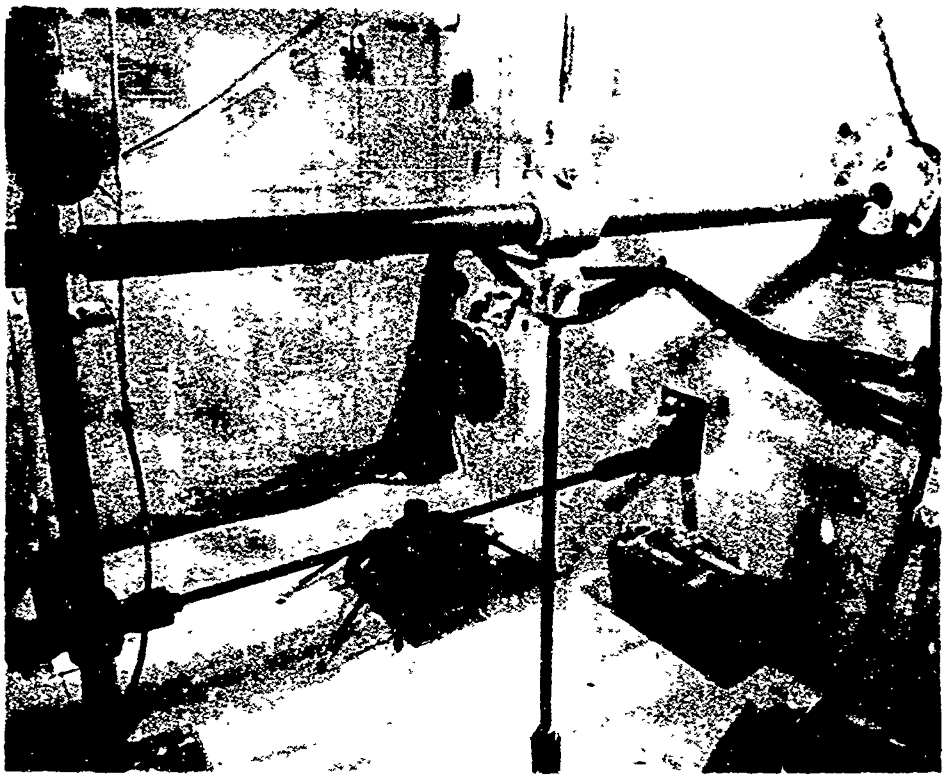

Fig. 2.14—Mouse cage.

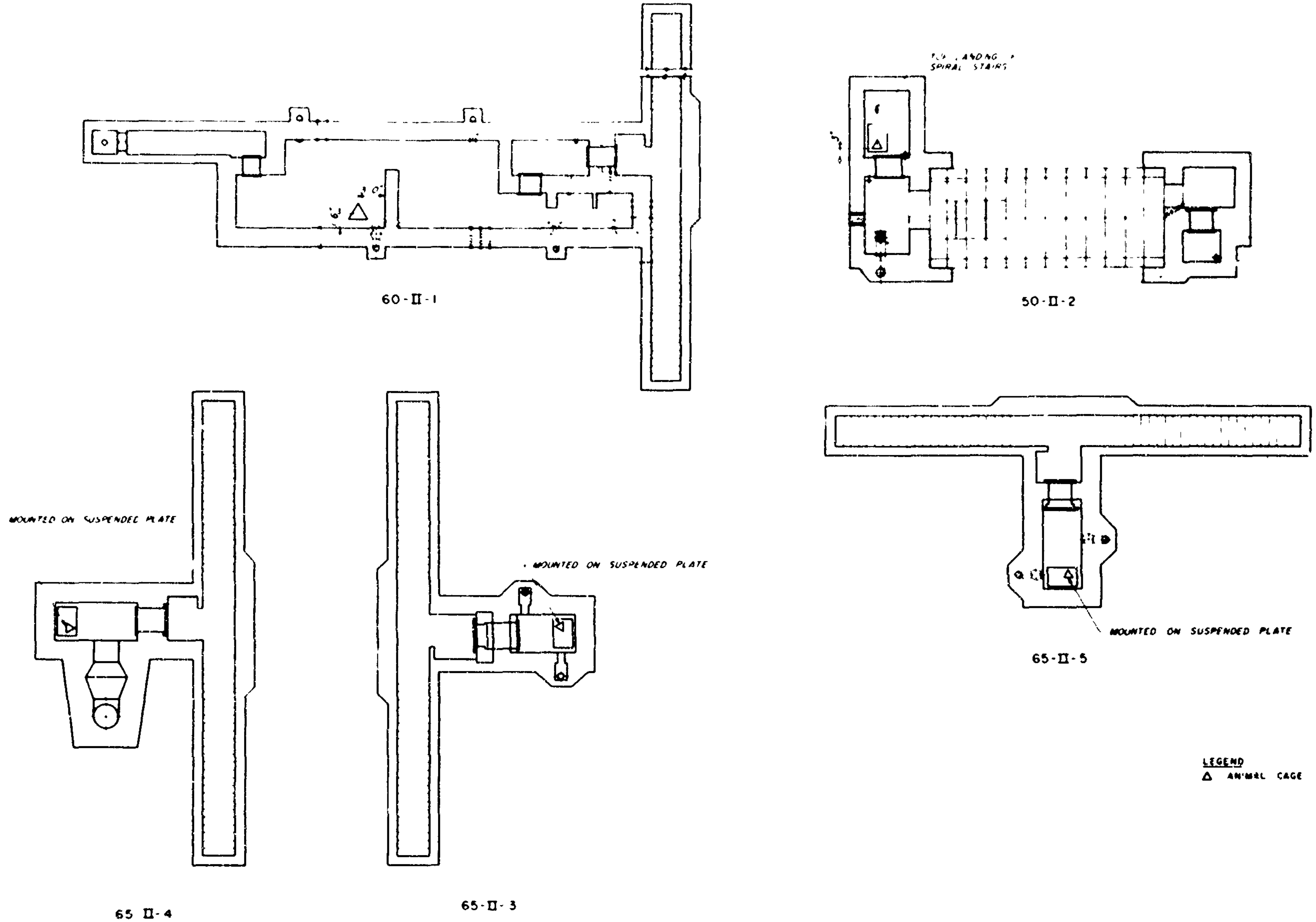

Fig. 2.15—Location of biological specimens.

Chapter 3

BLAST RESULTS

3.1 STRUCTURAL BLAST DAMAGE

3.1.1 Rectangular Concrete Shelter, Type 60, Structure II-1

(a) *Entranceways.* In the entrance facing GZ a $\frac{1}{64}$-in. crack occurred along the intersection of the roof slab and the interior wall. At the intersection of the exterior wall and the slab, the separation varies from $\frac{1}{64}$ in. at the top to $\frac{1}{32}$ in. at the bottom of the sloped portion of the slab. One hairline crack starts at the top of the roof slab and runs along the center line for about two-thirds of the sloped portion of the slab, at which point the crack branches off into two sections, one section leading to each wall. The stairs are separated from the interior wall by a crack that varies from hairline in size at the sixth riser from the top to $\frac{1}{16}$ in. at the bottom tread. The exterior wall is separated from the stairs by a similar crack, except that its size at the bottom tread is $\frac{1}{32}$ in. One hairline crack in the exterior wall is located at the eleventh riser from the top.

The landing roof slab has a $\frac{1}{32}$-in. crack along its intersection with the exterior wall. A $\frac{1}{32}$-in. transverse crack was observed to start at a point directly over the center of the blast door and continue out to a point located along the center-line of the landing; at this point the crack divides into two $\frac{1}{32}$-in. cracks, which continue across the slab to the exterior wall. At the corner of the opening in the interior wall, a diagonal crack starts and runs to the exterior wall near the sloped portion of the roof slab over the entrance away from GZ. Two $\frac{1}{64}$-in. transverse cracks are located at the GZ side of this opening. These cracks run the width of the landing. The interior wall has several vertical $\frac{1}{64}$-in. cracks located on the GZ side of the door opening. Two vertical $\frac{1}{64}$-in. cracks were observed in the exterior wall above the landing.

At the intersection of the roof slab and both walls on the side away from GZ, cracks were found varying in size from $\frac{1}{32}$ to $\frac{1}{16}$ and $\frac{1}{16}$ to 1 in. in width for the exterior and interior walls, respectively. There is a diagonal $\frac{1}{64}$-in. separation starting at the bottom of the sloped portion of the roof near the interior wall and continuing to the top of the slab at the exterior wall. The intersection of the interior wall and the stairs has a crack that is $\frac{1}{16}$-in. in width near the lower tread, increasing to $\frac{3}{8}$ in. at the seventh riser from the top, and decreasing again to $\frac{1}{8}$ in. near the top of the stairs. The crack along the exterior wall and the stairs is $\frac{1}{8}$ in. for three-quarters the height of the stairs; it decreases to $\frac{1}{16}$ in. at the second riser from the top. The interior wall of this entrance has a crack that starts at the intersection of the top of the roof slab and the wall and runs vertically downward toward the stairs. This crack is 1 in. in size at the roof and $\frac{1}{16}$ in. at its terminal point located approximately at the mid-height of the wall. Spalling is evident along the entire length of the crack. A $\frac{1}{16}$-in. vertical crack was formed above the fourth tread from the bottom; it runs the full height of the wall. Several vertical hairline cracks are located near the roof slab. The exterior wall has a $\frac{1}{16}$-in. crack located near the top four risers of the stairs.

The roof, stairs, and walls of the entranceways were scoured by the blast. Debris was deposited along the entire length of the entranceways. Two steel instrumentation mounting plates

were torn loose and deposited on the stairs facing away from GZ. The crack patterns for structure II-1 are shown in Figs. 3.1 to 3.3.

(b) *Antechamber.* One $^1/_{32}$-in. crack was formed in the roof slab of the antechamber, beginning directly over the center of the gastight door and continuing across three-quarters of the length of the room, at which point it flaired diagonally to the exterior and interior walls. This crack appears to be a continuation of the transverse crack in the roof slab of the entrance. The branch of the crack that leads toward the interior wall terminates at a point directly over the center line of the secondary blast door. This crack is also visible in the lower section of the lintel beam above the secondary blast and gastight doors.

(c) *Main Chamber.* The section of the main chamber adjacent to the secondary gastight door has minor structural damage. The crack that is present in the antechamber is continued into this section. It intersects a $^1/_{32}$-in. crack that starts at the interior corner of the small partition behind the gastight door and runs into the forward room of the main chamber. The floor, roof, and walls of the ventilation chamber were not damaged.

The forward room of the structure has a $^1/_{32}$-in. crack in the roof slab leading from the interior corner of the antechamber to a point near the top of the center of the lintel beam over the opening in the main-chamber partition. The crack is also present in the lintel beam. Diagonal hairline cracks start at the center of the roof slab and run toward the corners of the slab. The walls of the forward room are not damaged. The floor slab has a $^1/_{64}$-in. crack that starts at a point located at the front of the ventilating room and runs to the center of the room where a box-shaped crack has been formed around the survey point X-13. It then continues to the center of the opening in the main partition.

In the rear room of the main chamber, the $^1/_{32}$-in. crack in the roof slab of the forward room continues past the lintel beam and ends at a strain-gauge recess located in the center of the roof slab. Hairline cracks lead from the recess and run toward the rear walls of the structure. The $^1/_{64}$-in. crack in the floor slab of the forward room continues past the opening toward the center of the room. This crack intersects another $^1/_{64}$-in. crack that begins at a concrete deformator gauge mount and runs toward the rear of the structure. There is a $^1/_{64}$-in.-wide crack that connects the two concrete deformator mounts near the front of the rear room.

Appendix D contains the postshot dynamic analysis of the roof slab of the rectangular type 60 shelter. The analysis indicates that only minor cracking was expected under the applied blast load.

(d) *Exit Chamber, Tunnel, and Emergency Exit Shaft.* The only damaged section of the exit portion of the structure is the escape tunnel. Three continuous cracks were formed around the walls, roof, and floor slab. The width of these cracks varies from $^1/_{16}$ to $^1/_8$ in. The smallest crack is at the end wall of the main structure. The other two are toward the middle of the tunnel.

(e) *Doors.* All blast doors, including the emergency exit cover, were undamaged, and the locking mechanism and hinges functioned properly after the test.

Several days after the detonation, when the structure was first entered, the main blast door was found in an open position. No damage to the plate, hinges, or dogs could be observed. The door opened and closed in the same manner as before the test. It is believed that this door was closed but that the dogs were left in the open position at test time.

The fire door located past the main blast door suffered from the pressure which seeped behind the blast door. The front face exhibits extensive cracking and spalling. Two sections of the $^1/_2$-in. concrete facing, with an area of approximately 2 sq ft, were spalled off. The top hinge of the door was dislodged from its recess; the bottom hinge remained intact. The door bolting ensemble was broken after the test by the team recovering instrumentation and radiation data.

The gastight door was also damaged by the blast pressure. The center portion of the door deflected inward approximately $^1/_2$ in. The top spring type adjusting hinge was flattened out, causing the door to be off center.

(f) *Ventilation.* Inspection of the natural ventilation system showed that the ball type antiblast valves had operated. The spheres, which were located in the exhaust and intake pipes,

had circular indentations that were produced by the blast wave forcing them against the interior vent pipe. The sealing covers, which were located at the interior ends of the pipes, were all blown off and deformed. The three quick-acting shut-off valves, which were in the closed position before the test, were found to be in good working condition after the test. One of the valves located near the dust filter was open; the remaining two valves were in their original position after the test. The air distribution duct for ventilation was separated at one of its joints. The valve of the air exhaust pipe leading from between the main blast door and the fire door into the antechamber, which was in a closed position before the test, remained in the closed position and was in good operating condition. Owing to the position of the antiblast valve located in the exhaust pipe leading from between the fire and blast doors to the exterior wall into the entranceway, its operation after the test could not be checked.

(g) *Above-ground Portion of the Structure.* The exhaust and intake stacks were sheared off from 2 ft above to a few inches below grade. The main portions of the debris were found approximately 5 to 100 yards behind the structure away from GZ. The overhanging portion of the sand-pit roof slab was chipped and scoured on all four sides. One corner facing GZ was completely broken off, and the reinforcing bars were exposed. The remaining sections of the stacks and the sand pit were badly scoured.

(h) *Miscellaneous.* The electrical system within the structure was functioning properly after the test. The six light bulbs that were strung on an electrical cable were intact and in operating condition. An additional light bulb placed in an extension cable and mounted against the wall facing GZ was in good condition.

The siphon used as overflow for the emergency ventilation was found to have had all its condensation water evaporated after the test.

The radio equipment was recovered several days after the test and was in working condition at that time.

Blast damage incurred by structure II-1 is shown in Figs. 3.4 to 3.24.

3.1.2 Cylindrical Shelter, Type 50, Structure II-2

(a) *Main Entrance and Antechamber.* No damage was observed in the roof, floors, or walls of either the main entrance or the antechamber.

(b) *Main Chamber.* The circular precast rings in the main chamber were extensively damaged but did not collapse. The upper segments of rings 2 through 10 were displaced downward by varying amounts. There seems to have been no movement of rings 11 and 12 and the exit portions of the structure. The movement downward of ring 10 in relation to ring 11 is approximately $^3/_4$ in. There is a general increase of the downward displacement of all the inclusive rings between 10 and 2. Located at the joint between rings 2 and 3 is another sharp increase in the downward displacement of about $^1/_2$ in. Rings 1 and 2 and the main entrance and antechamber seem to have been displaced a greater amount than the remaining portion of the structure.

In addition to the downward movement of the rings, a flattening out of the rings occurred. The upper portion of the rings was forced downward, thereby causing an outward movement of the sides. This depression of the upper surface of the round rings produced an oblate shape, with the major axis running approximately between points 2 and 8 and the minor axis between points 5 and 11, Table 3.1. This oblate shape of the rings was predominant toward the center portion of the structure.

The postshot measurements taken along the ring diameters are indicated in Table 3.1.

All joints between rings 2 and 10 have developed cracking along parts of the circumference. Most of these cracks developed either in the lower half of the rings or on the side of the structure facing GZ. Several continuous circumferential cracks were formed at joints 2-3 and 10-11.

Extensive lamination or separation of the concrete between the interior faces of the rings and the circumferential surface of the reinforcement has developed along the upper quarters of the rings on the sides facing GZ and near their crowns. This separation may have extended be-

yond the interior rings of the reinforcement. If the structure had been uncovered, it would have been possible to verify whether these cracks extend completely through to the outer surface of the concrete.

A continuous laminated area starts at the upper quarter point facing GZ of ring 5 and terminates near the crown of the joint between rings 9 and 10. The width of this laminated section varies from 1 to 3 ft. An offshoot of this laminated area occurs at ring 8, where the crown of the ring has been deflected downward approximately $\frac{1}{2}$ in. below the crown of rings 7 and 9. In addition to the sections already described, several laminated areas were formed at the crown of rings 2 and 4 and also above the upper quarter point of ring 3 facing GZ.

Numerous longitudinal and transverse cracks were produced in the rings of the main chamber. Most of the laminated sections are bordered by these cracks. The main laminated section has a $\frac{1}{4}$-in. crack along its upper edge which starts at the mid-height of joint 2-3 and runs toward the laminated section. This crack meets the laminated section at joint 4-5 and then continues into the section. There is a $\frac{1}{64}$-in. crack beginning at the starting point of the above-described crack and following the lower edge of the laminated area to a point located at joint 6-7. A $\frac{1}{64}$- to $\frac{1}{16}$-in. longitudinal crack originates at the bottom of ring 10 and runs to a laminated section located at the bottom of ring 6. Several $\frac{1}{64}$-in. longitudinal cracks were produced at the upper quarter facing GZ of rings 4, 5, 6, and 7. A vertical crack, located on the side of, and running below, the laminated area of ring 2 on the GZ side of the structure, was observed. This crack has approximately 2-in. spalling on each of its sides. One $\frac{1}{32}$-in. vertical crack, similar to the one described above, is located along the side of the laminated section of ring 3 at its crown. Ring 8 also has a $\frac{1}{32}$- to $\frac{1}{16}$-in. vertical crack along the top edge of its laminated area. A large $\frac{1}{4}$- to $\frac{1}{2}$-in. vertical crack is located on the GZ side at the lower quarter point of ring 10. This crack has 2- to 3-in. spalling on each of its sides and also gives the impression that splitting of the ring was produced. Several vertical $\frac{1}{16}$- and $\frac{1}{32}$-in. cracks were formed in ring 11.

On the side of the structure away from GZ, cracking occurred between the upper quarter and the mid-height of ring 2. This crack has spalling continuously along each of its sides. A similar crack was produced in the lower quarter of rings 7 and 10. Several diagonal $\frac{1}{64}$- and $\frac{1}{32}$-in. cracks were formed at the upper section of rings 3 and 4. This is an indication of the vertical movement downward of that portion of the structure adjacent to the main entrance.

The crack patterns for the main chamber are shown in Figs. 3.25 and 3.26.

(c) *Exit Chamber and Emergency Exit Shaft.* The rear portion of the structure has no structural damage.

(d) *Doors.* All doors (the main sliding blast door, main entrance blast and gastight doors, exit chamber blast and gastight doors, and emergency exit trap door) were undamaged. The frames, hinges, and latching mechanisms were in proper operating condition.

(e) *Ventilation.* The flap-plate cover located at the interior end of the natural intake vent pipe, which was in the closed position during the test, was blown open but remained on the hinge. A circular indentation is present on the antiblast ball valve. The rubber hose that connected the natural ventilation pipe with the dust collector was blown off at the vent pipe end. The quick-acting shutoff valve between the natural ventilation pipe and intake fan, which was closed during the test, remained closed after the test and is in good operating condition. The quick-acting shutoff valve between the sand-pit filter and the intake fan was open during and after the test and functioned properly upon inspection. At the interior end of the exhaust pipe, the flap-plate sealing cover was in place after the test, but the rubber gasket had been squeezed out. Owing to the inaccessibility of the ball type antiblast valve in the natural exhaust vent pipe, its condition after the test could not be inspected.

(f) *Above-ground Portion of the Structure.* The portion of the ventilation system above the ground surface was badly damaged. The vent stack had the weather-protection cover blown off, leaving the reinforcement for the cover exposed. The reinforced-concrete surface of the stack facing GZ was scoured, and several $\frac{1}{64}$- to $\frac{1}{32}$-in. diagonal cracks were formed on this same face. The overhanging portion of the sand-pit roof slab on the sides of the pit parallel with the

blast line was blown off, and the reinforcement was exposed. The overhanging portion at the GZ side of the pit had the bottom face flaked off and deposited in the hole below. The rear face of the pit was slightly scoured. All ventilation holes in the sides of the pit were free of rubble.

(g) *Miscellaneous.* The two generators located in the main section of the structure were in operating condition, and the exhaust system showed no signs of pressure damage. The electrical system of the structure operated after the test. The bulb that was mounted in an extension cable and protected by a wire cage mounted on the wall opposite from GZ had its filament broken.

The portable transmitter-receiver radios were recovered several days after the test.

Several months after the test, an operational test of the antennas of structure II-2 was performed using the portable radios that had been located in structures II-1 and II-2. Owing to the failure of the standard radio batteries, 12-volt car batteries were used as replacements for this test.

The operational test was performed by connecting one portable radio to the interior end of the antenna of structure II-2. By mounting the second radio on the rear of a 1-ton pick-up truck, the distance between the two radios was increased by slowly driving the truck away from the shelter. Periodical transmissional tests were performed several hundred feet apart. The maximum distance for transmission was approximately 1500 ft.

The blast damage to structure II-2 is shown in Figs. 3.27 to 3.45.

3.1.3 Entrance and Entrance Chamber, Type 65, Structure II-3

(a) *Entranceway.* The concrete is cracked at the centerline of the roof slab of the entrance of structure II-3 toward GZ. A 1/16- to 3/32-in. crack starts at the free end of the roof slab and runs to a point three-quarters of the distance down the sloped portion of the roof, at which point it makes a 45° turn toward the exterior wall. The sloped section of the roof also has a 1/32-in. crack along the intersections of the roof slab and both retaining walls. Several transverse cracks in the roof slab, located above the fourth, fifth, and sixth treads and ranging from 1/64 to 1/32 in. in width, were observed. The stair has a 1/64- to 1/16-in. crack along its centerline, beginning at the bottom riser and continuing to a point located at the seventh riser from the top. Cracks 1/32 to 1/16 in. in width were produced along the entire intersections of the interior and exterior walls, respectively. One vertical 1/32-in. crack started at the roof slab and ran down the exterior wall to a steel loop. The loop had been cast into the wall at a point one-quarter the height of the wall above the second riser from the bottom of the stairs. Several 1/32-in. cracks running the full height of the wall are located above the seventh and tenth risers from the bottom. Two 1/32- and 1/8-in. cracks that start at the fifth and sixth risers from the top of the stairs meet at a common point at the top of the wall above the third riser. The interior wall of the entrance has cracks that are similar to but smaller than (hairline to 1/64 in. in width) those in the exterior wall.

The intersection of the roof slab and the exterior wall above the landing has a 1/32-in. crack. The interior wall of the landing has vertical 1/32-in. cracks located on the GZ side of the door. Several of these cracks terminate at the steel loops which are cast in the wall. On the interior wall on the opposite side of the door from GZ, there are several 3/16-in. vertical cracks.

The entrance leading away from GZ received the major portion of the damage. The roof slab has a 1/32-in. crack along the centerline of its sloped section similar to the centerline crack described for the other entrance. Cracks 1/64 and 1/32 in. were formed at the intersection of the roof slab and interior and exterior walls, respectively. The stairs have continuous cracks along their intersections with both walls. These cracks vary from zero inches at the bottom to about 3/4 in. at the middle and to about 1/8 in. at the top of the stairs. This is an indication of a bowing into the backfill of the two walls mid-way up the stairs. The interior wall has a 3/16- to 1/4-in. vertical crack above the second tread from the bottom running to the roof slab. There is spalling on both sides of this crack. It has several intersecting cracks which also have spalling along their entire length. Along the centerline of the interior wall and parallel to the plane of the stairs, there is a 1/16-in. crack with a 6-in. spalled section on each side of it. This crack, which has several 1/16-in. spalled cracks branching off, runs approximately

the length of the stairs, starting at the third riser from the bottom and terminating at a chipped-out section at the top of the wall. The exterior wall of the entrance away from GZ has numerous cracks varying in size from $\frac{1}{64}$ to $\frac{1}{8}$ in. in width. The major cracks located above the low portion of the stairs consist in several vertical $\frac{1}{16}$-in. cracks above the third and fourth treads. A $\frac{1}{8}$-in. crack, which is parallel to the plane of the stairs, approximately one-third up the height of the wall runs from the fourth to the eleventh tread. Several $\frac{1}{64}$- and $\frac{1}{32}$-in. cracks, perpendicular to the plane of the stairs, are located near the upper steps.

The roof, stairs, and walls of the entranceway were scoured during the test. Debris was deposited on the stairs and the landing. A steel instrumentation plate was deposited at the bottom of the stairs away from GZ.

The crack patterns for the entrance of structure II-3 are shown in Figs. 3.46 and 3.47.

(b) *Entrance Chamber.* No damage was observed in the walls, roof, or floor slab of the antechamber.

(c) *Doors.* The blast, fire-resistant, and gastight doors were undamaged. The door frames gave no evidence of structural failure. The grouted sections around the frame anchors were in the same condition after the test as before.

(d) *Ventilation.* The antiblast flap valve in the exhaust pipe was found in a slightly (approximately $\frac{1}{8}$ in.) open position. It could not be freed from this position after the blast. Close inspection of the flap-valve assembly could not be made owing to a grillage plate welded to the interior end of the pipe. It is quite possible that debris from the broken exhaust stack is lodged behind the flap plate thus holding it in position. The intake pipe cover plate was put in place by error in this test. The plate was partially blown off but remained in place. Inspection of the working of the flap valve was not possible.

(e) *Above-ground Portion of the Structure.* The ventilation intake and exhaust stacks were broken off at the ground surface. The dislodged sections were found 10 to 20 yards to the rear of the structure.

(f) *Miscellaneous.* The electrical system within the structure was found to be in operating condition after replacement of the light bulb. The light bulb, located on an extension cable and encased in a wire cage, had a broken filament. The glass around the filament was intact.

The blast damage to structure II-3 is shown in Figs. 3.48 to 3.56.

3.1.4 Entrance and Entrance Chamber, Type 65, Structure II-4

(a) *Entranceways.* The entranceway roof slab facing GZ has a $\frac{1}{64}$-in. transverse crack. This crack, which is at a 60° angle to the exterior wall, starts above the second tread from the bottom of the stairs and runs approximately three-quarters the span of the roof. There has been a separation of $\frac{1}{64}$ and $\frac{1}{32}$ to $\frac{3}{32}$ in. between the stairs and the interior and exterior walls, respectively. One vertical $\frac{1}{32}$-in. crack is located in the exterior wall above the third tread from the bottom running the full height of the wall. There was no damage to the interior wall of the entrance facing GZ.

The landing roof slab has several transverse cracks. One of these cracks is $\frac{1}{32}$ in. wide and is located near the opposite side of the door opening from GZ. Another, a diagonal crack, starts at the GZ side of the door opening and runs toward the center of the slab. The interior wall has numerous $\frac{1}{64}$- and $\frac{1}{32}$-in. diagonal cracks located on the side of the door opening away from GZ. On the exterior wall one crack was formed. This crack, running the full height of the wall, is $\frac{1}{32}$ in.

The entranceway facing away from GZ, as in the case of structure II-3, received most of the blast damage. The roof slab has a centerline crack starting at the upper end of the slab and running about one-half the sloped distance down the roof. At this point it makes a 90° angle and continues toward the exterior wall. Approximately 1 ft down the slope from where the above crack turns, another transverse crack, $\frac{1}{16}$ in. in width, runs the full width of the entrance. The four upper corners of the parapet around the entrance have $\frac{1}{32}$-in. diagonal cracks. The intersections of the stairs with both walls were opened. The interior wall has a $\frac{1}{32}$-in. crack along

the entire intersection, and the exterior wall has formed a crack that varies from $^1/_{32}$ in. at the bottom riser to hairline in size at the fifth riser from the top. The exterior wall of this entrance has three major vertical cracks running approximately the full height of the wall. The first two cracks are located over the second and third risers from the bottom and are $^1/_{16}$ in. wide. The third crack, $^1/_{32}$ in. wide was formed above the fourth riser. Several $^1/_{64}$-in. cracks perpendicular to the plane of the stairs were formed in the upper section of this wall.

In the interior wall, one diagonal $^1/_{16}$-in. crack, starting at the roof slab above the fourth riser from the bottom of the stairs, runs downward toward the first riser. Two vertical $^1/_{64}$-in. cracks are located above the fifth and eighth risers from the bottom. These cracks run from the roof slab to the mid-height of the wall. Also formed in the wall are two $^1/_{64}$-in. cracks perpendicular to the stairs at the upper section of the wall.

The roof, stairs, and wall of the entranceway were scoured by the blast. Debris was deposited on the stairs and landing during the test.

The crack patterns for the entranceway of structure II-4 are shown in Figs. 3.57 and 3.58.

(b) *Entrance Chamber.* The walls, roof, and floor slab of the antechamber were undamaged.

(c) *Doors.* The blast and combination fire-resistant gastight doors received no structural damage. The frames and the latching mechanisms for the two doors functioned properly after the test. The bolts passing through the sleeves were removed without difficulty after the blast.

(d) *Ventilation.* Investigation of the ball type antiblast valve indicated a circular indentation on the sphere which was produced by the blast pressure forcing it against the interior end of the vent pipe.

(e) *Above-ground Portion of the Structure.* The section of the ventilation stack extending 3 in. above the finish grade was undamaged. There was slight scouring of the top corner of the side of the stack facing GZ. The grillage over the surface end of the vent pipe was pulled from its position.

(f) *Miscellaneous.* The light bulb located on an extension cable mounted on the wall of the chamber facing GZ was broken. The bulb was replaced after the test, and the electrical system of the structure was then found to be in operating condition.

Blast damage to structure II-4 is shown in Figs. 3.59 and 3.60.

3.1.5 Entrance and Entrance Chamber, Type 65, Structure II-5

(a) *Entranceways.* At the intersections of the roof slab and the interior and exterior walls of the entrance toward structures II-3 and II-4, separations of $^1/_{64}$ in. and hairline, respectively, were observed running the full length of the sloped portion of the roof. One transverse crack, $^1/_{32}$ in. wide, the full width of the entrance is located above the third tread from the bottom. One diagonal hairline crack was formed, starting at the interior-wall terminal of the above-mentioned crack and running toward the exterior wall. This crack branches out into three individual cracks near the centerline of the slab. A hairline crack begins at a point located at the uppermost end of the slab and runs along the centerline approximately half way down the sloped surface of the slab. The intersection of the exterior wall and the stairs has a separation that varies from hairline at the bottom to $^1/_{16}$ in. at about the ninth riser from the bottom and then back to hairline at a point four risers above. The crack continues the remaining distance up the stairs as hairline in size. The interior wall has a $^1/_{64}$- to $^1/_{16}$-in. diagonal crack making about a 30° angle with the roof slab. This crack starts at the roof above the fourth riser from the bottom and runs to the landing wall where it terminates. Several vertical and diagonal cracks are located in the wall approximately half way up the stairs. Starting at the seventh riser from the top, there is a $^3/_{16}$-in. crack that runs to the intersection of the end of the roof slab and interior wall. The section of the wall above this crack is pushed into the backfill. Several parallel of $^1/_{64}$- and $^1/_{32}$-in. cracks are located above and below the above-mentioned separation. The exterior wall exhibits vertical cracking the full height of the wall above the second to fourth risers from the bottom inclusive. These cracks vary from hairline to $^1/_{16}$ in.

in width. Above the upper third of the wall hairline, $^1/_{16}$-in. vertical and diagonal cracks were observed.

One hairline crack running the full length of the landing was formed at the intersection of the roof slab and interior wall. Two diagonal cracks were produced in the interior wall of the landing on the opposite side of the door from structures II-3 and II-4.

In the entrance away from structures II-3 and II-4, a transverse $^1/_{32}$-in. crack was formed in the roof slab above the third riser. This crack also exhibits a $^1/_{32}$-in. vertical movement downward of the upper portion of the slab. Approximately 2 ft up the slope of the roof a transverse hairline crack was formed. A longitudinal hairline crack is located along the centerline of the sloped roof slab. At the intersection of the roof slab and interior and exterior walls, hairline and $^1/_{32}$- to $^1/_{16}$-in. cracks were produced. At three of the corners of the parapet around the entrance, diagonal cracks varying from $^1/_{64}$ to $^1/_2$ in. in size were formed. Along the intersection of the interior wall and the stairs, a $^1/_{64}$-in. to hairline separation occurred. A similar crack, varying from hairline at the bottom to $^1/_2$-in. at the top, was formed at the corner of the stairs and the exterior wall. The exterior wall has a cluster of hairline to $^1/_{16}$-in. vertical cracks located above the second to fifth riser from the bottom. Four vertical hairline cracks were produced in the upper portion of the wall. The uppermost portion of the exterior wall had extensive cracking. A diagonal crack running between the sixth riser from the top to a point located at the intersection of the end of the roof slab and the wall was observed. The section above this crack was deflected into the backfill by the blast. Several parallel cracks are located several feet below the above-mentioned crack. Additional cracks, which are perpendicular to the stairs, were formed.

The roof, stairs, and walls of the entire entranceway were scoured by the blast. Rubble from the exterior surface was found on both the stairs and the landing.

The crack patterns for the entrance of structure II-5 are shown in Figs. 3.61 and 3.62.

(b) *Entrance Chamber.* No damage was observed in the walls, floor, or roof slabs of the antechamber.

(c) *Doors.* The blast and gastight doors were not damaged. There were no cracks formed around the grouted sections of the gastight door. The hinges and latching mechanisms were in operating condition after the test.

(d) *Ventilation.* Investigation of the ball type antiblast valves located in the intake and exhaust stacks indicated a circular indentation which was produced by the pressure forcing the spheres against the interior vent pipes. Owing to the position of the antiblast valve located in the exhaust pipe leading from between the gastight and blast doors to the exterior wall into the entranceway, its operation after the test could not be checked.

(e) *Above-ground Portion of the Structure.* The section of the exhaust ventilation stack extending above the ground surface was broken off at a height approximately 2 ft above the ground. This stack lost its concrete cover. The intake ventilation stack was broken off about $1^1/_2$ ft below the ground and was moved about 3 ft back. The remaining portions of the superstructure were scoured.

(f) *Miscellaneous.* The electrical system was in operating condition after the test. The light bulb located on an extension and protected by a wire cage functioned when the electrical system was tested.

Blast damage to structure II-5 is shown in Figs. 3.63 to 3.66.

3.2 INSTRUMENTATION

3.2.1 French Instrumentation

Records were obtained from nonelectric equipment, including maximum dynamometers, glass disk diaphragms, caisson manometers, recording barometers, door lateral gauges, door deformeters, concrete deformeters, recording pendulums, and a recording hygrometer. No

postshot information was obtained from the peak thermometers, low-pressure manometer, tube manometer, choc marts, one-unit flux meters, or the 12- and 9-unit flux meters.

The 3.5.4 electronic equipment, as in the case of some of the nonelectronic measuring devices, failed to produce blast information. The principal reason for the failure of the recording system was evident from the photographic records. These records indicated a breakdown at the time of detonation between the timing signal circuit and galvanometer circuit. Several secondary reasons for failure of the equipment were (1) the failure of the fuses in the circuits which provided power for the paper advance mechanisms in two of the miniature recorders and (2) blackening of the photographic paper by nuclear radiation.

The results of the French instrumentation, with the exception of radiation instrumentation, are indicated in Tables 3.2 to 3.12 and Figs. 3.67 to 3.70. A more fully defined description of the test results, from which the instrumentation data have been accumulated, is given by Project 30.5b in WT-1535.

A complete description of the radiation results is given in Sec. 3.2.3 of this report.

3.2.2 U. S. Pressure Instrumentation

Of the 33 BRL self-recording pressure-time gauges installed, 29 good pressure-time records were obtained. The remaining four records gave only peak values. Two BRL self-recording VLP-time gauges were also installed to obtain pressure vs. time records within the structures; both gauges (one each in structures II-1 and II-2) gave very poor results.

The peak pressures and durations of the positive phase, as measured, are indicated in Table 3.13. The pressure vs. time curves for the instrumentation provided in the structures are shown in Fig. 3.71.

In addition to the pressure data obtained from the structure proper, blast-line pressure information has been made available from Project 30.5b.

Data that have been obtained summarize the peak side-on and dynamic pressures of the blast-line instrumentation, Tables 3.14 and 3.15 and Fig. 1.6. In addition to the peak values of the pressures at various stations along the blast line, the peak pressure vs. distance curves for the side-on and corrected dynamic pressures along the blast line are given in Fig. 3.72.

The pressure vs. time curves for the dynamic pressure gauges located at 500, 863, 981, and 1135 yd from GZ are indicated in Fig. 3.73. The definitions of the ordinate symbols for Fig. 3.73 are as follows:

$p_p^{*\prime}$ = total head pressure as measured
p' = side-on pressure as measured
$q_c^{*\prime}$ = dynamic pressure as measured
q^* = dynamic pressure (corrected)
M^* = Mach number

The pressure vs. time curves for the electronic incident air pressure (Wiancko) gauges located at 280, 300, 335, and 392 yd from GZ and the self-recording incident pressure gauges at 280, 300, and 392 yd from GZ are given in Fig. 3.74. The average pressure at the particular distance from GZ is as noted on the curve. Pressure vs. time curves for the self-recording incident pressure gauges located at 500, 863, 981, 1135, 1292, 1385, 1440, 1893, 2000, and 2667 yd from GZ are given in Fig. 3.75.

3.2.3 U. S. and French Radiation Instrumentation

Heavy instrumentation of the five French underground shelters was accomplished by the use of Edgerton, Germeshausen & Grier (EG&G) film packs, which were placed in the shelters to measure prompt-gamma-radiation doses at various locations within the shelters. Recovery was made in all shelters. Project 39.1b/39.5 neutron detectors were used to supplement this gamma information.

To compare French and American dosimetry techniques, French film plates and EG&G badges were placed together in the five French shelters used on shot Smoky. Each French plate consisted of eight film packs of various types taped to a piece of Plexiglas and wrapped in pack-

ing material covered with a dust-tight plastic bag The EG&G pack consisted of four types of film in a polyethylene case mounted in a lead and tin box.

French film types used were as follows:

Type	Range, r (accurate portion of curve) American process (approximate)	French process (approximate)
Kodak Periapical (K-P)		
a	2 to 200	0 to 2
b	2 to 200	100
Chassende Baroz 600 R (CB-600 R)		
a	20 to 500	150
b	20 to 1,000	600
Chassende Baroz 50,000 R (CB-50,000 R)		
a	100 to 10,000	1,000
b	200 to 40,000	10,000
c	5,000 to 70,000	40,000

Film types used by EG&G were:

Type	Range, r (accurate portion of curve)
Du Pont film pack, type 553	
Type 502	5 to 12
Type 510	8 to 250
Type 606	200 to 600
Eastman SO-1112	309 to 50,000

Two film packs on each French plate had a cadmium strip covering part of the packet. Table 3.16 gives French (cadmium readings) and EG&G dosimetry comparisons.

All French films were processed with the American dosimeters to a gamma of approximately 1.3.

French control films placed in standard EG&G badges were irradiated and developed to furnish calibration curves for the dose interpretation of the plates. It was thought that some of the French control film had been calibrated, but, since no means of identification could be found, these badges could not be distinguished from fresh film. Therefore a random series of K-P and CB-600 R film badges was cut in half and made light-tight. One series of these half-badges was then irradiated and processed with the other, nonirradiated (control), half. The results indicated that the Kodak badges chosen were all originally fresh film, and, since the controls showed no darkening above normal, a good calibration curve was obtained. Since some discrepancies appeared on the CB-600 R films, it was necessary to run two calibrations to obtain a curve. The CB-50,000 R film calibration looked very satisfactory, and the doses interpreted from the plates in the shelters indicated these doses to be in fair agreement with the American dosimeters.

A set of the remaining French badges was calibrated for processing in France to compare French and American processing techniques. Kodak Periapical calibration packs were placed in EG&G containers and were irradiated from 0.01 to 500 r on the EG&G Co^{60} calibration range, and the administered dose was written on the packs; the remaining Kodak packs that were returned were not irradiated.

Also included for return to France were nonirradiated controls plus irradiated CB-600 R films (with doses from 0.5 to 500 r irradiated in the same manner as the Kodak film) and CB-50,000 R films (with doses from 100 to 5×10^3 r).

As a final step in preparing film plates for return, all processed French films were mounted on clear plastic sheets, labeled, and bound in book form with a table of contents, thus making it possible to reread film densities directly from the pages without removing the films.

The results of the gamma-radiation film dosimeters are given in Fig. 3.76. The values of the radiation dosages given in the figure are average values of several dosimeters located near the indicated values. These values indicate the total gamma-radiation dosage accumulated over an approximate 52-hr period. The total dose vs. distance curve for the gamma film dosimeters located along the blast line is given in Fig. 3.77. The results obtained by Project 39.1 from gamma-radiation chemical dosimeters placed along the blast line are given in Table 3.17.

Of the four sulfur and gold detectors placed in the French structures (Fig. 2.11), only one gave reliable results. In structure II-2, readings of 3.315×10^7 and 1.588×10^{10} were obtained for the sulfur and gold-cadmium difference, respectively, for detector No. 162. These values are both in neutrons per square centimeter. In the same structure, detector No. 163 was not recovered. The two detectors placed in structure II-3, Nos. 164 and 169, were recovered too late to be readable. The foregoing information was abstracted from the Project 39.1a report, WT-1466. Results of all radiation-detection equipment are given by Projects 39.1, 39.1a, and 39.9 in reports ITR-1500, WT-1466, and ITR-1509, respectively.

3.3 GROUND-SHOCK SPECTRA

Peak displacement responses to shock of single-degree-of-freedom systems (reed gauges) of various natural frequencies are presented in Table 3.18 for shots Smoky, Whitney, Galileo, Charleston, and Stokes. As indicated in this table, peak displacement of reed gauges of known frequencies were recorded near the surface in the free-field and in an underground rectangular structure of Project 30.7 at the 1005-ft range.

These records show that the horizontal (radial) measurements are generally less than one-half the vertical measurements. The horizontal displacements recorded in the shelter are approximately the same as those for the free-field gauges adjacent to the structure. However, the vertical displacements in the shelter were considerably less than the free-field measurements, indicating attenuations in the vertical direction. In all cases high accelerations are associated with high frequencies and high displacements with the low frequencies.

Figures 3.78 and 3.79 are plots of vertical (Fig. 3.78) and horizontal displacements (Fig. 3.79) vs. frequency recorded at shots Smoky, Whitney, and Galileo for near-surface free-field values and values recorded inside the shelter during shot Smoky. This plot indicates that the data follow a consistent pattern.

3.4 BIOLOGICAL TEST RESULTS

3.4.1 General

The major portion of the samples were recovered two days after the test. The specimens in structure II-2 were recovered three days after the test.

After recovery and examination of the mice, if death had occurred, the body and spleen weights were recorded, and the entire organism was fixed in buffered Formalin. Average weights of the surviving animals for each location were taken daily by getting the total weight for each group and dividing by the number in the group.

3.4.2 Mortality

The immediate mortality of the mice was confined to structure II-2 where 19 of the 20 specimens placed on the top landing of the stairs were found dead upon recovery.

The location, number, time of recovery after the test, and time of death of the mice that had died between their recovery and 20 days after the test are given in Table 3.19. The table also includes the 19 mice of structure II-2 referred to above.

Of the control mice left unattended, none had died up until a period of 20 days after the test. As previously stated, each sample consisted of 20 mice.

Table 3.1 —DIAMETRICAL POSTSHOT MEASUREMENT OF PRECAST RINGS AND JOINTS

	Diametrically opposite points					
Location	1-7	2-8	3-9	4-10	5-11	6-12
Joint T1-1		7 ft 2 3/4 in.				
Ring -1		7 ft 2 1/2 in.	7 ft 2 1/2 in.	7 ft 2 1/2 in.		
Joint 1-2		7 ft 2 7/16 in.	7 ft 2 1/2 in.	7 ft 2 1/2 in.		
Joint 2-1		7 ft 2 3/4 in.	7 ft 3 in.	7 ft 2 7/8 in.		
Ring 2		7 ft 2 3/8 in.	7 ft 2 7/8 in.	7 ft 2 3/4 in.		
Joint 2-3	Concrete	7 ft 2 3/4 in.	7 ft 2 11/16 in.	7 ft 2 9/16 in.	Concrete	Concrete
Joint 3-2	seat	7 ft 2 15/16 in.	7 ft 3 3/16 in.	7 ft 3 1/16 in.	seat	seat
Ring 3	location	7 ft 2 15/16 in.	7 ft 3 1/4 in.	7 ft 3 1/16 in.	location	location
Joint 3-4		7 ft 2 13/16 in.	7 ft 3 1/4 in.	7 ft 2 7/8 in.		
Joint 4-3		7 ft 3 1/2 in.	7 ft 3 3/8 in.	7 ft 3 1/5 in.		
Ring 4		7 ft 3 1/4 in.	7 ft 3 1/4 in.	7 ft 2 15/16 in.		
Joint 4-5		7 ft 3 3/4 in.	7 ft 3 in.	7 ft 2 13/16 in.		
Joint 5-4		7 ft 3 7/16 in.	7 ft 3 in.	7 ft 2 7/8 in.		
Ring 5	7 ft 2 1/2 in.	7 ft 3 1/4 in.	7 ft 3 in.	7 ft 2 11/16 in.	7 ft 2 15/16 in.	G.L.*
Joint 5-6	7 ft 2 3/8 in.	7 ft 3 in	7 ft 2 13/16 in.	7 ft 2 5/8 in.	7 ft 1 11/16 in.	7 ft 1 13/16 in.
Joint 6-5	7 ft 2 7/16 in.	7 ft 3 in.	7 ft 3 in.	7 ft 2 7/8 in.	7 ft 2 1/8 in.	7 ft 2 1/4 in.
Ring 6	7 ft 2 5/16 in.	7 ft 2 15/16 in.	7 ft 2 13/16 in.	7 ft 2 5/8 in.	7 ft 1 3/4 in.	G.L.*
Joint 6-7	7 ft 2 5/16 in.	7 ft 2 7/8 in.	7 ft 2 3/4 in.	7 ft 2 5/8 in.	7 ft 1 5/8 in.	7 ft 1 3/4 in.
Joint 7-6	7 ft 2 1/8 in.	7 ft 3 3/16 in.	7 ft 2 1/8 in.	7 ft 3 1/4 in.	7 ft 2 in.	7 ft 1 13/16 in.
Ring 7	7 ft 2 1/8 in.	7 ft 3 1/16 in.	7 ft 3 1/16 in.	7 ft 2 15/16 in.	7 ft 1 3/4 in.	7 ft 1 5/8 in.
Joint 7-8	7 ft 2 1/8 in.	7 ft 3 in.	7 ft 2 15/16 in.	7 ft 2 5/8 in.	7 ft 1 5/8 in.	7 ft 1 3/4 in.
Joint 8-7	7 ft 2 3/8 in.	7 ft 3 5/16 in.	7 ft 3 3/8 in.	7 ft 3 3/16 in.	7 ft 1 3/4 in.	7 ft 1 7/8 in.
Ring 8	7 ft 2 3/16 in.	7 ft 3 1/4 in.	7 ft 3 3/8 in.	7 ft 3 in.	7 ft 1 13/16 in.	7 ft 1 3/4 in.
Joint 8-9	7 ft 2 in	7 ft 3 1/8 in.	G.L.*	7 ft 2 3/4 in.	7 ft 1 11/16 in.	7 ft 1 1/4 in.
Joint 9-8	7 ft 2 1/4 in.	7 ft 3 9/16 in.	7 ft 3 3/8 in.	7 ft 2 7/8 in.	7 ft 1 7/8 in.	7 ft 1 1/4 in.
Ring 9	7 ft 2 5/16 in.	7 ft 3 3/8 in.	7 ft 3 1/4 in.	7 ft 2 7/8 in.	7 ft 1 13/16 in.	7 ft 1 1/4 in.
Joint 9-10	7 ft 2 3/16 in.	7 ft 3 1/16 in.	7 ft 3 in.	7 ft 2 1/4 in.	7 ft 1 5/8 in.	7 ft 1 1/4 in.
Joint 10-9	7 ft 2 1/4 in.	7 ft 3 1/2 in.	7 ft 3 1/8 in.	7 ft 3 1/16 in.	7 ft 1 15/16 in.	7 ft 1 11/16 in.
Ring 10	7 ft 2 in.	7 ft 3 3/16 in.	7 ft 3 1/8 in.	7 ft 2 15/16 in.	7 ft 1 7/8 in.	7 ft 1 5/8 in.
Joint 10-11	7 ft 2 in.	7 ft 2 7/16 in.	7 ft 2 3/4 in.	7 ft 2 3/4 in.	7 ft 1 3/4 in.	7 ft 1 13/16 in.
Joint 11-10	7 ft 2 1/2 in.	7 ft 2 7/8 in.	7 ft 3 in.	7 ft 2 5/8 in.	7 ft 2 1/2 in.	G.L.*
Ring 11	7 ft 2 1/2 in.	7 ft 2 5/8 in.	7 ft 2 1/2 in.	7 ft 2 1/2 in.	7 ft 2 7/16 in.	G.L.*
Joint 11-12	7 ft 2 7/16 in.	7 ft 2 1/2 in.	7 ft 2 7/8 in.	7 ft 2 1/4 in.	7 ft 2 5/16 in.	G.L.*
Joint 12-11	7 ft 2 3/8 in.	7 ft 2 3/4 in.	7 ft 2 1/4 in.	7 ft 2 9/16 in.	7 ft 2 11/16 in.	G.L.*
Ring 12	7 ft 2 1/2 in.	7 ft 2 7/16 in.	7 ft 2 5/8 in.	7 ft 2 1/2 in.	7 ft 2 7/16 in.	7 ft 2 3/8 in.
Joint 12-T2†	7 ft 2 1/16 in.	7 ft 2 in.	7 ft 2 in.	7 ft 2 in.	7 ft 2 3/16 in.	7 ft 2 in.

*G.L., gauge location (no measurement because of gauge interferences).
†Grout along joint 12-T2.

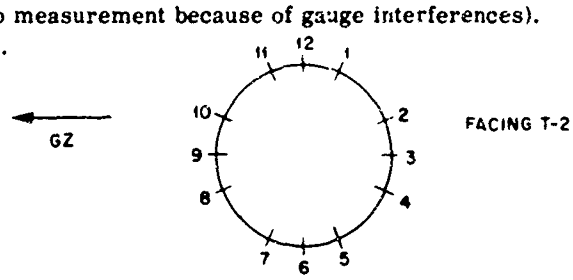

Table 3.2 — RESULTS OF FRENCH INSTRUMENTATION

Designation	Description	Results	Cause
3.2.1.1	Maximum dynamometer	See Table 3.3; 3 of 31 gauge records gave no results.	Probably pressure too low to depress pistons.
3.2.1.5	Glass disk diaphragms	See Table 3.4; disks in structures II-1, II-3, and II-4 were completely shattered.	Probably by debris carried by shock wave.
3.2.2.1	Low-pressure manometer	No rise in pressure after arrival of blast wave.	
3.2.2.2	Caisson manometer	See Table 3.5; manometer records in structure II-4 gave no results.	Glass in cover, metal cover and the recording arm were broken.
3.2.2.3	Recording barometer	See Table 3.6; barometer records in structure II-4 gave no results.	Recording pen was bent and glass in cover was shattered.
3.2.3.1	Tube manometer	No record obtained	Recording pen lifted from chart surface.
3.5.4	Pressure gauge	See Table 3.12.	Probably due to breakdown of timing signal and galvanometer circuit.
3.1.1.1	Door lateral gauge	See Table 3.7.	
3.1.1.2	Door deformeter	See Table 3.8.	
3.1.1.3	Concrete deformeter	See Table 3.9; one deflection recording exceeded the limit of the lead plate.	
3.1.1.4	Recording pendulum	See Figs. 3.67 to 3.70; no pendulum record for structure II-4.	Recording paper badly torn by point of pencil.
3.1.1.4	Choc mart	No results obtained.	Insufficient acceleration of structure.
3.5.4	Seismograph	Record not readable.	
3.5.4	Acceleration gauge	See Table 3.12.	Probably due to breakdown of timing signal and galvanometer circuit.
3.5.4	Deflection gauge	See Table 3.12.	Probably due to breakdown of timing signal and galvanometer circuit.
3.5.4	Strain gauge	See Table 3.12.	Probably due to breakdown of timing signal and galvanometer circuit.
3.3.1.1	1-Unit flux meter	No results obtained.	Due to missing elements, light, severe dust erosion, and missile damage.
3.3.1.2	Peak thermometer	See Table 3.10.	
3.3.1.4	12-Unit flux meter	No results obtained.	No color change.
3.3.1.4	9-Unit flux meter	No results obtained.	No color change.
3.3.2.1	Recording thermometer	See Table 3.11.	
3.3.2.2	Recording hygrometer	Recorded humidity was 47%.*	
3.5.4	Temperature gauge	See Table 3.12.	Probably due to breakdown of timing signal and galvanometer circuit.
3.4.1.1	Film badge	See Section 3.2.1.	
3.4.1.3	Dosimeter recorder	See Section 3.2.1.	
3.5.4	Temperatures and pressure	See Table 3.11.	Probably due to breakdown of timing signal and galvanometer circuit.
3.5.4	Temperature, pressure, and acceleration	See Table 3.12.	Probably due to breakdown of timing signal and galvanometer circuit.

*The actual value of humidity recorded by meterological services at the Nevada Test Site was 31 per cent.

Table 3.3 — DATA FROM MAXIMUM DYNAMOMETER (3.2.1.1)

Structure No.	Gauge No.	Displacement of segment, mm	Overpressure		Remarks
			kg/cm^2	psi	
II-1	1	18.25	9.125	129.8	None
	2	0.00			None
	3	0.00			None
	4	8.10	4.05	57.6	None
	5	17.10	8.55	121.6	None
	6	13.00	6.50	92.4	None
	7	14.00	7.00	99.6	None
	8	0.10	0.05	0.7	None
II-2	1	35.20	17.60	250.3	None
	2	66.00	33.00	469.3	Moderate sand blasting
	3	6.00	3.00	42.6	None
	4	0.10	0.05	0.7	None
	5	0.10	0.05	0.7	None
II-3	1	29.10	14.55	206.9	None
	2	14.00	7.00	99.6	None
	3	19.50	9.75	138.7	None
	4	41.50	20.75	295.1	None
	5	60.00	30.00	426.7	*
	6	23.20	11.60	164.9	None
II-4	1	14.50	7.25	103.1	None
	2	13.90	6.95	98.8	None
	3	21.80	10.90	155.0	None
	4	0.00			None
	5	33.50	16.75	238.2	None
	6	12.50	6.25	88.9	Moderate sand blasting
II-5	1	11.20	5.60	79.6	None
	2	16.50	8.25	117.3	None
	3	16.50	8.25	117.3	None
	4	13.50	6.75	96.0	None
	5	13.00	6.50	92.4	None
	6	17.50	8.75	124.4	None

*The ventilator was sheared by the blast wave and carried approximately 115 ft south of its original position. When found, the chimney had been overturned; so the face bearing the gauge was resting on the ground. The gauge suffered severe sand blasting.

Table 3.4—RESULTS OF GLASS-DISK PRESSURE INDICATOR (3.2.1.5)*

Structure No.	Assembly No.	Diameter of disks, mm	Remarks
II-1	6	56, 58, 60, 64, 68, 72, 76, 80	All disks completely shattered.
II-2	10	52, 54, 76, 80, 90, 100	No damage, glass intact.
II-3	9	76, 80, 90, 100	All disks completely shattered.
II-4	11	52, 54, 56, 58, 60, 64, 68, 72	All disks completely shattered.
II-5	12	56, 72, 76, 80	Disks completely shattered.
		58, 64, 68†	Many radial cracks converging near center of disk.
		60	Undamaged

*Information for the evaluation of pressures is not available at this time.
†Small elliptical hole 5.5 by 3.0 mm near point of convergence.

Table 3.5—RESULTS OBTAINED BY CAISSON MANOMETER (3.2.2.2)

Structure No.	Instrument No.	Atmospheric pressure, kg/cm^2	Maximum pressure, kg/cm^2	Overpressure, kg/cm^2
II-3	4	0.9	1.05	0.15 (2.12 psi)
II-4	5	0.9	No record	
II-5	6	0.9	1.02	0.12 (1.72 psi)

Table 3.6—RESULTS OF RECORDING BAROMETER (3.2.2.3)

Structure No.	Barometer No.	Atmospheric pressure, mm Hg	Maximum pressure, mm Hg	Overpressure mm Hg	Overpressure psi
II-1	6		709	72	1.4
II-2	4	643	760	117	2.3
II-3	8	643	740	97	1.9
II-4	9	639	No record*		
II-5	10	641	727	86	1.7

*Barometer damaged by excessive overpressure.

Table 3.7—DATA FROM LATERAL GAUGES (3.1.1.1)*

Structure No.	Lead plate No.	Gauge location	Depth of depression, mm	Remarks
II-1	1	Lintel	1.3	Smooth depression
	2	Sill	1.7	Smooth depression
	3	North jamb	0.0	
	4	South jamb	3.3	Smooth depression
	5	Lintel	9.0	Complete puncture
	6	Sill	0.7	Smooth depression (evidence of bounce)
	7	Lintel	6.8	Complete puncture
	8	Sill	0.4	Smooth depression
	9	North jamb	0.4	Smooth depression
	10	South jamb	0.4	Smooth depression
II-2	1	West jamb	2.4	Smooth depression
	2	East jamb	2.4	Smooth depression
	3	Lintel	0.3	Smooth depression
	4	Sill	Not readable	Faint impression
	5	West jamb	0.2	Depression not clearly defined
	6	East jamb	0.2	Smooth depression
	7	Lintel	0.3	Smooth depression
	8	Sill	1.6	Smooth depression
II-3	41	Lintel	1.1	Smooth depression
	42	Sill	Not readable	Faint impression
II-4	45	Lintel	0.5	Smooth depression
	46	Sill	0.8	Smooth depression
II-5	1	Lintel	Not readable	Faint impression
	2	Sill	0.1	Light scrape
	3	West jamb	1.9	Smooth depression
	4	East jamb	1.1	Smooth depression

*GZ direction is assumed north of structure.

Table 3.8—DATA FROM DOOR DEFORMETER (3.1.1.2)

Structure No.	Assembly No.	Lead plate No.	Depth of depression, mm	Remarks
II-1	B-3	A-61	2.0	Smooth depression
		A-62	2.7	Smooth depression
		A-64	2.8	Smooth depression
		A-65	2.0	Smooth depression
	B-4	A-66	0.4	Smooth depression
		A-67	0.5	Smooth depression
		A-68	0.6	Smooth depression
		A-69	0.9	Smooth depression
		A-70	1.3	Smooth depression
II-2	B-5	A-71	0.6	Smooth depression
		A-72	0.6	Smooth depression
		A-73	0.7	Smooth depression
		A-74	0.5	Smooth depression
		A-75	0.9	Smooth depression
II-3	B-8	A-86	4.0	Smooth depression
		A-87	4.3	Smooth depression
		A-88	4.5	Smooth depression
		A-89	4.1	Smooth depression
		A-90	4.2	Smooth depression
II-5	B-10	A-96	4.9	Smooth depression
		A-97	5.6	Smooth depression
		A-98	4.9	Smooth depression
		A-99	4.2	Smooth depression
		A-100	3.6	Smooth depression

Table 3.9—DATA FROM CONCRETE DEFORMETERS (3.1.1.3)

Structure No.	Lead plate No.	Depth of depression, mm	Remarks
II-1	1	1.6	The smoothness and symmetry of the depression indicate perpendicular penetration by the punch.
	2	0.7	After the first penetration, the punch made a series of four contacts about 0.240 mm in depth along a slide approximately 2.4 mm in length and 0.1 mm in depth.
II-2	1	18.6	The punch completely penetrated the plate. The total displacement of the ceiling was arrived at by adding the measurement of the deformation of the lead plate to the measurement of the length the punch protruded. This length was found by measuring the length of the scratch marks in the machinist's blue, which the punch had been coated with before-hand.
	2	6.9	This represents the first penetration of the punch.
		5.4	This penetration apparently occurred as a result of a change in position of the punch during the reaction to acceleration.
	3	0.8	The punch made a sliding contact. Size of the contact was approximately 5 by 4 mm.
II-3	1	1.3	First contact of the punch.
		0.9	Second contact of the punch.
II-4	1	0.5	The punch produced a sliding indentation.
II-5	1	0.9	The depression was very smooth.

Table 3.10—TEMPERATURE MEASUREMENTS USING MAXIMUM THERMOMETER (3.3.1.2)

Structure No.	Thermometer No.	Preshot, clinic type	Temp., °C (indicator type)	Postshot, clinic type	Temp., °C (indicator type)
II-1	3	28	26	28	26
	4	27	27	43	44
II-2	6	29	31	56	57.5
II-5	8	28	28	32	35.5

Table 3.11—RESULTS OBTAINED BY RECORDING THERMOMETER (3.3.2.1)

Structure No.	Thermometer No.	Temp., °C, at zero time	Temp., °C, following blast
II-1	6	25.5	27.5
	12	24.0	33.5
II-2	7	42.0	Final maximum temperature in this chamber rose to 57.5°C as a result of heat caused by the gasoline generator
	14	26.5	29
II-3	8	27	29
II-4	4	25	47
II-5	10	26	26

Table 3.12—SUMMARY OF PERFORMANCE OF ELECTRONIC RECORDER

Channel No.	Phenomenon measured	Recorder No.	Remarks
8	Strain	3971	No record, film blackened
9	Strain	3971	No record, film blackened
10	Strain	3971	No record, film blackened
11	Strain	3971	No record, film blackened
42	Displacement	3968	No record, film blackened
43	Displacement	3968	No record, film blackened
44	Displacement	3968	No record, film blackened
47	Displacement	320	No trace on paper
37	Acceleration	323	Poor record, intermittent trace
38	Acceleration	323	Poor record, intermittent trace
40	Acceleration	323	Poor record, intermittent trace
60	Acceleration	321	Poor record, intermittent trace
61	Acceleration	321	Poor record, intermittent trace
62	Acceleration	321	Poor record, intermittent trace
54	Earth pressure	326	No record, recorder did not run
55	Earth pressure	326	No record, recorder did not run
56	Earth pressure	325	Poor record, intermittent trace
48	Earth pressure	325	Poor record, intermittent trace
49	Earth pressure	325	Poor record, intermittent trace
50	Earth pressure	326	No record, recorder did not run
59	Earth pressure	326	No record, recorder did not run
52	Earth pressure	325	Poor record, intermittent trace
53	Earth pressure	325	Intermittent trace, no evidence of response
73	Air pressure	322	Poor record, intermittent trace
74	Air pressure	322	Poor record, intermittent trace
75	Air pressure	322	Poor record, intermittent trace
77	Air pressure	322	Poor record, intermittent trace
67	Air pressure	320	Poor record, intermittent trace
72	Air pressure	320	Poor record, intermittent trace
22 to 27	Temperature	324	No record, recorder did not run
14, 15, 16, 19, 20, 21	Temperature	324	No record, recorder did not run
30, 31, 33	Temperature	324	No record, recorder did not run

Table 3.13—RESULTS OF BRL SELF-RECORDING PRESSURE VS. TIME GAUGES

Structure No.	Gauge No.	Peak pressure, psi	Duration of positive phase, sec
II-1	1	90.0	0.228
	2	112.0	Peak pressure only
	3	2.2	0.130
	4	2.2	3.319
	5	110.0	0.236
	6	78.0	0.222
	7	132.0	0.174
	8	0.4	0.595
	9	0.36	0.722
	VLP-10	0.5	Poor record (recording stylus jumping caused by acceleration from the floor of the structure).
II-2	1	2.5	0.835
	2	0.7	1.175
	3	2.8	2.150
	4	250.0	1.340
	VLP-2	0.3	Gauge stopped recording after 481 msec.
II-3	1	115.0	0.188
	2	1.4	0.610
II-4	1	98.0	0.288
	2	104.0	0.850
	3	100.0	0.170
	4	90.0	0.260
	5	82.0	0.264
	6	78.0	0.203
	7	70.0	0.139
	8	94.0	0.188
	9	96.0	0.185
	10	110.0	0.185
	11	12.0	0.270
II-5	1	103.0	0.230
	2	104.0	0.259
	3	100.0	Peak pressure only
	4	112.0	0.230
	5	94.0	Peak pressure only
	6	78.0	Peak pressure only
	7	1.4	0.654

Table 3.14—BLAST-LINE MEASUREMENTS OF PEAK DYNAMIC PRESSURE

Distance from GZ, yd	Max. dynamic pressure* (corrected), psi
280	360
300	320
335	280
392	230
590	74
810	28
1440	1.5

*Taken from Fig. 3.72.

Table 3.15—BLAST-LINE MEASUREMENT OF PEAK OVERPRESSURE

Distance from GZ, yd	Type of gauge	Peak pressure, psi	Remarks
280	Self-recording	175.0	Poor record
	Electronic	165.0	Good record
300	Self-recording	165.0	Good record
	Electronic	145.0	Good record
	German	166	Peak pressure
335	Self-recording	116.0	Peak only
	Electronic	110.0	Good record
	German	101	Peak pressure
392	Self-recording	81.0	Good record
	Electronic	75.0	Good record
	German	59	Peak pressure
500	Self-recording	44.5	Good record
590		26.0	From pressure vs. distance curve
672	Electronic	18.2	Peak only
	German	18.2, 22.7	Peak pressure
810		11.5	From pressure vs. distance curve
863	Self-recording	8.8	Good record
	German	11.5, 14.2	Peak pressure
981	Self-recording	10.4	Good record
1135	Self-recording	6.4	Good record
1292	Self-recording	7.2	Good record
1385	Self-recording	6.3	Good record
1440	Self-recording	7.2	Good record
1893	Self-recording	4.9	Good record
2000	Self-recording	4.6	Good record
2667	Self-recording	2.8	Good record

Table 3.16 — COMPARISON OF FRENCH AND EG&G DOSIMETRY

Shelter No.	Inside location	5-ft French plate No.	5-ft French plate Av. dose, r (Cd)	5-ft EG&G badge No.	5-ft EG&G badge Dose, r	5-ft EG&G badge No.	5-ft EG&G badge Dose, r	3-ft EG&G badge No.	3-ft EG&G badge Dose, r
II-1	24	51	2.78	1979	1.5			1978	1.9
II-1	20 and 21	52	3.73	1970	1.8	1971	1.7	1972	2.3
II-1	16	53	24.50	1962	7.4	1963	7.4		
II-1	33	54	3.95	2564	2.7	2565	2.7	2566	2.7
II-1	35 and 36	55	18.80*	2570	8.7			2569	5.4
II-1	1	56	8.9×10^2*	1937	7.0×10^3†	1936	1.8×10^3‡	1935	1.6×10^3
II-1	39	57	35.	2580	31.0	2579	27.0	2578	31.0
II-2	5 and 6§	59	17.88	2512	26.0	2511	25.0	2510	19.0
II-2	19 and 20	60	26.00	1918	15.0	1917	13.0	1916	18.0
II-2	14 and 15	61	23.13	1909	42.0	1908	38.0	1907	30.0
II-2	9 and 10	62	205.50	2518	24.0	2519	22.0	2517	19.0
II-3	3 and 4	44 and 45	19.44	2521	22.0	2522	21.5		
II-3	8 and 9	46	27.50	2520	38.0	2528	35.0	2527	34.0
II-4	5 and 6	67	24.50				33.0¶		36.9**
II-4	9 and 10	68	24.38	2497	53.0	2498	53.0		
II-5	3 and 4	71	19.38	2476	28.0	2477	25.0		
II-5	8 and 9	72	34.13	2484	45.0	2486	46.0	2485	54.0

*Recovered one month later than the other badges.
†At 11 ft.
‡At 7 ft.
§3 and 4 were not recovered.
¶Average dose at 5 ft for Nos. 2494 and 2496.
**Average dose for Nos. 2493 and 2495.

Table 3.17 — BLAST-LINE GOAL-POST DATA*

Range, yd	Slant range (D), yd	D^2	Dose, r	RD^2
400	466			Lost
600	649			Lost
800	841			Lost
1000	1034			Lost
1200	1229	1.51×10^6	2870	4.33×10^9
1400	1426	2.03×10^6	2235	4.54×10^9
1500	1525	2.33×10^6	1700	3.96×10^9
1600	1623	2.63×10^6	1480	3.89×10^9
1700	1722	2.97×10^6	1420	4.22×10^9
1800	1821	3.32×10^6	1150	3.82×10^9
1900	1920	3.69×10^6	1325	4.89×10^9
2000	2019	4.08×10^6	1000	4.08×10^9

*Not plotted, results contaminated by fallout, recovery D + 3 days.

Table 3.18 — DISPLACEMENT SHOCK SPECTRUM

Radial Direction*				Vertical Direction*			
f cps	D in.	f cps	D in.	f cps	D in.	f cps	D in.
Shot Stokes, surface, 33-psi overpressure							
Gauge 1		Gauge 3		Gauge 2		Gauge 4	
2.56		2.66	0.199	2.56	0.710	2.74	0.516
8.82	0.137	8.87	0.0260	8.82	0.569	9.66	0.440
22.0	0.0318	22.2	0.0248	22.0	0.101	20.4	0.165
36.0	0.0451	36.5	0.0093	36.0	0.0498	32.8	0.0633
90.0	0.0231	92.0	0.0074	90.0	0.0385	88.0	0.0560
134	0.0056	132	0.0018	131	0.0128	133	0.0309
184	0.0121	176	0.0017	179	0.0088	185	0.0154
228	0.0027	224	0.0020	209	0.0030	220	0.0066
269	0.0065	279		268	0.0027	265	0.0026
339		312		303	0.0033	293	0.0012
Shot Smoky, inside shelter, 116-psi overpressure							
Gauge 5				Gauge 6			
2.72	2.25			2.54	1.62		
9.37	0.453			8.72	0.906		
22.3	0.113			21.9	0.336		
36.9	0.0451			37.0	0.0744		
95.0	0.0185			92.0	0.0167		
138	0.0101			138	0.0099		
184	0.0099			185	0.0034		
234	0.0041			246	0.0051		
285	0.0022			280	0.0039		
296	0.0031			363	0.0038		
Shot Smoky, surface, 116-psi overpressure							
Gauge 9				Gauge 7		Gauge 8	
2.55	1.95			2.60	5.45	2.53	4.53
9.12	0.359			8.56	1.52	8.82	1.46
22.4	0.189			22.4	0.845	22.6	0.5[illegible]5
33.9	0.131			37.4	0.254	37.1	0.2[illegible]5
93.0	0.0227			91.0	0.132	93.0	0.103
107	0.0149			132	0.0673	137	0.0450
181	0.0107			187	0.0221	180	0.0199
203	0.0042			238	0.0106	236	0.0122
293	0.0055			280	0.0112	294	0.0055
357	0.0027			335	0.0066	328	0.0066
Shot Galileo, surface, 130-psi overpressure							
Gauge 11				Gauge 10		Gauge 12	
2.35	0.653			2.48	4.10	2.47	4.25
8.63	0.377			8.26	0.946	8.23	1.22
22.5	0.164			22.7	0.320	21.0	0.475
36.5	0.0453			37.1	0.314	35.0	0.280
95.0	0.0349			94.0	0.140	94.0	0.121
138	0.0184			138	0.0441	136	0.0267
186	0.0103			187	0.0446	178	0.0442
237	0.0032			234	0.0098	229	0.0161
294	0.0046			272	0.0139	300	0.0121
317	0.0029			365	0.0046	339	0.0053

Table 3.18 — (Continued)

Radial direction*				Vertical direction*			
f	D	f	D	f	D	f	D
cps	in.	cps	in.	cps	in.	cps	in.
Shot Whitney, surface, 146-psi overpressure							
Gauge 4†				Gauge 3†			
2.74	1.60			2.66	3.10		
9.66	0.260			8.87	1.47		
20.4	0.119			22.2	0.788		
32.8	0.0834			36.5	0.348		
86.0	0.0187			92.0	0.141		
134	0.0118			132	0.0992		
185	0.0088			176	0.0402		
220	0.0064			227	0.0090		
269	0.0026			284	0.0152		
314	0.0054			330	0.0080		
Shot Charleston, surface‡							
Gauge 5 (20-psi overpressure)		Gauge 9 (18-psi overpressure)		Gauge 6 (20-psi overpressure)		Gauge 8 (18-psi overpressure)	
2.72	0.263	2.55	0.265	2.54		2.53	0.728
9.37	0.111	9.12	0.0838	8.72	0.280	8.82	0.368
22.3	0.0900	22.4	0.0691	21.9	0.221	22.6	0.194
36.9	0.0404	33.9		37.0		37.1	0.0828
95.0	0.0190	93.0	0.0096	92.0	0.0246	93.0	0.0208
138	0.0100	107	0.0050	138	0.0093	137	0.0048
184	0.0014	181	0.0023	185	0.0062	180	0.0025
234	0.0030	203	0.0020	246	0.0023	236	0.0015
285	0.0026	293	0.0019	280	0.0023	294	0.0015
296	0.0020	357	0.0009	363	0.0007	328	0.0016
Gauge 11 (15-psi overpressure)				Gauge 10 (15-psi overpressure)		Gauge 12 (12-psi overpressure)	
2.35	0.879			2.48	0.407	2.47	0.492
8.63	0.262			8.26	0.163	8.23	0.177
22.5	0.195			22.7	0.0726	21.0	0.207
36.5	0.0804			37.1	0.0231	35.0	0.0786
95	0.0246			94.0		94.0	0.0193
138	0.0033			138		136	0.0101
186	0.0020			187		178	0.0053
237	0.0019			234		229	0.0005
294	0.0011			272		300	
317	0.0007			365	0.0009	339	0.0006

*f, natural frequency; D, peak displacement.

†Canister tops were about 18 in. below ground level in hard ground. Two other gauges bolted to concrete pads in the same vicinity were knocked loose and data were lost.

‡Tangential direction for gauge 7 (20-psi overpressure): insignificant displacement.

Table 3.19 — MORTALITY RESULTS OF BIOLOGICAL TESTS

Structure No.	Time of recovery after test, days	Number and time of deaths
II-1	2	None
II-2	3	19 before recovery and 1 on day of recovery
II-3	2	1 on 2 days after recovery
II-4	2	1 each on 12 and 17 days after recovery
II-5	2	1 each on 1, 8, 11, and 13 days after recovery

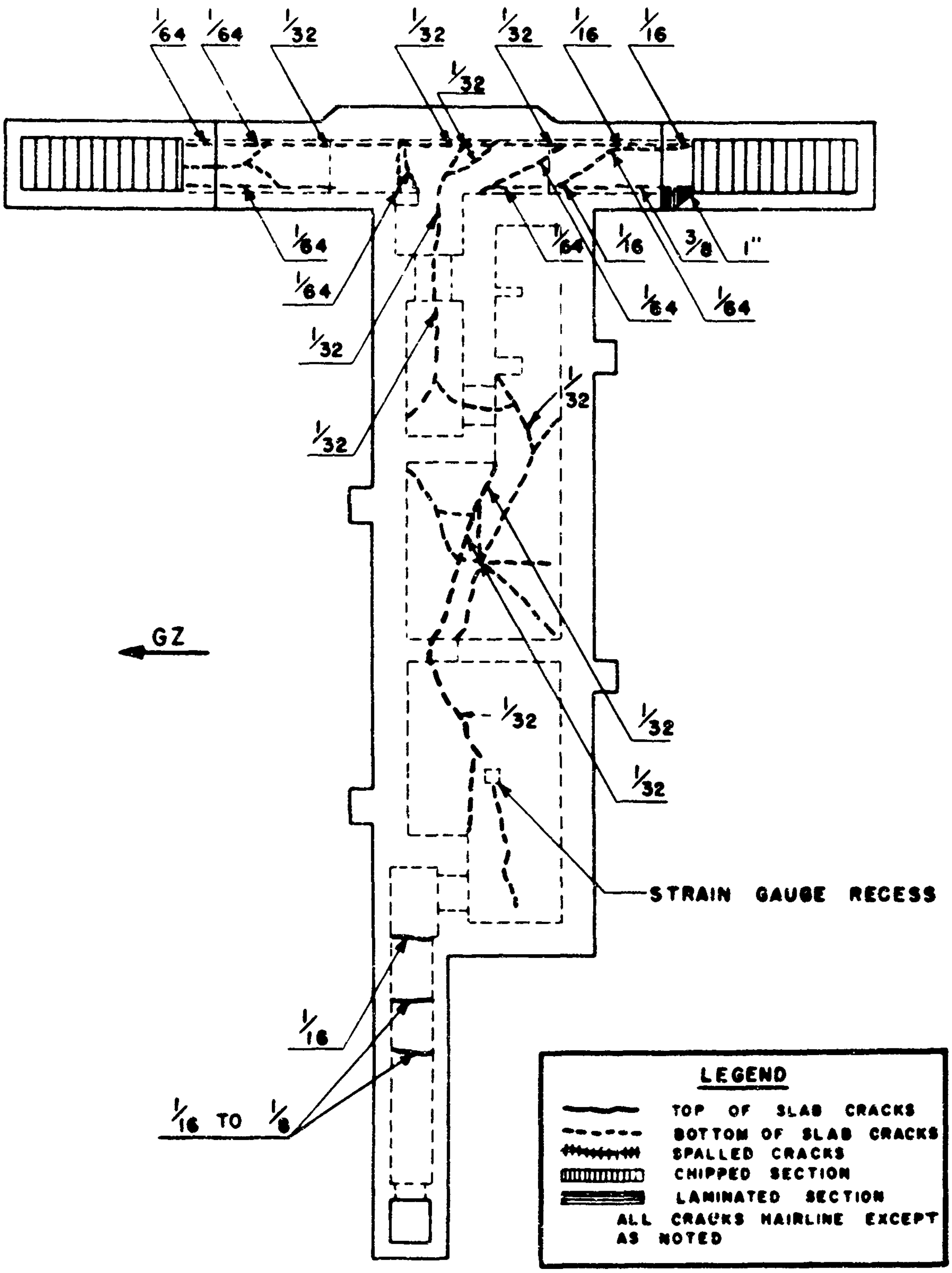

Fig. 3.1—Roof-slab crack pattern, structure II-1.

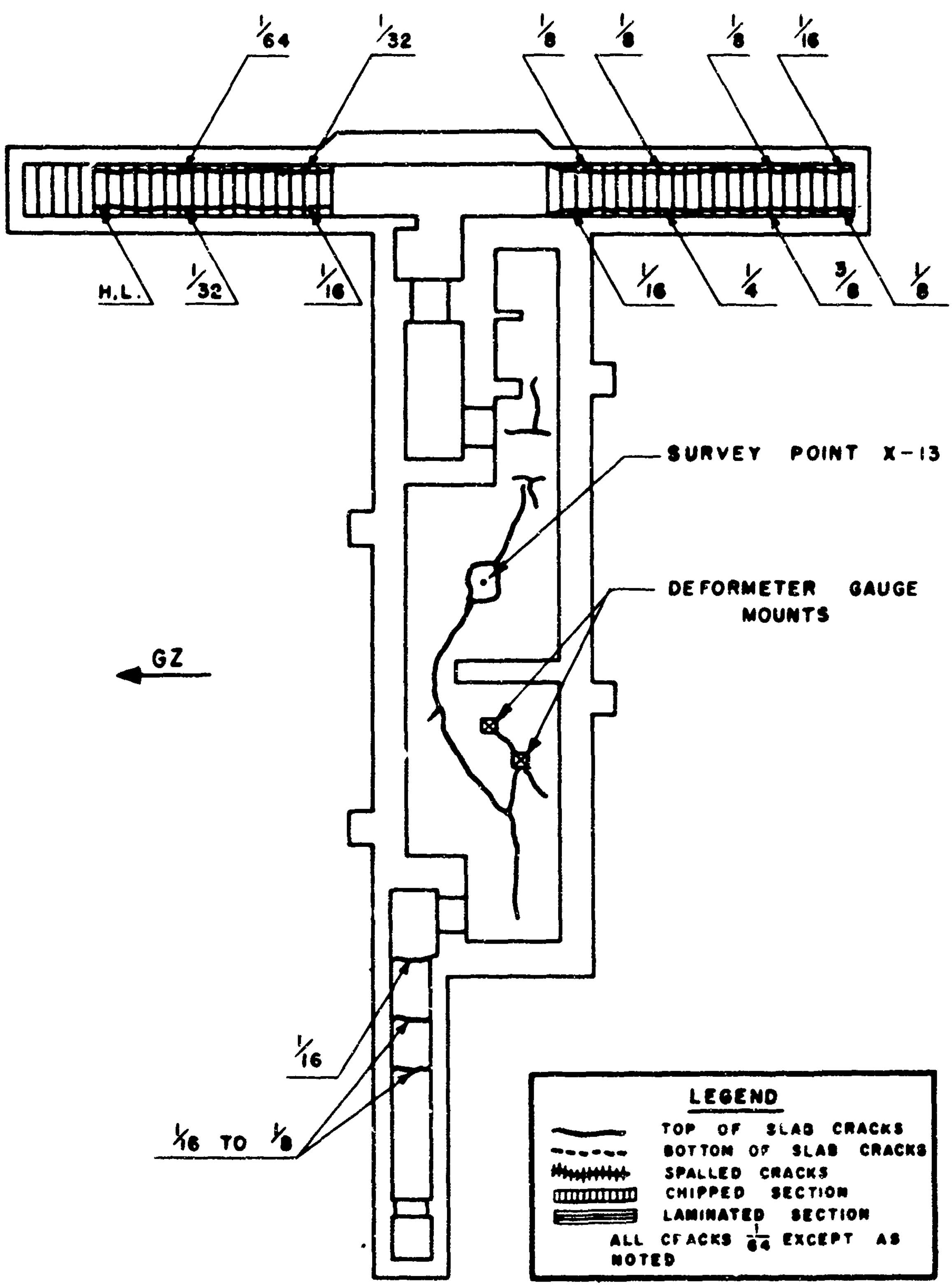

Fig. 3.2—Floor-slab crack pattern, structure II-1.

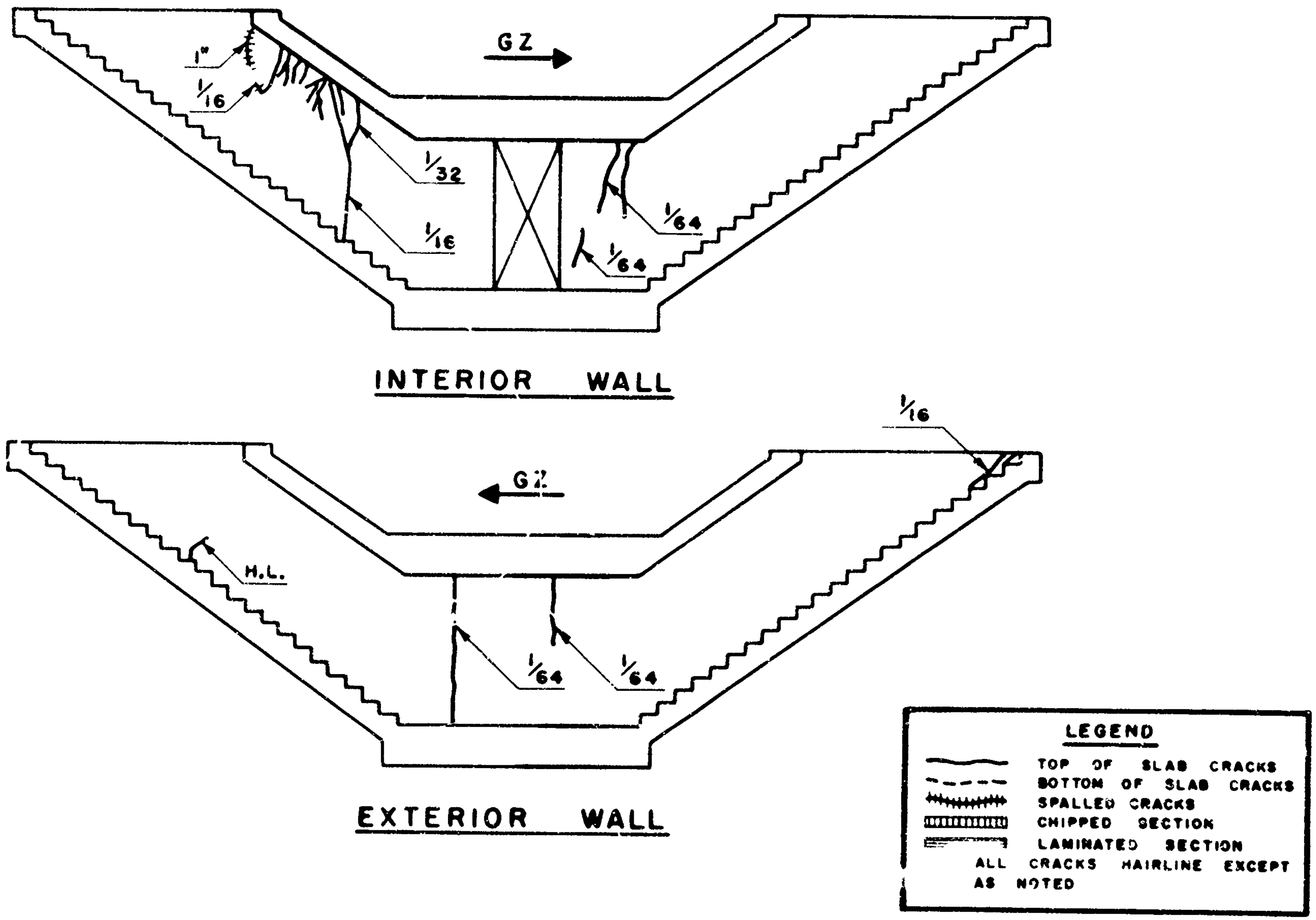

Fig. 3.3—Entrance crack pattern, structure II-1.

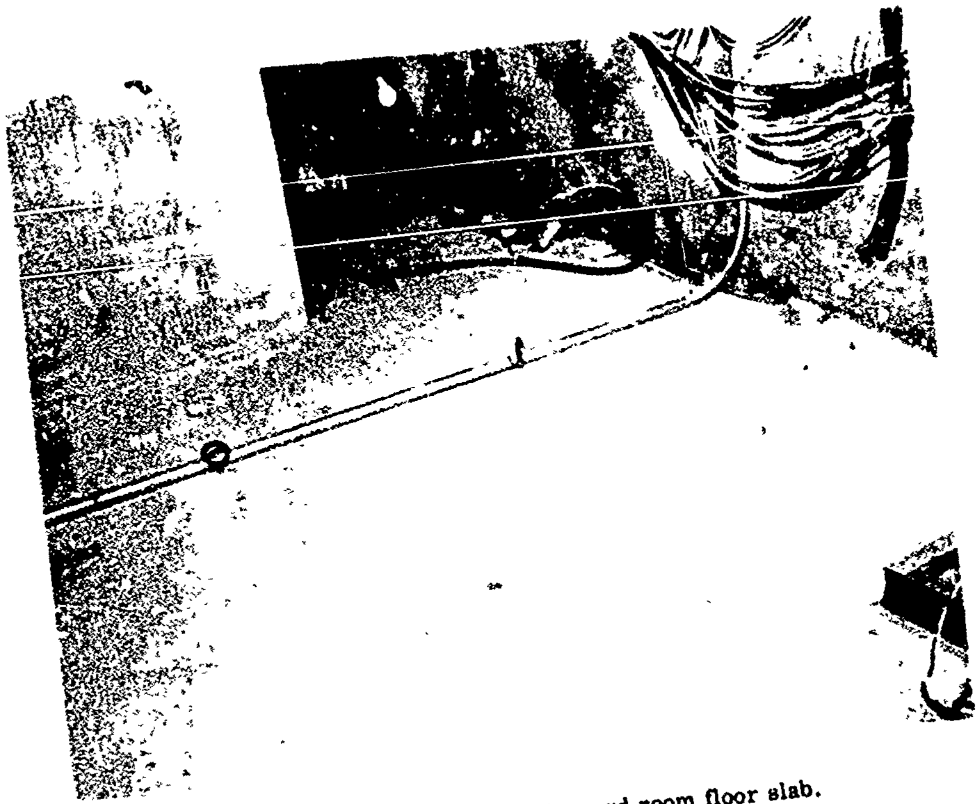

Fig. 3.4—Blast damage of forward room floor slab.

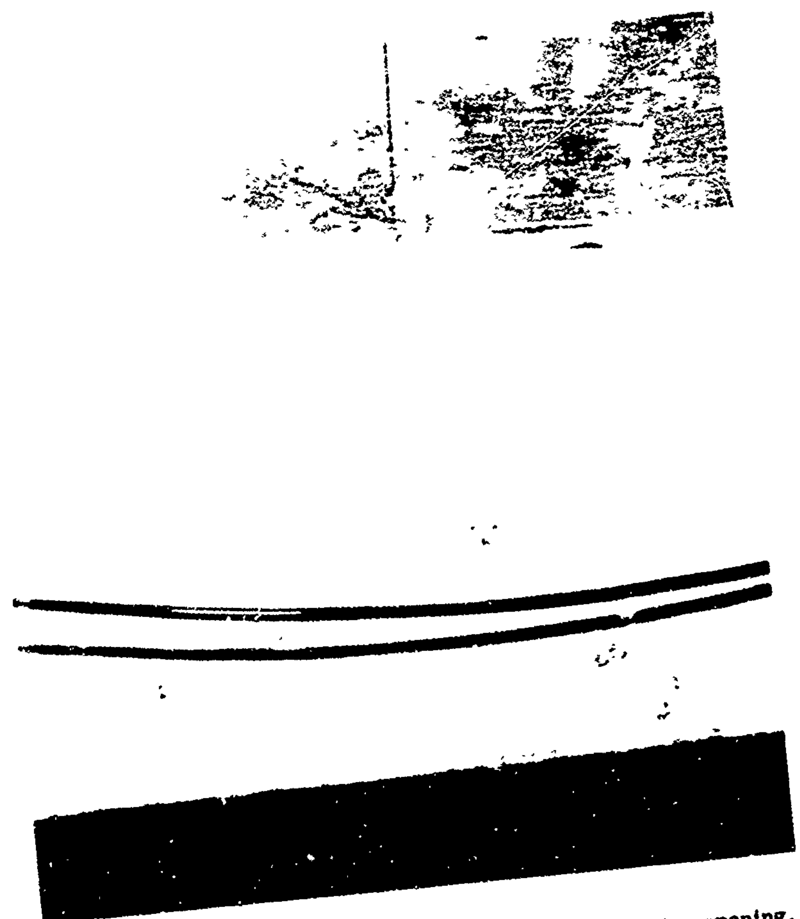

Fig. 3.5—Blast damage of lintel beam at main partition opening.

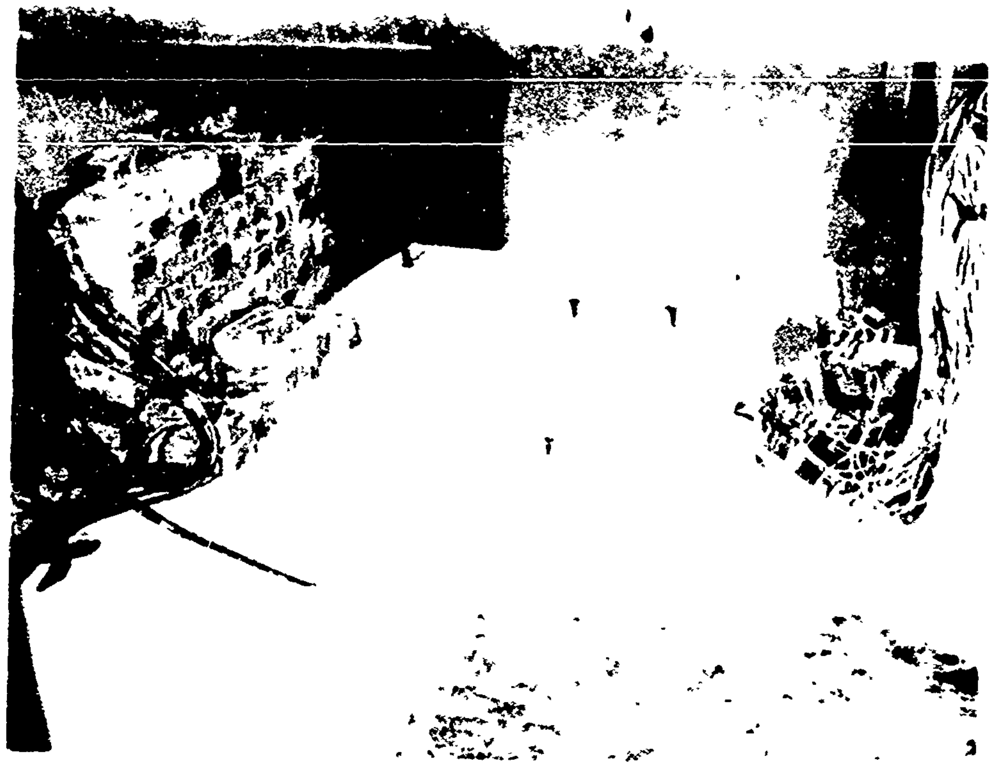

Fig. 3.6—Blast damage of rear room floor slab.

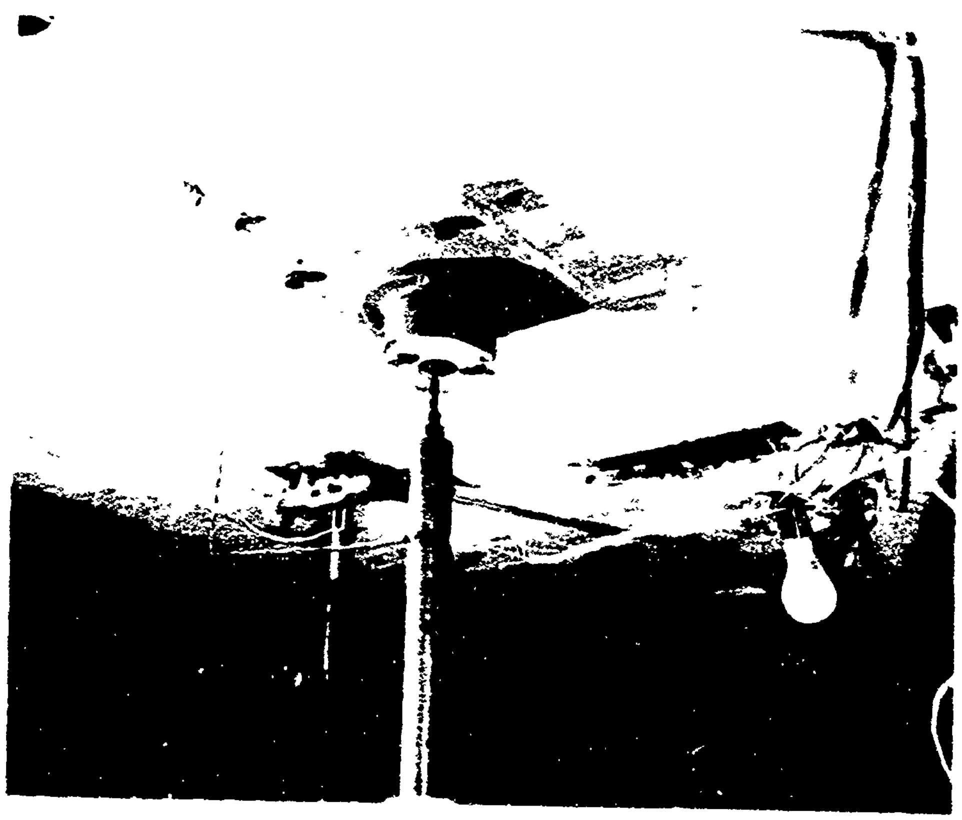

Fig. 3.7—Roof-slab cracks of the rear section of the main chamber.

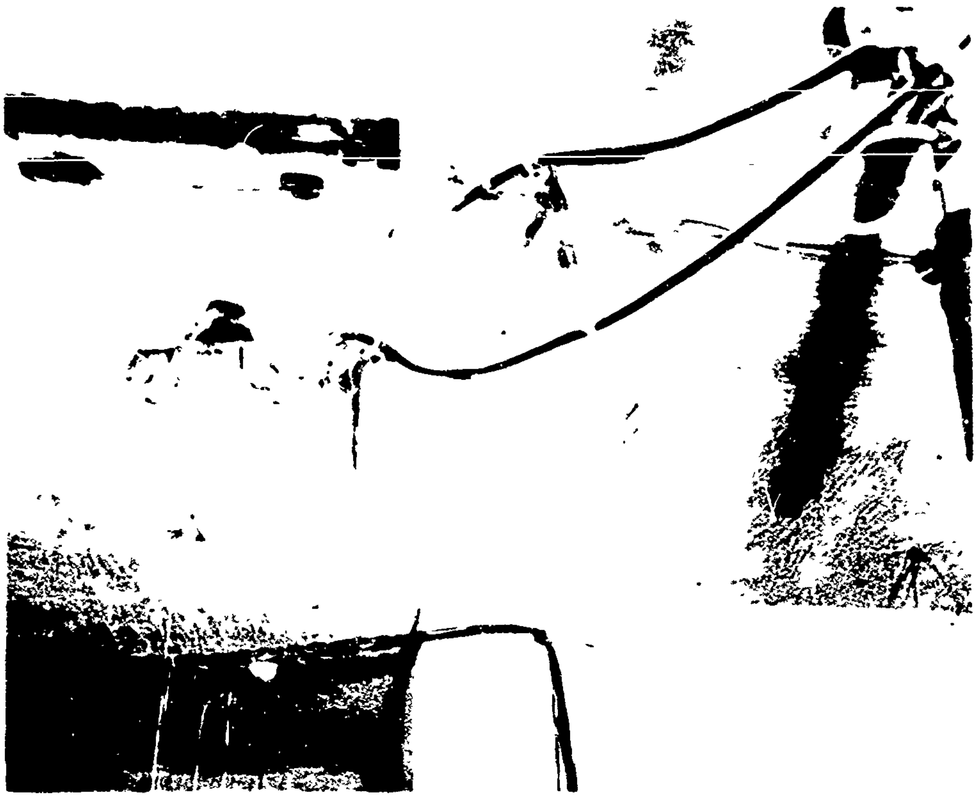

Fig. 3.8—Roof-slab cracks of the rear section of the main chamber.

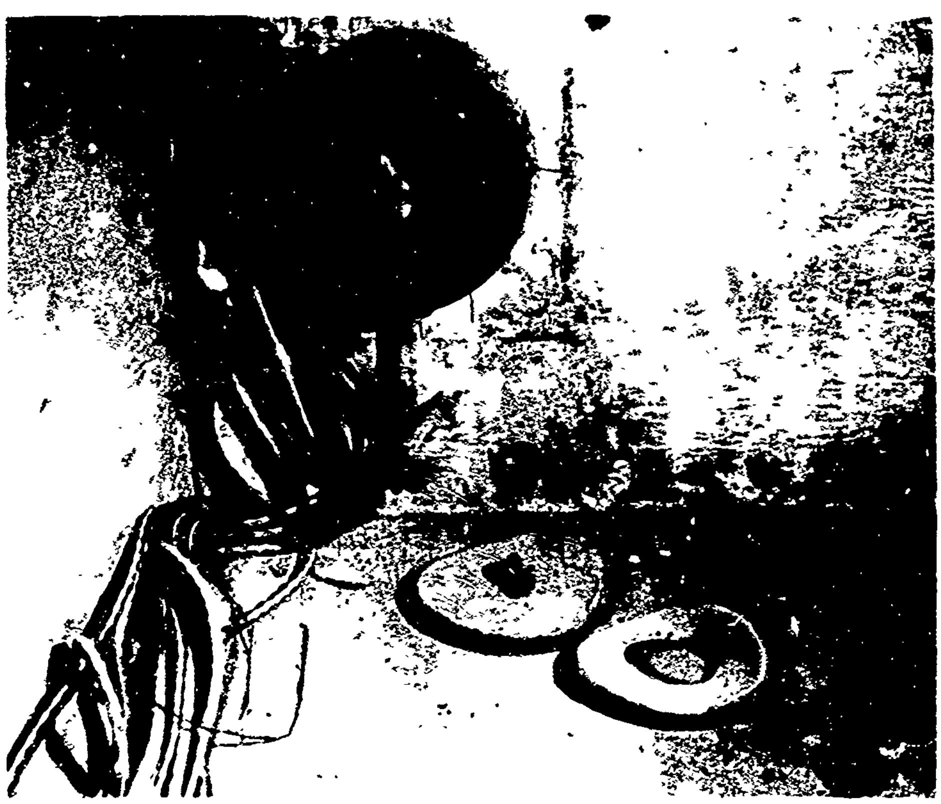

Fig. 3.9—Blast results of interior end of intake ventilation pipe.

Fig. 3.10—Over-all view of blast results of interior end of exhaust pipe.

Fig. 3.11—Internal blast results of interior end of exhaust pipe.

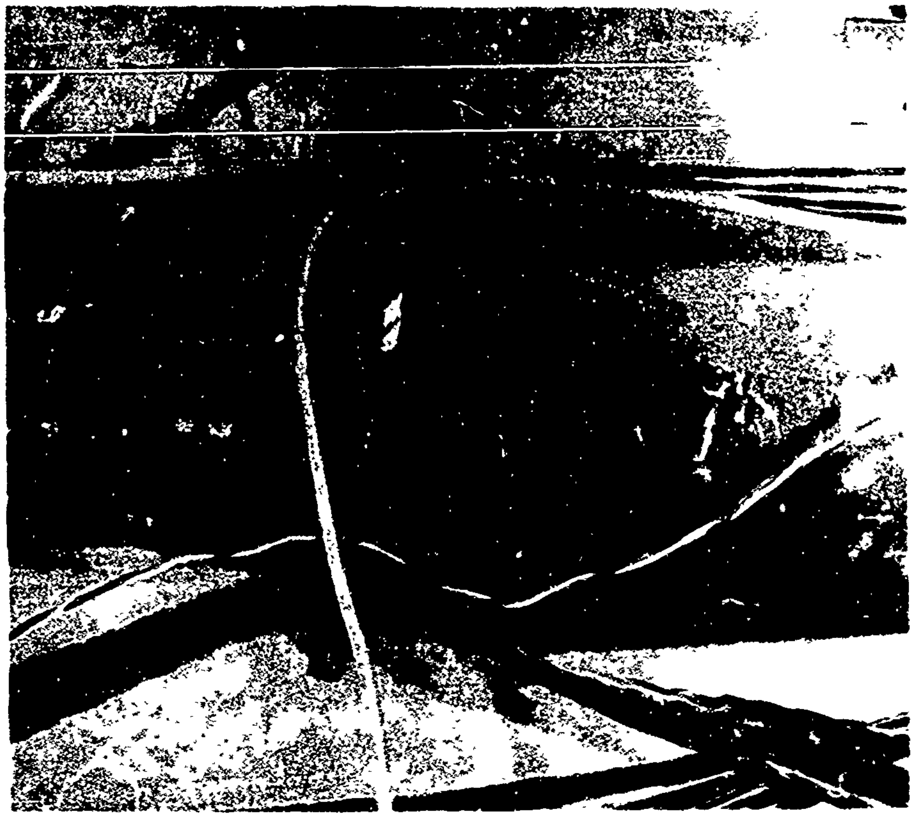

Fig. 3.12 — Blast damage to ventilation duct connections.

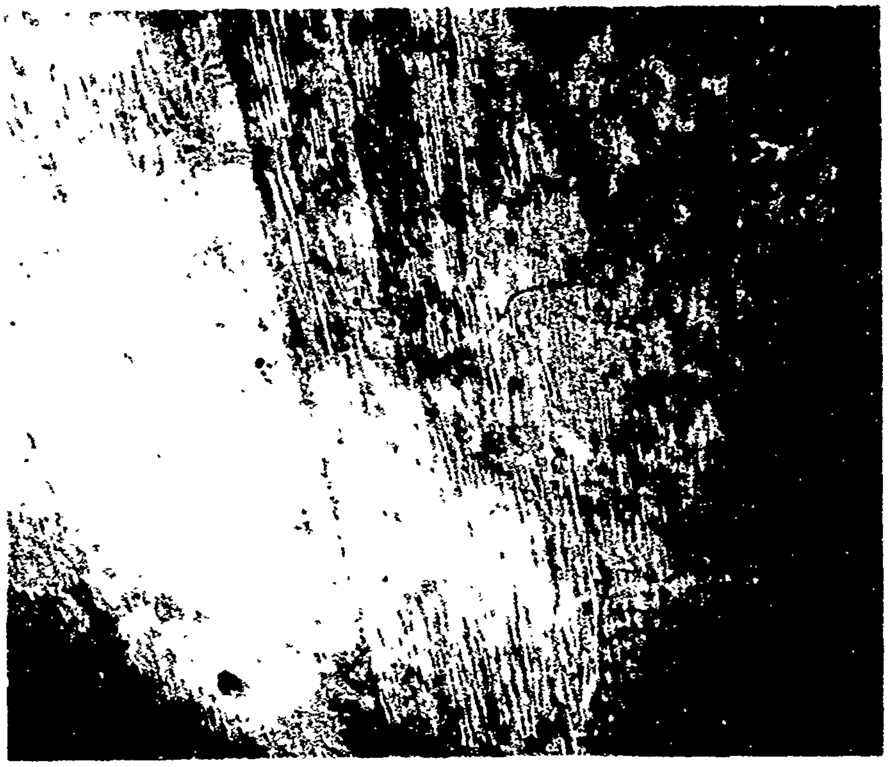

Fig. 3.13 — Roof-slab cracks of forward section of main chamber.

Fig. 3.14—Blast damage of main entrance.

Fig. 3.15—Blast damage of main entrance.

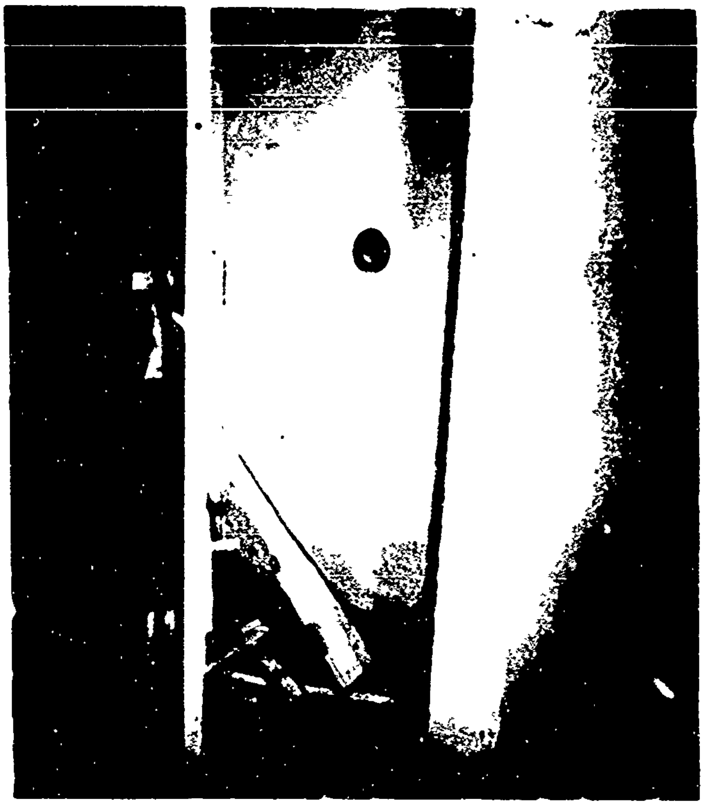

Fig. 3.16 — Debris resulting from blast at the main entrance.

Fig. 3.17 — Blast debris and damage of the entrance facing away from GZ.

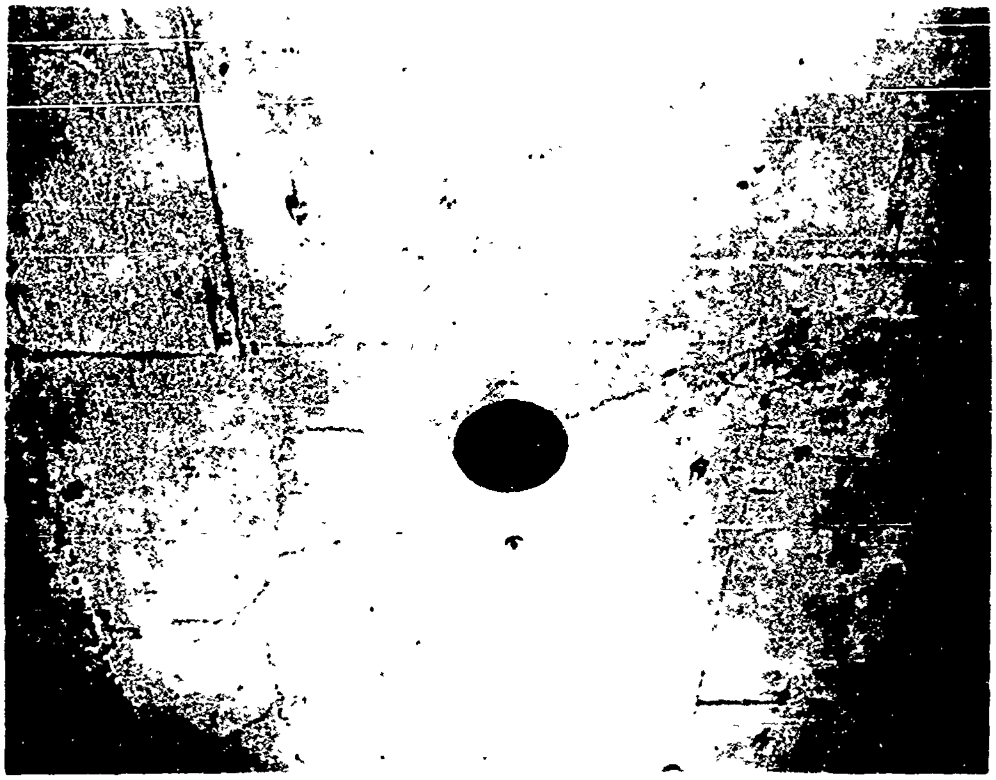

Fig. 3.18—Cracks formed in roof slab of landing.

Fig. 3.19—Blast results of exit tunnel.

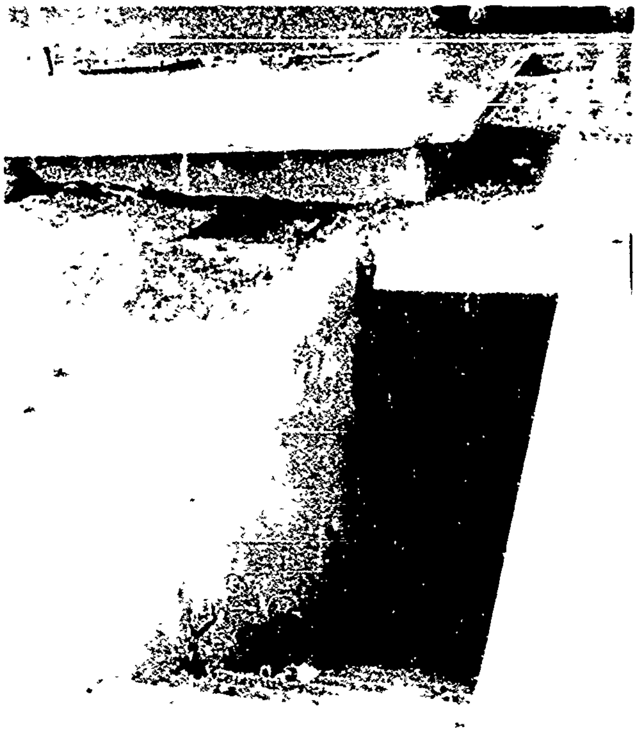

Fig. 3.20 — Debris and damage produced by the blast wave in the entrance facing away from GZ.

Fig. 3.21 — Detail view of chipped-out section at top of entrance facing away from GZ.

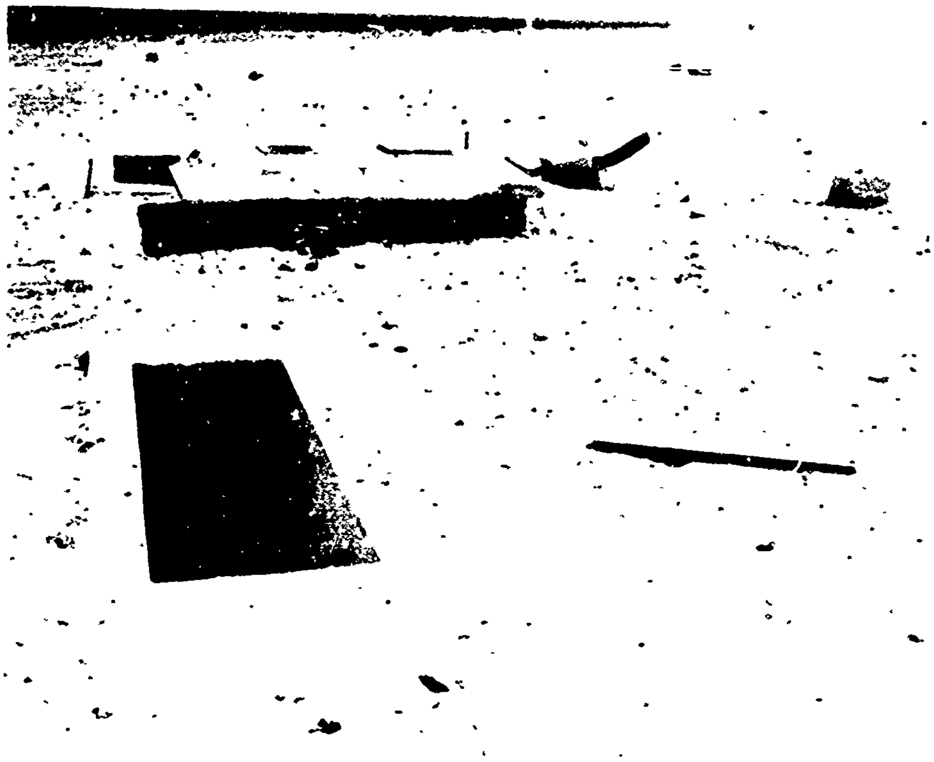

Fig. 3.22 — Postshot view of sand pit and main entrance.

Fig. 3.23 — Postshot view of sand pit.

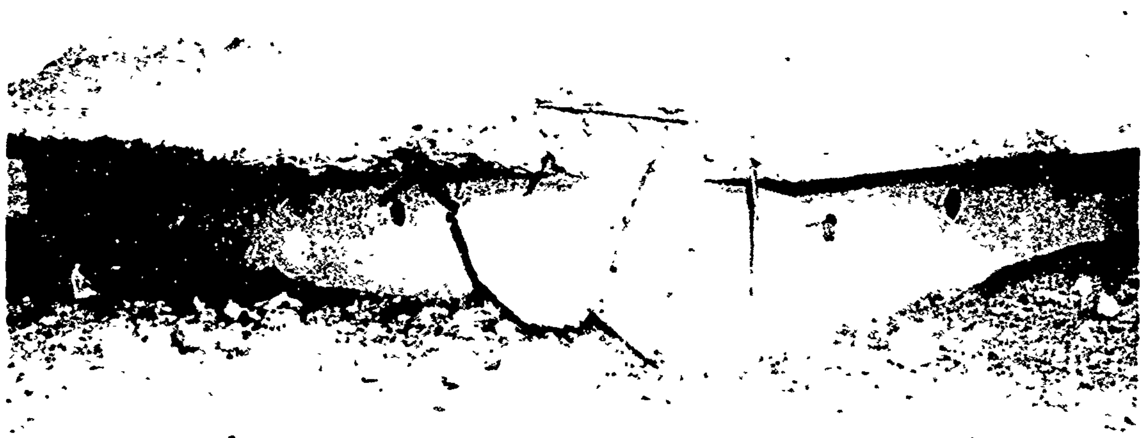

Fig. 3.24 — Postshot view of the corner of the sand-pit facing GZ.

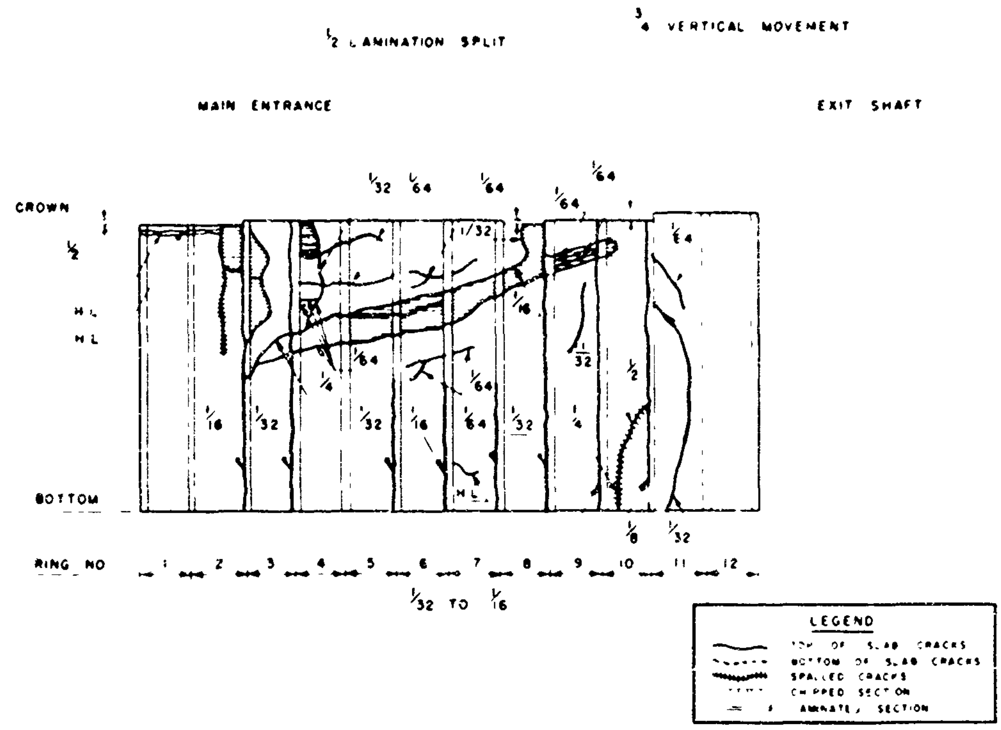

Fig. 3.25 — Developed vertical elevation facing GZ, structure II-2.

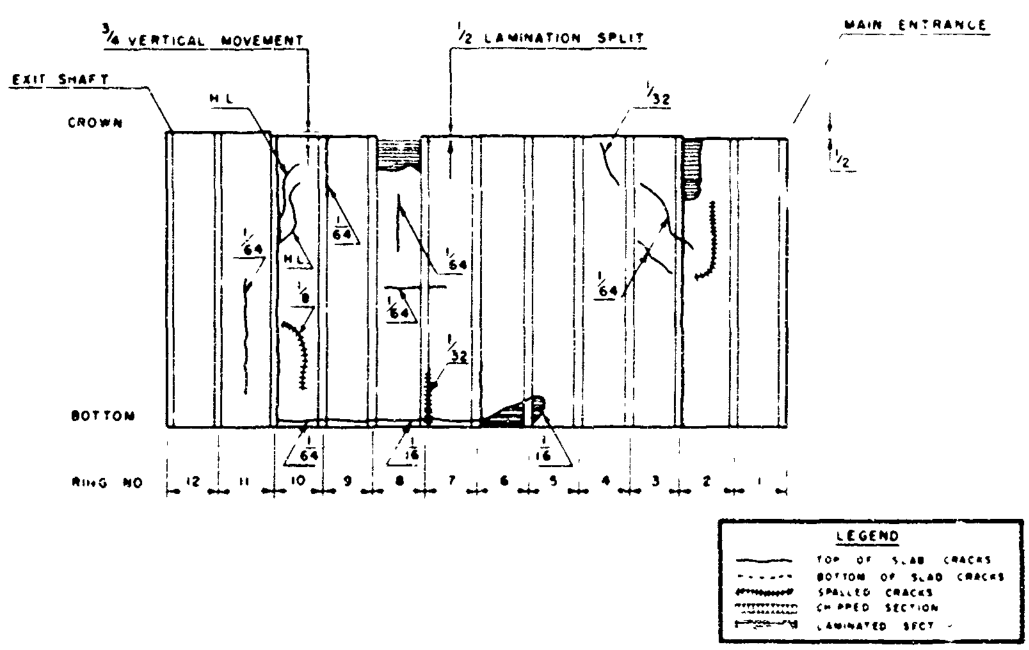

Fig. 3.26 — Developed vertical elevation facing away from GZ, structure II-2.

Fig. 3.27—Spalling and cracking on GZ side of ring 10.

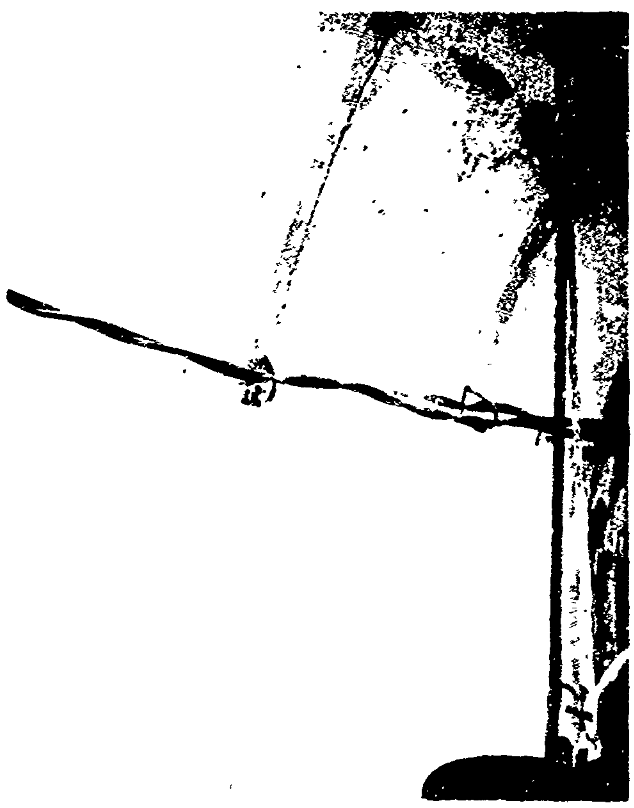

Fig. 3.28—Cracking of ring 10 on side facing away from GZ.

Fig. 3.29 — Vertical movement of ring 10 in relation to ring 11 at their crowns.

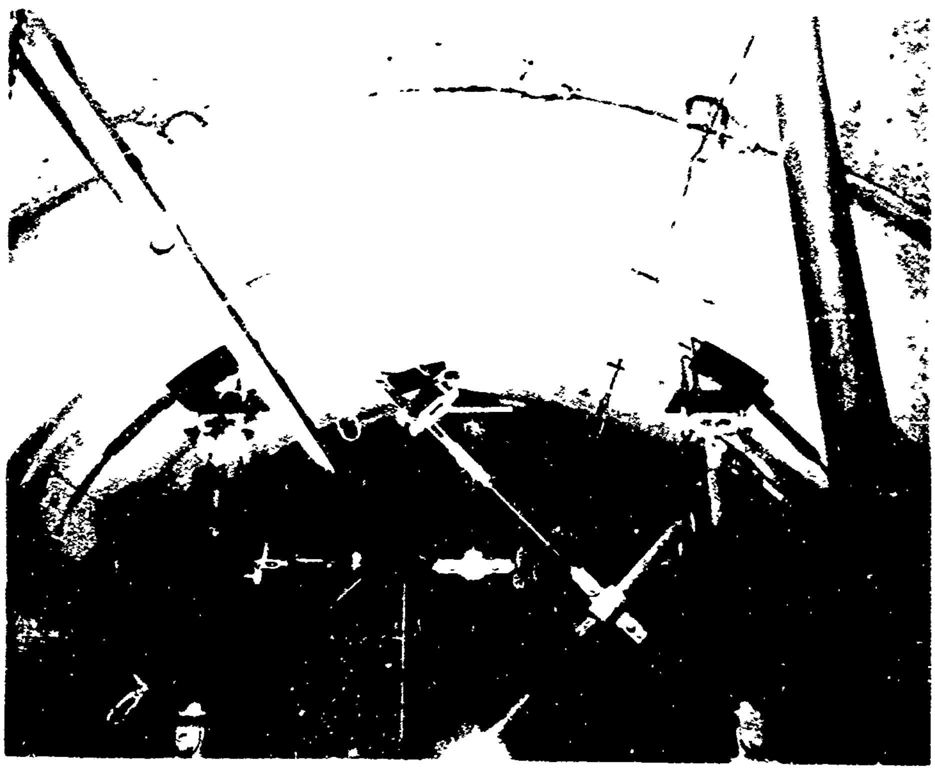

Fig. 3.30 — Cracking and spalling of joint 8-9 and ring 8 at crown.

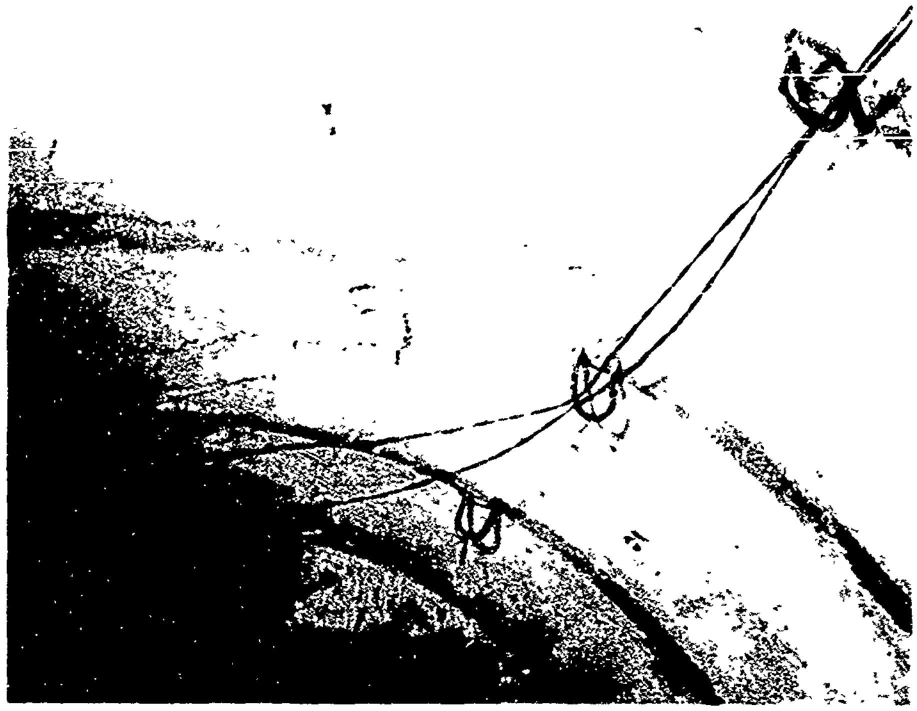

Fig. 3.31—Spalling and cracking of rings 2 and 3 at their crowns.

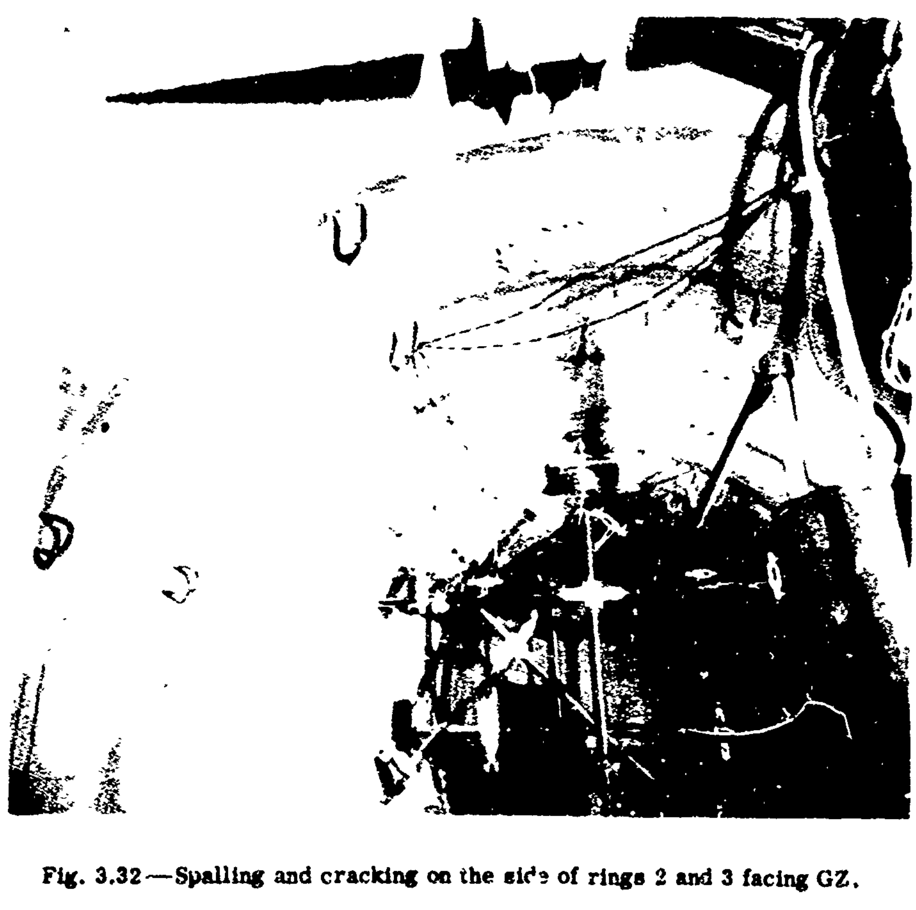

Fig. 3.32—Spalling and cracking on the side of rings 2 and 3 facing GZ.

Fig. 3.33—Separation of joint between rings 2 and 3, side facing GZ.

Fig. 3.34—Separation of concrete seats between rings 3 and 4, side facing GZ.

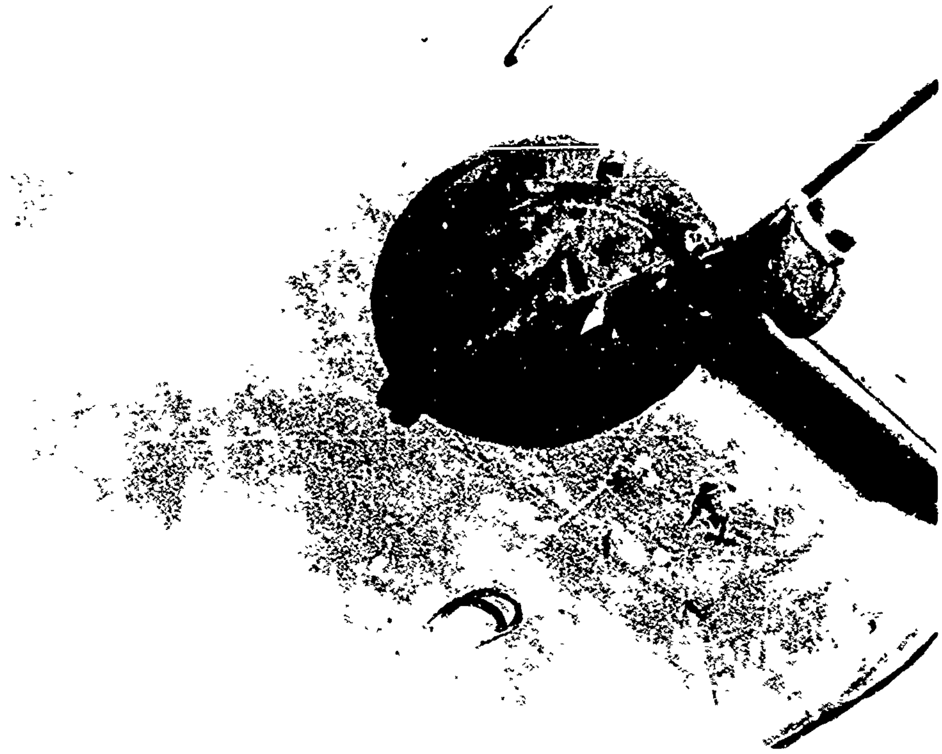

Fig. 3.35—Interior end of exhaust pipe after detonation.

Fig. 3.36—Detail view of intake-pipe flap plate after detonation.

Fig. 3.37—General view of interior end of intake pipe after detonation.

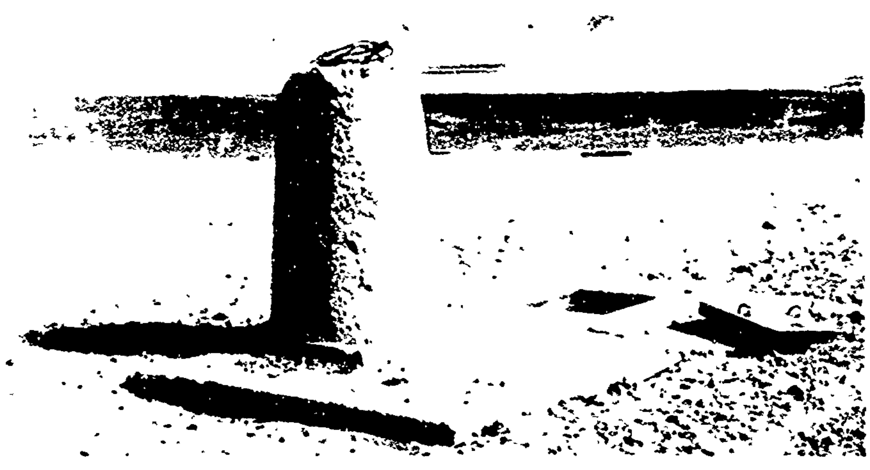

Fig. 3.38—Postshot view of the above-ground portion of the exhaust stack and exit shaft.

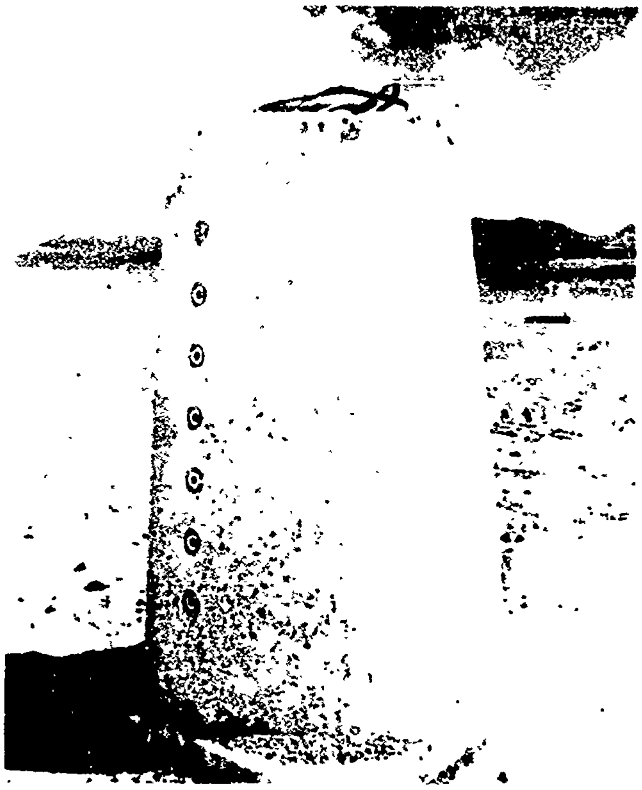

Fig. 3.39 — Sand blasting of exhaust stack, facing GZ.

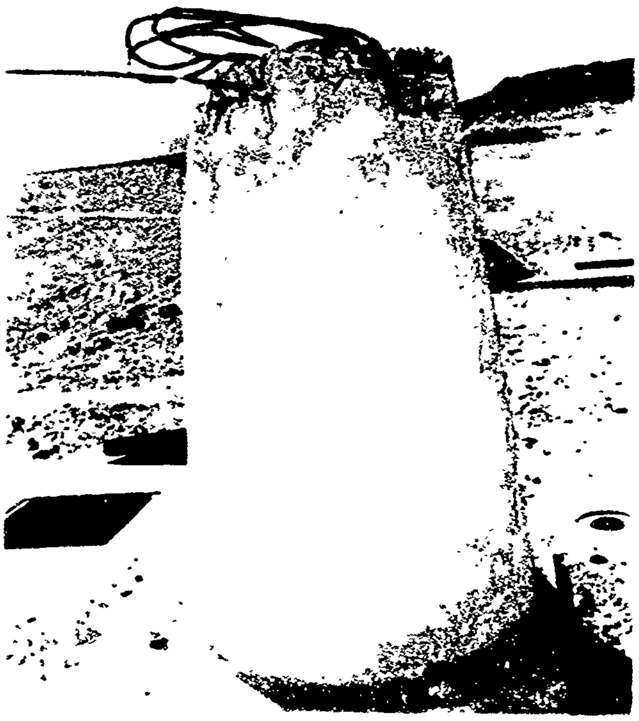

Fig. 3.40 — Blast damage to the exhaust stack, side parallel to blast line.

Fig. 3.41—Blast damage to exposed surface of front reflection shield of sand-pit.

Fig. 3.42—Blast damage to unexposed surface of front reflection shield of sand-pit.

Fig. 3.43 — Blast damage to above-ground portion of structure facing GZ.

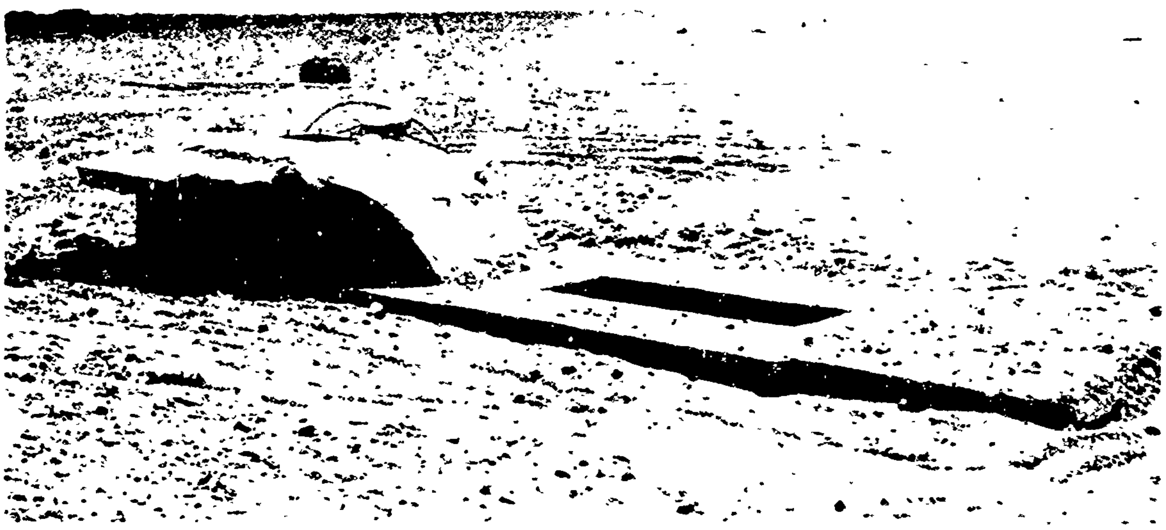

Fig. 3.44 — Detail view of blast damage to main entrance and sand-pit.

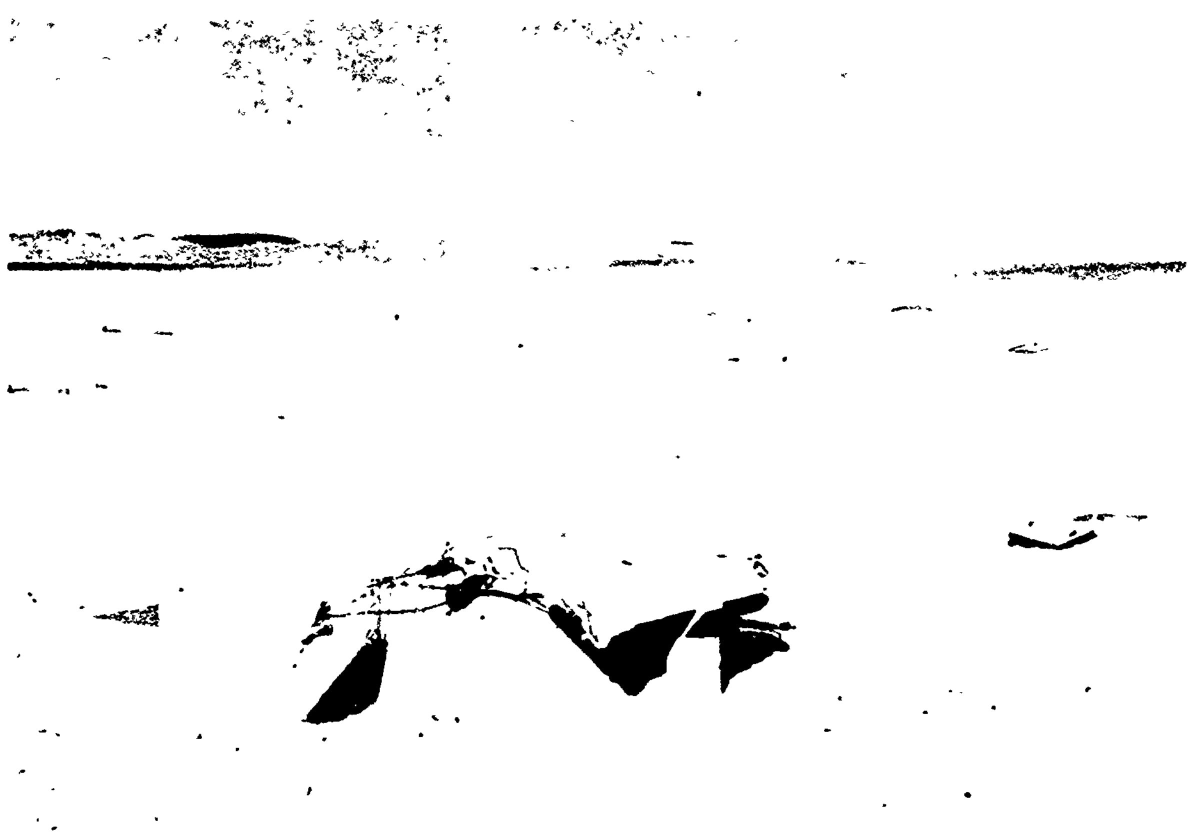

Fig. 3.45—General view of above-ground portion of the structure, facing away from GZ.

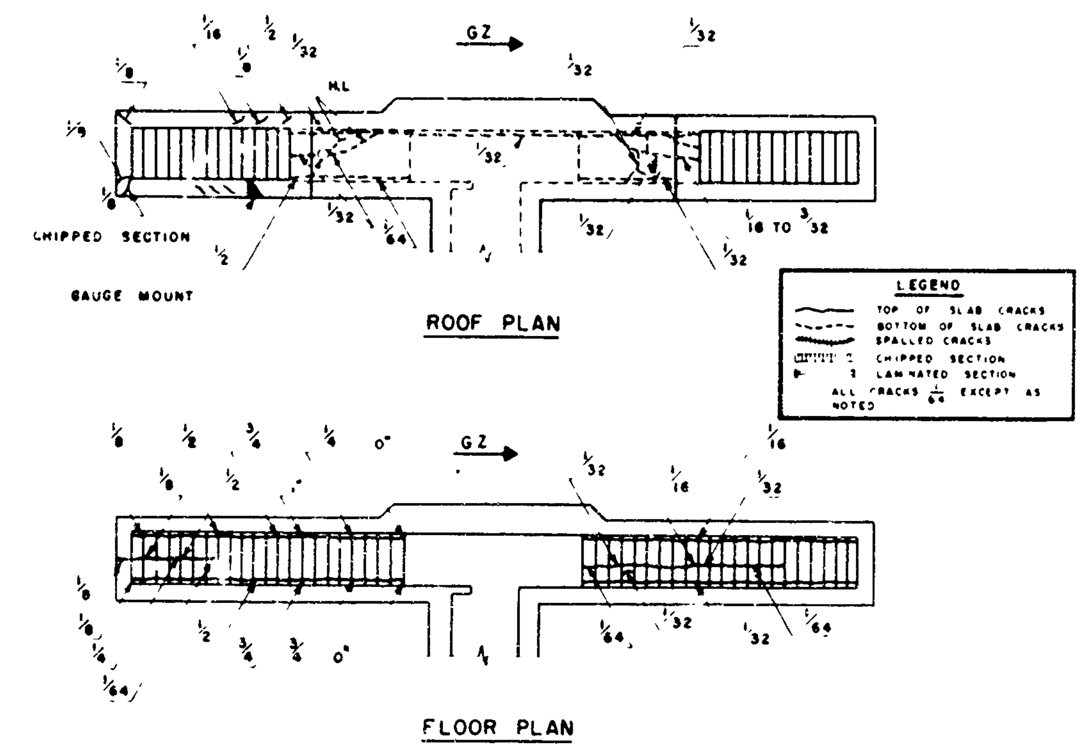

Fig. 3.46 — Entrance crack pattern, structure II-3.

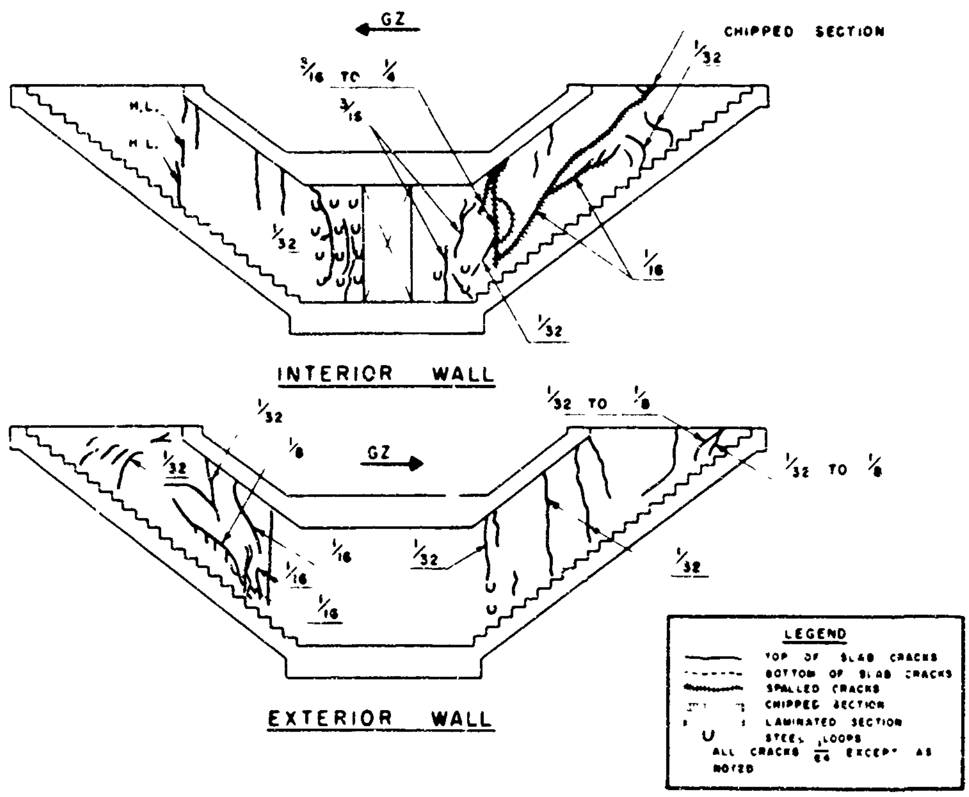

Fig. 3.47 — Entrance crack pattern, structure II-3.

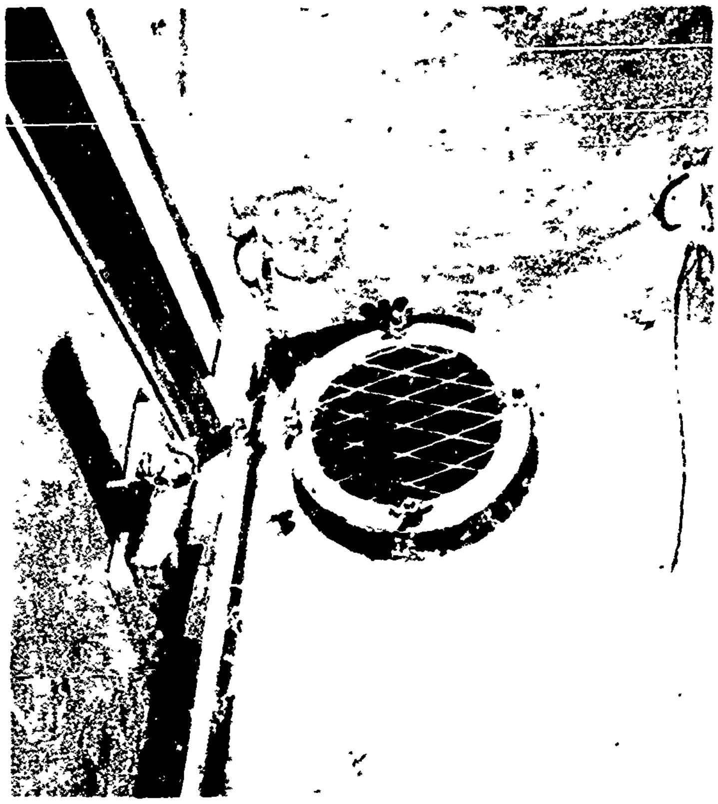

Fig. 3.48 — Interior end of exhaust valve after detonation.

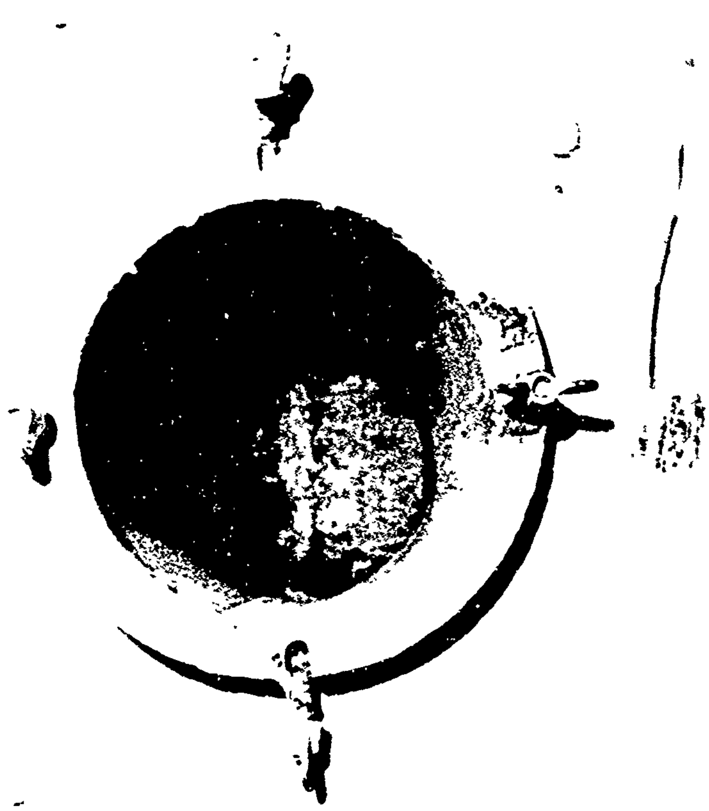

Fig. 3.49 — Postshot view of interior end of intake pipe.

Fig. 3.50 — Blast damage to roof slab of entrance landing.

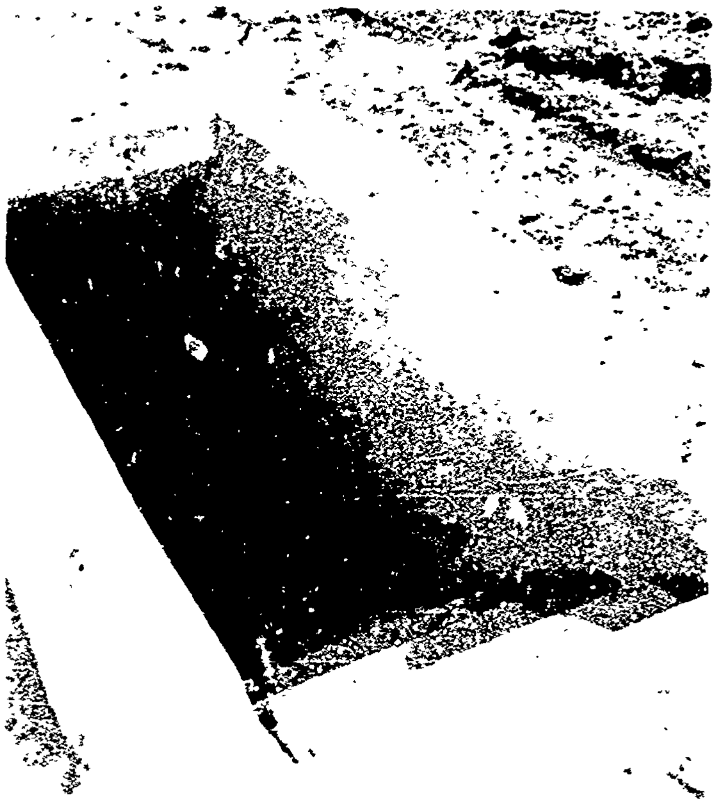

Fig. 3.51 — Blast damage to walls of entrance facing GZ.

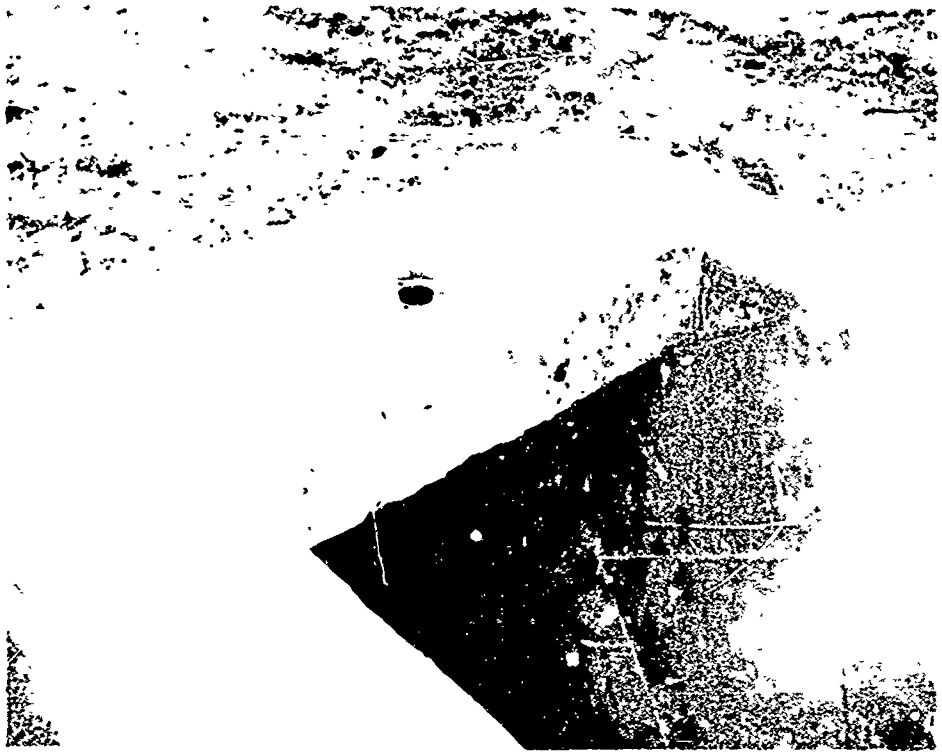

Fig. 3.52—Detail view of end of roof slab of entrance facing GZ.

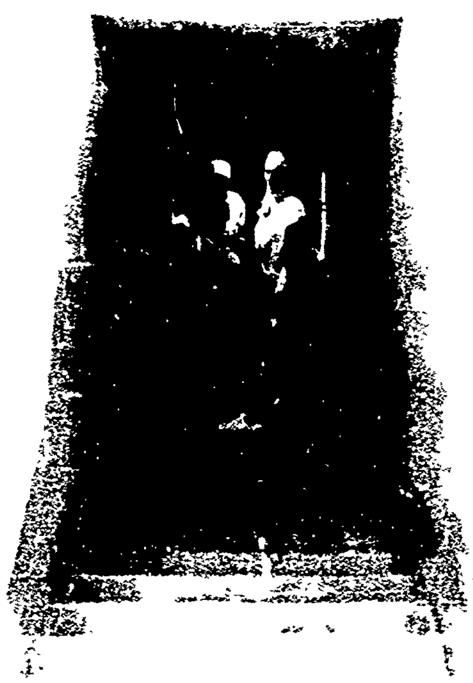

Fig. 3.53—Blast oam ge of entrance facing GZ.

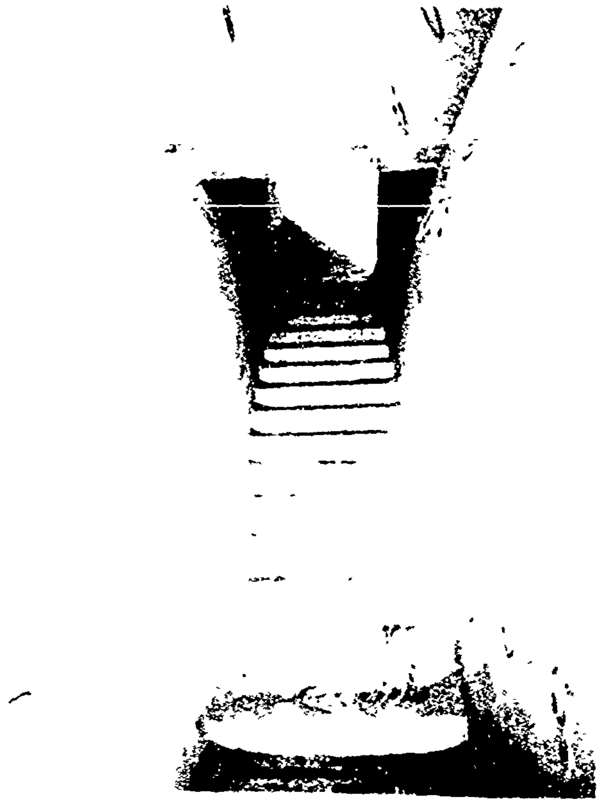

Fig. 3.54 — Blast debris deposited on stairs of entrance facing GZ.

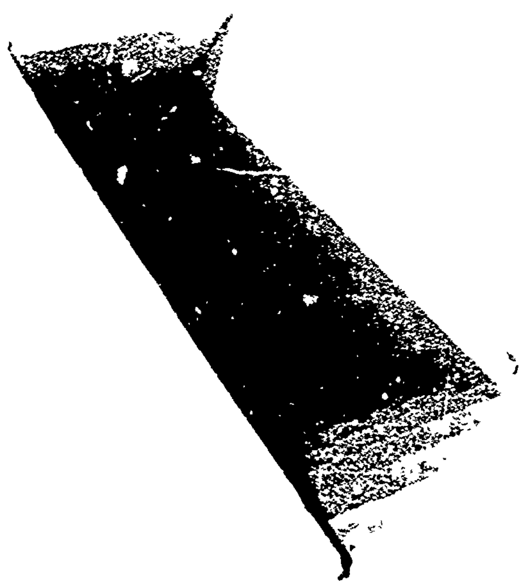

Fig. 3.55 — Blast damage to surface section of entrance facing away from GZ.

Fig. 3.56—Blast debris deposited on stairs of entrance facing away from GZ.

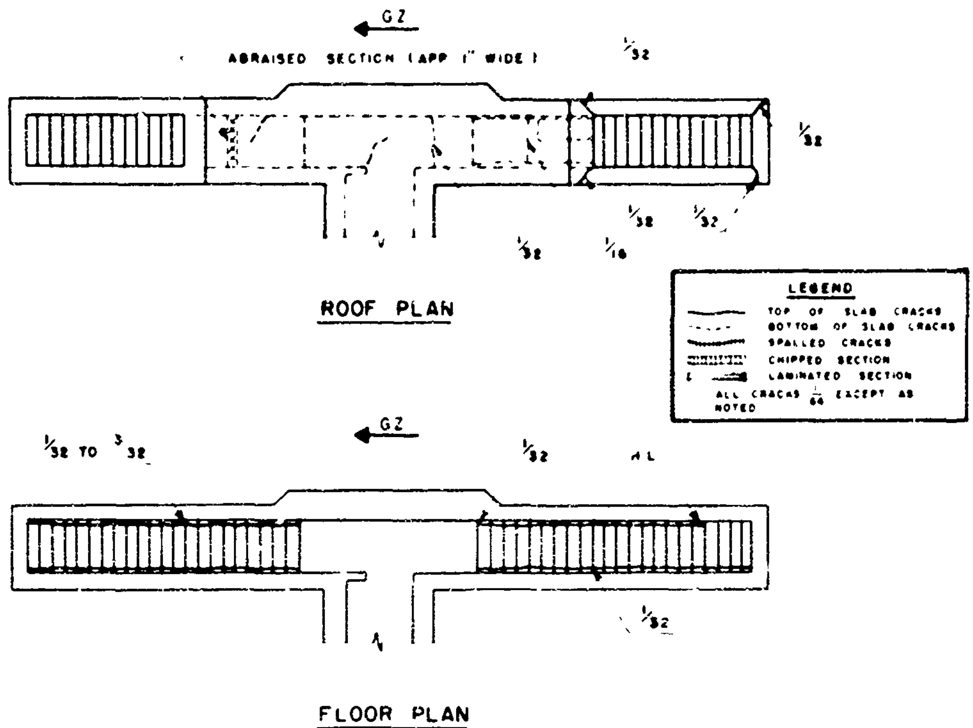

Fig. 3.57—Entrance crack pattern, structure II-4.

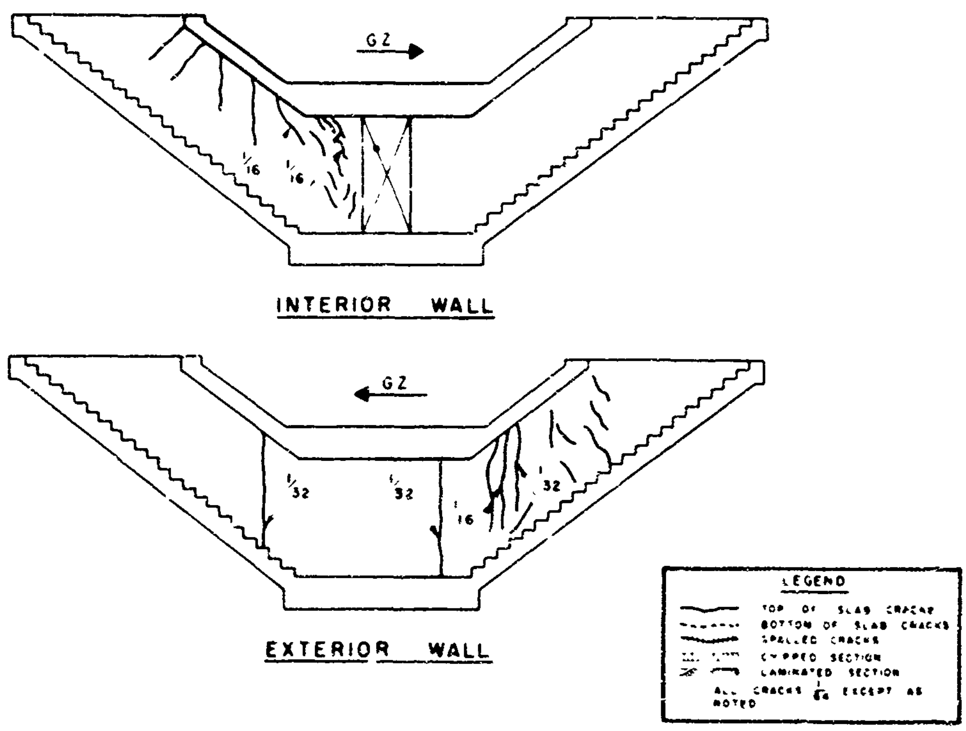

Fig. 3.58—Entrance crack pattern, structure II-4.

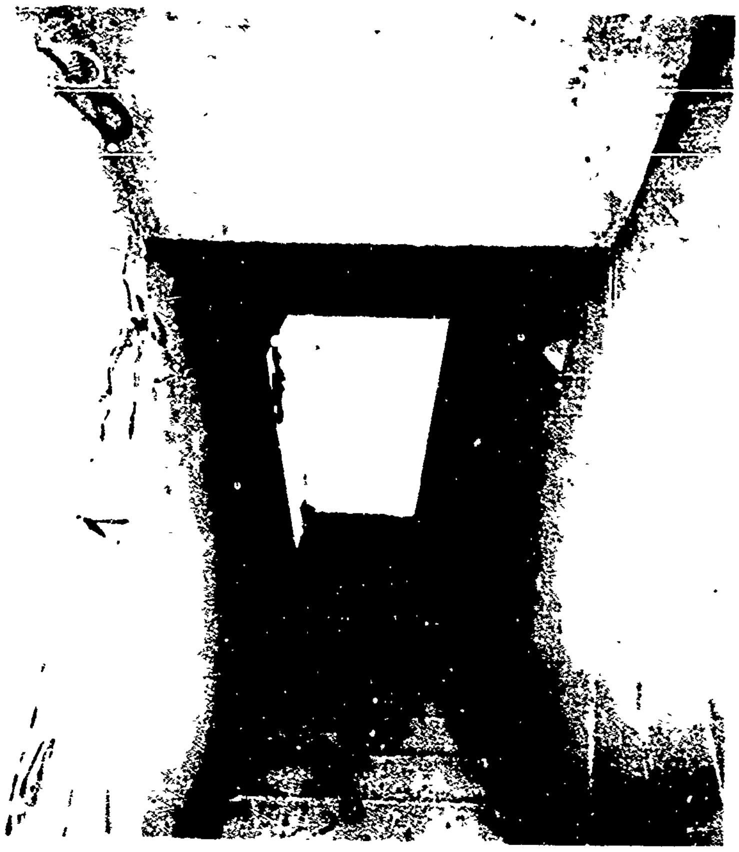

Fig. 3.59 — Blast debris and damage of entrance facing away from GZ.

Fig. 3.60 — Blast results of ball type antiblast valve.

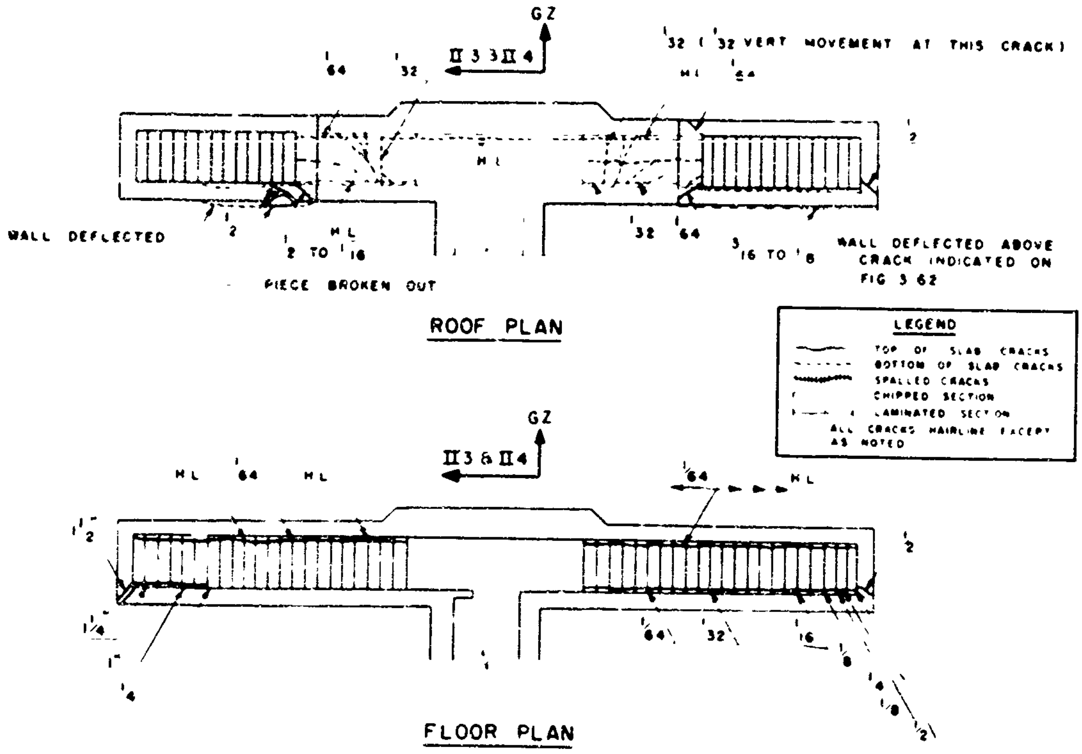

Fig. 3.61—Entrance crack pattern, structure II-5.

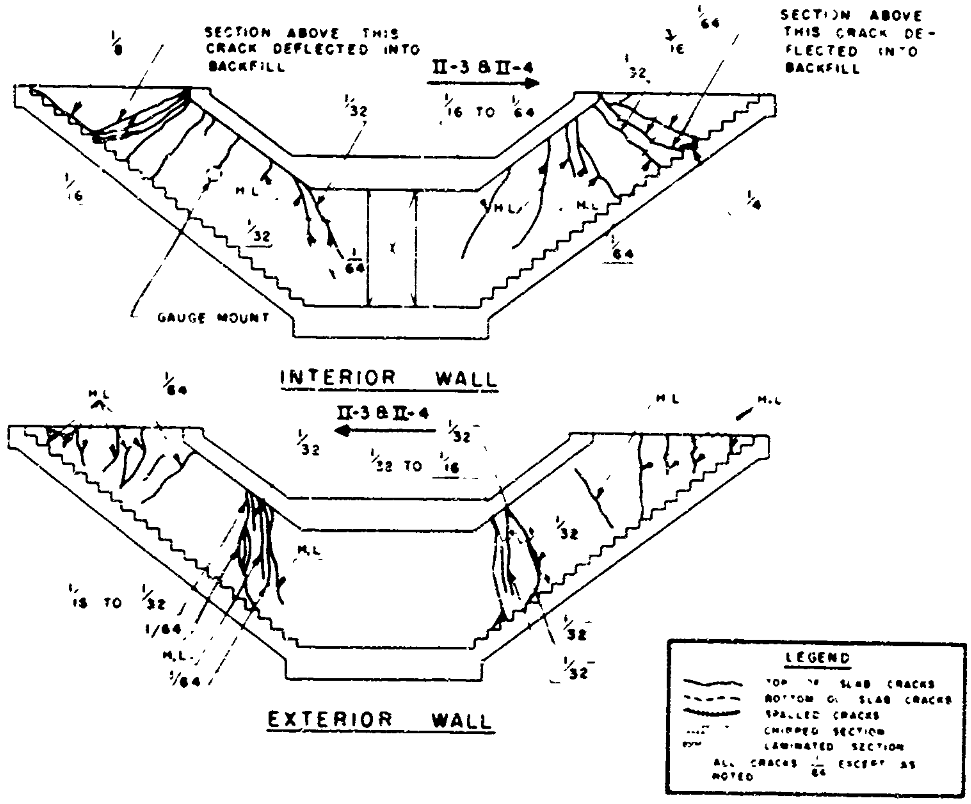

Fig. 3.62—Entrance crack pattern, structure II-5.

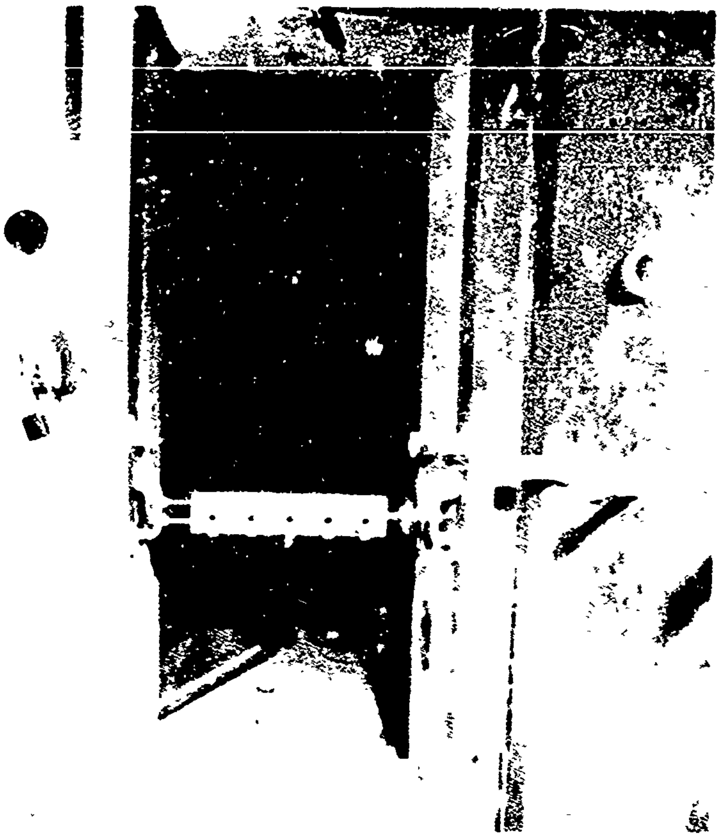

Fig. 3.63 — Postshot view of interior surface of main blast door.

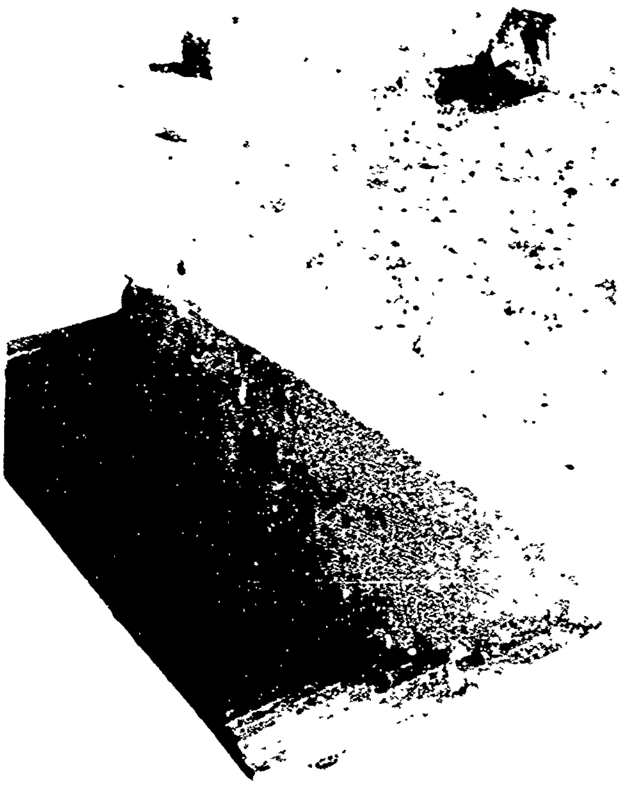

Fig. 3.64 — Blast damage to upper portion of entrance facing structures II-3 and II-4.

Fig. 3.65 — Blast debris and damage to lower portion of entra ıce facing structures II-3 and II-4.

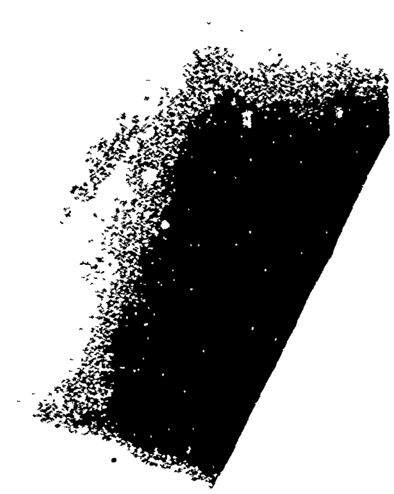

Fig. 3.66 — Blast damage to upper portion of entrance facing blast line.

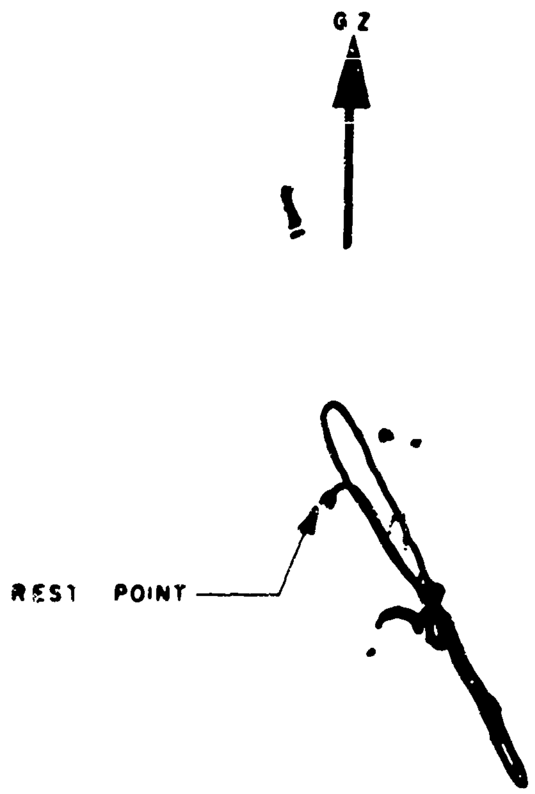

Fig. 3.67—Record, recording pendulum, structure II-1.

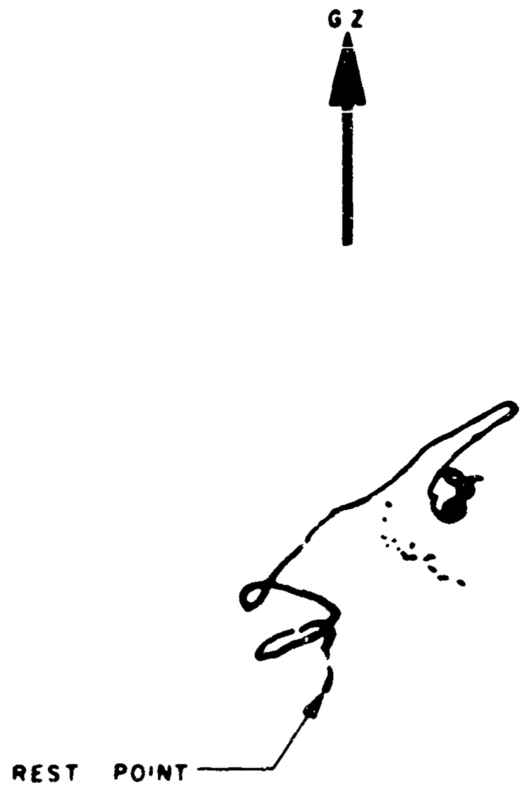

Fig. 3.68—Record, recording pendulum, structure II-2.

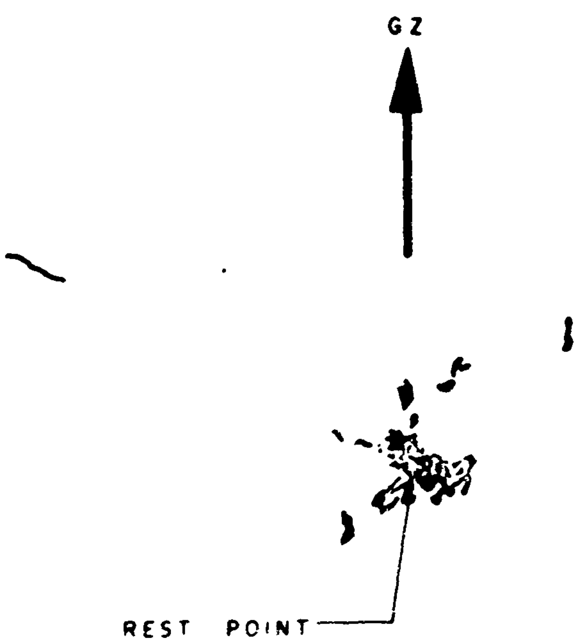

Fig. 3.69—Record, recording pendulum, structure II-3.

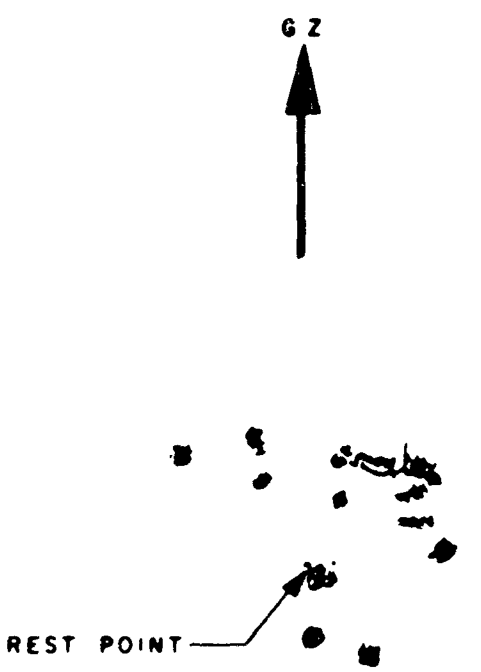

Fig. 3.70—Record, recording pendulum, structure II-5.

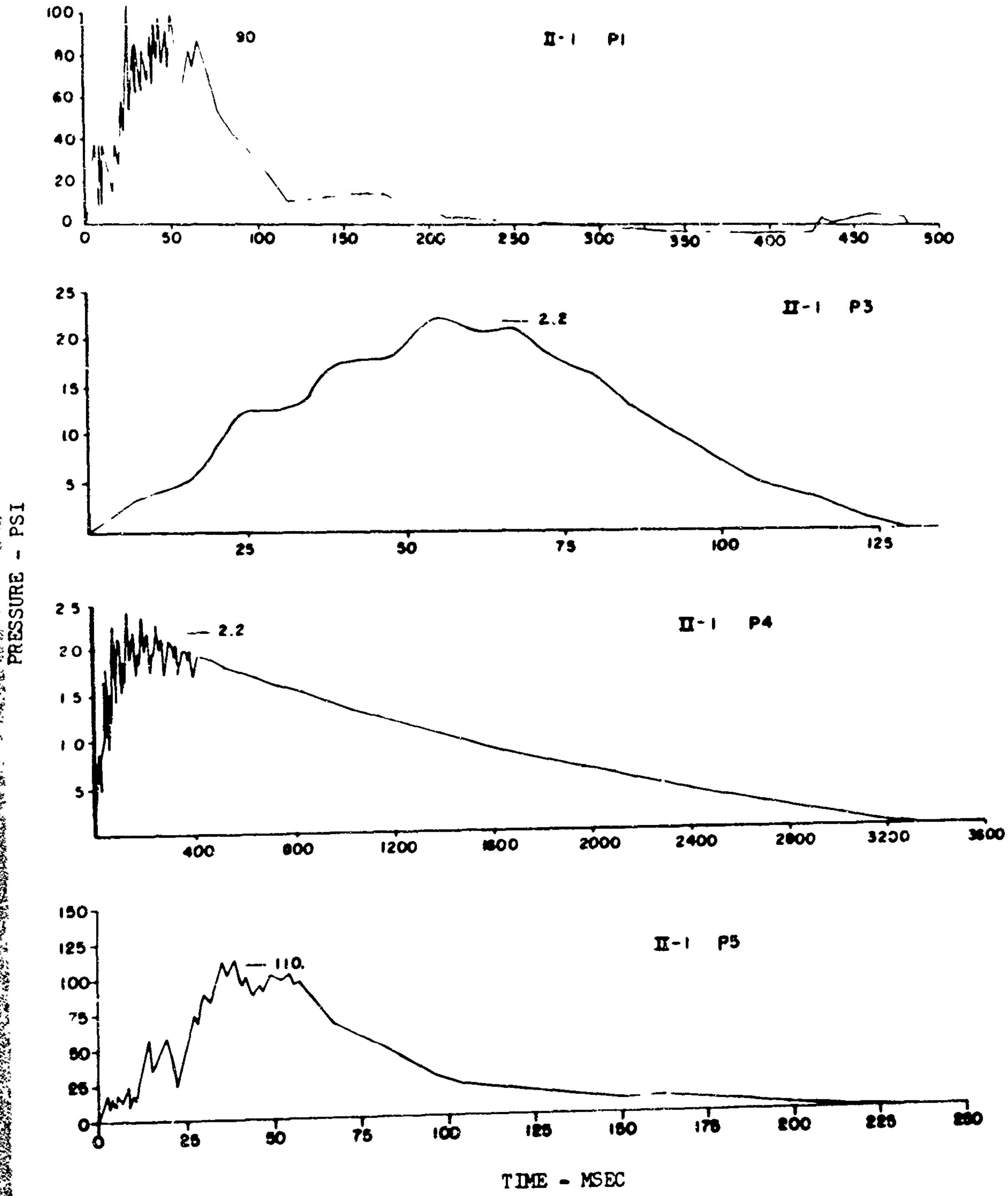

Fig. 3.71—Pressure vs. time; self-recording pressure gauge records.

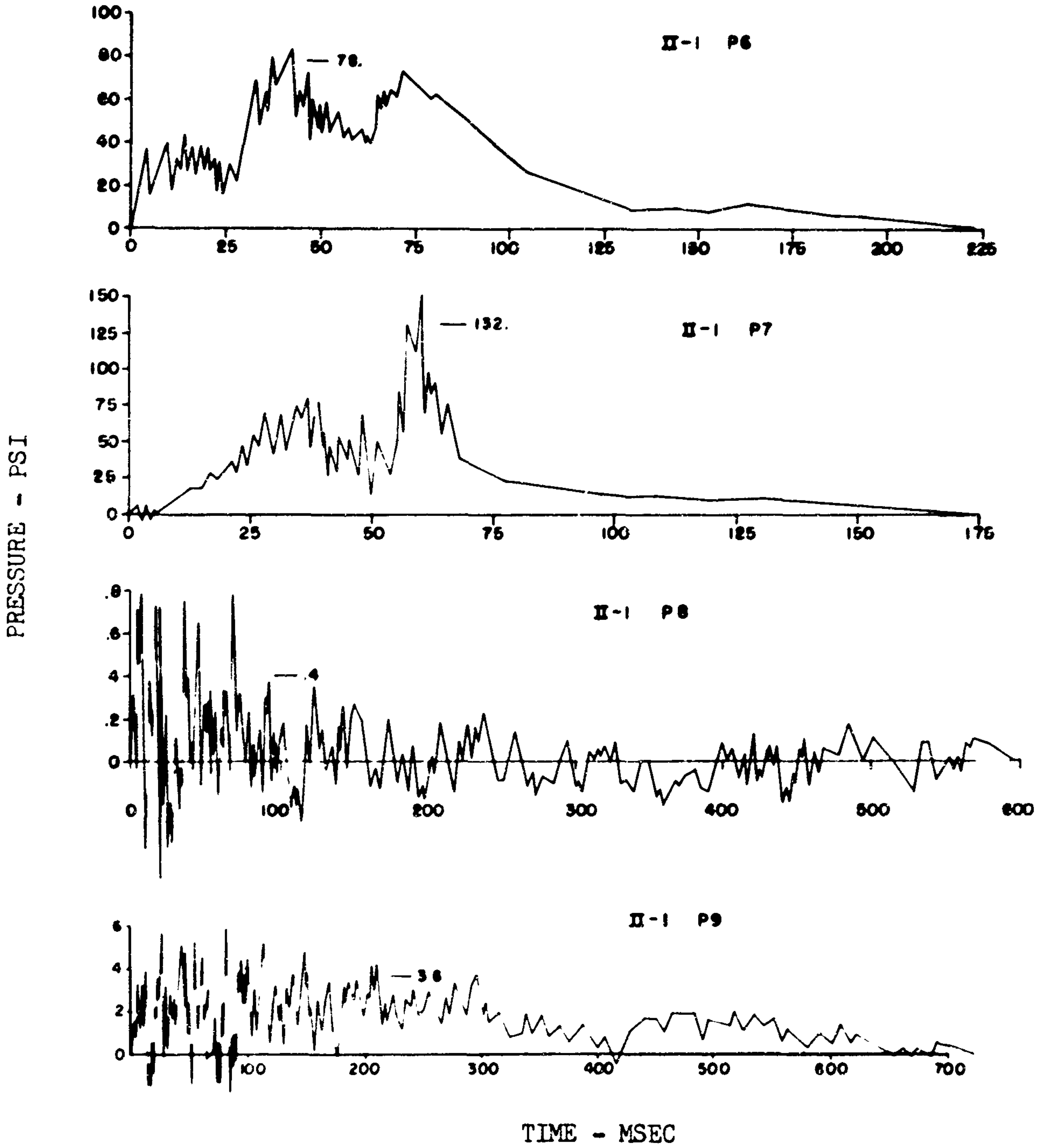

Fig. 3.71—(Continued)

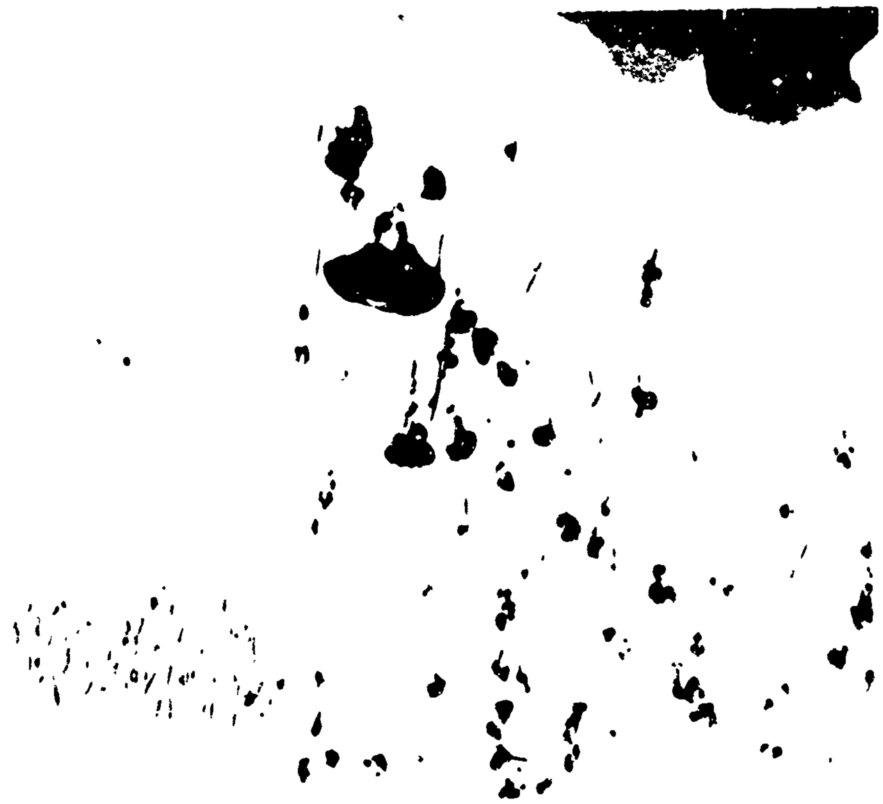

II-I VLP-10 0 50 PSI

Fig. 3.71—(Continued)

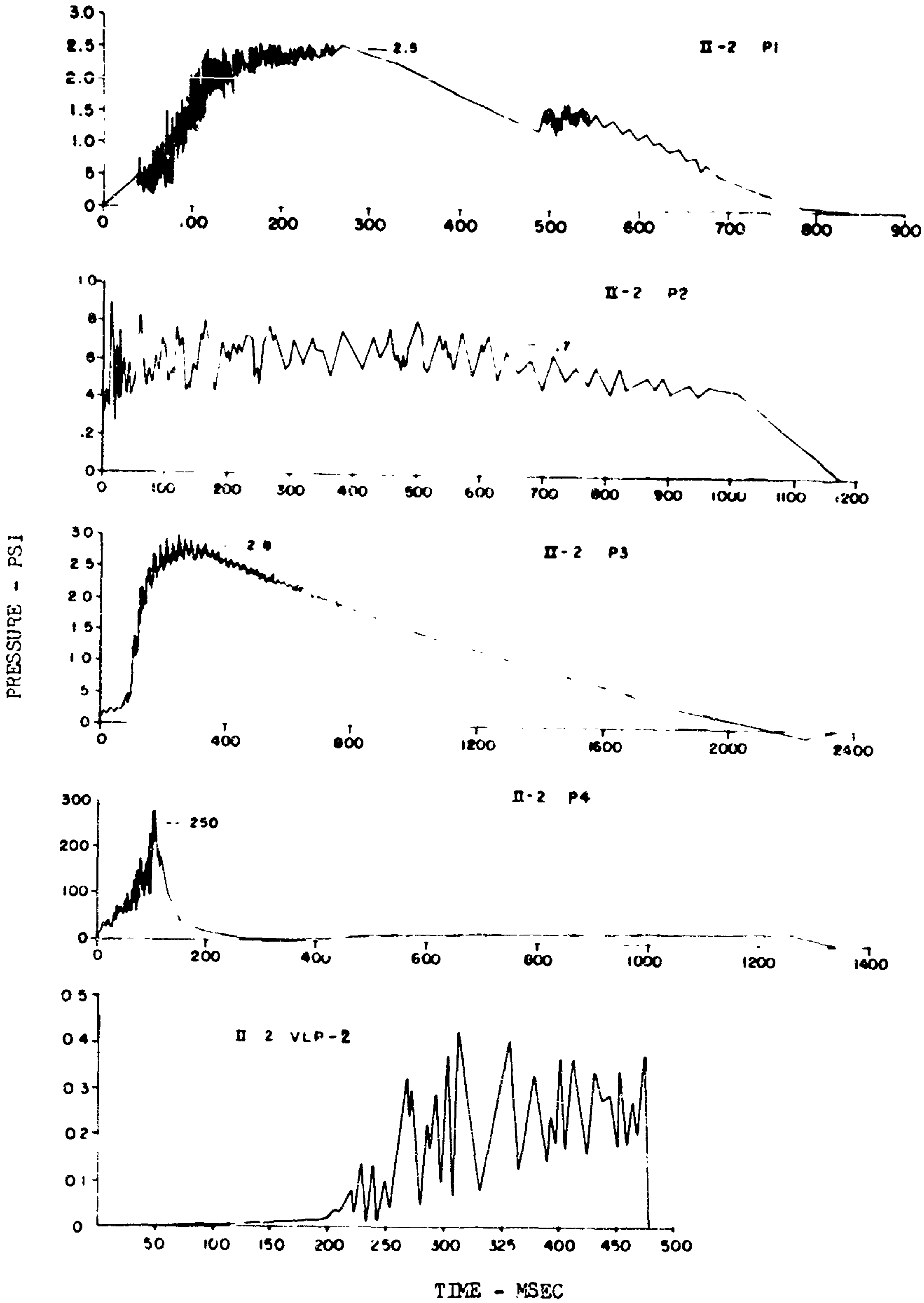

Fig. 3.71—(Continued)

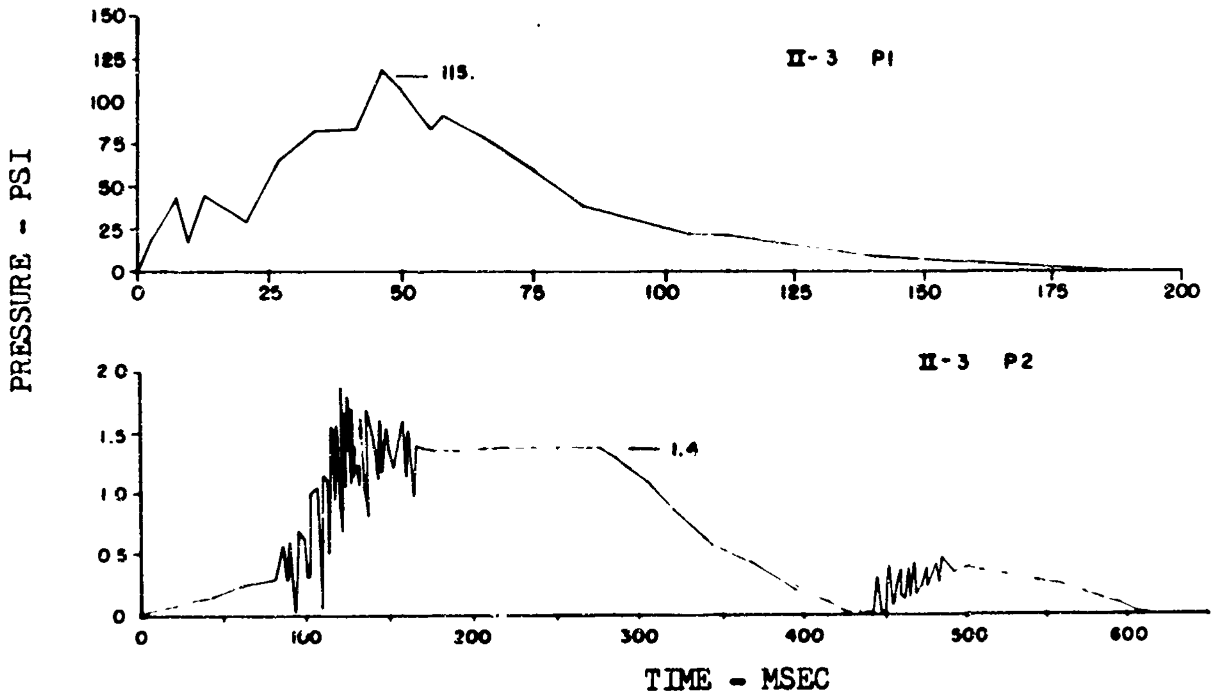

Fig. 3.71—(Continued)

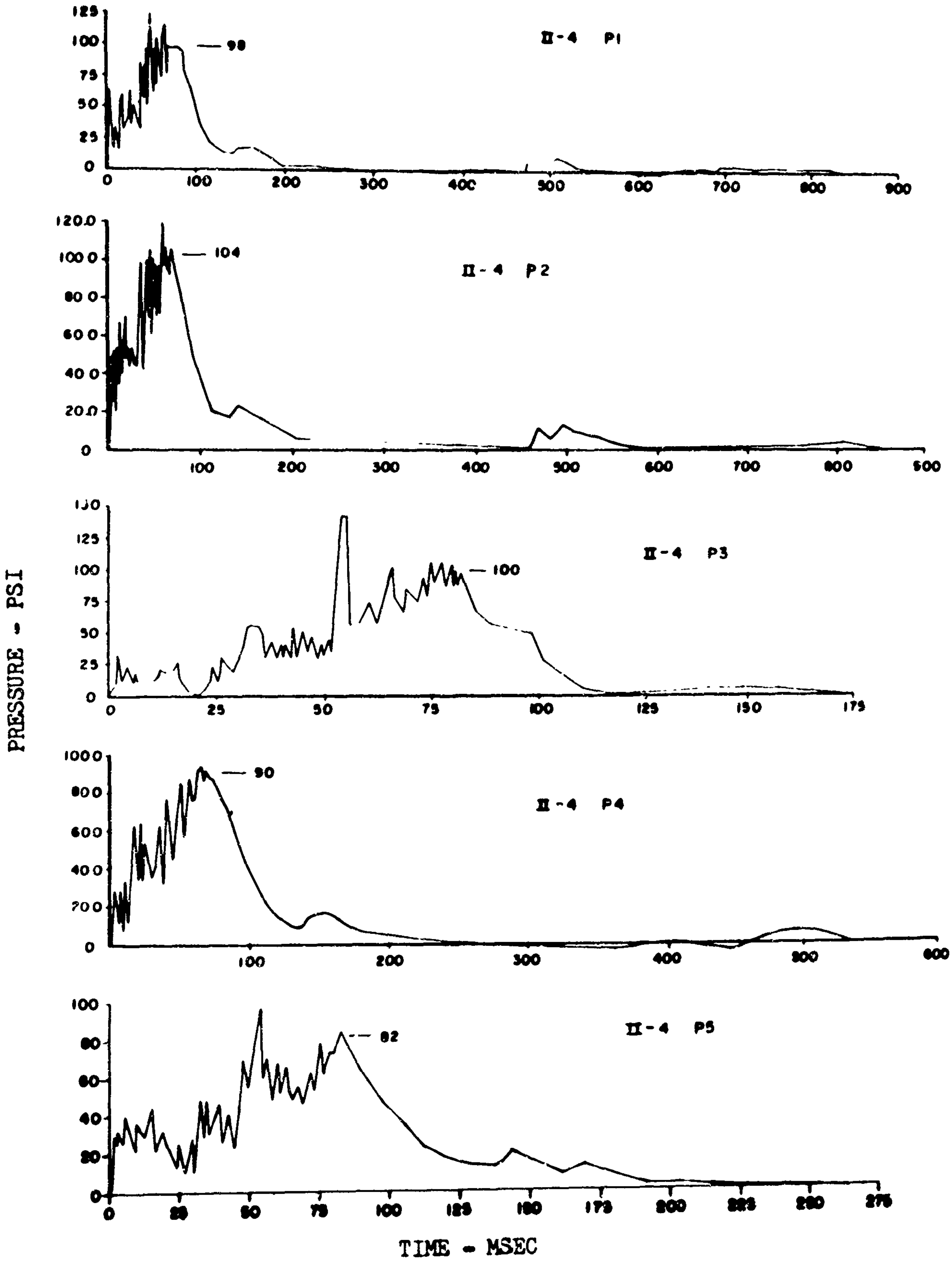

Fig. 3.71—(Continued)

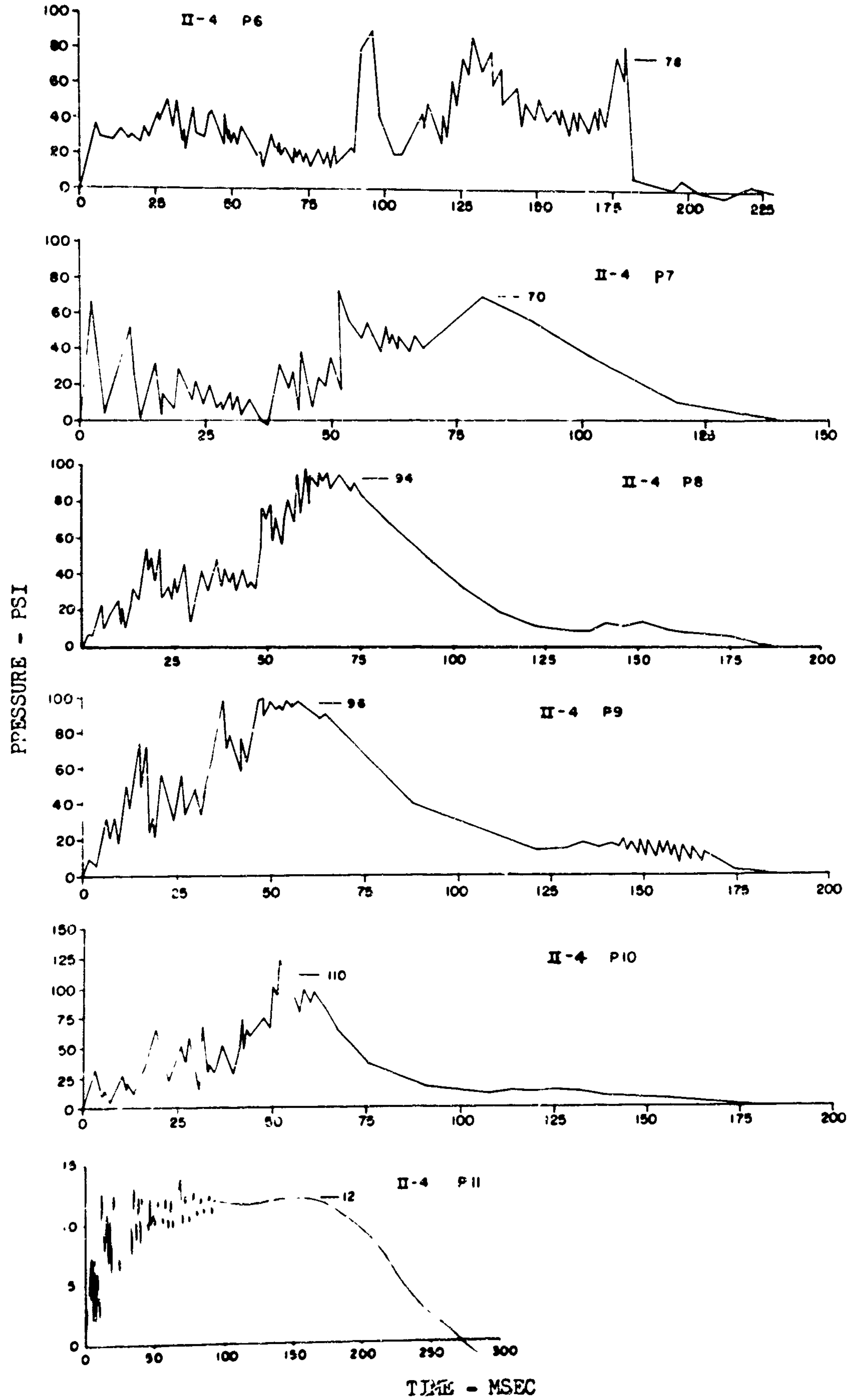

Fig. 3.71—(Continued)

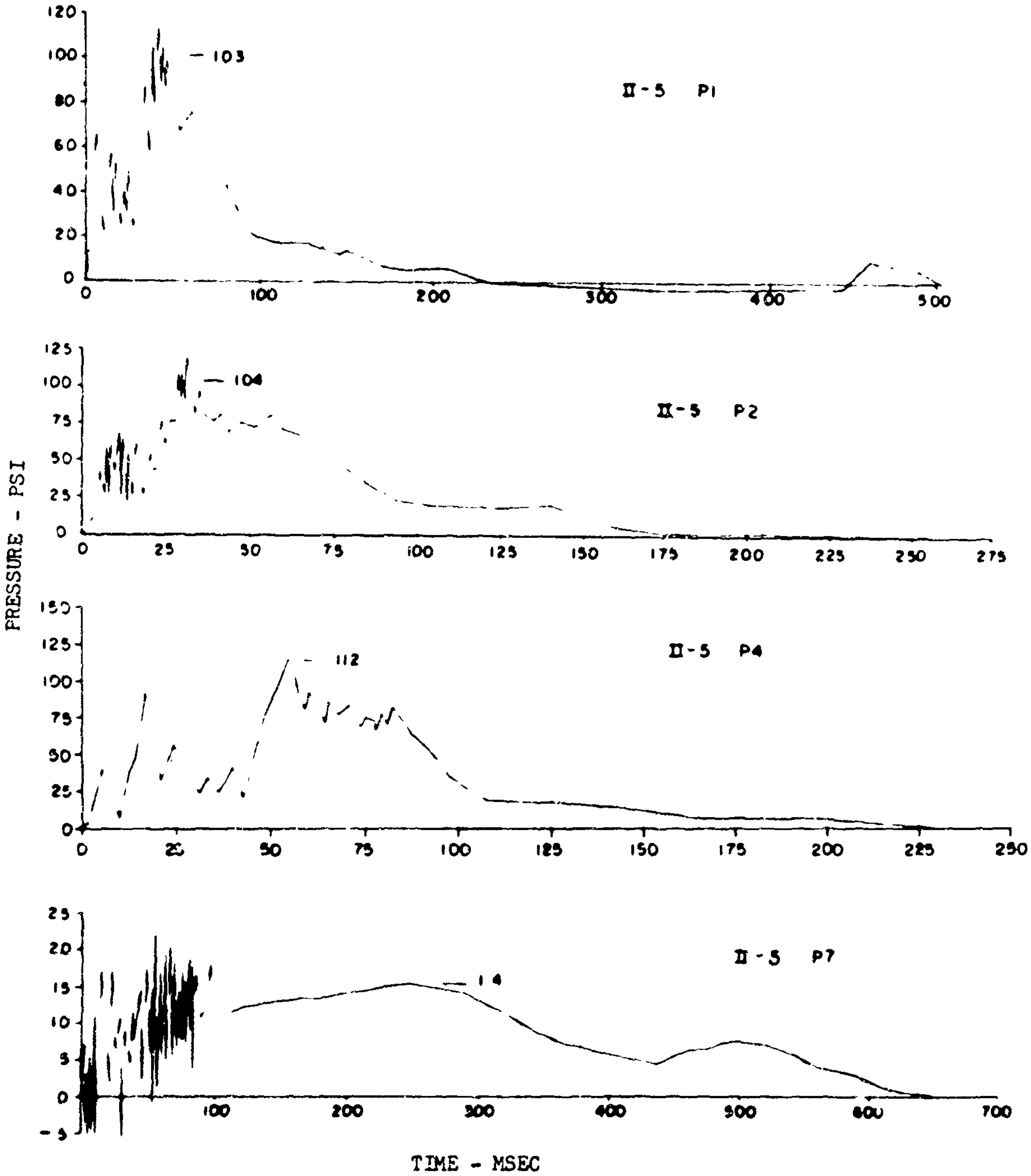

Fig. 3.71—(Continued)

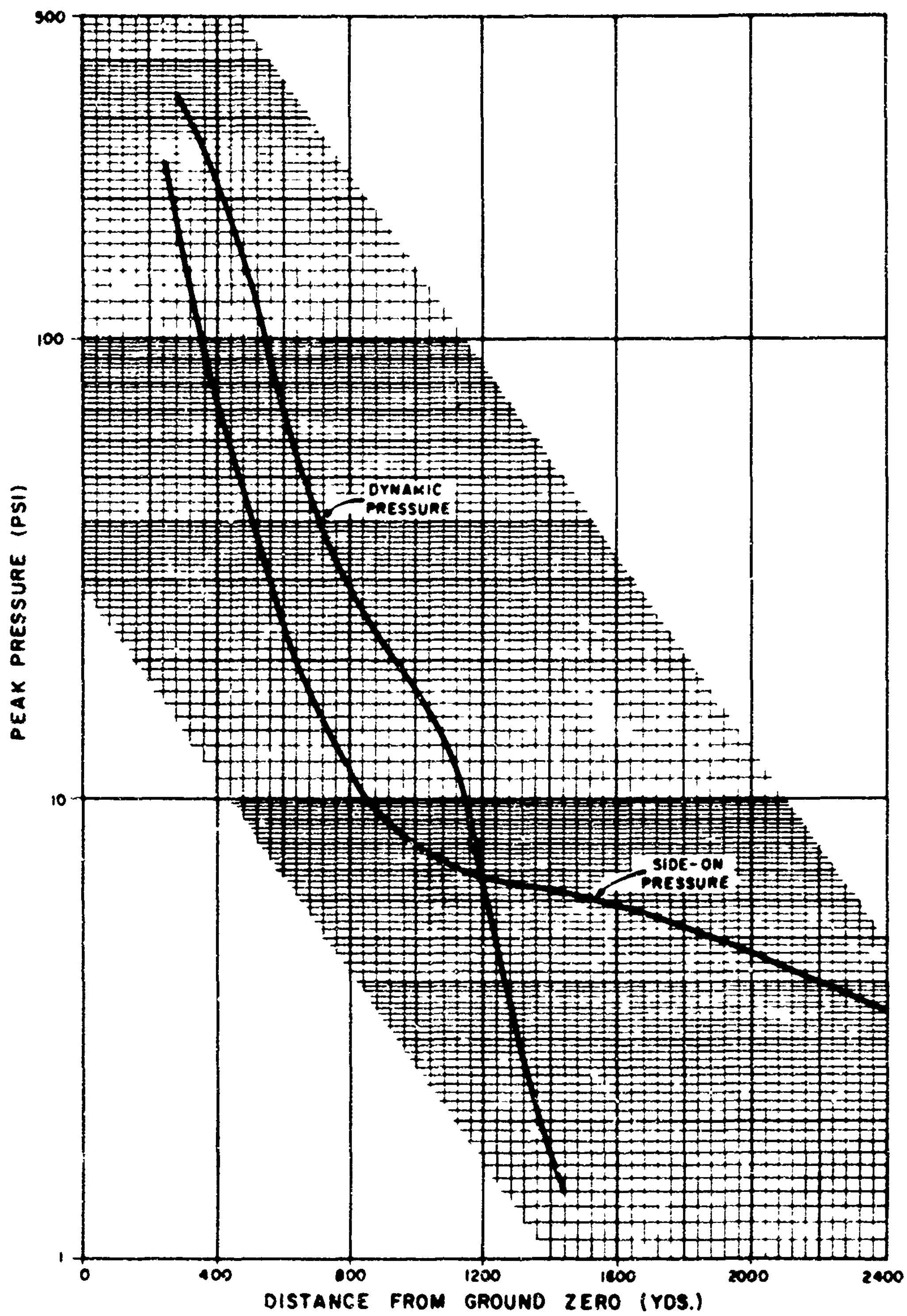

Fig. 3.72 -- Blast-line pressure vs. distance curve.

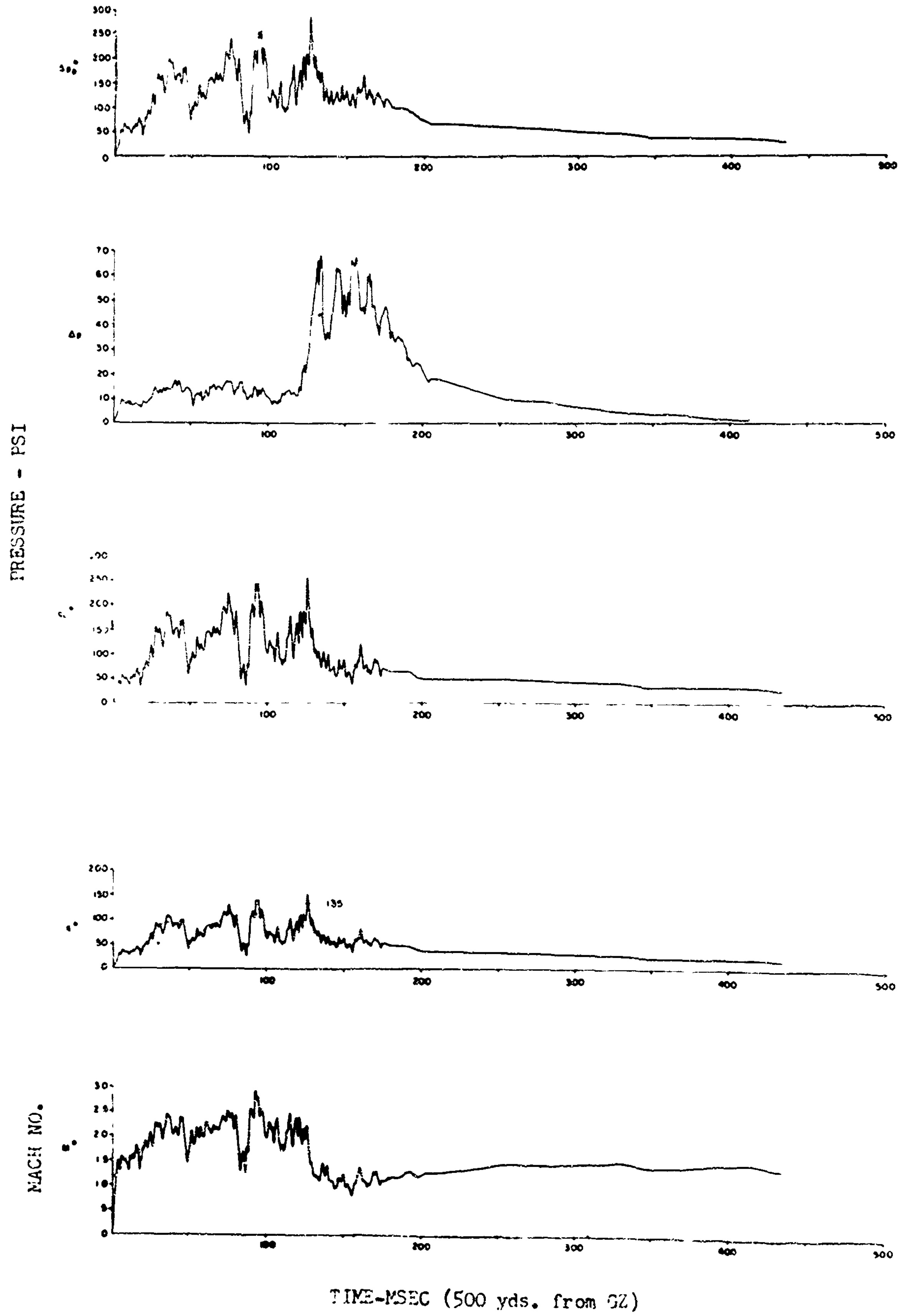

Fig. 3.73—Blast-line pressure, Mach number vs. time; self-recording dynamic pressure gauge records.

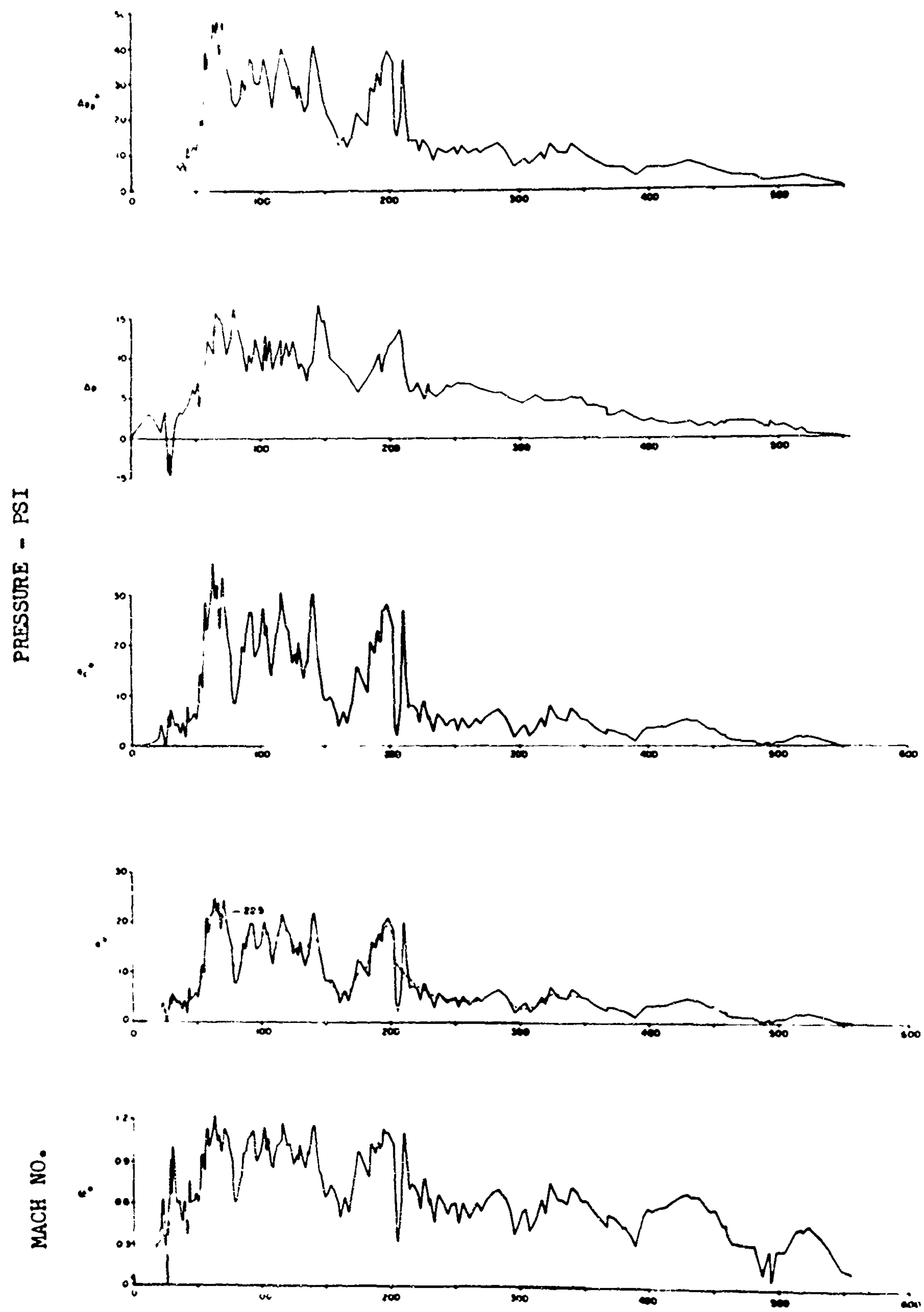

TIME-MSEC (863 yds. from GZ)

Fig. 3.73—(Continued)

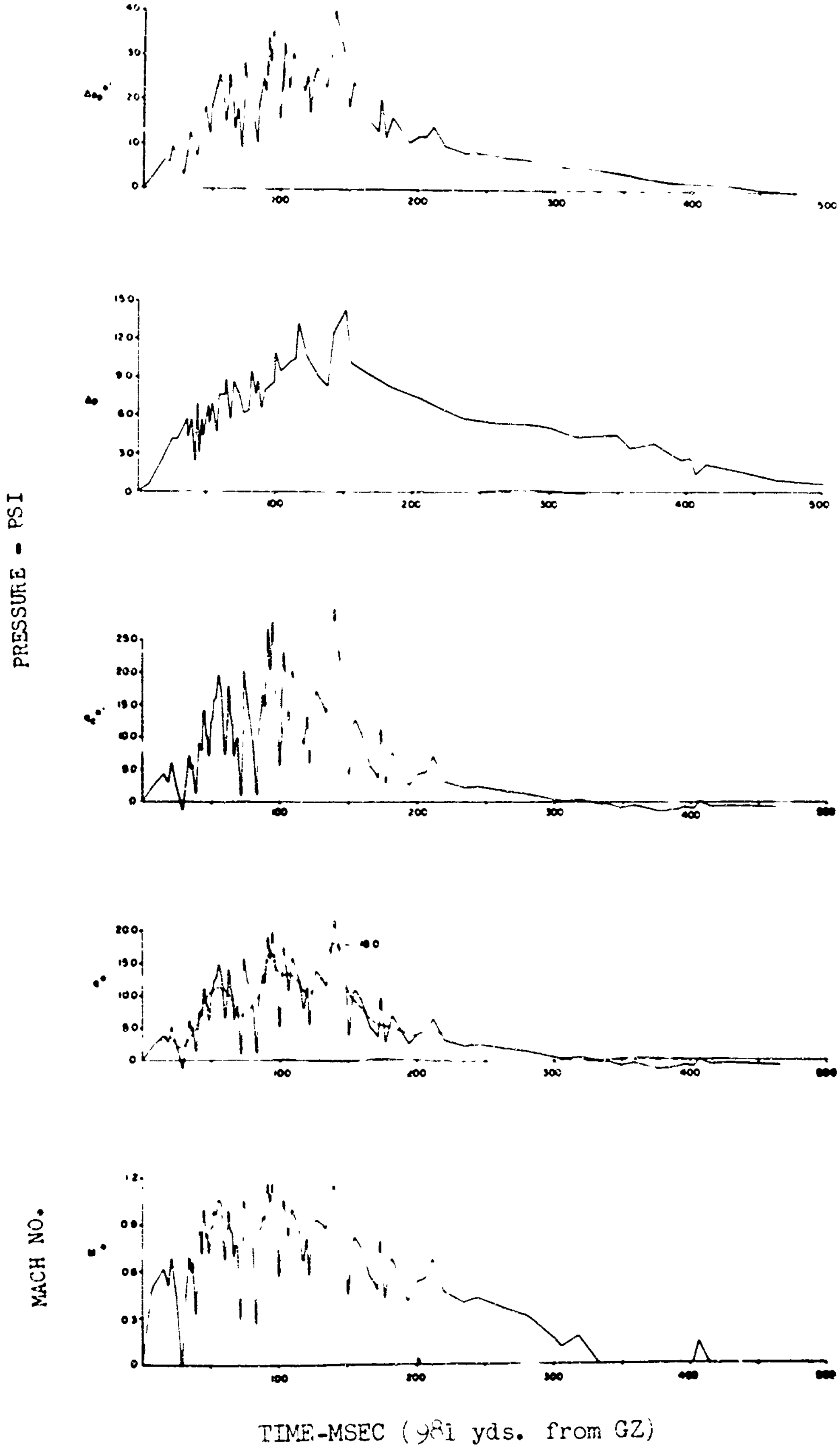

Fig. 3.73—(Continued)

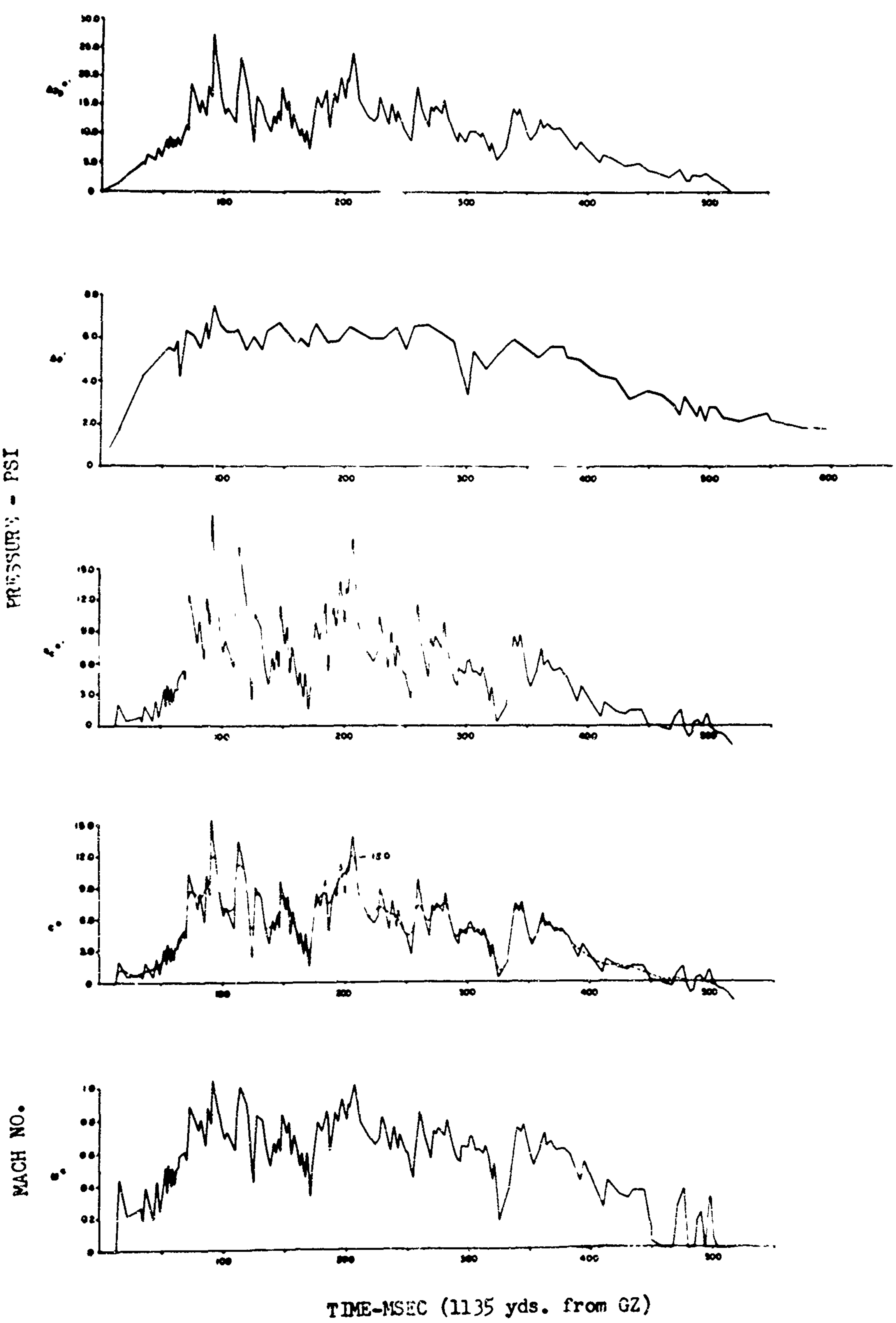

Fig. 3.73—(Continued)

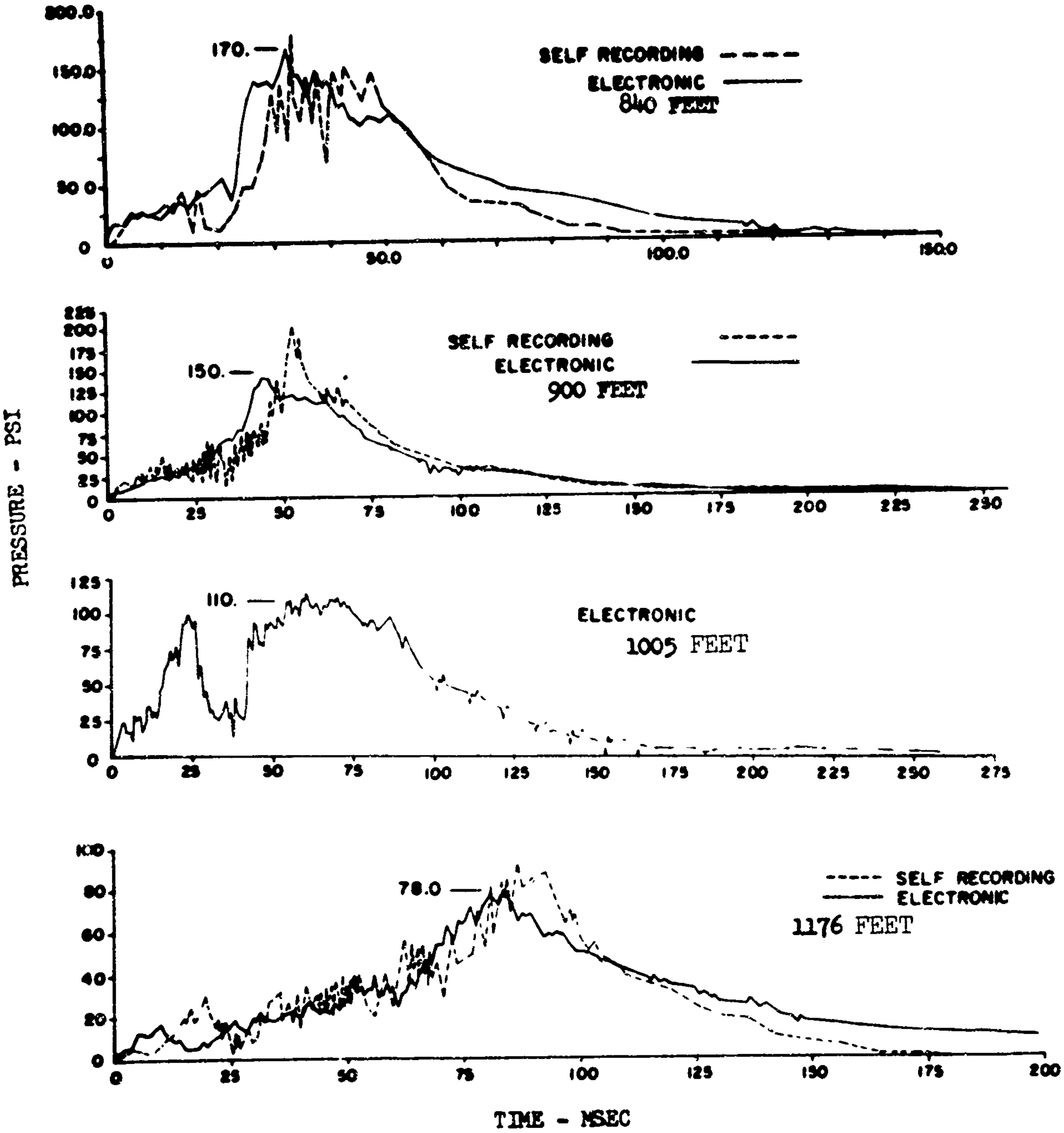

Fig. 3.74—Blast-line pressure vs. time; electronic and self-recording pressure gauge records.

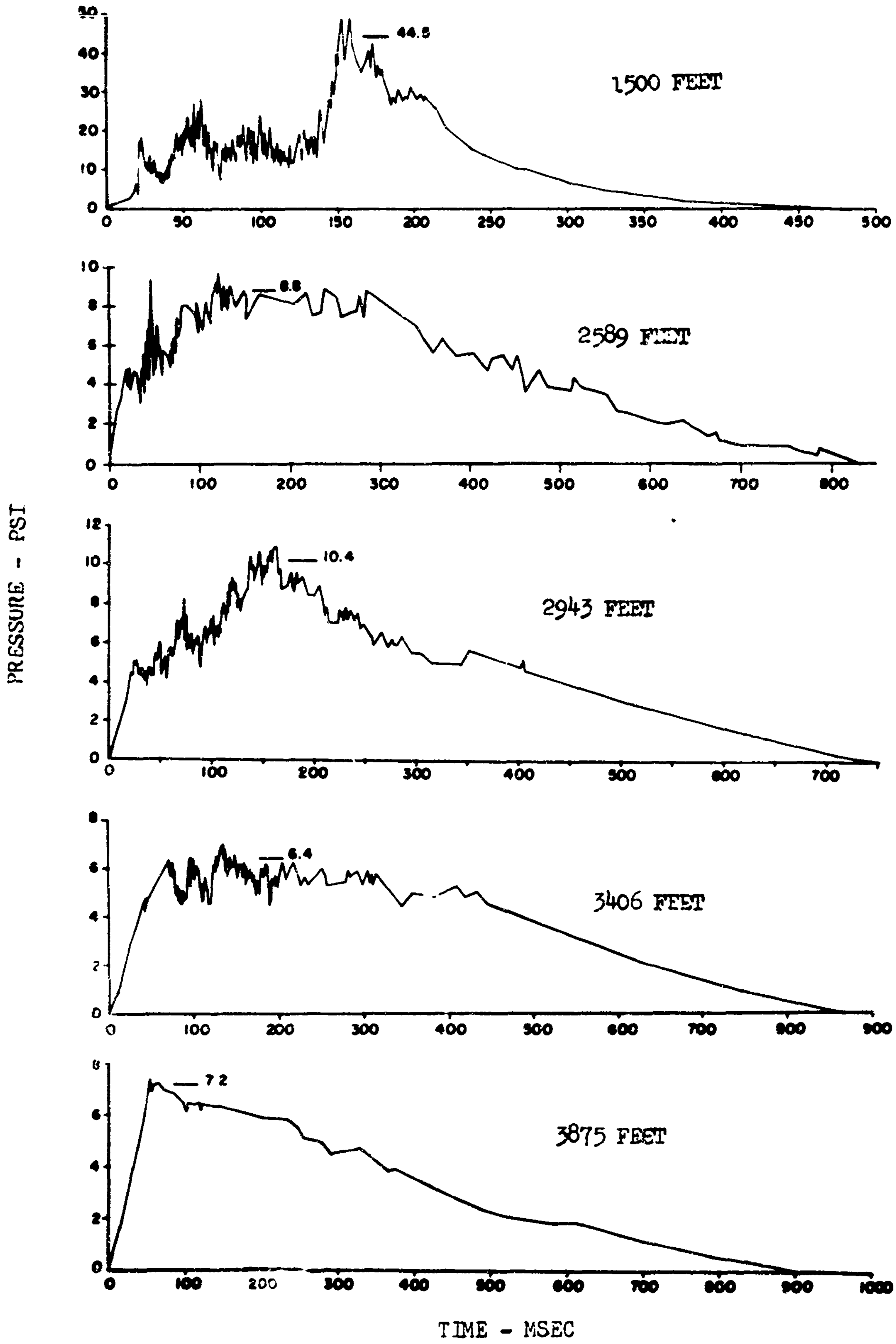

Fig. 3.75—Blast-line pressure vs. time; self-recording pressure gauge records.

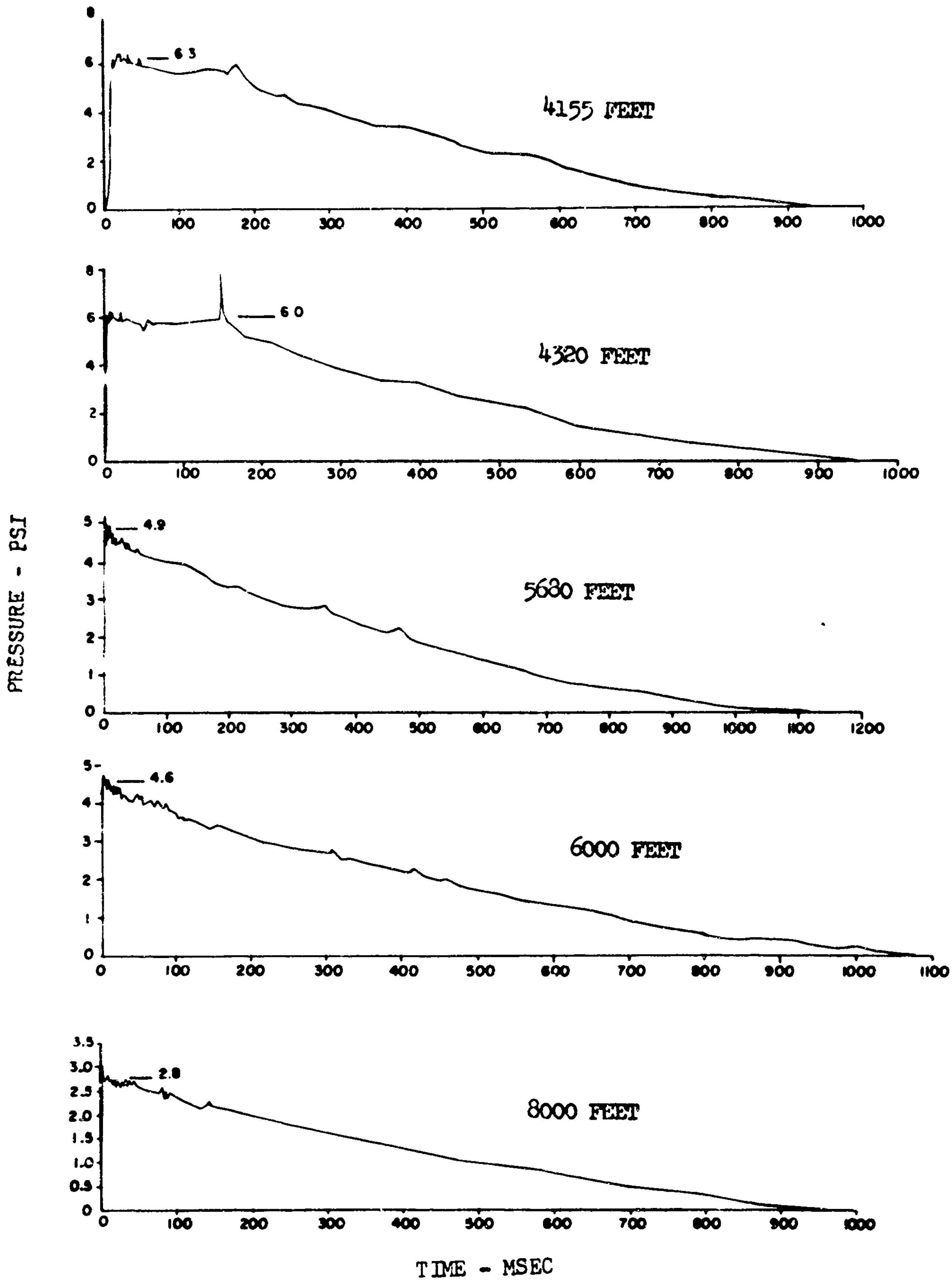

Fig. 3.75—(Continued)

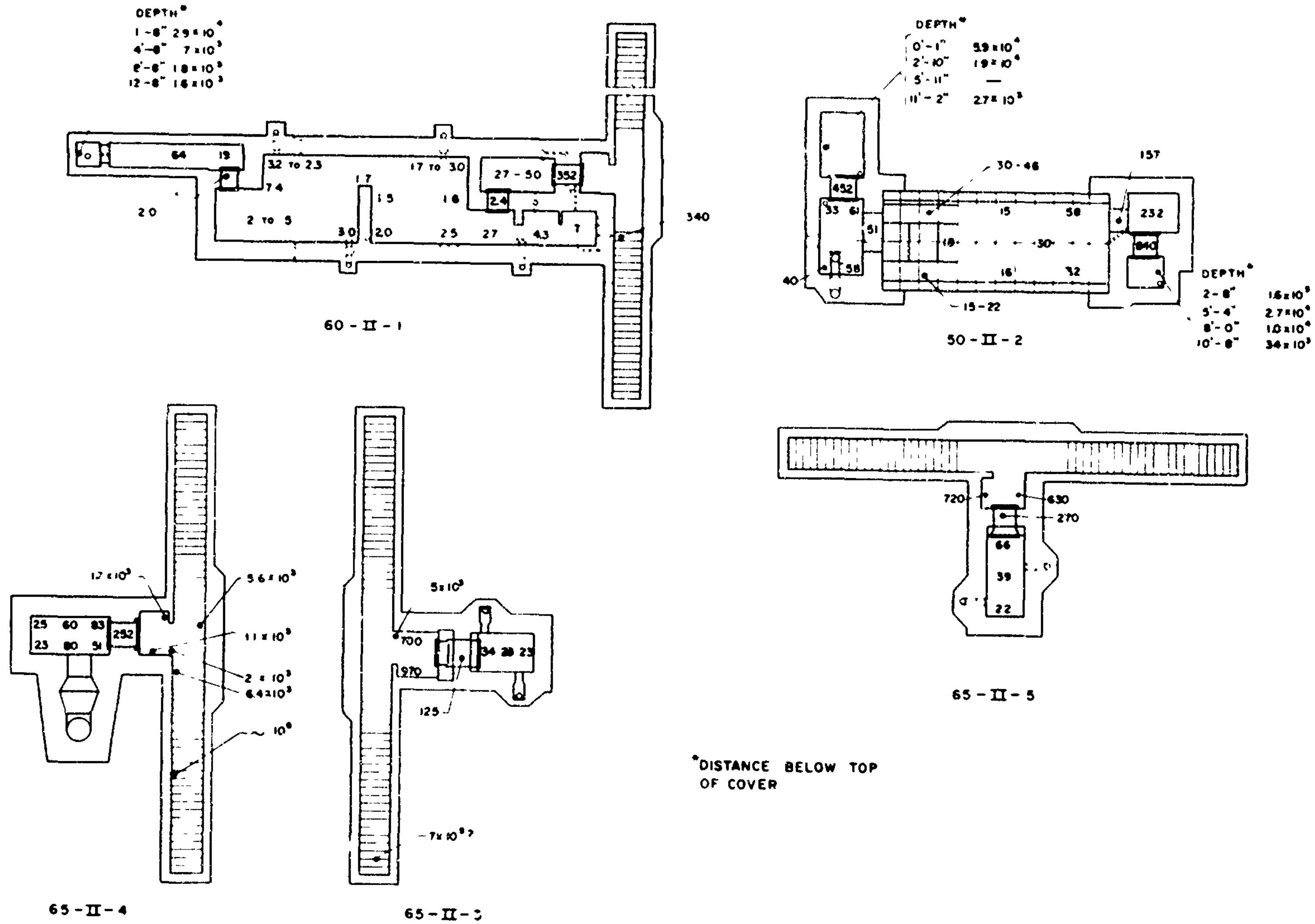

Fig. 3.76—Approximate total gamma dosages during first 52 hr after detonation.

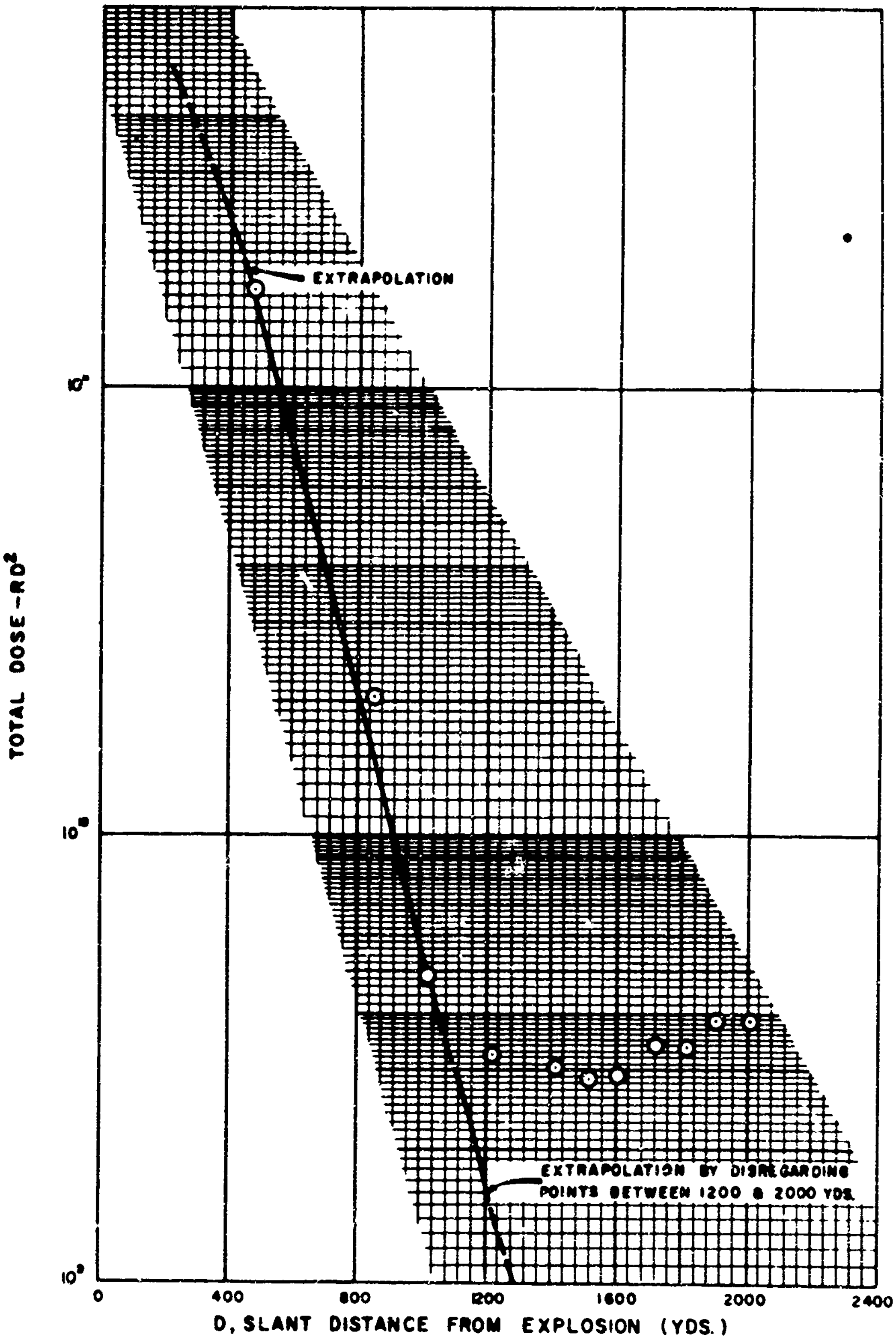

Fig. 3.77—Blast-line total gamma dose vs. distance curve.

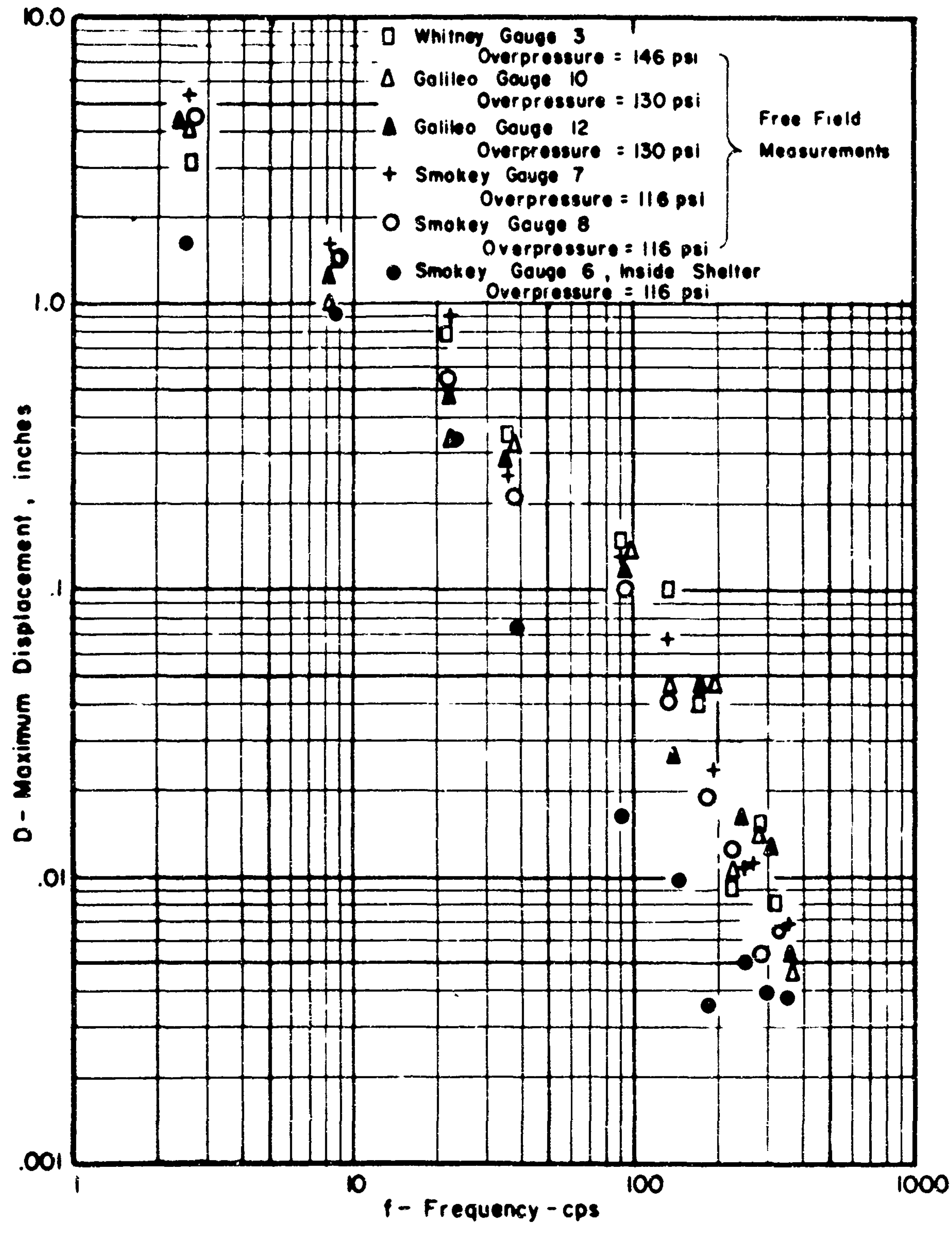

Fig. 3.78—Displacement shock spectrum, vertical direction.

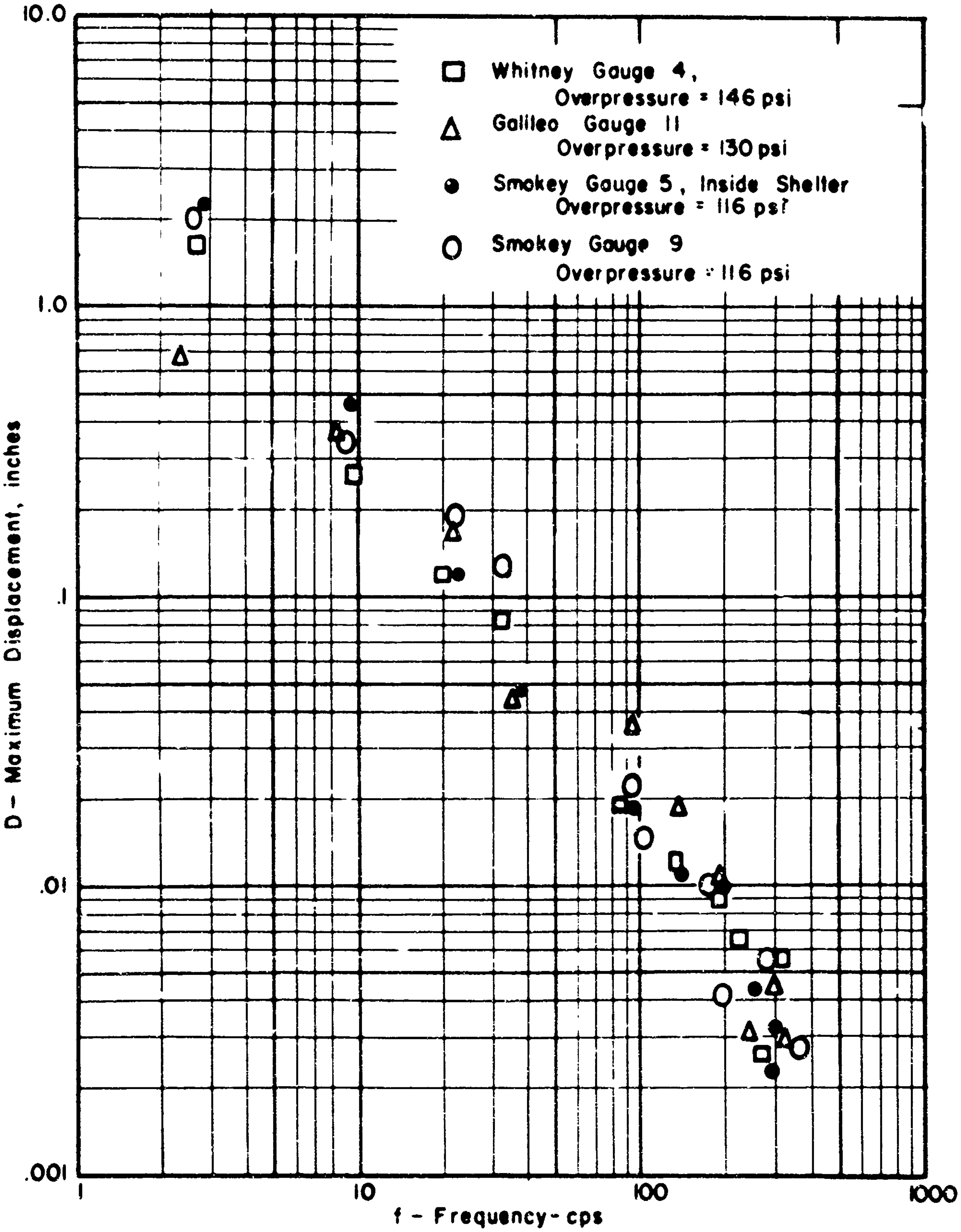

Fig. 3.79—Displacement shock spectrum, horizontal direction.

Chapter 4

SUMMARY

4.1 GROUND AND STRUCTURE DISPLACEMENTS

Although visual observation indicated no gross movements of the main body of any of the five structures tested, the shock spectra data (Sec. 3.3) indicate substantial transient vertical and horizontal motions. It is reasonable to assume that a part of these are permanent. Comparison of preshot and postshot field-location survey data has not been made since reliable postshot surveys were not available at the time of writing of this report.

4.2 EXTERNAL PRESSURE

As indicated by Fig. 1.6, the actual incident overpressure at the predicted pressure levels of 132.3 and 118.0 psi was approximately 12 per cent lower than predicted and approximately 20 per cent less than the static design overpressure of 147 psi.

4.3 INTERNAL PRESSURE

The overpressure in the interior of a structure is a function of the external pressure and duration, the interior volume of the structure, the size and configuration of the openings leading to the interior, and the type of blast closure employed. If the first four factors are equal or can be evaluated, then the relative efficiencies of the various blast valves can be approximated by analyzing the interior pressures obtained.

In the two full-scale test structures, shelters II-1 and II-2, the maximum recorded internal pressures were 0.4 and 0.7 psi, respectively. Both of these structures had the sealing covers on the interior ends of the ventilation pipes blown off by the shock wave. The maximum internal pressures recorded in shelters II-3 and II-5 were both equal to 1.4 psi, even though two basically different types of blast closures were used. It is to be noted that the external pressure level was slightly higher at shelter II-3. The ventilation pipe and blast closure in shelter II-4 was similar in design to that in shelters II-1, II-2, and II-5, but was of a much larger size. Maximum internal pressure recorded in shelter II-4 was 12.0 psi. The interior volumes of shelters II-3, II-4, and II-5 were approximately equal.

4.4 STRUCTURAL DAMAGE

With the exception of structure II-2, all the test structures sustained very slight damage in the shelter areas. Cracking was observed in all structures, but major damage occurred only to those portions exposed to the shock front such as the entrances and the ventilation projections. A detailed description of the structural damage due to blast is given in Sec. 3.1.

The damage to structure II-2 should be evaluated with consideration to the short duration of the test overpressure as compared to that which would result from a large yield weapon.

A postshot dynamic analysis of the roof slab of the rectangular type 60 shelter is included as Appendix D of this report. This analysis utilizes current ultimate strength theory and was performed using the materials strengths as determined from test results, the reinforcement placement and structure dimensions as obtained from the as-built drawings, and the recorded incident pressure on the blast line at the location of the structure as the loading. The analysis indicates that only minor cracking was to have been expected and agrees with the actual postshot condition.

4.5 RADIATION

The permissible level of the initial radiation with the structures was assumed by SNPC to be 20 to 70 rem. No readings of the initial radiation were obtained as separate values, but, as can be seen from Fig. 3.76, the values for the total gamma dosage during the first 52 hr after the detonation at various points within the five test structures were within the prescribed allowable for the initial radiation. Structure II-1, the full-scale rectangular type 60 shelter for 50 persons, had values of total gamma radiation within the first 52 hr ranging from approximately 2 to 9 r for individual dosimeters. The radiation level within the antechamber of this structure was comparable to the radiation level present in structures II-3 and II-5. Structure II-4 had a slightly higher interior level, probably due to the large ventilation pipe extending to the surface.

The radiation level within structures II-2 was generally higher than that of structure II-1. This is explained by noting that the radiation attenuation of 10 in. of concrete and 4 ft 9 in. of soil (structure II-2) is less than that offered by 24 in. of concrete and 3 ft 11 in. of soil (structure II-1).

At the pressure range at which their structures were to be tested, the above-ground incident gamma dosage was assumed in the French design to be in the range from 2 to 7×10^4 r. This dosage is consistent with results obtained by extrapolation of the curves given in "The Effects of Atomic Weapons," but is slightly lower than the data presented in "The Effects of Nuclear Weapons." However, from Fig. 3.77 the actual total gamma dosage was found to be approximately 1.3×10^6 r at a slant distance of 410 yd from the point of explosion.

The attenuation factor of 1000, assumed in the design, is conservative when using "The Effects of Atomic Weapons" as a guide. The actual attenuation factor for gamma radiation indicated by the interior measurement is 100,000 in this test. Free-field and interior gamma measurements are not available.

4.6 THERMAL EFFECTS

It was not possible to obtain thermal measurements from the instrumentation provided. The nonelectronic gauges exposed to the thermal wave were scoured by debris carried by the blast wave and were unreadable. In some cases the recording elements were removed from their mountings by the blast wave. Owing to a breakdown in the 3.5.4 electronic recorder, no results were obtained from the electronic temperature gauges.

Residual thermal effects were not apparent from visual observation.

4.7 DEBRIS AND DUST

The postshot photos taken before the entranceways were cleaned indicate that deposited debris was comparatively light. A dust layer varied in thickness from approximately $^1/_4$ in. to a maximum of 2 in. in places where drifting occurred. Some rubble was also present. Interior dust was observed only at the bases of the ventilation ducts. Owing to the natural surface of the test area, it was difficult to ascertain the extent of debris on the ground surface.

All vertical or inclined surfaces facing GZ (ventilation projections, stairs, walls, etc.) were scoured by sand and debris carried by the blast wave. Above-ground projections that were broken off were deposited from 5 to 100 yd away from their original positions (see Sec. 3.1).

4.8 LIMITATIONS IN APPLICATION OF TEST RESULTS

Although the magnitude of the effects (overpressure vs. time, thermal and nuclear radiation) is different for small nuclear weapons than for the large thermonuclear weapons now available and the physical environment at the Nevada Test Site is not typical of most populated areas, the data obtained from these weapons tests are very useful in estimating response and evaluating the parameters used in design. For this reason the records of blast overpressure, ground-shock motions, radiation, and other weapons effects are of prime importance. However, the results cannot be used directly for proof test purposes except in special cases.

Appendix A

CONSTRUCTION

A.1 GENERAL

All work was done under contract to the U. S. Atomic Energy Commission. The contractor for the construction of the five reinforced-concrete shelters was the Sierra Construction Company of Las Vegas, Nevada. Reynolds Electric & Engineering Company supplied the concrete aggregate and miscellaneous work required to make the structures ready for the test. Holmes & Narver, Inc., provided over-all supervision and coordination as field representatives of the AEC.

The Federal Civil Defense Administration and the Service National de la Protection Civile were continuously represented at the Site by an Ammann & Whitney field representative, who provided inspection and advisory service for the construction groups. This service was supplemented by visits to the Site at critical times by the Project Officer.

Construction, in general, was geared to a very rapid time schedule. This schedule was closely adhered to despite the many difficulties that were experienced. The schedule called for a maximum of 75 calendar days, starting on Apr. 6, 1957. Excavation was started on April 24 and the backfilling was scheduled to be completed on June 20. The schedule, as indicated above, could not be completely adhered to because of problems that developed during construction. These problems will be more fully defined in Secs. A.4.1 through A.4.8 of this report.

Figures A.1 through A.19 are photographs of the five shelters at the time of their construction. Dates are included to show construction progress. Deviations from the drawings and specifications are recorded in Appendix C, "As-built Drawings." Table A.1 indicates the schedule adhered to during the construction phase of the operation.

A.2 MATERIALS

A.2.1 Concrete

Concrete was mixed at a central mixing plant operated by Reynolds Electrical & Engineering Company. The plant was a permanent batcher type installation and was located approximately 15 miles from the structures. The concrete was trucked to the structures by conventional transit-mix trucks. During the batching, the mixing water, as predetermined by the concrete mix design, was added to the dry mix, and the concrete was mixed during transportation. The concrete was placed by the use of one or more of the three following methods: (1) by dumping into a $^3/_8$ or $^1/_2$ C.Y. bucket and placing by crane, (2) by dumping into tremies for wall pours, or (3) by placing directly with the use of concrete chutes. Hunts paraffin-base curing compound was used to cure the concrete.

A total of 72 standard 6- by 12-in. cylinders was taken from all the structures for 7-, 28-, and 90-day compression tests. A total of 39 $7\frac{7}{8}$-in. concrete cubes and 30 concrete test beams were tested at 7, 28, and 90 days. The tests on all three items were performed by Nevada Testing Laboratories. In addition to the specimen tests, the Schmidt Concrete Hammer was used to check the uniformity of the concrete and to determine the correlation between the rebound values and the ultimate concrete strength of the structures.

The results of the concrete strengths as recorded for the concrete cylinders, beams, and cubes are contained in Tables A.2 to A.4. Average results of these tests are summarized in Table A.5. The hammer test results are given in Table A.6. Table A.7 gives the typical concrete-mix design used during construction.

A.2.2 Concrete Components

(a) *Cement.* The cement used in construction was predominantly type II Portland cement. Owing to the limited amount of time for the construction of structure II-2, Hi-Early cement was used for the erection of shafts T_1 and T_2.

(b) *Coarse Aggregate.* The coarse aggregate, $1\frac{1}{2}$-in. graded aggregate, was stockpiled at the batching plant. Owing to the handling procedure and transportation methods from the crusher, which were products of Site conditions and the limited amount of time for construction, segregation of the aggregate was evident in the stockpile and batched concrete. Some aggregates were observed to have maximum dimensions ranging to $2\frac{1}{2}$ in.

(c) *Fine Aggregate.* The fine aggregate had additional wind-blown fines, not indicated in Table A.7, primarily because of the conditions at the Test Site.

A.2.3 Concrete Forms

Wall and roof slab forms consisted of plywood panels of $\frac{5}{8}$- and $\frac{3}{4}$- in. stock. Some of this material had been used several times before being used on the French test structures and was then used as many as three times during construction of the five test structures. Dimension stock for studs was 2 by 4 in.

A.2.4 Reinforcing Steel

Reinforcing steel used in the structures consisted of French supplied ADx and TOR bars. The fabrication of the steel was subcontracted by Sierra Construction Co. to Fontana Steel Co. All reinforcing steel was cut and bent at the Site. The field fabrication shop was located near the concrete mixing plant, which was situated approximately 15 miles from the construction Site. The transportation of the fabricated steel between the shop and the structures was accomplished by flat-bed trucks. Although the bending operation was generally adequate, there are deficiencies between the actual construction and the original contract plans. None of these appear to have been critical in terms of the test results. All deviations from the construction drawings of the fabrication and/or placement of the steel have been noted on the "As-built Drawings," Appendix C.

The yield and ultimate stresses and the percentage of elongation of 8-in. test specimens, as tested by Smith-Emery Co. of Los Angeles, Calif., are given in Table A.8.

A.2.5 Structural Steel and Steel Wire

The structural-steel components of the structure consisted essentially of door frames, ventilation equipment, and miscellaneous end items. These items were supplied by the French Government. Several items, as described in Sec. A.4, were damaged during shipment from France to the Site. All members were repaired before their installation.

The steel wire used to post-tension the concrete circular structure (II-2) was tested, and the results are shown in Table A.8.

A.3 SOIL TESTS AND DESCRIPTION

The subsoil, upon visual investigation, was found to be a heterogeneous mixture of various sizes of sand and gravel particles with interstitial clay and silt; it may be loosely described as a calcinated conglomerate. The formation contained a cementing agent, apparently of calcium carbonate origin. This agent, in conjunction with the clay particles, produced a state of high consolidation. The soil condition described above was below 1 to $1\frac{1}{2}$ ft of typical desert top soil. The depth of the calcium carbonate mixture was of an indefinite vertical extent.

To determine the dimension, shape, and peculiarities of cut, cross-sections of the excavations were taken at all the structures. These are shown in Fig. A.21.

To evaluate the compaction achieved by the backfilling method, in-place density tests were performed on pre- and postconstructional soil conditions that existed at the structures.

The results of the tests are indicated in Table A.9.

A.4 THE CONSTRUCTION OF THE STRUCTURES THROUGH THEIR COMPONENT ITEMS

A.4.1 General

The following sections deal with the procedures used in construction of the component items of the structures and the resulting conditions that existed at the completion of the construction phase of the operation. Also included in this section are all deviations from the drawings and specifications and any additions that were deemed necessary to complete the structures in a satisfactory manner.

A.4.2 Excavation

The predominant characteristic of the soil, with regard to the excavation, was its natural cementation. This characteristic made it virtually impossible to excavate using conventional back-hoeing equipment, and all existing soil had to be loosened by caterpillar-propelled rippers or explosive charges before removal by a caterpillar-drawn scraper, Fig. A.20. Excavation was carried down approximately 3 in. below the elevation of the bottom of the base slabs for structures II-1, II-3, II-4, and II-5 and approximately 1 ft below the bottom elevation of the 4-in. setting bed of structure II-2. Required grade was obtained by backfilling, leveling, and compacting using the construction equipment. All additional excavation for the dry wells was by hand.

A.4.3 Floor Slabs

The forms for the floor slabs of the cast-in-place portions of the five French test structures were set holding the exterior dimensions of the structures. French reinforcing steel was then placed within the formwork directly over the natural ground. Concrete blocks of the required thicknesses were used to support the bottom layer of steel.

Because of the nature of the reinforcement pattern, no "chairs" were required to support the top mats. In structure II-1 a system of stirrups in the floor slab of the main chamber and emergency exit tunnel dictated the distance between layers of reinforcement. The top mat reinforcement for structures II-2, II-3, II-4, and II-5 was tied directly to the vertical wall steel, which had to be placed and poured in with the floor slab. Because of the relatively small spans between the vertical wall reinforcement, intermediate supports of the top mat were omitted.

Immediately prior to pouring the floor slabs of all structures, the existing natural ground within the formwork was thoroughly moistened to prevent excess absorption.

For structure II-1 the first pour consisted of the floor slab of the emergency exit shaft, emergency exit tunnel, and main shelter and the base slab of the entrance ways, including the stairs. Structures II-3, II-4, and II-5 had the floor slab of the main chamber and the base slab of the entranceways poured at the same time.

Structure II-2, an entirely different type structure, had two separate cast-in-place portions. The floor slabs of both of these sections (shaft T1 and shaft T2) were poured at the same time.

Placement of reinforcement for all five structures was tedious and in many ways did not conform to United States standards. Some deviations from the contract drawings therefore occurred, and these deviations can be found in Figs. C.1.1 through C.6.4.

A.4.4 Walls and Roof Slabs

Owing to the intricacy of the reinforcement pattern, it was found advantageous to complete as much as possible of the remainder of the structures in a single pour. Therefore, the second pour of structure II-1 consisted of the emergency exit shaft walls, emergency exit tunnel walls and roof slab, main shelter exterior wall, partitions and roof slab, and entranceway walls and roof slab. Horizontal construction joints were permitted at the top of the roof slab for the intake and exhaust stacks and for the sand-filter pit. These parts of the structures were subsequently completed the following week.

Structures II-3 and II-5 were also poured complete, with the exception of the portions of the intake and exhaust stacks extending above the roof slab. Structure II-4 was completed in its entirety by the second pour.

Both shafts T1 and T2 of structure II-2 were poured on August 6. Owing to the proximity of the proposed shot date, it was found necessary to use High-Early strength cement for these portions of the structure. Sand and coarse aggregate were batched and brought to the construction Site in standard concrete mixers. There cement and water were added. This procedure was required because of the length of travel time from the batching plant and the extremely high rate of evaporation. The above-grade portion of the exhaust stack on shaft T2 was poured two days later.

All deviations from the contract drawings of that portion of the structure above the floor slab are shown in Figs. C.1.1 through C.6.4.

A.4.5 Post-tensioning of Structure II-2

The design of the cylindrical structure required that 12 precast cylindrical elements be post-tensioned by means of 8 cables. The sequence of operations, as outlined by the Freyssinet Company, Inc., was as follows:

(1) One cable consisting of 12 wires, each 0.196 in. in diameter, was inserted in each of the 8 preformed holes. Since this operation was accomplished prior to grouting the segments, the 8 cables were protected from the grout by pipe sleeves at the joints between the rings.

(2) Prior to stressing the cables, a male plug was inserted and seated snugly in each of the female anchorages. The 12 wires of each cable were spaced around the plug so that each wire was in one of the plug's longitudinal grooves.

(3) Two jacks were connected to the ends of two cables diametrically opposite each other in order that these cables be simultaneously tensioned.

(4) An initial 500-psi hydraulic pressure was applied. With this pressure maintained in the jacks, a set distance of 8 in. was marked on the wires at the jack end (J) and 6 in. was marked at the plug end (P).

(5) The required pressure was then applied in stages, Tables A.10 to A.12, until a maximum jack pressure of 5600 psi was produced. The elongation at the jacking end and pull in at the plug end were measured. The net elongation of the wire is the required quantity.

(6) After the proper elongation had been obtained for a pair of cables, the pressure was locked in the tensioning cylinder, and a specified pressure was applied to the plugging piston.

(7) The pressure was then released, and the jacks were removed and transferred to the next pair of cables.

In the post-tensioning operation a jack pressure of 5300 psi applied to the cables produced a bearing stress of 122 psi on the faces of the precast cylinders. The maximum jack pressure of 5600 psi was applied to cables 1 and 2 (see Table A.10) to allow for friction between the precast members and the base slab.

Stages 1 and 2 of the above procedure were performed at some time prior to jacking. Immediately before the post-tensioning operation, a mixture of 1 to 1 grout was hand trowelled into the eleven $1\frac{1}{2}$-in. joints between rings. Wet burlap was placed over the grouted joints. Steps 3 through 7 were then carried out with the grout in a workable condition.

A.4.6 Patching

During the construction of structures II-3, II-4, and II-5, the steel loops for hanging instruments were cast into the walls, roof, and floor slabs. After removal of the interior formwork, the ends of these loops were broken out of the concrete. The areas around the broken-out sections were subsequently patched. Structure II-2 also had loops cast in the cast-in-place portions, but owing to the time element no patching was done after removal of the formwork.

A.4.7 Doors

Minor defects were apparent in each of the three different makes of doors. Although the Dumoulin doors for structures II-1, II-2, and II-5 had the simplest construction details, the blast doors had no provisions for adjustment of the dogs or hinges. Consequently, if either the flat-plate door or the door frame became warped during shipment or erection, it was exceedingly difficult to close the door properly. This situation occurred in the door for structure II-5 and was partially remedied by grinding the door and door frame down so that the door could be closed with the aid of hand tools, Fig. 3.63.

Before arrival of the Dumoulin fire door for structure II-1 at the Test Site, some cracking of the soft fire-resistant concrete had occurred because of improper crating and handling during shipping. No difficulty of operation was experienced with the Dumoulin gastight doors.

In structure II-3 three doors (blast, fire-resistant, and gastight) manufactured by the Bauche Co. were used. During preshot trial operation of the mechanical equipment, two handles welded to the latching dogs were broken off by hand pressure (no tools). One each was broken off the fire door and the gastight door. For the test, the broken handles were put on the inside face of the doors to permit the doors to be closed and dogged from the outside.

The fire door was slightly warped and did not set flush against the door frame. The top corner away from the hinges was $\frac{3}{16}$ in. from the door frame; consequently the adjustment given by the beveled slots in the door frame was insufficient, and the two dogs away from the hinges had to be beveled off to allow the door to be latched.

A slightly different problem arose with the dogs on the blast door. With the door open it is possible to put the dogs in a closed position. If then the door is shut with the dogs inadvertently in the closed position, the dogs are slammed against the door frame, and the latches tend to be deformed. If bending of the dogs occurs, it is impossible to latch the door. This situation arose and was remedied in the field by wedging the assembly straight.

Structure II-4 had two doors manufactured by Society Cheops. The blast door and combination fire-resistant gastight door each had four latching pins that were inserted in circular recesses in the door frame. The blast door had no provisions for adjustment of the sliding bolts, and therefore the recesses in the door frame were enlarged to allow the bolts to seat properly. Adjustment provided on the other door was insufficient, and these holes too were enlarged by grinding.

A.4.8 Ventilation Equipment

No difficulty was experienced in the installation of the ventilation equipment for structures II-4 or II-5. In structure II-3 the dimension of $1\frac{1}{8}$ in. from the roof to the top of the vent pipe was changed to 2 in. to allow turning of the top wing nut that holds the sealing cover.

Some minor difficulty occurred in the assembly of the ventilation system of structure II-1. Since cast-in-place ventilation equipment is joined by prefabricated open duct work in the interior of shelter II-1, any error of placement before pouring requires an adjustment of the connecting parts. In II-1 some bending and adjustment of the ductwork from exhaust stack No. 1 to the ventilator unit was required. This ventilator was shimmed in position.

The slip joints for the air distribution ductwork had insufficient overlap. Some joints that had come apart repeatedly were fastened together with sheet metal screws to hold them during construction.

In the circular structure, shelter II-2, the natural-ventilation air-intake pipe shifted slightly during placing of the concrete. To correct the misalignment, a section was chipped from the wall of the chamber to accommodate the electric intake motor, and the piece of galvanized ductwork from the sand filter was cut and resoldered to allow a tight connection. The gastight door could not be fully opened because of the air distribution duct, which extended into the main chamber.

Table A.1—SCHEDULE OF CONSTRUCTION (1957)

		Floor slab				Walls, roof slab, and entranceways				
	Excavation	Forms	Steel	Concrete		Interior forms	Steel	Exterior forms	Concrete	
Structure	Date	Date	Date	Date	Quantity	Date	Date	Date	Date	Quantity
II-1	4/30	5/4	5/20	5/21	68	6/3	6/9	6/13	6/13	188
II-2*										
Shaft T1	5/1	7/8	7/26	7/26	8	7/28	8/3	8/6	8/6	30
Shaft T2	5/1	7/8	7/26	7/26	9	7/27	8/2	8/3	8/6	37
II-3	4/30	5/4	5/21	5/23	31	5/26	6/6	6/7	6/7	70
II-4	5/1	5/14	6/3	6/4	41	6/5	6/10	6/11	6/12	88
II-5	5/2	5/13	5/31	5/31	33	6/5	6/20	6/22	6/24	70

*Precast circular segment setting bed poured 5/14; precast circular segments placed 6/23; precast circular segments post-tensioned 6/24.

Table A.2—LABORATORY TEST RESULTS (CYLINDERS)*

		Test results, psi		
Structure	Member	7 days	28 days	90 days
II-1	Floor slab	2160	3340	
		2220	3330	
		2190	3080	
	Walls and roof	2340	3480	3740
		2180	3430	3880
		2340	3310	3940
II-2†	Floor slab (T2)	3160		
		3150		
		2880	3180	
	Floor slab (T1)		3410	
			3450	
	Wall and roof (T2)	3130	3720	4080
			3740	4220
				4070
	Wall and roof (T1)	2850	3410	3970
			3300	3800
				3950
II-3	Walls and roof	1920	2740	3410
		1900	2610	3180
		1920	2830	3370
II-4	Floor and stairs	1930	3000	
		2070	2350	
		2030	2590	
	Walls and roof	2250	3190	3550
		2180	3370	3420
		1850	3220	3540
II-5	Floor and stairs	2340	3020	
		2120	2920	
		2250	2850	
		2550	3280	3120
		2470	3240	3460
		2480	3180	3410

*All concrete has type II Portland cement except as noted.

†Portland Hi-Early cement.

Table A.3— LABORATORY TEST RESULTS (CUBES)*

Structure	Member	Test results, psi 7 days	28 days
II-1	Walls and roof	2614	3317
		2510	3257
		2328	3592
II-2†	Floor slab (T2)	2870	
		2980	
		2760	
			3010
	Floor slab (T1)		2690
			2795
	Walls and roof (T2)	3200	3160
			3220
	Walls and roof (T1)	3010	3700
			3540
II-3	Walls and roof	2165	2971
		2104	3258
		2117	2800
II-4	Floor and stairs	2390	2807
			2657
	Walls and roof	2387	3182
		2177	3121
		2441	3000
II-5	Walls and roof	2509	2950
		3054	3006
		2299	3232

*All concrete has type II Portland cement except as noted.

†Portland Hi-Early cement.

Table A.4— LABORATORY TEST RESULTS (BEAMS)*

Structure	Member	Test results, psi 28 days	90 days
II-1	Roof	596	500
		546	544
		481	559
II-2†	Roof (T2)	485	650
			545
	Roof (T1)	405	555
			560
II-3	Roof	382	476
		522	568
		443	527
II-4	Roof	564	577
		530	548
		534	554
II-5	Roof	374	‡
		460	460
		114	436

*All concrete has type II Portland cement except as noted.

†Portland Hi-Early cement.

‡No results were obtained from cylinder tested.

Table A.5— AVERAGE VALUES OF CONCRETE TEST DATA*

Specimen	Structure	Test results, psi 7 days	28 days	90 days
Cylinders	II-1	2238	3328	3853
	II-2†	3400	3459	4015
	II-3	1913	2727	3320
	II-4	2052	2953	3503
	II-5	2368	3082	3330
Cubes	II-1	2517	3389	
	II-2†	2924	3171	
	II-3	2129	3010	
	II-4	2324	2955	
	II-5	2617	3063	
Beams	II-1		541	534
	II-2†		445	578
	II-3		449	523
	II-4		543	560
	II-5		816	448

*All concrete has type II Portland cement except as noted.
†Portland Hi-Early cement.

Table A.6 — CONCRETE HAMMER TESTS (Equivalent Cylinder Strength, psi)*

Structure	Hammer No.	Wall facing GZ Preshot	Wall facing GZ Postshot	Wall away from GZ Preshot	Wall away from GZ Postshot	Roof slab Preshot	Roof slab Postshot	Floor slab Preshot	Floor slab Postshot
II-1	1	3400	3600	3250	2400	3550	2600	1500	1800
	2		5980		5430		7810		3720
II-2	1	3900	2700	3700	2650	3750	2500	3950	2550
	2		6600		6710		6900		
II-3	1	3250	2950	3100	2350	3650	2450	1700	1600
	2		3720		4520		7260		3840

*Hammer No. 1 supplied by Holmes & Narver, Inc. (#1639); hammer No. 2 supplied by FCDA.

Table A.7—TYPICAL CONCRETE-MIX DESIGN

Sieve size	Per cent passing U. S. standard sieve: Fine aggregate	Coarse aggregate	Combined
1.5 in.		100.0	100.0
¾ in.		59.0	76.4
⅜ in.		11.6	49.2
#4	100.0	1.4	43.3
#8	78.8		33.5
#16	57.0		24.2
#30	32.9		14.0
#50	17.9		7.8
#100	4.3		1.8
F. M.	3.091	7.280	5.498
Specific gravity (S. and S.D.)	2.47	2.665	

Mix design for one cubic yard of concrete – 3000 psi
Absolute volume of aggregate in one cubic yard of concrete – 19.73 cu ft
Weight of one cubic yard batch of aggregate – 3240 lb

	Per cent	Batch wt., lb		Absolute vol., cu ft
Gravel			2000	12.03
Sand, dry	39	1188		7.70
Free water in sand, 6.2 gal	4.35	52		0.84
		1240	1240	
Water, added 28.5 gal			237	3.80
Cement, 5.5 sacks			517	2.63
			Total	27.00

Maximum slump = 5 in.

Table A.8—LABORATORY TEST RESULTS OF REINFORCEMENT AND POST-TENSIONING WIRES

Type	Size, mm	Yield stress, psi: Average	Low	High	Ultimate stress, psi: Average	Low	High	Elongation,* %: Average	Low	High
ADx	10	52,037	46,550	55,750	72,862	64,550	76,900	25.62	23.50	27.00
ADx	12	43,125	40,800	44,500	57,600	66,650	58,500	29.87	28.00	33.00
TOR	12									
TOR	16	65,062	62,750	68,250	79,050	76,900	80,200	15.00	13.00	16.00
TOR	20	61,687	58,450	64,600	74,787	72,050	77,750	16.25	16.00	17.00
TOR	32	60,562	58,050	62,350	72,262	75,000	78,800	19.12	18.00	20.00
Cable wires		219,583	217,500	221,800	251,150	250,150	253,450	5.6	5.6	6.2

*Per cent elongation for 8-in. specimen.

Table A.9—IN-PLACE DENSITY TEST RESULTS

Structure	In-place density, lb/cu ft: Existing soil, av.	Backfill at mid-height	Backfill at final grade	Location of mid-height reading*
II-1	121	102	135	North
II-2	121	134	131	North
II-3	119	102	136	South
II-4	119	125	136	South
II-5	123	119	121	South

*North, side of structure facing GZ; south, side of structure facing away from GZ.

Table A.10—OVER-ALL LENGTH OF PRECAST CYLINDERS DURING POST-TENSIONING OPERATION

Cable No.	Relative distance between ends of precast segments: At 500 psi* (1)	At 4600 psi* (2)	At 5000 psi* (3)	At 5300 psi* (4)	At 5600 psi* (5)
1	20 ft 1 in.	19 ft 11¾ in.	19 ft 11⅛ in.		19 ft 11⅛ in.
2	20 ft 0 in.	19 ft 9½ in.	19 ft 9½ in.		19 ft 9½ in.
3	19 ft 11 in.		19 ft 10⅝ in.	19 ft 10⅝ in.	
4	19 ft 10½ in.		19 ft 10 in.	19 ft 10 in.	
5	19 ft 10⅛ in.		19 ft 10 in.	19 ft 10 in.	
6	19 ft 10⅛ in.		19 ft 10 in.	19 ft 10 in.	
7	19 ft 9½ in.		19 ft 9⅜ in.	19 ft 9⅜ in.	
8	19 ft 10⅞ in.		19 ft 10⅞ in.	19 ft 10⅞ in.	

*Hydraulic pressure produced in the jack.

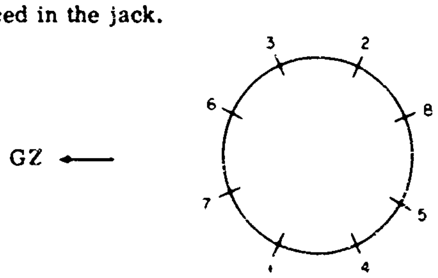

Location of cables

Table A.11 — GAUGE LENGTH DURING POST-TENSIONING OPERATION

Cable No.	Relative distance between gauge mark and reference point									
	At 500 psi* (6)		At 4600 psi* (7)		At 5000 psi* (8)		At 5300 psi* (9)		At 5600 psi* (10)	
	J	P	J	P	J	P	J	P	J	P
1	8 in.	6 in.	10 7/8 in.	5 3/4 in.	11 in.	5 3/4 in.			11 3/4 in.	5 3/4 in.
2	8 in.	6 in.	10 5/8 in.	5 3/4 in.	11 in.	5 3/4 in.			11 7/8 in.	5 3/4 in.
3	8 in.	6 in.			9 3/4 in.	5 11/16 in.	9 13/16 in.	5 11/16 in.		
4	8 in.	6 in.			9 7/8 in.	5 11/16 in.	9 7/8 in.	5 11/16 in.		
5	8 in.	6 in.			9 13/16 in.	5 11/16 in.	9 7/8 in.	5 11/16 in.		
6	8 in.	6 in.			9 3/4 in.	5 11/16 in.	9 13/16 in.	5 11/16 in.		
7	8 in.	6 in.			9 5/8 in.	5 3/4 in.	9 7/8 in.	5 3/4 in.		
8	8 in.	6 in.			9 11/16 in.	5 3/4 in.	9 7/8 in.	5 3/4 in.		

NOTE: J, distance between jack end gauge mark and reference point; P, distance between plug end gauge mark and reference point.

*Hydraulic pressure produced in the jack.

Table A.12 — RELATIVE AND ABSOLUTE ELONGATION, AND STRESSES OF POST-TENSION CABLES

Cable No.	Δ_1 (11) (in.)	Δ_2 (12) (in.)	Δ_3 (13) (in.)	Δ_4 (14) (in.)	Δ_5 (15) (in.)	Wire stress (psi)
1	1 7/8	3 3/4	1/4	3 1/2	1 5/8	205,770
2	2 1/2	3 7/8	1/4	3 5/8	1 1/8	125,740
3	3/8	1 13/16	5/16	1 1/2	1 1/4	139,710
4	1/8	1 7/8	5/16	1 9/16	1 5/16	146,690
5	1/8	1 7/8	5/16	1 9/16	1 7/16	160,660
6	1/8	1 13/16	5/16	1 1/2	1 3/8	153,680
7	1/8	1 7/8	1/4	1 5/8	1 1/2	167,650
8	0	1 7/8	1/4	1 5/8	1 5/8	205,770

Δ_1 Relative movement of end of the precast segments due to change in jack pressure from 500 psi to 5300 or 5600 psi, (1) to (4) or (5).

Δ_2 Absolute movement of gauge mark at jack end due to elongation of cable, pull in of plug end and relative movement of precast segments Δ_1. J (9) or J (10) to J (6).

Δ_3 Pull in at plug end. P (6) to P (9) or P (10).

Δ_4 Movement of gauge mark at jack end due to elongation of cable and relative movement of precast segments Δ_2 (12) to Δ_3 (13).

Δ_5 Absolute elongation of cables.

Stress in cable is based on E = 28,500,000.

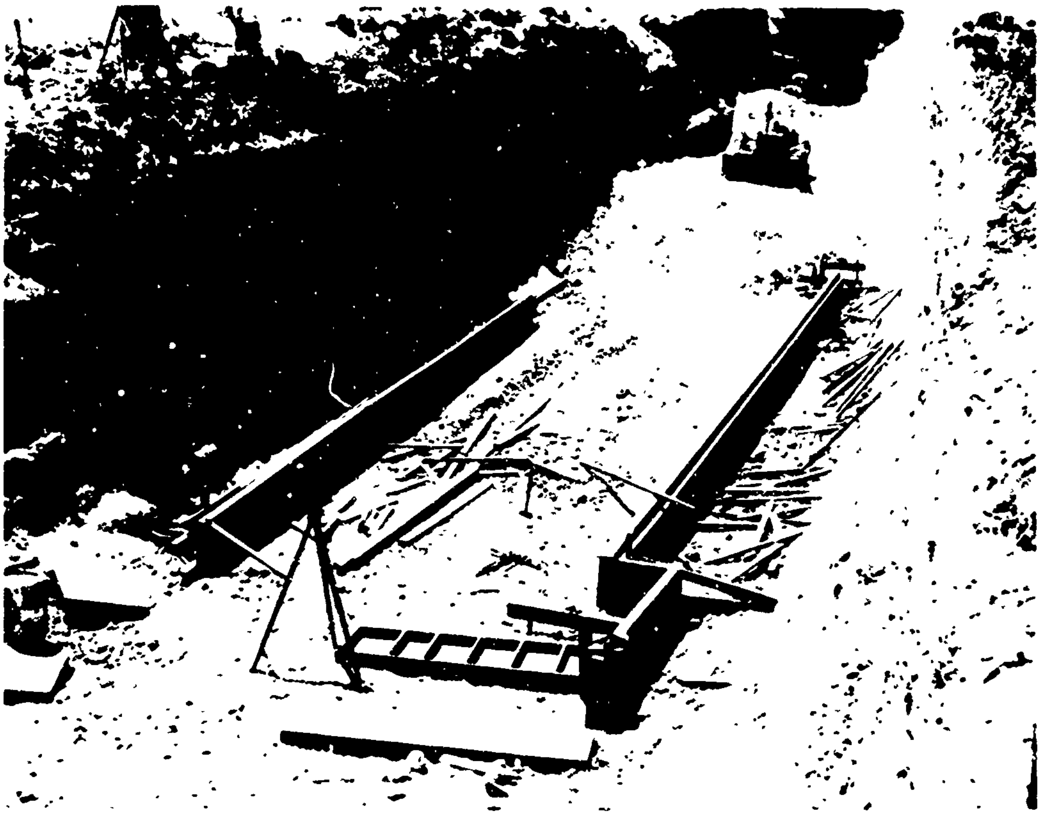

Fig. A.1—Structure II-1, partially erected base slab formwork (May 2, 1957).

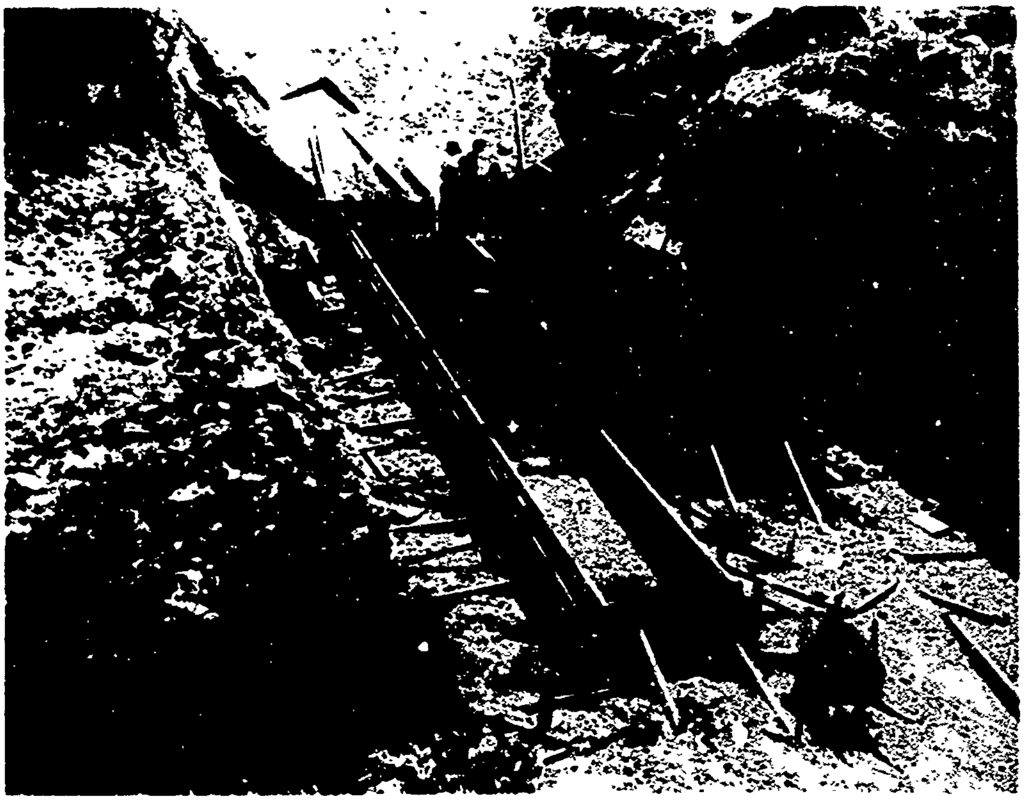

Fig. A.2—Structure II-1, partially placed base slab reinforcement (May 9, 1957).

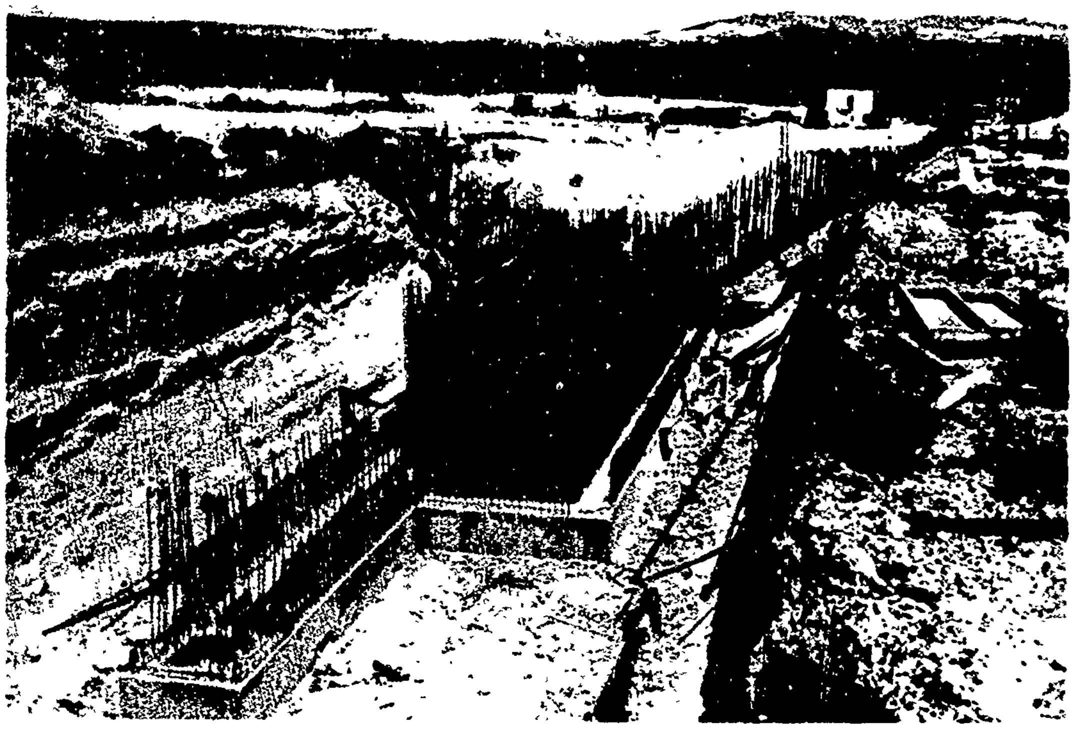

Fig. A.3—Structure II-1, base slab poured; interior formwork partially erected (May 27, 1957).

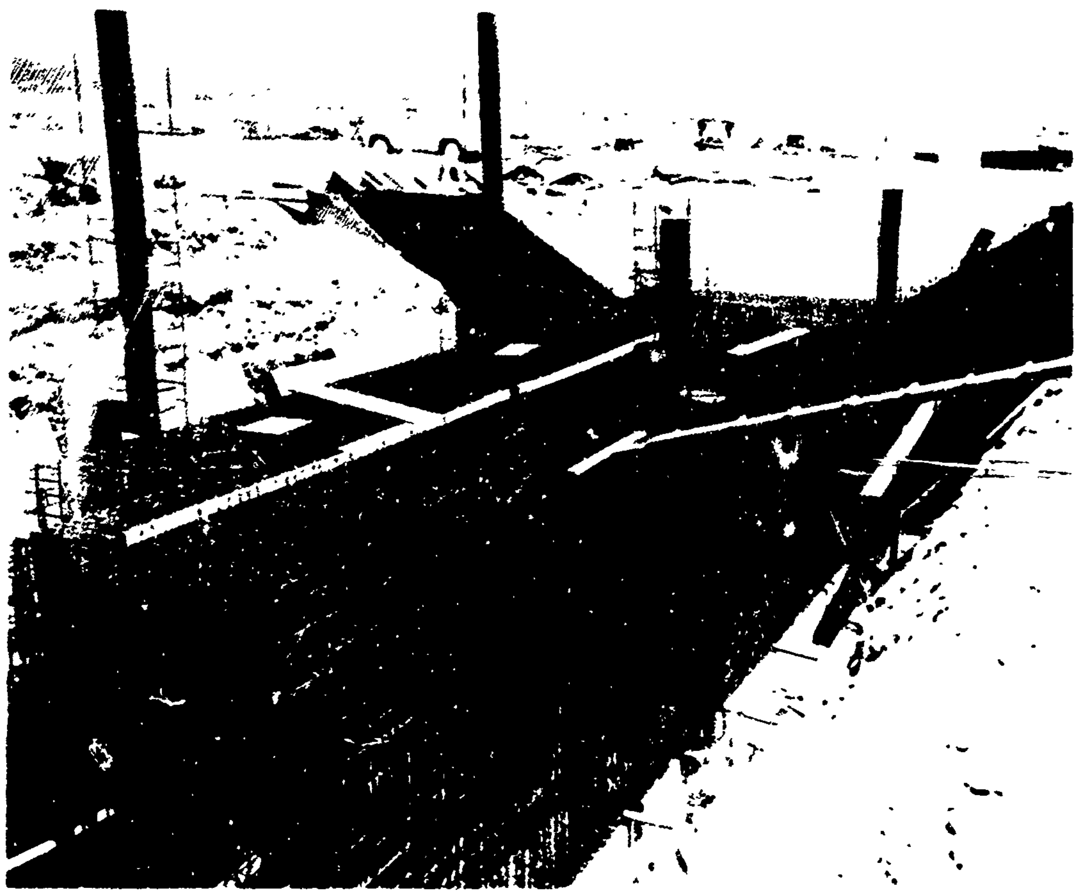

Fig. A.4—Structure II-1, roof slab and wall reinforcement placed (June 7, 1957).

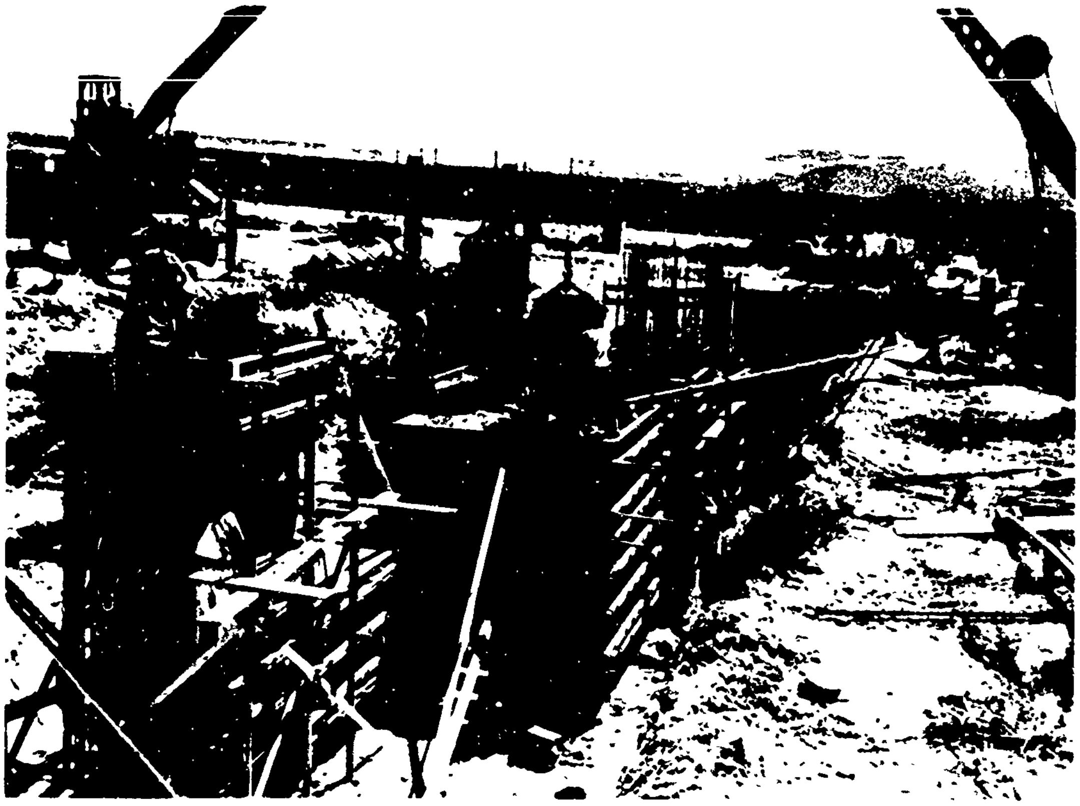

Fig. A.5—Structure II-1, concrete placement for structure above base slab (June 13, 1959).

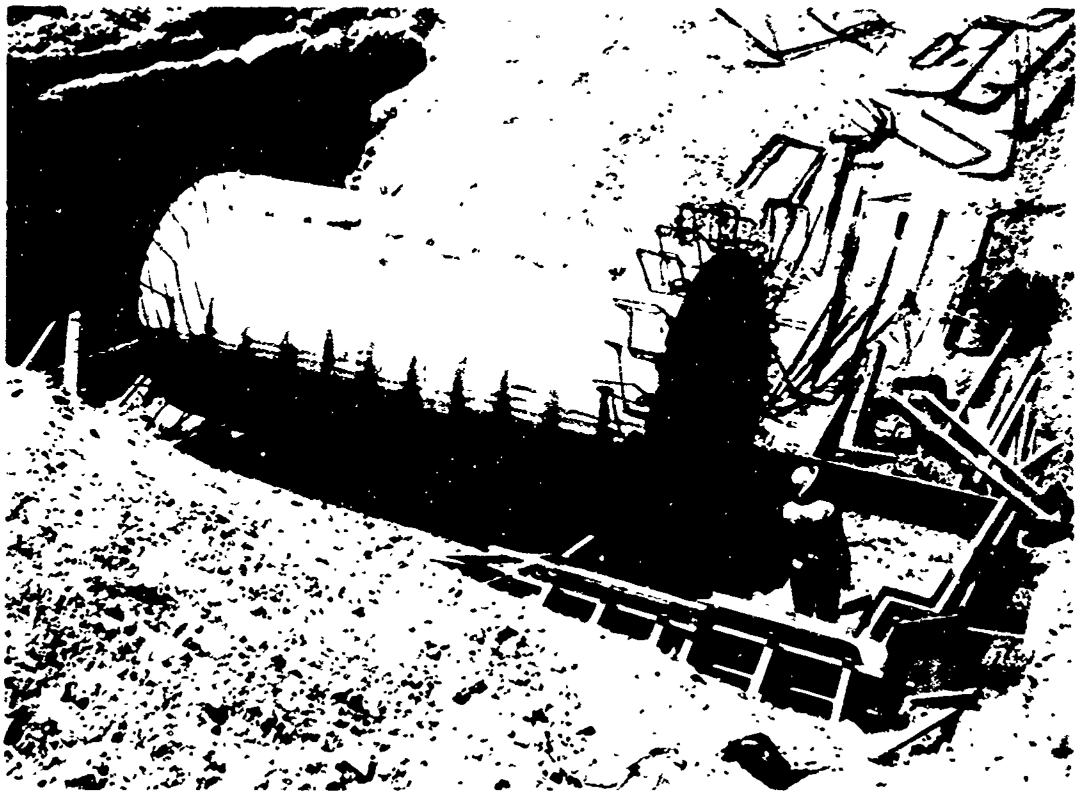

Fig. A.6—Structure II-2, precast circular segments placed (July 9, 1957).

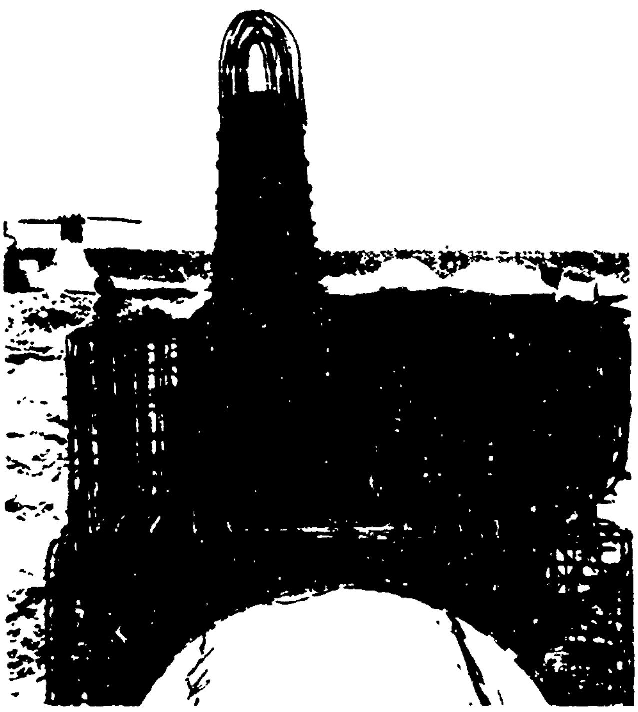

Fig. A.7—Structure II-2, reinforcement of upper section of shaft T-1 (Aug. 1, 1957).

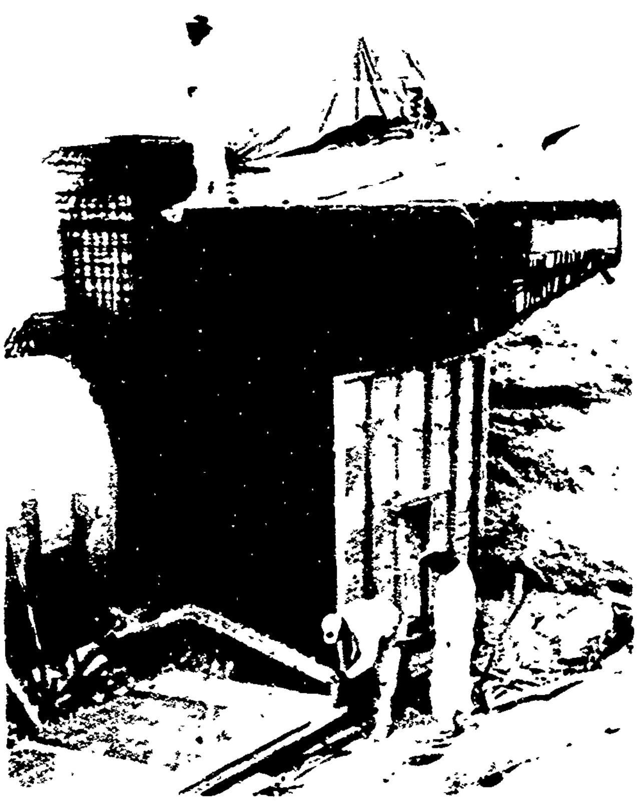

Fig. A.8—Structure II-2, erecting exterior formwork for shaft T-2 (Aug. 2, 1957).

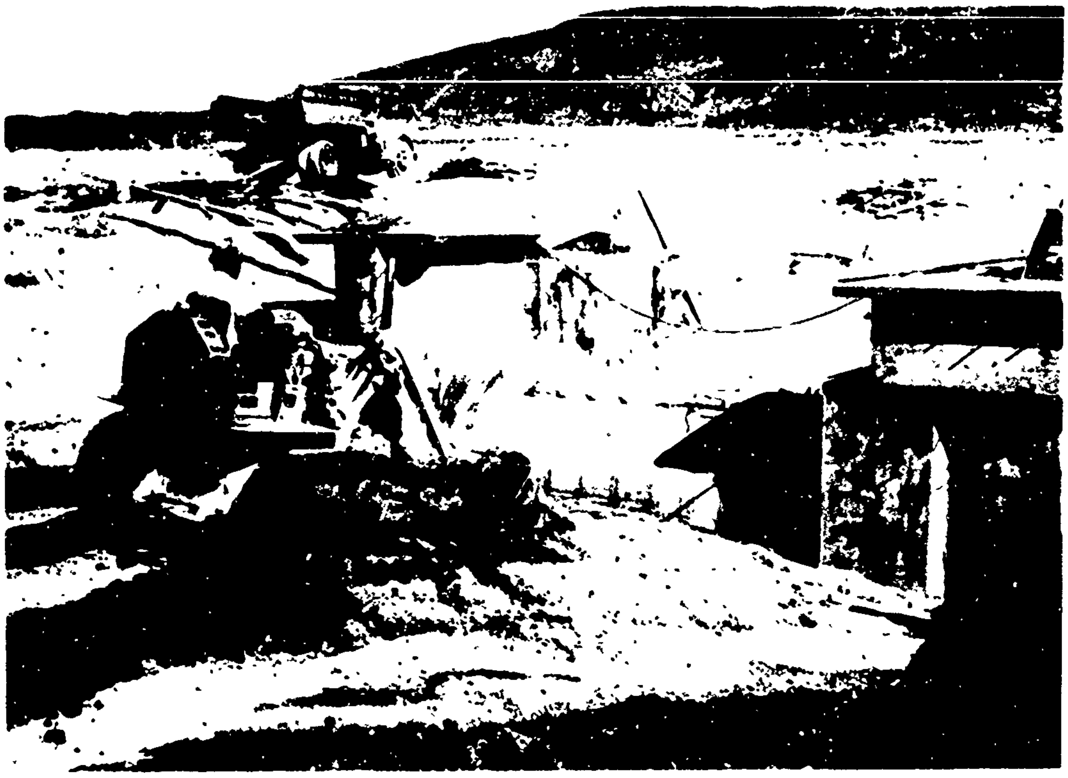

Fig. A.9—Structure II-2, during backfilling (Aug. 7, 1957).

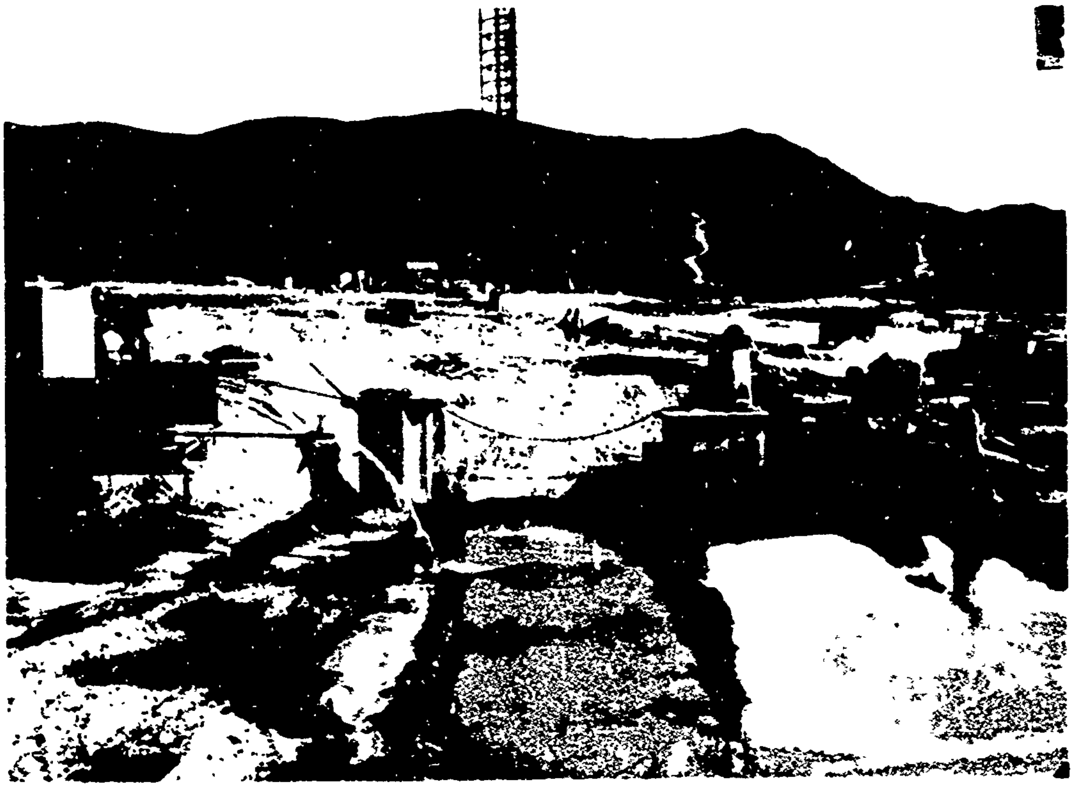

Fig. A.10—Structure II-2, typical backfill saturation procedure (Aug. 7, 1957).

Fig. A.11—Structure II-2, standard compaction procedure near structure (Aug. 7, 1957).

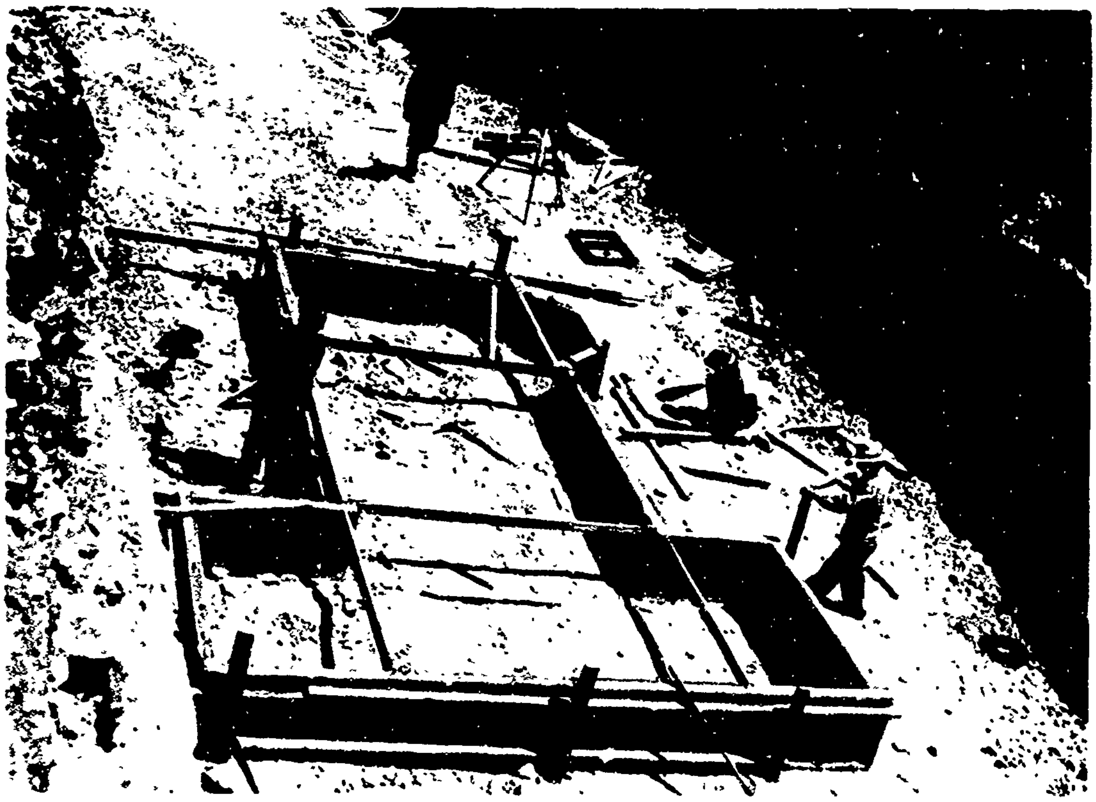

Fig. A.12—Structure II-3, erecting base slab formwork (May 3, 1957).

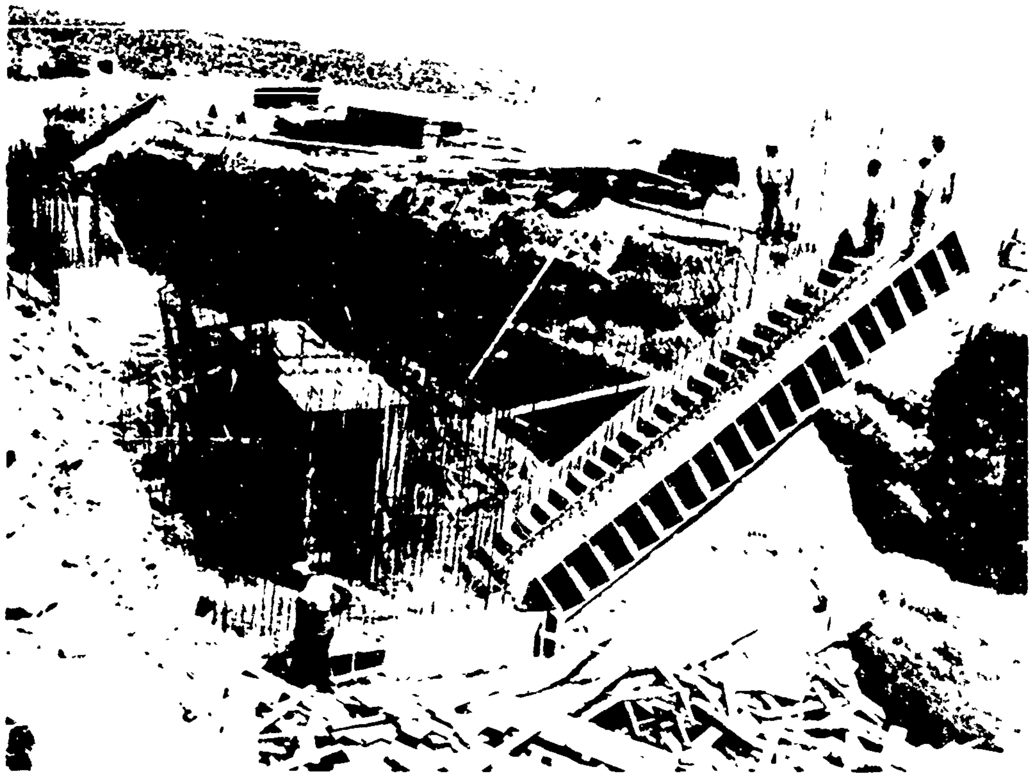

Fig. A.13—Structure II-3, stripping base slab formwork (May 27, 1957).

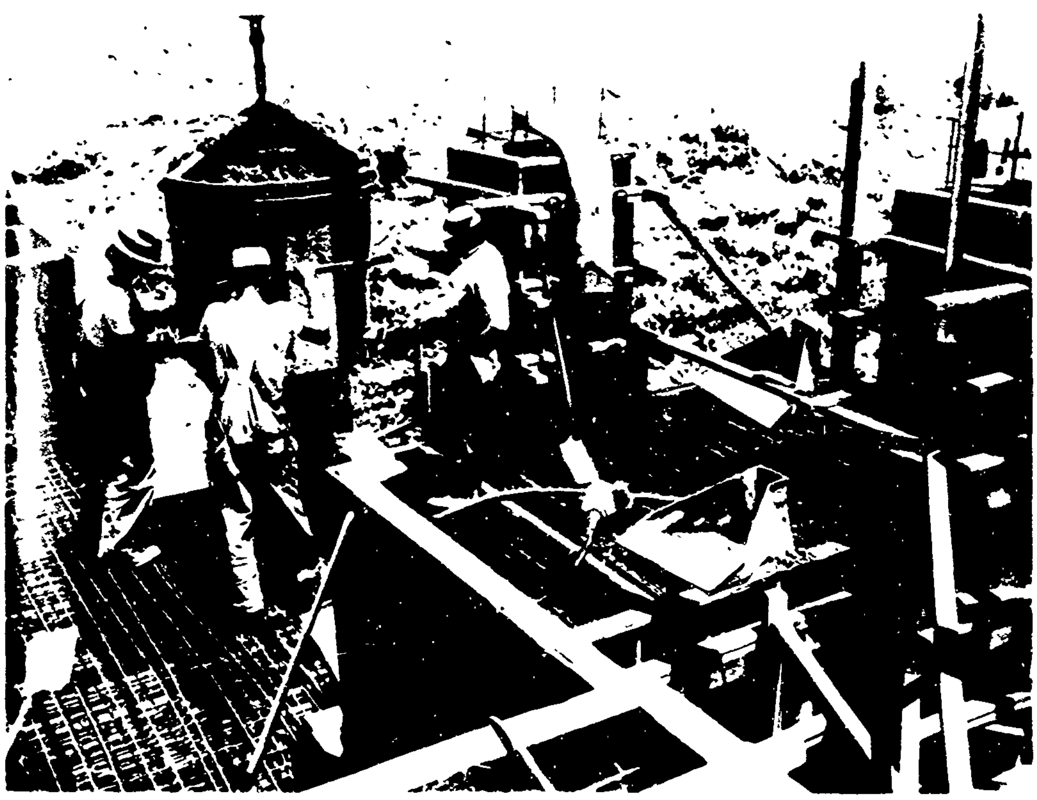

Fig. A.14—Structure II-3, concrete placement in walls and roof slab (June 7, 1957).

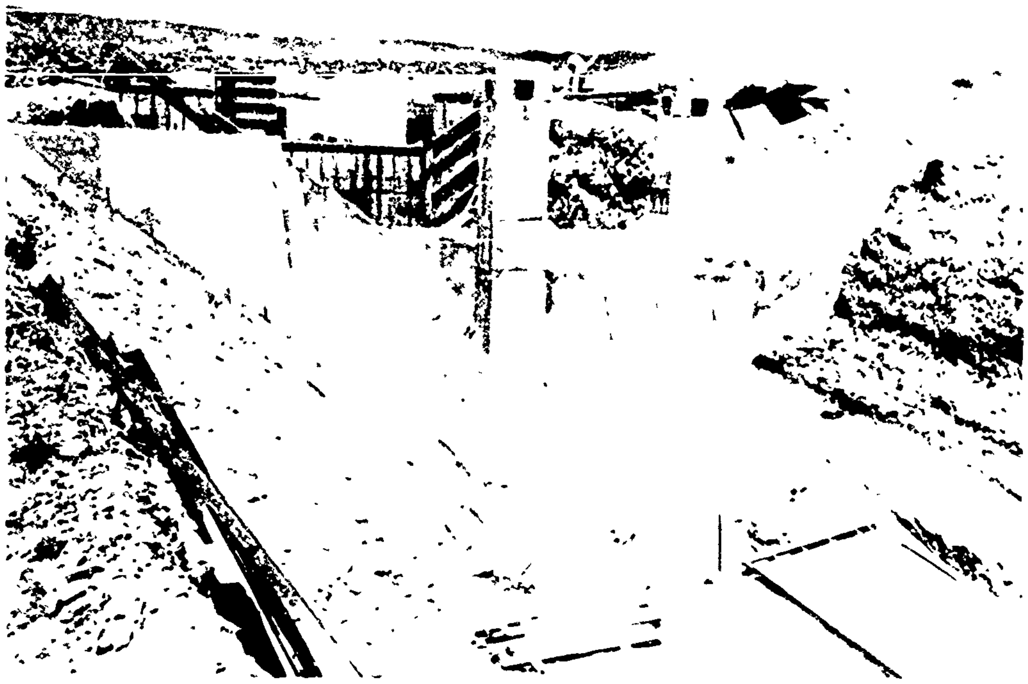

Fig. A.15—Structure II-3, before backfilling (June 13, 1957).

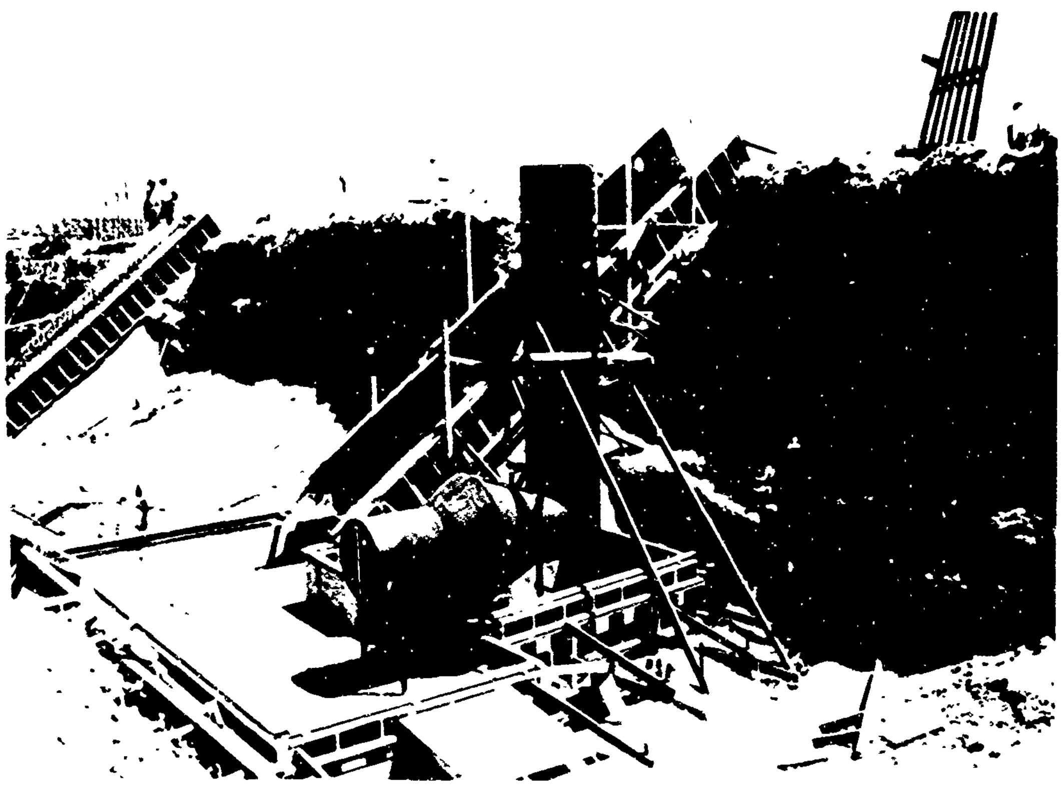

Fig. A.16—Structure II-4, base slab formwork with ventilation pipe in place (May 27, 1957).

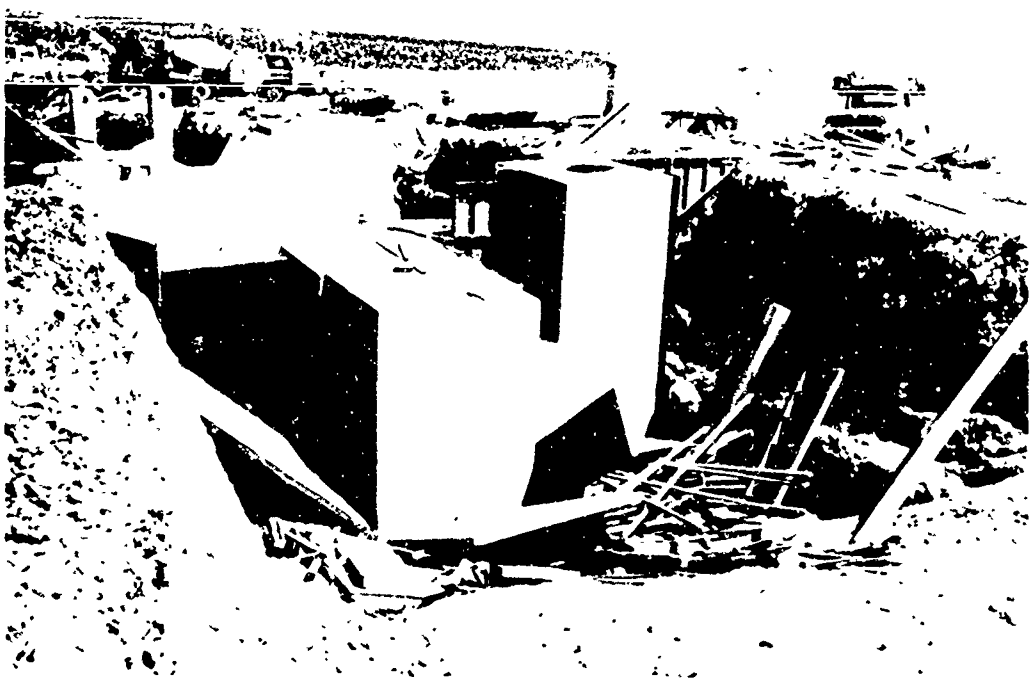

Fig. A.17—Structure II-4, stripping exterior formwork (June 13, 1957).

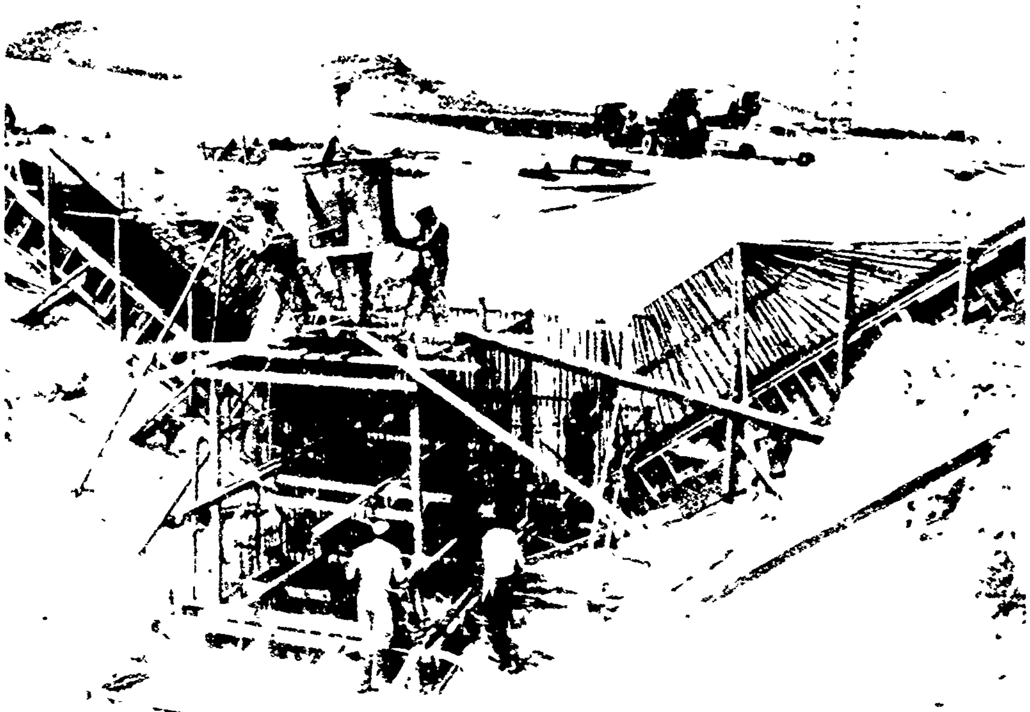

Fig. A.18 - Structure II-5, concrete placement in base slab (May 31, 1957).

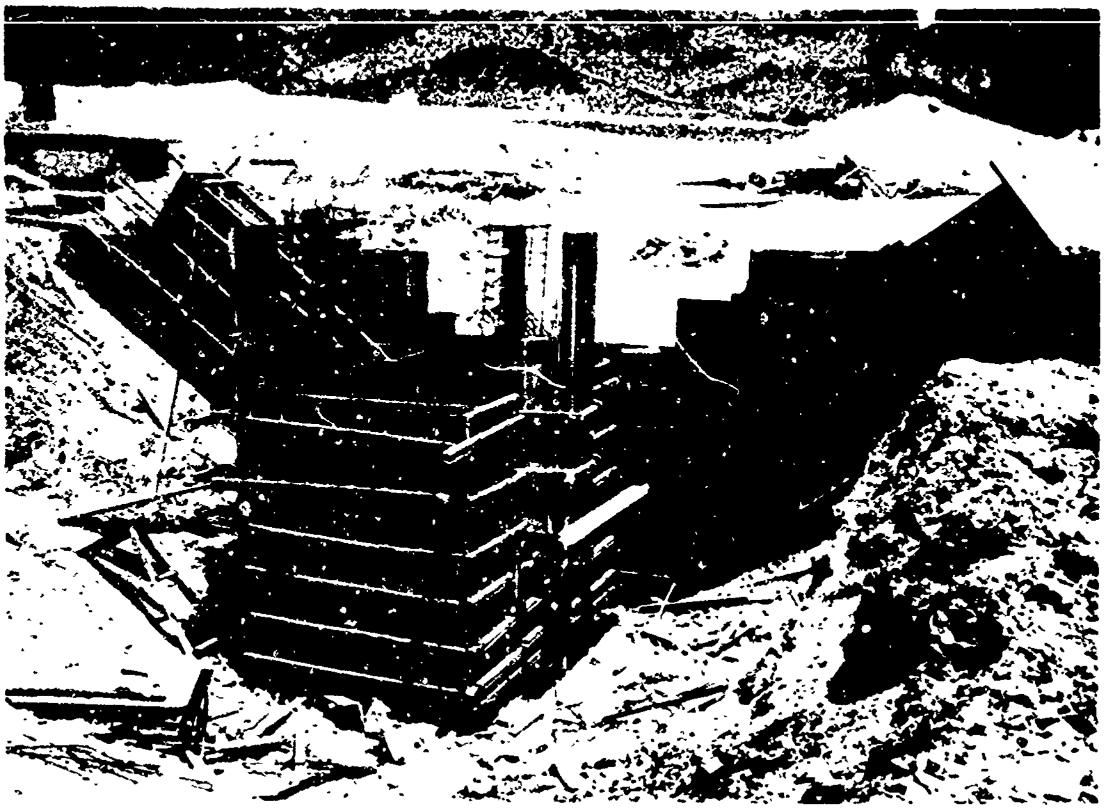

Fig. A.19—Structure II-5, before concrete placement (June 23, 1957).

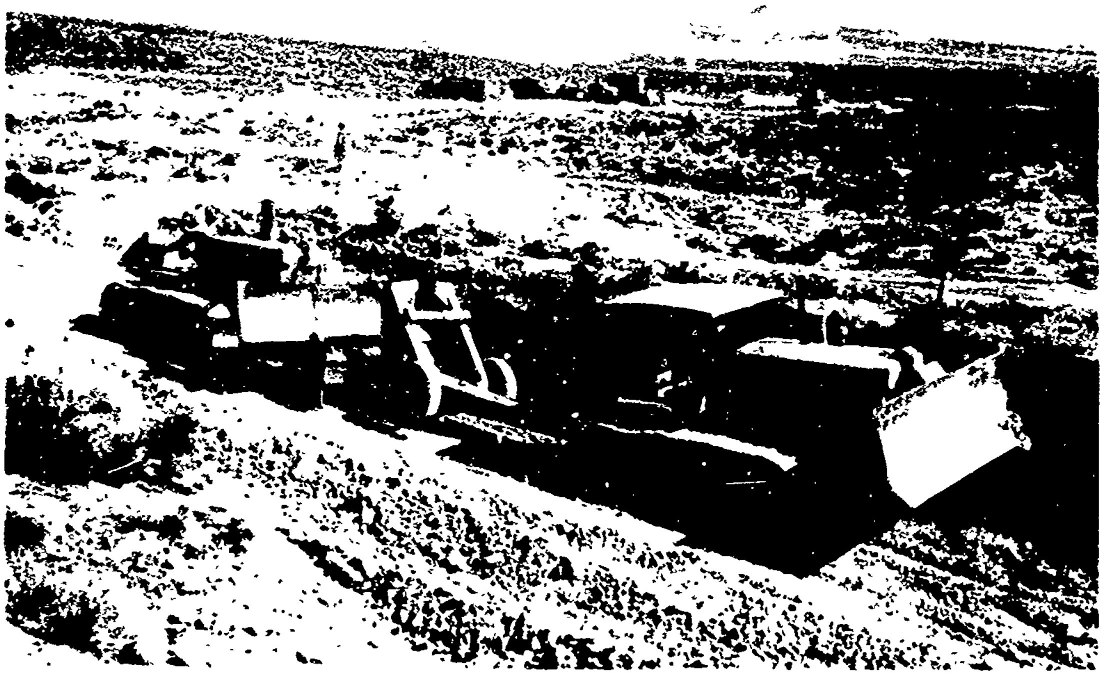

Fig. A.20—Typical excavation equipment.

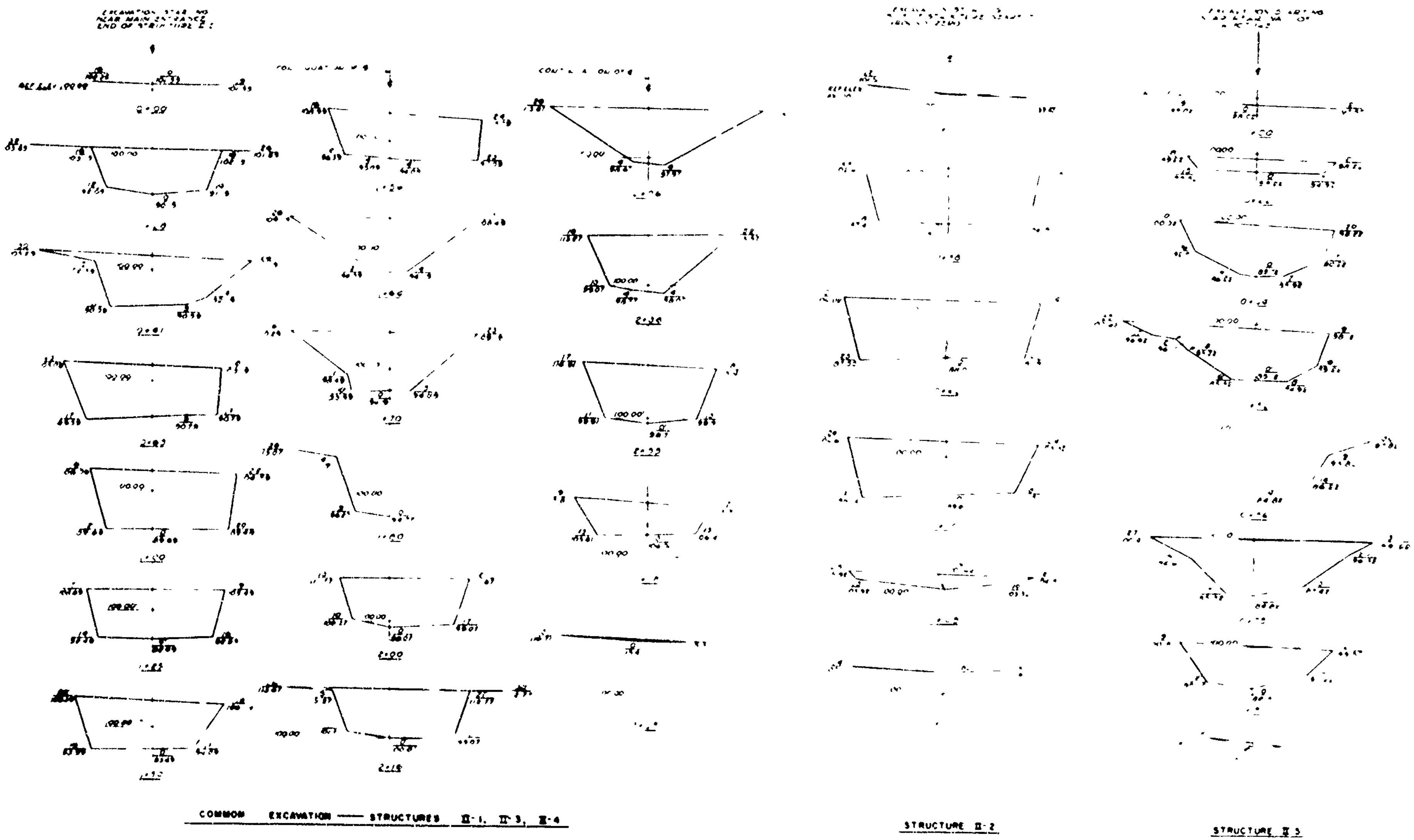

Fig. A.21—Structures II-1, II-2, II-3, II-4, and II-5, excavation.

Appendix B

SNPC DESIGN CALCULATION FOR RECTANGULAR CONCRETE SHELTER, TYPE 60*

Technical Consultant: M. Antoine Martin
Chief Engineer of the Bridge and Highway Department
Ministry of the Interior, Service National de la Protection Civile

B.1 GENERAL

The type 60 shelter is a reinforced concrete box 60 cm thick on all faces.

It is designed for an overpressure of 10 kg/cm^2, due to the blast wave of an atomic or thermonuclear bomb and a reversal of $^1/_{16}$ of the maximum overpressure.

The forces have been calculated based on the diagram of Mr. Pigeaud, with a reduction of 20 per cent of the moment in the center to take care of the partial fixity of the slab on its supports. The compression in the slabs is neglected, and the ratio of the modulus of elasticity of concrete and steel is assumed to be $m = 15$.

Allowable Stresses

Concrete	
Allowable compression stress	125 kg/cm^2
Allowable shear stress without stirrups	10 kg/cm^2
Steel	
Steel Tor	40 kg/mm^2
Smooth round ADx steel with diameter ≤ 10 mm	29 kg/mm^2
Bond	
Bond stresses between Tor and concrete	33 kg/cm^2

Notations

ω' = area of main steel (A_s)
x = circumference of main steel
n_a' = stress in main steel
n_b = compressive stress in extreme fiber of concrete (f_c')
h = total height of concrete section (t)
h' = distance between extreme compressive concrete fiber and centroid of the main steel (d)

*Reinforcement drawn and calculated by the Central Service of Technical Studies of Bridges and Highways – M. Robinson, ingenieur et chief; M. Prunier, ingenieur ordinaire. The calculations were furnished in French and translated by Ammann & Whitney.

z = level arm of elastic couple (jd)
b = width of section (b)
ω_e' = area of secondary reinforcement

B.2 MAIN BODY OF THE SHELTER

B.2.1 Applied Forces

(a) Horizontal Slabs. In the first positive phase, the roof of the shelter is loaded, due to the blast wave, by an overload of 100 tons/m^2, by the load of the earth above and by its own dead load.

Weight of 1 m^3 of earth, 2 tons/m^3
Weight of 1 m^3 of reinforced concrete, 2.5 tons/m^3

(b) Vertical Slabs. At a particular pressure level the walls of the shelter are loaded on one side by earth pressure that is assumed to be between 25 and 40 per cent of the vertical pressure at that same pressure level.

B.2.2 Roof of the Shelter

For purposes of analysis, the roof of the shelter is taken as various elementary slabs that are limited by the interior walls, the exterior walls, and the visible or incorporated lintel beams of the slab.

An analysis will be made of the 3.30 × 3.00 m, 2.60 × 1.20 m (entrance chambers), and 4.00 × 1.20 m (water closet, etc.) slabs.

The maximum vertical applied pressure has the following values:

Blast-wave overpressure	100 tons/m^2
Weight of overburden (earth), 1.5 × 2	3 tons/m^2
Weight of concrete (dead load), 0.6 × 2.5	1.5 tons/m^2
(Rounding off value)	0.5 tons/m^2
	105 tons/m^2

(a) Slabs, 3.30 × 3.00 m.

$a = 3.00$ m $\quad \rho = a/b = 0.91 \quad 1/\rho = b/a = 1.1$

$b = 3.30$ m

$P = 3 \times 3.3 \times 105 = 1039.5$ tons

(1) Bending moments at center of slab.

$M_1 = 0.039$

$M_2 = 0.0315$ (Pigeaud diagram)

In the direction of the short span

$$M_a = 0.8 \times (0.039 + 0.15 \times 0.0315) \times 1039.5 = 36.4 \text{ ton-m/m}$$

In the direction of the long span

$$M_b = 0.8 \times (0.0315 + 0.15 \times 0.039) \times 1039.5 = 31.1 \text{ ton-m/m}$$

(2) Shear stresses at the supports. At the center of the long side

$$T_a = \frac{1039.5}{2 \times 3.30 + 3.00} = 108.3 \text{ tons/m}$$

At the center of the short side

$$T_b = \frac{1039.5}{3 \times 3.30} = 105 \text{ tons/m}$$

(3) Stresses. The reinforcement is analyzed in the direction of the short span for which the stresses are maximum.

At the center:

$M = 36.4$ ton-m/m
$T = 0$
$h = 60$ cm
$h' = 56$ cm
$y = 15.6$ cm
$z = 50.8$ cm
$n_b = 92$ kg/cm^2
$n_a' = 35.7$ kg/mm^2

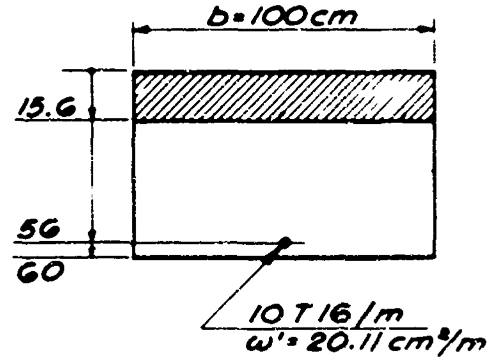

At supports:

$T = 108.3$ tons/m
$\omega' = 22.62$ cm^2/m
$x = 75.4$ cm/m
$h = 60$ cm
$h' = 54.8$ cm
$y = 16.2$ cm
$z = 49.4$ cm
$T/bz = 21.9$ kg/cm^2
$T/xz = 29.2$ kg/cm^2
$\omega_e' = 15.7$ cm^2/m
$e = 20$ cm
$n_e' = 28.0$ kg/mm^2

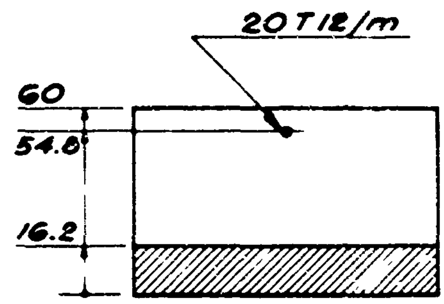

(Ten stirrups of round Adx with a diameter of 10 mm per meter at 20 cm on centers)

(b) Slabs, 2.60 × 1.20 m (entrance chamber).

$$\rho = a/b = 0.462$$

$$1/\rho = b/a = 2.16$$

$$P = 2.60 \times 1.20 \times 105 = 327.6 \text{ tons}$$

(1) Bending moments at center of slab.

$$M_1 = 0.0465$$

$$M_2 = 0.007$$

In the direction of the short span

$$M_a = 0.8 \times (0.0465 + 0.15 \times 0.007) \times 327.6 = 12.5 \text{ ton-m/m}$$

In the direction of the long span

$$M_b = 0.8\ (0.007 + 0.15 \times 0.0465) \times 327.6 = 3.7 \text{ ton-m/m}$$

(2) Shear stresses at the supports. At the center of the long side

$$T_a = \frac{327.6}{2 \times 2.60 \times 1.20} = 51.2 \text{ tons/m}$$

At the center of the short side

$$T_b = \frac{327.6}{3 \times 2.60} = 42 \text{ tons/m}$$

(3) Stresses Stresses in the direction of the short span.

At the center:

$M = 12.5$ ton-m/m
$h = 60$ cm
$h' = 56$ cm
$y = 11.6$ cm
$z = 52.1$ cm
$n'_a = 24.0$ kg/mm^2

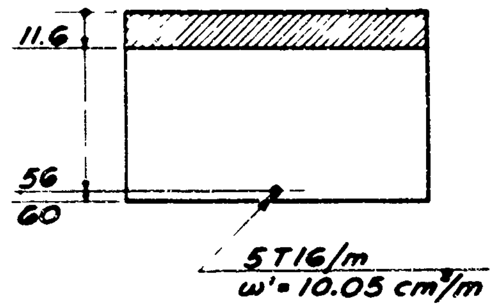

At supports:

$T = 51.2$ tons/m
$\omega' = 11.31$ cm^2/m
$x = 37.7$ cm/m
$h = 60$ cm
$h' = 56$ cm
$y = 12.3$ cm
$z = 51.9$ cm
$T/bz = 9.9$ kg/cm^2
$T/xz = 26.2$ kg/cm^2

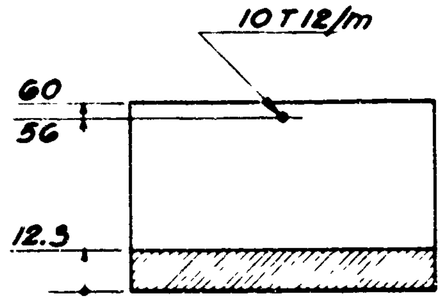

Stresses in the direction of the long span. The reinforcement at the center and at the supports is the same as the reinforcement in the other direction, even though the forces are smaller.

(c) Slab, 4.00 × 1.20 m. This slab forms the cover of the annexes of the shelter (water closet, etc.). The slab is supported by a projection of the interior wall, which is known as pilaster C4. Therefore the design of the 1.20 × 4.00 m slab is conservative.

(1) Bending moments at center of slab

$\rho = a/b = 0.30 \qquad 1/\rho = b/a = 3.33$

$P = 4.00 \times 1.20 \times 105 = 504$ tons

$M_1 = 0.036$

$M_2 = 0.0014$

Moment in the direction of the short span

$M_a = 0.8\,(0.036 + 0.15 \times 0.0014) \times 504 = 14.6$ ton-m/m

$M_b = 0.8\,(0.0014 + 0.15 \times 0.036) \times 504 = 2.7$ ton-m/m

(2) Shear stresses at the supports. At the center of the long side

$$T_a = \frac{504}{2 \times 4.0 + 1.2} = 54.8 \text{ tons/m}$$

At the center of the short side

$$T_b = \frac{504}{3 \times 4.0} = 42.0 \text{ tons/m}$$

(3) Stresses. Stresses in the direction of the short span.

At the center:

M = 14.6 cm/m
h = 60 cm
h' = 56 cm
y = 11.6 cm
z = 52.1 cm
n'_a = 27.9 kg/mm^2

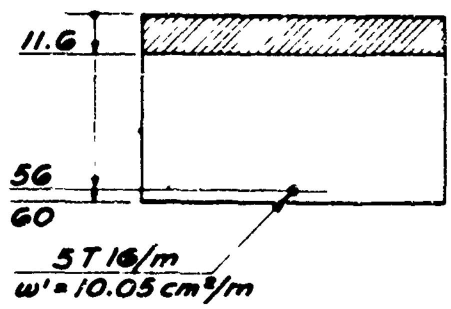

At supports:

T = 54.8 tons/m
h = 60 cm
h' = 56 cm
ω' = 11.31 cm^2/m
x = 37.7 cm/m
y = 12.3 cm
z = 51.9 cm
T/bz = 10.8 kg/cm^2
T/xz = 28.0 kg/cm^2

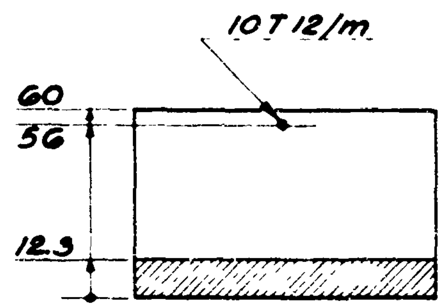

REMARK: The total shear as given by T/bz surpasses the allowable stresses, but, in reality, bearing on the partition wall diminishes this shearing stress.

Stresses in the direction of the long span. The principal reinforcement is identical to that placed in the other direction, even though the forces are smaller. The secondary reinforcement is unnecessary.

B.2.3 Floor of the Shelter

The roof-slab loading on the shelter is transmitted to the floor slab by the walls and then on to the ground.

If the reaction of the ground on the floor slab were uniform, the reinforcement of the floor slab would be identical to that of the roof slab (the dead load of the walls and of the floor slab is negligible). But, at the center of the slabs, cracks due to bending can only form after cracks due to bending at the supports at the walls. The cracks at the center would then bring a considerable deformation of the floor slab, and the floor slab would no longer be in direct contact with the ground. For that reason Tor 12's were used in the floor slab where Tor 16's were used in the roof slab, but the same Tor 12 layers were retained at the supports at the walls.

B.2.4 Walls of the Shelter

These are considered as slabs partially fixed in the perpendicular walls, the floor slab, and the roof slab.

The slab most heavily loaded will be analyzed. This slab measures 7.70 × 2.30 m.

(a) Applied Forces. The least favorable assumption corresponds to a horizontal pressure equal to 40 per cent of the overpressure at that pressure level. The dead load of the earth being small in comparison to the overpressure, the slightly trapezoidal diagram of forces is assumed to be a rectangular diagram, the intensity of which is equal to the pressure of the level of the floor of the shelter.

Blast-wave overpressure	100 tons/m^2
Weight of overburden	8.8 tons/m^2
(Rounding off value)	0.2 ton/m^2
Pressure at the level of the floor	109 tons/m^2

Horizontal loads on the walls = 109 × 0.4 = 43.6 tons/m²

(b) Stresses. (1) Bending moments at center.

$$\rho = a/b = 2.30/7.70 = 0.30$$

$$1/\rho = b/a = 3.35$$

$$P = 7.70 \times 2.30 \times 43.6 = 772.2 \text{ tons}$$

$$M_1 = 0.0355$$

$$M_2 = 0.003$$

Moments in the direction of the short span

$$M_a = 0.8 \times (0.0355 + 0.15 \times 0.033) \times 772.2 = 22.2 \text{ ton-m/m}$$

In the direction of the long span

$$M_b = 0.8 \times (0.003 + 0.0355 \times 0.15) \times 772.2 = 5.2 \text{ ton-m/m}$$

(2) Shear stresses at the supports. At the center of the long side

$$T_a = \frac{772.2}{2 \times 7.70 + 2.30} = 43.6 \text{ tons/m}$$

At the center of the short side

$$T_b = \frac{772.2}{3 \times 7.7} = 33.4 \text{ tons/m}$$

(3) Stresses. Stresses in the direction of the short span (vertical reinforcement).

At the center:

M = 22.2 ton-m/m
h = 60 cm
h' = 56 cm
y = 12.2 cm
z = 51.9 cm
n'_a = 37.8 kg/mm²

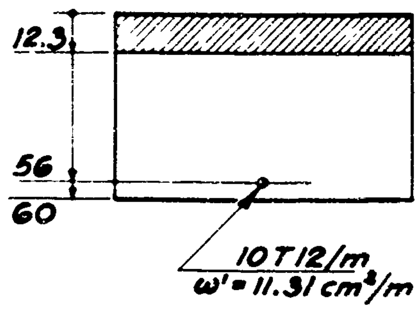

At supports:

T = 43.6 tons/m
ω' = 11.31 cm²/m
x = 37.7 cm/m
h = 60 cm
h' = 56 cm
y = 12.3 cm
z = 51.9 cm
T/bz = 8.4 kg/cm²
T/xz = 22.3 kg/cm²

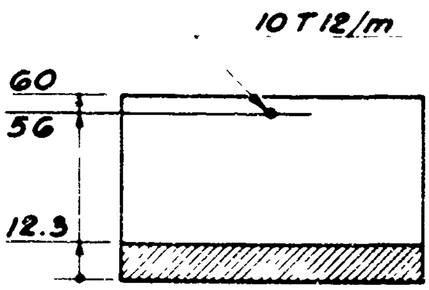

Secondary reinforcement: none

Stresses in the direction of the long span (horizontal reinforcement).

At supports:

$T = 33.4$ tons/m
$\omega' = 7.54$ cm^2/m
$x = 25.1$ cm/m
$h = 60$ cm
$h' = 54.8$ cm
$y = 10.2$ cm
$z = 51.4$ cm
$T/bz = 6.5$ kg/cm^2
$T/xz = 25.9$ kg/cm^2

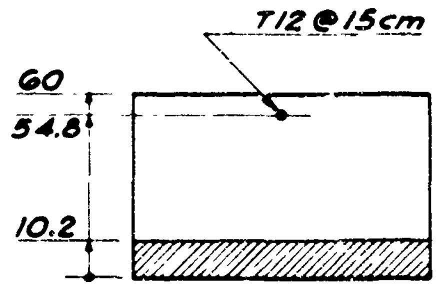

At the center: The reinforcement consists of T12 at 12 cm on centers for a small moment.

B.2.5 Partition Walls

The partition walls that close the entrance chamber must be able to resist the complete overpressure if the door, F1, stays open at the moment of the explosion.

The partition that is directly in front of the door, F1, measures 2.30 m in height, 0.40 m in thickness, and 1.20 m in width between the exterior wall and the vertical lintel beam (pilaster), C3.

The perpendicular partition wall measures 2.30 m in height, 60 cm in thickness, and 1.10 m in width between the exterior wall and the vertical lintel beam (pilaster), C4. The first partition wall is analyzed as follows:

(a) Stresses. (1) Bending moments at center.

$a = 1.20$ m

$b = 2.30$ m

$\rho = 0.522 \qquad 1/\rho = 1.91$

$P = 2.30 \times 1.20 \times 100 = 276$ tons

$M_1 = 0.047$

$M_2 = 0.010$

Moment in the direction of the short span

$$M_a = 0.8\ (0.047 + 0.15 \times 0.01) \times 276 = 10.7 \text{ ton-m/m}$$

Moment in the direction of the long span

$$M_b = 0.8\ (0.01 + 0.15 \times 0.047) \times 276 = 3.8 \text{ ton-m/m}$$

(2) Shearing stresses at the supports. At center of long side

$$T_a = \frac{276}{2 \times 2.30 + 1.20} = 47.6 \text{ tons/m}$$

At center of the short side

$$T_b = \frac{276}{3 \times 2.30} = 40.0 \text{ tons/m}$$

(3) Stresses. Stresses in the direction of the short span (horizontal reinforcement).

At the center:

M = 10.7 ton-m/m
h = 40 cm
h' = 36 cm
y = 9.3 cm
z = 32.9 cm
n'_a = 28.8 kg/mm²

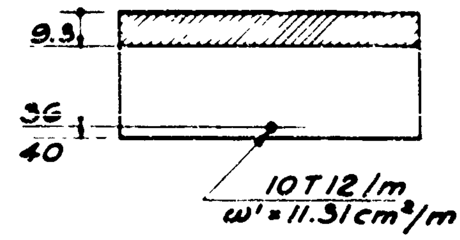

At supports:

T = 47.6 tons/m
ω' = 20.1 cm²/m
x = 50.3 cm/m
h = 40 cm
h' = 36 cm
y = 11.9 cm
z = 32.0 cm
T/bz = 14.9 kg/m²
T/xz = 29.6 kg/m²
ω'_a = 15.7 cm²/m
e = 25 cm
n'_e = 23.7 kg/mm²

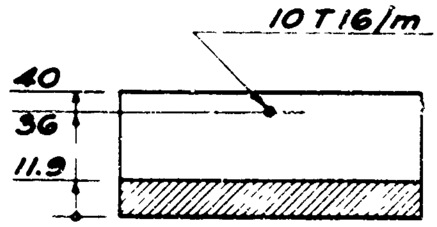

(Ten stirrups of ADx with a diameter of 10 mm per meter at 25 cm on centers)

Stresses in the direction of the long span (vertical reinforcement).

At the center:

M = 3.8 ton-m/m
h = 40 cm
h' = 34.8 cm
y = 6.9 cm
z = 32.5 cm
n'_a = 20.7 kg/mm²

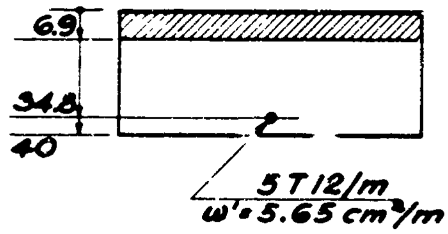

At supports:

T = 40.0 tons/m
ω' = 11.31 cm²/m
x = 37.7 cm/m
h = 40 cm
h' = 34.6 cm
y = 9.3 cm
z = 31.5 cm
T/bz = 12.7 kg/cm²
T/xz = 35.7 kg/cm²
ω'_e = 7.85 cm²/m
e = 15 cm
n'_e = 24.3 kg/mm²

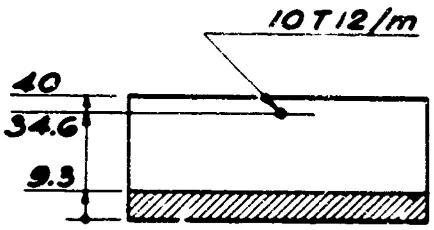

(Five stirrups of ADx with a diameter of 10 mm per meter at 15 cm on centers)

B.2.6 Lintel Beams

The openings F1, F2, and S2 are framed by four lintel beams (heavy reinforcement on four sides of the openings). Lintel beams are placed in the roof slab and in the floor slab. Lintel beam C1 is placed at the opening of 1.0 m between the two rooms that measure 3.30 × 3.00 m. Lintel beam C2 is placed at the opening of 1.2 m between the main room and the water closet. Two other vertical lintel beams (pilasters), C3 and C4, serve as supports for the two partition walls that close the entrance chamber.

(a) Opening F1. (1) Horizontal lintel beams (in roof slab). The corresponding opening measures 0.70 × 1.8 m and the lintel beam is 0.92 m high and 0.50 m thick.

The lintel beam is subjected to the reaction of the slab of the entrance chamber, the roof slab over the vestibule, to its dead load, and to the overpressure that it supports directly.

Reaction of the slab of the entrance chamber. The worst possible condition exists if a uniform reaction equal to the maximum shearing stress at the center of the small side of the slab is assumed, that is, 42 tons/m.

Reaction of the 1.40 × 1.20 m roof slab over the vestibule. This slab is exposed to the atmosphere by means of the stairs and the landing. However, it is assumed that the latter are collapsed in such a manner that the vestibule slab transmits a maximum stress into the lintel beam. The room being supported on three sides, the average reaction is

$$\frac{105 \times 1.2 \times 1.40}{2 \times 1.20 + 1.40} = 46.4 \text{ tons/m}$$

Load directly supported by the lintel beam

$$0.50 \times 105 = 52.5 \text{ tons/m}$$

Dead load

$$0.5 \times 0.32 \times 2.5 = 0.4 \text{ tons/m}$$

Total load

$$p = 42 + 46.4 + 63 + 0.4 = 141.3 \text{ tons/m}$$

Stresses. Taking an equal moment at the center and at the fixed edge which is equal to $\pm pL^2/10$

$$M = \pm \frac{141.3 \times (0.70)^2}{10} = \pm 6.9 \text{ ton-m/m}$$

Shearing stress at the support

$$T = \frac{141.3 \times 0.70}{2} = 49.5 \text{ tons}$$

At supports:

$M = -6.9$ ton-m/m
$T = 49.5$ tons
$\omega' = 5.63$ cm^2
$x = 18.8$ cm
$h = 92$ cm
$h' = 88$ cm
$y = 15.65$ cm
$z = 82.8$ cm
$n'_a = 14.7$ kg/mm^2
$T/bz = 12.0$ kg/cm^2
$T/xz = 31.8$ kg/cm^2
$\omega'_e = 3.83$ cm^2
$e = 15$ cm
$n'_e = 23.5$ kg/mm^2

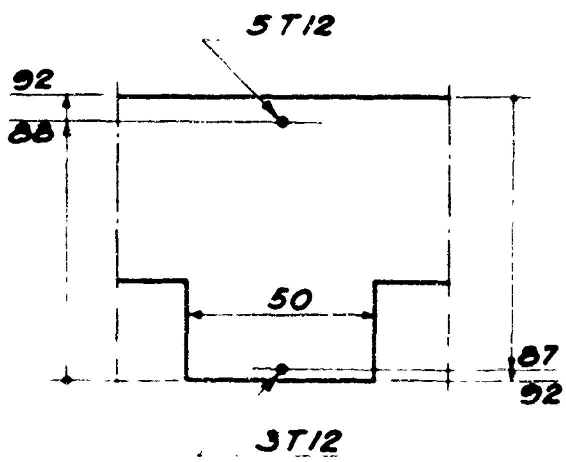

[One stirrup (A10) plus 1 tie (T12) at 15 cm on centers]

At the center:

$M = +6.9$
$\omega' = 3.4$ cm^2
$h = 92$ cm
$h' = 87$ cm
$y = 12.3$ cm
$z = 82.9$ cm
$n'_a = 24.5$ kg/mm^2

(2) Vertical lintel beams (pilasters). The lintel beam situated at the earth side of door opening F1 is justified as follows: It measures 1.80 m long, 0.50 m thick, and 0.80 m in height. (Note: Fire door recess has been deducted from total thickness.)

The beam serves as a support of the vertical 60-cm wall exterior of the entrance chamber and the vertical 40-cm wall of the vestibule.

Reaction of the exterior wall of the entrance chamber. This wall measures 2.30 × 2.60 m. The horizontal thrust equal to 40 per cent of the vertical pressure gives a maximum reaction at the center of the vertical side of 2.30 m equal to

$$\frac{43.6 \times 2.30 \times 2.60}{2 \times 2.60 + 2.30} = 34.8 \text{ tons/m}$$

Reaction of the wall of the vestibule. This wall measures 2.30 × 1.20 m. Assuming the destruction of the stairs and the landing, this slab, supported on three sides, is subjected only to forces of dead load and the horizontal thrust of the earth.

The average reaction is

$$\frac{43.6 \times 2.30 \times 1.20}{2.30 + 2 \times 1.20} = 25.6 \text{ tons/m}$$

Load directly supported: The lintel beam (pilaster) finally supports the load

$$43.6 \times 0.50 = 21.8 \text{ tons/m}$$

Total load

$$p = 34.8 + 25.6 + 21.8 = 82.2 \text{ tons/m}$$

Stresses

$$M = \pm\frac{pL^2}{10} = \pm\frac{82.2 \times (1.80)^2}{10} = \pm 26.6 \text{ ton-m/m}$$

$$T = \frac{pL}{2} = 82.2 \times 0.90 = 74.0 \text{ tons}$$

At supports:

M = −26.6 ton-m
T = 74.0 tons
ω' = 11.31 cm^2
x = 37.7 cm
h = 80 cm
h' = 74.8 cm
y = 19.4 cm
z = 68.3 cm
n'_a = 34.4 kg/mm^2
T/bz = 21.7 kg/cm^2
T/xz = 28.7 kg/cm^2
ω'_e = 6.28 cm^2
e = 15 cm
n'_e = 25.9 kg/mm^2

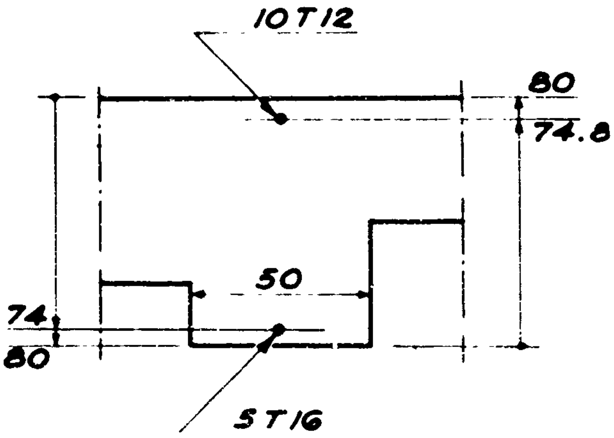

(Three stirrups plus 1 tie (ADx), 10 mm at 15 cm on centers)

At the center:

M = +26.6 ton-m
ω' = 10.0 cm^2
h = 80 cm
h' = 74 cm
y = 16.55 cm
z = 67.0 cm
n'_a = 39.7 kg/mm^2

(b) Opening F2. The stresses of the partition walls of the entrance chamber are transmitted to the vertical lintel beams (pilasters) C3 and C4. The horizontal lintel beams of opening F2, in particular the lintel beam in the roof slab, measures 0.70 m long, 0.50 m thick, and 0.95 m in height.

The lintel beam is subjected to the reaction of the slabs of the entrance chamber and the annexes, to the pressure that is directly applied, and to its dead load.

Reaction of the slab of the entrance chamber. A uniform reaction is taken which is equal to the maximum shearing stress, 51.2 tons/m [see Sec. B.2.2(b)(2)].

Reaction of the slab of the annexes. In like manner, a uniform equal reaction is taken which is equal to the maximum shearing stress, 54.8 tons/m [see Sec. B.2.2(c)(2)].

Load directly applied

$$0.50 \times 105 = 52.5 \text{ tons/m}$$

Dead load

$$0.35 \times 0.50 \times 2.5 = 0.4 \text{ ton/m}$$

Total load applied on lintel beam

$$p = 51.2 + 54.8 + 52.5 + 0.4 = 158.9 \text{ tons/m}$$

Stresses. Bending moments.

$$M = \pm\frac{pL^2}{10} = \pm\frac{158.9 \times (0.70)^2}{10} = \pm 7.8 \text{ ton-m}$$

Shearing stresses at the supports.

$$T = \frac{pL}{2} = \frac{157.9 \times 0.70}{2} = 56.6 \text{ tons}$$

At supports:

M = −7.8 ton-m
T = 55.6 tons
ω' = 5.65 cm^2
x = 18.8 cm
h = 95 cm
h' = 89.8 cm
y = 15.8 cm
z = 84.5 cm
n'_a = 16.3 kg/mm^2
T/bz = 13.2 kg/cm^2
T/xz = 36.0 kg/cm^2
ω'_e = 3.83 m^2
e = 10 cm
n'_e = 17.2 kg/mm^2

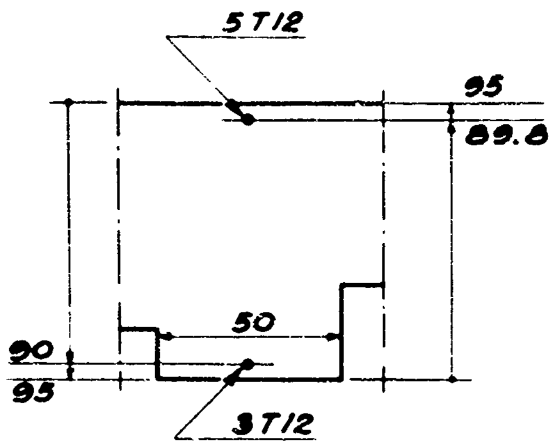

(One stirrup (A10) plus 1 tie (T12), at 10 cm on centers)

At the center:

M = + 7.8 ton-m
ω' = 3.39 cm^2
h = 95 cm
h' = 90 cm
y = 12.6 cm
z = 85.8 cm
n'_a = 26.7 kg/mm^2

(c) Lintel Beam C1. The beams (C1) are located at the opening that is 1.0 m wide, which connects the two large rooms of the shelter.

The lower lintel beam is incorporated in the floor; the upper lintel beam protrudes 0.40 m below the ceiling of the shelter.

The lower lintel beam would be subjected to the same forces as the upper lintel beam if the reaction of the ground on the floor was uniform. However, its failure would bring large deformations incompatible with the condition that the floor remain in contact with the ground. This is why the lower lintel beam will be reinforced as the upper beam even though its height is less.

The upper lintel beam is 0.40 m thick, 1.00 m long, and 1.00 m high.

The lintel beam (C1) serves as a support for the two 3.30 × 3.00 m slabs, carries its dead load, and carries the overpressure that is directly applied to it.

Reactions of the 3.30 × 3.00 m slabs. The lintel beam is located at the end of the short side of the slabs (the common short side). Along this side the reaction has a parabolic distribution, with the maximum at the center and zero at the ends. It is safe to replace this variable reaction by a uniform distributed reaction equal to the average reaction taken along the perimeter of the rectangle.

$$\frac{105 \times 3.30 \times 3.00}{2 \times 3.30 + 2 \times 3.00} = 82.5 \text{ tons/m}$$

Therefore, for the two slabs, the total is 165 tons/m.

Pressure directly supported by the lintel beam

$$105 \times 0.40 = 42 \text{ tons/m}$$

Dead load protruding under the slab

$$0.40 \times 0.40 \times 2.5 = 0.4 \text{ ton/m}$$

Total load

$$p = 165 + 42 + 0.4 = 207.4 \text{ tons/m}$$

Stresses.

$$M = \pm \frac{pL^2}{10} = \pm \frac{207.4 \times (1.00)^2}{10} = 20.74 \text{ ton-m}$$

$$T = \frac{pL}{2} = 207.4 \times 0.50 = 103.7 \text{ tons}$$

At supports:

M	=	$-$ 20.7 ton-m
T	=	103.7 tons
ω'	=	12.56 cm^2
x	=	35.2 cm
h	=	100 cm
h'	=	94.8 cm
y	=	25.5 cm
z	=	86.3 cm
n'_a	=	19.1 kg/mm^2
T/bz	=	30.0 kg/cm^2
T/xz	=	34.1 kg/cm^2
ω'_e	=	4.71 cm^2
e	=	10 cm
n'_e	=	25.5 kg/mm^2

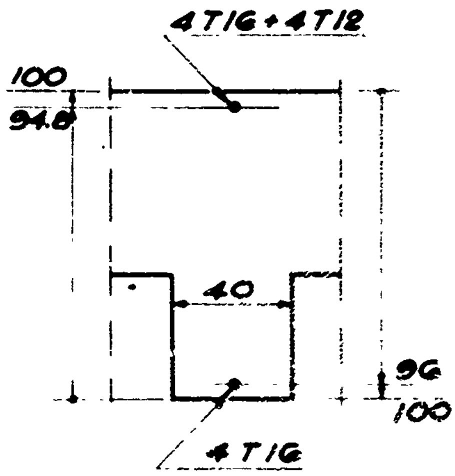

[Two stirrups plus 1 tie (ADx), 10 mm at 10 cm on centers]

At the center:

$M = +20.74$ ton-m
$\omega' = 8.04\ cm^2$
$h = 100$ cm
$h' = 96$ cm
$y = 21.3$ cm
$z = 88.9$ cm
$n'_a = 28.7\ kg/mm^2$

(d) Lintel Beam C2. The lintel beam (C2) is located at the opening of 1.20 × 2.30 m, which gives access to the annexes (water closet, etc.). The upper lintel beam is incorporated in the roof slab and the lower one in the floor slab. Only the former will be analyzed, the latter being identically reinforced. They are 0.60 m wide.

The beam serves as a support for the 3.30 × 3.00 m slab and the slab of the annexes. It also receives the overpressure that is directly applied to it.

Reaction of the 3.30 × 3.00 m slab. The same reaction as that of the lintel beam (C1) is taken, that is, 82.5 tons/m.

Reaction of the slab of the annexes. Since the lintel beam (C2) acts as the support of one of the short sides of the annex slab, a uniform average reaction is taken which is equal to 80 per cent of the maximum shearing stress along this side, this is 0.8 × 42 = 33.6 tons/m.

Directly applied pressure

$$105 \times 0.60 = 63.0 \text{ tons/m}$$

Total load

$$p = 82.5 + 33.6 + 63.0 = 179.1 \text{ tons/m}$$

Stresses.

$$M = \pm\frac{pL^2}{10} = \pm\frac{179.1 \times (1.2)^2}{10} = \pm 25.8 \text{ ton-m}$$

$$T = 179.1 \times 0.60 = 107.5 \text{ tons}$$

At supports:

$M = -25.8$ ton-m
$T = 107.5$ tons
$\omega' = 20.36\ cm^2$
$x = 67.9$ cm
$h = 60$ cm
$h' = 53.6$ cm
$y = 18.8$ cm
$z = 47.3$ cm
$n'_a = 26.8\ kg/mm^2$
$T/bz = 37.9\ kg/cm^2$
$T/xz = 33.5\ kg/cm^2$
$\omega'_e = 7.85\ cm^2$
$e = 10$ cm
$n'_e = 29.0\ kg/mm^2$

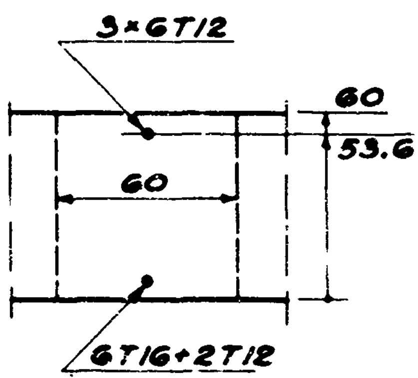

[Six stirrups (ADx), 10 mm at 10 mm on centers]

At the center:

$M = +29.8$ ton-m
$\omega' = 14.32\ cm^2$
$h = 60$ cm
$h' = 55.5$ cm
$y = 16.7$ cm
$z = 49.9$ cm
$n'_a = 38.1\ kg/mm^2$

(e) Lintel Beam (Pilaster) C3. The vertical lintel beam serves as a support for the 1.20 × 2.30 m partition wall of the entrance chamber. It is 2.30 m long, 0.70 m high, and 0.60 m thick.

The reaction is maximum at the center and has a value of 47.6 tons/m. The uniform reaction obtained by taking the average reaction of the perimeter is assumed to be approximately the maximum:

$$p = \frac{100 \times 2.30 \times 1.20}{2 \times 2.30 + 2 \times 1.20} = 39.4 \text{ tons/m}$$

Stresses.

$$M = \pm \frac{pL^2}{10} = \pm \frac{39.4 \times (2.3)^2}{10} = \pm 20.8 \text{ ton-m}$$

$$T = \frac{pL}{2} = 39.4 \times 1.15 = 45.3 \text{ tons}$$

At supports:

$M = -20.8$ ton-m
$T = 45.3$ tons
$\omega' = 10.05\ cm^2$
$x = 25.1$ cm
$h = 70$ cm
$h' = 64.4$ cm
$y = 15.6$ cm
$z = 59.2$ cm
$n'_a = 31.5\ kg/mm^2$
$n_b = 74.8\ kg/cm^2$
$T/bz = 12.8\ kg/cm^2$
$T/xz = 30.4\ kg/cm^2$
$\omega'_e = 6.97\ cm^2$
$e = 20$ cm
$n'_e = 22\ kg/mm^2$

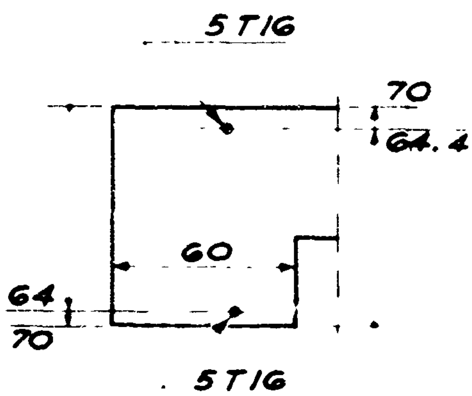

[One tie (T12) plus 3 stirrups (ADx), 10 mm at 20 cm on centers]

At the center:

$M = +20.8$ ton-m
$\omega' = 10.5\ cm^2$
$h = 70$ cm
$h' = 64$ cm
$y = 15.6$ cm
$z = 58.8$ cm
$n'_a = 35.4\ kg/mm^2$

(f) Lintel Beam (Pilaster) C4. The lintel beam (C4) serves as a support for the door (F2) and for the 1.10 × 2.30 m partition wall of the entrance chamber. It is 2.30 m long, 1.10 m high, and 0.30 m thick.

Reaction of the partition wall. The average reaction of the perimeter is used:

$$\frac{100 \times 2.30 \times 1.10}{2 \times 2.30 + 2 \times 1.10} = 37.2 \text{ tons/m}$$

Reaction of the door. The presence of the horizontal lintel beams of the door is neglected and the average reaction on the perimeter of the rectangle bounded by the floor slab, the roof slab, the lintel beam (C2), and the 1.20 × 2.30 m partition wall is used.

$$\frac{100 \times 2.30 \times 1.20}{2 \times 2.30 + 2 \times 1.20} = 39.4 \text{ tons/m}$$

Directly applied pressure

$$100 \times 0.30 = 30 \text{ tons/m}$$

Total load

$$p = 37.2 + 39.4 + 30 = 106.6 \text{ tons/m}$$

Stresses

$$M = \pm \frac{pL^2}{10} = \pm \frac{106.6 \times (2.30)^2}{10} = \pm 56.4 \text{ ton-m}$$

$$T = \frac{p}{2} = 106.6 \times 1.15 = 122.6 \text{ tons}$$

At support:

$M = -56.4$ ton-m
$T = 122.6$ tons
$\omega' = 16.08 \text{ cm}^2$
$x = 40.2$ cm
$h = 110$ cm
$h' = 103.8$ cm
$y = 33.6$ cm
$z = 92.6$ cm
$n'_a = 37.9 \text{ kg/mm}^2$
$n_b = 110.9 \text{ kg/cm}^2$
$T/bz = 44.1 \text{ kg/cm}^2$
$T/xz = 32.9 \text{ kg/cm}^2$
$\omega'_e = 6.78 \text{ cm}^2$
$e = 15$ cm
$n'_e = 29.3 \text{ kg/mm}^2$

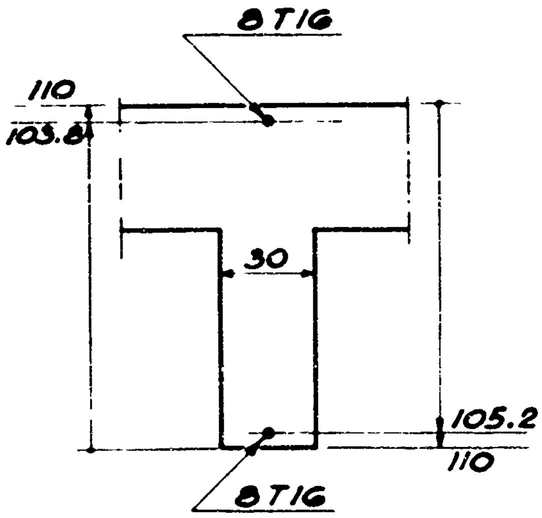

[Two stirrups plus 1 tie (T12), at 15 cm on centers]

At the center:

$M = +56.4$ ton-m
$\omega' = 16.08 \text{ cm}^2$
$h = 110$ cm
$h' = 105.2$ cm
$y = 33.6$ cm
$z = 93.9$ cm
$n'_a = 37.4 \text{ kg/mm}^2$

B.3 EMERGENCY EXIT TUNNEL AND SHAFT

B.3.1 General

The following is the analysis for the typical sections of the emergency exit tunnel and shaft. The equations for slabs, as obtained from the following assumptions, will apply:

1. The normal forces are neglected.
2. An assumption is made that the reaction of the ground on the base slab is uniform.

The equations are valid if the typical section of the slabs is taken at a distance at least one-half the span of the slabs away from the ends (that is, 0.80 m for both tunnel and shaft).

Adhering to these conditions, the equations used are as follows:

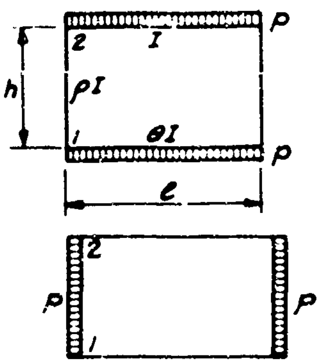

$$M_1 = -\frac{pL^3}{4}\,\frac{3\rho L + (2-\theta)h}{\Delta}$$

$$M_2 = -\frac{pL^3}{4}\,\frac{3\rho L + (2\theta - 1)h}{\Delta}$$

$$M_1 = -\frac{ph^3}{4}\,\frac{3\rho L + h}{\Delta}$$

$$M_2 = -\frac{ph^3}{4}\,\frac{3\rho L + \theta h}{\Delta}$$

with $\Delta = (3\rho L + 2h)(3\rho L + 2\theta h) - \theta h^2$

B.3.2 Emergency Exit Tunnel

The floor slab and the roof slab are 0.40 m thick, and the vertical walls are 0.30 m.
The lengths of L and h are measured from center line to center line of the corresponding slabs.

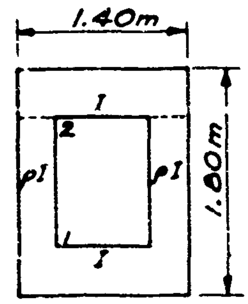

$L = 1.10$ m

$h = 1.40$ m

$\theta = 1$

$\rho = \left(\frac{0.30}{0.40}\right)^3 = 0.422$

$\Delta = (3 \times 0.422 \times 1.10 + 2 \times 1.40)$
$\times (3 \times 0.422 \times 1.10 + 2 \times 1.40) - (1.40)^2 = 15.6\ \text{m}^2$

(a) Floor and Roof Slabs. The vertical pressure p is calculated for the floor slab.

Dead load of slab:	$(2 \times 0.40 \times 1.40 + 2 \times 1.00 \times 0.30) \times 2.5$	= 4.3 tons/m
Overpressure	1.40×1.00	= 140.0 tons/m
Earth load (overburden)	$2 \times 3.00 \times 1.4$	= 8.4 tons/m
		= 152.7 tons/m

Reaction of ground p.

$$p = \frac{152.7}{1.40} = 109\ \text{tons/m}^2$$

(b) Tunnel Walls. The pressure at the level of the floor slab is equal to

$$100\ \text{tons} + 2 \times 3.00\ \text{m} = 106\ \text{tons/m}^2$$

Therefore, the thrust is

(Coefficient of thrust = 0.25) $106 \times 0.25 = 26.5\ \text{tons/m}^2$

(Coefficient of thrust = 0.40) $106 \times 0.40 = 42.4\ \text{tons/m}^2$

(c) Bending Moments. (1) Moments due to pressure of the slab. Fixed-end moments.

$$M_1 = -\frac{pL^3}{4}\,\rho\,\frac{3\rho L + (2-\theta)h}{\Delta} = -2.75\ \text{ton-m/m}$$

$$M_2 = -\frac{pL^3}{4}\rho\frac{3\rho L + (2\theta - 1)h}{\Delta} = -2.75 \text{ ton-m/m}$$

Moments in the roof and floor slabs. At fixed-end

$$M = M_1 = M_2 = -2.75 \text{ ton-m/m}$$

At mid-span

$$M = (pL^2/8)\ M_1 = +13.75 \text{ ton-m/m}$$

Moments in the tunnel walls.

$$M = M_1 = M_2 = -2.75 \text{ ton-m/m}$$

(2) Moments due to thrust of the earth (overburden). Fixed-end moments. With the coefficient of 0.25

$$M_1 = M_2 = -\frac{ph^3}{4}\theta\frac{3\rho L + h}{\Delta} = -3.25 \text{ ton-m/m}$$

With coefficient of 0.40

$$M_1 = M_2 = -5.20 \text{ ton-m/m}$$

Moments in the roof and floor slabs. With the coefficient of thrust of 0.25

$$M = -3.25 \text{ ton-m/m}$$

With the coefficient of thrust of 0.40

$$M = 5.20 \text{ ton-m/m}$$

Moments in the tunnel walls. At fixed ends

$$M = -3.25 \text{ ton-m/m}$$

$$M = -5.20 \text{ ton-m/m}$$

At mid-span, coefficient of thrust of 0.25

$$M = -3.25 + \frac{26.5 \times (1.40)^2}{8} = +3.25 \text{ ton-m/m}$$

At mid-span, coefficient of thrust of 0 40

$$M = -5.20 + \frac{42.4 \times (1.40)^2}{8} = +5.20 \text{ ton-m/m}$$

(3) Resultant Moments. Roof and floor slabs. At fixed end

$$-6.00 \text{ ton-m/m} > M > -7.95 \text{ ton-m/m}$$

At mid-span

$$+8.55 \text{ ton-m/m} < M < +10.50 \text{ ton-m/m}$$

Tunnel walls. At fixed end

$$-6.00 \text{ ton-m/m} > M > -7.95 \text{ ton-m/m}$$

At mid-span

$$+0.50 \text{ ton-m/m} < M < +2.45 \text{ ton-m/m}$$

(d) Shearing Stresses. (1) Roof and floor slabs.

$$T = 109 \times 0.40 = 43.6 \text{ tons/m}$$

(2) Tunnel walls. The maximum thrust gives the worst condition

$$T = 42.4 \times 0.50 = 21\ 2 \text{ ton-m/m}$$

(e) Stresses. (1) Roof and floor slabs. The least favorable stresses are given.

At fixed end

M = − 7.95 ton-m/m
T = 43.6 tons/m
y = 11.0 cm
z = 32.35 cm
n'_a = 15.4 kg/mm^2
T/bz = 13.5 kg/cm^2
T/xz = 33.5 kg/cm^2

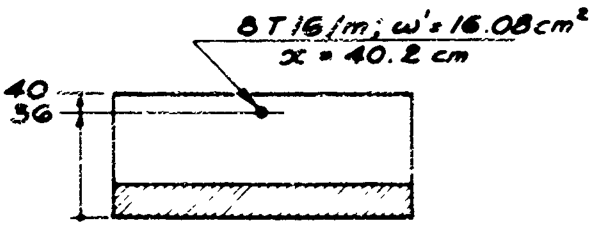

Stirrups: 8 single-leg stirrups (ADx) of 10 mm per meter spaced at 12.5 cm on centers.

$\omega'_e = 6.28 \text{ cm}^2$

$$n'_e = \frac{43\ 600 \times 12.5}{628 \times 32.35} = 26.8 \text{ kg/mm}^2$$

At mid-span

M = + 10.50 ton-m/m
h' = 36 cm
y = 8.6 cm
z = 33.1 cm
n'_a = 35.1 kg/mm^2

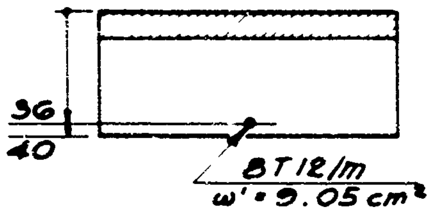

(2) Tunnel walls. At fixed end

M = − 7.95 ton-m/m
T = 21.2 tons/m
h' = 26 cm
y = 9.03 cm
z = 23.0 cm
n'_a = 21.5 kg/mm^2
n_b = 76.1 kg/cm^2
T/bz = 9.2 kg/cm^2
T/xz = 23 0 kg/cm^2
No stirrups

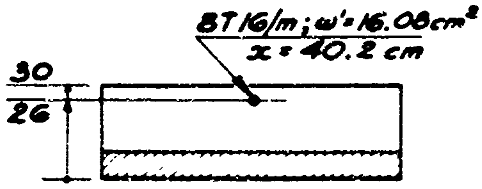

At mid-span. This section is reinforced with four T12 ($\omega' = 4.52 \text{ cm}^2$, $x = 15.1$ cm), which is an area and a perimeter greater than one-third of that supplied by the reinforcement at the mid-span of the slabs. However, the moment at this section is less than one-third of the moment at the mid-span, and the reinforcement is adequate.

B.3.3 Emergency Exit Shaft

The floor slab measures 1.40 × 1.40 m and the walls of the shaft are 0.30 m thick.

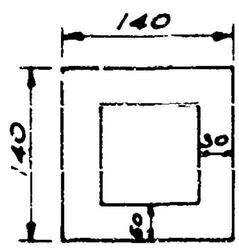

$$\rho = \upsilon = 1$$

It is uniformly loaded by a pressure p, which is assumed equal to the maximum pressure (43.3 tons/m²) on the total height.

The formulas for the slab are simplied as follows:

$$M_1 = M_2 = -\frac{pL^2}{24}$$

$$M_1 = M_2 = -\frac{ph^2}{24}$$

with h = L = 1.10 m

(a) Bending Moments. The stresses are identical on all surfaces.

(1) At fixed end

$$M = -\frac{pL^2}{24} - \frac{ph^2}{24} = -43.3 \times \frac{(1.10)^2}{12} = -4.4 \text{ ton-m/m}$$

(2) At mid-span

$$M = -4.4 + \frac{43.3 \times (1.10)^2}{8} = +2.2 \text{ ton-m/m}$$

(b) Shearing Stresses. On all surfaces; at fixed end

$$T = 43.3 \times 0.40 = 17.3 \text{ tons/m}$$

(c) Stresses. (1) At fixed end

M = – 4.4 ton-m/m
T = 17.3 tons/m
h′ = 26 cm
y = 6.6 cm
z = 23.8 cm
n'_a = 24.6 kg/mm²
T/bz = 7.3 kg/cm²
T/xz = 29.0 kg/cm²
No stirrups

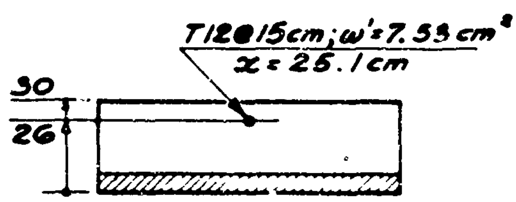

(2) At mid-span. The bending moment (and the shearing stress because the tension face changes sides) is one-half as large as that at the fixed end. Therefore the steel area is also one-half as large. T12 at 30 cm on centers are sufficient.

Appendix C

AS-BUILT DRAWINGS

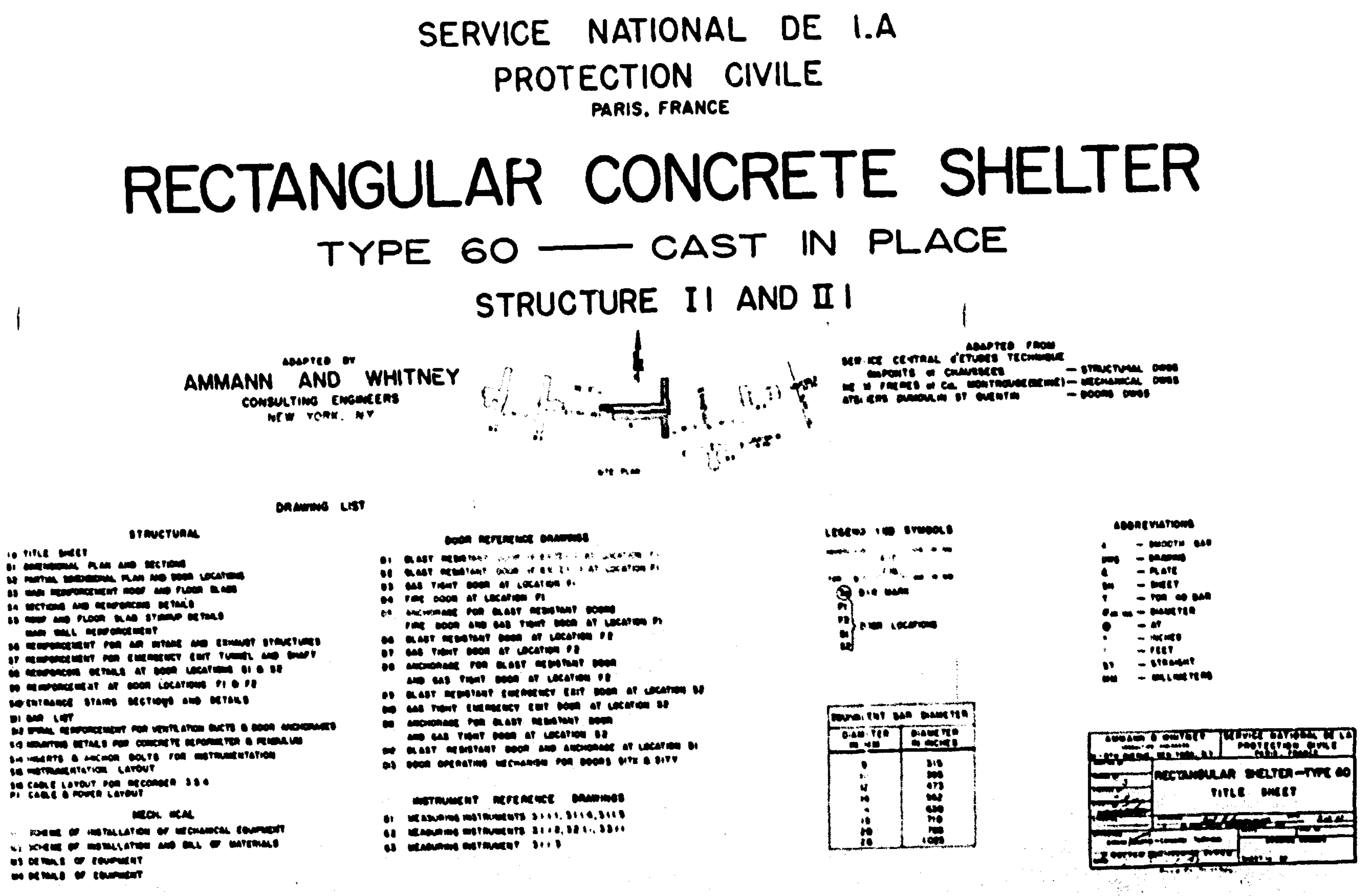

Fig. C.1—Rectangular shelter, type 60, title sheet.

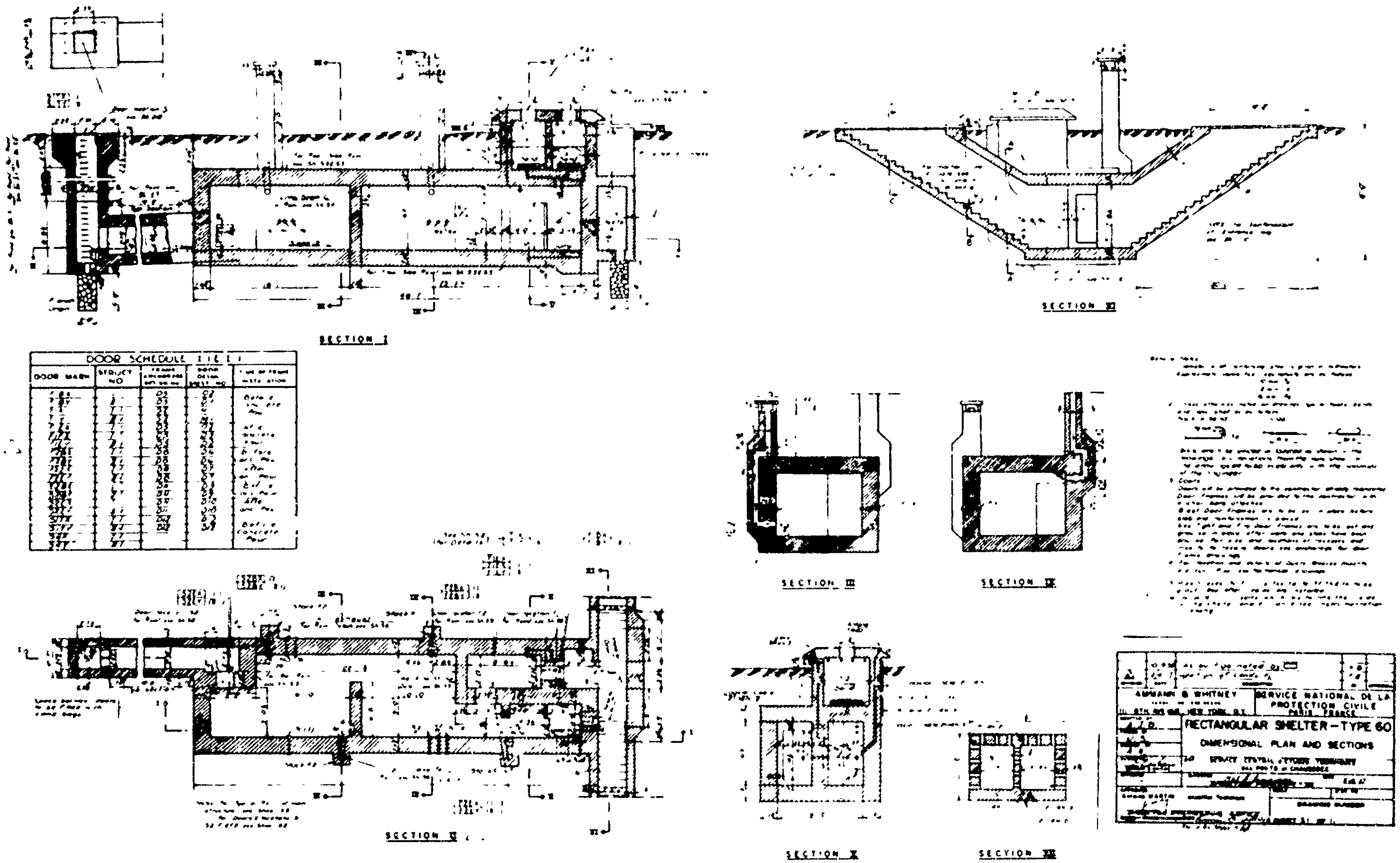

Fig. C.1.1 —Rectangular shelter, type 60, dimensional plan and section.

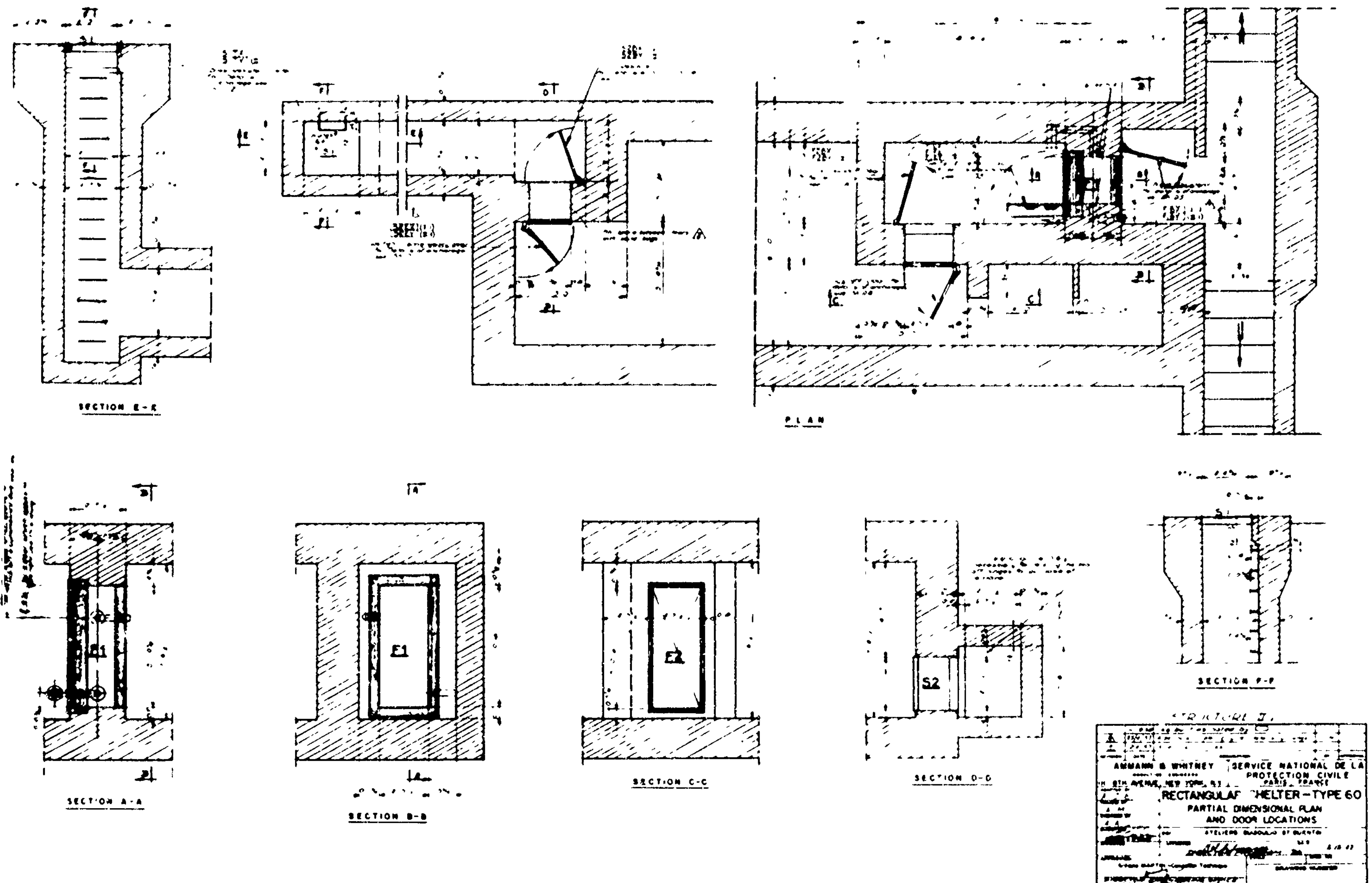

Fig. C.1.2—Rectangular shelter, type 60, partial dimensional plan and door locations.

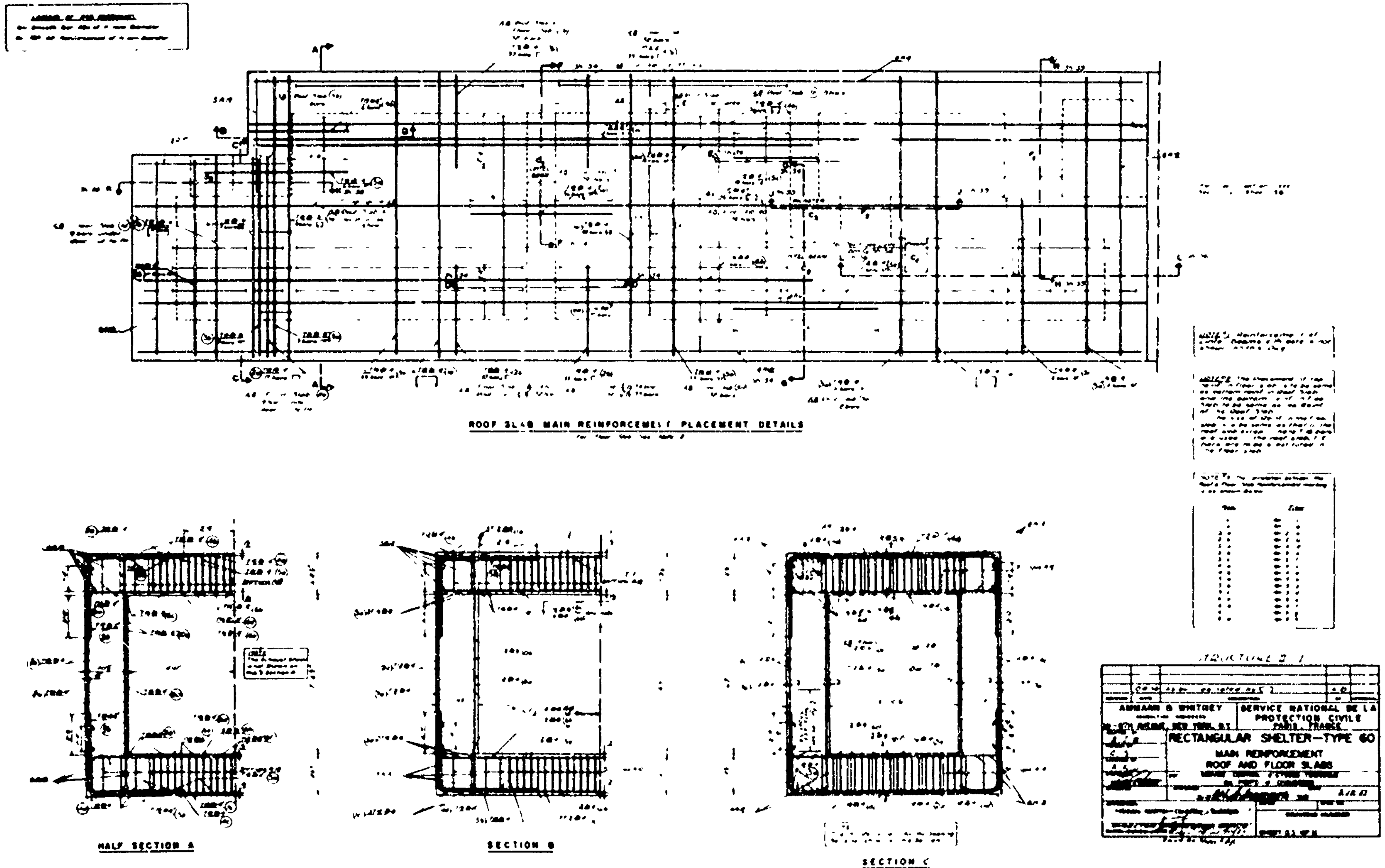

Fig. C.1.3—Rectangular shelter, type 60, main reinforcement roof and floor slabs.

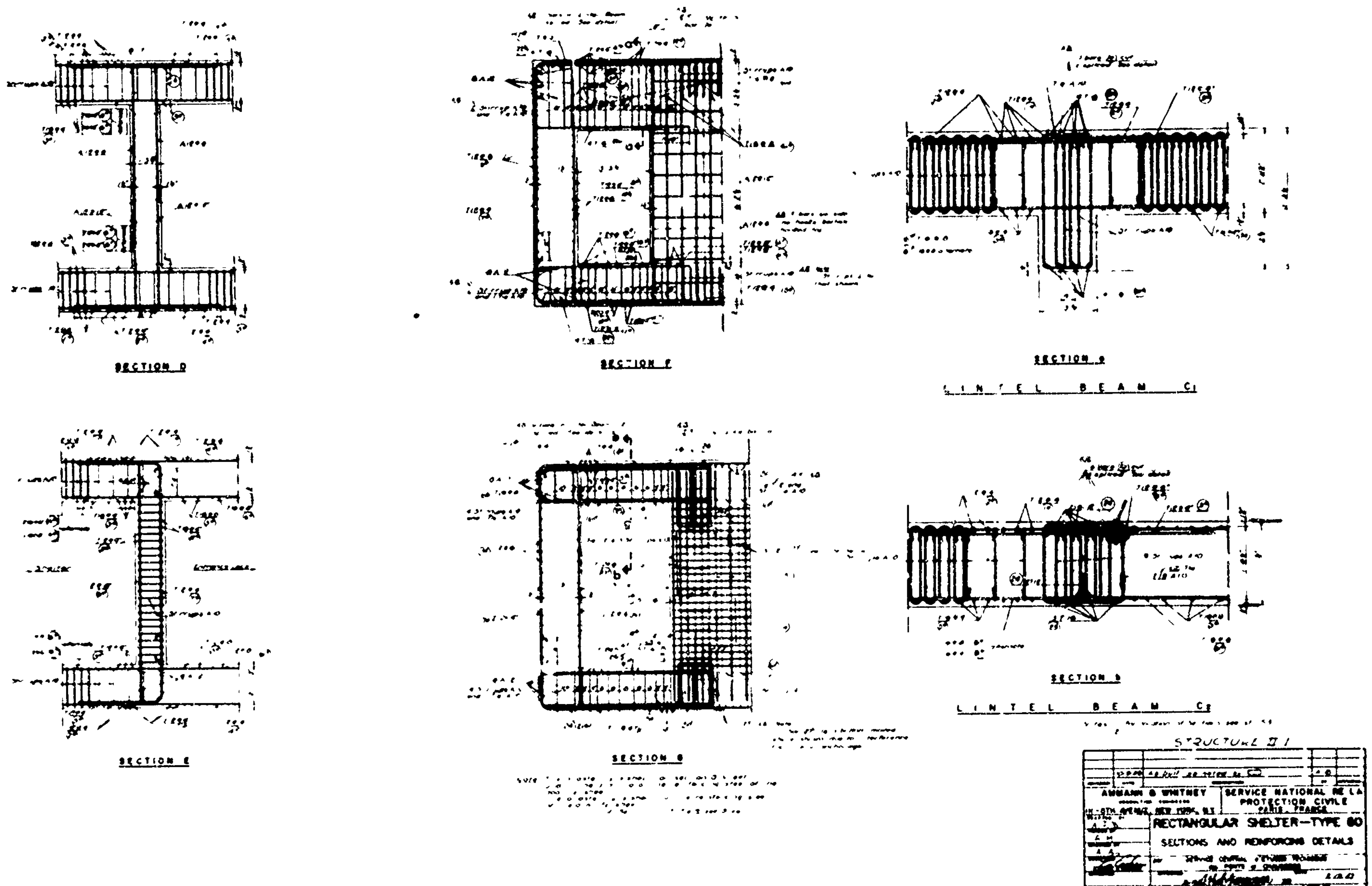

Fig. C.1.4—Rectangular shelter, type 60, sections and reinforcing details.

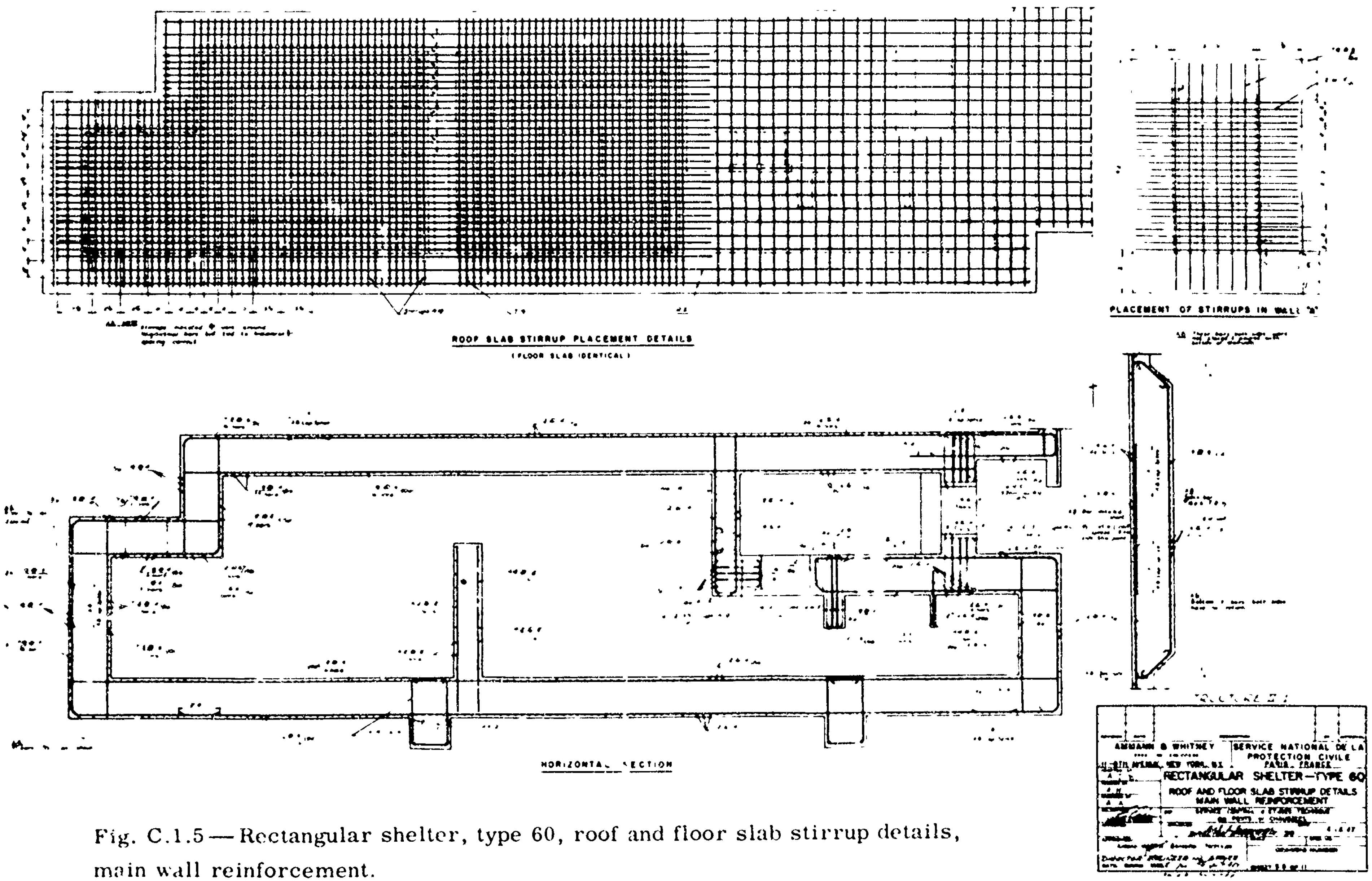

Fig. C.1.5 — Rectangular shelter, type 60, roof and floor slab stirrup details, main wall reinforcement.

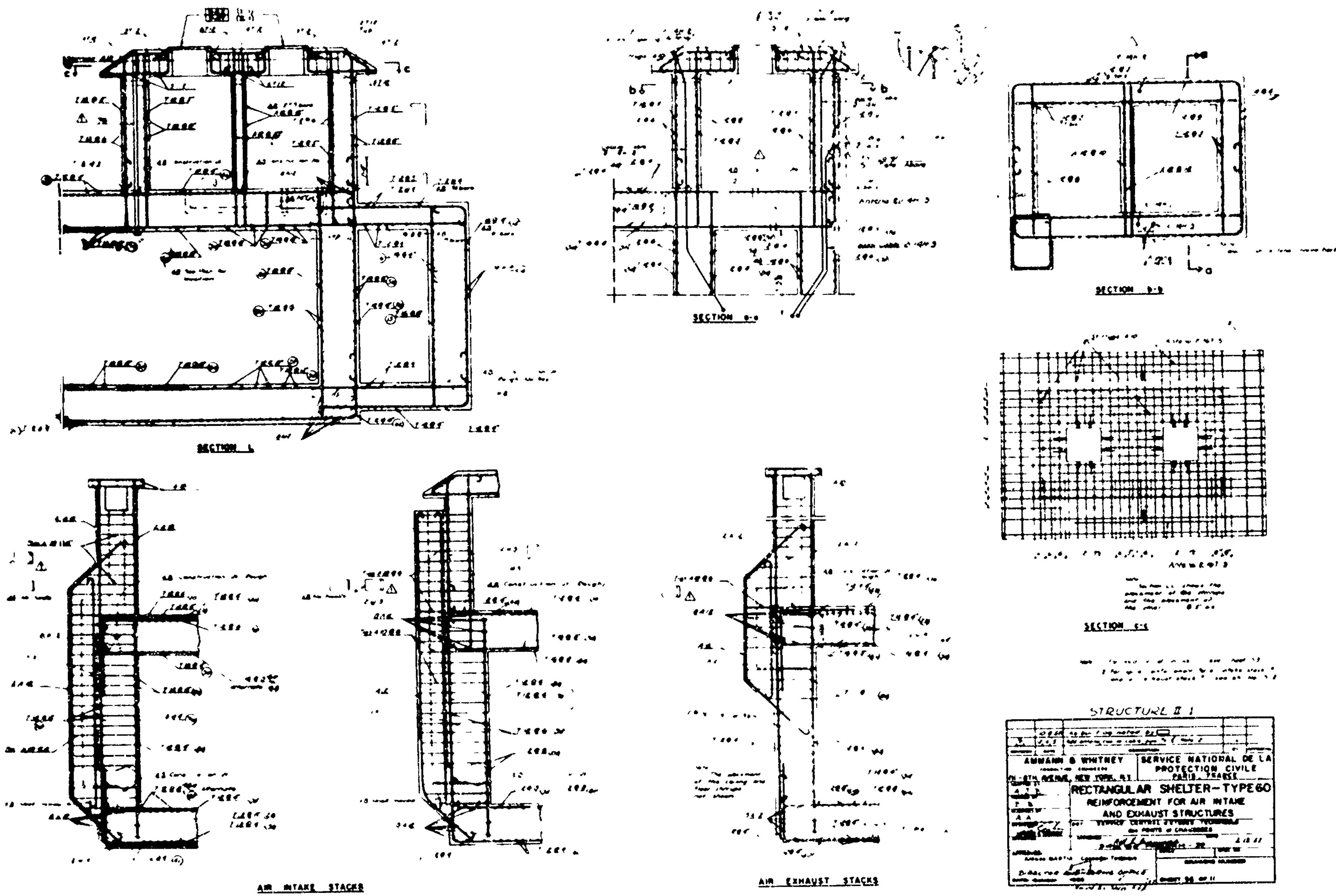

Fig. C.1.6—Rectangular shelter, type 60, reinforcement for air intake and exhaust structures.

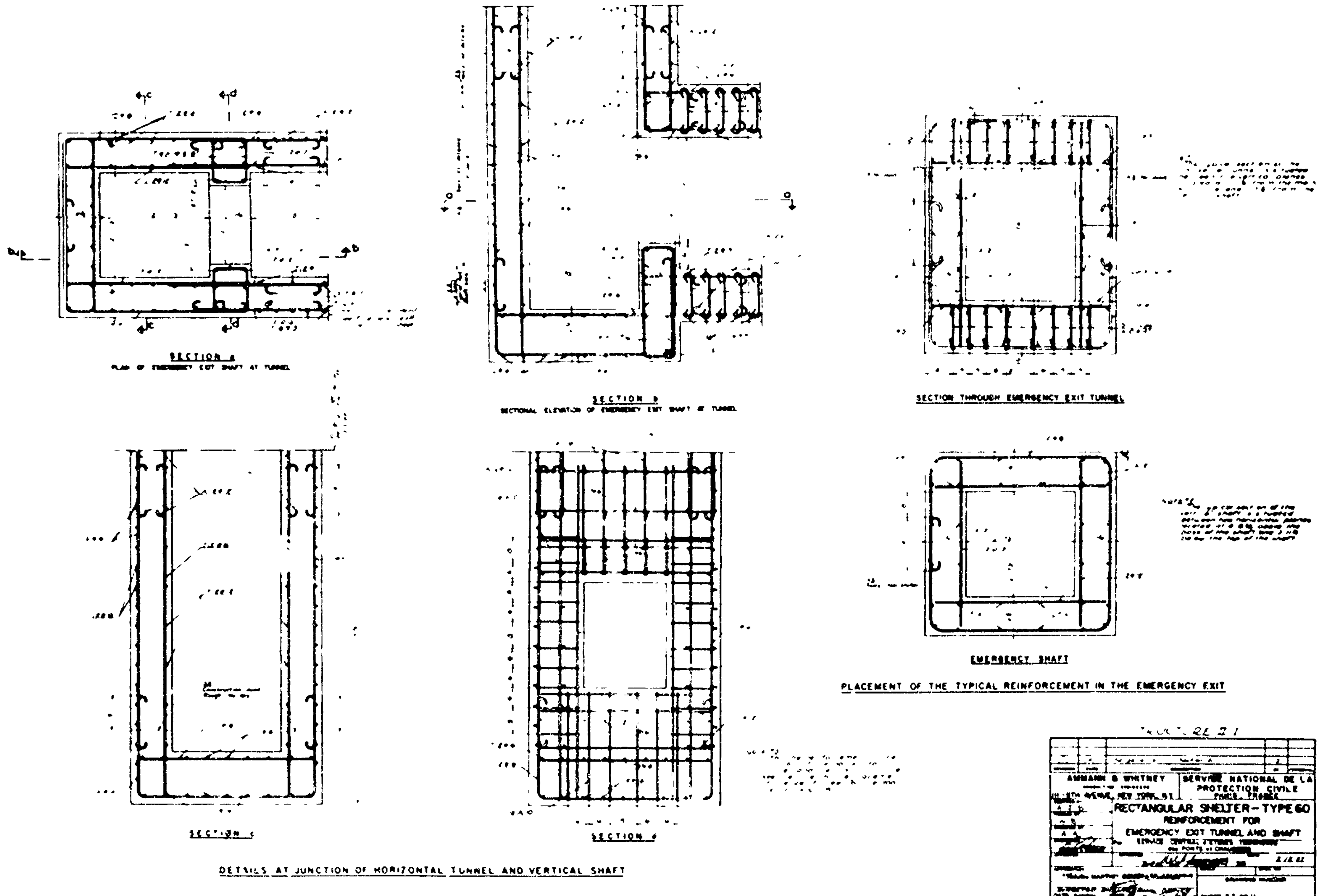

Fig. C.1.7—Rectangular shelter, type 60, reinforcement for emergency exit tunnel and shaft.

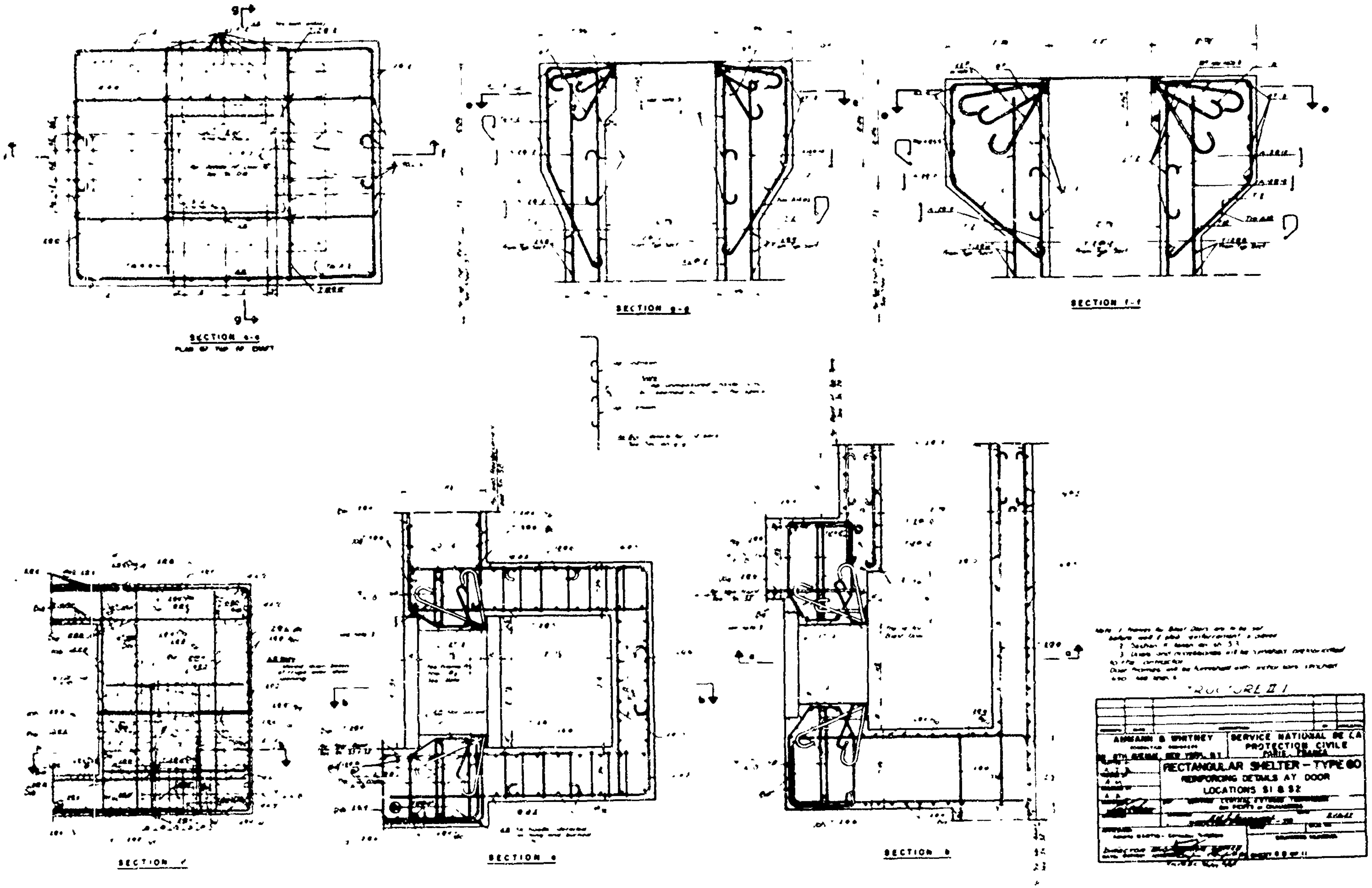

Fig. C.1.8—Rectangular shelter, type 60, reinforcing details at door locations S1 and S2.

Fig. C.1.10—Rectangular shelter, type 60, entrance stairs, sections and details.

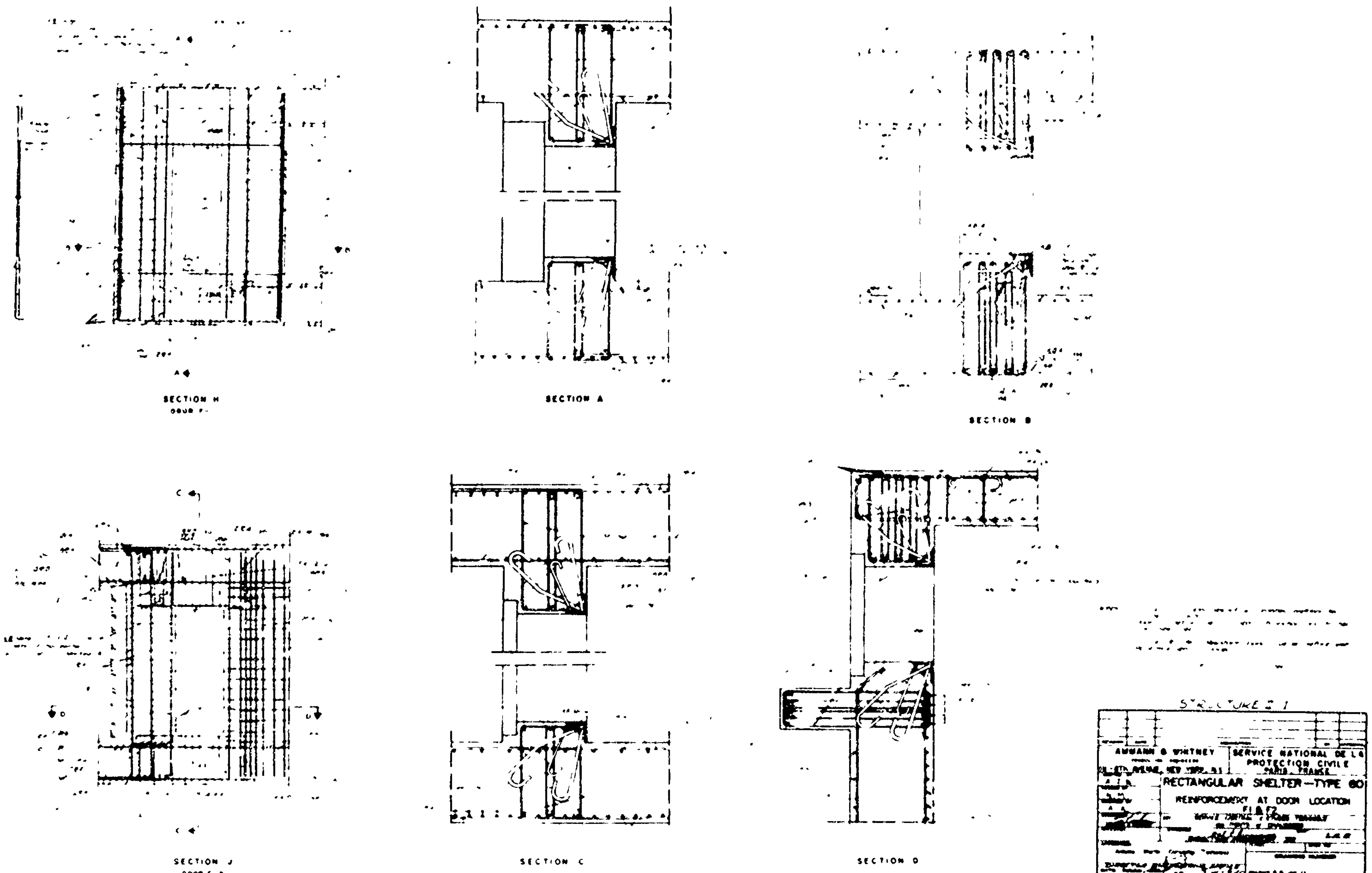

Fig C.1.9—Rectangular shelter, type 60, reinforcement at door locations F1 and F2.

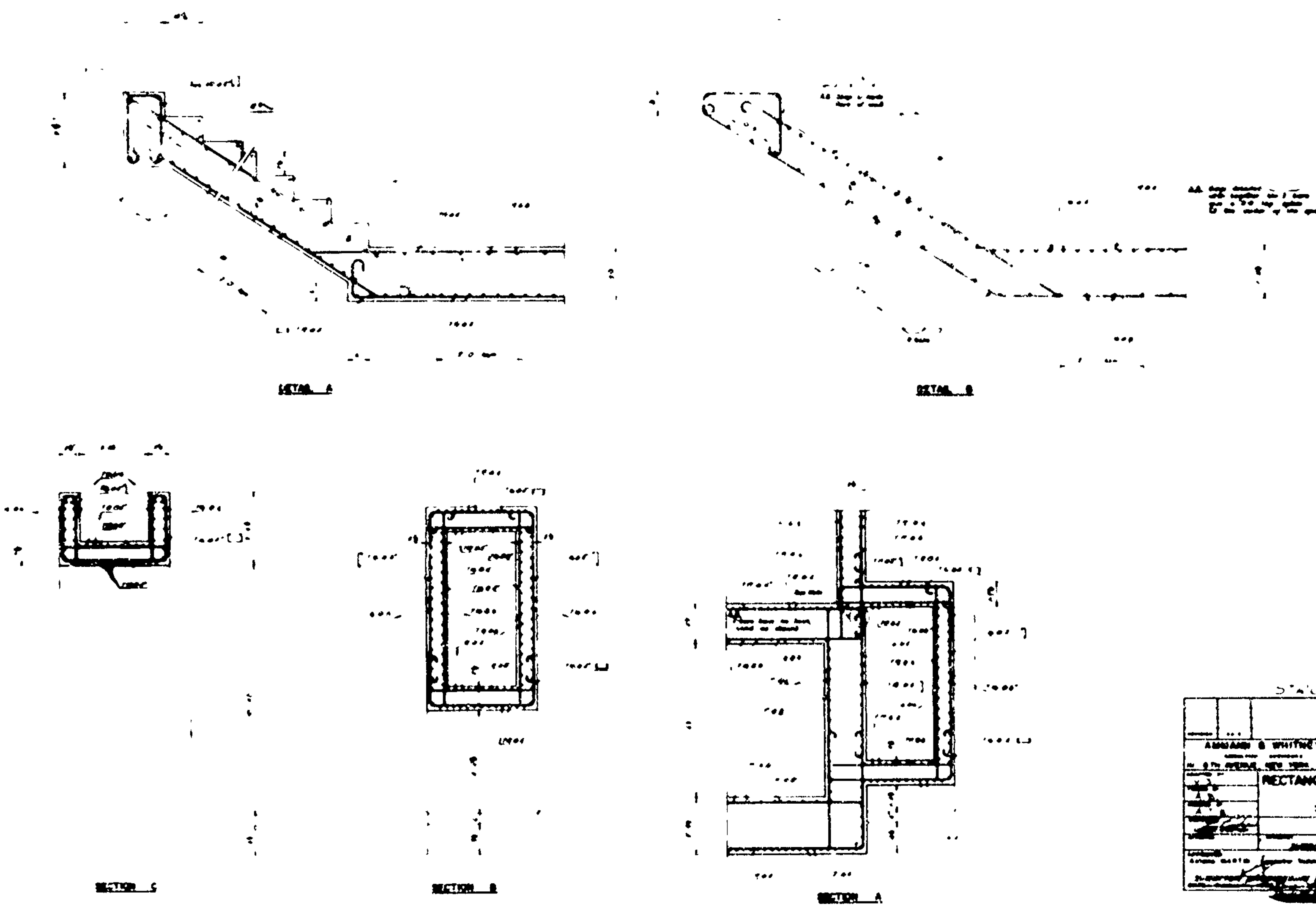

STRUCTURAL # 7

AMMANN & WHITNEY

SERVICE NATIONAL DE LA PROTECTION CIVILE
PARIS, FRANCE

RECTANGULAR SHELTER– TYPE 60
ENTRANCE STAIRS
SECTIONS AND DETAILS

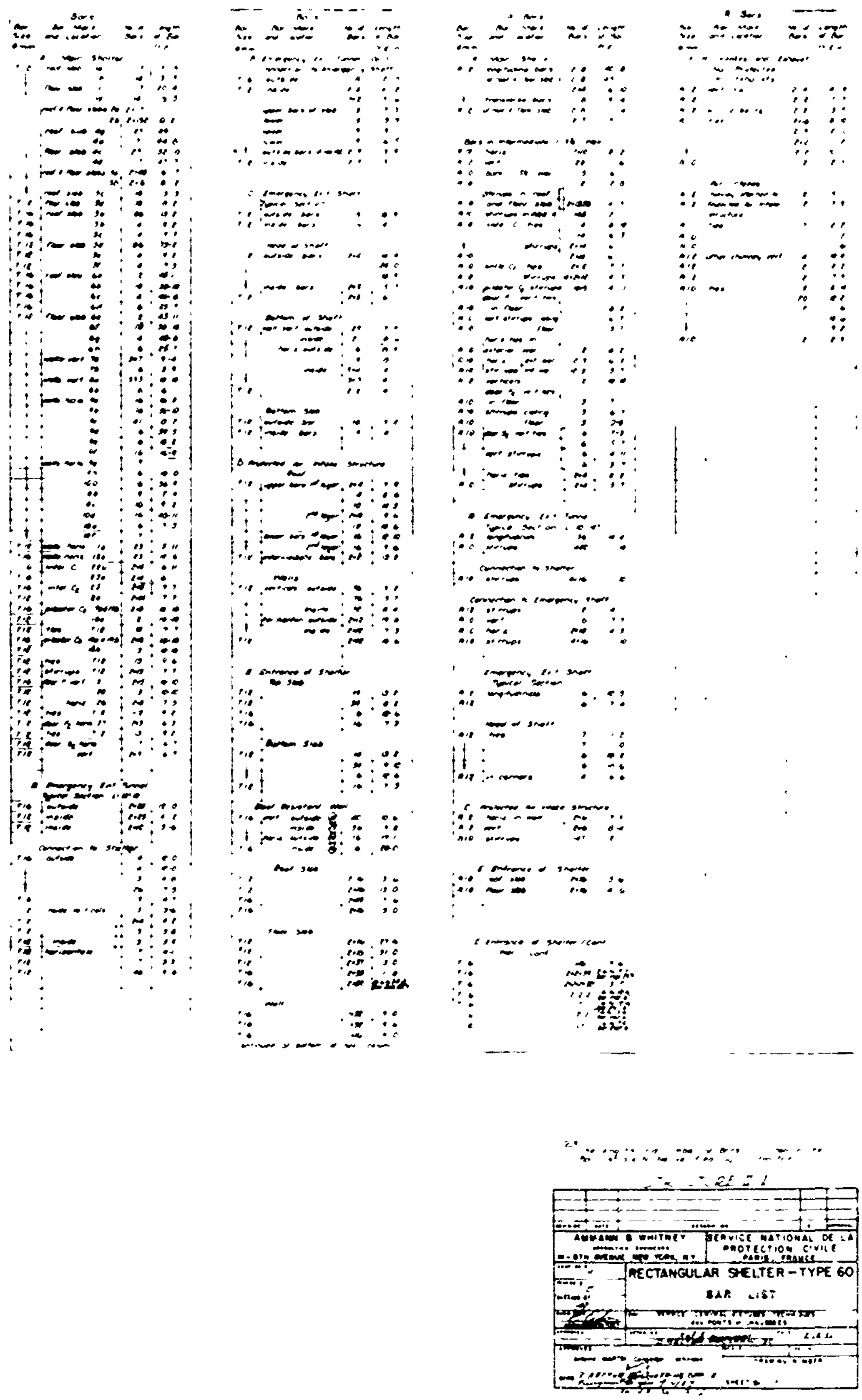

Fig. C.1.11 — Rectangular shelter, type 60, bar list.

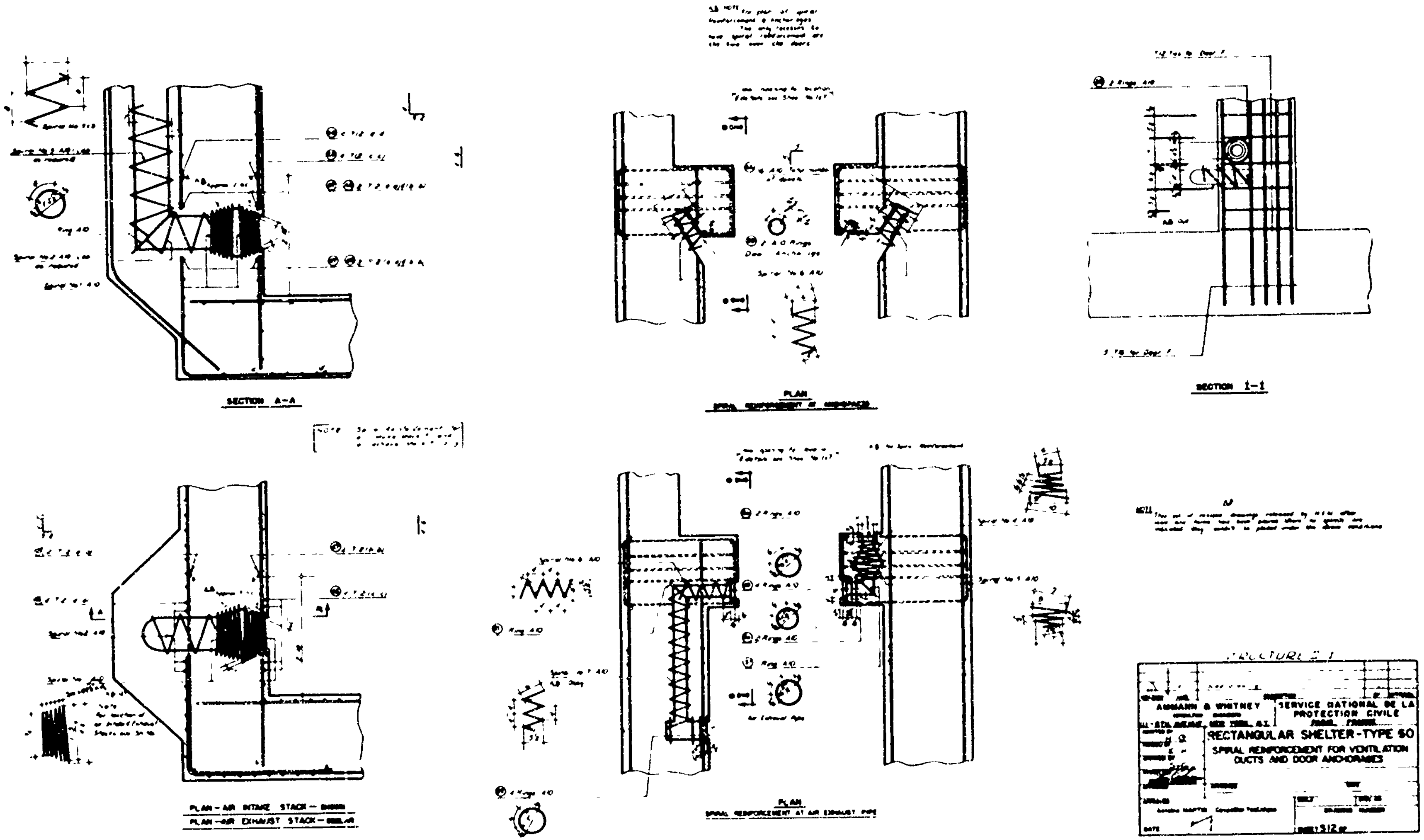

Fig. C.1.12 — Rectangular shelter, type 60, spiral reinforcement for ventilation ducts and door anchorages.

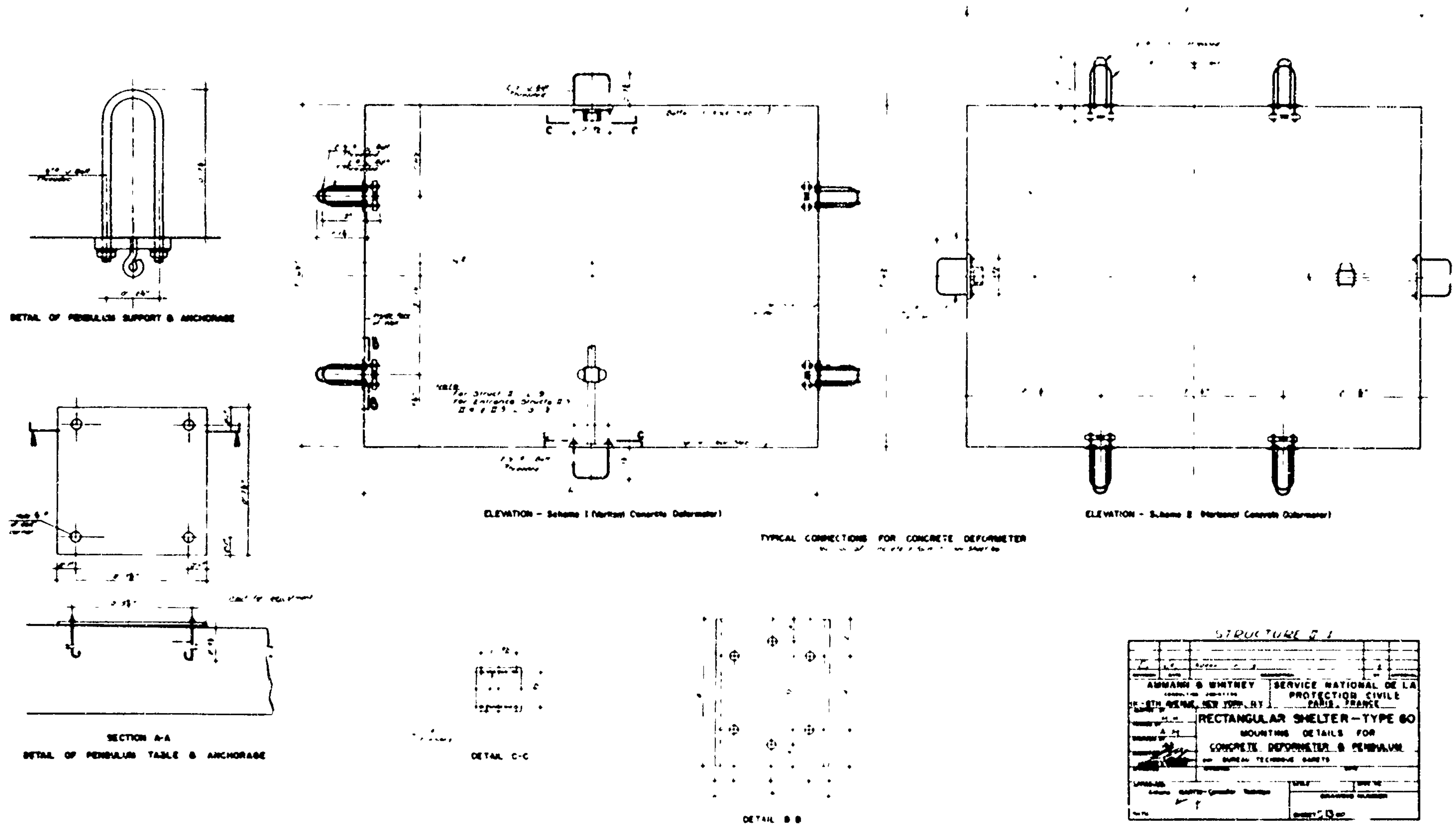

Fig. C.1.13--Rectangular shelter, type 60, mounting details for concrete deformeter and pendulum.

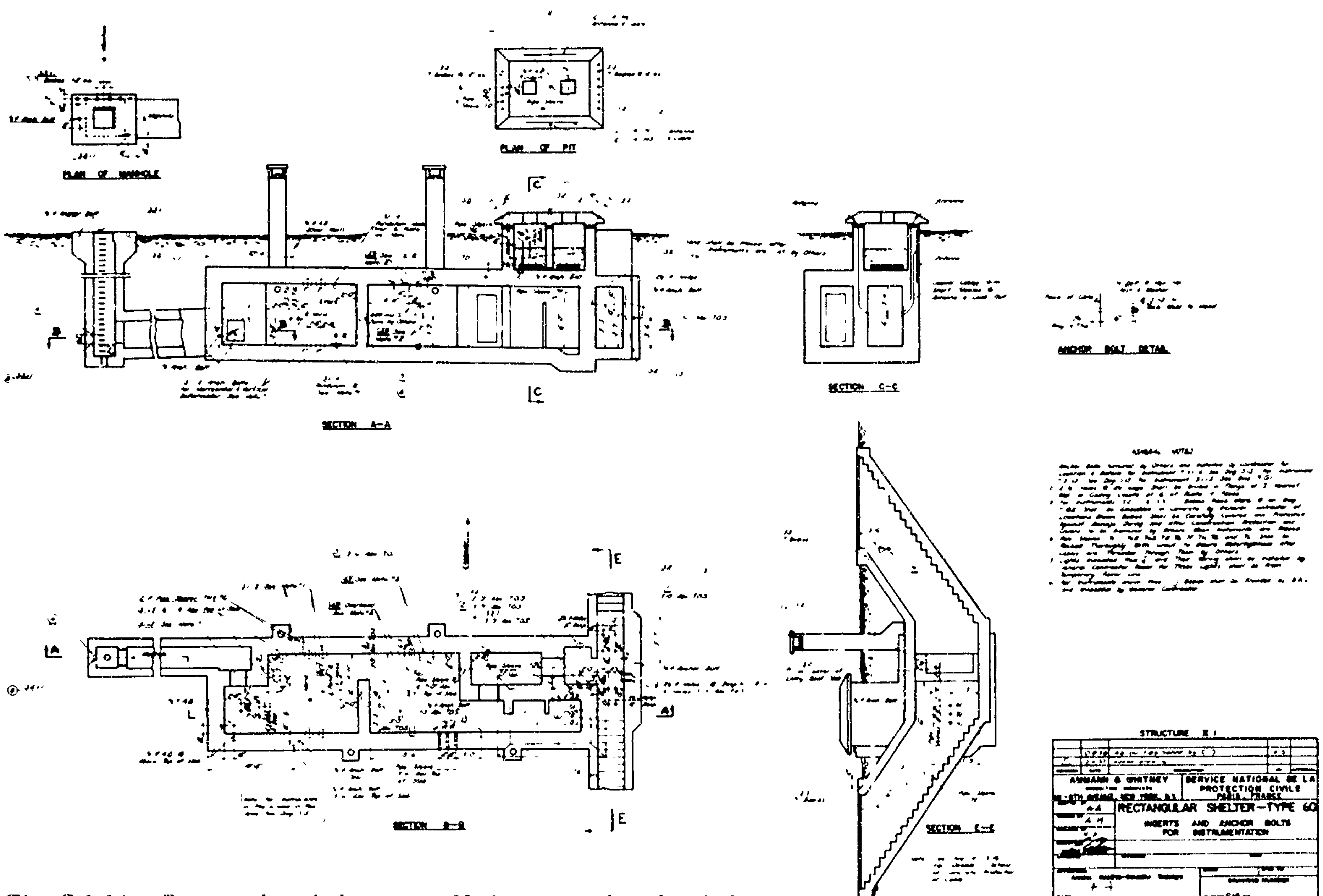

Fig. C.1.14—Rectangular shelter, type 60, inserts and anchor bolts for instrumentation.

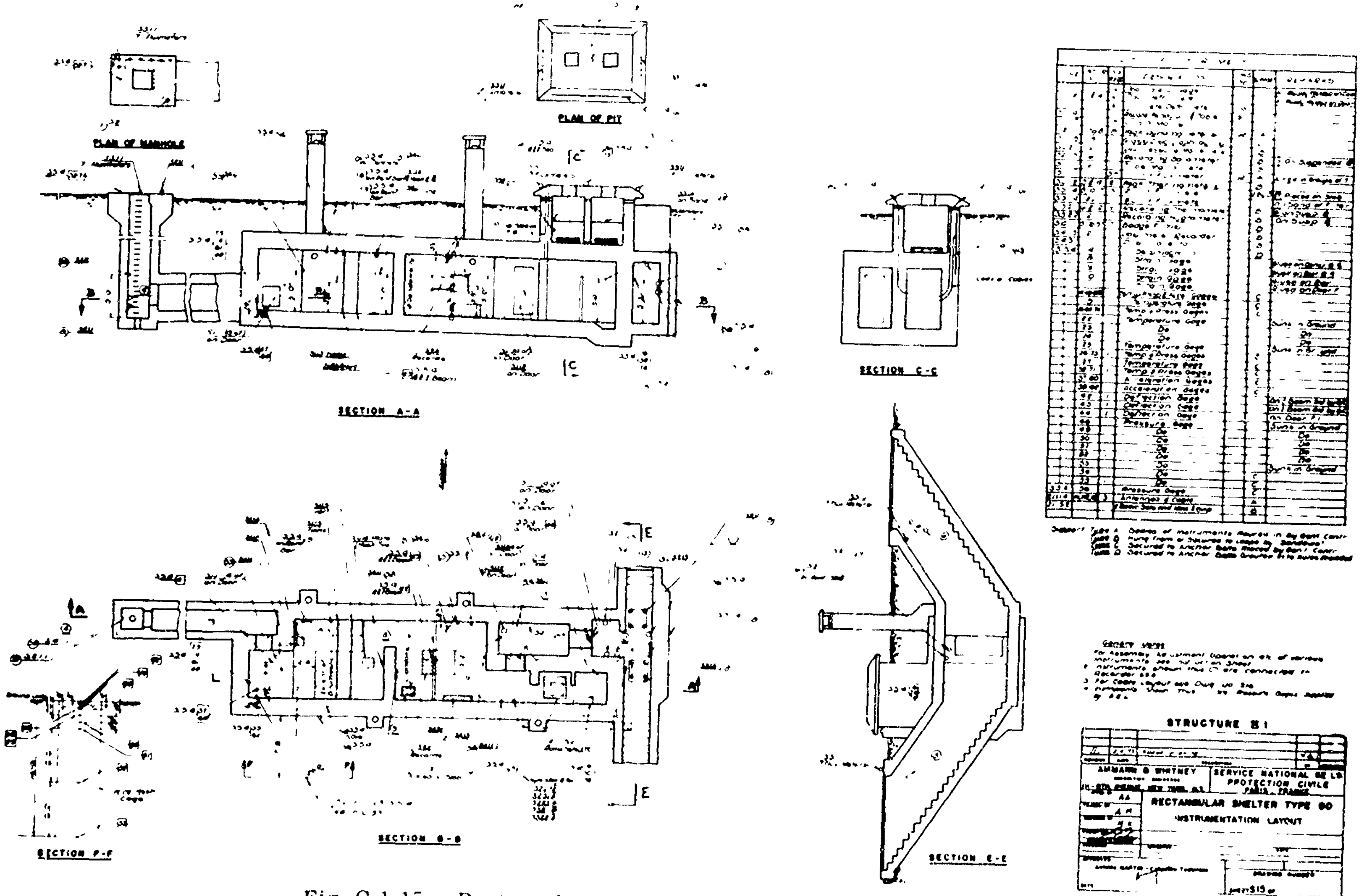

Fig. C.1.15—Rectangular shelter, type 60, instrumentation layout.

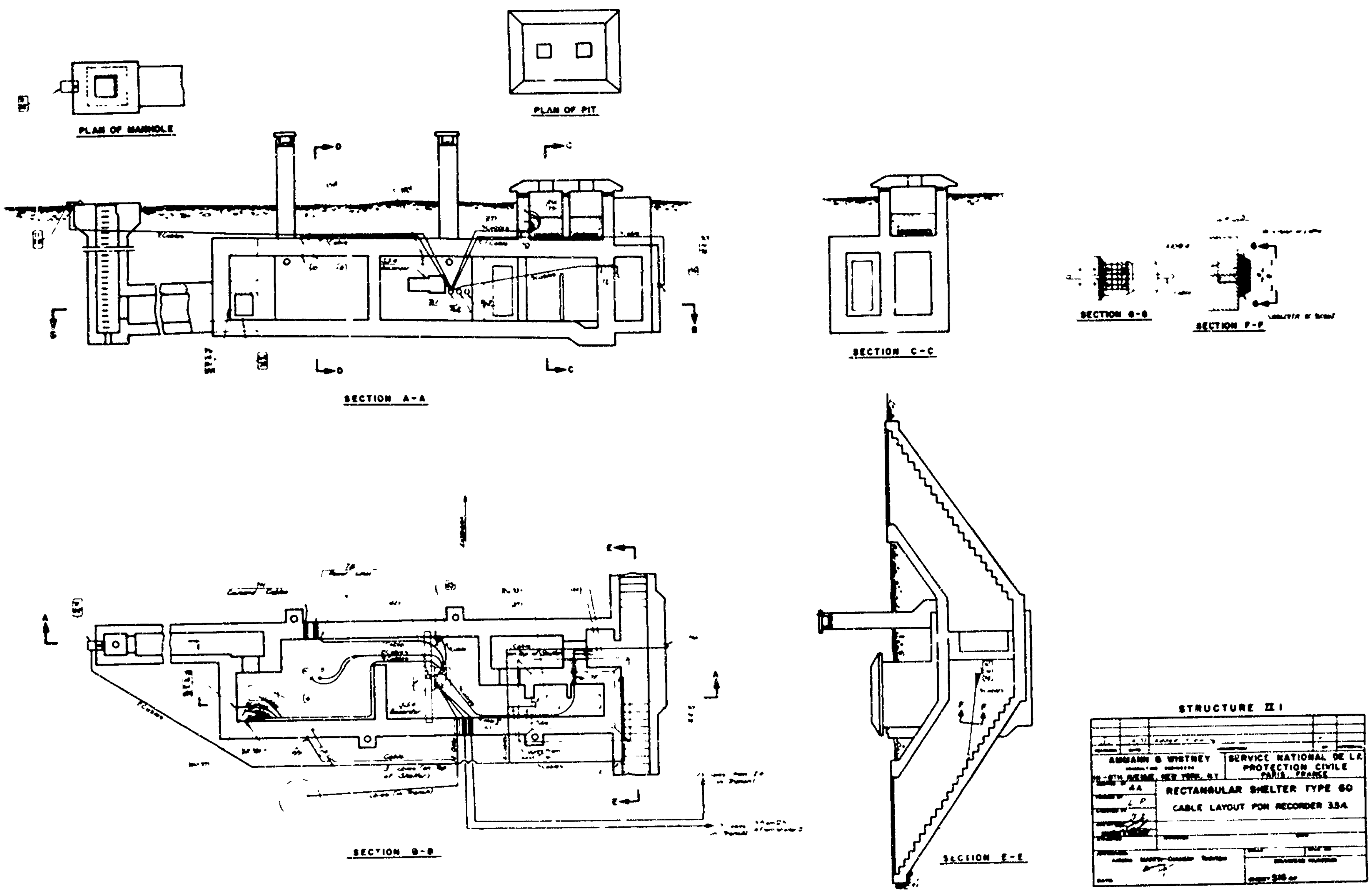

Fig. C.1.16—Rectangular shelter, type 60, cable layout for recorder 3.5.4.

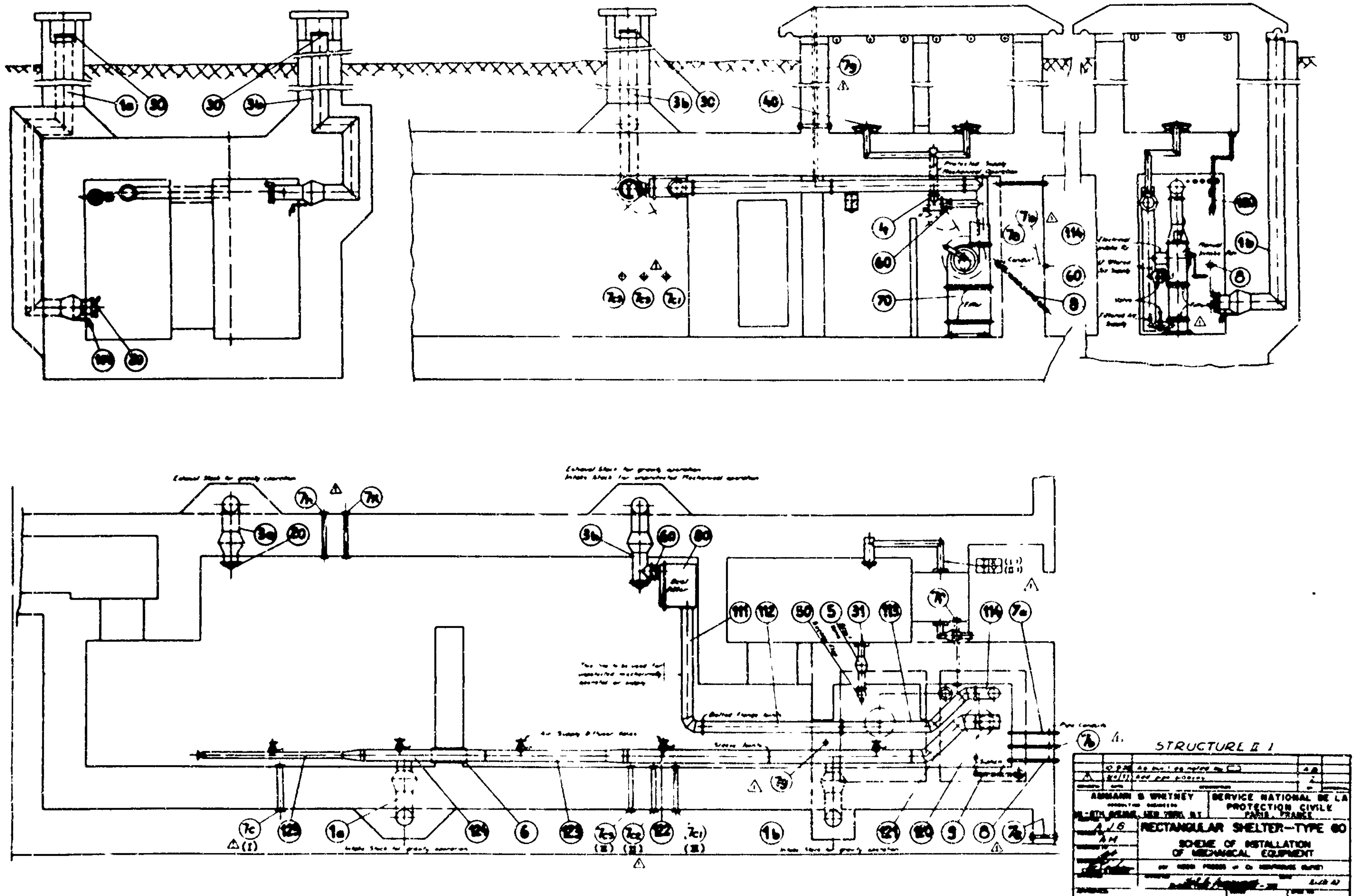

Fig. C.1.17—Rectangular shelter, type 60, scheme of installation of mechanical equipment.

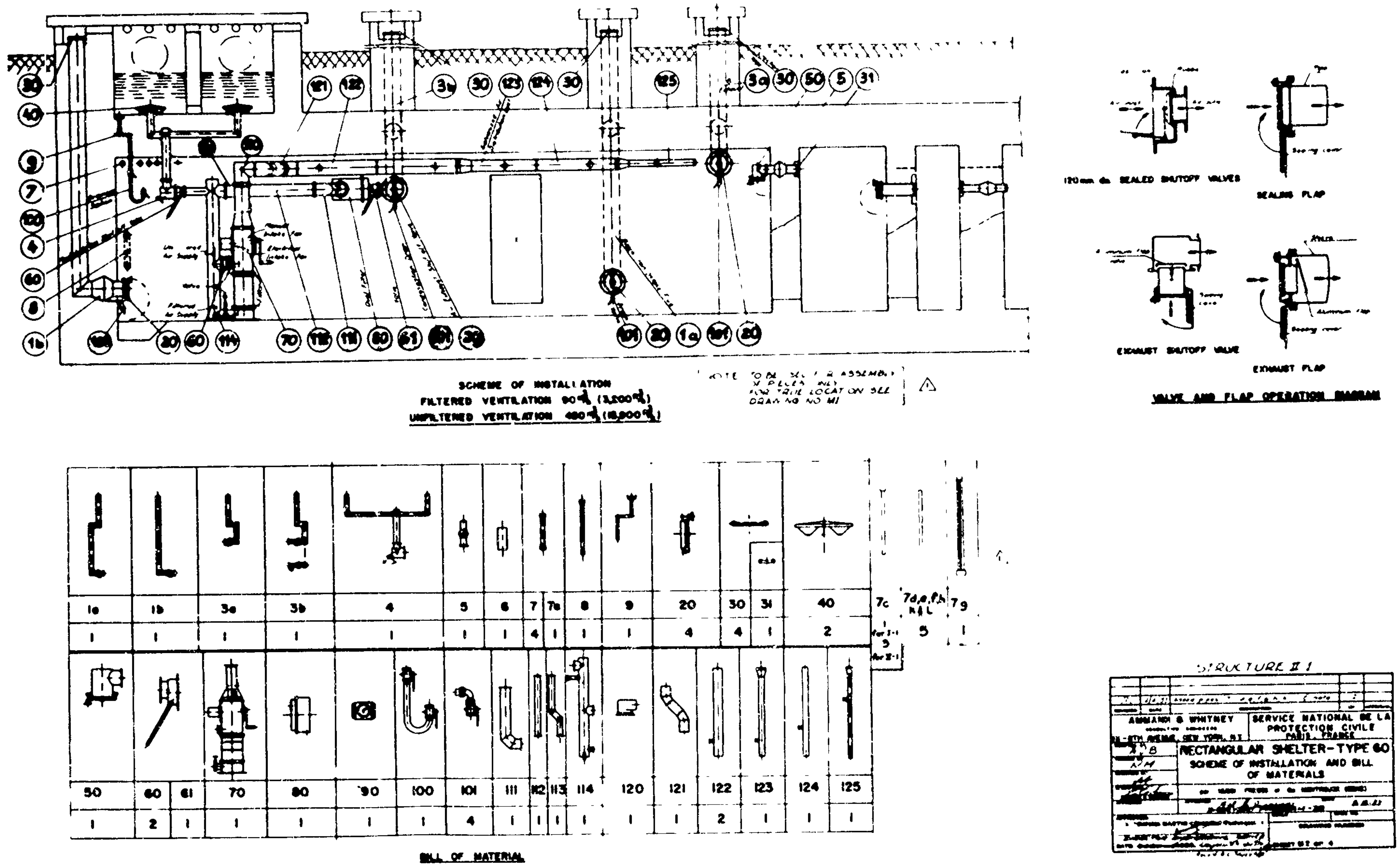

Fig. C.1.18—Rectangular shelter, type 60, scheme of installation and bill of materials.

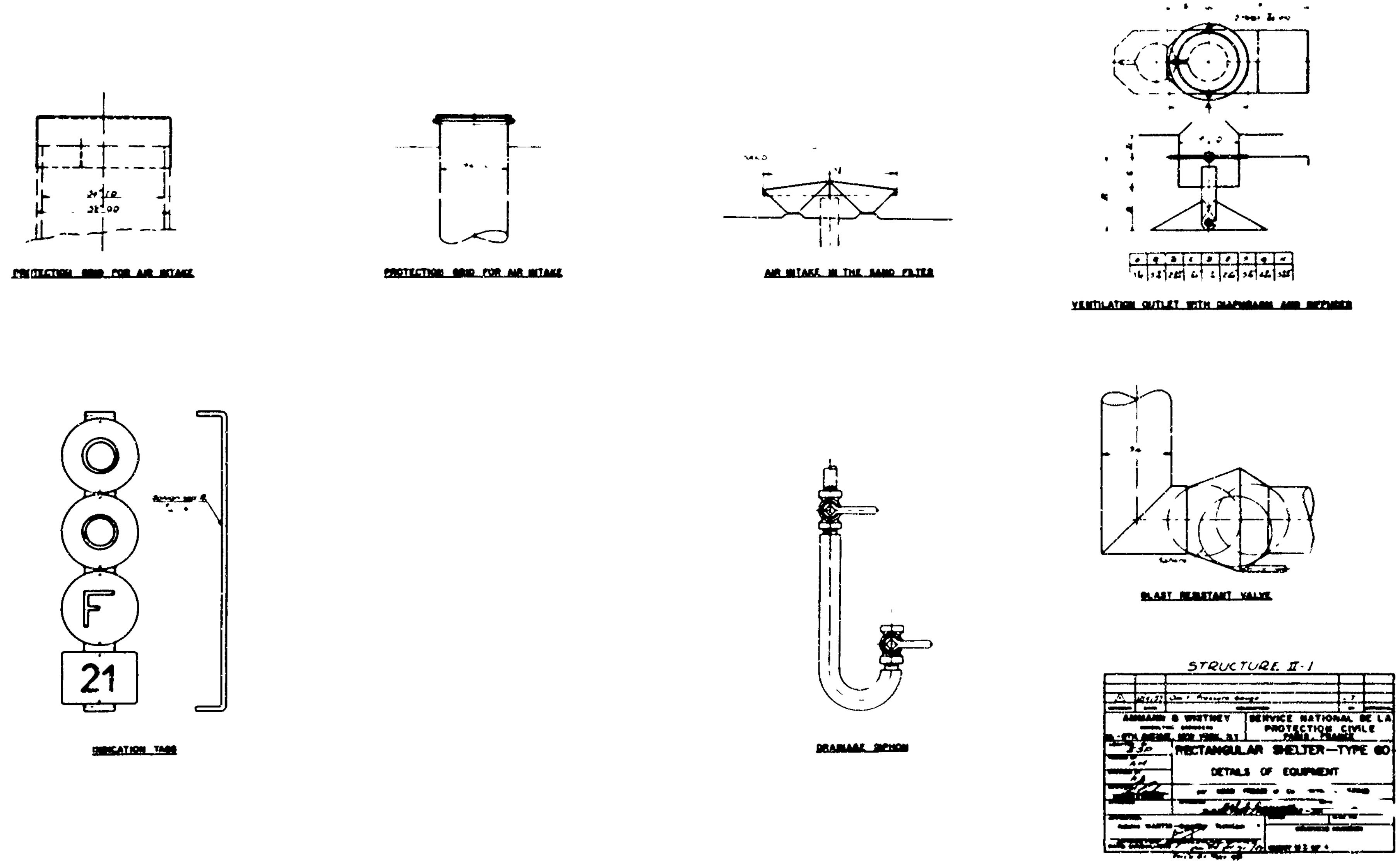

Fig. C.1.19—Rectangular shelter, type 60, details of equipment.

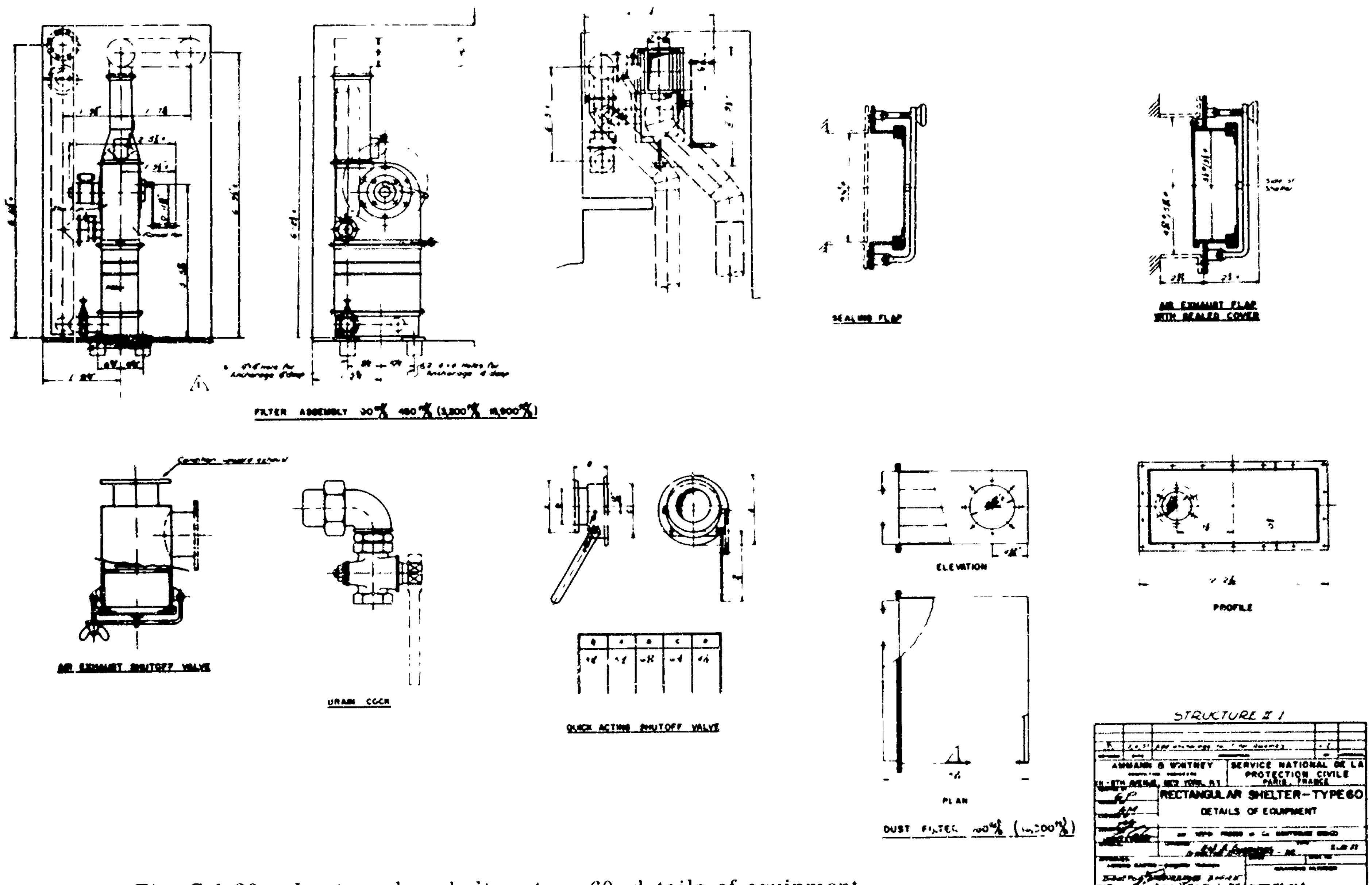

Fig. C.1.20—Rectangular shelter, type 60, details of equipment.

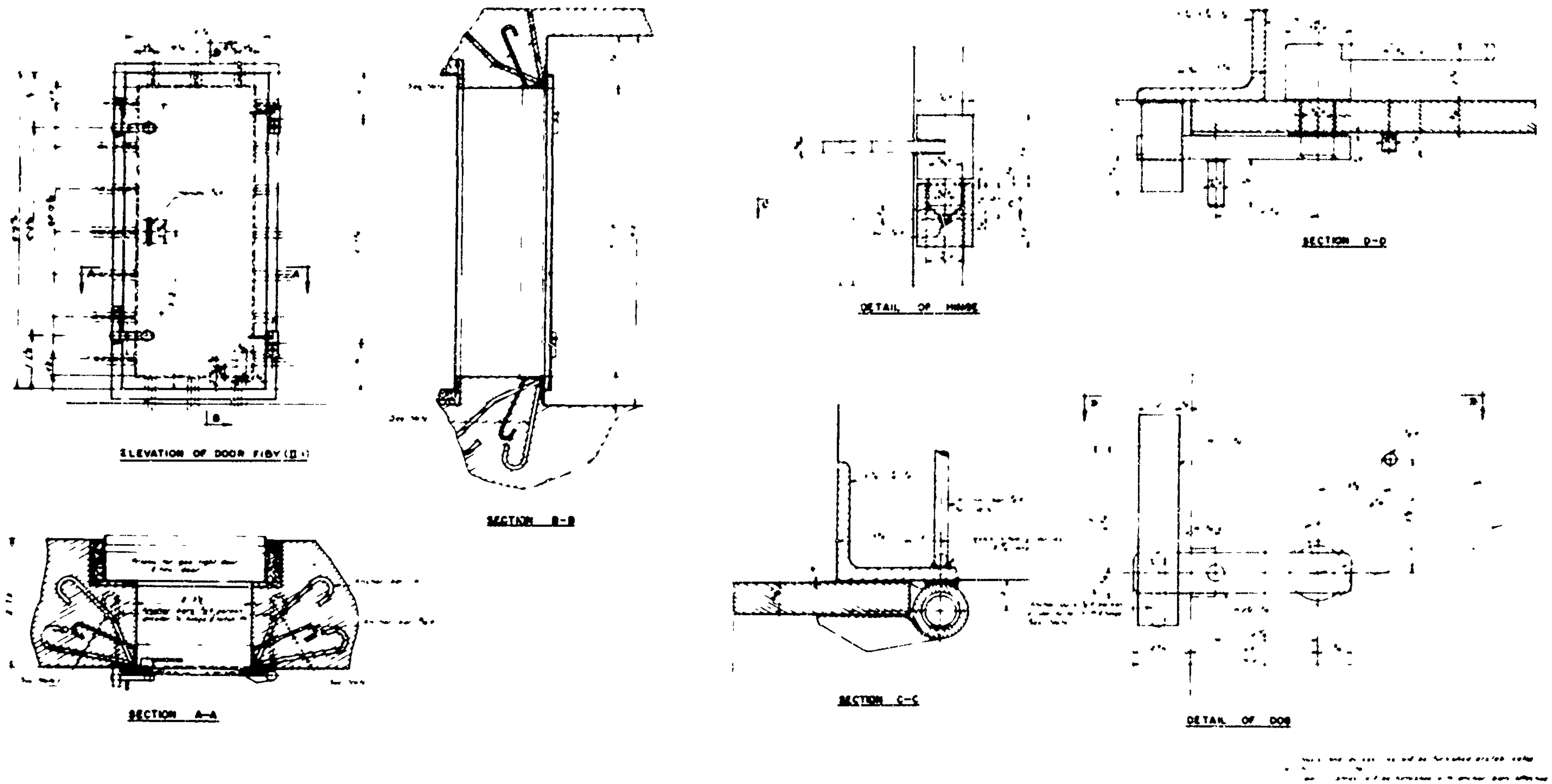

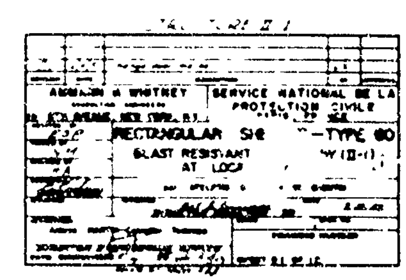

Fig. C.1.21 — Rectangular shelter, type 60, blast-resistant door F1BY, structure II-1, at location F1.

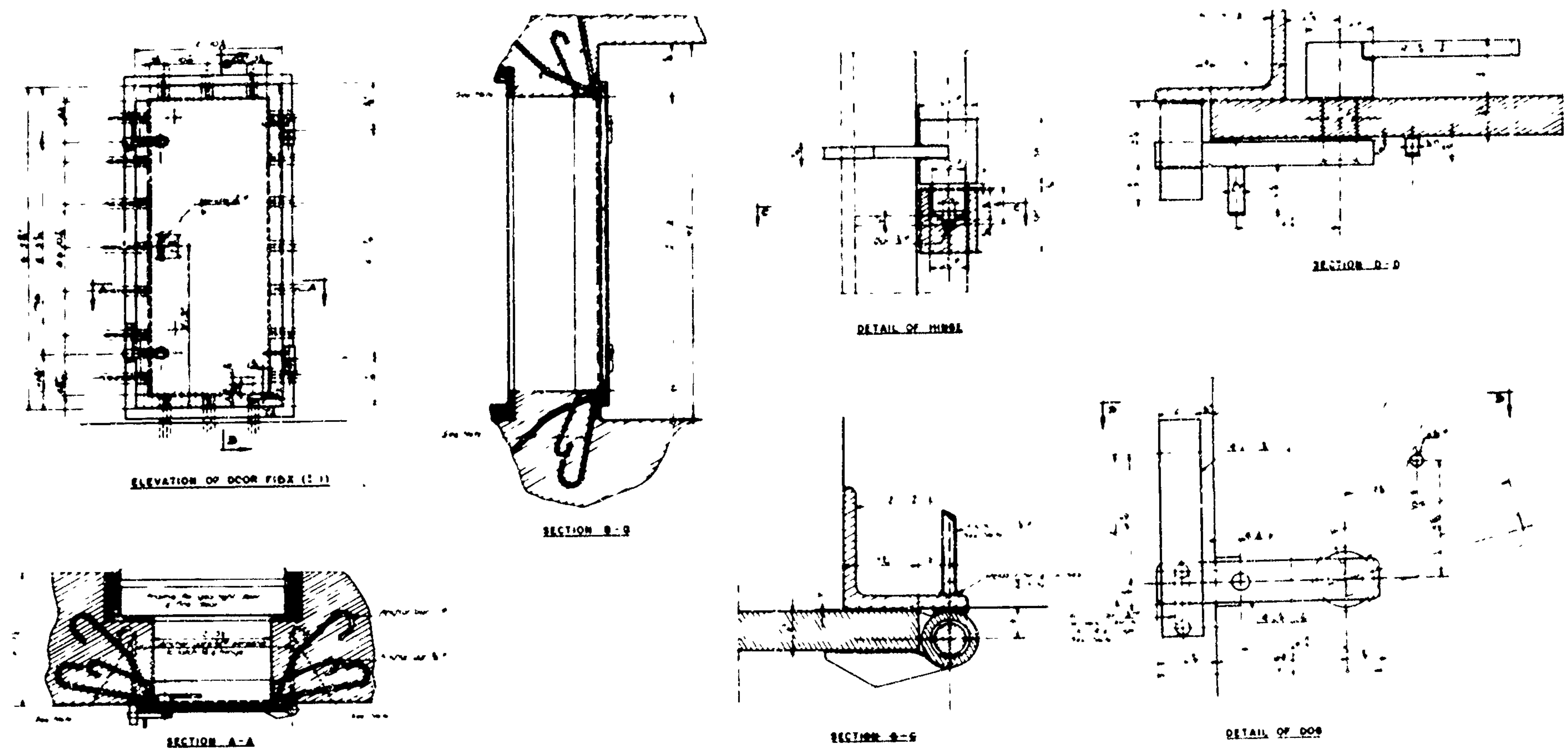

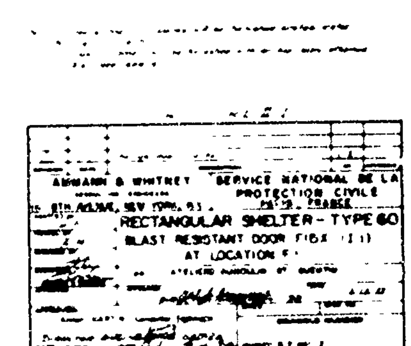

Fig. C.1.22—Rectangular shelter, type 60, blast-resistant door F1BX, structure 1-1, at location F1.

Fig. C.1.24 — Rectangular shelter, type 60, fire door at location F1.

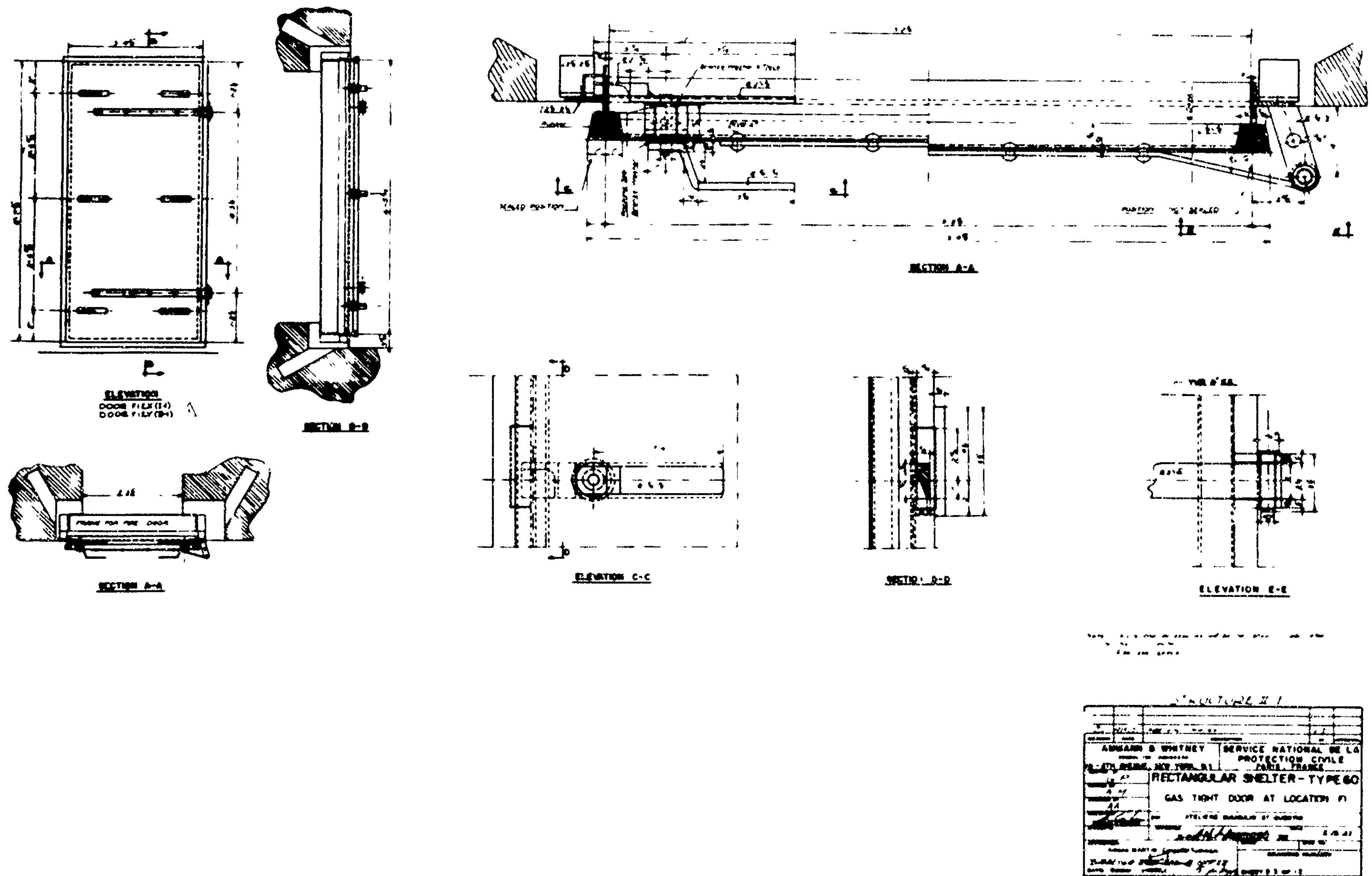

Fig. C.1.23 — Rectangular shelter, type 60, gastight door at location F1.

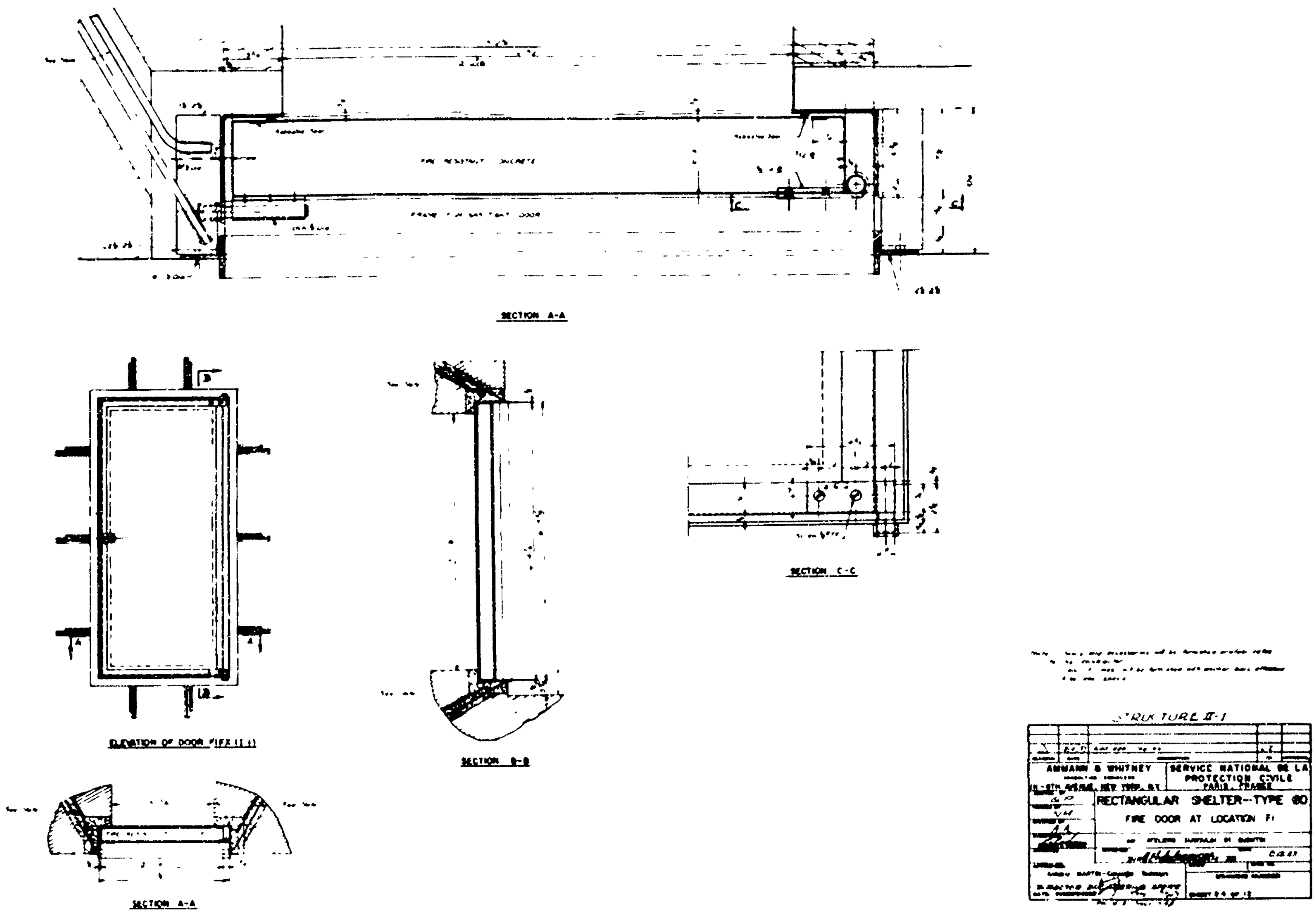

Fig. C.1.24—Rectangular shelter, type 60, fire door at location F1.

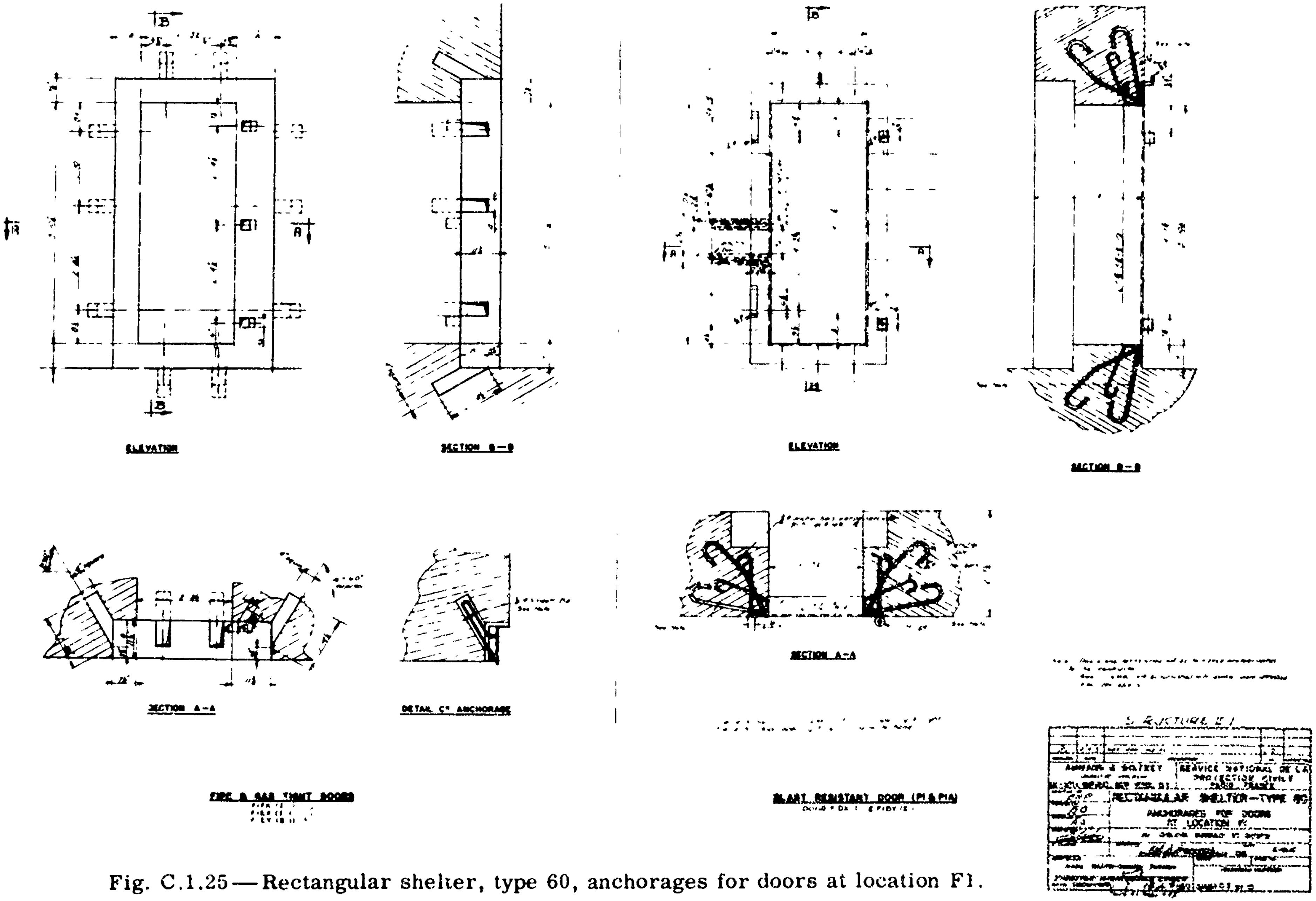

Fig. C.1.25—Rectangular shelter, type 60, anchorages for doors at location F1.

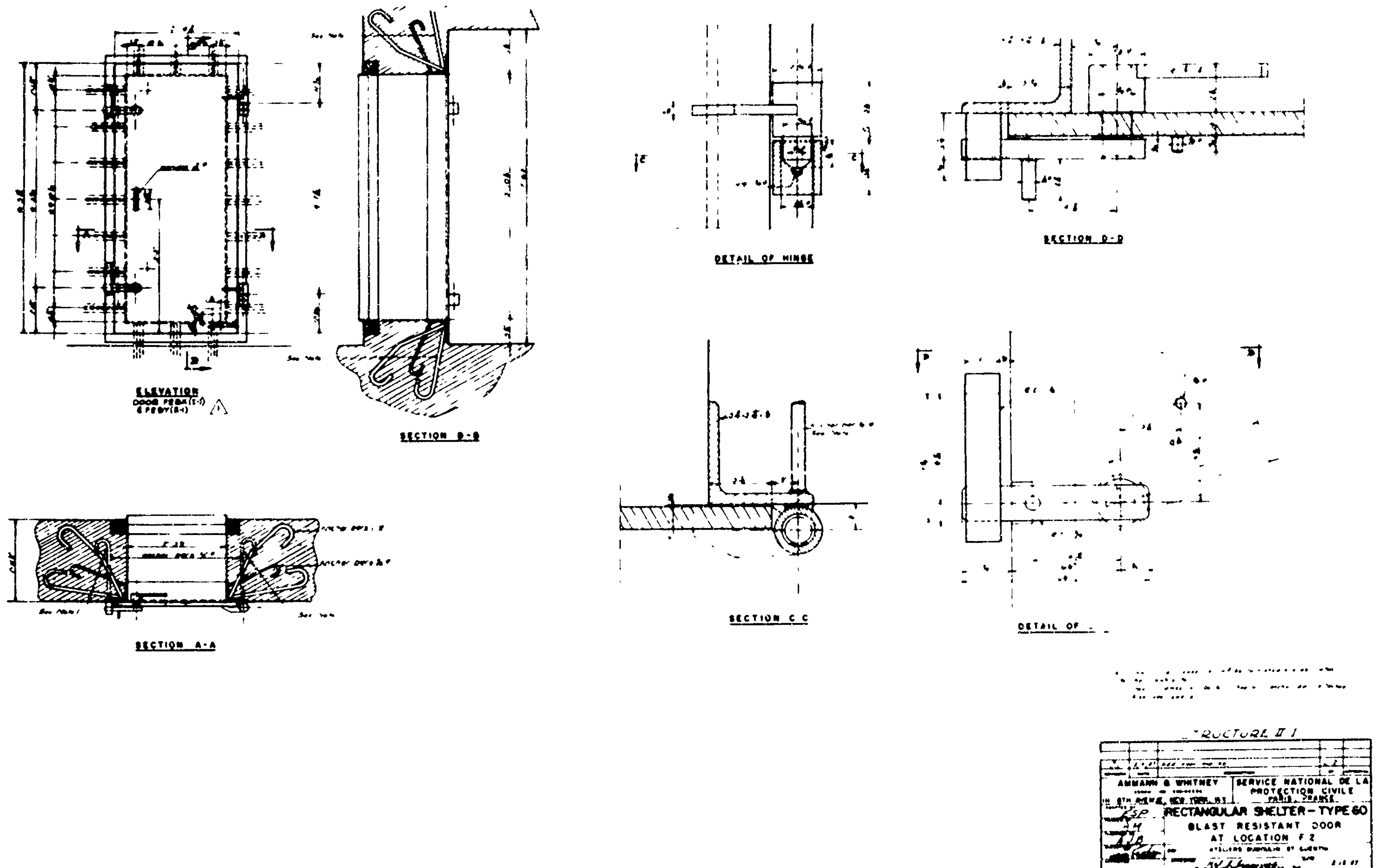

Fig. C.1.26 — Rectangular shelter, type 60, blast-resistant door at location F2.

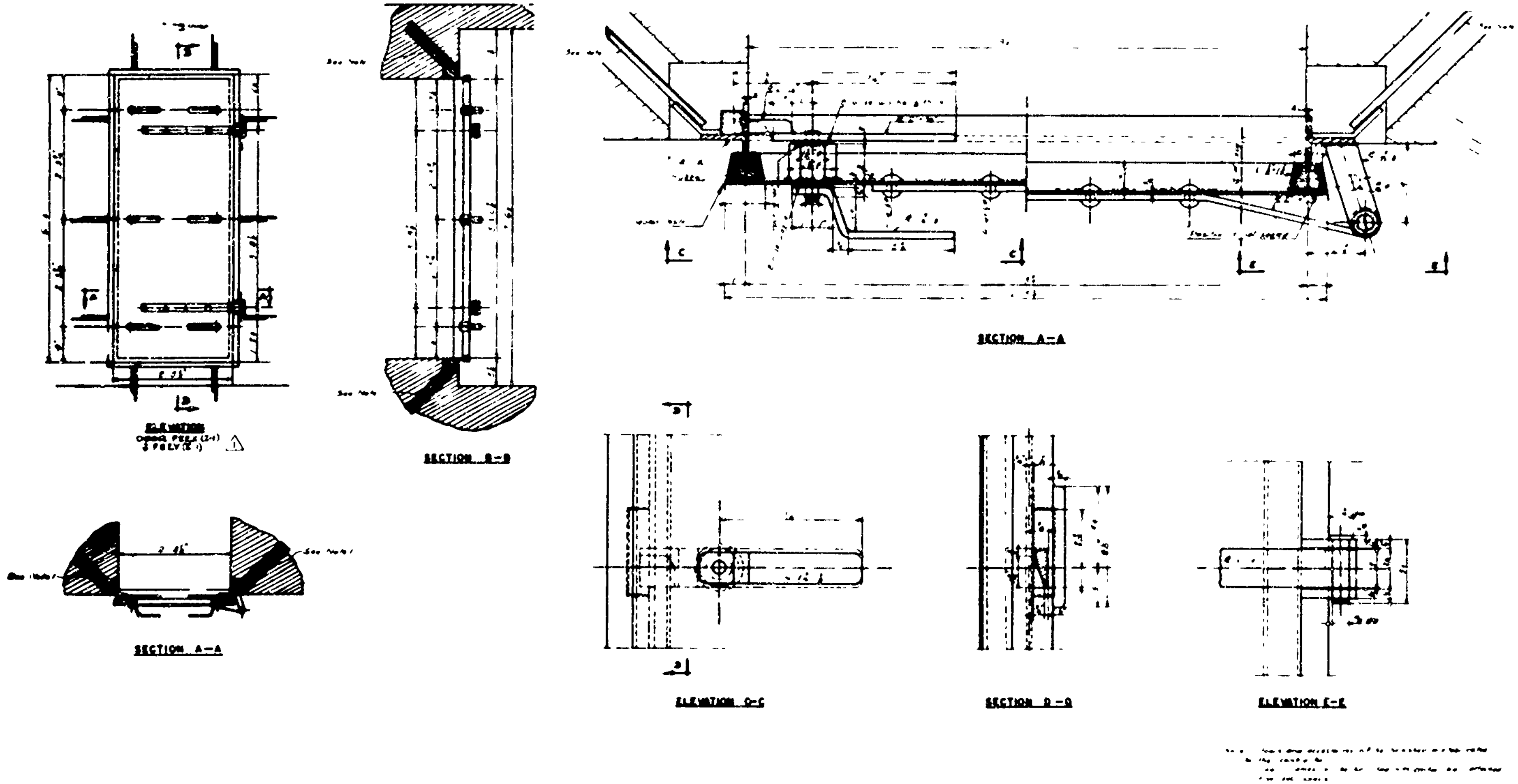

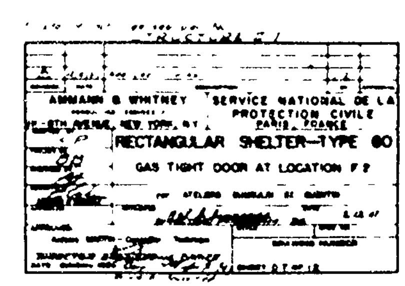

Fig. C.1.27—Rectangular shelter, type 60, gastight door at location F2.

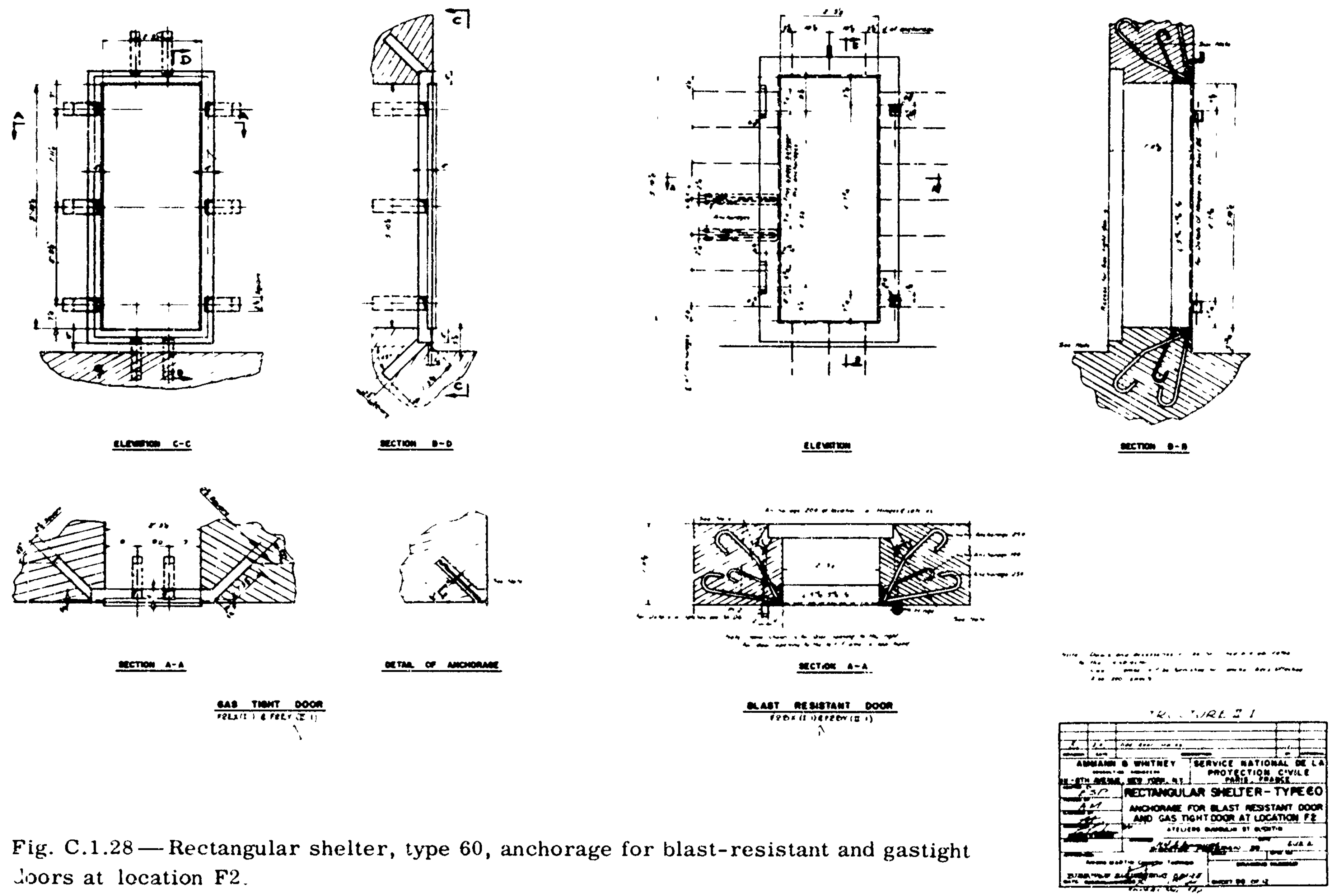

Fig. C.1.28 — Rectangular shelter, type 60, anchorage for blast-resistant and gastight doors at location F2.

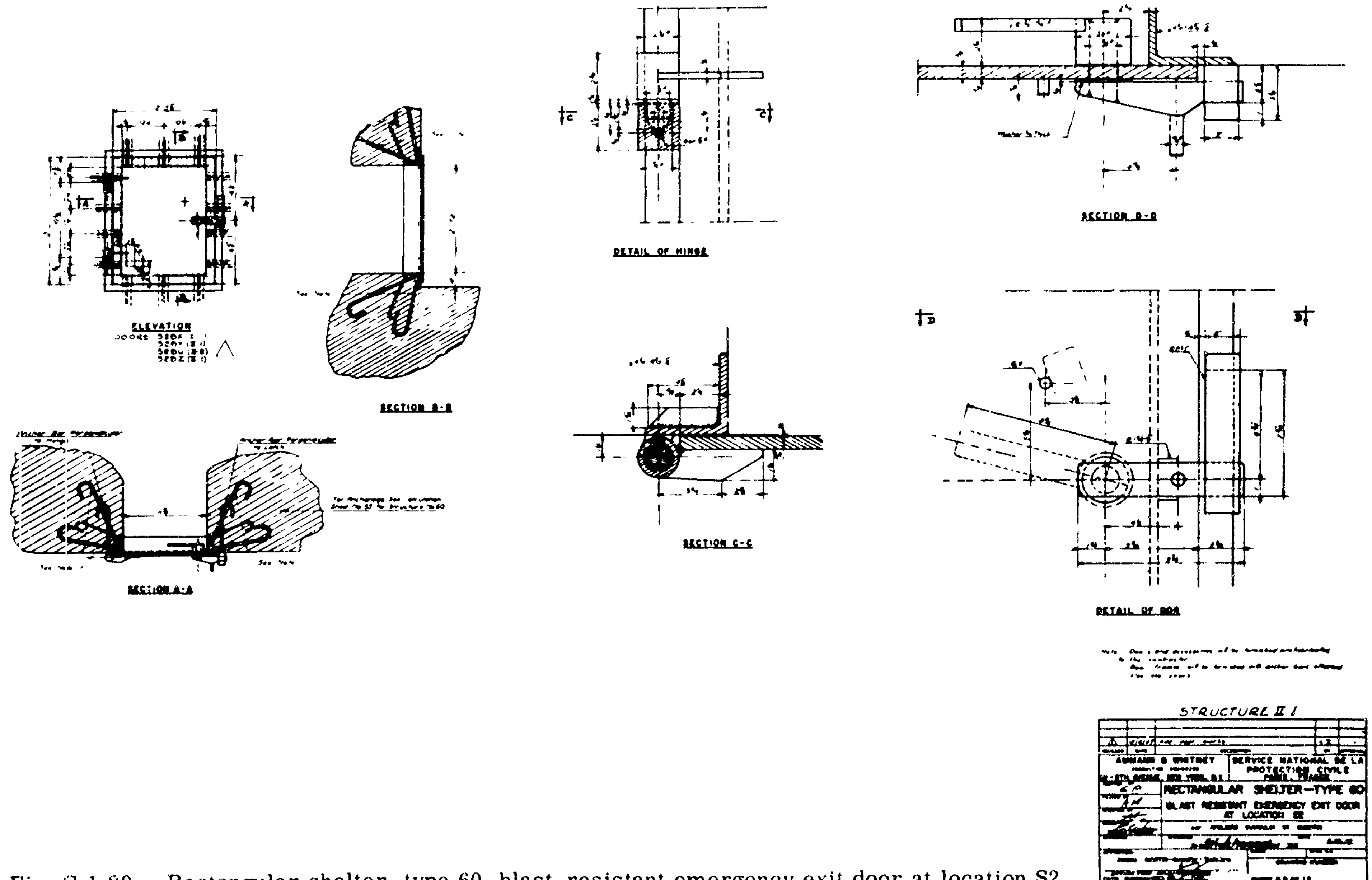

Fig. C.1.29—Rectangular shelter, type 60, blast-resistant emergency exit door at location S2.

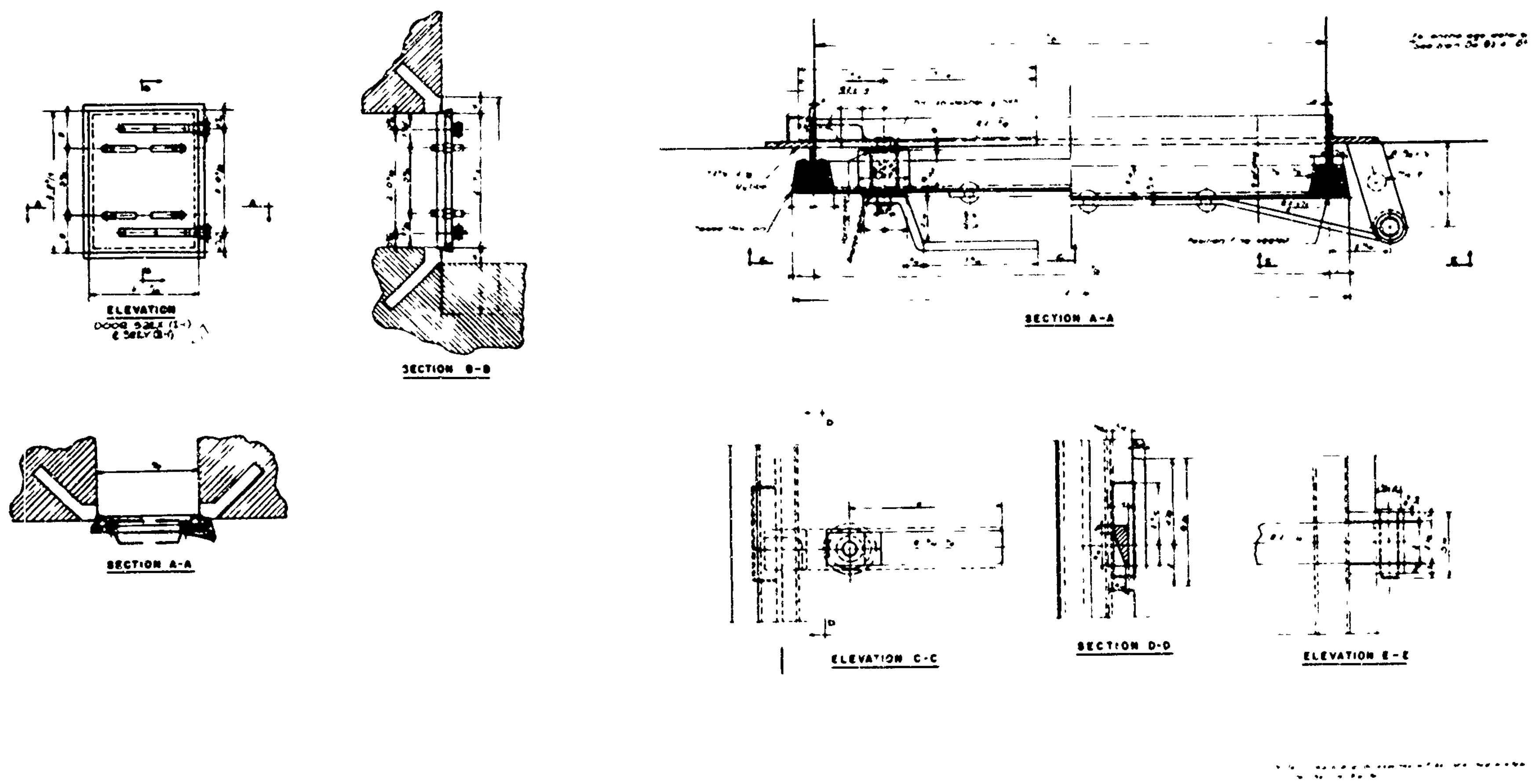

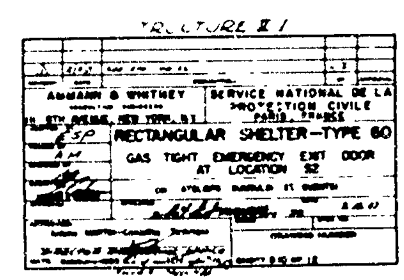

Fig. C.1.30 — Rectangular shelter, type 60, gastight emergency exit door at location S2.

Fig. C.1.32—Rectangular shelter, type 60, blast-resistant door and anchorage at location S1.

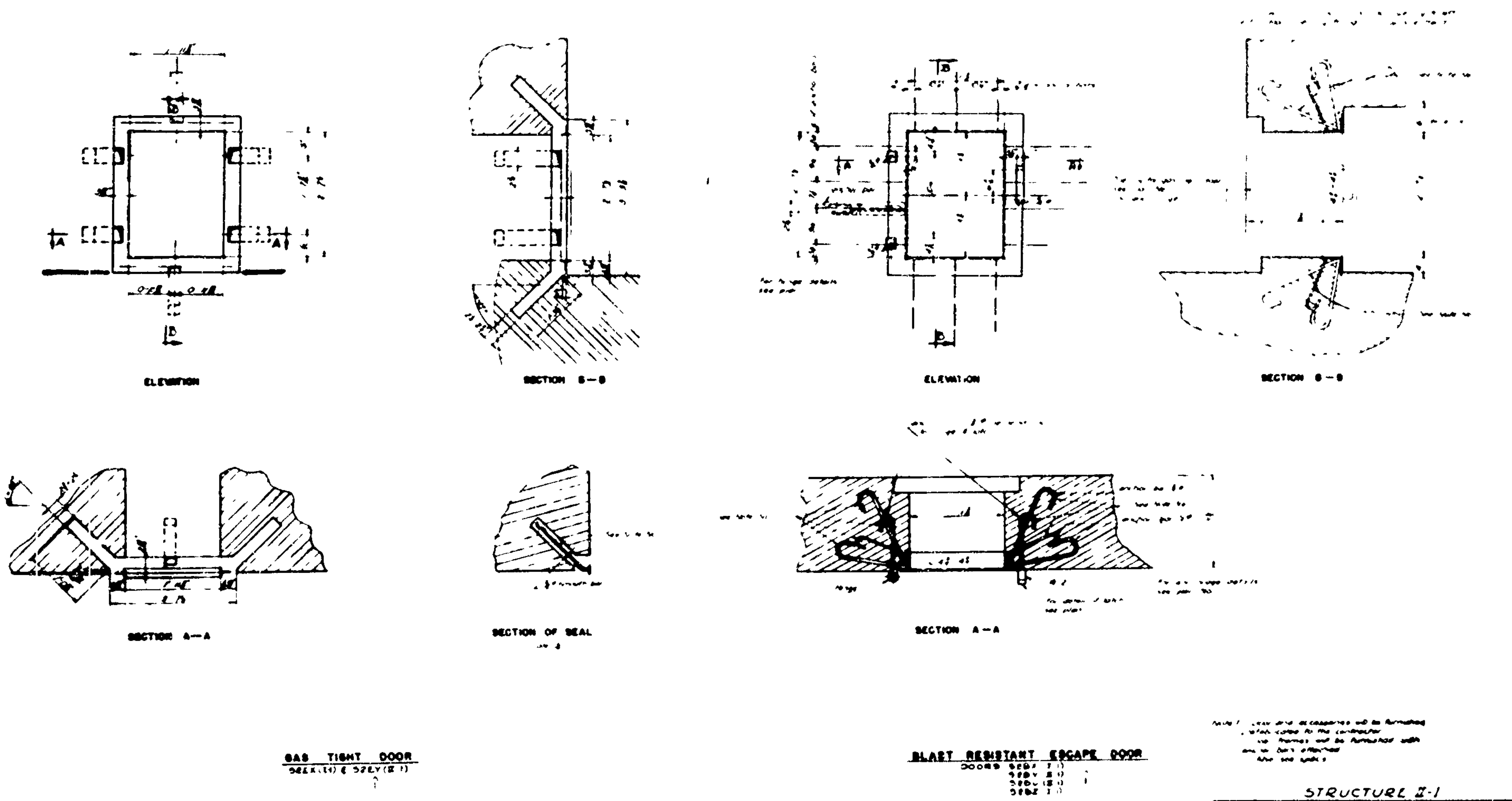

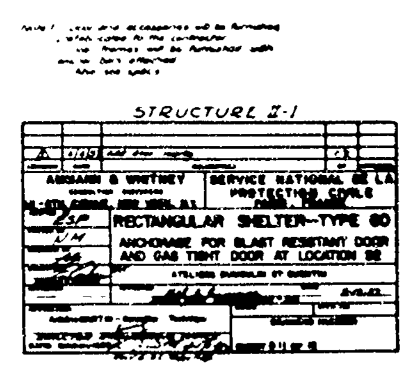

Fig. C.1.31—Rectangular shelter, type 60, anchorage for blast-resistant and gastight doors at location S2.

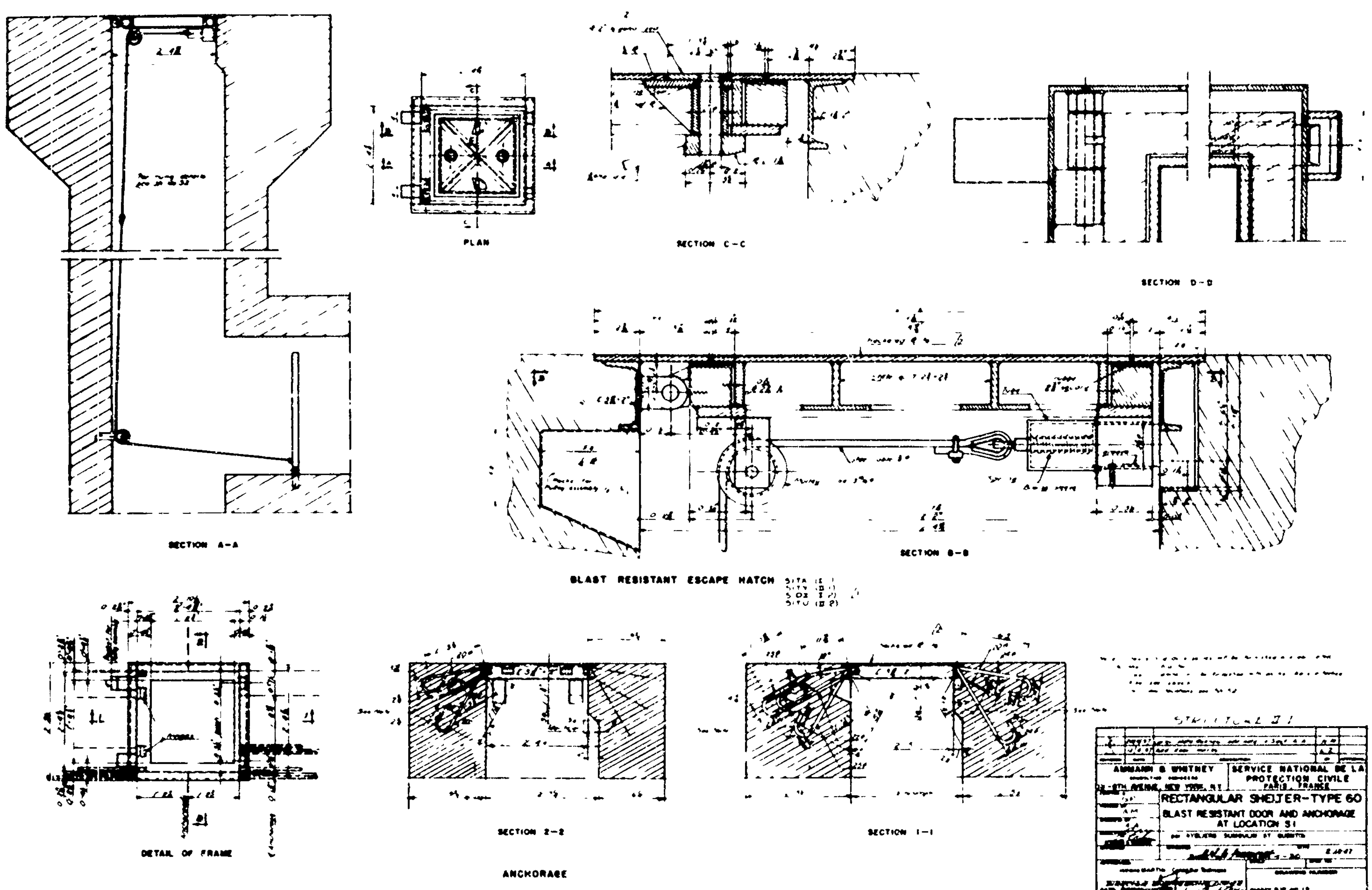

Fig. C.1.32—Rectangular shelter, type 60, blast-resistant door and anchorage at location S1.

Fig. C.2 — Circular concrete shelter, type 50, title sheet.

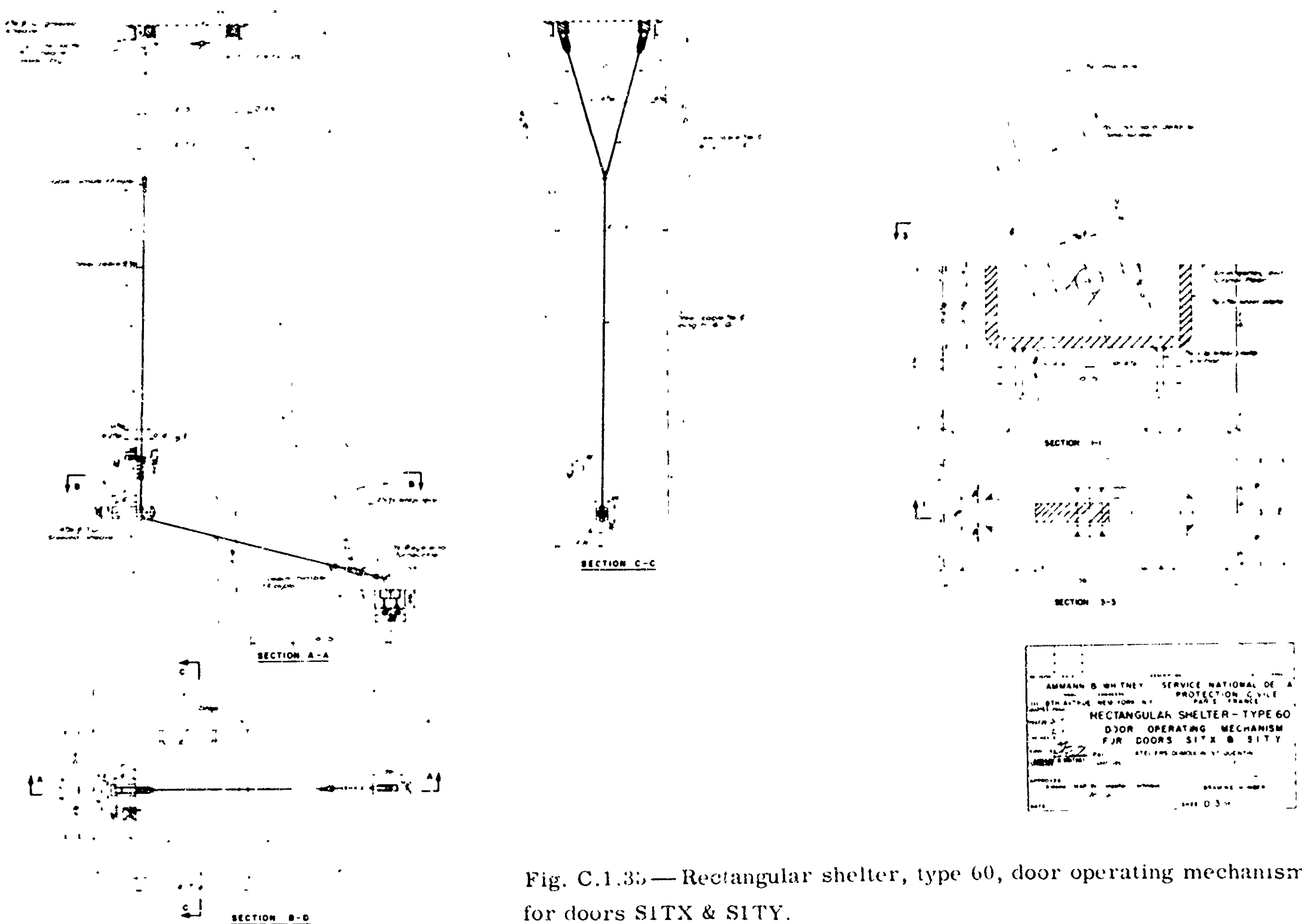

Fig. C.1.35 — Rectangular shelter, type 60, door operating mechanism for doors S1TX & S1TY.

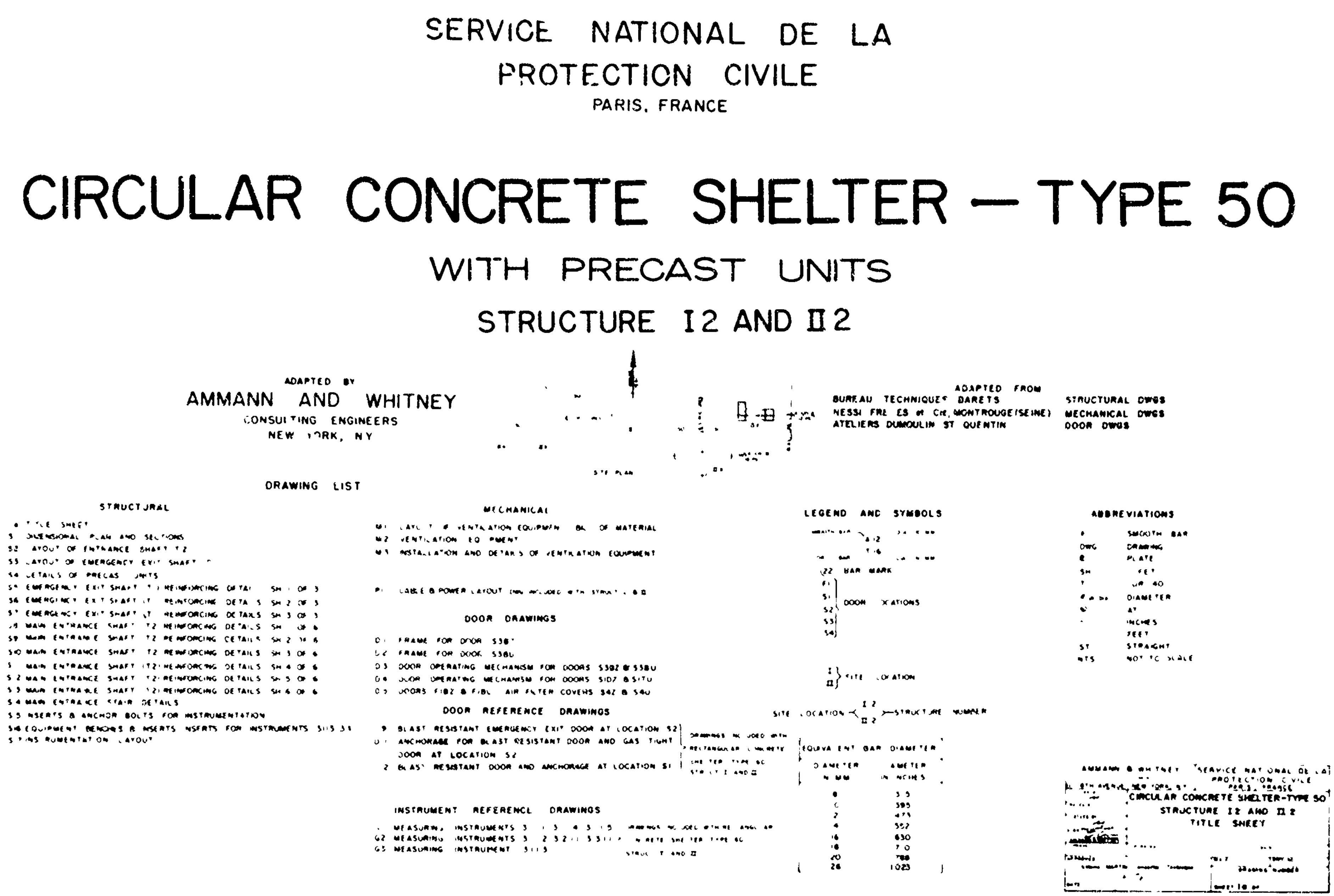

Fig. C.2 — Circular concrete shelter, type 50, title sheet.

Fig. C.2.2—Circular shelter, type 50, structures I-2 and II-2, layout of entrance shaft T2.

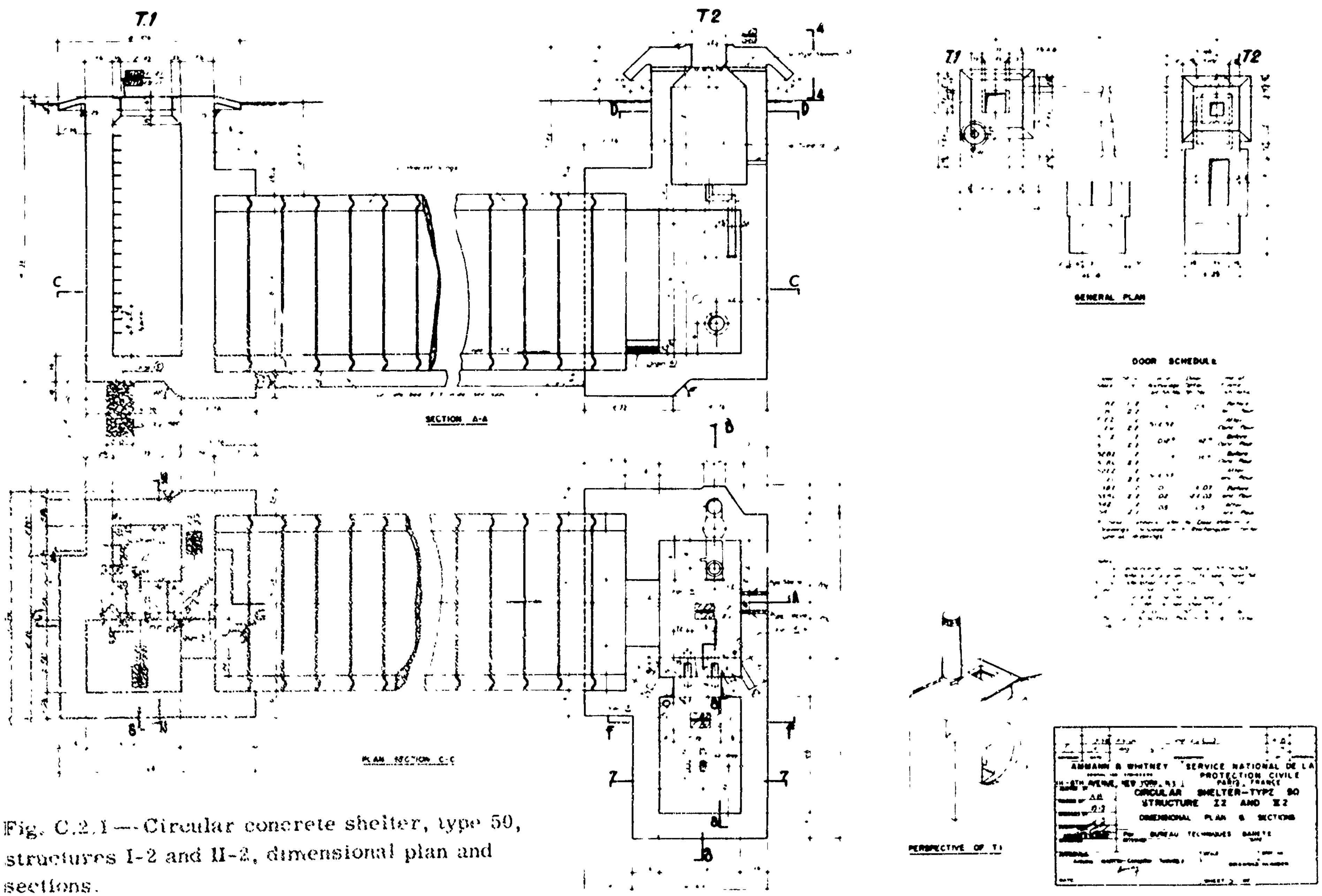

Fig. C.2.1—Circular concrete shelter, type 50, structures I-2 and II-2, dimensional plan and sections.

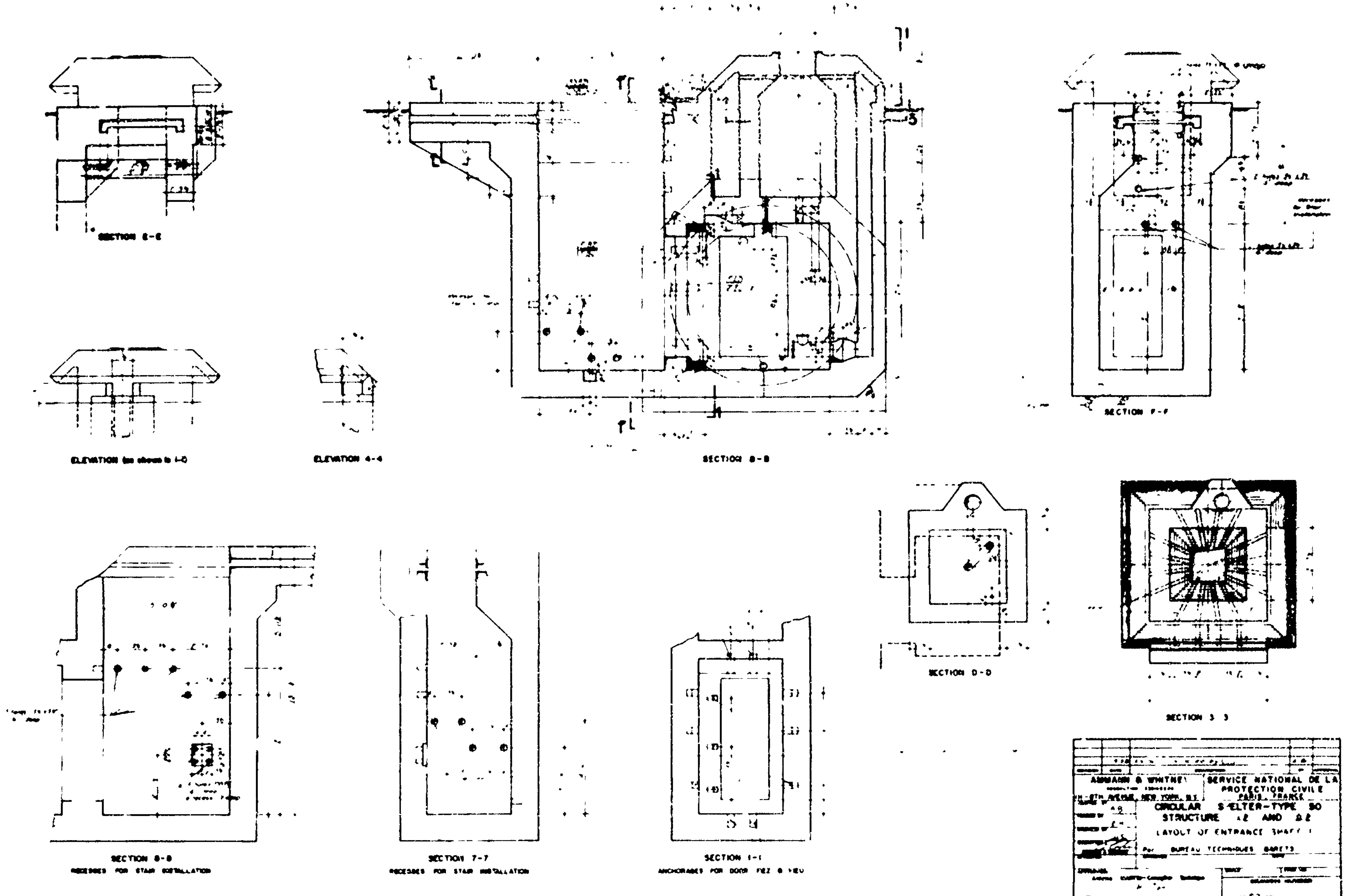

Fig. C.2.2—Circular shelter, type 50, structures I-2 and II-2, layout of entrance shaft T2.

Fig. C.2.4—Circular concrete shelter, type 50, structures I-2 and II-2, details of precast units.

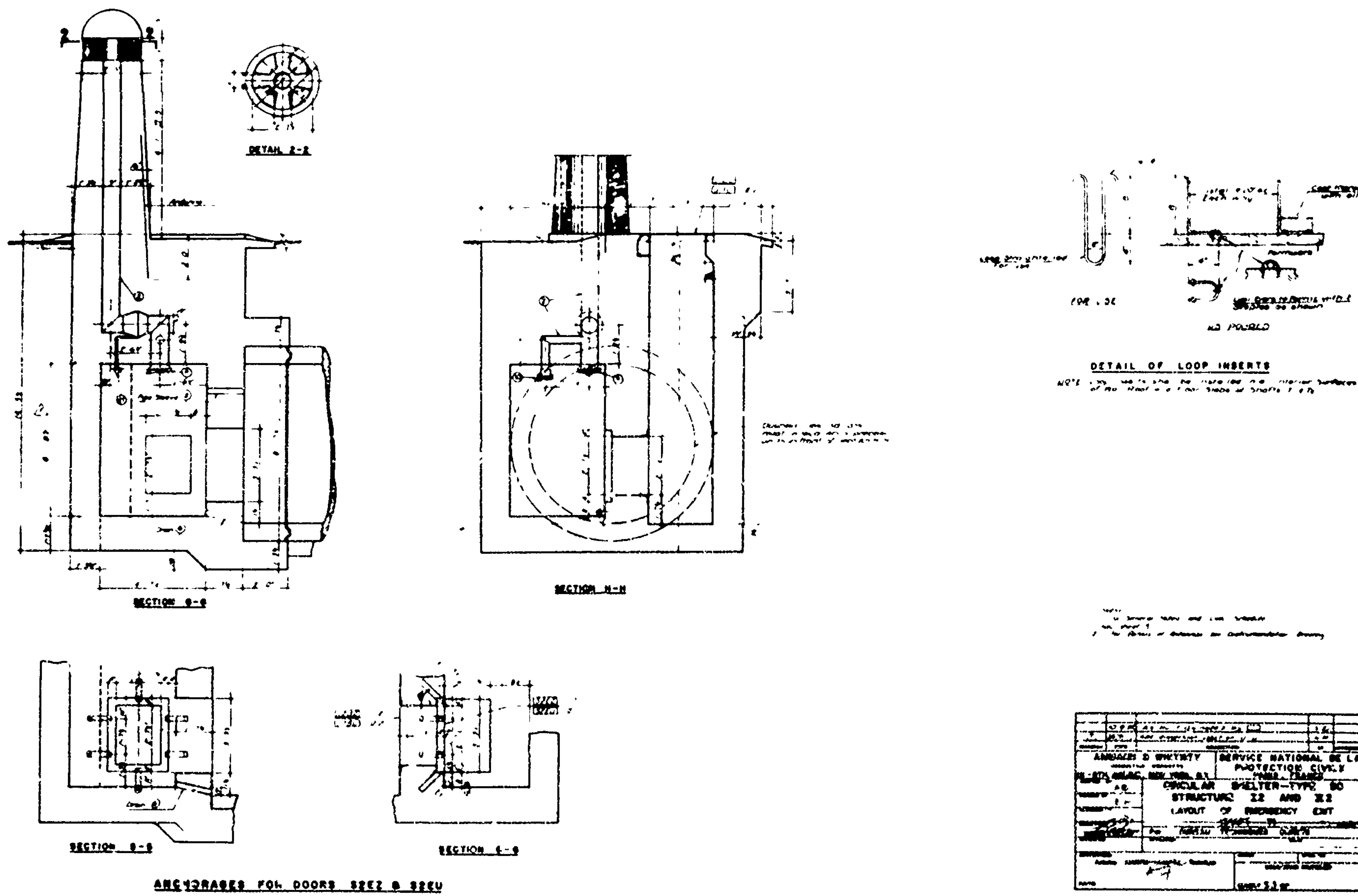

Fig. C 2.3—Circular concrete sheiter, type 50, structures I-2 and II-2, layout of emergency exit shaft T1.

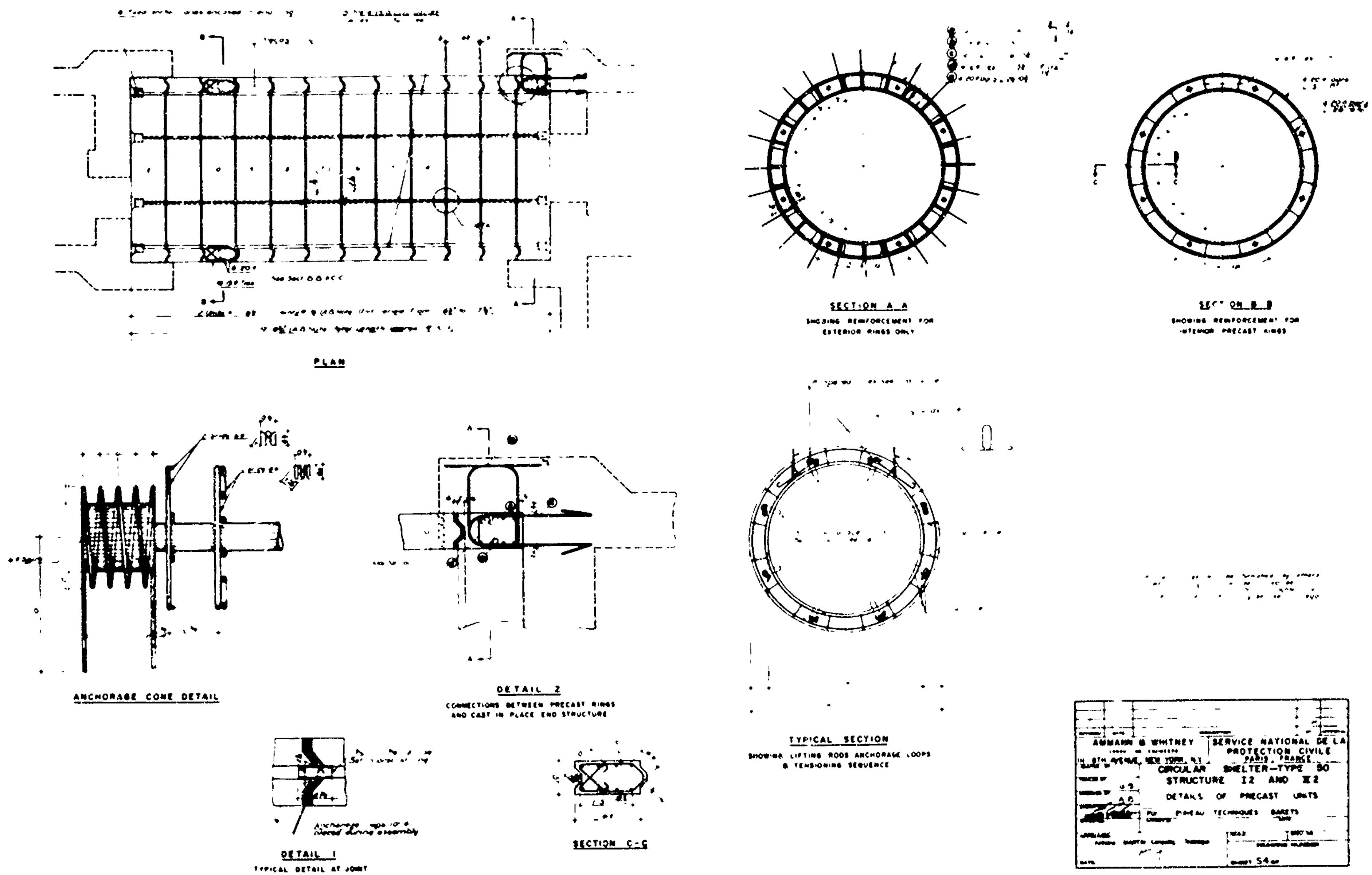

Fig. C.2.4—Circular concrete shelter, type 50, structures I-2 and II-2, details of precast units.

Fig. C.2.5—Circular shelter, type 50, structures I-2 and II-2, emergency exit shaft (T1) reinforcing details (2 of 3).

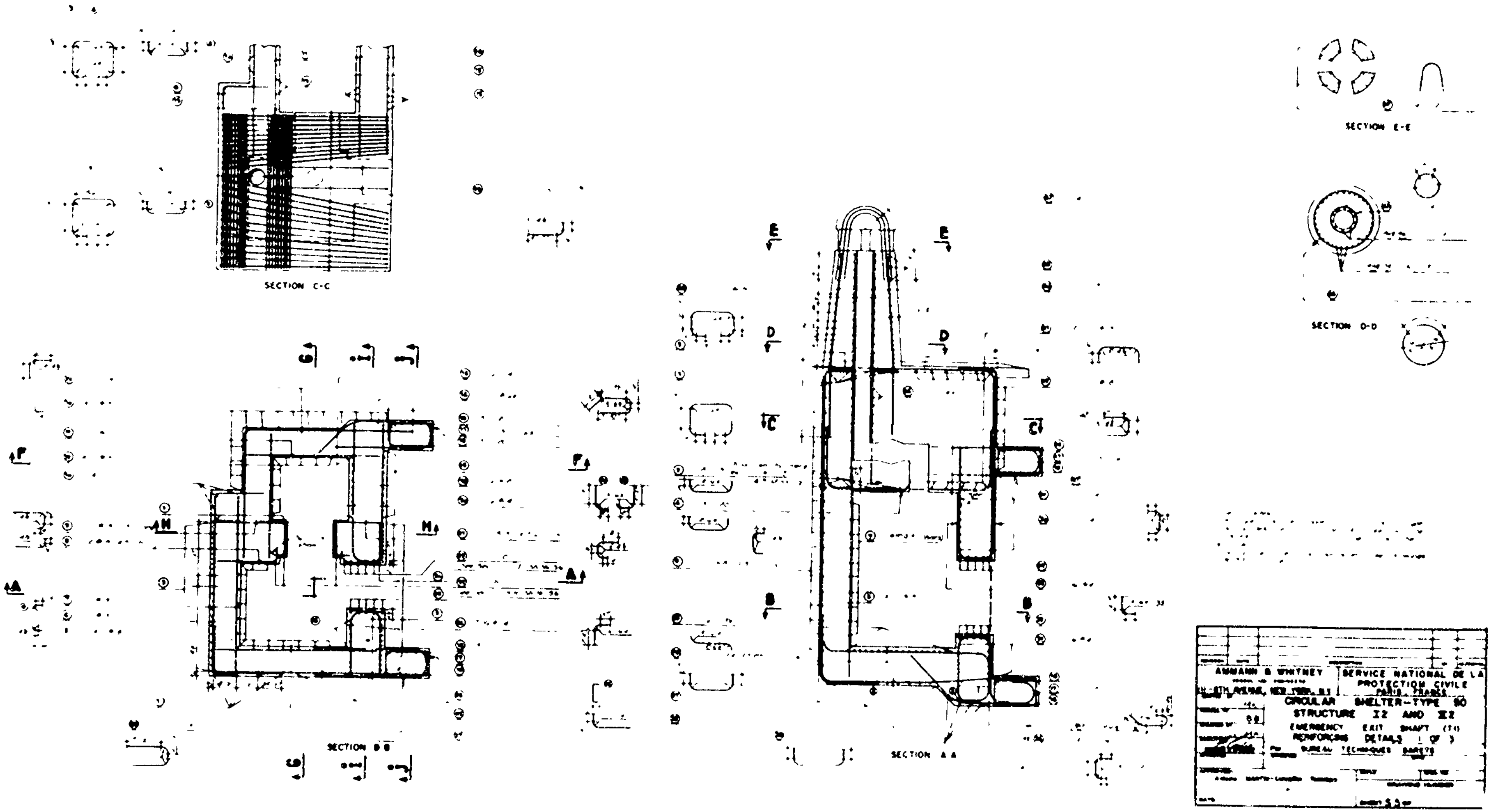

Fig. C.2.5—Circular shelter, type 50, structures I-2 and II-2, emergency exit shaft (T1) reinforcing details (1 of 3).

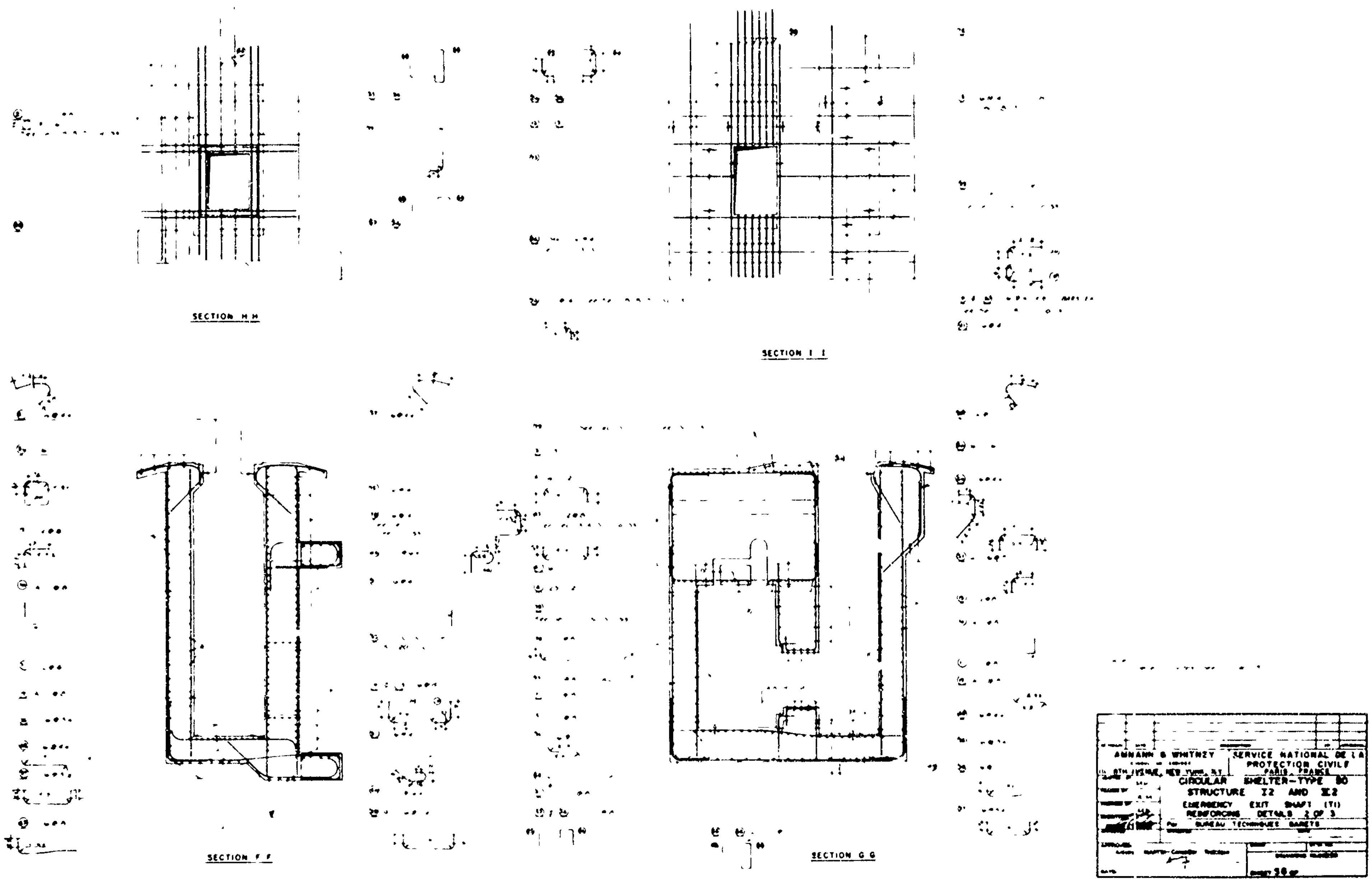

Fig. C.2.6—Circular shelter, type 50, structures I-2 and II-2, emergency exit shaft (T1) reinforcing details (2 of 3).

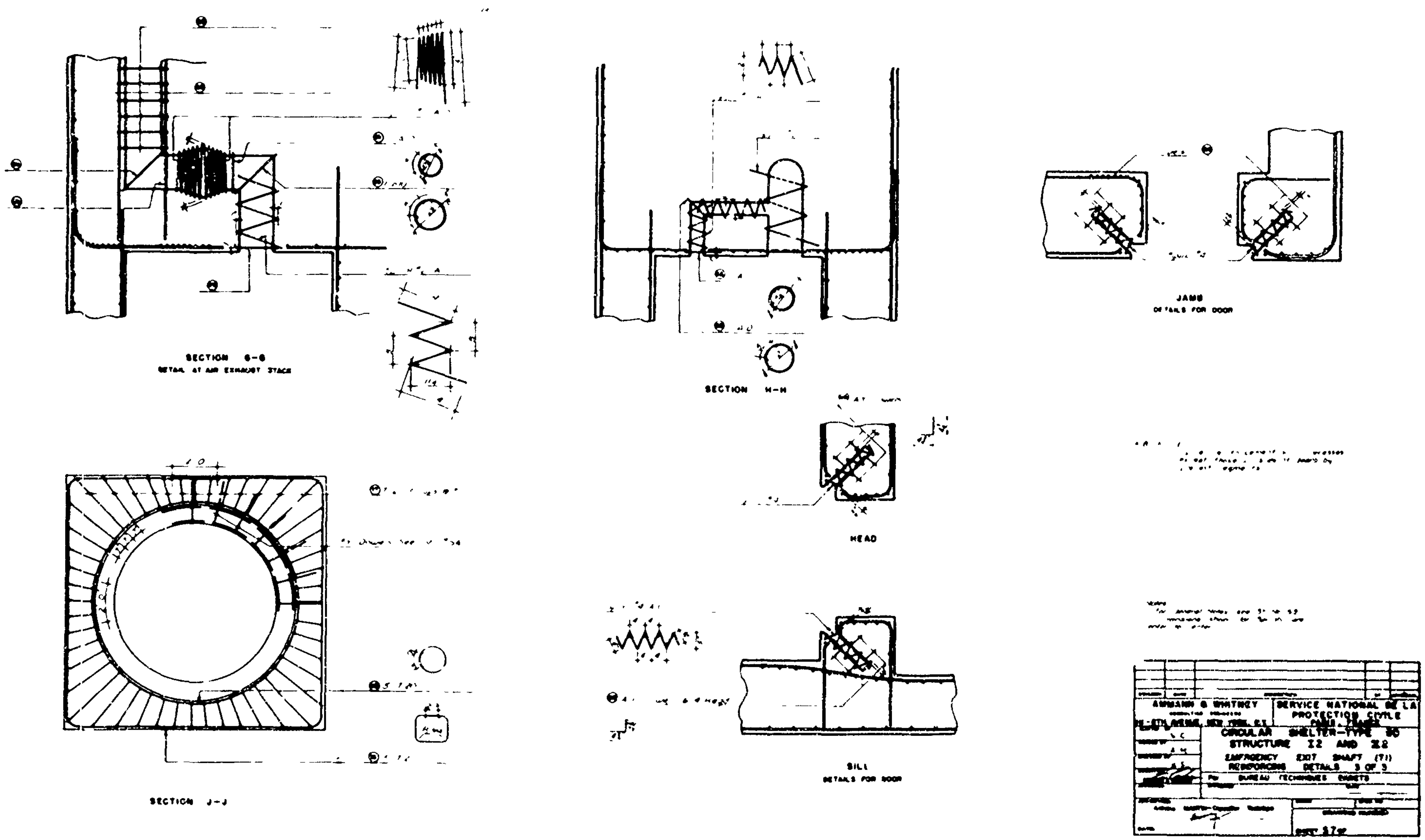

Fig. C.2.7—Circular shelter, type 50, structures I-2 and II-2 emergency exit shaft (T1) reinforcing details (3 of 3).

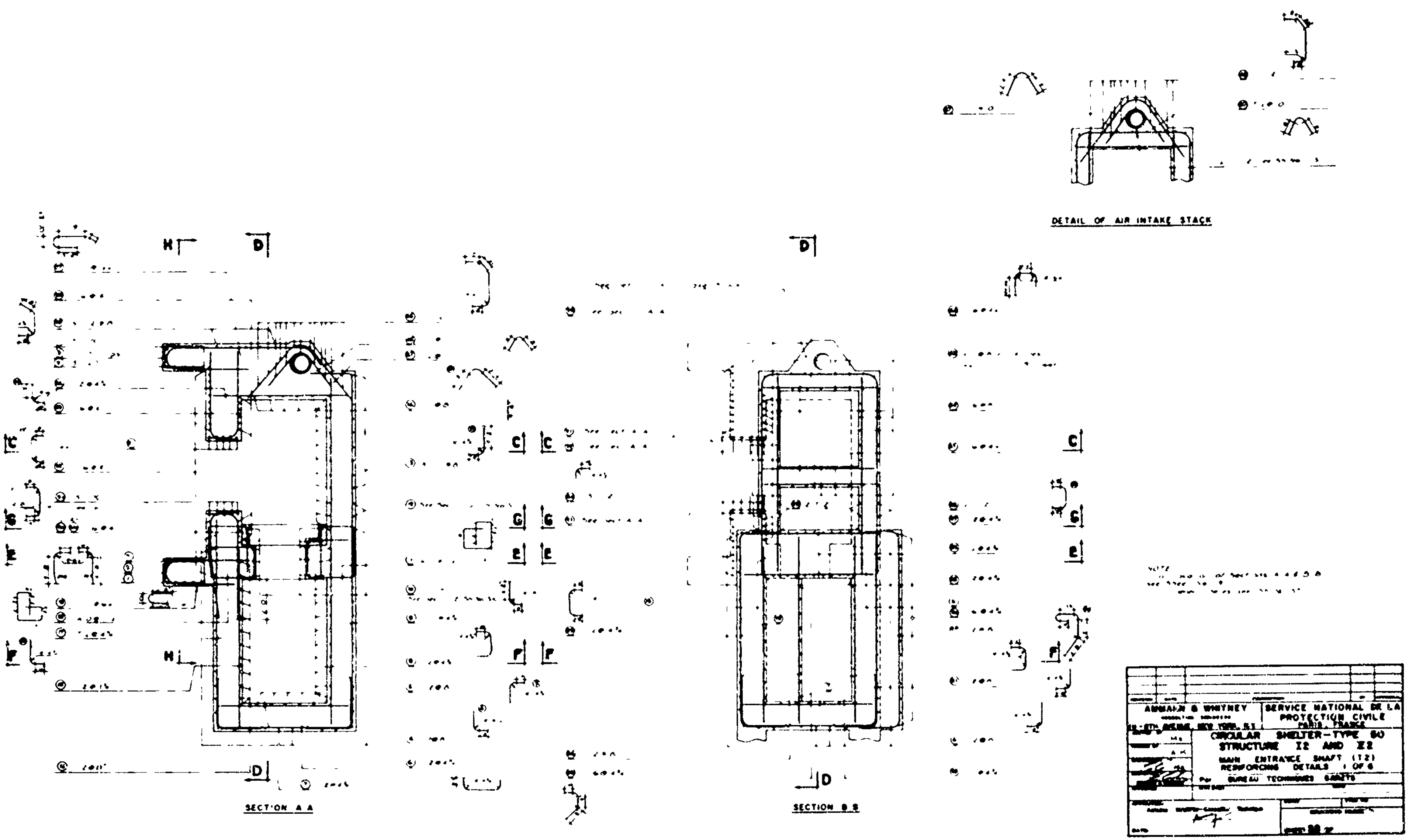

Fig. C.2.8 — Circular shelter, type 50, structures I-2 and II-2, main entrance shaft (T2) reinforcing details (1 of 6).

Fig. C.2.10 — Circular shelter, type 50, structures I-2 and II-2, main entrance shaft (T2) reinforcing details (3 of 6).

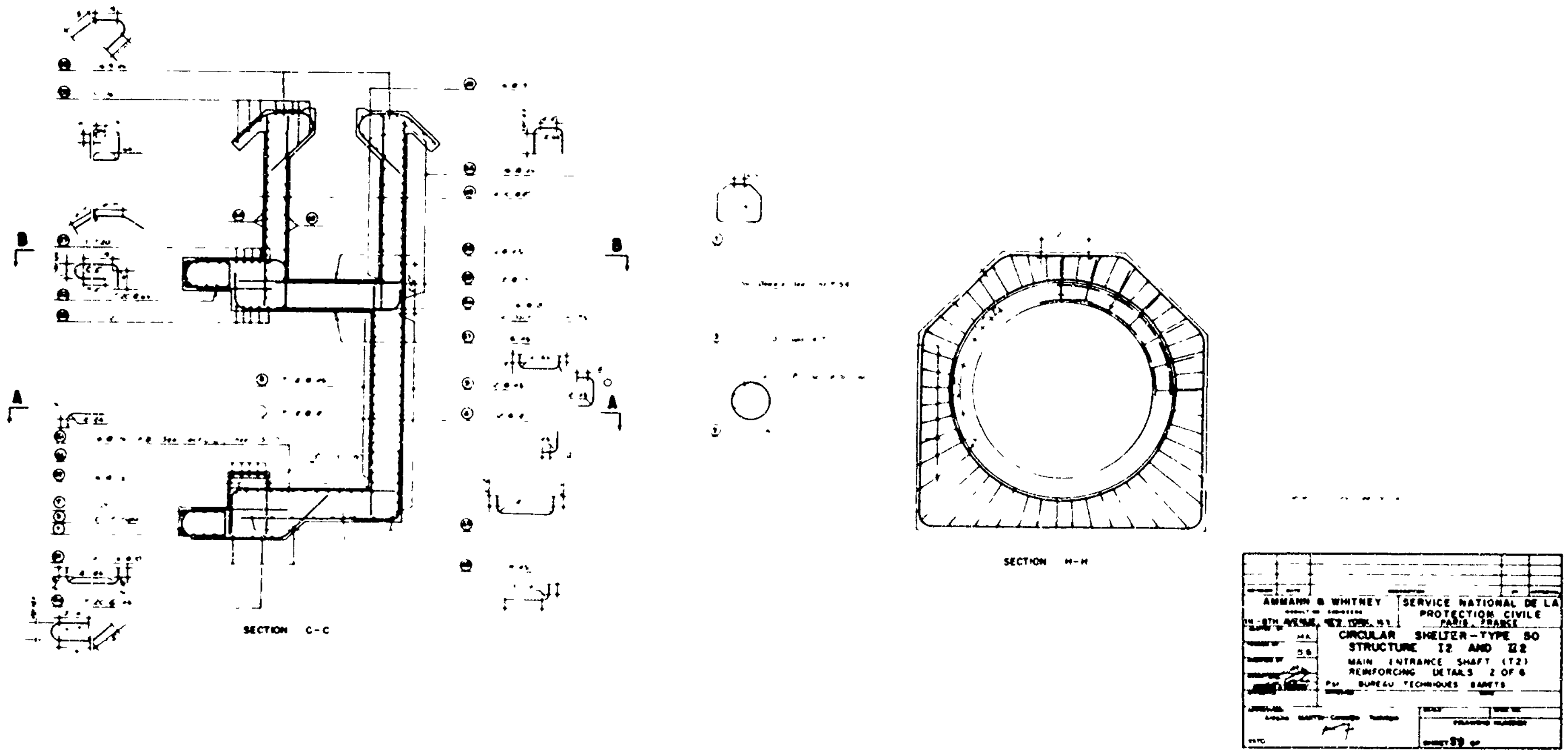

Fig. C.2.9 — Circular shelter, type 50, structures I-2 and II-2, main entrance shaft (T2) reinforcing details (2 of 6).

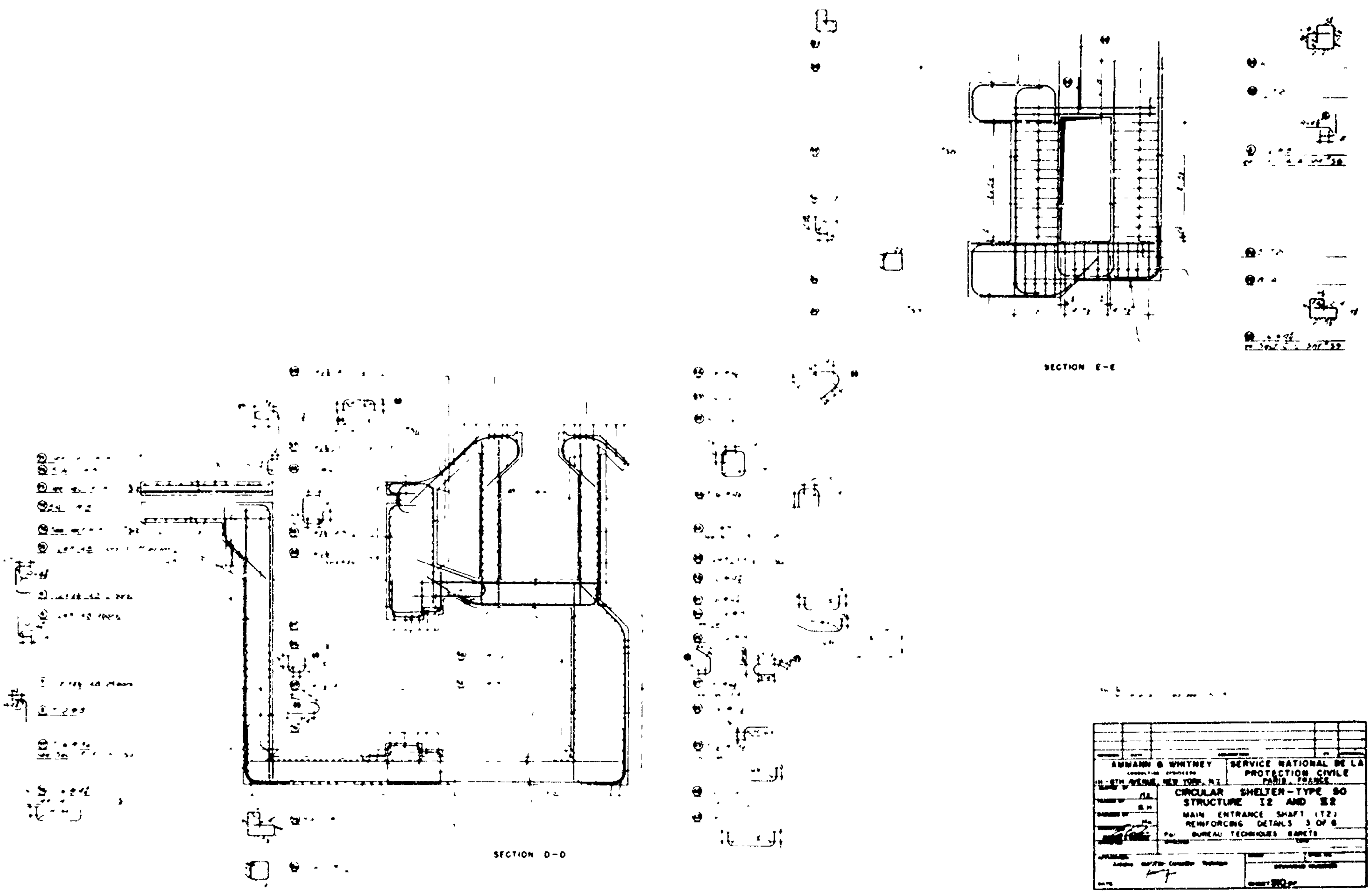

Fig. C.2.10—Circular shelter, type 50, structures I-2 and II-2, main entrance shaft (T2) reinforcing details (3 of 6).

details (5 of 6).

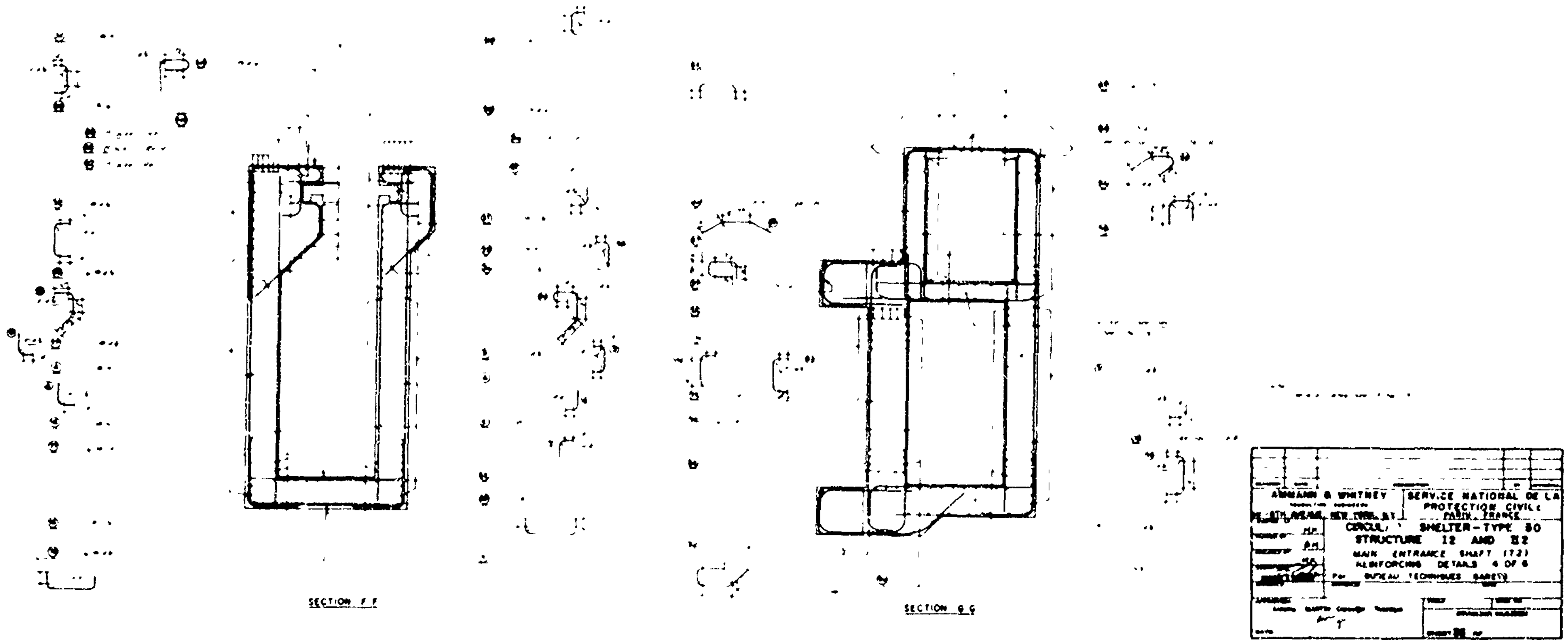

Fig. C.2.11 — Circular shelter, type 50, structures I-2 and II-2, main entrance shaft (T2) reinforcing details (4 of 6).

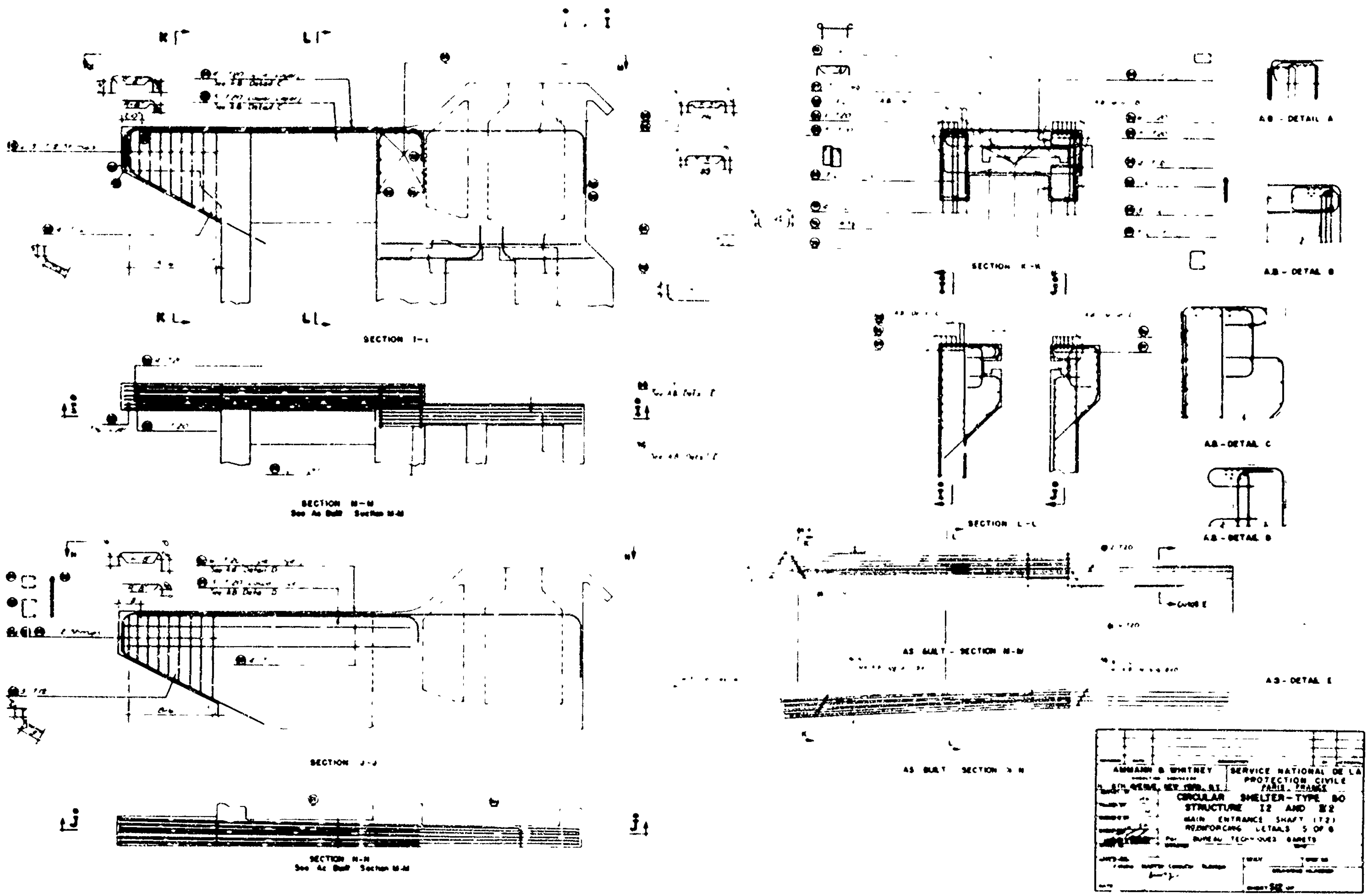

Fig. C.2.12—Circular shelter, type 50, structures I-2 and II-2, main entrance shaft (T2) reinforcing details (5 of 6).

Fig. C.2.14—Circular shelter, type 50, structures I-2 and II-2, main entrance stair details.

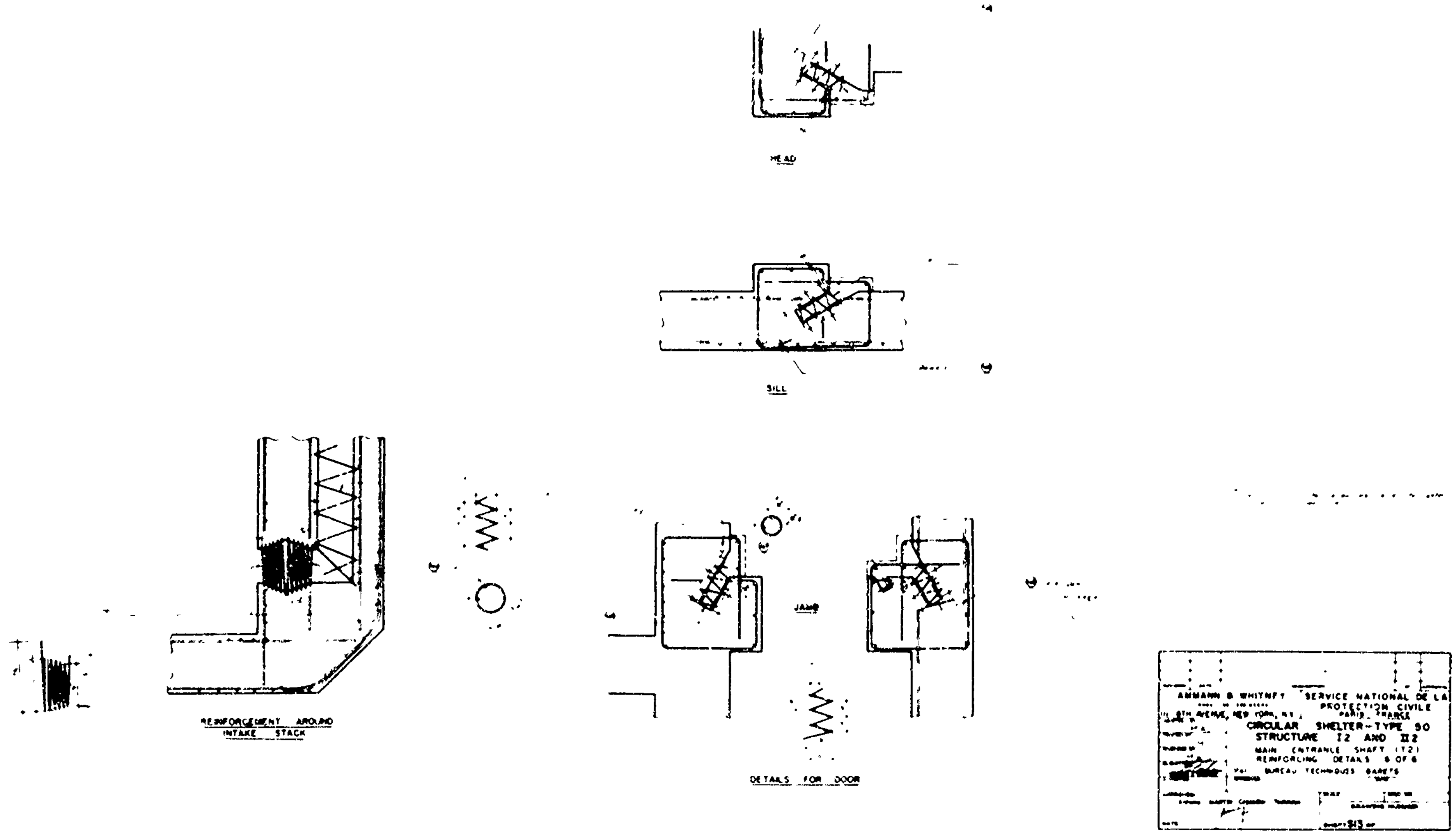

Fig. C.2.13—Circular shelter, type 50, structures I-2 and II-2, main entrance shaft (T2) reinforcing details (6 of 6).

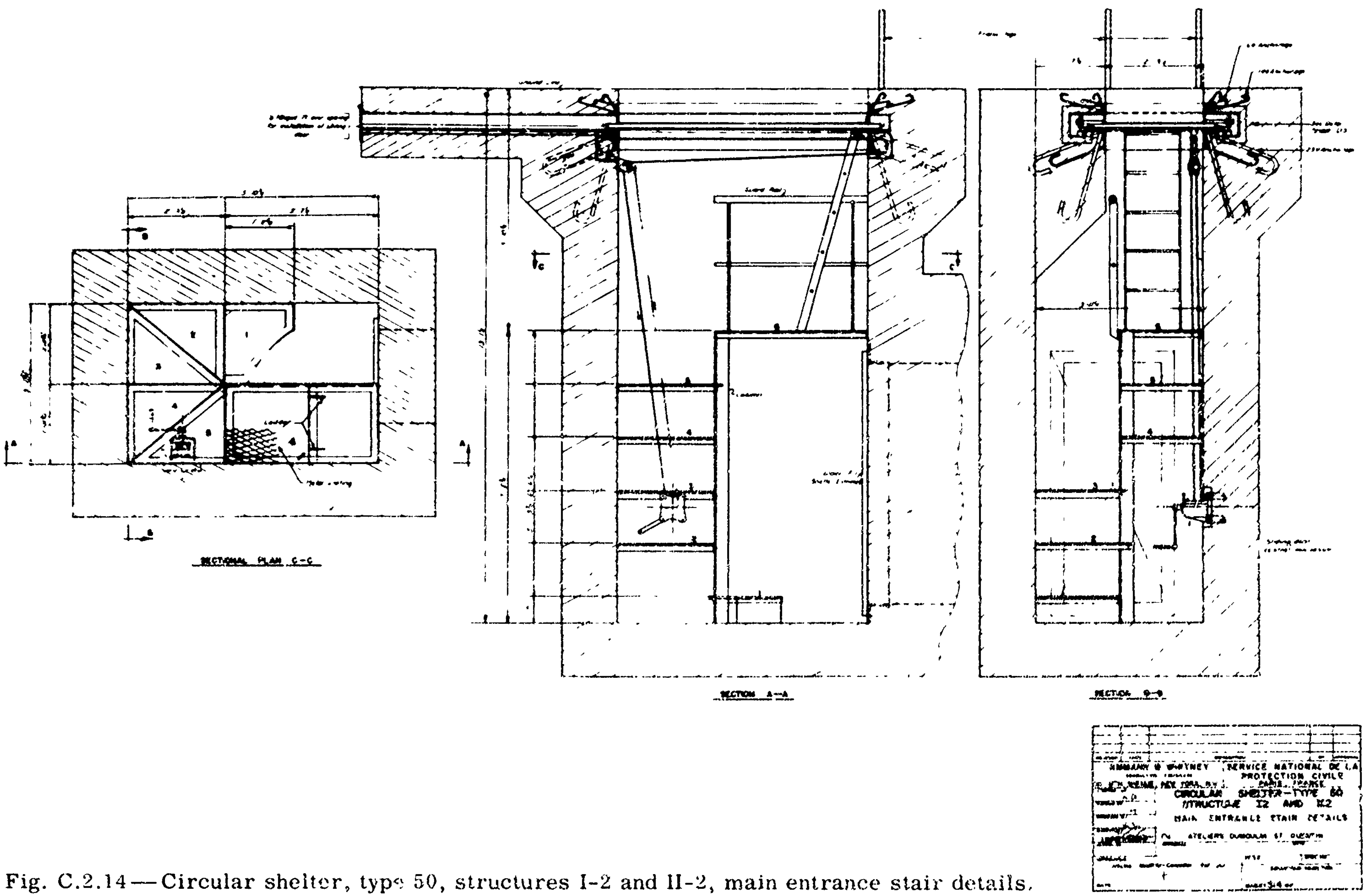

Fig. C.2.14—Circular shelter, type 50, structures I-2 and II-2, main entrance stair details.

instruments 3.1.1.3 and 3.4.1.1.

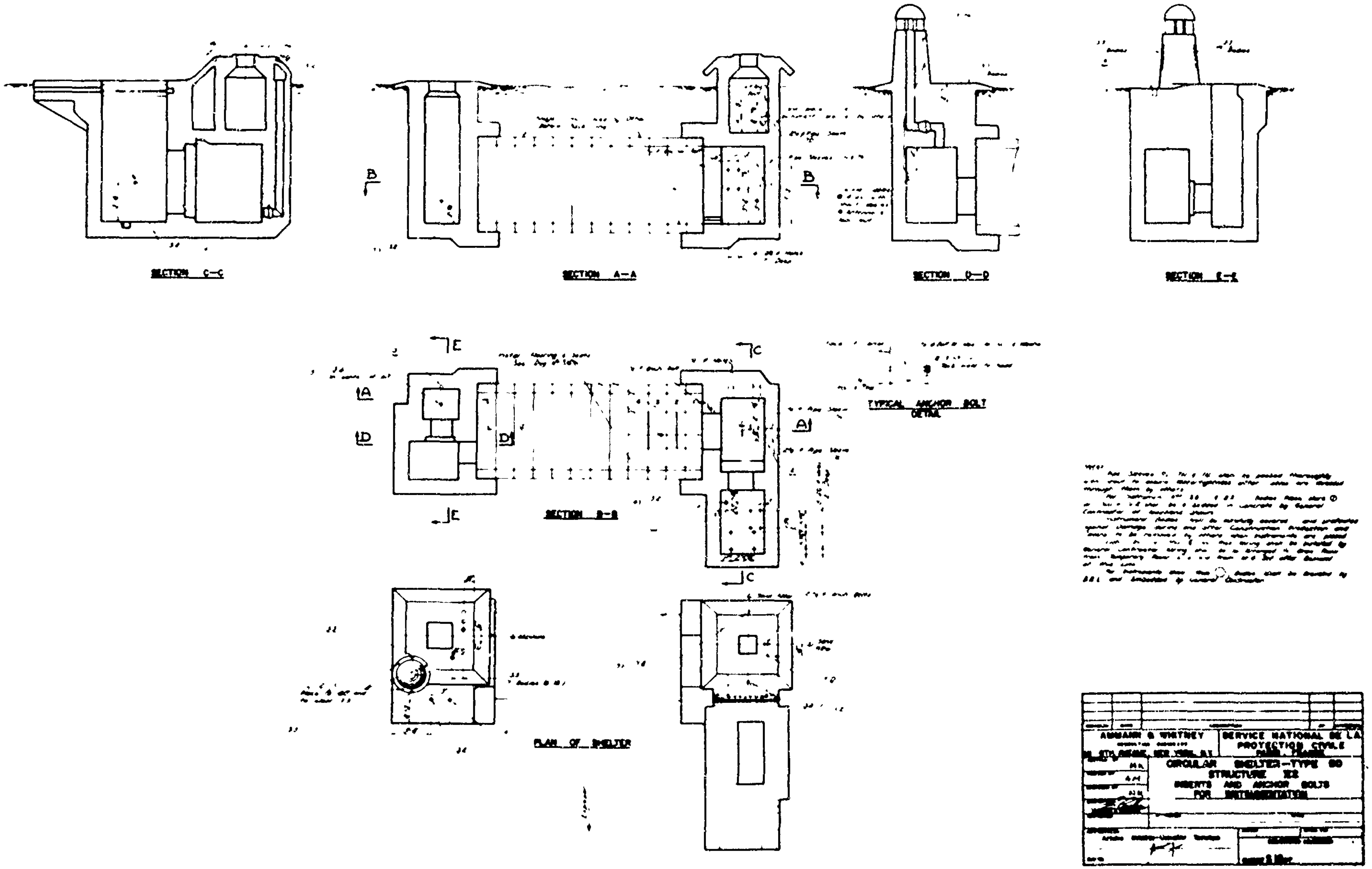

Fig. C.2.15—Circular shelter, type 50, structures I-2 and II-2, inserts and anchor bolts for instrumentation.

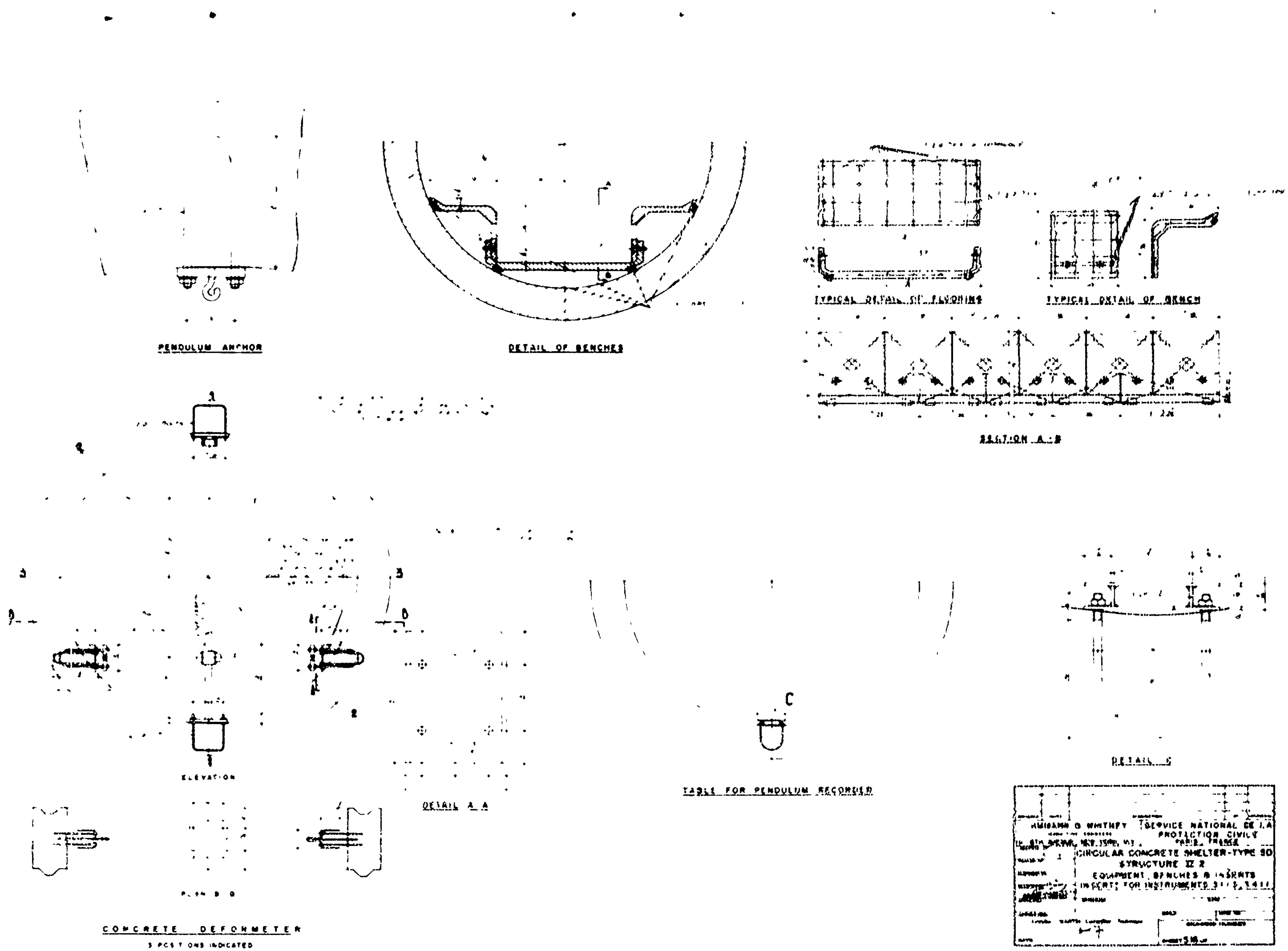

Fig. C.2.16—Circular concrete shelter, type 50, structure II-2, equipment, benches, and inserts for instruments 3.1.1.3 and 3.4.1.1.

of materials.

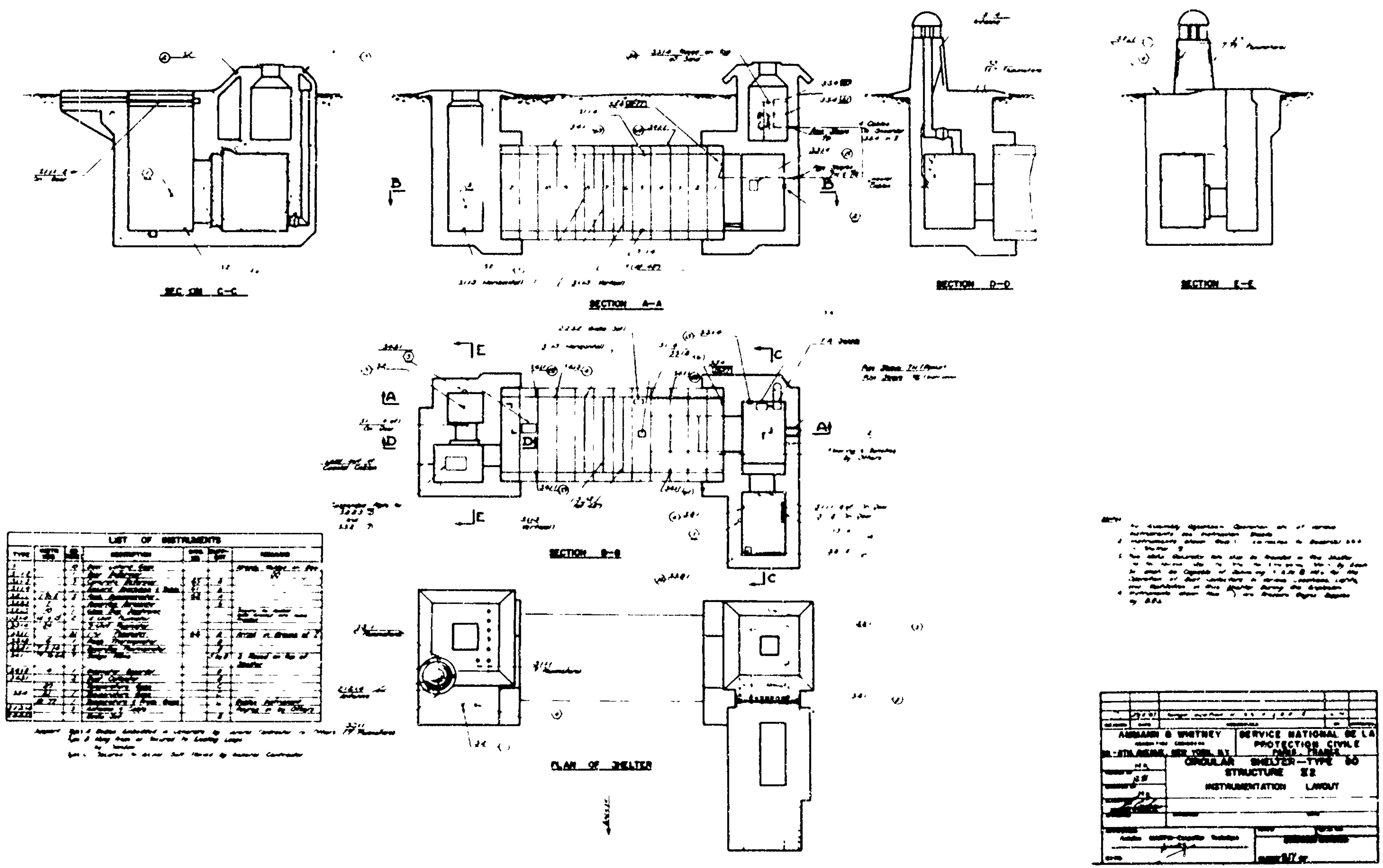

Fig. C.2.17—Circular shelter, type 50, structure II-2, instrumentation layout.

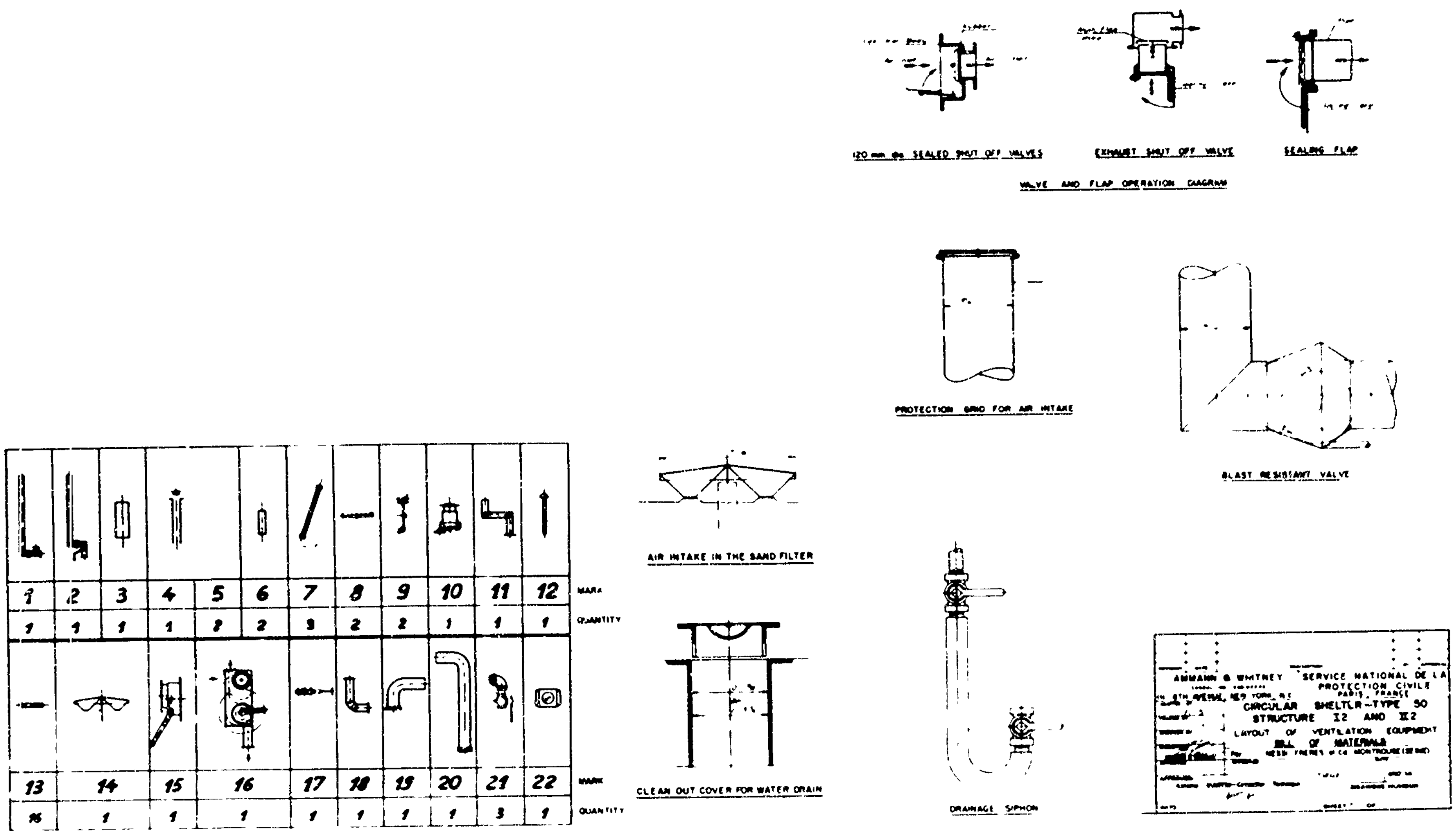

Fig. C.2.18—Circular shelter, type 50, structures I-2 and II-2, layout of ventilation equipment and bill of materials.

of ventilation equipment.

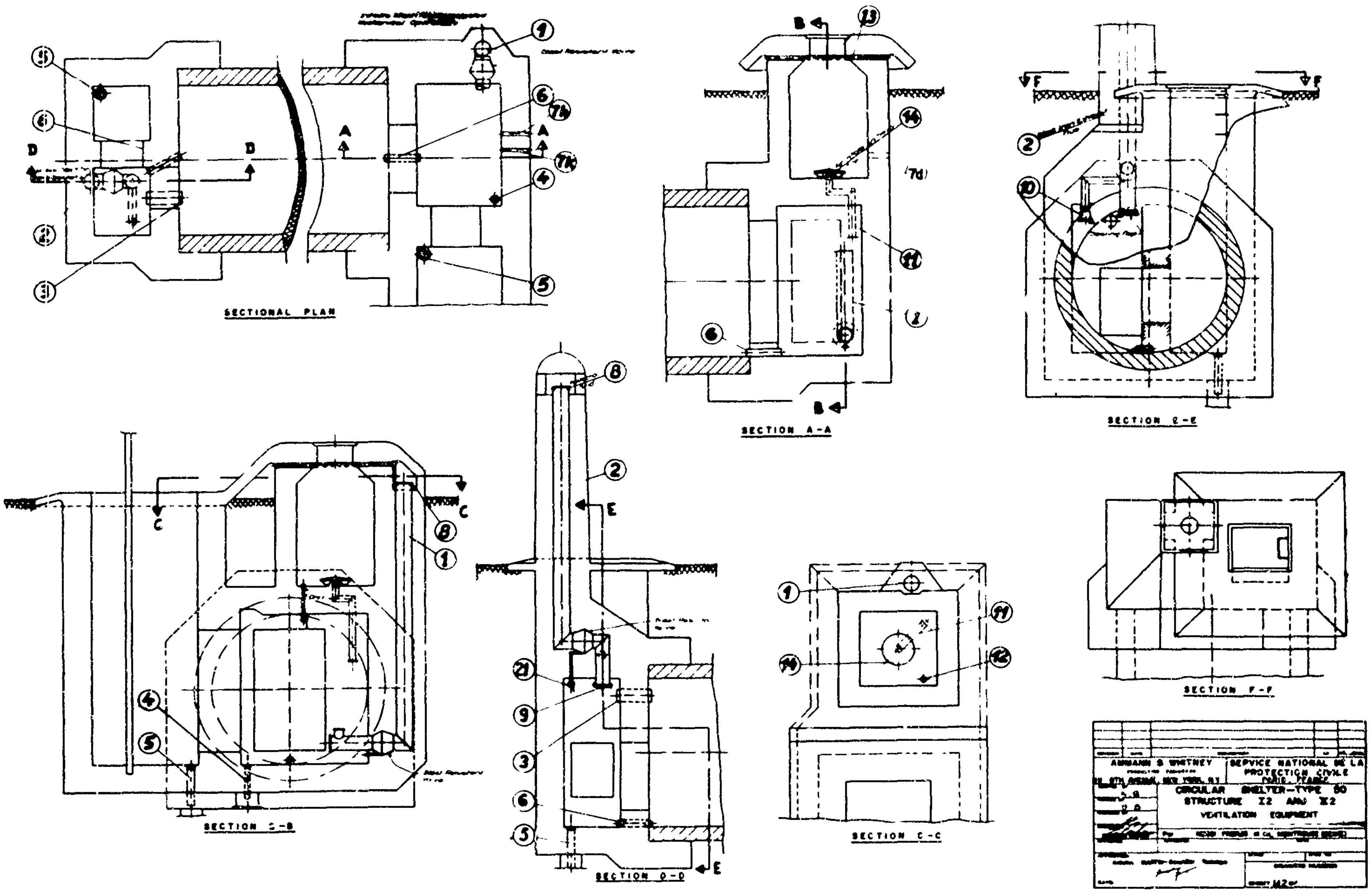

Fig. C.2.19—Circular shelter, type 50, structures I-2 and II-2, ventilation equipment.

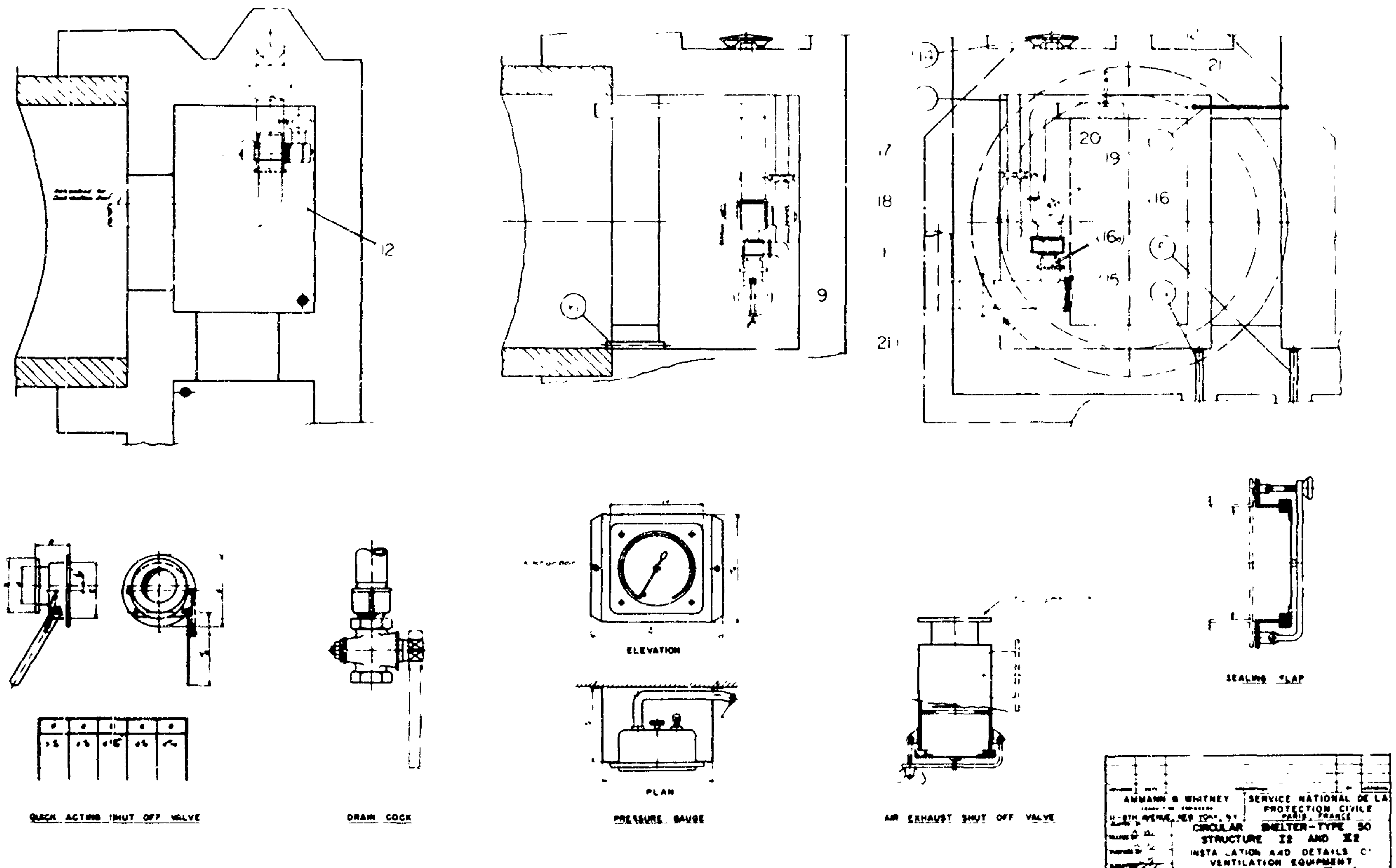

Fig. C 2.20—Circular shelter, type 50, structures I-2 and II-2, installation and details of ventilation equipment.

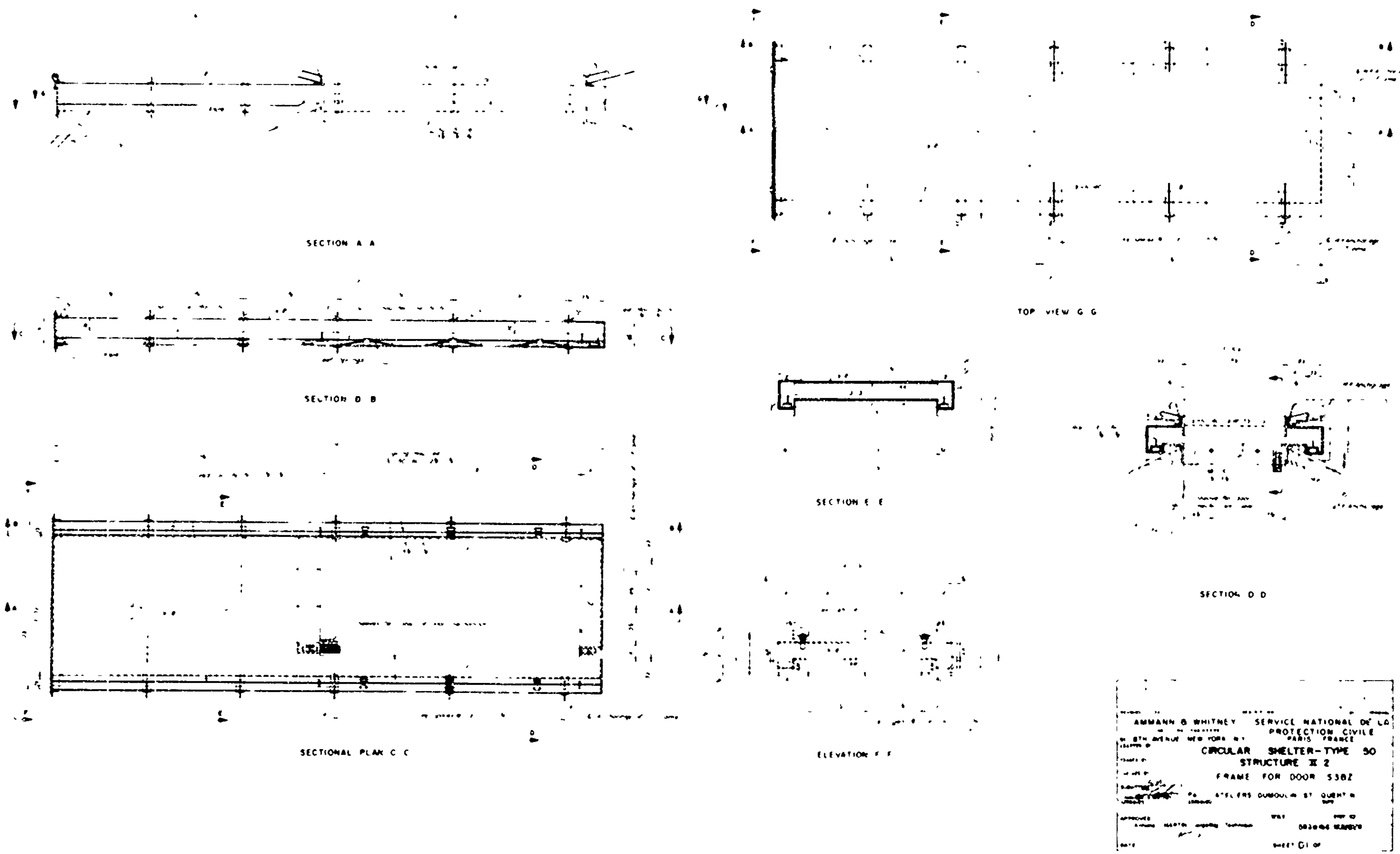

Fig. C.2.21—Circular shelter, type 50, structures I-2 and II-2, frame for door S3BZ.

Fig. C.2.22—Circular shelter, type 50, structure II-2, frame for door S3BU.

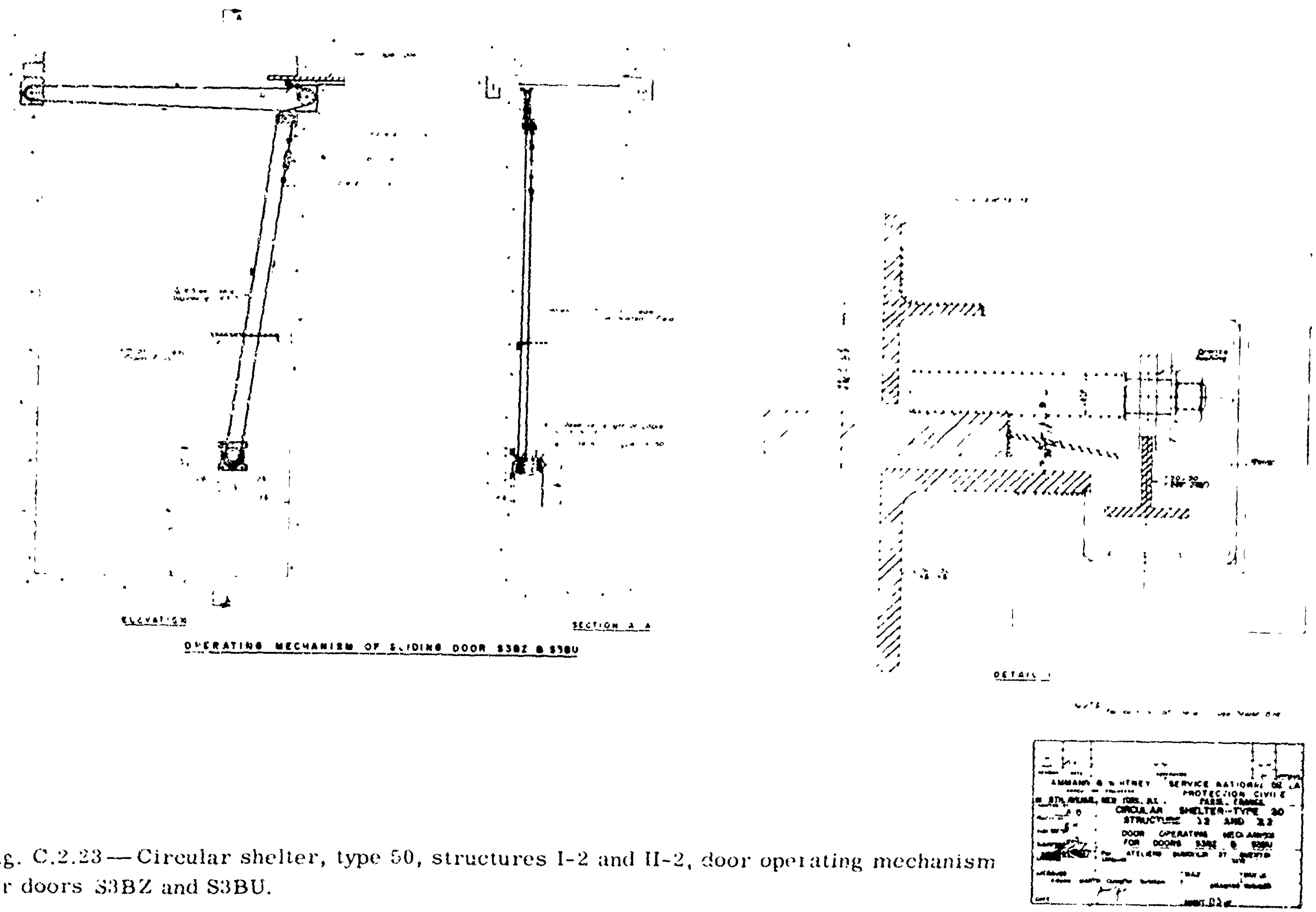

Fig. C.2.23—Circular shelter, type 50, structures I-2 and II-2, door operating mechanism for doors S3BZ and S3BU.

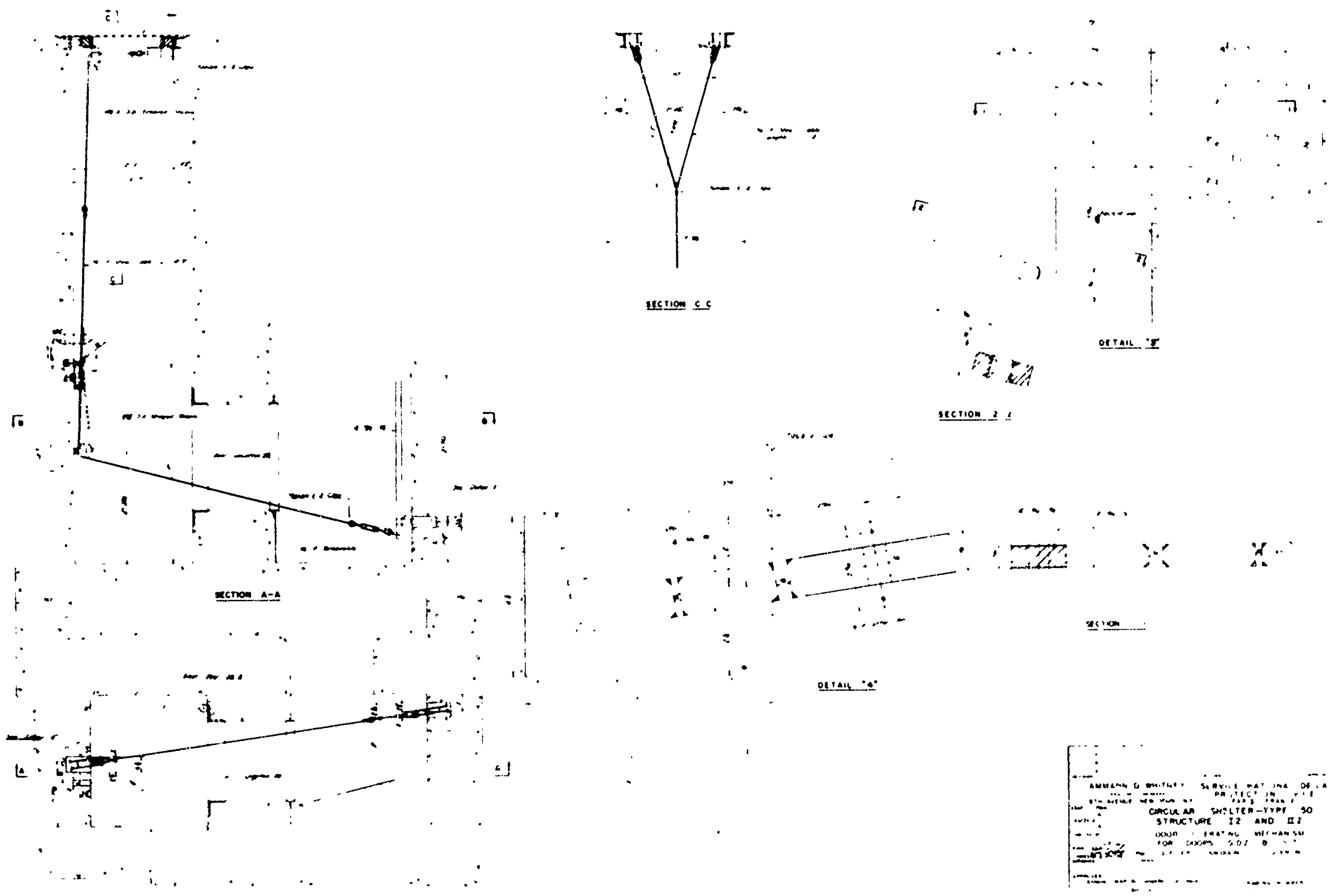

Fig. C.2.24—Circular shelter, type 50, structures I-2 and II-2, door operating mechanism for doors S1DZ and S1TU.

Fig. C.2.— Entrance and entrance chamber, type 65, structures 3, 4, and 5, title sheet

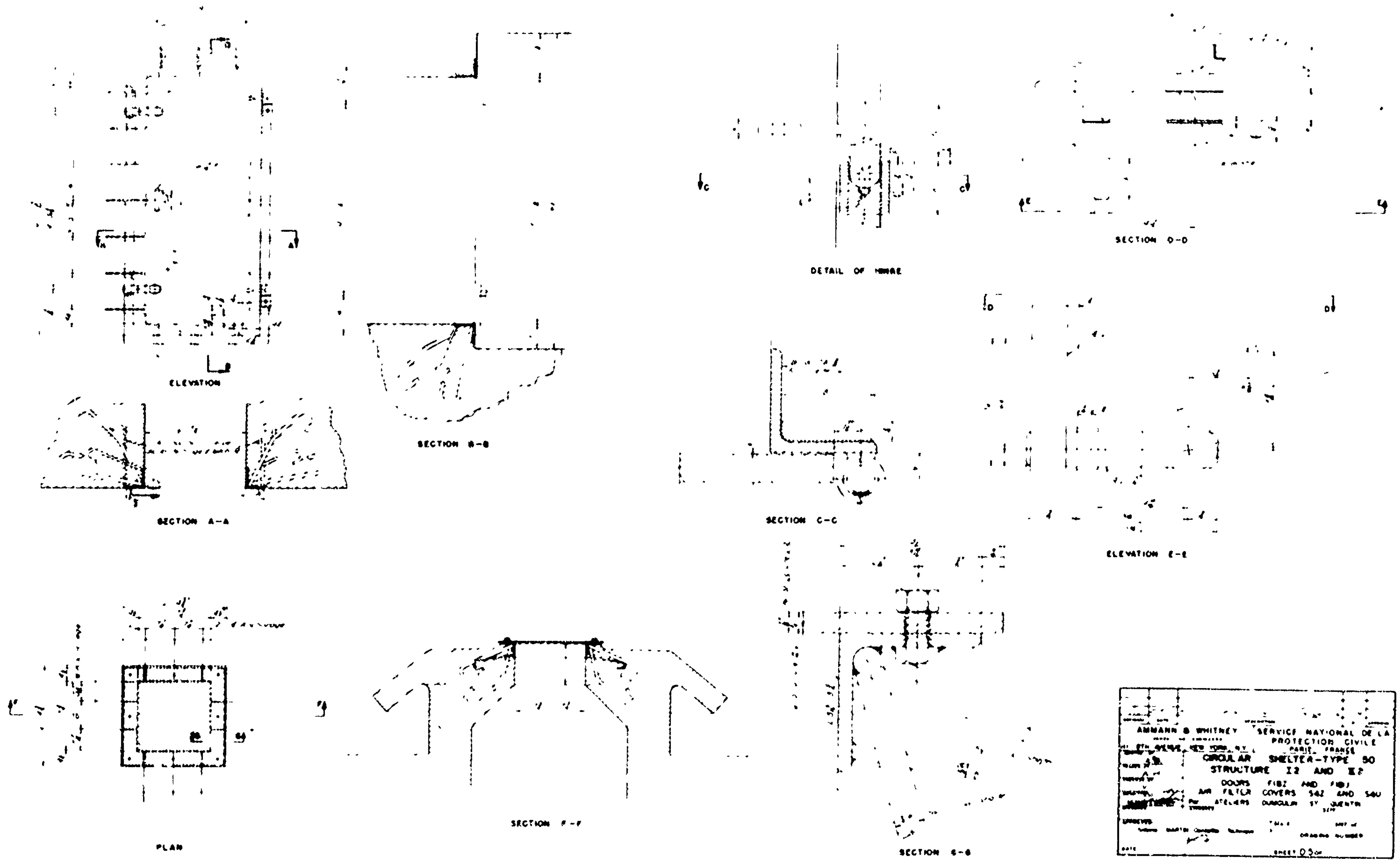

Fig. C.2.25 — Circular shelter, type 50, structures I-2 and II-2, doors F1BZ and F1BU air filter covers S4Z and S4U.

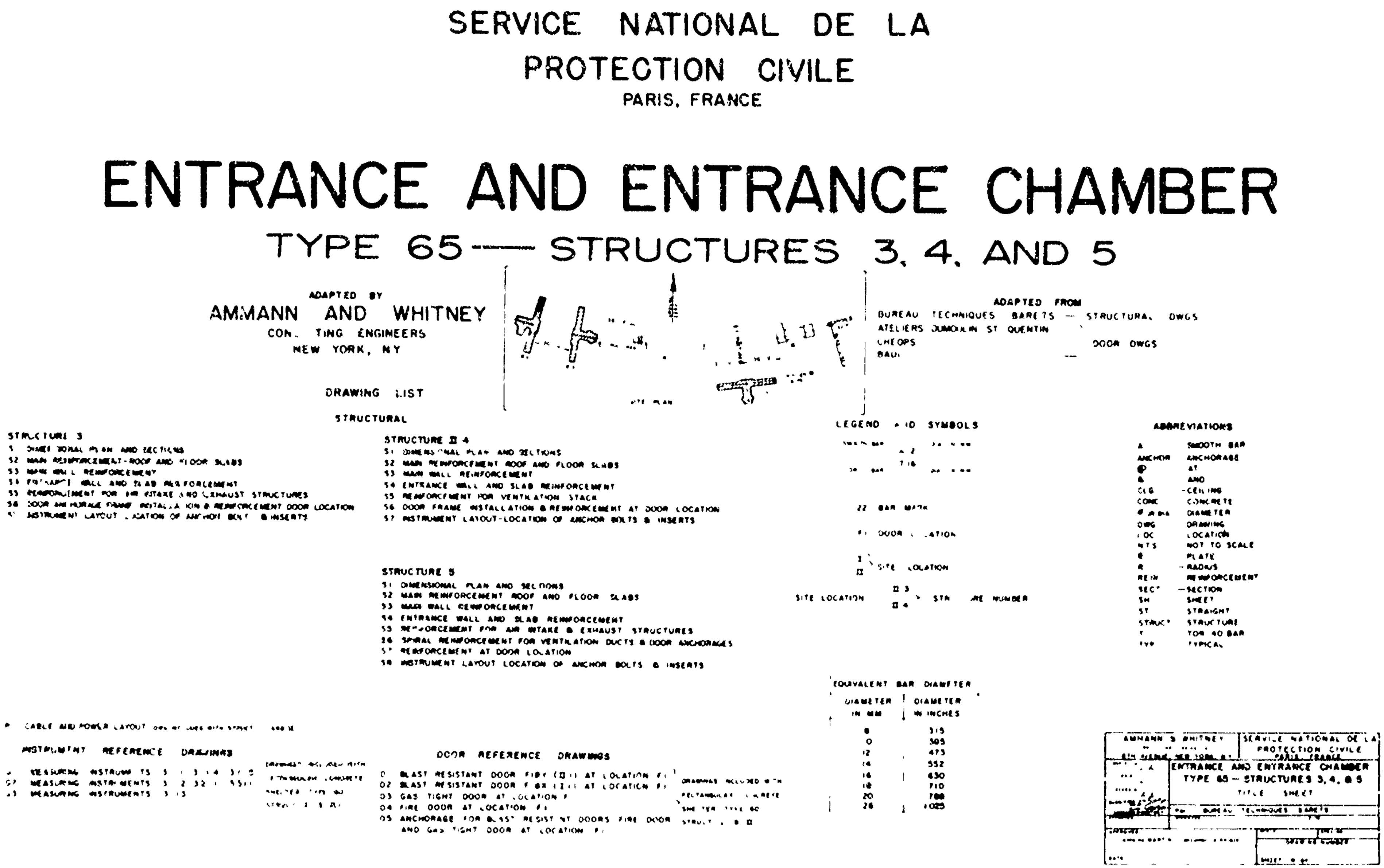

Fig. C.2 — Entrance and entrance chamber, type 65, structures 3, 4, and 5, title sheet

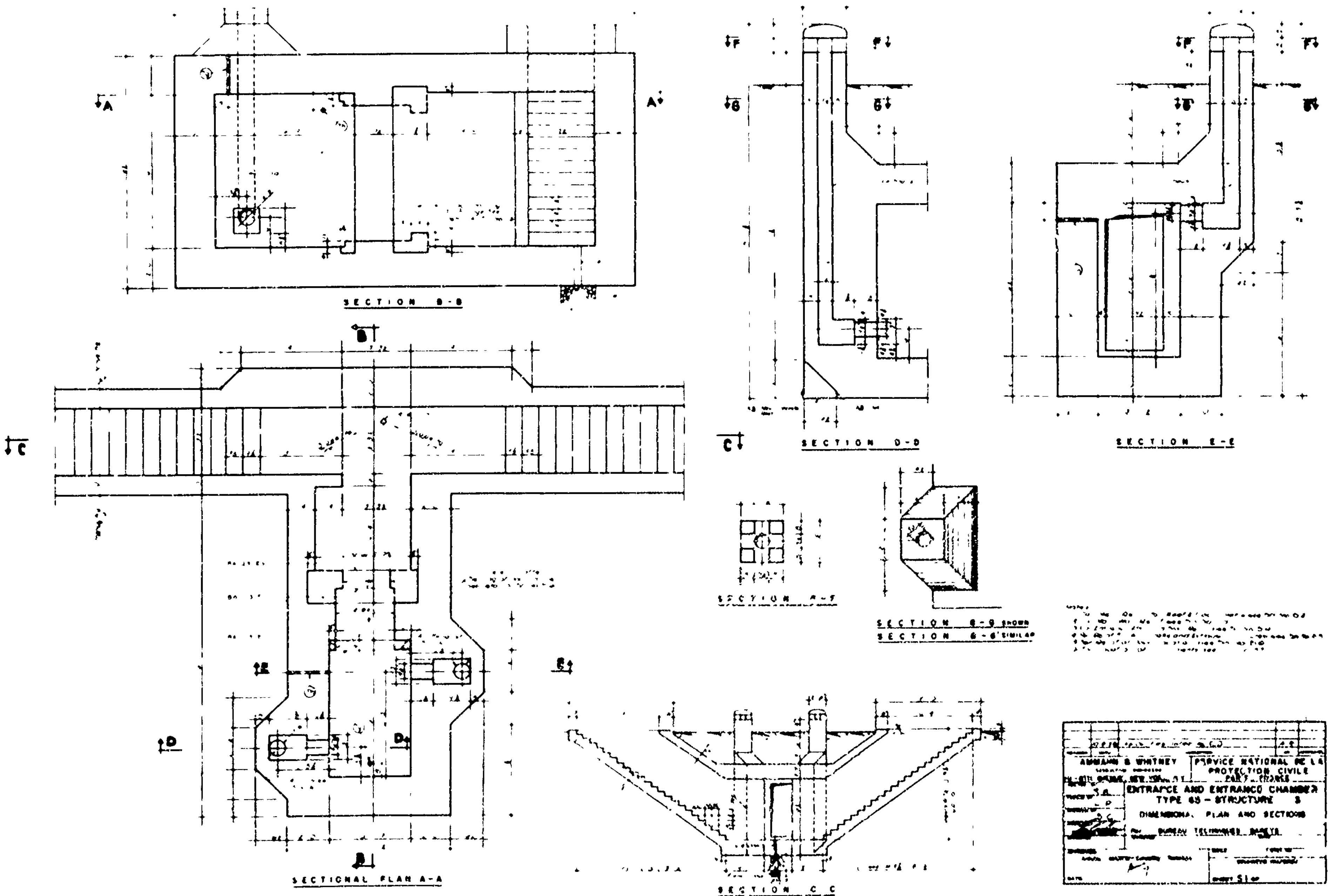

Fig. C.3.1 — Entrance and entrance chamber, type 65, structure 3, dimensional plan and sections.

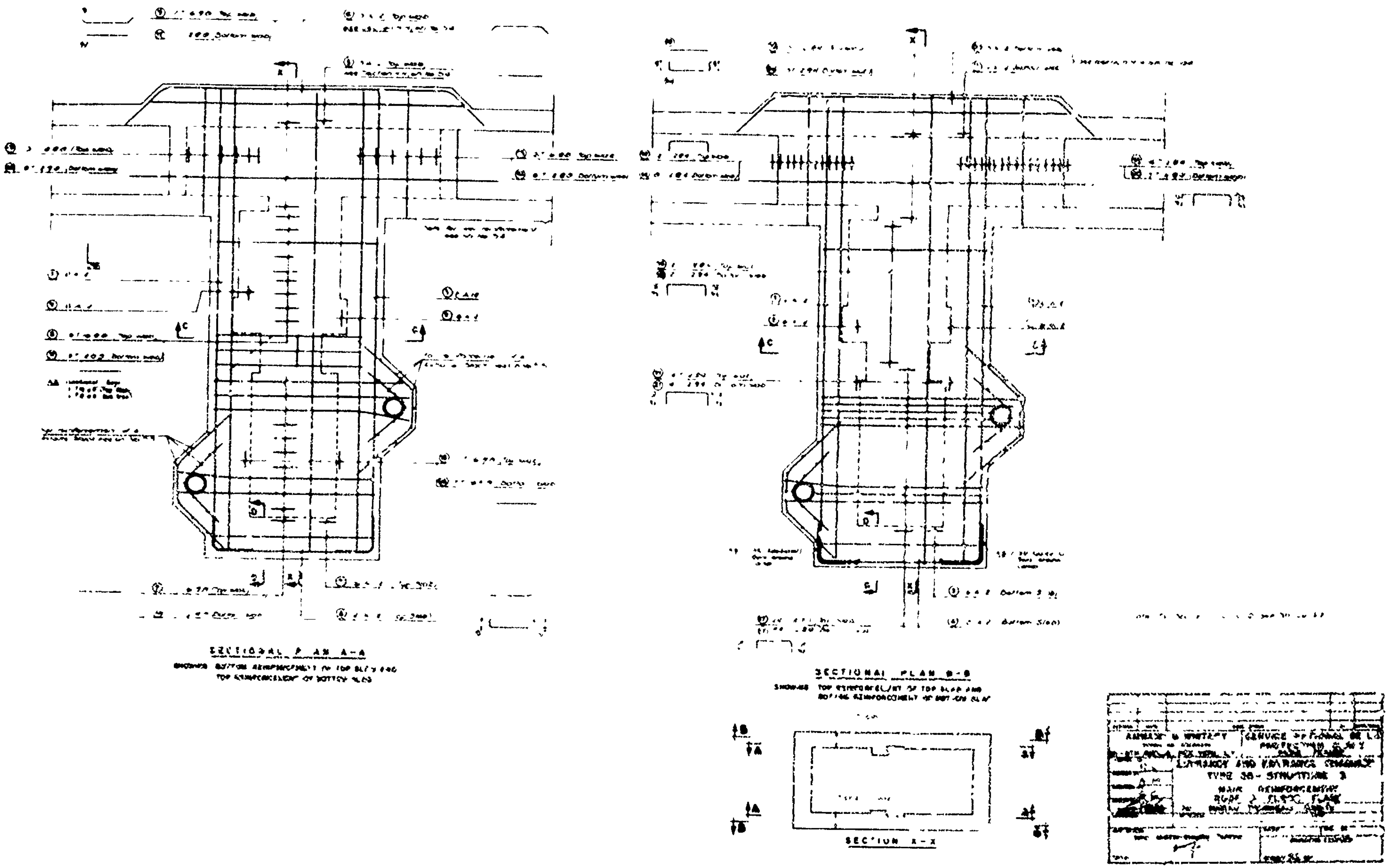

Fig. C.3.2—Entrance and entrance chamber, type 65, structure 3, main reinforcement roof and floor slabs.

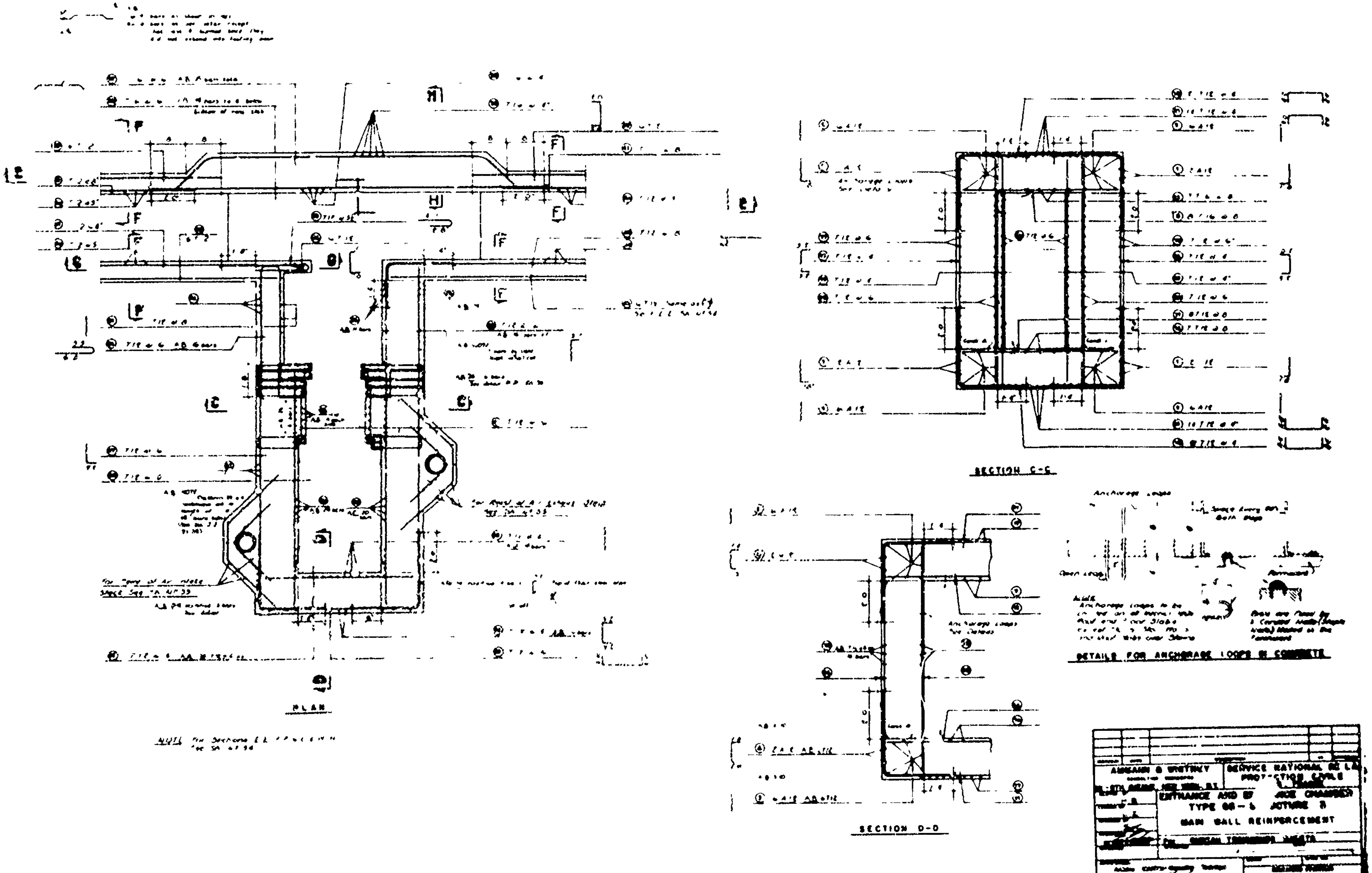

Fig. C.3.3 — Entrance and entrance chamber, type 65, structure 3, main wall reinforcement.

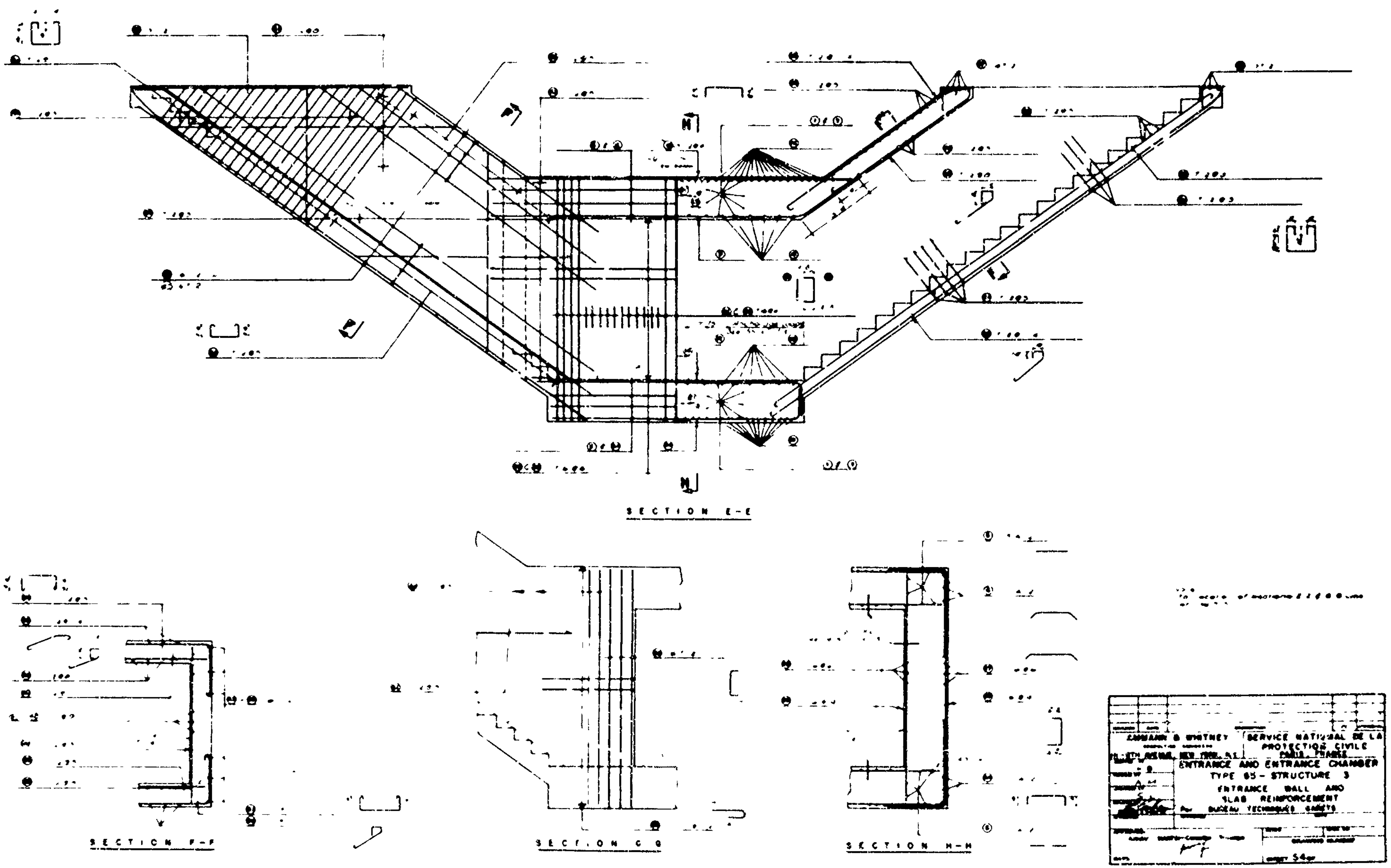

Fig. C.3.4—Entrance and entrance chamber, type 65, structure 3, entrance wall and slab reinforcement.

and reinforcement at door location.

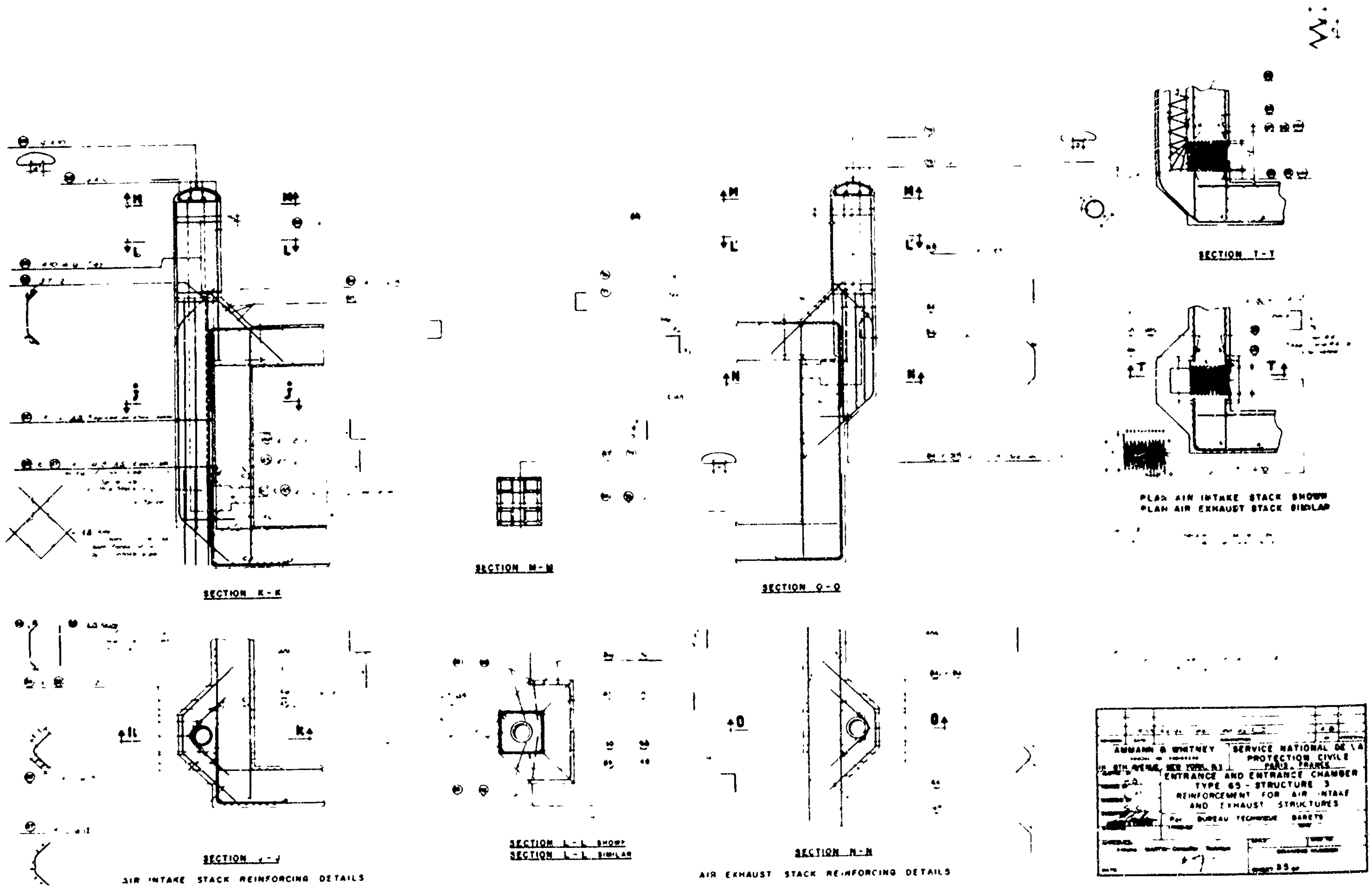

Fig. C 3.5—Entrance and entrance chamber, type 65, structure 3, reinforcement for air intake and exhaust structures.

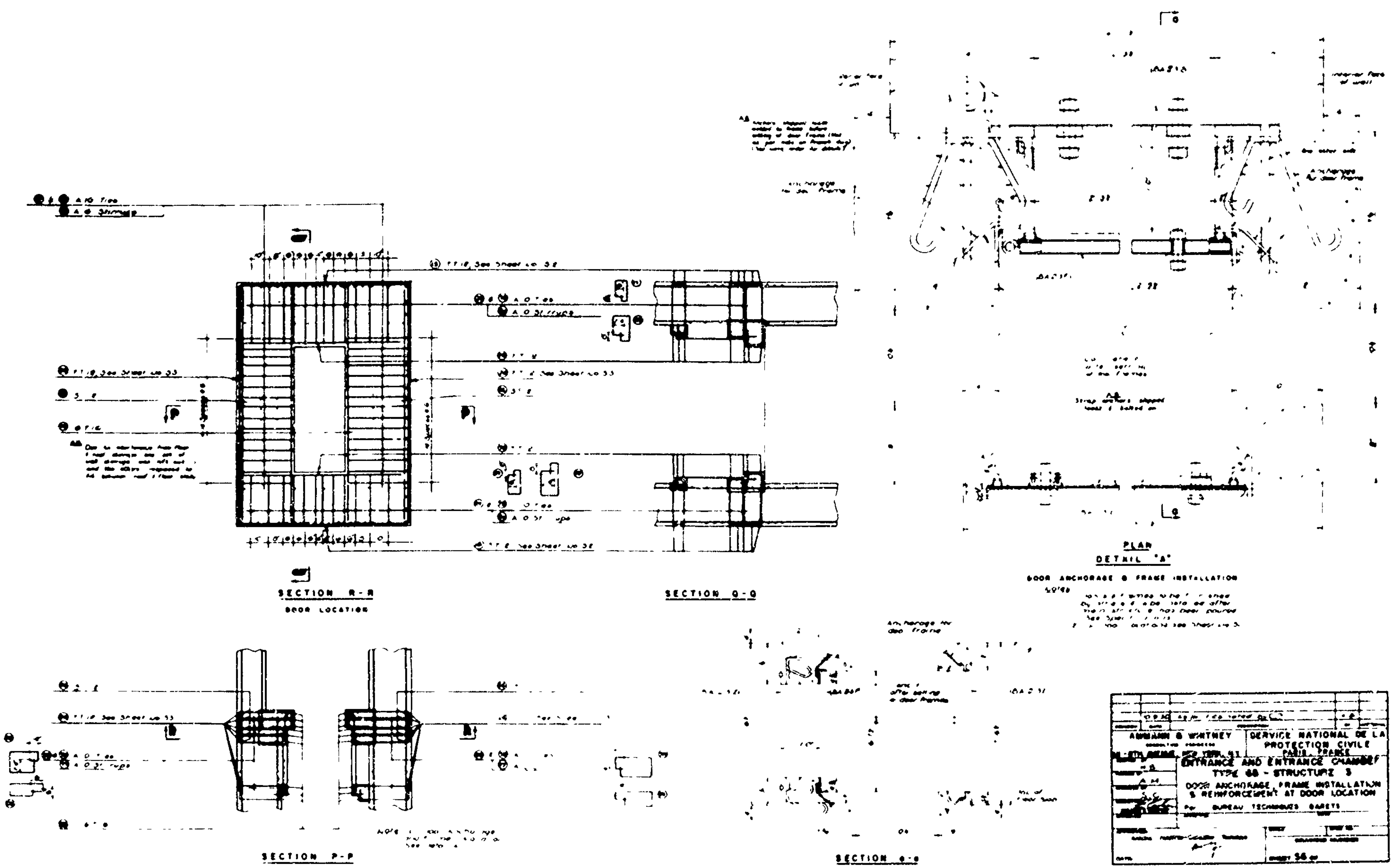

Fig. C.3.6—Entrance and entrance chamber, type 65, structure 3, door anchorage, frame installation, and reinforcement at door location.

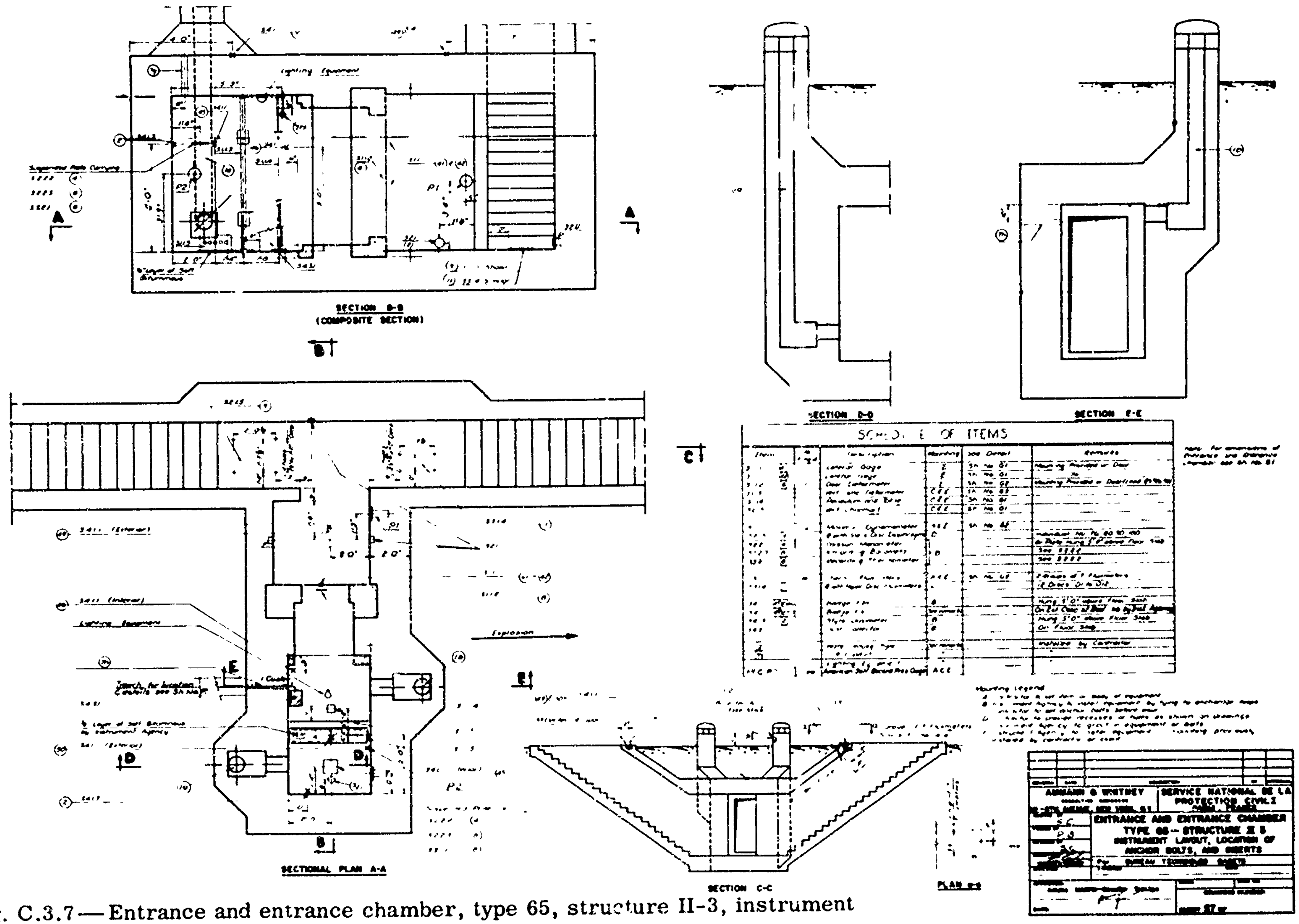

Fig. C.3.7 — Entrance and entrance chamber, type 65, structure II-3, instrument layout, location of anchor bolts, and inserts.

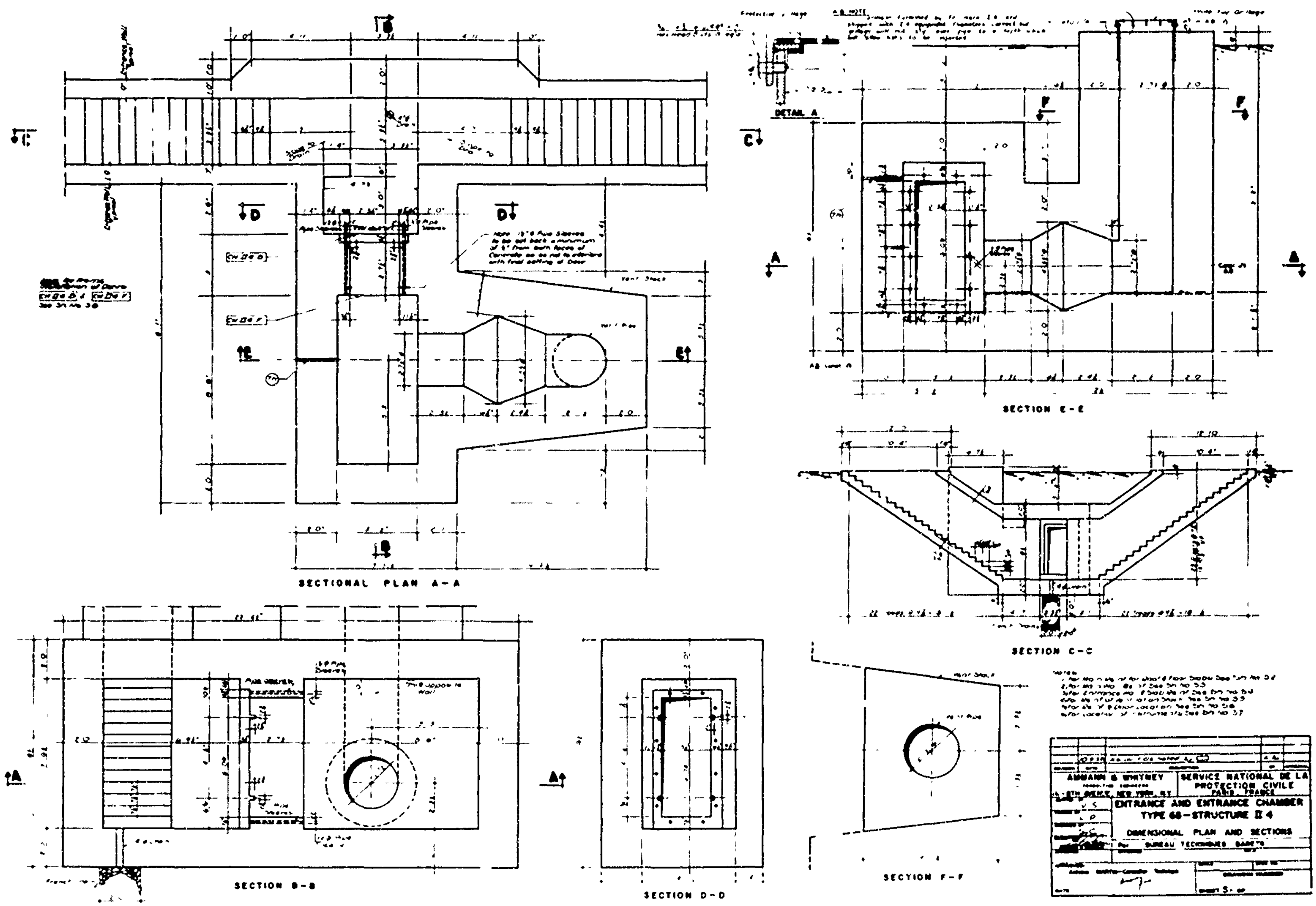

Fig. C.4.1—Entrance and entrance chamber, type 65, structure 'I-4, dimensional plan and sections.

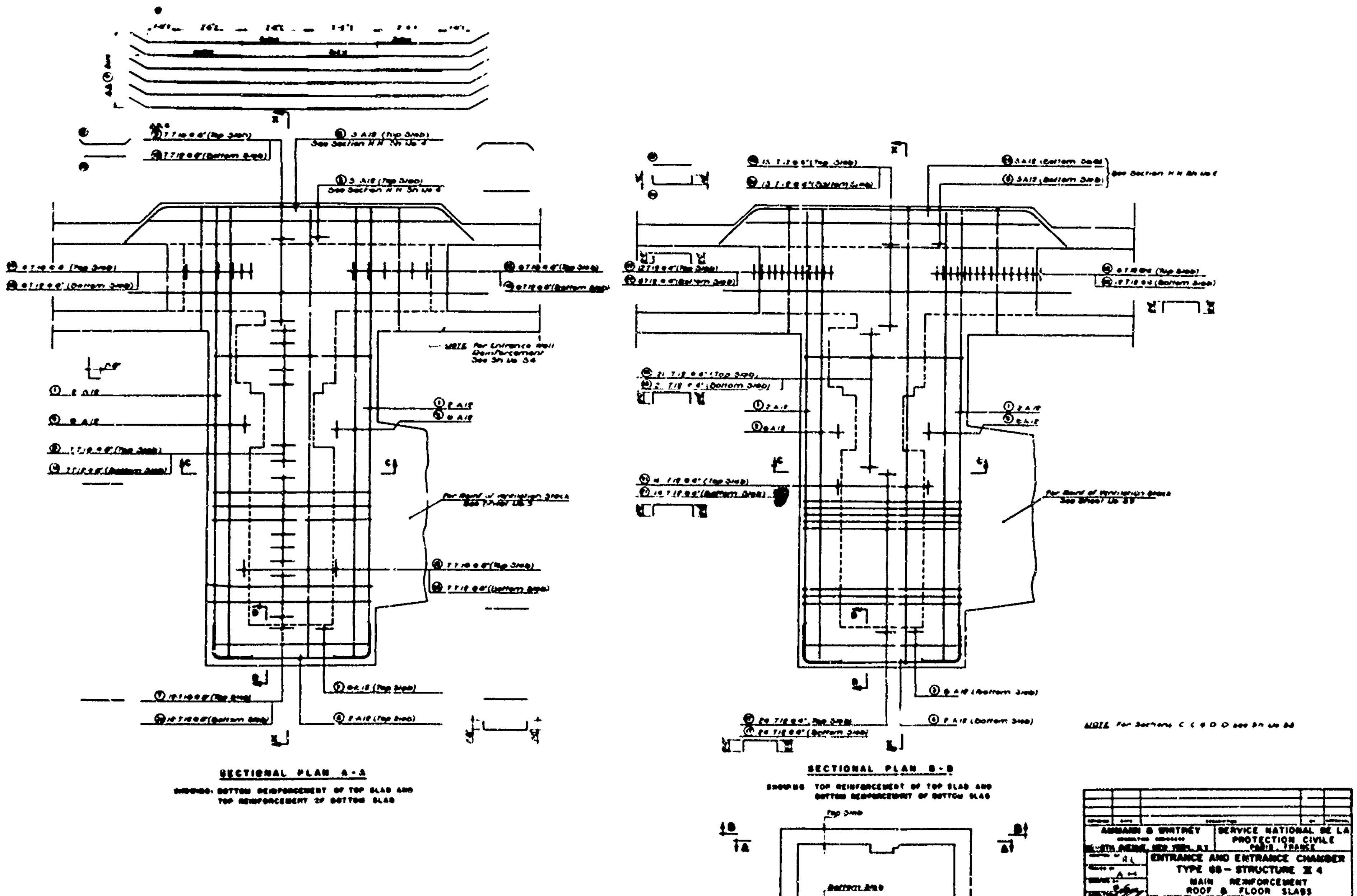

Fig. C.4.2—Entrance and entrance chamber, type 65, structure II-4, main reinforcement roof and floor slabs.

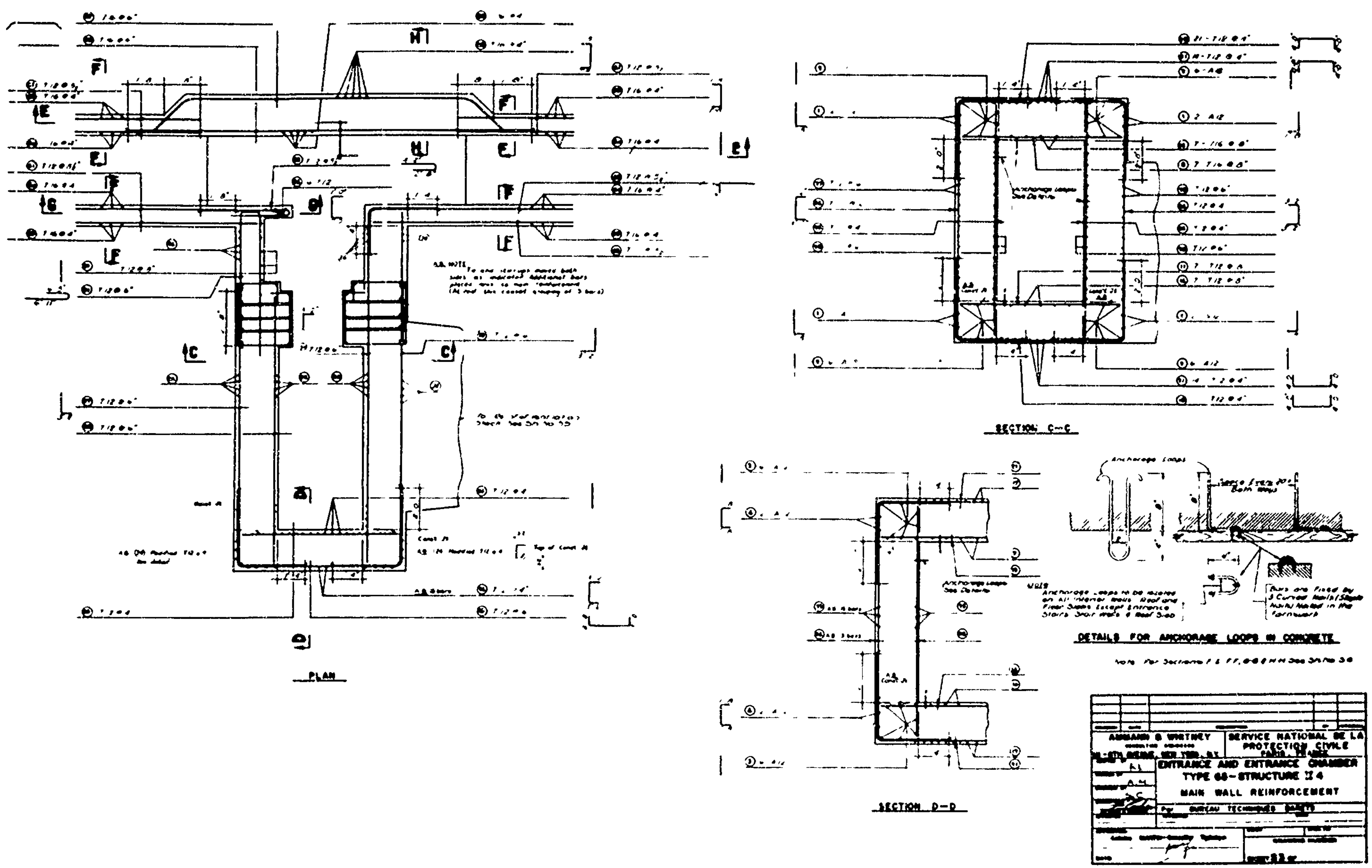

Fig. C.4.3—Entrance and entrance chamber, type 65, structure II-4, main wall reinforcement.

stack.

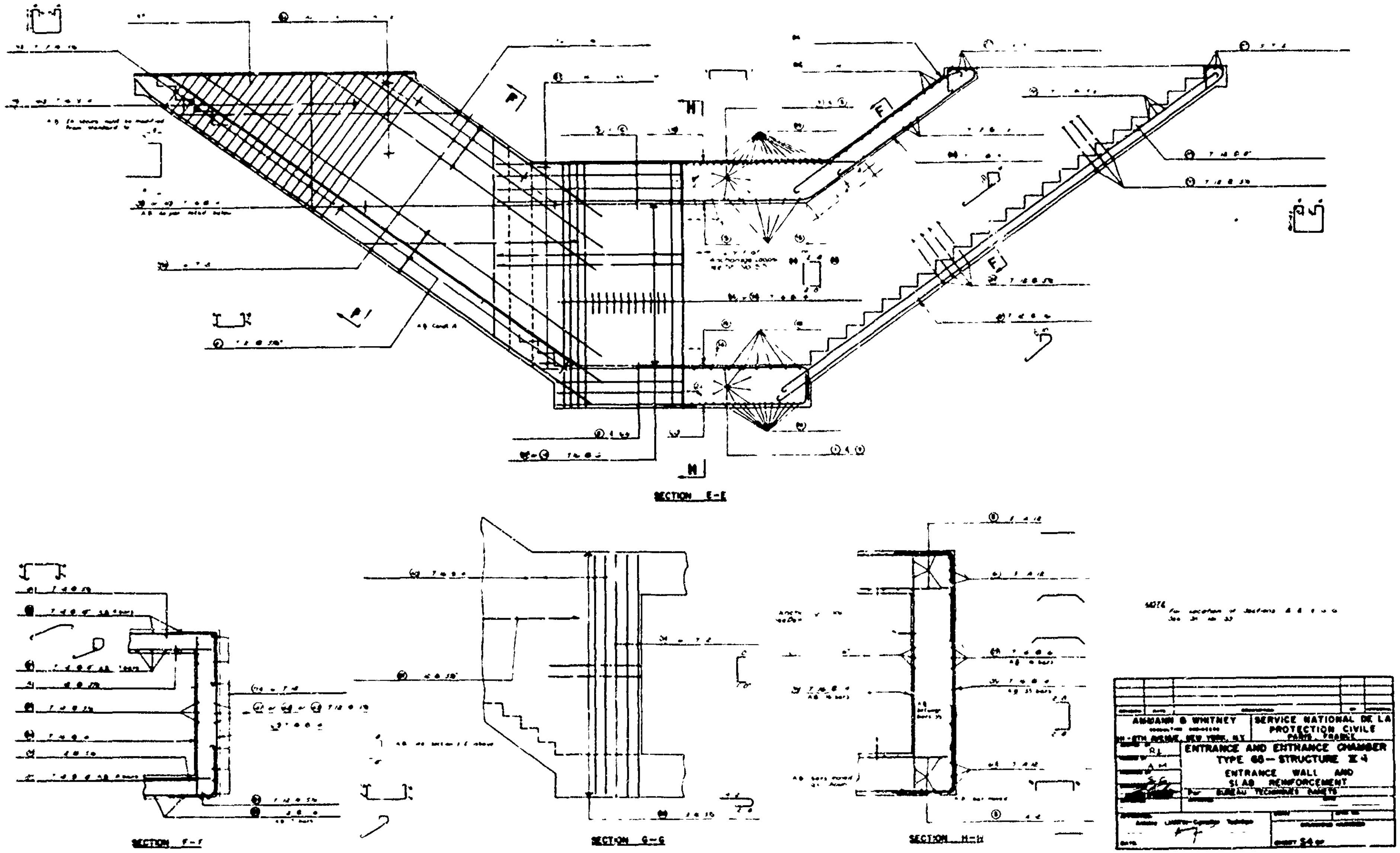

Fig. C.4.4—Entrance and entrance chamber, type 65, structure II-4, entrance wall and slab reinforcement.

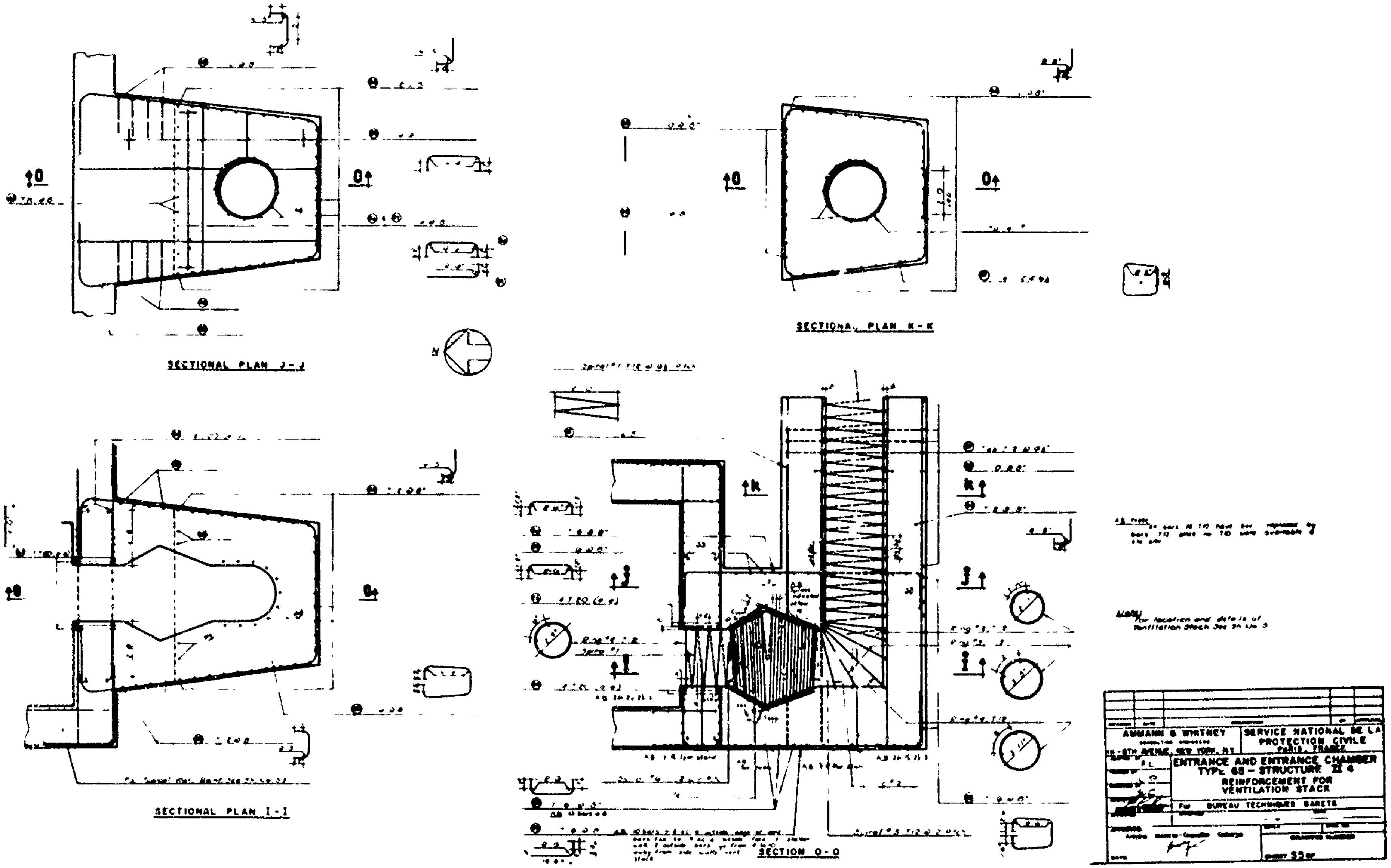

Fig. C.4.5—Entrance and entrance chamber, type 65, structure II-4, reinforcement for ventilation stack.

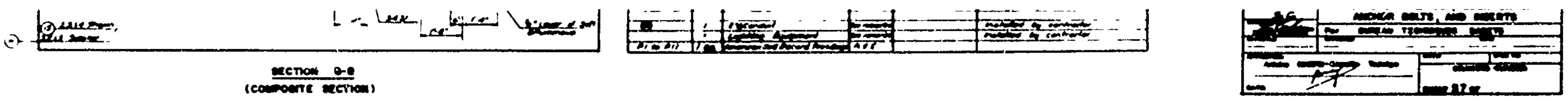

Fig. C.4.7 — Entrance and entrance chamber, type 65, structure II-4, instrument layout, location of anchor bolts, and inserts.

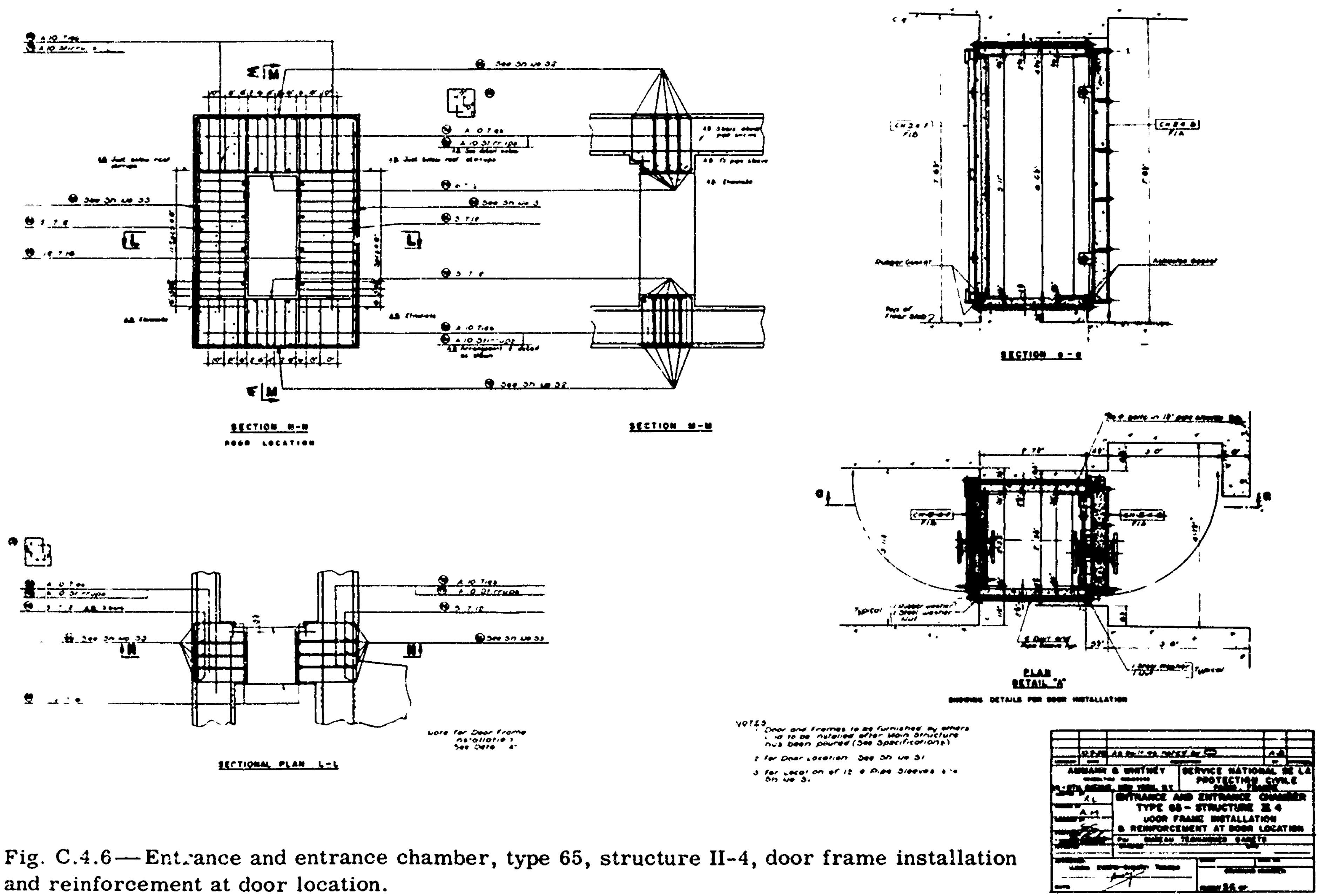

Fig. C.4.6 — Ent.ance and entrance chamber, type 65, structure II-4, door frame installation and reinforcement at door location.

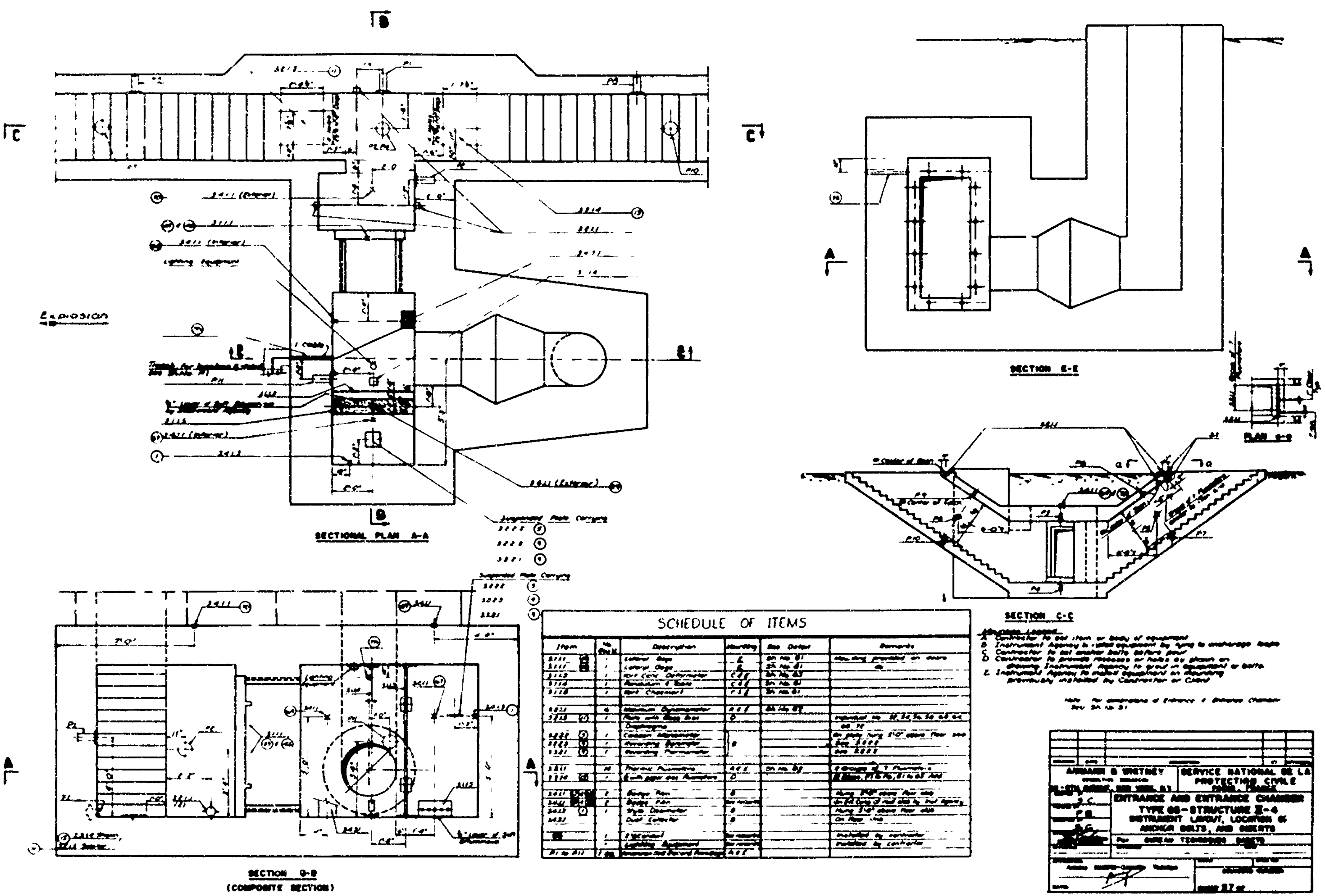
SECTIONAL PLAN A-A
Explosion
SECTION B-B
(COMPOSITE SECTION)
SECTION E-E
SECTION C-C
PLAN G-G
SCHEDULE OF ITEMS
Item
Description
Remarks
AMMANN & WHITNEY
SERVICE NATIONAL DE LA PROTECTION CIVILE
ENTRANCE AND ENTRANCE CHAMBER
TYPE 66-STRUCTURE II-4
INSTRUMENT LAYOUT, LOCATION OF
ANCHOR BOLTS, AND INSERTS

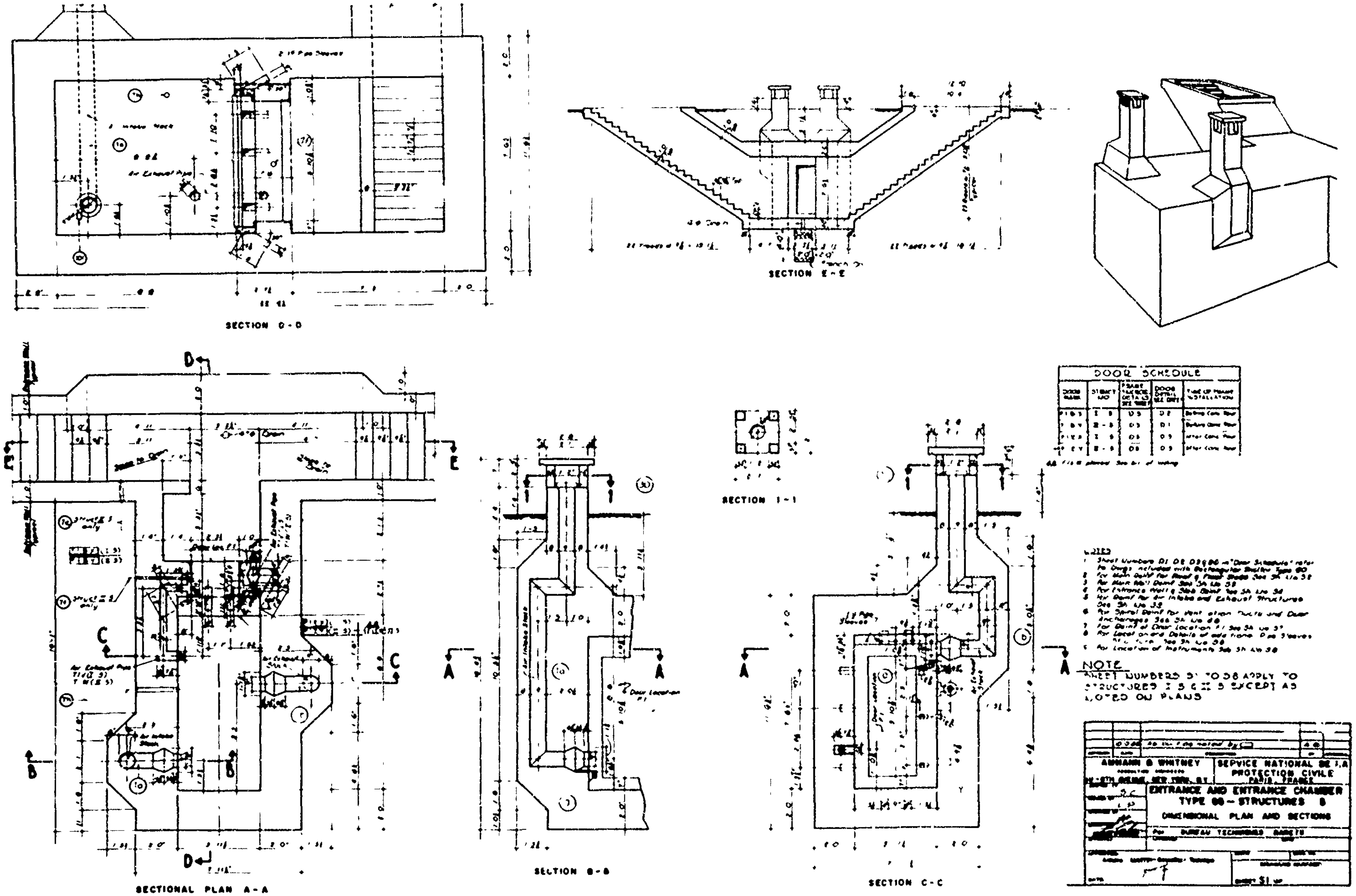

Fig. C.5.1—Entrance and entrance chamber, type 65, structure 5, dimensional plan and sections.

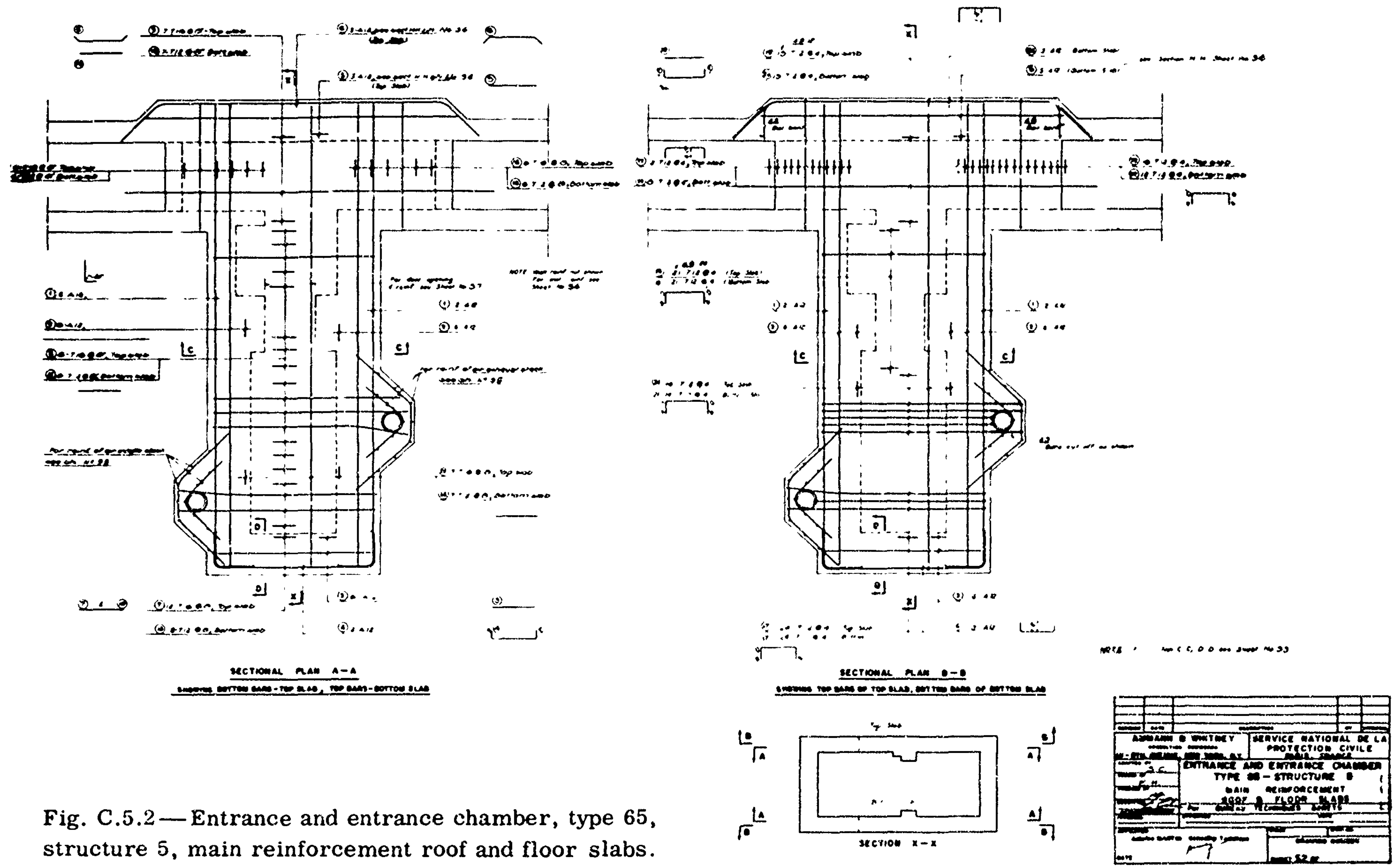

Fig. C.5.2—Entrance and entrance chamber, type 65, structure 5, main reinforcement roof and floor slabs.

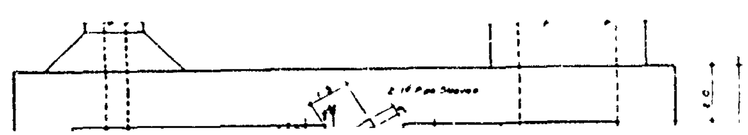

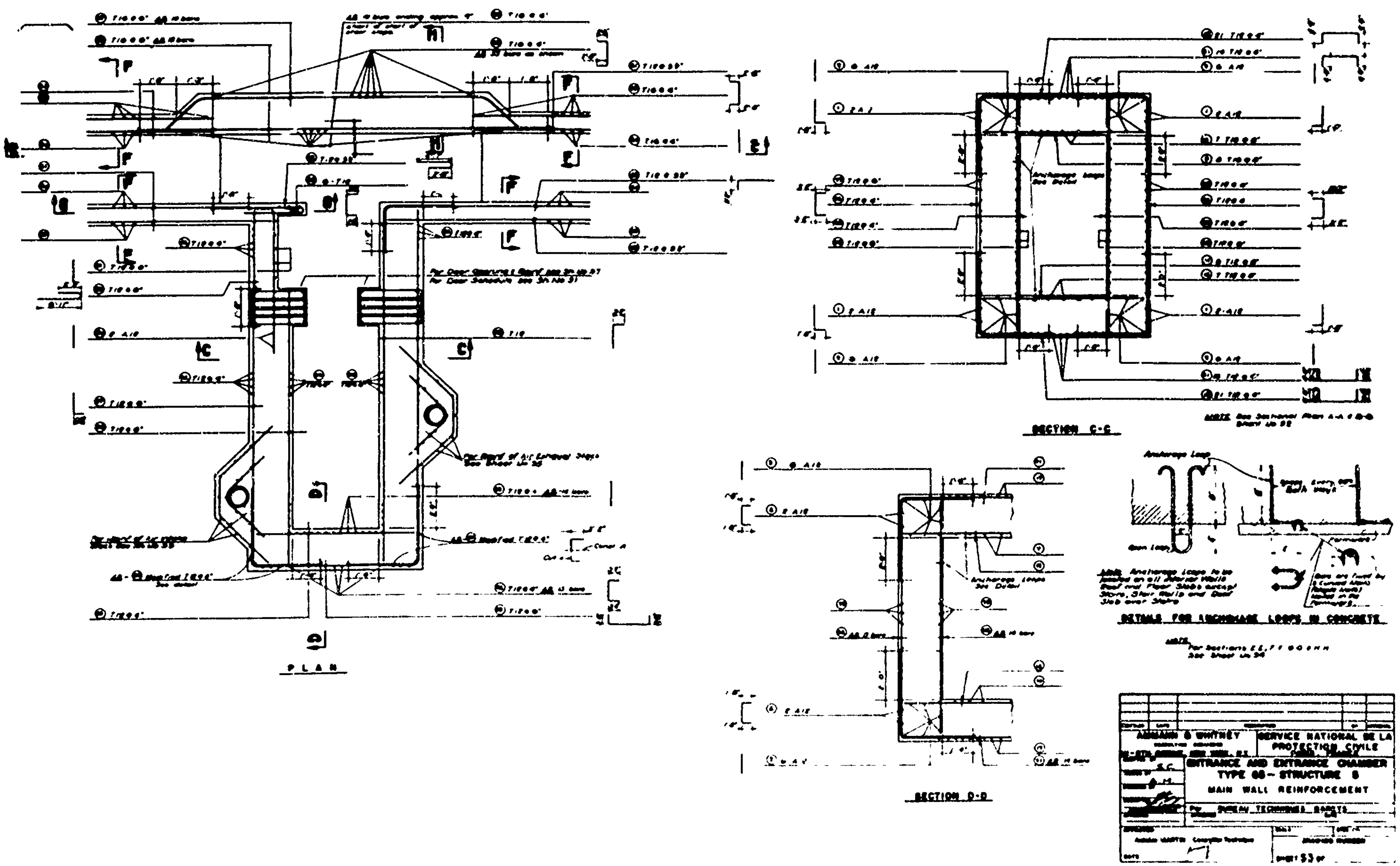

Fig. C.5.3—Entrance and entrance chamber, type 65, structure 5, main wall reinforcement.

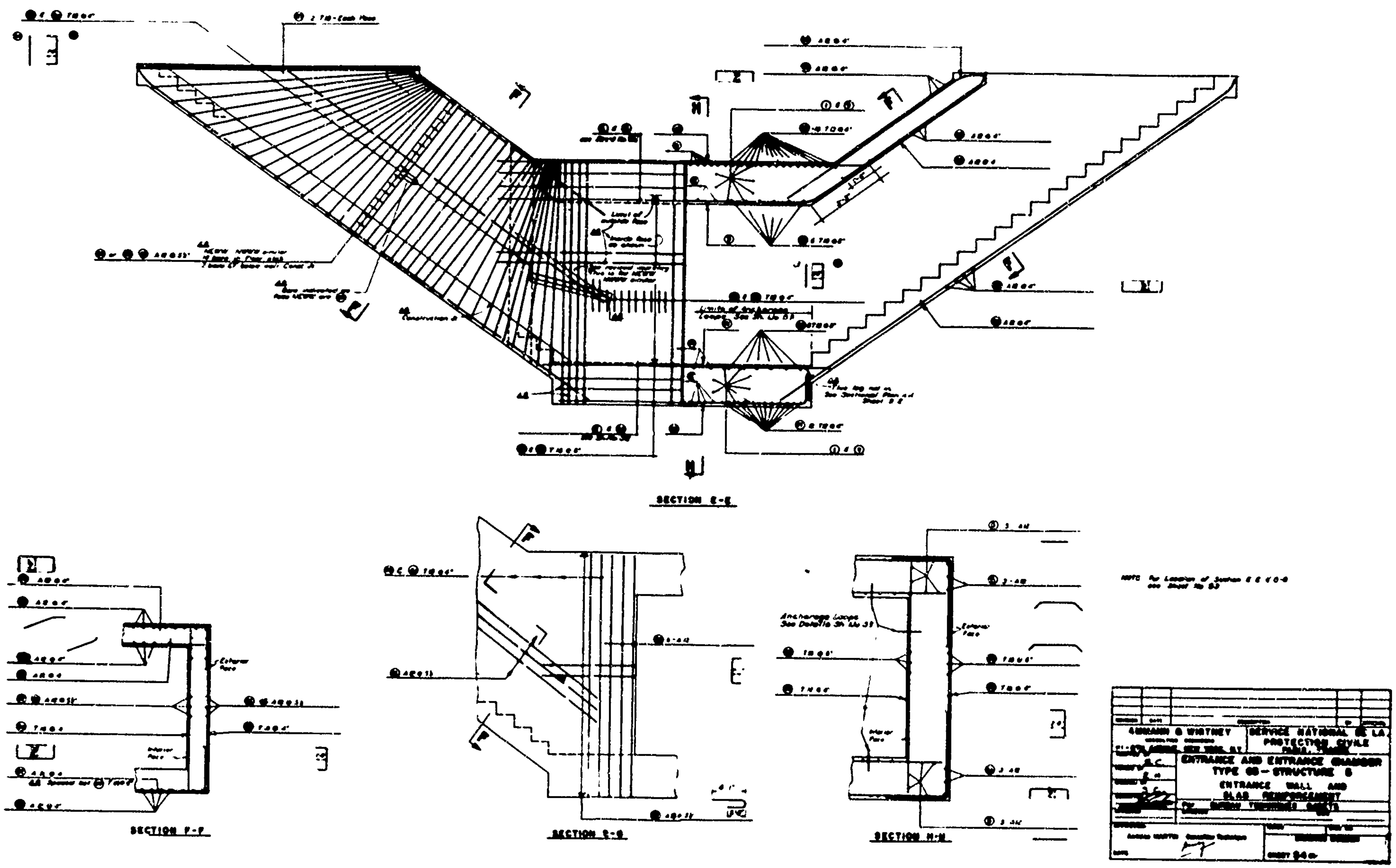

Fig. C.5.4—Entrance and entrance chamber, type 65, structure 5, entrance wall and slab reinforcement.

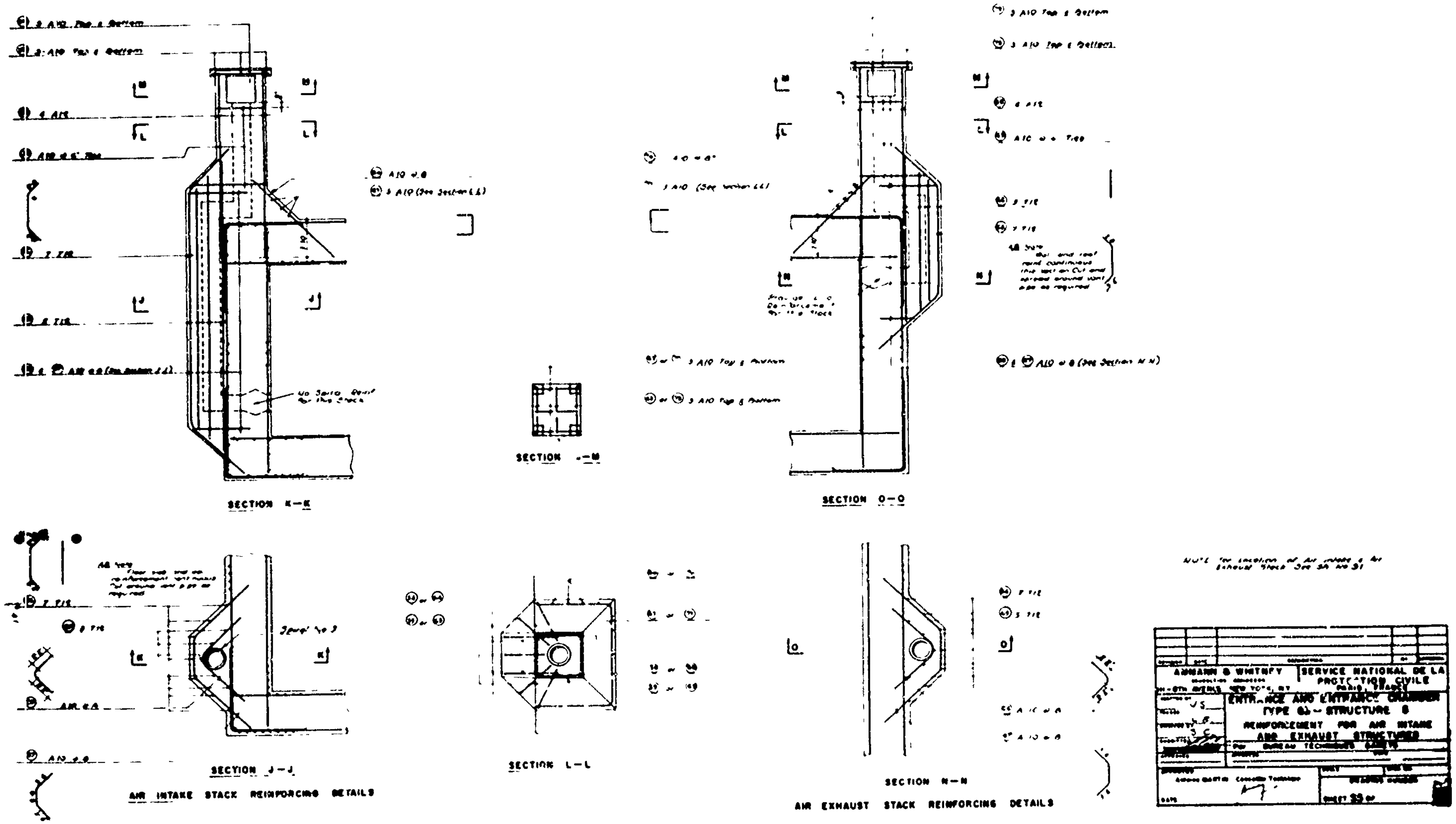

Fig. C.5.5—Entrance and entrance chamb^r, type 65, structure 5, reinforcement for air intake and exhaust structures.

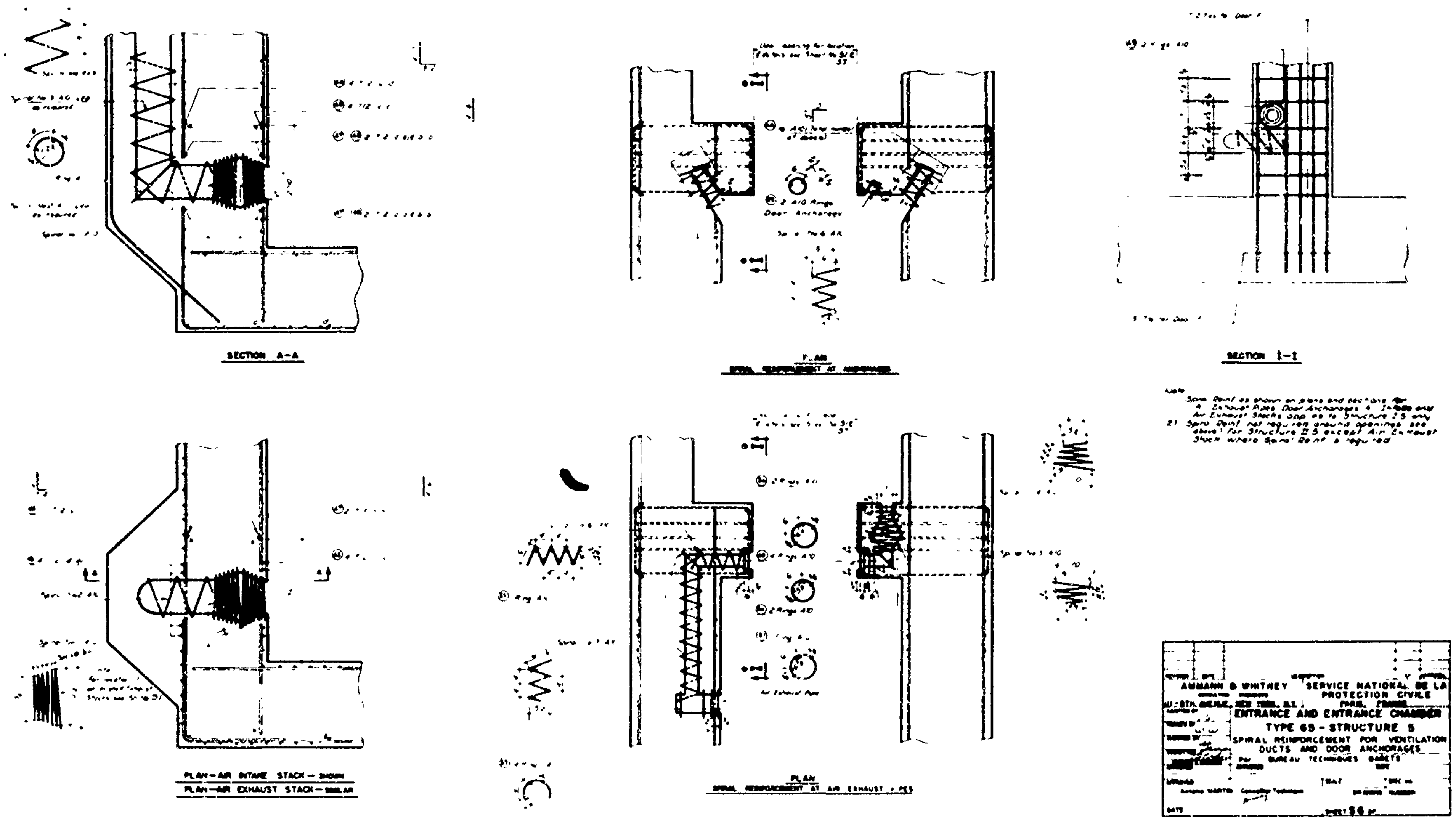

Fig. C.5.6—Entrance and entrance chamber, type 65, structure 5, spiral reinforcement for ventilation ducts and door anchorages.

Fig. C.5.8—Entrance and entrance chamber, type 65, structure II-5, instrument layout, location of anchor bolts, and inserts.

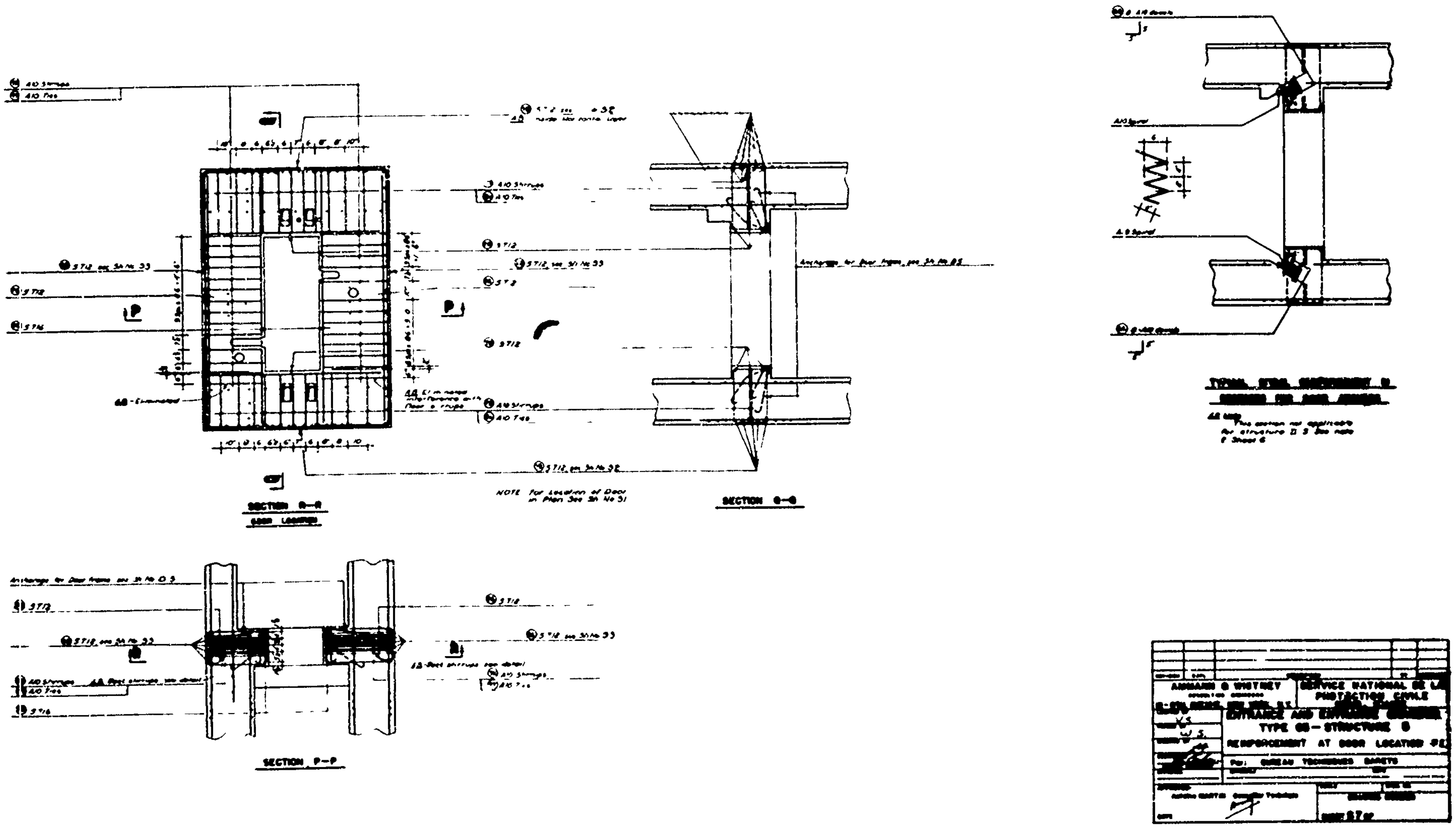

Fig. C.5.7—Entrance and entrance chamber, type 65, structure 5, reinforcement at door location F1.

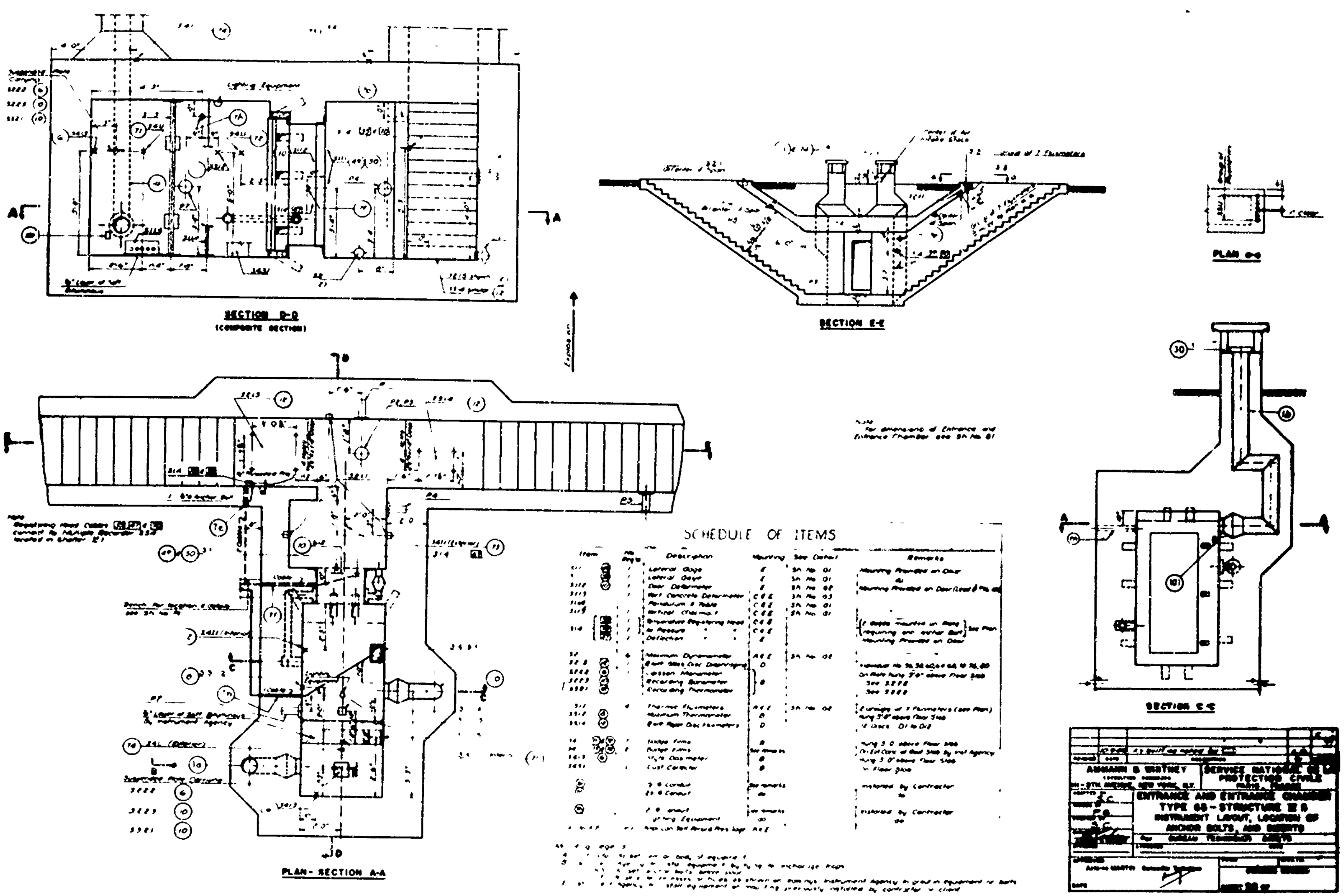

Fig. C.5.8—Entrance and entrance chamber, type 65, structure II-5, instrument layout, location of anchor bolts, and inserts.

Fig. C.6.2 — Measuring instruments 3.1.1.1, 3.1.1.4, and 3.1.1.5.

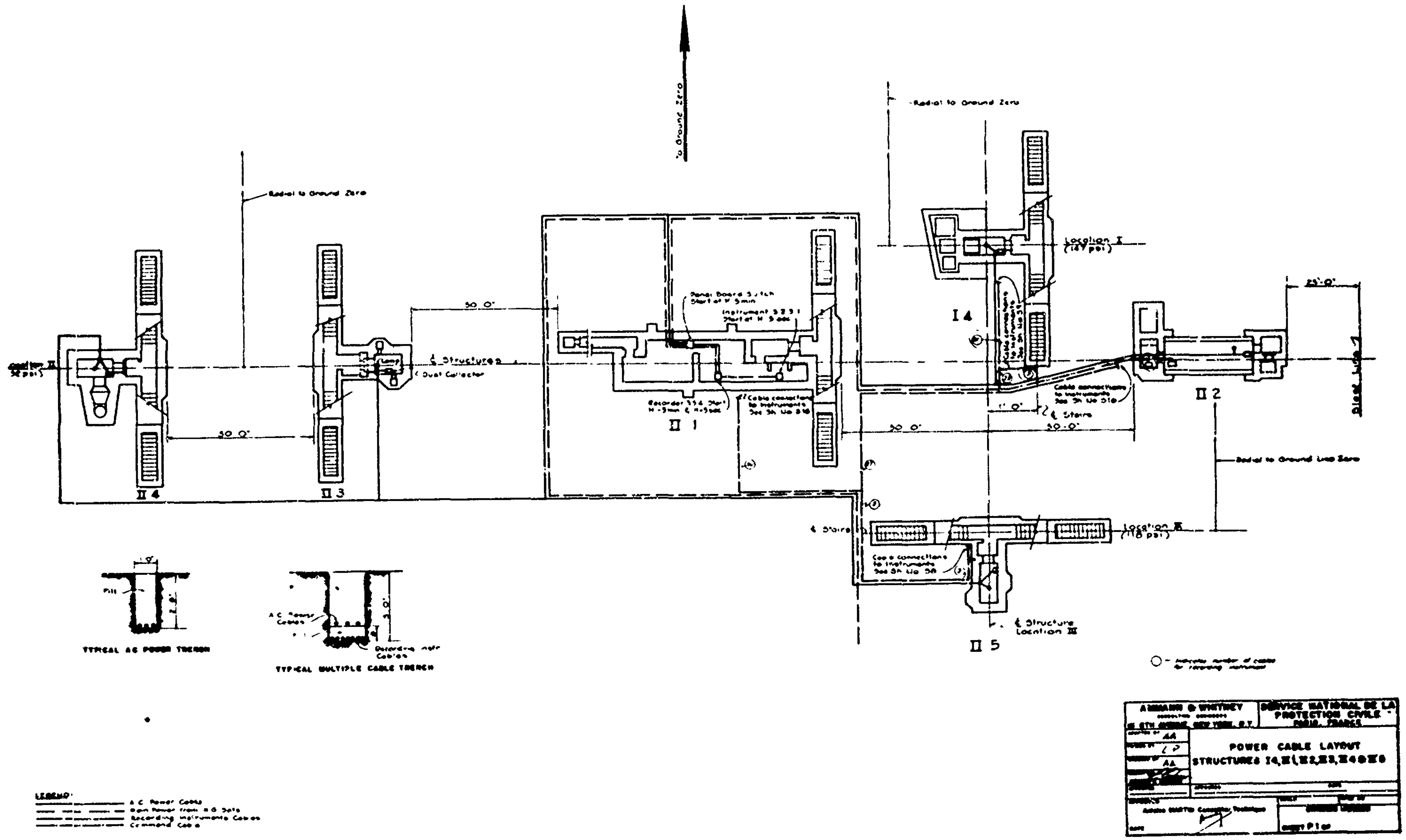

Fig. C.6.1 — Power cable layout for structures I-4, II-1, II-2, II-3, II-4, and II-5.

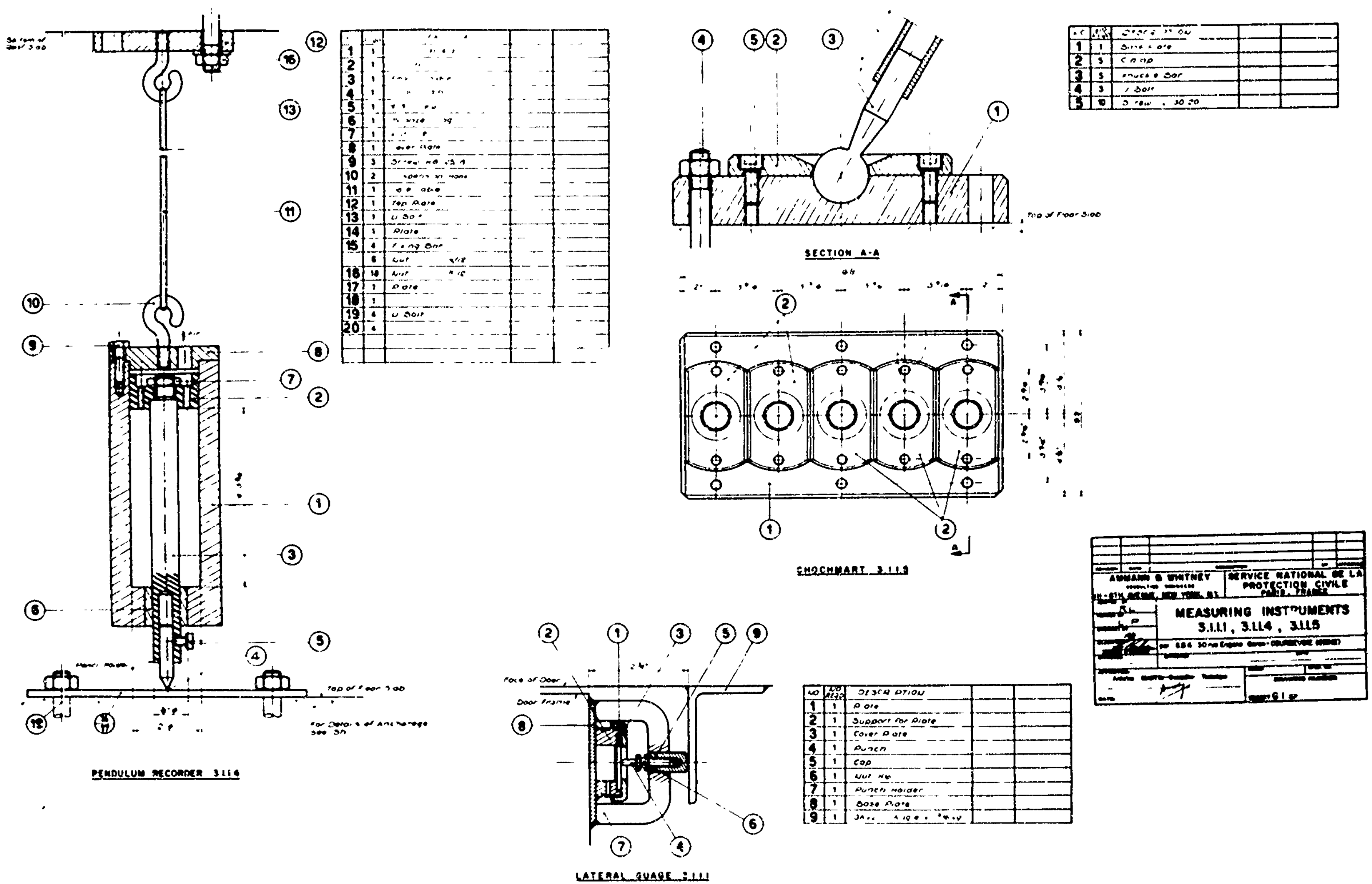

Fig. C.6.2—Measuring instruments 3.1.1.1, 3.1.1.4, and 3.1.1.5.

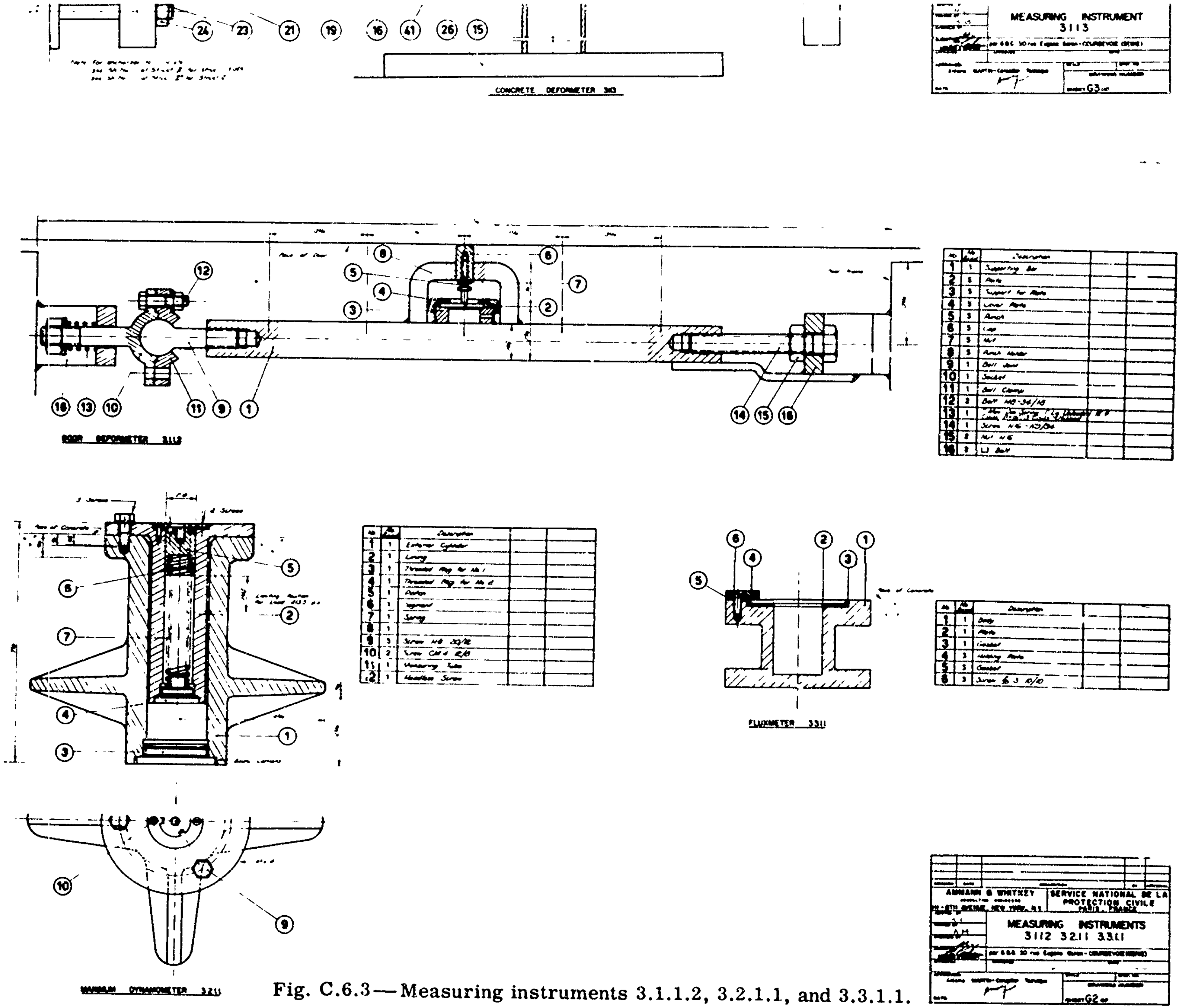

Fig. C.6.3—Measuring instruments 3.1.1.2, 3.2.1.1, and 3.3.1.1.

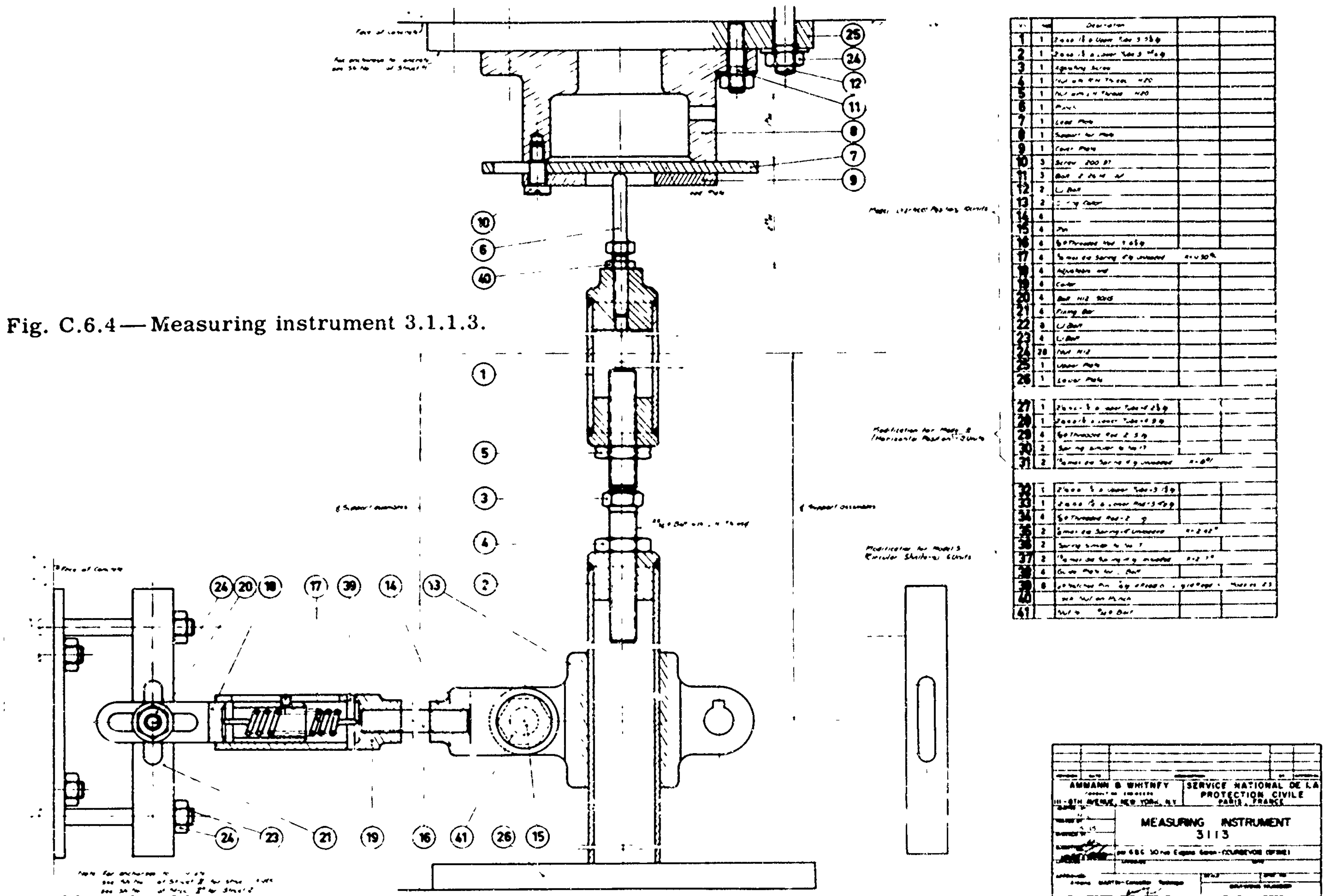

Fig. C.6.4—Measuring instrument 3.1.1.3.

Appendix D

ANALYSIS OF RECTANGULAR CONCRETE SHELTER, TYPE 60, STRUCTURE II-1

D.1 GENERAL

The shelter was designed by French engineers to withstand a static loading condition (Sec. 1.4). A shelter of this type was constructed at the theoretical 132.3-psi overpressure level and tested during shot Smoky of Operation Plumbbob. On the basis of the limited damage incurred, it was deemed advisable to analyze the roof slab of this shelter by the conventional ultimate strength theory in order to ascertain whether this method would substantiate the actual damage sustained by the member.

D.2 BLAST LOADING

For the purpose of analysis, the blast loading on the roof slab of this structure was assumed to be the actual free-air pressure-time load as recorded on the blast line at the location of this structure. The earth cover was assumed not to attenuate the free-air overpressure.

D.3 STRENGTH CRITERIA

As stated before, the structure was analyzed for dynamic behavior using ultimate strength theory.

The compressive strength of the concrete was 3800 psi and was determined as the average value obtained from the 90-day test cylinders (preshot). Reinforcing steel used in the roof slab was Tor-40 deformed reinforcement sent from France.

This type reinforcement has two diametrically opposite continuous spiral ribs running along its length. These square raised-pattern ribs have a height and width of one-tenth of the bar core diameter. The static unit stress at yield of 65,000 psi was also the average of values obtained from the test specimens. The dynamic design tensile and compressive yield stresses for steel and the dynamic ultimate compressive stress for concrete were increased over the static values to account for the rapid strain rates* caused by the blast loading.

---

* See SH.D.6, f'_{dc} and f_{ds}. The dynamic increase factors used in this analysis are the average values recommended in the manual EM-1110-345-414. More accurate values can be obtained by considering the actual times of yield and utilizing Figs. 4.15 and 4.20 of the above-referenced manual.

D.4 ANALYSIS

In general, the analysis of the various members of the structure which are exposed to the blast consist in the solution of the equation of motion,

$$F - R = M_e \ddot{X}$$

where F = applied blast force
R = internal resistance of the structural member
M_e = mass of an equivalent one-degree-of-freedom system[1]
$\ddot{X}$ = acceleration of the mass

This equation of motion can be readily solved by any of several numerical integration[2] methods. The numerical method illustrated in this appendix for the analysis of the roof slab of the shelter is the "acceleration impulse extrapolation method," described in reference 1.

Poisson's ratio for reinforced concrete usually is taken to vary between 0.10 and 0.166. In this analysis Poisson's ratio has been taken as zero. Another analysis using Poisson's ratio equal to 0.3 was also performed in order to ascertain the actual effect that this constant has on the final results. Comparison of results indicates that the effect of Poisson's ratio may be considered negligible over the entire range from elastic to plastic behavior of the structural member.

D.5 DESIGN AND STRUCTURE

Architecturally, the shelter was constructed as shown in Chap. 1, Fig. 1.1. The as-built drawings shown in Appendix C, Figs. C.1.1 to C.1.33, show the actual reinforcement arrangement placed in the field. As is clearly indicated by these drawings, there is very little deviation from the original reinforcement details. No modifications other than those recorded on the as-built drawings were made to any of the structures.

NOMENCLATURE

A_s = area of reinforcement
a = depth of compression block of the slab
b = width of the slab
d = distance from extreme compressive fiber to the centroid of the tension force in tensile reinforcement
E = modulus of elasticity
f'_c = static ultimate unit stress of concrete
f'_{dc} = dynamic ultimate unit stress of concrete
f_s = static unit stress of reinforcement at yield
f_{ds} = dynamic unit stress of reinforcement at yield
I_c = moment of inertia of cracked section
I_u = moment of inertia of uncracked section
K = stiffness of member
L_1 = clear span (member in short direction)
L_2 = clear span (member in long direction)
m = mass of the member
$M_{\mathbb{C}}$ = moment at the centerline of the member
M_s = moment at the support of the member
n = ratio of modulus of elasticity of steel to that of concrete
r = unit resistance of the member
R = total resistance of the member
T = period of vibration of the member
ult = ultimate
x = deflection of the member

ANALYSIS

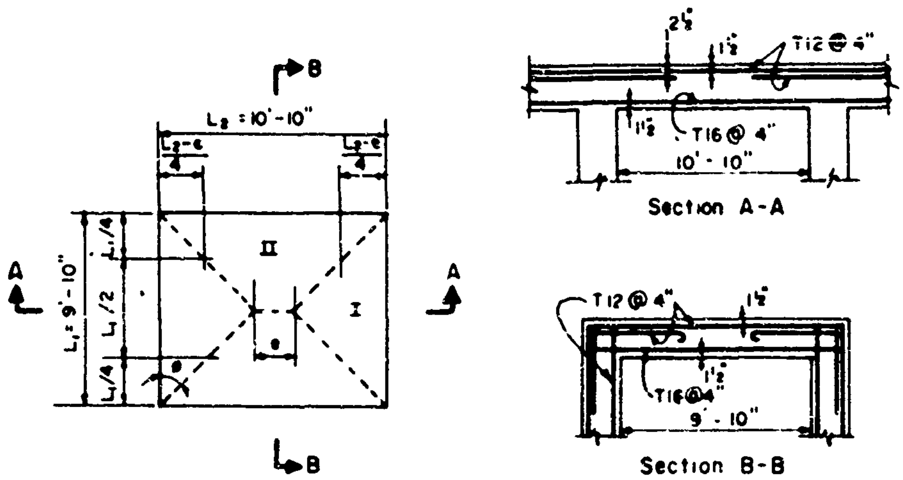

NOTE: The ultimate resistance of section I is governed by the continuous portion of the slab. The ultimate resistance of section II is governed by the moment capacity of the wall below the roof slab. Assume the outer strips of sections I and II have one-half the moment and shear capacity of their respective middle strips.

ν = Poisson's ratio = 0 (for reinforced concrete)
f'_c = 3,800 psi (90-day results) } av. values of test results
f_s = 65,000 psi
f'_{dc} = 3,800 (1.3) = 4.95 ksi
f_{ds} = 65,000 (1.1) = 71.5 ksi
d = 24 in. − 2 in. = 22 in. } av. values for both directions
d′ = 24 in. − 4 in. = 20 in.
t = 24 in.

Diameter:

Millimeters	12	16
Inches	0.473	0.630

<u>Section I:</u>

By trial and error solution, use

ϕ = 45.75°

X = tan ϕ (4.92) = 5.05 ft

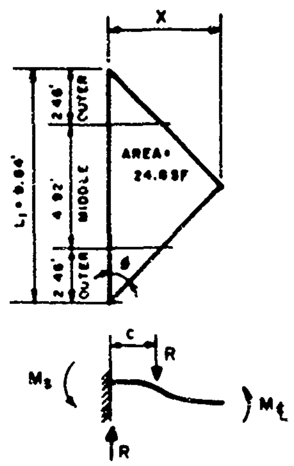

Positive steel (per foot)

$$A'_{\mathrm{\cent}} = \frac{\pi}{4}(0.63)^2(3) = 0.935 \text{ sq in./ft} = A'_S$$

Negative steel (per foot)

$$A'_S = \frac{\pi}{4}(0.473)^2(6) = 1.052 \text{ sq in./ft}$$

$$A'_{\mathrm{\cent}} = \frac{\pi}{4}(0.473)^2(3) = 0.526 \text{ sq in./ft}$$

Negative moment capacity (per foot)

$$a = \frac{A_s f_{ds}}{0.85 b f'_{dc}} = \frac{1.052(71.5)}{0.85(12)(4.95)} = 1.49 \text{ in. (Ref. 3)}$$

$$M'_{s\,ult} = A'_s f_{ds}\left(d - \frac{a}{2}\right)$$

$$= 1.052(71.5)\left(22 - \frac{1.49}{2}\right)\left(\frac{1}{12}\right) = 133.3 \text{ kf/ft}$$

Positive moment capacity (per foot)

$$a = \frac{0.935}{1.052}(1.49) = 1.322 \text{ in.}$$

$$M'_{\mathrm{℄}\,ult} = 0.935(71.5)\left(22 - \frac{1.322}{2}\right)\left(\frac{1}{12}\right) = 118.9 \text{ kf/ft}$$

Total positive and negative moments

$$(M'_S + M'_{\mathrm{℄}})\frac{3}{4}L_1$$

$$\Sigma M_{ult} = (133.3 + 118.9)(0.75)(9.83) = 1860 \text{ kf}$$

Total resistance of Section I

$$R_{ult} = \frac{\Sigma M}{c} = \frac{1860}{0.333(5.05)} = 1105 \text{ k}$$

Unit resistance

$$r_{ult} = \frac{1105}{0.5(5.05)(9.83)} = 44.6 \text{ ksf} = 310 \text{ psi}$$

<u>Section II:</u>

Wall reinforcement (per foot)

$$A+ = \frac{\pi}{4}(0.473)^2(3) = 0.526 \text{ sq in.}$$

$$A- = \frac{\pi}{4}(0.473)^2(6) = 1.052 \text{ sq in.}$$

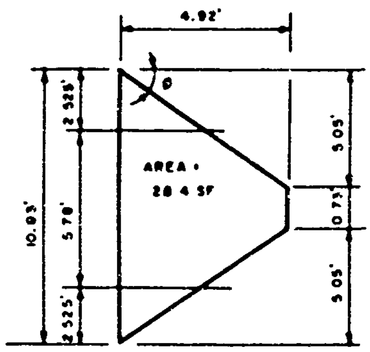

Negative moment (per foot)

Assume maximum loading on roof slab = 310 psi. Assumed resistance,

$$R = \left[2\left(\frac{1}{2}\right)(4.92)(5.05) + (4.92)(0.73)\right]44.6 = 1265 \text{ k}$$

$$P = R' = \frac{1265}{5.78 + 2.52} = 153 \text{ k/ft}$$

Negative moment capacity (per foot)

$$M'_S = d' A'_S f_S + 0.85 f'_c ab\left(\frac{d'}{2} + \frac{t}{2} - \frac{a}{2}\right) \qquad a = 1.49 \text{ in.}$$

$$= (20)(0.526)(71.5) + 0.85(4.95)(1.49)(12)\left(\frac{20}{2} + \frac{24}{2} - \frac{1.49}{2}\right)$$

$$= 75.2 + 75.3(10 + 12 - 0.745)$$

$$= 75.2 + 1600 = 1675 \text{ ki/ft} \approx 140 \text{ kf/ft}$$

Positive moment capacity (per foot)

$$M_{\mathfrak{c}} = A_S f_S\left(d - \frac{a}{2}\right)$$

$$A_{\mathfrak{c}} = \frac{\pi}{4}(0.63)^2(3) = 0.935 \text{ sq in./ft} \qquad a = 1.322 \text{ in.}$$

$$M_{\mathfrak{c}} = 0.935(71.5)\left(22 - \frac{1.322}{2}\right)$$

$$= 1427 \text{ ki/ft.} = 119 \text{ kf/ft}$$

Total positive and negative moments

$$\Sigma M_{ult} = (M'_S + M_{\mathfrak{c}})\left[e + \frac{3}{4}(L_2 - e)\right]$$

$$= (140 + 119)\left[0.73 + \frac{3}{4}(10.83 - 0.73)\right]$$

$$= 259(8.31) = 2160 \text{ kf}$$

Moment arm

$$C = \frac{24.8\left(\frac{4.92}{3}\right) + 3.6\left(\frac{4.92}{2}\right)}{\frac{1}{2}(0.73 + 10.83)(4.92)} = \frac{49.6}{28.4} = 1.75 \text{ ft}$$

Total resistance; Section II

$$R = \frac{\Sigma M}{c} = \frac{2160}{1.75} = 1240 \text{ k}$$

Unit resistance; Section II

$$r = \frac{1240}{28.4} = 43.7 \text{ ksf} \cong 44.6 \text{ ksf}$$

Av. unit resistance of total slab

$$r_{av.} = \frac{1240 + 1105}{53.2} = 44.0 \text{ ksf}$$

Ultimate resistance of slab for moment

$$R_{ult} = 2(53.2)(44.0) = 4690 \text{ k}$$

Assume member is fixed all around

$$\frac{L_2}{L_1} = \frac{b}{a} = \frac{10.83}{9.83} = 1.101 \qquad \text{(Use 1.1)}$$

Sec. I: $M_{S1} = 0.0543\ q\ L_1^2$ (Ref. 4, p. 240)

$M_{\mathfrak{c}1} = 0.0166\ q\ L_1^2$

Sec. II: $M_{S2} = 0.0585\ q\ L_1^2$

$M_{\mathfrak{c}2} = 0.0217\ q\ L_1^2$

Sec. I: $$q_{S1} = \frac{M_{S1}}{0.0543\ L_1^2} = \frac{133.3}{0.0543(9.84)^2} = 25.3 \text{ ksf} = 176 \text{ psi}$$

$$q_{\mathfrak{c}1} = \frac{M_{\mathfrak{c}1}}{0.0166\ L_1^2} = \frac{118.9}{0.0166(9.84)^2} = 74.0 \text{ ksf}$$

Sec. II: $$q_{S2} = \frac{M_{S2}}{0.0585\ L_1^2} = \frac{140}{0.0585(9.84)^2} = 24.8 \text{ ksf} = 172 \text{ psi}$$

$$q_{\mathfrak{c}2} = \frac{M_{\mathfrak{c}2}}{0.0217\ L_1^2} = \frac{119.0}{0.0217(9.84)^2} = 56.8 \text{ ksf}$$

Negative steel of Section II yields first. Section II, first yield, q = 172 psi:

$$R_1 = 24.8(10.83)(9.83) = 2640 \text{ k}$$

$$E = 1000\ f_c' = 3.8 \times 10^6$$

$$p^- = \frac{1}{2}\left[\frac{1.052 + 0.935}{12(22)}\right] = 0.00376$$

$$p^+ = \frac{1}{2}\left[\frac{0.935 + 1.052}{12(22)}\right] = \frac{0.00376}{0.00752} \text{ (Total)}$$

$$n = \frac{30 \times 10^6}{3.8 \times 10^6} = 7.9$$

$$p_{av.} = 0.00376; \ F = 0.022 \text{ (Ref. 2)}$$

$$I_{uncracked} = \frac{1}{12}\ bt^3 = \frac{1}{12}\ (12)(24)^3 = 13{,}800$$

$$I_{cracked} = Fbd^3 = 0.022(12)(22)^3 = \frac{2{,}810}{16{,}610} \text{ (Total)}$$

$$I\ av. = 8300 \text{ in.}^4$$

$$t^3 = \frac{12I}{b} = \frac{12}{12}\ (8300) = 8300$$

$$x_1 = \frac{0.0181qL_1^4}{Et^3} = \frac{0.0181(172)(9.83 \times 12)^4}{3.8(10^6)\ 8300} = 0.01918 \text{ in.} = 0.00160 \text{ ft}$$

$$K_1 = \frac{R_1}{x_1} = \frac{2640}{0.00160} = 1.65 \times 10^6 \text{ k/ft}$$

For q = 24.8 ksf

$$M_{S1}' = 133.3\left(\frac{24.8}{25.3}\right) = 130.8 \text{ k}'/\text{ft}$$

$$M'_{\mathfrak{C}1} = 118.9\left(\frac{24.8}{74.0}\right) = 39.8 \text{ kf/ft}$$

$$M'_{\mathfrak{C}2} = 119.0\left(\frac{24.8}{56.8}\right) = 52.0 \text{ kf/ft}$$

Second yield, member clamped on side L_1 and simply supported on side L_2

$M_{\mathfrak{C}2} = 0.0217qL_1^2$ (Ref. 4; p. 235)

$M_{S1} = 0.0788qL_1^2$

$M_{\mathfrak{C}1} = 0.0304qL_1^2$

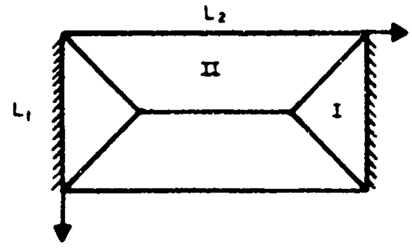

Remaining moment capacities

$$M_{\mathfrak{C}2} = M_{\mathfrak{C}2ult} - M'_{\mathfrak{C}2} = 119.0 - 52.0 = 67 \text{ kf/ft}$$

$$M_{S1} = M_{S1ult} - M'_{S1} = 133.3 - 130.8 = 2.5 \text{ kf/ft}$$

$$M_{\mathfrak{C}1} = M_{\mathfrak{C}1ult} - M'_{\mathfrak{C}1} = 118.9 - 39.8 = 79.1 \text{ kf/ft}$$

Loads to cause yield

$$q_{\mathfrak{C}2} = \frac{M_{\mathfrak{C}2}}{0.0217L_1^2} = \frac{67}{0.0217(9.83)^2} = 32.0 \text{ ksf}$$

$$q_{S1} = \frac{M_{S1}}{0.0788L_1^2} = \frac{2.5}{0.0788(9.83)^2} = 0.33 \text{ ksf} = 2.29 \text{ psi}$$

$$q_{\mathfrak{C}1} = \frac{M_{\mathfrak{C}1}}{0.0304L_1^2} = \frac{79.1}{0.0304(9.83)^2} = 26.9 \text{ ksf}$$

Second yield, negative steel of Section I

$$\Delta R_2 = 0.33(10.83)(9.83) = 35.2 \text{ k}$$

$$R_2 = 2640 + 35.2 = 2675 \text{ k}$$

$$\Delta x_2 = \frac{0.0303qL_1^4}{Et^3} = \frac{0.0303(2.29)(9.83 \times 12)^4}{3.8(10^6)(8300)} = 0.000426 \text{ in.} = 0.0000355 \text{ ft}$$

$$x_2 = 0.00160 + 0.0000355 = 0.00164 \text{ ft}$$

$$K_2 = \frac{\Delta R_2}{\Delta x_2} = \frac{35.2}{3.55 \times 10^{-5}} = 0.990 \times 10^6 \text{ k/ft}$$

$$\Delta M_{\mathfrak{C}1} = 79.1\left(\frac{0.33}{26.9}\right) 0.97 \text{ kf/ft}$$

$$\Delta M_{\mathfrak{C}2} = 67\left(\frac{0.33}{32.0}\right) 0.69 \text{ kf/ft}$$

$$M''_{\mathfrak{C}1} = 39.8 + 0.97 = 40.8 \text{ kf/ft}$$

$$M''_{\mathfrak{C}2} = 52.0 + 0.69 = 52.7 \text{ kf/ft}$$

Third yield, member simply supported all around

$M_{\mathfrak{C}1} = 0.0359qL_1^2$ (Ref. 4, p. 232)

$$M_{\mathrm{¢}2} = 0.0446qL_1^2$$

$$M_{\mathrm{¢}1} = M_{\mathrm{¢}1ult} - M''_{\mathrm{¢}1} = 118.9 - 40.8 = 78.1 \text{ kf/ft}$$

$$M_{\mathrm{¢}2} = M_{\mathrm{¢}2ult} - M''_{\mathrm{¢}2} = 119.0 - 52.7 = 66.3 \text{ kf/ft}$$

$$q_{\mathrm{¢}1} = \frac{M_{\mathrm{¢}1}}{0.0359L_1^2} = \frac{78.1}{0.0359(9.83)^2} = 22.5 \text{ ksf}$$

$$q_{\mathrm{¢}2} = \frac{M_{\mathrm{¢}2}}{0.0446L_1^2} = \frac{66.3}{0.0446(9.83)^2} = 15.37 \text{ ksf} = 106.7 \text{ psi}$$

Third yield, positive steel of Section II

$$\Delta R_3 = 15.37(9.83)(10.83) = 1636 \text{ k}$$

$$R_3 = 2675 + 1636 = 4311 \text{ k}$$

$$\Delta x_3 = \frac{0.0584(106.7)(9.83 \times 12)^4}{3.8(10^6)(8300)} = 0.0382 \text{ in.} = 0.00318 \text{ ft}$$

$$x_3 = 0.00164 + 0.00318 = 0.00482 \text{ ft}$$

$$K_3 = \frac{\Delta R_3}{\Delta x_3} = \frac{1636}{3.18 \times 10^{-3}} = 5.14 \times 10^5 \text{ k/ft}$$

$$\Delta M_{\mathrm{¢}1} = 78.1\frac{15.37}{22.5} = 53.4 \text{ kf/ft}$$

$$M''_{\mathrm{¢}1} = 40.8 + 53.4 = 94.2 \text{ kf/ft}$$

NOTE: Since "e" is small, the failure at the fourth yield is localized. Consequently, the stiffness of the entire slab at the fourth yield is very nearly equal to that of the slab at the third yield. For purposes of this analysis, we have assumed that the stiffnesses at the fourth yield is equal to that at the third yield. The ultimate resistance of the slab remains unchanged.

The resistance vs. deflection curve is shown in Fig. D.1.

Dynamic Analysis

Dead load (assume overburden = 100 pcf)

$$F_{dl} = R_{dl} = [(0.15 \times 2) + (0.10 \times 4)]\ (9.83)(10.83) = 74.5 \text{ k}$$

Mass

$$\triangle \text{ Section I} \quad 2\left(\frac{1}{2}\right)(9.83)(5.05)\ [(2)(0.15) + 4(0.1)]\ \frac{1}{32.2} = 1.08$$

$$\text{Section II} \quad 2(28.4)\ [(2)(0.15) + 4(0.1)]\ \frac{1}{32.2} = \underline{1.23}$$

$$m = 2.31 \text{ k-sec}^2\text{/ft}$$

Equivalent mass (Ref. 5)

$$\text{1st yield} = m_1 = \left[0.610 + 0.156\left(\frac{b}{a} - 1.0\right)\right]\ m$$

$$= [0.610 + 0.156\ (1.1 - 1.0)]\ 2.31 = 1.445 \text{ k-sec}^2\text{/ft}$$

$$\text{4th yield} = m_4 = \left[0.630 + 0.160\left(\frac{b}{a} - 1.0\right)\right]\ m$$

$$= [0.630 + 0.160\ (1.1 - 1.0)]\ 2.31 = 1.490 \text{ k-sec}^2\text{/ft}$$

NOTE: Use the same equivalent mass for m_2 and m_3 as was used for m_4.

$$5\text{th yield} - m_5 - \frac{1}{2}\Sigma m_\Delta + \frac{(4b-3a)}{(6b-4a)}\Sigma m_\Delta$$

$$= \frac{1}{2}(7.08) + \left[\frac{4(10.83) - 3(9.83)}{6(10.83) - 4(9.83)}\right](1.23)$$

$$= 0.54 + \left[\frac{43.3 - 29.5}{65.0 - 39.3}\right](1.23)$$

$$= 0.54 + \left[\frac{13.8}{25.7}\right](1.23)$$

$$= 0.54 + 0.66 = 1.20 \text{ k-sec}^2/\text{ft}$$

NOTE: Assume the dead load and preliminary part of the pressure curve, Fig. D.2, to t = 13.5 msec (time 0.00 of dynamic analysis No. 1) act as a static load.

Period

$$T = 2\pi\sqrt{m_e/k_1} = 2\pi\sqrt{\frac{1.445 \times 10^{-6}}{1.65}} = 5.88 \times 10^{-3}$$

$$\Delta t = T/10 = 5.88 \times 10^{-4} \text{ -- use } 0.00025 \text{ sec}$$

Static load, analysis No. 1 (see Fig. D.2)

$$F_{static} = F_{d.l.} + F_{p.p.} = 74.5 + 30(0.144)(106.4)$$

$$= 75 + 460 = 535 \text{ k}$$

$$x_{static} = x_{d.l.} + x_{p.p.} = 0.00160\left(\frac{535}{2640}\right) = 0.000324 \text{ ft}$$

Analysis constants

$$\Delta t^2 = (25 \times 10^{-5})^2 = 625 \times 10^{-10} = 0.625 \times 10^{-7} \text{ sec}^2$$

$$\Delta t^2/m_1 = \frac{0.625 \times 10^{-7}}{1.445} = 0.432 \times 10^{-7}$$

$$\Delta t^2/m_2 = \frac{0.625 \times 10^{-7}}{1.490} = 0.420 \times 10^{-7}$$

$$x_{n+1} = 2x_n - x_{n-1} + a_n(\Delta t^2) \qquad \text{(Ref. 1)}$$

$$F = P(0.144)(106.4) - 460 = 15.32P - 460$$

$$a_n = \frac{F_n - R_n}{m} \qquad \text{(Ref. 1)}$$

$$a_0 = \frac{1}{m_e}\left[\frac{F_0}{2} + \frac{F_1 - F_0}{6}\right] = \frac{1}{1.445}\left[0 + \frac{54}{6}\right] = 6.23$$

$$x_0 = a_0\Delta t^2 = (6.23)(0.625 \times 10^{-7}) = 0.389 \times 10^{-6}$$

Static load, analysis No. 2

$$F_{static} = F_{d.l.} + F_{p.p.} = 74.5 + 32(0.144)(106.4) = 75 + 490$$

$$F_{static} = 565 \text{ k}$$

$$x_{static} = x_{d.l.} + x_{p.p.} = 0.00160\left(\frac{565}{2640}\right) = 0.00342 \text{ ft}$$

Analysis constants

$$a_0 = \frac{1}{m_e}\left[\frac{F_0}{2} + \frac{F_1 - F_0}{6}\right] = \frac{1}{1.445}\left[0 + \frac{185}{6}\right] = 21.35$$

$$x_0 = a_0 \Delta t^2 = (21.35)(0.625 \times 10^{-7}) = 1.335 \times 10^{-6}$$

Dynamic analysis No. 1 is not given herein. Solution of this analysis indicated that the resistance damped out and returned to vibrate about the load curve. Subsequently, comparison of dynamic analysis No. 1 with dynamic analysis No. 2 indicated that the maximum resistance of dynamic analysis No. 2 was greater than that obtained from analysis No. 1.

NOTE: Dynamic analysis indicates that, if a damping factor were included in the analysis, the resistance would vibrate about the load curve and by the time the peak pressure was reached the applied load would be static in nature. At the first reversal the maximum dynamic resistance is 1458 kip. At the second reversal R_n is 1634 kip. This indicates an increase of approximately 11 per cent. However, the damping factor for the first cycle is approximately 15 per cent, thereby indicating that the peak dynamic resistance occurs at the first reversal. For purposes of this analysis, we have taken the peak dynamic load as that which was obtained from the second reversal (at $t = 92.5 \times 10^{-6}$ sec) of dynamic analysis No. 2. This value is conservative, the actual loading probably being less than 1400 kip.

$$R_{static} = 565 \text{ k}; \ R_{dynamic\ load} = 1634 \text{ k}$$

$$R_T = 1634 + 565 = 2199 \text{ k}$$

Deflection at third yield

$$x_3 = 0.00482 + 0.00342 = 0.005162 \text{ ft} = L/1906$$

Check of Shear

NOTE: For diagonal tension assume the critical section for shear is at "d" distance from the interior face of the walls (Ref. 6).

As can be seen from the dynamic analysis presented in Table D.1, the slab remained elastic under the applied blast load. Because of this, the slab was first analyzed using shear coefficients for a slab fixed on four sides.

Elastic behavior

$$t = 24 \text{ in.}$$

$$x = d = 22.5 \text{ in.} = 1.875 \text{ ft}$$

$$R_T = 2199 \text{ k}$$

$$w = \frac{2199}{106.4} = 20.6 \text{ ksf}$$

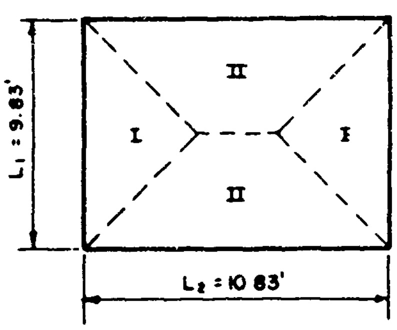

$$V_{s2} = \frac{wL_1}{2.10} = \frac{20.6(9.83)}{2.10} = 96.4 \text{ k/ft (Ref. 4, p. 240)}$$

$$V_{d2} = V_{s2} - wd$$

$$V_{d2} = 96.4 - (20.6)(1.875) = 57.8 \text{ k/ft}$$

The actual unit shear is

$$v = \frac{V_{d2}}{bd} = \frac{57.8}{(12)(22.5)} = 214 \text{ psi} = 3.47\sqrt{f'_c}$$

If the structure had been more heavily loaded, the yield lines would have developed. For this condition one must assume that the maximum shears are those obtained as the capacities for the strongest section.

The shear at "d" distance from the support is obtained as follows:

$$A_{tot} = 28.4 \text{ sq ft}$$

$$A_1 = \frac{(6.98 + 10.83)(1.875)}{2}$$

$$= 16.7 \text{ sq ft}$$

$$A_2 = A_{tot} - A_1$$

$$= 11.7 \text{ sq ft}$$

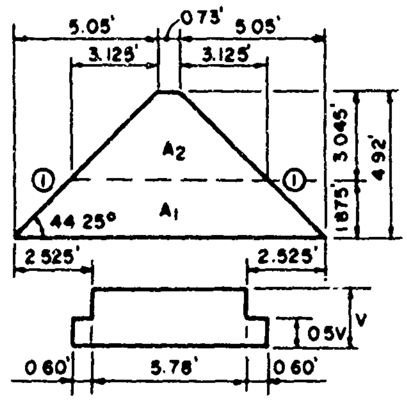

Total shear at "d" from support (line ① – ①):

$$V_T = 11.7(44.0) = 515 \text{ k}$$

Shear per foot

$$V = \frac{515}{5.78 + 2(0.60/2)} = 80.8 \text{ k/ft}$$

Actual unit shear

$$v = \frac{80.8}{12(22.5)} = 299 \text{ psi} = 4.85 \sqrt{f_c'}$$

REFERENCES

1. Engineering and Design, Design of Structures to Resist the Effects of Atomic Weapons, Principles of Dynamic Analysis and Design, EM 1110-345-415, U. S. Army Corps of Engineers.
2. Unpublished charts prepared by Ammann & Whitney.
3. C. S. Whitney, Plastic Theory of Reinforced Concrete Design, Trans. Am. Soc. Civil Engrs., Vol. 107 (1940).
4. Beton Kalendar, 1958.
5. C. S. Whitney, B. G. Anderson, and E. Cohen, Design of Blast Resistant Construction for Atomic Explosions, J. Am. Concrete Inst., Proc. (51) (March 1955).
6. Current Ammann & Whitney criteria for the determination of ultimate shear requirements for beams and flat slabs.

Table D.1 — DYNAMIC ANALYSIS NO. 2

n	t ($\times 10^{-4}$), sec	F_n, kip	R_n, kip	$F_n - R_n$, kip	$\Delta t^2/m$ ($\times 10^{-7}$)	$a_n \Delta t^2$ ($\times 10^{-6}$)	$x_n + 1$ ($\times 10^{-6}$), ft	
0	0	0			0.432	1.34		$\Delta R_1 = 2640^k$
1	2.5	185	2	183		7.91	1.34	$\Delta x_1 - 1600 \times 10^{-6}$
2	5.0	354	17	337		14.56	10.59	$K_1 = 1.65 \times 10^{-6}$
3	7.5	522	57	465		20.09	34.40	
4	10.0	722	129	593		25.62	78.30	
5	12.5	728	244	484		20.91	147.82	
6	15.0	732	393	339		14.64	238.25	
7	17.5	737	566	171		7.39	343.32	
8	20.0	742	752	−10		−0.43	455.78	
9	22.5	749	937	−188		−8.12	567.81	
10	25.0	757	1108	−351		−15.16	671.72	
11	27.5	765	1255	−490		−21.17	760.47	
12	30.0	772	1366	−594		−25.66	828.05	
13	32.5	779	1435	−656		−28.34	869.97	
14	35.0	786	1458	−672		−29.03	883.55	← first reversal
15	37.5	794	1432	−638		−27.56	868.10	
16	40.0	802	1361	−559		−24.15	825.09	
17	42.5	809	1251	−442		−19.09	757.93	
18	45.0	817	1108	−291		−12.57	671.68	
19	47.5	826	945	−119		−5.14	572.86	
20	50.0	834	773	61		2.64	468.72	
21	52.5	842	606	236		10.20	367.22	
22	55.0	848	455	393		16.98	275.92	
23	57.5	855	333	522		22.55	201.60	
24	60.0	861	247	614		26.52	149.83	
25	62.5	869	206	663		28.64	124.58	
26	65.5	877	211	666		26.77	127.97	
27	67.5	884	264	620		26.78	160.13	
28	70.0	892	361	531		22.94	219.07	
29	72.5	900	498	402		17.37	301.95	
30	75.0	907	664	243		10.50	402.20	
31	77.5	915	846	69		2.98	512.95	
32	80.0	923	1034	−111		−4.80	626.68	
33	82.5	930	1214	−284		−12.27	735.61	
34	85.0	938	1373	−435		−18.79	832.27	
35	87.5	946	1502	−556		−24.02	910.14	
36	90.0	952	1591	−639		−27.60	963.99	
37	92.5	960	1634	−674		−29.12	990.24	← second reversal
38	95.0	967	1629	−662		−28.60	987.37	
39	97.5	975	1577	−602		−26.01	955.90	
40	100.0	983	1482	−499		−21.56	898.42	

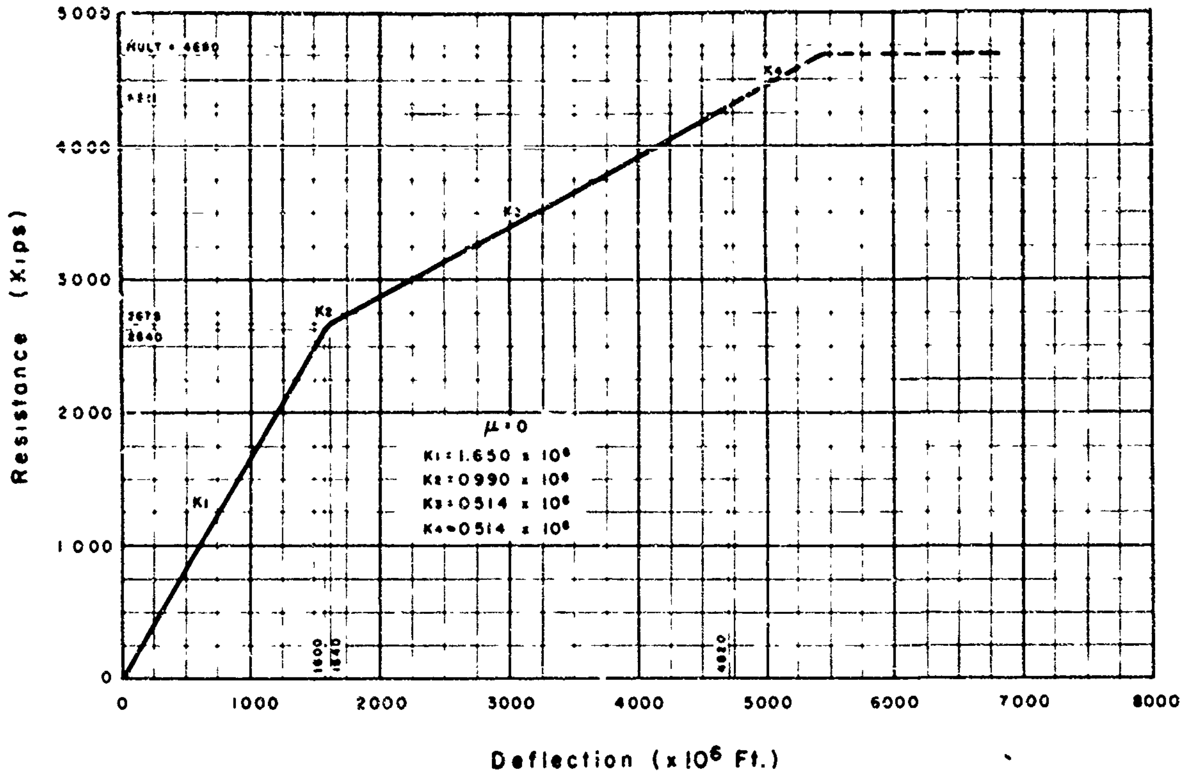

Fig. D.1 — Resistance vs. deflection curve.

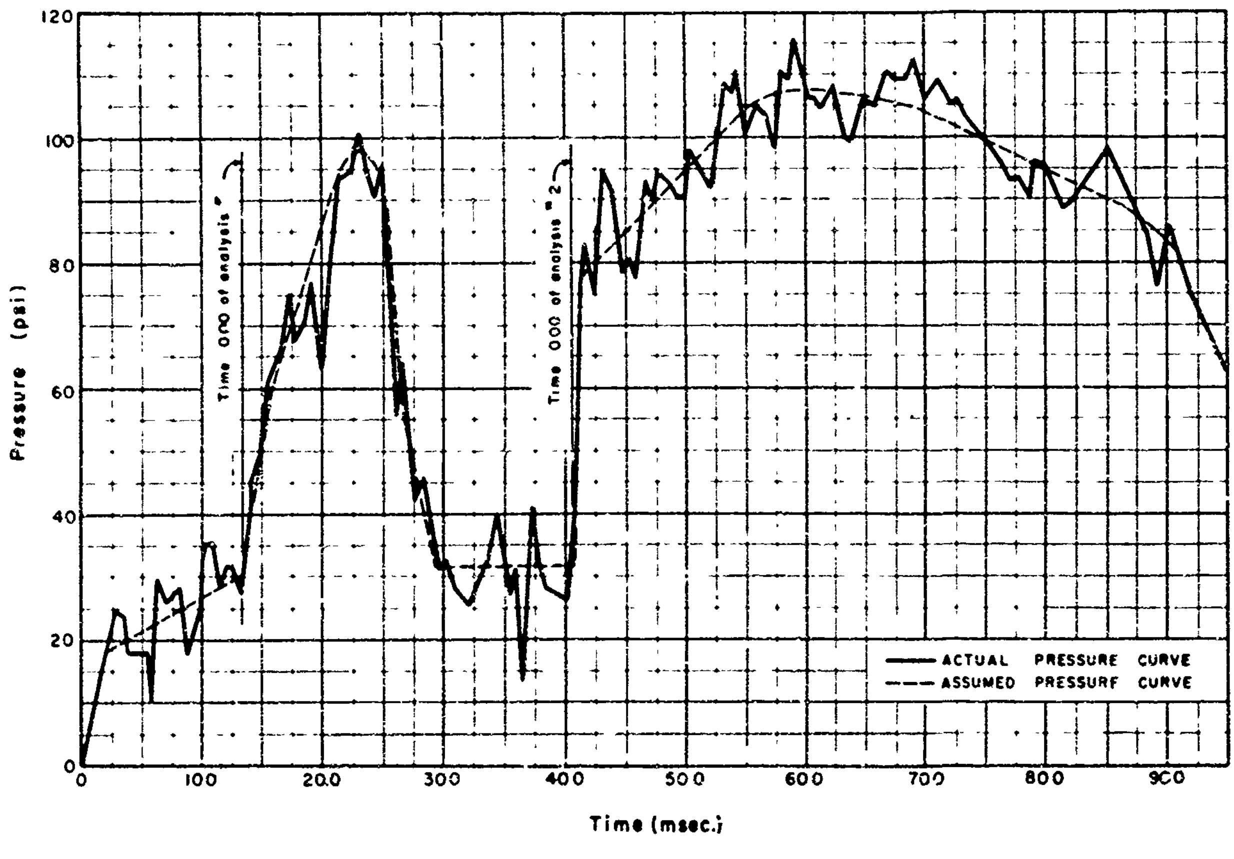

Fig D.2 — Free-field pressure vs. time curve.

Appendix E

TECHNIQUES FOR FILM-BADGE MEASUREMENT*

E.1 GENERAL

Film-badge dosimetry measurements were made primarily for the Civil Effects Test Group. In addition, some measurements were made for the Department of Defense; the Los Alamos Scientific Laboratory; Holmes & Narver, Inc.; the Naval Radiological Defense Laboratory; and Edgerton, Germeshausen & Grier, Inc. Instrumentation was generally made to determine dose vs. distance (RD^2 vs. D) for a given event. Measurements were also made shelters and various other structures and test devices. Methods were essentially the same as those used on Operation Teapot (EG&G Report 1387). The controls required to ensure uniformity of measurements and the sensitometric problems encountered during the program are discussed in the following pages.

Measurements were made with four special types of film in two dental packets. The films used were Du Pont 502, 510, and 606, and Eastman SO1112. An Eastman neutron-monitoring film was tried at the beginning of the operation, but its use was discontinued because of extreme gamma darkening.

A 7-curie Co^{60} source was used to furnish irradiated controls for the interpretation of film badges used for each event. These badges were handled and processed with the field badges.

E.2 CALIBRATION

A Co^{60} gamma calibration system (shown in Fig. E.1) was arranged so that 10 badge assemblies were consecutively administered in three sets, logarithmically progressive exposures from 0.05 to 5×10^3 r. Table E.1 indicates the time of exposure, the dose rate, and the dose administered to the film. The readings listed in the table are accurate to 5 per cent.

Thirty badges were administered doses from 0.05 to 5×10^3 r; 18 of the badge doses overlapped for standardization. The distance necessary to obtain the required doses with one exposure per series remained identical for each corresponding badge.

The source was placed in a cradle at one end of a calibration range table in such a manner that the center of the source beam passed through the center of the badges. The source was adjusted to the same position for each exposure so that, once the correct distances were established, they were automatically reproduced each time.

Distances were determined with a 25-r Victoreen R-meter, which was recently calibrated by National Bureau of Standards. Exposures were timed to obtain midscale readings for greatest accuracy. The badges were placed directly behind each other in a straight and level line

*The information contained in this appendix has been extracted from Edgerton, Germeshausen & Grier, Inc., report No. 321 to the AEC.

away from the source; the calibrated positions were determined by use of identical dummy assemblies for attenuation. Total opening and closing time of the source was approximately 4 sec. This length of time could cause, at the most, a 2 per cent error on the 200-sec exposures, and negligible error on all the others. It is believed an over-all accuracy of better than 5 per cent was maintained on administered doses.

Actual shot calibrations were made the morning of a shot on film badges that were assembled and handled with the field badges. All badges were developed together, with gray scales spaced at equal intervals throughout the reel. Ranges accurately covered by the dosimeter films were:

Du Pont 502	0.1 to 10 r
Du Pont 510	8 to 300 r
Du Pont 606	200 to 600 r
Eastman SO1112	800 to 5×10^4 r

The Du Pont film packet is shown in Fig. E.2.

It was necessary to consider a total possible error of ± 20 per cent because of the accuracy limitations on administered doses, reading, and development. In addition, film irradiated in the field tends to darken beyond the density obtainable with gamma calibration alone. This is believed to be caused by some type of reciprocity failure, neutron effects (at closer range), thermal and pressure effects, or overdarkening due to secondaries. Finally, solar effects must be taken into consideration because film that has remained in the heat of the Nevada sun does not behave in the same way as fresh film.

E.3 HANDLING OF FILM BADGE

Since each film badge consists of many parts, an assembly line was set up to handle exposed film efficiently. EG&G badge parts are: a light-tight package containing the film; a plastic box that serves as an electron diffuser; a special metal box made of a lamination of tin on the inside with lead on the outside, which functions as a filter to make the film energy independent; a polyethylene bag to protect the badge against weather and contamination; and an identification tab (see Fig. E.2). The total assembly was then wrapped in aluminum foil for protection against thermal radiation.

After recovery of the film badges from the field, the outside plastic cases containing the film and identification tab were sorted and arranged numerically. The embossed film number and the number of films in each badge were listed on a loading order data sheet.

The next step was to arrange the film packets in numerical order in a special dispenser from which they were removed to be individually fastened together in the improved, more functional edge-taping machine developed by EG&G for this purpose (Fig. E.3). After being taped on this machine, approximately 200 complete badges—or 800 pieces of film—could be assembled on a single reel and processed together. Although a single reel could contain more film, it was found this amount was the most convenient to handle.

After completion of the processing operation, the density of each film was measured on a densitometer (Fig. E.4). Personnel working in pairs read the densities and simultaneously determined the equivalent roentgen exposures from the curves that were made from the calibration badges. The evaluated dosages were tabulated according to the proper film-badge number and transferred to the data sheets for analysis.

E.4 FILM PROCESSING

Because of the similarity between visible-light and gamma-radiation (short wave length) sensitometry, precautions applicable to one must be applied to the other in the processing operation. In both cases, the relation between exposure and developed density can be determined by means of a D–log E curve.

The shape of the curve is dependent upon the degree of development of the irradiated film in that, as development is increased, a given exposure will produce increasing values of density until the point is reached where density will be unaffected by a further increase in development. This point of complete development should theoretically be reached for optimum accuracy in sensitometric work. However, owing to the severe limitation that would be noticed in the high-density range and to densitometer errors that may result from high-density readings, any advantages gained may be offset.

Although more control is required in the actual developing phase if development is not carried to completion, several advantages can be noticed from partial development of the film. A family of D-log E characteristic curves for different development times of a typical medium-speed emulsion is presented in Fig. E.5. The curve designated infinity represents development to completion. It can be seen from the curves of the incompletely developed films that the range of exposures over which the film is responsive is extended considerably, covering nearly two orders of magnitude beyond that exhibited by the completely developed film.

As shown in Fig. E.5, the maximum density which an incompletely developed film can attain is approximately 2.8. A further increase in exposure, rather than increasing the density to the saturation point, produces a definite reduction of density, or a reversal in exposure response. This effect becomes more pronounced as development is decreased, until a point is reached where the reversal is minimized.

Observation of the curves for the incompletely developed emulsions indicates that two distinct slopes are present, and as development is reduced, both slopes tend to become more nearly equal. The first slope of the curve is commonly referred to as the gamma of the D-log E curve.

Gamma initially increases very rapidly with an increase in development time; this rate subsequently becomes less, and finally levels off with no further change. This leveling point is known as gamma infinity, or complete development. The second slope region of the curve is less well defined because it is seldom a straightforward logarithmic response (Fig. E.6). Its average slope, however, exhibits considerably less change for different developing times than does the value of gamma.

E.4.1 Problems of Processing Control

Fresh developer must enter the emulsion by diffusion. Once in the emulsion, the developer reacts with the exposed silver halides and forms complexes that must diffuse out of the emulsion before new developer can enter. Since the mild acid contained in the complexes retards development, violent action is often necessary to separate these acids from the surface. Once they have been removed, they diffuse throughout the developer and become neutralized or rendered inactive by components of the solution placed there to serve as such a buffer.

If a film being developed remains idle in the solution, the acid-retarding development will gradually be reduced by the buffer and development to completion can ultimately occur. However, when the film being processed is removed from the developer before complete development takes place, physical aid is necessary to remove the complexes from the emulsion surface. The method presently employed makes use of ten double-squeegee wipers to provide agitation to the solution near the emulsion surface. This agitation is caused by the film moving past a series of ten knifelike edges similar to soft rubber windshield wipers. These blades are held in near contact with the emulsion surface and set up a turbulent flow pattern of developer as the film and a layer of developer move past them. Design of this agitation system is such that there is little chance of damage to the film.

E.4.2 Controlled Processing of Radiation Film Badges

Figure E.6 is a plot of a comparison of two D-log E curves. The dashed line represents the response of several SO1112 films subjected to a series of 400-μsec visible light exposures; the solid line is the response curve of a series of calibrated Co^{60} exposures. Exposure values are given in arbitrary units. Although further experimental work must be performed before conclusive evidence can be drawn from the results of Fig. E.6, the similarity of the D-log E

curve for the SO1112 film indicates that white-light exposures may be used for process control of gamma-radiation exposures.

The development of SO-1112 emulsions was carried out to a high contrast in an effort to reduce the exposure-evaluation errors. With the contrast shown in Fig. E.6, the evaluation errors are ±3 per cent in the lower region of the curve, and ±7 per cent in the upper slope region. The resulting D–log E curves display a wide range in gamma-radiation exposure, especially in comparison to the accepted useful range produced as a result of development to completion.

E.4.3 Processing Procedure

Included with the cobalt calibration badges were several SO1112 white-light standards. All badges were run through the taping machine and developed to a gamma of 1.3, as follows:

Emulsion Type MF, No. 1112; MCS 5000; N.D. 1.3
Color: White
Developer: D-76, No. 4
Temperature: 70°F
Time: 2 min 39 sec, 10 double-squeegee wipers, used at $8\frac{1}{4}$ ft/min

The development gamma at the head of the series was 1.3, and at the tail was 1.29.

E.5 ANALYSIS

The reels of processed badges are mounted on rewinds and wound across the reading surface of an Ansco-Macbeth densitometer. Two central readings are made and recorded for each film. With the readings complete, the calibration films are first compared to previous runs, and then the shot films to their calibration film. From the results of these comparisons, analysis charts and graphs can be drawn, and from these comprehensive summaries, the shot doses and the accuracy of the system are determined.

Table E.1 — FILM-BADGE CALIBRATION

	Time, sec		
Dose, r	200	2×10^3	2×10^4
0.05	0.00025		
0.1	0.0005		
0.2	0.001		
0.5	0.0025	0.00025	
1	0.005	0.0005	
2	0.01	0.001	
5	0.025	0.0025	0.00025
10	0.05	0.005	0.0005
20	0.1	0.01	0.001
50	0.25	0.025	0.0025
100		0.05	0.005
200		0.1	0.01
500		0.25	0.025
10^3			0.05
2×10^3			0.1
5×10^3			0.25
		Dose rate (r/sec)	

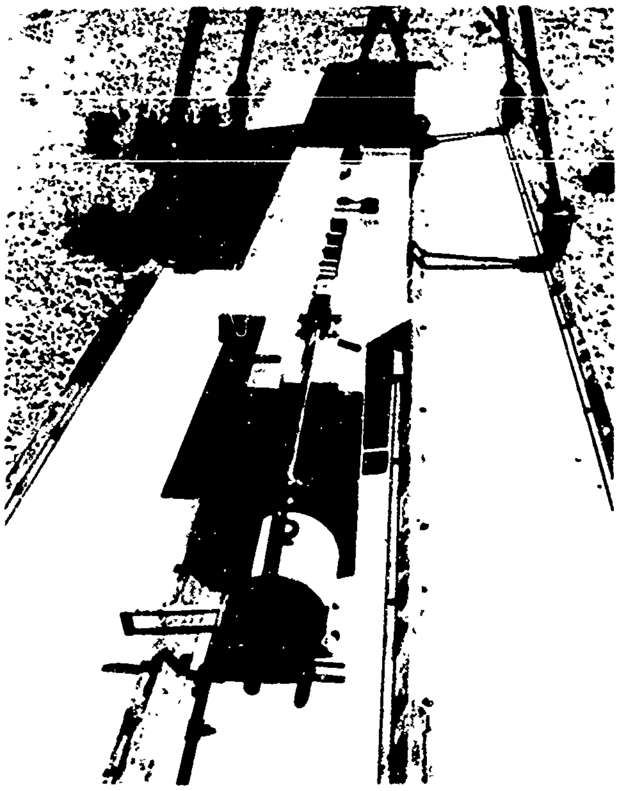

Fig. E.1 — Cobalt-60 gamma calibration system.

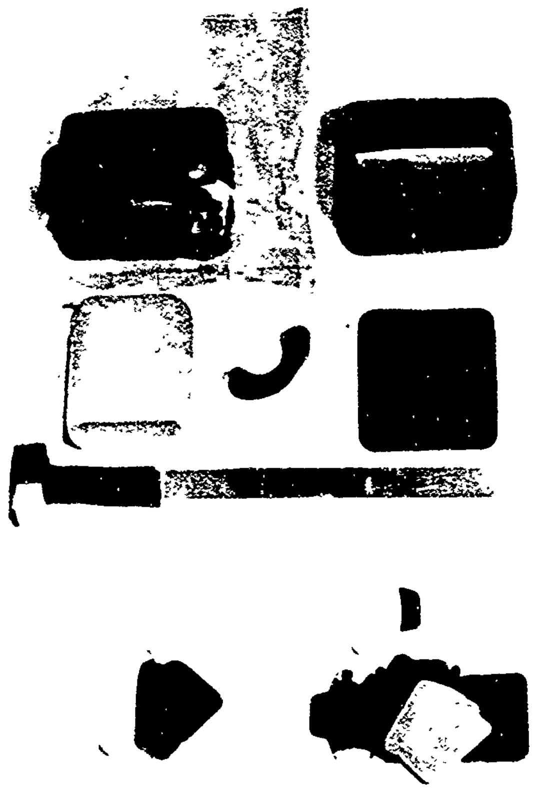

Fig. E.2 — Du Pont film packet and EG&G film badge.

Fig. E.3 — EG&G taping machine.

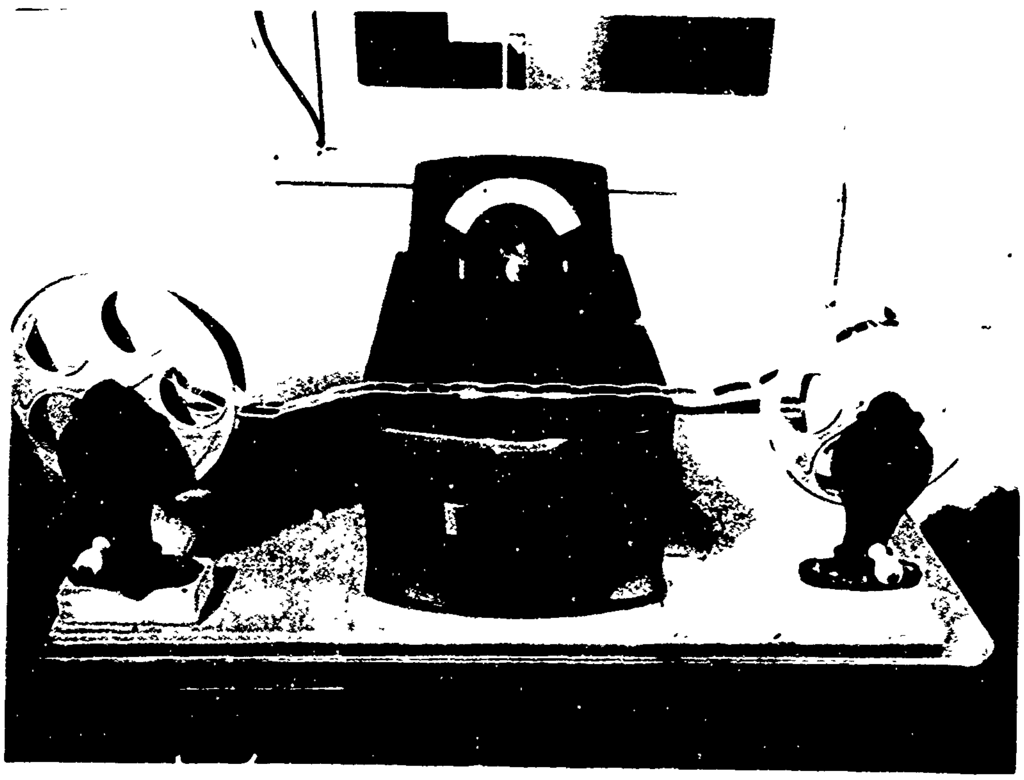

Fig. E.4 — Densitometer.

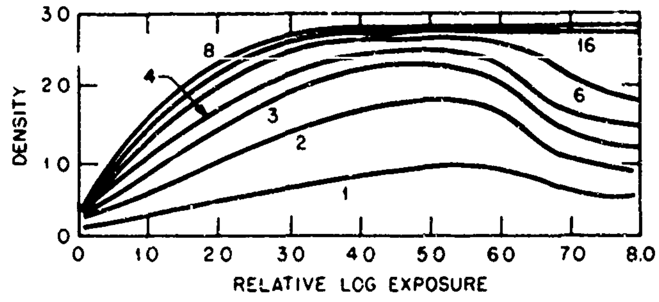

Fig. E.5—Effect of development time on the shape of the characteristic curve of a typical medium-speed film. (Mees, Theory of the Photographic Process, p. 261, The Macmillan Company, 1952.)

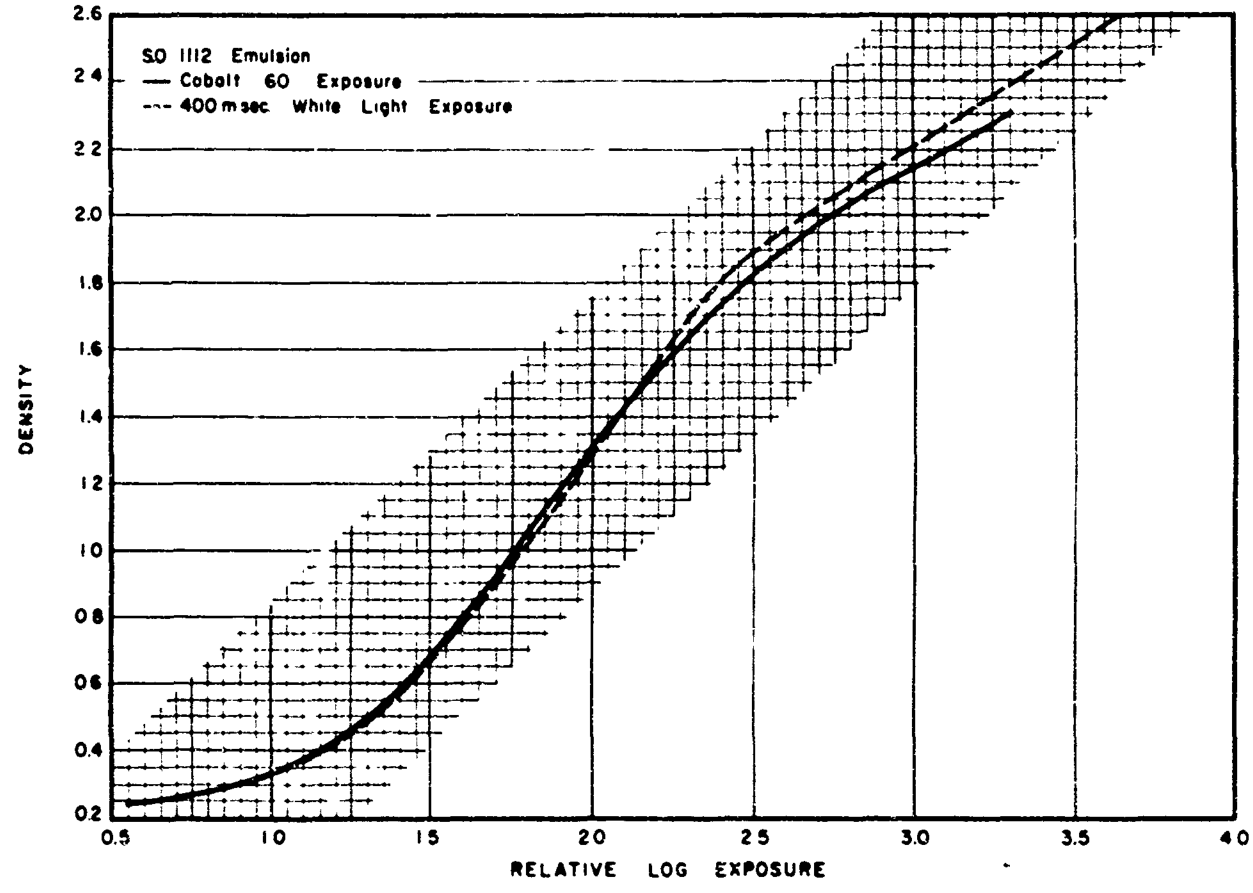

Fig. E.6—Comparison of white light and gamma radiation exposure densities.